frontiers | Research Topics

Case reports in thoracic oncology 2022

Edited by
Caroline Hayhurst, Kohei Fujita and Yaron Perry

Published in
Frontiers in Oncology

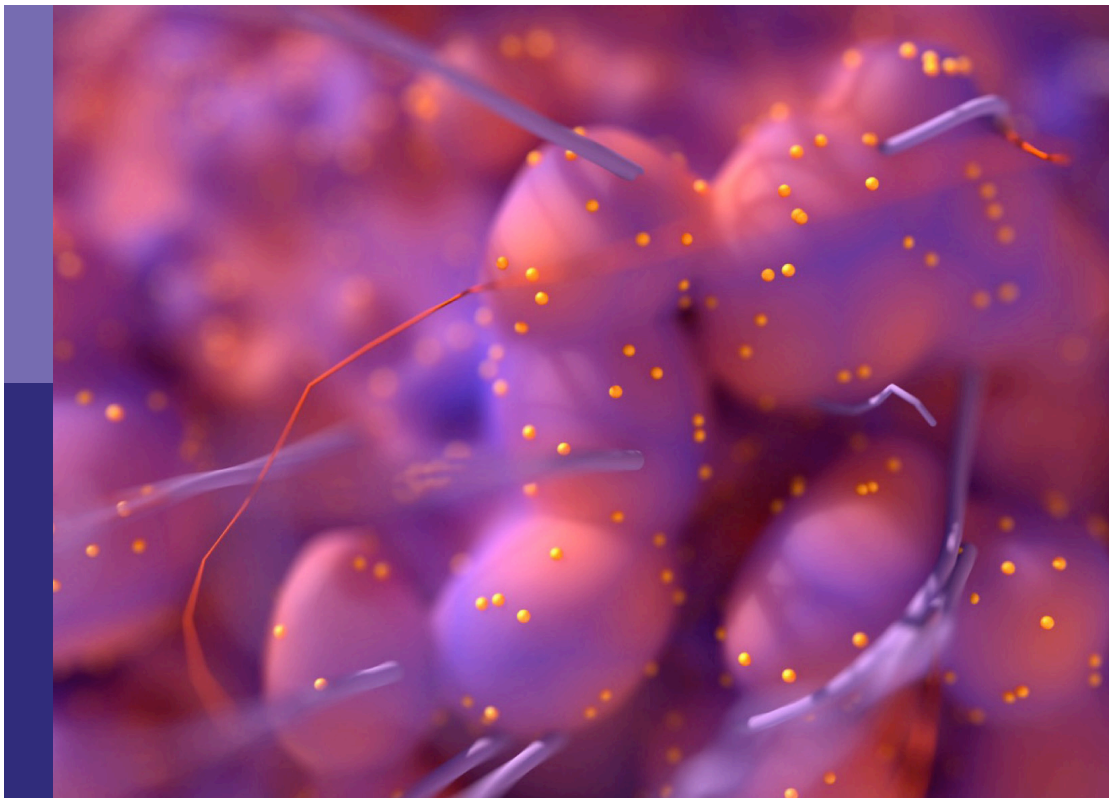

ISSN 1664-8714
ISBN 978-2-8325-4271-2
DOI 10.3389/978-2-8325-4271-2

About Frontiers

Frontiers is more than just an open access publisher of scholarly articles: it is a pioneering approach to the world of academia, radically improving the way scholarly research is managed. The grand vision of Frontiers is a world where all people have an equal opportunity to seek, share and generate knowledge. Frontiers provides immediate and permanent online open access to all its publications, but this alone is not enough to realize our grand goals.

Frontiers journal series

The Frontiers journal series is a multi-tier and interdisciplinary set of open-access, online journals, promising a paradigm shift from the current review, selection and dissemination processes in academic publishing. All Frontiers journals are driven by researchers for researchers; therefore, they constitute a service to the scholarly community. At the same time, the *Frontiers journal series* operates on a revolutionary invention, the tiered publishing system, initially addressing specific communities of scholars, and gradually climbing up to broader public understanding, thus serving the interests of the lay society, too.

Dedication to quality

Each Frontiers article is a landmark of the highest quality, thanks to genuinely collaborative interactions between authors and review editors, who include some of the world's best academicians. Research must be certified by peers before entering a stream of knowledge that may eventually reach the public - and shape society; therefore, Frontiers only applies the most rigorous and unbiased reviews. Frontiers revolutionizes research publishing by freely delivering the most outstanding research, evaluated with no bias from both the academic and social point of view. By applying the most advanced information technologies, Frontiers is catapulting scholarly publishing into a new generation.

What are Frontiers Research Topics?

Frontiers Research Topics are very popular trademarks of the *Frontiers journals series*: they are collections of at least ten articles, all centered on a particular subject. With their unique mix of varied contributions from Original Research to Review Articles, Frontiers Research Topics unify the most influential researchers, the latest key findings and historical advances in a hot research area.

Find out more on how to host your own Frontiers Research Topic or contribute to one as an author by contacting the Frontiers editorial office: frontiersin.org/about/contact

Case reports in thoracic oncology: 2022

Topic editors

Caroline Hayhurst — University Hospital of Wales, United Kingdom
Kohei Fujita — Division of Respiratory Medicine, Center for Respiratory Diseases, National Hospital Organization Kyoto Medical Center, Japan
Yaron Perry — University at Buffalo, United States

Citation

Hayhurst, C., Fujita, K., Perry, Y., eds. (2024). *Case reports in thoracic oncology: 2022*. Lausanne: Frontiers Media SA. doi: 10.3389/978-2-8325-4271-2

Table of contents

08 Editorial: Case reports in thoracic oncology: 2022
Yaron Perry

11 Rapid response to monotherapy with MEK inhibitor trametinib for a lung adenocarcinoma patient harboring primary *SDN1-BRAF* fusion: A case report and literature review
Yang Yu, Min Yu, Yanying Li, Xiaojuan Zhou, Tian Tian, Yijia Du, Zegui Tu and Meijuan Huang

17 Pseudo-progression with osimertinib after definitive chemoradiation in unresectable epidermal growth factor receptor mutation positive of stage III non-small cell lung cancer: A case report
Fei Ren, Yao Wang, Yongsheng Gao and Xiangjiao Meng

23 *EML4-ALK* rearrangement in primary malignant fibrous histiocytoma of the lung treated with alectinib: A case report
Shuai Zhang, Xuqiang Liao and Jiawei Chen

30 Drug-induced liver injury associated with dacomitinib: A case report
Xuanxuan Wang, Anqi Huang, Yun Lu, Suyu Gao, Wen Hu and Hong Cheng

36 A pulmonary enteric adenocarcinoma patient harboring a rare EGFR exon 19 P753S mutation: Case report and review
Xiaohu Xu, Dong Chen, Xiao Wu and Qi Wang

43 Lung cancer patients with nephropathy as the first manifestation: Literature review and clinical study report
Qianqian Xu, Guming Zou, Li Zhuo, Hongmei Gao and Wenge Li

51 Case report: Novel *junctional sarcoplasmic reticulum protein 1* intergenic region–*anaplastic lymphoma kinase* fusion in a patient with lung adenocarcinoma responds to alectinib
Feng Xue, Shengyuan Xu, Cailing Jiang, Mafei Kang, Muhammad Usman and Lin Zhu

57 Secondary mutant ALK-I1171s in pituitary metastases from a patient with ALK fusion-positive advanced lung adenocarcinoma: A case report and literature review
Dan Han, Kewei Zhao, Qin Yang, Liling Zhang and Shihong Fei

63 Case report: Using DNA short tandem repeats to confirm nongestational origin of pulmonary choriocarcinoma
Filipa Ferreira da Silva, Rita Barata, Inês Rolim, Catarina Carvalheiro, Nuno Gil and Marcos Pantarotto

68 Case report: A case report and literature review about Pathological transformation of lung adenosquamous cell carcinoma
Liang Ge-ge, Geng Cuicui, Li Leiqiang, Tian Yongcang, Ma Jiangang, Ou Yiwen and Sun Li-zhe

76 *EGFR* mutations and high PD-L1 expression of lung squamous cell carcinoma patients achieving pCR following neoadjuvant immuno-chemotherapy: Case report
Xiangyu Xu, Zixia Shi, Dan Fu, Depei Huang and Zheng Ma

83 Case report: Complete resection of invasive thymoma invading the superior vena cava and right atrium under cardiopulmonary bypass support
Xiangxin Zhang, Liang Chen, Wenyong Zhou, Zhexin Wang, Chong Wang, Jianxin Shi and Feng Yao

88 Case report: Immunovirotherapy as a novel add-on treatment in a patient with thoracic NUT carcinoma
Linus D. Kloker, Branko Calukovic, Katrin Benzler, Alexander Golf, Sebastian Böhm, Sven Günther, Marius Horger, Simone Haas, Susanne Berchtold, Julia Beil, Mary E. Carter, Tina Ganzenmueller, Stephan Singer, Abbas Agaimy, Robert Stöhr, Arndt Hartmann, Thomas Duell, Sandra Mairhofer, Fabian Fohrer, Niels Reinmuth, Lars Zender and Ulrich M. Lauer

97 Case report: A rapid response to immunotherapy in a thoracic SMARCA4-deficient undifferentiated tumor with respiratory failure
Liyong Shi, Lianshun Lin, Yin Ding, Yiming Zeng and Xiaoyang Chen

104 Case report: *EML4::NTRK3* gene fusion in a patient with metastatic lung adenocarcinoma successfully treated with entrectinib
Chiara Lazzari, Lorenza Pecciarini, Claudio Doglioni, Federica Pedica, Ana Maria Samanes Gajate, Alessandra Bulotta, Vanesa Gregorc and Maria Giulia Cangi

111 Case report: BRAF A598-T599insV mutation as a potential resistance mechanism to alectinib in ALK-rearranged lung adenocarcinoma
Thomas Pasau, Els Wauters, Isabelle Wauters, Fabrice Duplaquet, Lionel Pirard, Claudia Pop-Stanciu, Nicky D'Haene, Michael Dupont, Thierry Vander Borght, Benoît Rondelet and Sebahat Ocak

118 Primary pulmonary T-cell lymphoma after operation for small intestinal stromal tumor: A case report
Zhiwei Peng, Li Yi, Yahong Tao, Zhiyong Chen, Ze Lin, Anjing He, Mengni Jin, Fanrong Liu and Minjing Zuo

123 *RET* fusion mutation detected by re-biopsy 7 years after initial cytotoxic chemotherapy: A case report
Kei Morikawa, Hiroshi Handa, Junko Ueno, Hajime Tsuruoka, Takeo Inoue, Naoki Shimada, Junki Koike, Seiji Nakamura, Yoshiharu Sato and Masamichi Mineshita

129 Case report: Rechallenge with EGFR–TKIs after immunotherapy in EGFR–mutated non–small cell lung cancer with leptomeningeal metastasis
Chunfa Qian, Yuhai Zhang, Wanwan Cheng, Qingchao Zhang, Mengzhen Li and Shencun Fang

134 Case report: Radiofrequency ablation combined with biopsy for Cushing's syndrome due to ectopic ACTH lesions in the lung
Xiao Zhang, Liangliang Meng, Yueyong Xiao and Zenan Chen

140 Case Report: The first case of primary pulmonary collision tumor comprising mixed squamous cell and glandular papilloma and glomus tumor
Chan Yang, Shuang Li, Zuoyu Liang and Lili Jiang

147 Case report: an initially unresectable stage III pulmonary sarcomatoid carcinoma qith EGFR mutation achieving pathological complete response following neoadjuvant therapy with osimertinib plus chemotherapy
Xiguang Liu, Yating Zheng, Shijie Mai, Yu Tong, Lili Yang, Mengli Huang and Ruijun Cai

154 Case Report: A case of radioactive iodine-refractory thyroid cancer accompanying cervical lymph node metastasis treated with US-guided RFA combined with ^{125}I seed implantation
Yuanpeng Zhai, Yu Shao and Qian Li

161 Small cell lung cancer transformation and tumor heterogeneity after sequential targeted therapy and immunotherapy in EGFR-mutant non-small cell lung cancer: A case report
Meng-Hang Yang, Jia Yu, Chen-Lei Cai and Wei Li

166 Case report: Liquid biopsy, the sooner the better?
Quentin Dominique Thomas, Julien Colard-Thomas, Delphine Delansay, Fanny Leenhardt, Jerome Solassol, Julie A. Vendrell and Xavier Quantin

172 Case report: Rare intrapulmonary malignant mesothelioma complicated with myositis
Dandan Gong, Jian Yu and Xiaodong Jiang

177 Successful treatment of extensive-stage small cell lung cancer with concurrent pleural and pericardial effusions: Case report
Ayaka Kashima, Yosuke Fukuda, Miri Shimamura, Miharu Ijichi and Hironori Sagara

182 Case report: Imaging findings of true thymic hyperplasia at ^{18}F-FDG PET/CT in an infant
Jiazhong Ren, Zheng Fu and Yaqing Zhao

186 Successful treatment of a patient with advanced lung adenocarcinoma (EGFR-T790M and C797S cis) with lazertinib: A case report and literature review
Yue Fang, Qiankun Zhang, Weimin Wang, Juanjuan Tong and Xialin Li

193 Case report: Identification of acute promyelocytic leukemia during osimertinib resistance followed by granulocyte colony-stimulating factor and pembrolizumab
Huohuan Tian, Linhui Yang, Wang Hou, Yu Wu, Yang Dai, Jiang Yu and Dan Liu

199 Case Report: A case of synchronous right upper lobe adenocarcinoma and left lower lobe squamous cell carcinoma treated with immune checkpoint inhibitor plus chemotherapy
Yujiao Liu, Han Yu, Youhong Dong and Dongdong Zhang

205 Case report: A rare case of sintilimab-induced gastric stenosis and literature review
Kunkun Song, Haoxu Dong, Shujun Jiang, Xiaohu Xu, Chao Zhang, Qian Chen and Qi Wang

211 Extraskeletal Ewing's sarcoma of the mediastinum: Case report
Aldo Caltavituro, Roberto Buonaiuto, Fabio Salomone, Rocco Morra, Erica Pietroluongo, Pietro De Placido, Marianna Tortora, Annarita Peddio, Fernanda Picozzi, Margaret Ottaviano, Mirella Marino, Sabino De Placido, Giovannella Palmieri and Mario Giuliano

219 Chemo-immunotherapy for metastatic non-squamous NSCLC in a patient with HIV infection: A case report
Alessandro Inno, Emanuela Lattuada, Giovanni Foti and Stefania Gori

223 Case report: Primary mediastinal Ewing's sarcoma presenting with chest tightness
Manman Cui, Duchang Zhai, Yan Liu, Xiuzhi Zhou, Tingting Wang, Lihuan Wang, Wu Cai, Guohua Fan and Shenghong Ju

227 Nonfunctional ectopic adrenocortical carcinoma in the lung: A case report and literature review
Limin Nie, Shuyun Wang, Zongfeng Feng, Yuping Sun, Zhen Wang, Qi Dang, Aiqin Gao and Yajuan Lv

234 Case report: Pulmonary synovial sarcoma in a long-term survivor of childhood Hodgkin lymphoma
Konstantin Shilo, Peter J. Kneuertz, David Liebner and Wei Chen

239 Acquired ALK G1202R-, ALK I1171N-, or EML4-ALK-mediated resistance to ensartinib in lung adenocarcinoma but responded to lorlatinib: A case report
Zhifeng Ye and Junhua Guo

243 Case report: The stroma-rich variant of Castleman's disease of hyaline-vascular type with atypical stromal cell proliferation and malignant potential: An exceptional rare case occurred in mediastinal lymph node
Xiaoxin Shi, Mengying Liao, Xiaomin Yin, Yaoli Chen, Chuqiang Huang, Weihua Yin and Jian Li

250 Long-term survival with anlotinib as a front-line treatment in an elderly NSCLC patient: A case report
Jingyi Wang, Xiaoqing Li, Juan Zhou, Dan Qiu, Mengyao Zhang, Lan Sun and Shengwen Calvin Li

257 Case Report: Termination of unplanned pregnancy led to rapid deterioration of non-small-cell lung cancer during osimertinib treatment
Qizhi Ma, Pei Shu, Kexun Zhou and Yongsheng Wang

frontiers | Frontiers in Oncology

TYPE Editorial
PUBLISHED 20 March 2024
DOI 10.3389/fonc.2024.1369799

OPEN ACCESS

EDITED AND REVIEWED BY
Lizza E.L. Hendriks,
Maastricht University Medical Centre,
Netherlands

*CORRESPONDENCE
Yaron Perry
yperry@buffalo.edu

RECEIVED 13 January 2024
ACCEPTED 15 January 2024
PUBLISHED 20 March 2024

CITATION
Perry Y (2024) Editorial: Case reports in thoracic oncology: 2022.
Front. Oncol. 14:1369799.
doi: 10.3389/fonc.2024.1369799

Editorial: Case reports in thoracic oncology: 2022

Yaron Perry[1,2,3]*

[1]Division of Thoracic Surgery, Buffalo General Hospital, Buffalo, NY, United States, [2]Division of Thoracic Surgery, Erie County Medical Center, Buffalo, NY, United States, [3]Department of Surgery, Jacobs School of Medicine and Biomedical Sciences, University at Buffalo, Buffalo, NY, United States

KEYWORDS

case report, thoracic oncology, unique findings, novel therapies, unique pathology

Editorial on the Research Topic
Case reports in thoracic oncology: 2022

When I was asked by the editorial board of Frontiers to help edit a whole Research Topic on "*case reports in thoracic oncology*," I was caught by surprise. In an era of large databases and unlimited access to medical information, is there still a role for case reports?

Physicians began describing interesting cases involving all specialties in the early days of humanity, Ancient Egyptian medicine (c. 1600 BCE) has papyrus records of case reports as well as reports by Hippocrates (460–370 BCE) (1). Case reports describe important scientific observations that are missed or undetected in clinical trials and provide individual clinical insights. A case report of Kaposi's sarcoma in a young homosexual man was the initial main observation to the finding of acquired immune deficiency syndrome (2). In 1817, James Parkinson wrote an article titled "An essay on the shaking palsy," later it lead to the discovery of the disease carrying his name (Parkinson's disease) (3). Case reports linked the anorexic agents fenfluramine and dexfenfluramine with primary pulmonary hypertension led to clinical trials that investigated the mechanism and incidence of this adverse effect, causing their withdrawal from the market (4, 5). Hemolytic-uremic syndrome is a severe condition associated with Escherichia coli and characterized by hemolytic anemia, thrombocytopenia, and acute renal failure. At the start of an outbreak, a case series reported dramatic resolution of symptoms of Escherichia coli-associated hemolytic-uremic syndrome after treatment with monoclonal antibody eculizumab (6). This case series led to the adoption of eculizumab as a treatment option. In 1985, the American Medical Association reprinted 51 papers from the Journal of the American Medical Association that had significantly changed the science and practice of medicine during the 150 years of the organization's existence (7); five of these papers were case reports.. But in the last decade, most professional journals and scientific editorial committees are publishing mainly case studies, double-blind control studies, cohort studies, large database reports, and original scientific work, while case reports are scattered and usually limited to a single page of imaging or rare occasions and account for less than 2% of the journal content. In the second half of the 20th century, the significance of a case report as a type of research article was downgraded due to low ranking in the evidence hierarchy (8).

As a thoracic surgeon, I recently admitted a young patient to our thoracic surgery service: a very fit 27-year-old police officer who initially presented with pneumonia and parapneumonic effusion. Within a matter of hours, his condition deteriorated so that he

needed mechanical ventilation and pressors support. He was treated by multiple medical teams from internal medicine, infectious disease, and intensive care and multiple surgeons; he was stabilized and treated with a chest drain. Because he was not improving, I looked through the literature and found a case report describing the same clinical picture with isolation of very rare bacteria—*Streptococcus constellatus* (9). The patient in the described case report was treated aggressively with surgical exploration and drainage of the pleural space with decortication, leading to expansion of the lung and recovery. The initial Gram stain of cultures from our patient were indicative of *Streptococcus* but without the final species isolation. On the basis of the case report, I took the patient to the operating room and performed an extensive decortication of his pleural space with expansion of the lung and clearance of infected tissue and fluid, which ultimately resulted in complete recovery of the patient within 48 hours. The final cultures documented that the bacterium was the rare *Streptococcus constellatus*.

Having learned from a case report, which led to saving my patient's life, I was very enthusiastic to contribute and collect many case reports from my colleagues in the thoracic oncology field. Publication of their experiences with rare cases will hopefully contribute to the care of patients with rare manifestations in the future.

We carefully collected case reports, such as a case that describes a rare/unconventional treatment from a group in the Department of Radiology, The First Medical Center, Chinese People's Liberation Army (PLA) General Hospital, Beijing, China; they describe radiofrequency ablation combined with biopsy for Cushing's syndrome due to ectopic adrenocorticotropic hormone lesions in the lung (this Research Topic). We included an article describing a new conventional treatment with rare side effects from a group in the Department of Pharmacy, Zhongnan Hospital of Wuhan University, Wuhan, China; they describe liver injury associated with dacomitinib (this Research Topic). Clinicians should pay particular attention to the possibility of drug-induced liver injury during dacomitinib treatment. A group from the Department of Pathology, Peking University Shenzhen Hospital, Shenzhen, China, described a rare manifestation of a known disease (this Research Topic): a case of a stroma-rich variant of Castleman's disease of the hyaline-vascular type featuring atypical hyperplasia of the stromal cells and malignant behavior. In addition, a group from the Department of Thoracic Oncology, State Key Laboratory of Biotherapy, Cancer Center, West China Hospital, Sichuan University, Chengdu, China, report on the efficacy of new targeted immunotherapy in lung cancer (this Research Topic). In this research, a patient with non-small cell lung cancer with primary SDN1-BRAF fusion responded well to continuous trametinib monotherapy. Further research is required to understand the biochemical and oncogenic mechanisms and identify the targeted strategy in NSCLC patients harboring BRAF fusions, but this case may lead to a new mode of treatment.

Treatments such as insulin for diabetes and cholesterol-lowering drugs for coronary heart disease first appeared as scattered case report descriptions in the literature. Their subsequent persistence in the literature and scientific trials with expansion to larger patient populations led these novel therapies to become the standard of care. In the same way, the field of thoracic oncology can benefit from novel targeted therapies that are rapidly evolving. The publishing of case reports in thoracic oncology will increase descriptions of new diseases from which clues to etiology can be derived. Indeed, the first clues about tobacco smoking and lung cancer came from surgical patient series in the 1920s and 1930s, though formal case-control and cohort studies came only decades later (10). Case reports can lead to new therapies, recognition of side effects, or as in my patient, serve to educate. Case histories are like a lesson from the clinicopathological conference: "do not make the same mistake I did." Cases with an unfavorable outcome can be collected to see whether that outcome might have been prevented (11).

By giving this platform to many clinicians in the field of thoracic oncology to publish their unique findings, I hope that many novel therapies will be established for the care of our future patients.

This is what it is all about.

I hope you will find these case reports informative and helpful.

Happy New Year!

Author contributions

YP: Conceptualization, Writing – original draft, Writing – review & editing.

Acknowledgments

Special thanks to Dr. Karen Dietz for her editorial support.

Conflict of interest

The author declares that the research was conducted in the absence of any commercial or financial relationships that could be construed as a potential conflict of interest.

Publisher's note

References

1. Garrison FH. *An introduction to the history of medicine: with medical chronology, suggestions for study and bibliographic data. 4th ed*. Philadelphia: W.B. Saunders (1929). p. 996. p. p.

2. Gottlieb GJ, Ragaz A, Vogel JV, Friedman-Kien A, Rywlin AM, Weiner EA, et al. A preliminary communication on extensively disseminated Kaposi's sarcoma in young homosexual men. *Am J Dermatopathol* (1981) 3(2):111–4. doi: 10.1097/00000372-198100320-00002

3. Goetz CG. The history of Parkinson's disease: early clinical descriptions and neurological therapies. *Cold Spring Harb Perspect Med* (2011) 1(1):a008862. doi: 10.1101/cshperspect.a008862

4. Atanassoff PG, Weiss BM, Schmid ER, Tornic M. Pulmonary hypertension and dexfenfluramine. *Lancet* (1992) 339(8790):436. doi: 10.1016/0140-6736(92)90129-Q

5. Douglas JG, Munro JF, Kitchin AH, Muir AL, Proudfoot AT. Pulmonary hypertension and fenfluramine. *Br Med J (Clin Res Ed)* (1981) 283(6296):881–3. doi: 10.1136/bmj.283.6296.881

6. Lapeyraque AL, Malina M, Fremeaux-Bacchi V, Boppel T, Kirschfink M, Oualha M, et al. Eculizumab in severe shiga-toxin-associated HUS. *N Engl J Med* (2011) 364 (26):2561–3. doi: 10.1056/NEJMc1100859

7. Meyer HS, Lundberg GDAmerican Medical Association. *Fifty-one landmark articles in medicine: the JAMA centennial series* Vol. xiv. . Chicago: American Medical Association (1985). p. 486. p. p.

8. Martyn C. Case reports, case series and systematic reviews. *QJM* (2002) 95 (4):197–8. doi: 10.1093/qjmed/95.4.197

9. Vulisha AK, Sam R, Nur H, Bhardwaj N, Sirineni S. Aggressive presentation of Streptococcus constellatus. *Cureus* (2021) 13(4):e14534. doi: 10.7759/cureus.14534

10. Doll R. Uncovering the effects of smoking: historical perspective. *Stat Methods Med Res* (1998) 7(2):87–117. doi: 10.1177/096228029800700202

11. Vandenbroucke JP. Case reports in an evidence-based world. *J R Soc Med* (1999) 92(4):159–63. doi: 10.1177/014107689909200401

frontiers | Frontiers in Oncology

TYPE Case Report
PUBLISHED 19 August 2022
DOI 10.3389/fonc.2022.945620

OPEN ACCESS

EDITED BY
Giuseppe Palmieri,
University of Sassari, Italy

REVIEWED BY
Panagiotis Paliogiannis,
University of Sassari, Italy
Tilman Brummer,
University of Freiburg, Germany

*CORRESPONDENCE
Meijuan Huang
hmj107@163.com

SPECIALTY SECTION
This article was submitted to Thoracic Oncology, a section of the journal Frontiers in Oncology

RECEIVED 16 May 2022
ACCEPTED 26 July 2022
PUBLISHED 19 August 2022

CITATION
Yu Y, Yu M, Li Y, Zhou X, Tian T, Du Y, Tu Z and Huang M (2022) Rapid response to monotherapy with MEK inhibitor trametinib for a lung adenocarcinoma patient harboring primary *SDN1-BRAF* fusion: A case report and literature review. *Front. Oncol.* 12:945620. doi: 10.3389/fonc.2022.945620

Rapid response to monotherapy with MEK inhibitor trametinib for a lung adenocarcinoma patient harboring primary *SDN1-BRAF* fusion: A case report and literature review

Yang Yu[1], Min Yu[1], Yanying Li[1], Xiaojuan Zhou[1], Tian Tian[2], Yijia Du[2], Zegui Tu[2] and Meijuan Huang[1]*

[1]Department of Thoracic Oncology and State Key Laboratory of Biotherapy, Cancer Center, West China Hospital, Sichuan University, Chengdu, China, [2] West China school of medicine, Sichuan University, Chengdu, China

BRAF gene has been identified as an oncogenic driver and a potential target in various malignancies. *BRAF* fusions are one subtype of *BRAF* alterations with a rare frequency. Here, we first report a previously treated advanced lung adenocarcinoma patient with *de novo SND1-BRAF* fusion who achieves partial response to the MAK inhibitor trametinib. We also provide a literature review on targeted therapies for *BRAF* fusions.

KEYWORDS

***BRAF* fusion, *SDN1-BRAF*, lung adenocarcinoma, trametinib, MAPK pathway**

Introduction

BRAF gene encodes the RAF kinase and activates the MAPK pathway. It has emerged as an oncogenic driver and a potential therapeutic target in a wide variety of solid tumors (1, 2). Based on signaling mechanism, kinase activity, and sensitivity to inhibitors, *BRAF* mutations have been categorized into three functional classes: RAS-independent kinase-activating V600 monomers (class I), RAS-independent kinase-activating dimers (class II), and RAS-dependent kinase-inactivating heterodimers (class III) (3, 4). *BRAF* alterations occur in 4.4% of non-small cell lung cancer (NSCLC) patients (1). The most prevalent variant is the BRAF *V600* mutation, accounting for 1%–2% of BRAF-mutated NSCLC patients (5). However, *BRAF* fusions, one subtype of *BRAF* class II mutations, are only identified in 0.2% of NSCLC samples (1). The Food and Drug Administration (FDA) has approved dabrafenib plus trametinib to treat NSCLC patients with *BRAF*

V600 mutation (6). In contrast, *BRAF* fusions are not yet eligible for targeted therapies (4).

Unlike *BRAF* mutation, *BRAF* gene fusions activate the MAPK signaling pathway by inducing the removal of the auto-inhibitory N-terminal moiety (7). *BRAF* fusions exist in numerous solid tumors, including melanoma, glioma, thyroid cancer, pancreatic carcinoma, NSCLC, and colorectal cancer (1, 8). *BRAF* fusions can take on various forms. Ross et al. and Zehir et al. have reported 44 distinct types of *BRAF* fusions in multiple solid tumors, especially in NSCLC, such as *EPS15-BRAF*, *NUP214-BRAF*, *ARMC10-BRAF*, *BTF3L4-BRAF*, *AGK-BRAF*, *GHR-BRAF*, *ZC3HAV1-BRAF*, *TRIM24-BRAF*, *GK-BRAF*, *PJA2-BRAF*, *SND1-BRAF*, *MRPS33-BRAF*, and *PARP12-BRAF (*1, 9). Unfortunately, reports on anti-*BRAF* therapies for NSCLC with *de novo BRAF* gene fusion are scarce.

The study shows a rapid response to trametinib monotherapy in the advanced lung adenocarcinoma patient with *de novo* SND1-BRAF fusion for the first time.

Case report

A 60-year-old man was admitted to West China Hospital, Sichuan University in February 2017 with symptoms of expectoration and shortness of breath for 1 month. He was a current smoker (30 packs/years) with no family history of cancer. High concentration levels of serum carcinoembryonic antigen (CEA) (63.92 ng/ml) and neuron-specific enolase (NSE) (23.35 ng/ml) were revealed by blood tests. Right lung masses and solid nodules were visible on a chest computed tomography (CT) scan, which also revealed enlargement of the right hilar and mediastinal lymph nodes, focal thickening of the right pleura, and right pleural effusions. He underwent a CT-guided biopsy of the right lung mass, and the lesion was pathologically diagnosed as adenocarcinoma. Immunohistochemical examination of the right pleural effusions showed positivity of CK7, Napsin A, P63, and TTF-1 and negativity of CK5/6, ALK-V, and ROS-1, PD-L1 tumor proportion score (TPS) of 30% , which confirms that the metastatic adenocarcinoma originated from the lung. Next-generation sequencing (NGS) (Burning Rock, Guangzhou, China) with a panel of 295 cancer-related genes was conducted to examine the tumor tissue. The outcome was positive for *SND1-BRAF* (S10:B9) fusion (abundance 3.8%), whereas *EGFR*, *ALK*, *ROS1*, and other sensitive genes were all negative.

According to the Eighth Edition of the TNM Classification for Lung Cancer, the patient was classified as stage cT4N3M1a (cIVA) lung cancer. Therefore, the patient underwent four cycles of cisplatin/pemetrexed combined with bevacizumab as the first-line therapy. Then, the patient received maintenance treatment of pemetrexed/bevacizumab until the disease spread to his right thoracic cavity and left the adrenal gland. The disease progression was revealed in March 2020 through the chest and abdomen CT. The best response was partial response (PR) with a PFS of 36 months during first-line therapy. The major treatment-associated adverse events were Grade 1 gingival bleeding and Grade 2 leukopenia and neutropenia. Pembrolizumab (200 mg, Q3W) was administered to the patient as the second-line therapy. However, the patient's right thoracic solid nodules continued to grow. Several treatment lines failed, including pembrolizumab (200 mg, Q3W) plus docetaxel (110 mg, Q3W) and pembrolizumab (200 mg, Q3W) plus anlotinib (10 mg D1–14, Q3W).

Laboratory results revealed an increased NSE level of 24.5 ng/ml in July 2021, and multiple lesions on the CT scan suggested disease progression. It should be noted that the NSE concentration remained normal throughout last year. Furthermore, a percutaneous right lung biopsy guided by CT confirmed the patient's adenocarcinoma diagnosis. Whole-exome sequencing (WES) (Berry Oncology Corporation, Beijing, China) was conducted to analyze the biopsy specimen. The result showed the positivity of *SND1-BRAF* (S10:B9) and *BRAF-RNF150*(B8:R2)fusions with a PD-L1 TPS of 10% in August 2021. The patient received the MEK inhibitor trametinib (2 mg daily) from 1 September 2021. His cough was significantly relieved following 1-week trametinib treatment. The only adverse effect, which appeared 3 weeks after taking trametinib, was scattered acne with itching over the head and face (CTCAE 1 grade). After 4 months, the CT scan confirmed the patient with PR with a dramatic tumor shrinkage of 57% (Figure 1). He is now treated with trametinib. The overall timeline of diagnosis and treatment is displayed in Figure 2.

Discussion

BRAF fusions occur at a rare frequency (1, 10). Moreover, there are no anti-*BRAF* treatment guidelines for lung cancer patients with *BRAF* fusions. The situation is further worsened by the dearth of case reports on anti-*BRAF* targeted therapy. Our patient is the first reported NSCLC case with *de novo SND1-BRAF* fusion responding to the MEK inhibitor trametinib.

Despite the rarity of *BRAF* gene fusions, the alterations can be found in several solid tumors, including melanoma, glioma, thyroid cancer, pancreatic carcinoma, NSCLC, and colorectal cancer (1, 11). In contrast to *BRAF* monomer mutations, which often result in the mutation of the kinase domain sand, BRAF fusion proteins retain the normal kinase domain sand while inducing the loss of the auto-inhibitory N-terminal moiety (7) (Figure 3). Moreover, *BRAF* fusions exhibit variability due to their distinct partners, which have been documented in several papers (1, 9). However, there are no literature reports on *BRAF-RNF150*. Its role and mechanism in tumorigenesis and tumor development are still being investigated. *SND1-BRAF* fusion has been found in pancreatic cancer and lung adenocarcinoma. Nevertheless, no clinical investigation has shown any instances of *SND1-BRAF* fusion in solid malignancies. Preclinical research on pancreatic acinar cell carcinoma revealed that trametinib could significantly inhibit the growth of *SND1-BRAF*

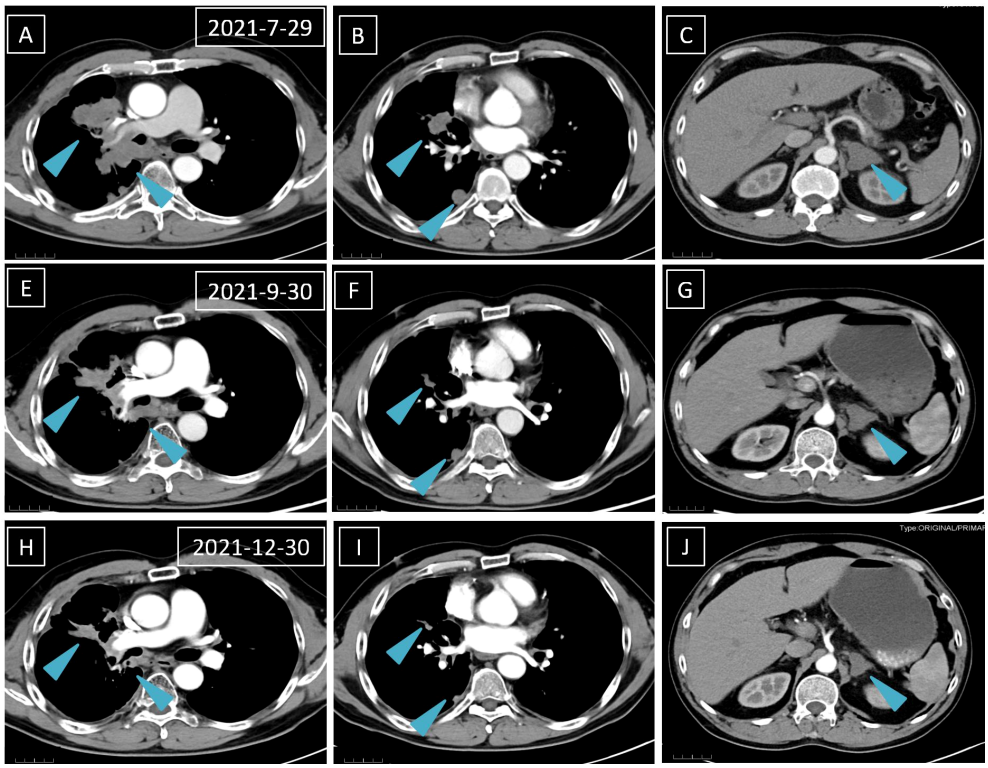

FIGURE 1
A computed tomography scan is performed before **(A–C)**, 1 month after **(D–F)**, and 4 months after **(H–J)** trametinib treatment. The blue arrows mean lung and left adrenal gland nodules.

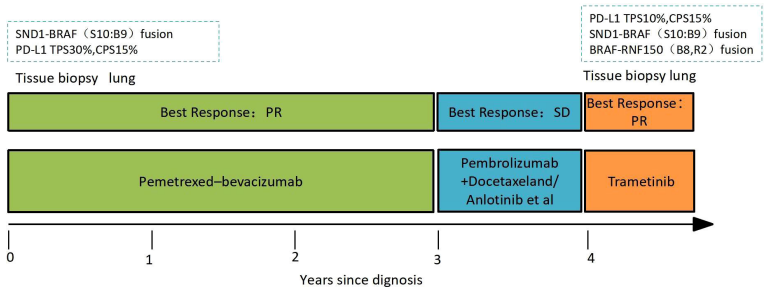

FIGURE 2
Timeline and duration of each regimen.

transformed cells. At the same time, TAK-632 exhibited a weak suppressive effect, and sorafenib showed no inhibitory effect (12). Hutchinson et al. studied *PAPSS1-BRAF* or *KIAA1549-BRAF* transfected 293H cells treated with vemurafenib or trametinib *in vitro* (13). The finding revealed that the mutant-specific *BRAF* inhibitor trametinib, rather than vemurafenib, might block the downstream signaling induced by the *PAPSS1-BRAF* or *KIAA1549-BRAF* fusion. Botton et al. found that six melanoma cell lines harboring *BRAF* fusions were resistant to first- and second-generation RAF inhibitors (14). By contrast, next-generation αC-IN/DFG-OUT RAF inhibitors blunted the activation of all cell lines, and showed synergistic effects when combined with the MEK inhibitors. Similarly, Usta et al. screened MAPK inhibitors using the *KIAA1549-BRAF* transfected glioma cell line (15) The result revealed that MEK inhibitors inhibited the MAPK signaling pathway with the lowest IC_{50}s, followed by

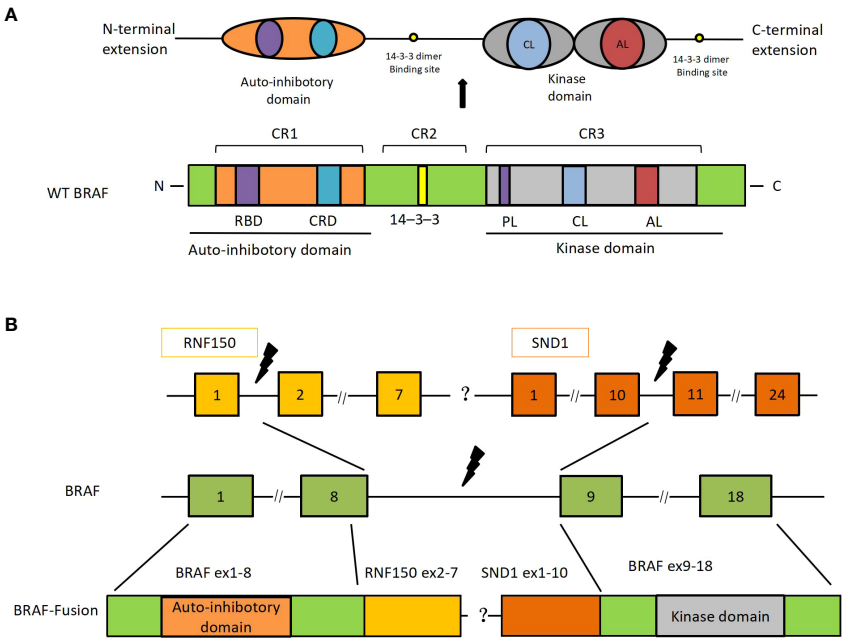

FIGURE 3
SND1-BRAF transcript fusion in metastatic lung adenocarcinoma. **(A)** The primary structure of *BRAF* and its functional domains. **(B)** *BRAF-RNF150* and *SND1-BRAF* fusions. RBD, ras-binding domain; CRD, cysteine-rich domain; PL, phosphate-binding loop; CL, catalytic loop; AL, activation loop; SND, staphylococcal nuclease domain; Ex, exon.

ERK and next-generation RAF inhibitors. A synergistic effect was observed in the combination of RAF and MEK inhibitors. In addition, Vojnic et al. identified four individuals with *EGFR*-mutated lung cancers that acquired BRAF rearrangements and showed secondary resistance to anti-*EGFR* therapy (16). The study further induced the *AGK-BRAF* fusion in H1975 (L858R +T790M), PC9 (ex19del), and HCC827 (ex19del) cell lines, and the cells also displayed osimertinib resistance. Furthermore, trametinib could synergistically suppress the proliferation of these cell lines when combined with osimertinib (16). Clinical references for our regimen included various studies describing anti-*BRAF* targeted therapies on different forms of *BRAF* fusions (Table 1). Pan-RAF inhibitors were an effective agent for targeting the *BRAF* fusions as demonstrated both in animal models and *in vitro*. Yao et al. reported that a dual RAF inhibitor BGB659 could inactivate RAF fusion proteins by blocking the ERK signaling pathway (22). Similarly, Peng et al. showed that LY3009120, a pan-RAF and RAF dimer inhibitor,

TABLE 1 Literature review on anti-*BRAF* therapies used in solid tumors with *BRAF* gene fusions.

Case	Histologic diagnosis	Age/ Gender	Sample source	BRAF fusion	Therapy	PFS (month)	Response	OS (month)
Chew et al. (17)	Melanoma	40/F	Lung metastasis	SKAP2-BRAF	Trametinib	3 m	PR	4 m
Menzies et al. (18)	Melanoma	47/F	Brain metastasis	PPFIBP2-BRAF	Trametinib	NA	PR	8 m
	Melanoma	65/M	Subcutaneous calf metastasis	KIAA1549-BRAF	Trametinib	NA	SD (enlargement)	8 m
Subbiah et al. (19)	Spindle cell neoplasm	55/F	Primary tumor	KIAA1549-BRAF	Bevacizumab + temsirolimus + sorafenib	NA	SD (reduction)	NA
Isaacson et al. (20)	Papillary urothelial carcinoma	69/M	Liver metastasis	NRF1-BRAF	Trametinib	3 m	PR	NA
del Bufalo et al. (21)	Gangliogliomas	2/M	Primary tumor	KIAA1549-BRAF +BRAF V600E	Vemurafenib	NA	NA (reduction)	NA
Zhu YC et al. (10)	Lung cancer	60/M	Primary tumor	TRIM24-BRAF	Vemurafenib	3.5 m	PR	9 m
Wang CY et al. (14)	Lung cancer	66/M	Pleural metastasis	LIMD1-BRAF	Trametinib	7.4 m	PR	NA

M, male; F, female; PFS, progression-free survival; OS, overall survival; PR, partial response; SD, stable disease; NA, not available.

could inhibit RAF isoforms (*ARAF*, *BRAF*, and *CRAF*) and occupy protomers in RAF dimers (23). Another *BRAF*-specific dimer breaker called PLX8394 was discovered by Yao et al. It showed a superior safety profile in clinical practice and preferentially suppressed the ERK signaling pathway in tumors driven by dimeric *BRAF* mutants while sparing RAF function in normal cells (24).

In conclusion, drugs targeting the MAPK pathway, particularly MEK inhibitors whose antitumor benefits have been shown in preclinical research and clinical case reports, may effectively treat *BRAF* fusion-related cancers (15). In addition, ERK and next-generation RAF inhibitors may have a synergistic antitumor impact across distinct classes of MAPK inhibitors. In this research, the NSCLC patient with primary *SDN1-BRAF* fusion receives continuous trametinib monotherapy, and it is encouraging to observe PR. Further research is required to understand the biochemical and oncogenic mechanisms and identify the targeted strategy in NSCLC patients harboring *BRAF* fusions.

Data availability statement

The original contributions presented in the study are included in the article/supplementary material. Further inquiries can be directed to the corresponding author.

Ethics statement

Written informed consent was obtained from the individual (s) for the publication of any potentially identifiable images or data included in this article.

Author contributions

MH, Corresponding author, contributed to the conception of the study and helped perform the analysis with constructive discussions. YY contributed significantly to manage and treat these patients, analysis and wrote the manuscript. MY, YL, XZ, TT, YD, ZT helped manage and treat this patient. All authors contributed to the article and approved the submitted version.

Acknowledgments

We would like to thank TopEdit (www.topeditsci.com) for English language editing of this manuscript.

Conflict of interest

The authors declare that the research was conducted in the absence of any commercial or financial relationships that could be construed as a potential conflict of interest.

Publisher's note

All claims expressed in this article are solely those of the authors and do not necessarily represent those of their affiliated organizations, or those of the publisher, the editors and the reviewers. Any product that may be evaluated in this article, or claim that may be made by its manufacturer, is not guaranteed or endorsed by the publisher.

References

1. Ross JS, Wang K, Chmielecki J, Gay L, Johnson A, Chudnovsky J, et al. The distribution of BRAF gene fusions in solid tumors and response to targeted therapy. *Int J Cancer* (2016) 138(4):881–90. doi: 10.1002/ijc.29825

2. Pakneshan S, Salajegheh A, Smith RA, Lam AK. Clinicopathological relevance of BRAF mutations in human cancer. *Pathology* (2013) 45(4):346–56. doi: 10.1097/PAT.0b013e328360b61d

3. Fois SS, Paliogiannis P, Zinellu A, Fois AG, Cossu A, Palmieri G. Molecular Epidemiology of the Main Druggable Genetic Alterations in Non-Small Cell Lung Cancer. *Int J Mol Sci* (2021) 22(2):612. doi: 10.3390/ijms22020612

4. Lin Q, Zhang H, Ding H, Qian J, Lizaso A, Lin J, et al. The association between BRAF mutation class and clinical features in BRAF-mutant Chinese non-small cell lung cancer patients. *J Transl Med* (2019) 17(1):298. doi: 10.1186/s12967-019-2036-7

5. Bracht JWP, Karachaliou N, Bivona T, Lanman RB, Faull I, Nagy RJ, et al. II, and III in NSCLC Patients Included in the SLLIP Trial: The Need for a New Pre-Clinical Treatment Rationale. *Cancers (Basel)* (2019) 11(9):1381. doi: 10.3390/cancers11091381

6. Planchard D, Besse B, Groen HJM, Hashemi SMS, Mazieres J, Kim TM, et al. Phase 2 Study of Dabrafenib Plus Trametinib in Patients With BRAF V600E-Mutant Metastatic NSCLC: Updated 5-Year Survival Rates and Genomic Analysis. *J Thorac Oncol* (2022) 17(1):103–15. doi: 10.1016/j.jtho.2021.08.011

7. Weinberg F, Griffin R, Fröhlich M, Heining C, Braun S, Spohr C, et al. Identification and characterization of a BRAF fusion oncoprotein with retained autoinhibitory domains. *Oncogene* (2020) 39(4):814–32. doi: 10.1038/s41388-019-1021-1

8. Palanisamy N, Ateeq B, Kalyana-Sundaram S, Pflueger D, Ramnarayanan K, Shankar S, et al. Rearrangements of the RAF kinase pathway in prostate cancer, gastric cancer and melanoma. *Nat Med* (2010) 16(7):793–8. doi: 10.1038/nm.2166

9. Zehir A, Benayed R, Shah RH, Syed A, Middha S, Kim HR, et al. Mutational landscape of metastatic cancer revealed from prospective clinical sequencing of 10,000 patients. *Nat Med* (2017) 23(6):703–13. doi: 10.1038/nm.4333

10. Zhu YC, Wang WX, Xu CW, Zhuang W, Du KQ, Chen G, et al. A Patient With Lung Adenocarcinoma With BRAF Gene Fusion and Response to Vemurafenib. *Clin Lung Cancer* (2019) 20(3):e224–8. doi: 10.1016/j.cllc.2019.02.020

11. Wang CY, Hsia JY, Li CH, Ho CC, Chao WR, Wu MF. Lung Adenocarcinoma With Primary LIMD1-BRAF Fusion Treated With MEK Inhibitor: A Case Report. *Clin Lung Cancer* (2021) 22(6):e878–80. doi: 10.1016/j.cllc.2021.05.003

12. Chmielecki J, Hutchinson KE, Frampton GM, Chalmers ZR, Johnson A, Shi C, et al. Comprehensive genomic profiling of pancreatic acinar cell carcinomas identifies recurrent RAF fusions and frequent inactivation of DNA repair genes. *Cancer Discovery* (2014) 4(12):1398–405. doi: 10.1158/2159-8290.CD-14-0617

13. Hutchinson KE, Lipson D, Stephens PJ, Otto G, Lehmann BD, Lyle PL, et al. BRAF fusions define a distinct molecular subset of melanomas with potential sensitivity to MEK inhibition. *Clin Cancer Res* (2013) 19(24):6696–702. doi: 10.1158/1078-0432.CCR-13-1746

14. Botton T, Talevich E, Mishra VK, Zhang T, Shain AH, Berquet C, et al. Genetic Heterogeneity of BRAF Fusion Kinases in Melanoma Affects Drug Responses. *Cell Rep* (2019) 29(3):573–588.e7. doi: 10.1016/j.celrep.2019.09.009

15. Usta D, Sigaud R, Buhl JL, Selt F, Marquardt V, Pauck D, et al. A Cell-Based MAPK Reporter Assay Reveals Synergistic MAPK Pathway Activity Suppression by MAPK Inhibitor Combination in BRAF-Driven Pediatric Low-Grade Glioma Cells. *Mol Cancer Ther* (2020) 19(8):1736–50. doi: 10.1158/1535-7163

16. Vojnic M, Kubota D, Kurzatkowski C, Offin M, Suzawa K, Benayed R, et al. Acquired BRAF Rearrangements Induce Secondary Resistance to EGFR therapy in EGFR-Mutated Lung Cancers. *J Thorac Oncol* (2019) 14(5):802–15. doi: 10.1016/j.jtho.2018.12.038

17. Chew SM, Lucas M, Brady M, Kelly CM. SKAP2-BRAF fusion and response to an MEK inhibitor in a patient with metastatic melanoma resistant to immunotherapy. *BMJ Case Rep* (2021) 14(6):e238494. doi: 10.1136/bcr-2020-238494

18. Menzies AM, Yeh I, Botton T, Bastian BC, Scolyer RA, Long GV. Clinical activity of the MEK inhibitor trametinib in metastatic melanoma containing BRAF kinase fusion. *Pigment Cell Melanoma Res* (2015) 28(5):607–10. doi: 10.1111/pcmr.12388

19. Subbiah V, Westin SN, Wang K, Araujo D, Wang WL, Miller VA, et al. Targeted therapy by combined inhibition of the RAF and mTOR kinases in malignant spindle cell neoplasm harboring the KIAA1549-BRAF fusion protein. *J Hematol Oncol* (2014) 7:8. doi: 10.1186/1756-8722-7-8

20. Isaacson AL, Guseva NV, Bossler AD, Ma D. Urothelial carcinoma with an NRF1-BRAF rearrangement and response to targeted therapy. *Cold Spring Harb Mol Case Stud* (2019) 5(3):a003848. doi: 10.1101/mcs.a003848

21. del Bufalo F, Carai A, Figà-Talamanca L, Pettorini B, Mallucci C, Giangaspero F, et al. Response of recurrent BRAFV600E mutated ganglioglioma to Vemurafenib as single agent. *J Transl Med* (2014) 12:356. doi: 10.1186/s12967-014-0356-1

22. Yao Z, Torres NM, Tao A, Gao Y, Luo L, Li Q, et al. BRAF Mutants Evade ERK-Dependent Feedback by Different Mechanisms that Determine Their Sensitivity to Pharmacologic Inhibition. *Cancer Cell* (2015) 28(3):370–83. doi: 10.1016/j.ccell.2015.08.001

23. Peng SB, Henry JR, Kaufman MD, Lu WP, Smith BD, et al. Inhibition of RAF Isoforms and Active Dimers by LY3009120 Leads to Anti-tumor Activities in RAS or BRAF Mutant Cancers. *Cancer Cell* (2015) 28(3):384–98. doi: 10.1016/j.ccell.2015.08.002

24. Yao Z, Gao Y, Su W, Yaeger R, Tao J, Na N, et al. RAF inhibitor PLX8394 selectively disrupts BRAF dimers and RAS-independent BRAF-mutant-driven signaling. *Nat Med* (2019) 25(2):284–91. doi: 10.1038/s41591-018-0274-5

frontiers | Frontiers in Oncology

TYPE Case Report
PUBLISHED 30 August 2022
DOI 10.3389/fonc.2022.971192

OPEN ACCESS

EDITED BY
Yuan-Zheng Xia,
China Pharmaceutical University, China

REVIEWED BY
Fubing Wu,
Nanjing Medical University, China
Xiaolin Huang,
Guangxi Medical University Cancer Hospital, China

*CORRESPONDENCE
Xiangjiao Meng
mengxiangjiao@126.com
Yongsheng Gao
gys-777@163.com

SPECIALTY SECTION
This article was submitted to Thoracic Oncology, a section of the journal Frontiers in Oncology

RECEIVED 16 June 2022
ACCEPTED 05 August 2022
PUBLISHED 30 August 2022

CITATION
Ren F, Wang Y, Gao Y and Meng X (2022) Pseudo-progression with osimertinib after definitive chemoradiation in unresectable epidermal growth factor receptor mutation positive of stage III non-small cell lung cancer: A case report. *Front. Oncol.* 12:971192. doi: 10.3389/fonc.2022.971192

Pseudo-progression with osimertinib after definitive chemoradiation in unresectable epidermal growth factor receptor mutation positive of stage III non-small cell lung cancer: A case report

Fei Ren[1], Yao Wang[1], Yongsheng Gao[2]* and Xiangjiao Meng[1,3]*

[1]Department of Radiation Oncology, Shandong Cancer Hospital and Institute, Shandong First Medical University and Shandong Academy of Medical Sciences, Jinan, China, [2]Department of Pathology, Shandong Cancer Hospital and Institute, Shandong First Medical University and Shandong Academy of Medical Sciences, Jinan, China, [3]Department of Radiation Oncology, Shandong Cancer Hospital and Institute Affiliated to Shandong University, Jinan, China

Epidermal growth factor receptor tyrosine kinase inhibitors (EGFR TKIs) have been widely used in the treatment of locally advanced non-small cell lung cancer (NSCLC). The phenomenon of pseudoprogression in targeted therapy in EGFR-mutation NSCLC patients is rare. Here, we reported an EGFR-mutation-positive lung adenocarcinoma patient who was admitted to a hospital for cough and chest distress accompanied by shortness of breath. He underwent four cycles of chemotherapy with pemetrexed combined with carboplatin and concurrent radiotherapy in the third and fourth cycles. Then, he was treated by osimertinib maintenance therapy. After 11.5 months of osimertinib treatment, he was assessed to progressive disease by computed tomography. He underwent fiber bronchoscopy, and the biopsy pathology showed extensive necrosis without tumor cells. Until now, the patient has continued on osimertinib for 7 months without relapse or metastasis. As far as we know, we are the first to report pseudoprogression in osimertinib maintenance after definitive chemoradiation. This study reminds the clinicians to distinguish pseudoprogression from osimertinib-induced progression and avoid abandoning effective treatments.

KEYWORDS

pseudoprogression, osimertinib, EGFR mutation, NSCLC, case report

Introduction

At present, immune checkpoint inhibitors and targeted drugs have become widely used in locally advanced non-small cell lung cancer (NSCLC) (1, 2). Pseudoprogression is a special phenomenon, which is manifested by increased volume or appearance of new lesions with subsequent narrowing of the mass (3). The overall rate of pseudoprogression in immunotherapy was 5.0% (95% CI: 3.4%, 6.7%) in NSCLC patients (4). Two case reports showed three ALK-positive NSCLC patients who developed pseudoprogression by magnetic resonance imaging (MRI) after alectinib treatment (5, 6). Data are scarce on pseudoprogression in epidermal growth factor receptor (EGFR) mutation NSCLC patients associated with targeted drug monotherapy. In this study, we reported a patient with lung adenocarcinoma who developed pseudoprogression in osimertinib maintenance after definitive chemoradiation.

Case presentation

This patient is a 65-year-old man who was hospitalized for cough and chest distress accompanied by shortness of breath. He was a previously healthy never smoker and had no family history of tumors. No significant abnormalities were observed on physical examination. Carcinoembryonic antigen (CEA) and cytokeratin 19 fragments were high and procalcitonin was in the normal range. Chest computed tomography (CT) and positron emission tomography/computed tomography (PET/CT) showed the right lower lobe lung cancer (35 mm×60 mm) (SUVmax = 14.1) with the right hilar and mediastinal lymph node metastasis (Figures 1A–2D). Cranial-enhanced MRI showed no brain metastases. He underwent fiber bronchoscopy, and the biopsy pathology showed adenocarcinoma. The gene mutation test indicated EGFR exon 21 L858R mutation. He was diagnosed with EGFR-mutation-positive stage IIIB (cT3N2M0) lung adenocarcinoma. He underwent four cycles of chemotherapy with pemetrexed (800 mg on day 1, every 3 weeks) combined with carboplatin (500 mg on day 2, every 3 weeks) and concurrent lung tumor and metastatic lymph node radiotherapy (RT) (60 Gy/30 fractions) in the third and fourth cycles. After chemoradiation, reexamination CT showed partial response (Figure 2A). Then, he was enrolled in a clinical trial, which evaluates the efficacy and safety of osimertinib maintenance after definitive chemoradiation in unresectable EGFR mutation positive stage III NSCLC (LAURA trial) (7). During osimertinib treatment, the therapeutic effect evaluated by CT was always stable disease (SD) (Figures 2B–D). After 11.5 months of osimertinib treatment, he reviewed the chest enhanced CT showing the mass enlarged, which was inhomogeneous reinforcement (Figures 3A, B). He was assessed as having progressive disease (PD) according to the evaluation criteria of RECIST 1.1. The increased CT value after enhanced CT is 23 hounsfield unit (HU), whereas the increased value is 33 HU before osimertinib. Tumor markers were in the normal range. He underwent fiber bronchoscopy, and no tumor cells were detected by the aspiration cytology of the mediastinal lumps; the biopsy pathology showed extensive necrosis without tumor cells (Figure 3C). PET/CT showed no high fluorodeoxyglucose avidity (SUVmax = 3.4) to avoid inaccurate puncture due to tumor heterogeneity (Figures 3D, E). Therefore, the therapeutic effect was SD. Now, the patient has continued on osimertinib for 7 months without relapse or metastasis (Figure 3F). The overall course of treatment is shown in Figure 4, and the compliance of this patient was quite high.

Discussion

In our study, we are the first to report pseudoprogression in osimertinib maintenance after definitive chemoradiation. However, it is not clear whether the necrosis was caused by RT or osimertinib treatment or both. Radiation therapy can cause vascular endothelial damage, leading to the increase in vascular permeability and the release of some pro-inflammatory cytokines, concomitant with the upregulation of vascular endothelial growth factor (VEGF), and ultimately facilitating7 radioactive injury lesion expansion (8). A case report showed a stage IIIA adenocarcinoma patient who developed pseudoprogression at 4 months after stereotactic body radiotherapy (SBRT) (9). Michael C Stauder et al. reported that the pseudoprogression occurred at 12 months after stereotactic ablative RT (10). Another study showed that the median time for developing an enlarged lesion in the area of SBRT was 12 months in patients without tumor recurrence (11). This suggests that the possibility of radionecrosis can occur at several months to one year after RT.

Osimertinib, a third-generation EGFR tyrosine kinase inhibitor (TKI), is now the first-line treatment for EGFR-mutation-positive advanced NSCLC (1, 2). VEGF and EGFR have many overlapping and parallel downstream pathways, and the activation of EGFR can upregulate the expression of VEGF and VEGFR and facilitate VEGFR activating (12). The combination therapy of anti-angiogenic drugs and EGFR-TKIs can simultaneously block the VEGFR/EGFR pathway, which has synergistic effects to enhance the antitumor effect (13, 14). In a clinical trial, osimertinib combined with bevacizumab showed that the overall response rate was 80% (95% CI, 67–91%), and the median progression free survival (PFS) was 19 months (95% CI, 15–24 months) (15). However, VEGF expression is affected by many factors, including cytokines (e.g., tumor necrosis factor-α [TNF-α], transforming growth factor-β [TGF-β], EGF, fibroblast cytokines, and interleukin-1), oncogene expression (e.g., EGFR,

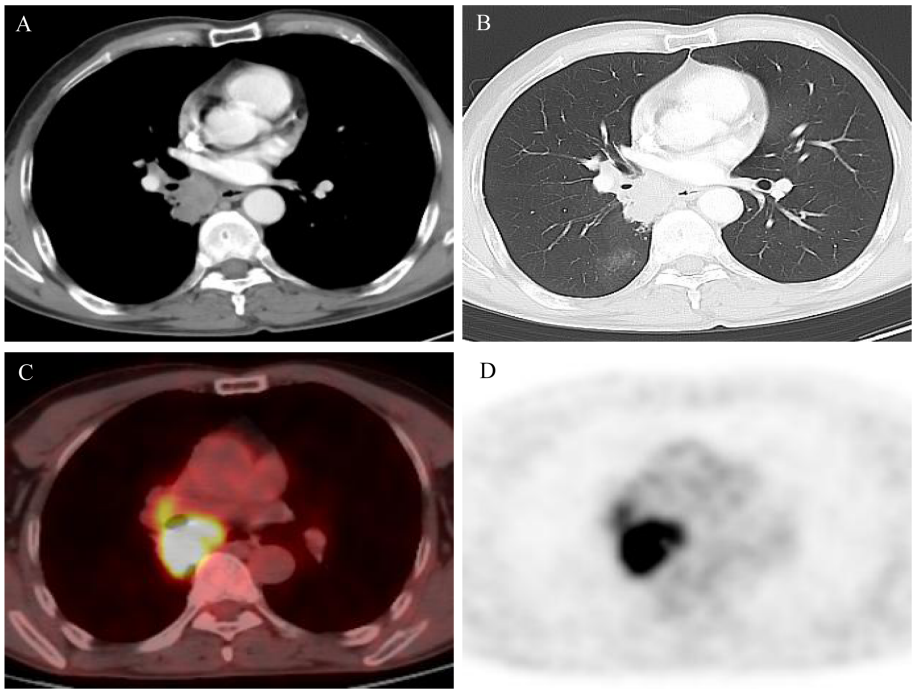

FIGURE 1
(A, B) Computed tomography (CT) scan at diagnosis showed a lung mass in the right lower lobe and mediastinum; **(C, D)** positron emission tomography/computed tomography (PET/CT) scan at diagnosis showed high fluorodeoxyglucose avidity.

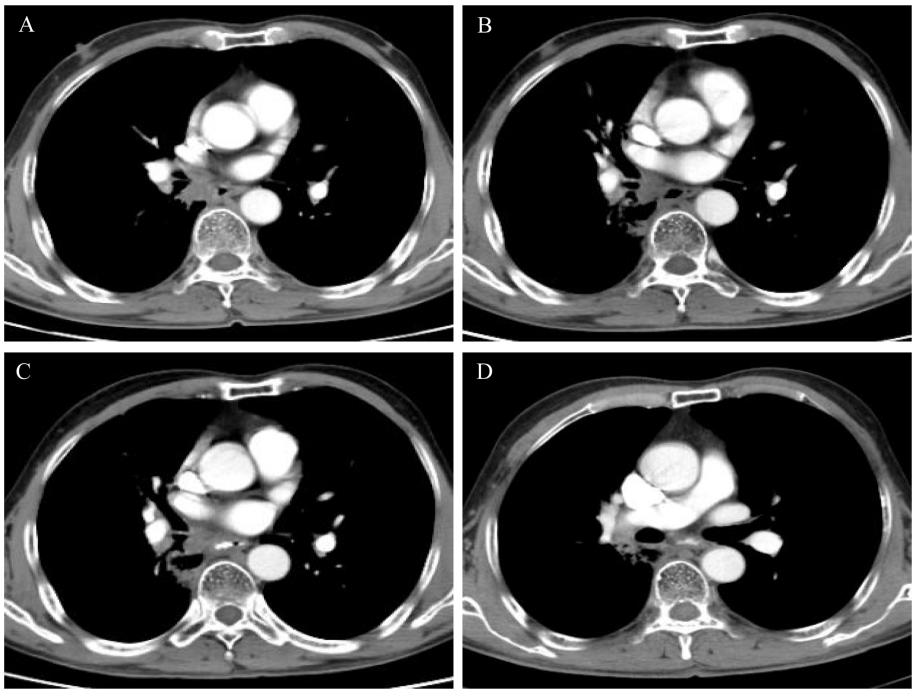

FIGURE 2
(A) Computed tomography (CT) scan after chemoradiation showed partial response; **(B–D)** CT scan showed stable disease during osimertinib treatment.

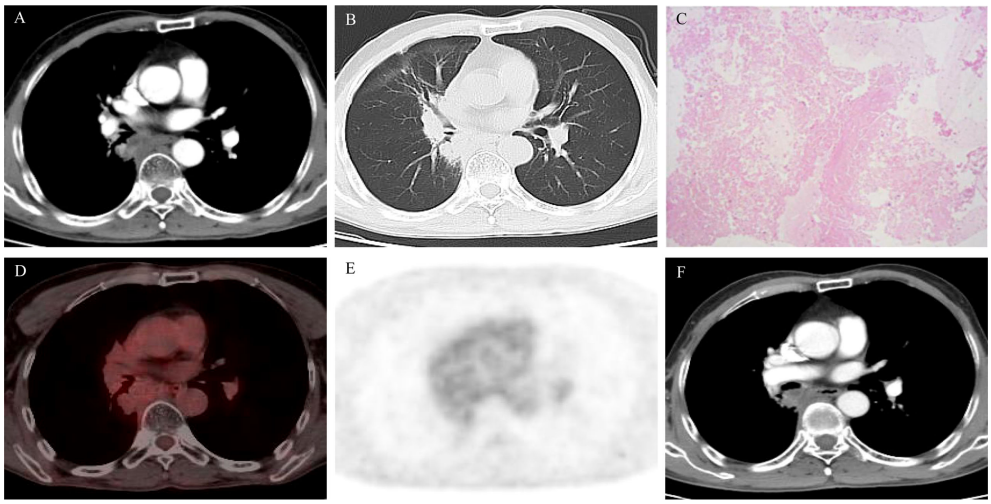

FIGURE 3
(A, B) Computed tomography (CT) scan after 11.5 months of osimertinib therapy showed enlarged primary mass; **(C)** hematoxylin and eosin (H&E) stain of the mediastinal biopsy tissue sample demonstrating extensive necrosis without tumor cells; **(D, E)** PET/CT scan after 11.5 months of osimertinib therapy showed no fluorodeoxyglucose avidity; **(F)** CT scan after 18.5 months of osimertinib treatment showed no relapse or metastasis.

erbB2/human EGFR 2 [HER2], ras, and src), and hypoxia (16). The EGF/EGFR pathway is one of the many factors that regulate VEGF expression. EGFR inhibition alone does not block VEGF, thereby allowing tumor angiogenesis (17). We cannot make the certain claim that pseudo-progression was due to endothelial injury.

The patient's enhanced CT demonstrated the mediastinum invasion by lung tumor with unclear pericardial demarcation. He was diagnosed as EGFR-mutation-positive unresectable locally advanced lung adenocarcinoma. The standard treatment of unresectable locally advanced NSCLC is concurrent chemoradiotherapy (CCRT) (18). In a retrospective study of EGFR mutation positive of stage IIIB lung adenocarcinoma, there were no statistically significant differences in the 5-year overall survival (OS) rates between TKIs and CCRT groups (30% vs. 26%) (19). Phase I trial of erlotinib combined with CCRT and the SWOG S0023 trial also failed to prove any benefit of TKI addition (20, 21). In unresectable EGFR-mutated positive stage III NSCLC patients, the initial results indicated that the median PFS of EGFR TKI and CRT was significantly longer than that of CRT alone (26.1 months vs. 6.9 months, log-rank $P = 0.023$) (22). In the RECEL trial, compared with etoposide/cisplatin concurrent RT, the median PFS with erlotinib concurrent RT was significantly longer (24.5 vs. 9.0 months [$P < 0.001$]) (23). The LAURA trial will assess the efficacy of osimertinib after definitive chemoradiation in EGFR mutation NSCLC patients (7).

In conclusion, this is the first report of pseudoprogression in osimertinib maintenance after definitive chemoradiation. The mechanism of pseudoprogression after osimertinib treatment is still unclear, but the significance of this study suggests that clinicians should not easily interrupt osimertinib treatment when imaging progression occurs during osimertinib, and further determine pathological examination and PET-CT before making decisions.

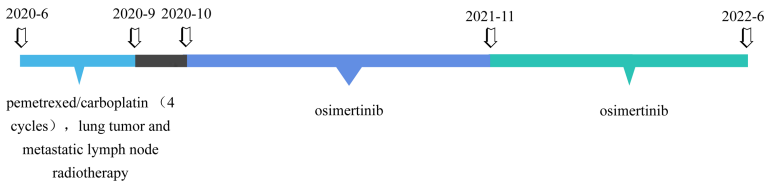

FIGURE 4
Timeline of the interventions and outcomes.

There are very few relevant studies about the mechanism and possibility of whether EGFR-TKI targeted therapy combined with RT increases pseudoprogression compared with RT alone; it deserves further exploration and discussion.

Data availability statement

The original contributions presented in the study are included in the article/supplementary material. Further inquiries can be directed to the corresponding authors.

Ethics statement

The studies involving human participants were reviewed and approved by the Ethics Committee of Shandong Cancer Hospital and Institute. The patients/participants provided their written informed consent to participate in this study.

Author contributions

FR performed the literature search and wrote the original draft, FR and YW collected and analyzed the data, and XM and YG revised the manuscript critically for important scientific content. All authors contributed to the article and approved the submitted version.

Funding

This work was supported by CSCO-Haosen Cancer Research Fund (No. Y-HS202102-0089).

Acknowledgments

We thank the patient and his family for giving consent to this case report.

Conflict of interest

The authors declare that the research was conducted in the absence of any commercial or financial relationships that could be construed as a potential conflict of interest.

Publisher's note

References

1. Iams WT, Porter J, Horn L. Immunotherapeutic approaches for small-cell lung cancer. *Nat Rev Clin Oncol* (2020) 17(5):300–12. doi: 10.1038/s41571-019-0316-z

2. Wu YL, Planchard D, Lu S, Sun H, Yamamoto N, Kim DW, et al. Pan-Asian adapted clinical practice guidelines for the management of patients with metastatic non-small-cell lung cancer: a CSCO-ESMO initiative endorsed by JSMO, KSMO, MOS, SSO and TOS. *Ann Oncol* (2019) 30(2):171–210. doi: 10.1093/annonc/mdy554

3. Jia W, Gao Q, Han A, Zhu H, Yu J. The potential mechanism, recognition and clinical significance of tumor pseudoprogression after immunotherapy. *Cancer Biol Med* (2019) 16(4):655–70. doi: 10.20892/j.issn.2095-3941.2019.0144

4. Park HJ, Kim KW, Pyo J, Suh CH, Yoon S, Hatabu H, et al. Incidence of pseudoprogression during immune checkpoint inhibitor therapy for solid tumors: A systematic review and meta-analysis. *Radiology* (2020) 297(1):87–96. doi: 10.1148/radiol.2020200443

5. Ou SH, Klempner SJ, Azada MC, Rausei-Mills V, Duma C. Radiation necrosis presenting as pseudoprogression (PsP) during alectinib treatment of previously radiated brain metastases in ALK-positive NSCLC: Implications for disease assessment and management. *Lung Cancer* (2015) 88(3):355–9. doi: 10.1016/j.lungcan.2015.03.022

6. Ou SH, Weitz M, Jalas JR, Kelly DF, Wong V, Azada MC, et al. Alectinib induced CNS radiation necrosis in an ALK+NSCLC patient with a remote (7 years) history of brain radiation. *Lung Cancer* (2016) 96:15–8. doi: 10.1016/j.lungcan.2016.03.008

7. Lu S, Casarini I, Kato T, Cobo M, Özgüroğlu M, Hodge R, et al. Osimertinib maintenance after definitive chemoradiation in patients with unresectable EGFR mutation positive stage III non-small-cell lung cancer: LAURA trial in progress. *Clin Lung Cancer* (2021) 22(4):371–5. doi: 10.1016/j.cllc.2020.11.004

8. Zhuang H, Shi S, Yuan Z, Chang JY. Bevacizumab treatment for radiation brain necrosis: mechanism, efficacy and issues. *Mol Cancer* (2019) 18(1):21. doi: 10.1186/s12943-019-0950-1

9. Frechette KM, Brown LC, Aubry MC, Wigle DA, Olivier KR. Pseudoprogression after stereotactic body radiotherapy. *J Thorac Oncol* (2014) 9 (4):e29–30. doi: 10.1097/JTO.0000000000000067

10. Stauder MC, Rooney JW, Neben-Wittich MA, Garces YI, Olivier KR. Late tumor pseudoprogression followed by complete remission after lung stereotactic ablative radiotherapy. *Radiat Oncol* (2013) 8:167. doi: 10.1186/1748-717X-8-167

11. Dunlap NE, Yang W, McIntosh A, Sheng K, Benedict SH, Read PW, et al. Computed tomography-based anatomic assessment overestimates local tumor recurrence in patients with mass-like consolidation after stereotactic body radiotherapy for early-stage non-small cell lung cancer. *Int J Radiat Oncol Biol Phys* (2012) 84(5):1071–7. doi: 10.1016/j.ijrobp.2012.01.088

12. Hirata A, Ogawa S, Kometani T, Kuwano T, Naito S, Kuwano M, et al. ZD1839 (Iressa) induces antiangiogenic effects through inhibition of epidermal growth factor receptor tyrosine kinase. *Cancer Res* (2002) 62(9):2554–60.

13. Perdrizet K, Leighl NB. The role of angiogenesis inhibitors in the era of immune checkpoint inhibitors and targeted therapy in metastatic non-small cell lung cancer. *Curr Treat Options Oncol* (2019) 20(3):21. doi: 10.1007/s11864-019-0617-6

14. Naumov GN, Nilsson MB, Cascone T, Briggs A, Straume O, Akslen LA, et al. Combined vascular endothelial growth factor receptor and epidermal growth factor receptor (EGFR) blockade inhibits tumor growth in xenograft models of EGFR inhibitor resistance. *Clin Cancer Res* (2009) 15(10):3484–94. doi: 10.1158/1078-0432.CCR-08-2904

15. Yu HA, Schoenfeld AJ, Makhnin A, Kim R, Rizvi H, Tsui D, et al. Effect of osimertinib and bevacizumab on progression-free survival for patients with metastatic EGFR-mutant lung cancers: A phase 1/2 single-group open-label trial. *JAMA Oncol* (2020) 6(7):1048–54. doi: 10.1001/jamaoncol.2020.1260

16. Tabernero J. The role of VEGF and EGFR inhibition: implications for combining anti-VEGF and anti-EGFR agents. *Mol Cancer Res* (2007) 5(3):203–20. doi: 10.1158/1541-7786.MCR-06-0404

17. Niu G, Wright KL, Huang M, Song L, Haura E, Turkson J, et al. Constitutive Stat3 activity up-regulates VEGF expression and tumor angiogenesis. *Oncogene* (2002) 21(13):2000–8. doi: 10.1038/sj.onc.1205260

18. Jiang L, Meng X, Zhao X, Xing L, Yu J. Perspective on treatment for unresectable locally advanced non-small cell lung cancer with oncogene-driven mutation: a narrative review. *Transl Lung Cancer Res* (2020) 9(5):2137–44. doi: 10.21037/tlcr-20-722

19. Hsia TC, Liang JA, Li CC, Chien CR. Comparative effectiveness of concurrent chemoradiotherapy versus EGFR-tyrosine kinase inhibitors for the treatment of clinical stage IIIb lung adenocarcinoma patients with mutant EGFR. *Thorac Cancer* (2018) 9(11):1398–405. doi: 10.1111/1759-7714.12847

20. Choong NW, Mauer AM, Haraf DJ, Lester E, Hoffman PC, Kozloff M, et al. Phase I trial of erlotinib-based multimodality therapy for inoperable stage III non-small cell lung cancer. *J Thorac Oncol* (2008) 3(9):1003–11. doi: 10.1097/JTO.0b013e31818396a4

21. Kelly K, Chansky K, Gaspar LE, Albain KS, Jett J, Ung YC, et al. Phase III trial of maintenance gefitinib or placebo after concurrent chemoradiotherapy and docetaxel consolidation in inoperable stage III non-small-cell lung cancer: SWOG S0023. *J Clin Oncol* (2008) 26(15):2450–6. doi: 10.1200/JCO.2007.14.4824

22. Aredo JV, Mambetsariev I, Hellyer JA, Amini A, Neal JW, Padda SK, et al. Durvalumab for stage III EGFR-mutated NSCLC after definitive chemoradiotherapy. *J Thorac Oncol* (2021) 16(6):1030–41. doi: 10.1016/j.jtho.2021.01.1628

23. Xing L, Wu G, Wang L, Li J, Wang J, Yuan Z, et al. Erlotinib versus Etoposide/Cisplatin with radiation therapy in unresectable stage III epidermal growth factor receptor mutation-positive non-small cell lung cancer: A multicenter, randomized, open-label, phase 2 trial. *Int J Radiat Oncol Biol Phys* (2021) 109(5):1349–58. doi: 10.1016/j.ijrobp.2020.11.026

frontiers | Frontiers in Oncology

TYPE Case Report
PUBLISHED 05 September 2022
DOI 10.3389/fonc.2022.978327

OPEN ACCESS

EDITED BY
Kohei Fujita,
National Hospital Organization Kyoto Medical Center, Japan

REVIEWED BY
Janaki Deepak,
University of Maryland, United States
Song Xu,
Tianjin Medical University General Hospital, China

*CORRESPONDENCE
Jiawei Chen
chenjiawei59@126.com

†These authors have contributed equally to this work

SPECIALTY SECTION
This article was submitted to Thoracic Oncology, a section of the journal Frontiers in Oncology

RECEIVED 25 June 2022
ACCEPTED 18 August 2022
PUBLISHED 05 September 2022

CITATION
Zhang S, Liao X and Chen J (2022) *EML4-ALK* rearrangement in primary malignant fibrous histiocytoma of the lung treated with alectinib: a case report. *Front. Oncol.* 12:978327. doi: 10.3389/fonc.2022.978327

EML4-ALK rearrangement in primary malignant fibrous histiocytoma of the lung treated with alectinib: A case report

Shuai Zhang[1†], Xuqiang Liao[2†] and Jiawei Chen[1*]

[1]Department of Radiation Oncology, Hainan General Hospital, Hainan Affiliated Hospital of Hainan Medical University, Haikou, China, [2]Department of Thoracic Surgery, Hainan General Hospital, Hainan Affiliated Hospital of Hainan Medical University, Haikou, China

Primary malignant fibrous histiocytoma of the lung (PMFHL) is extremely rare. It is more common in the right lung and has no specific symptoms. Lymph node metastasis is rare, but hematogenous metastasis is more common. The common metastatic sites are the brain and bone. In this study, a 59-year-old male patient was diagnosed with PMFHL with brain metastasis due to persistent cough and blood in the sputum for the past week. Genetic testing revealed *EML4-ALK* gene rearrangement (fusion). We first used alectinib in a patient with advanced PMFHL with *EML4-ALK* gene rearrangement (fusion) accompanied by brain metastasis. The treatment was effective and successfully delayed the development of the disease. Satisfactory results were observed, with an overall survival time of 19 months. Therefore, genetic testing in PMFHL and the choice of treatment plan are important. Local treatment methods, including surgery and radiotherapy, are important when the disease is less advanced. Multidisciplinary discussion is recommended for the best prognosis.

KEYWORDS

treatment, malignant fibrous histiocytoma (MFH), alectinib, lung, case report

Introduction

Malignant fibrous histiocytoma (MFH) is the most common malignant mesenchymal tumor in adults. MFH can occur in a variety of organs, especially the trunk part of the extremities and the deep musculature of the retroperitoneum, but it rarely originates in the lung and more often metastasizes to the lung from other organs (1). Surgery is the main treatment for primary MFH of the lung (PMFHL). The effectiveness of adjuvant radiotherapy after surgery is unclear.

The pathology of PMFHL is divided into the fibroblast type, histiocytic type, and inflammatory cell type. The postoperative gross specimens are mostly large tumors with a diameter of >5 cm, with pseudocapsules and gray–white sections with necrosis in the

center. Fibrillar cells and collagen fibers are arranged in bundles of spokes, and histiocytic cells with large variation, mononuclear and multinucleated giant cells, and foam cells with nuclear atypia are observed under light microscopy. The immunohistochemical characteristics are as follows: α1-antitrypsin and α1-antichymotrypsin, vimentin (+), S-100 protein (-), and myosin (-) (2). Because the growth of PMFHL is a centrifugal spherical enlargement phenomenon, the surrounding normal tissue is compressed and changed in layers, forming a relatively tight "compression zone", and a tissue reaction phenomenon occurs around the "compression zone" to form a pseudocapsule (3).

Because of its complex and heterogeneous pathological features, the lack of specific immunohistochemical markers, and no lineage specificity, the clinical diagnosis of PMFHL is controversial. We strongly recommend that core needle biopsy is required for pathological tissue. In this paper, we report a rare case of PMFHL with brain metastasis and EML4-ALK gene rearrangement (fusion). We investigated the clinical diagnosis, treatment characteristics, and prognosis of this disease and analyzed the application value and challenges of genetic testing and targeted drugs over the whole course of treatment.

Case description

All procedures performed in human participants followed the ethical standards of the institutional and/or national research committee(s) and with the Helsinki Declaration (as revised in 2013). Written informed consent was obtained from the patient.

The patient, a 59-year-old male, was admitted to the Department of Thoracic Surgery on January 22, 2019, with coughing with no obvious cause, white sticky sputum with occasional bloody sputum, chest tightness but no chest pain, hemoptysis, shortness of breath, headache, and dizziness. The patient had a history of smoking for more than 30 years (1-2 packs/day). Chest computed tomography (CT) showed irregular soft tissue nodules and mass shadows in the right middle and lower lobes near the hilar area and the anterior basal segment of the right lower lobe. The larger nodule was located next to the right hilum, with a larger cross-section of approximately 5.7 cm × 4.5 cm and a lobular shape. The boundary between the lesion and the right hilum was unclear, straddling the oblique fissure pleura, with uneven enhancement on enhanced scanning, and bronchial stenosis in the middle and lower lobes of the right lung was narrow. The right hilar lymph nodes were enlarged, and the mediastinal lymph nodes were slightly enlarged (Figure 1). Positron-emission tomography (PET/CT) results showed the following: 1. increased ^{18}F-fluorodeoxyglucose (FDG) metabolism in nodules and masses at the right middle and lower lobe near the hilar area with a maximum standardized uptake value (SUV max) of 13.1, the right psoas muscle area, the gastrosplenic space, and the left inferior abdominal wall; multiple round-like nodules in the right lung with elevated FDG metabolism; a left parietal nodular lesion surrounded by flaky edema and increased FDG metabolism; uneven bone density in the left iliac bone with increased FDG metabolism; and multiple nodules in the left renal parenchyma with increased FDG metabolism, all suggesting malignant tumor lesions; and 2. slightly larger bilateral hilar and mediastinal lymph nodes, increased FDG metabolism, and the possibility of metastasis. Follow-up examination was recommended (Figure 2). Fiberoptic bronchoscopy examination showed that in the right bronchus, the right middle bronchial mucosa was swollen and bulged, cauliflower-like masses grew in the right middle lobe and the lower lobe segment of the bronchial lumen, the lumen was completely occluded, and the lesion was greater than 2 cm from the protuberance (Figure 3). Pathology of the specimen under bronchoscopy showed a malignant tumor (middle right, lower right). After immunohistochemical labeling, a malignant soft tissue tumor was reported (middle right, lower right), which was consistent with MFH. The nucleus of the tumor cells was irregularly shaped, mainly shuttle-shaped, large nucleated cells were observed, and nuclear divisions were easily observed and diffusely distributed. Immunohistochemical labeling showed vimentin (+), α1-antitrypsin (+), α1-antichymotrypsin (+), CK19 (some +), S-100 (-), desmin (-), MyoD1 (-), HHF35 (-), Fli-1 (-), ALK (-), CK7 (-), myogenin (-), SMA (-), CD34 (-), CD56 (-), Bcl-2 (-), CD99 (partial +), Ki-67>60%, CK (-), TFF-1 (-), napsin A (-), P63 (-), P40 (-), CK7 (-), and CK20 (-). See Figure 4 for details. After a multidisciplinary discussion, the patient was considered to have MFH with multiple systemic metastases, without surgical indications and with poor chemotherapy efficacy. We recommended genetic testing to evaluate whether targeted immunotherapy was appropriate. The results of genetic testing showed that the ALK gene had the *EML4-ALK* (E6:A20) gene rearrangement (fusion) with an abundance of 8.93% (Figure 5). The tumor mutation burden (TMB) was 1.6 mutations/Mb. Microsatellite instability results showed microsatellite stability. Programmed death-ligand 1 (PD-L1) was detected using immunohistochemistry (clone number 22C3). The tumor proportion score (TPS) was 80%. Considering the possibility of *ALK* gene mutation, the efficacy of first-line alectinib was better than that of crizotinib, and the immunotherapy effect was poor. He was started on alectinib 600 mg orally twice daily. The symptoms completely disappeared after 1 month of administration.

The patient was hospitalized on December 3, 2019, due to right limb weakness with numbness. Cranial magnetic resonance (MR) showed that the nodular-shaped abnormal signal of the

Abbreviations: PMFHL, Primary malignant fibrous histiocytoma of the lung; MFH, Malignant fibrous histiocytoma; CT, computed tomography; PET/CT, positron-emission tomography; FDG, ^{18}F-fluorodeoxyglucose; TMB, tumor mutation burden; PD-L1, programmed death-ligand 1; TPS, tumor proportion score; MR, magnetic resonance.

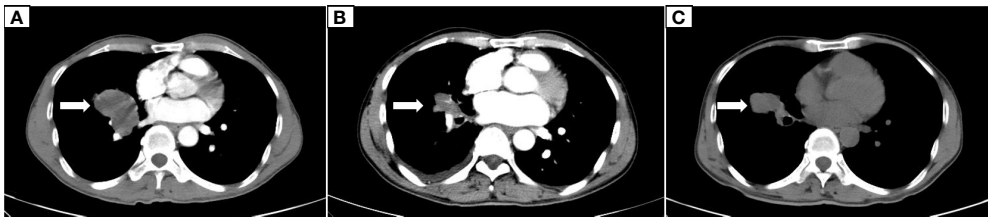

FIGURE 1
Dynamic changes on chest CT. **(A)** The initial CT scan on January 23, 2019, showed an irregular soft tissue mass measuring 5.7 cm × 4.5 cm in the middle and lower lobes of the right lung. **(B)** A CT scan on December 9, 2019, showed that the right lung lesion was reduced to 2.5 cm × 1.5 cm. **(C)** A CT scan on May 5, 2020, showed progression of the right lung lesion, which had grown to 4.5 cm × 3.5 cm.

left parietal lobe was significantly larger than before, with an increase in the small amount of edema in the surrounding area. The tumor was considered to be metastatic (Figure 6). Because the patient had stable pulmonary lesions and progressing craniocerebral lesions, neurosurgeons considered resection of the left parietal lobe metastases, and the patient was informed of the above conditions. The patient did not consent to surgical resection due to the risk of surgery. Stereotactic radiotherapy for brain metastases was approved by the radiotherapy physician. Varian's EDGE (edge cancer treatment) was used, and volume-modulated radiotherapy was performed at a prescribed dose of 12 Gy three times. After radiotherapy, the symptoms of right limb weakness and numbness completely improved, but right limb weakness developed, which was accompanied by limb numbness and uncoordinated movement, 3 months later. Reexamination of brain MRI on March 23, 2020, showed a small, nodular abnormal signal in the left frontal parietal lobe, which was slightly larger than before, with a fuzzy edge. It was

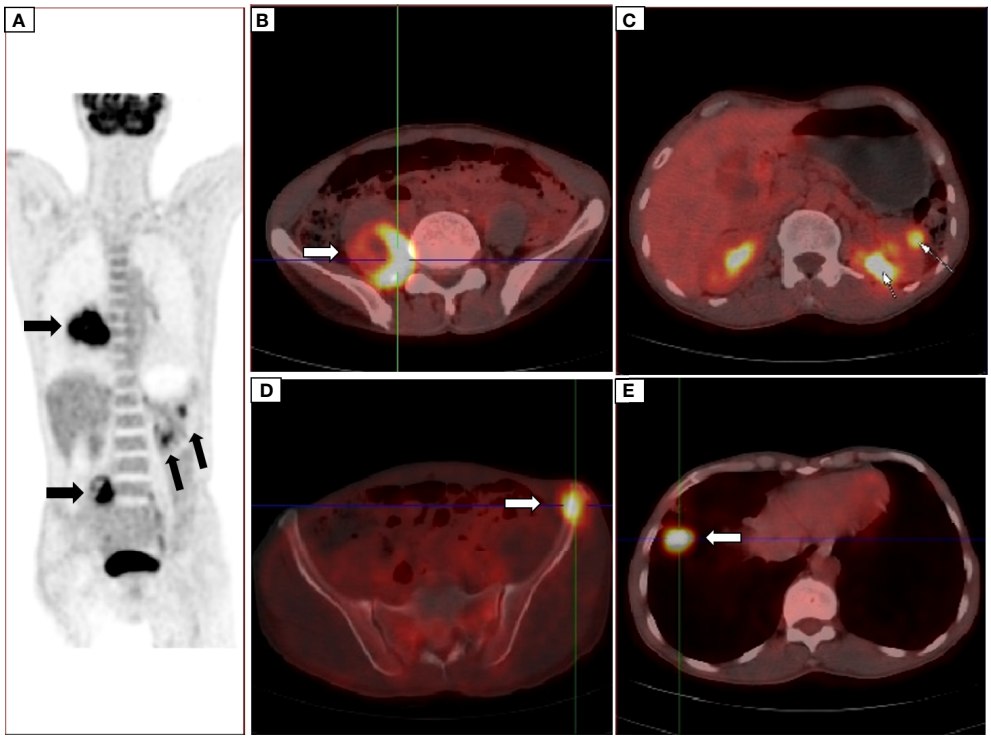

FIGURE 2
PET/CT showed nodules in the right middle and lower lobes near the hilar area **(A)** the right psoas muscle area **(B)** and the gastrosplenic space and multiple nodules in the left renal parenchyma **(C)** uneven density of the left iliac bone **(D)** multiple round nodules in the right lung **(E)** and increased FDG metabolism, suggesting malignant lesions.

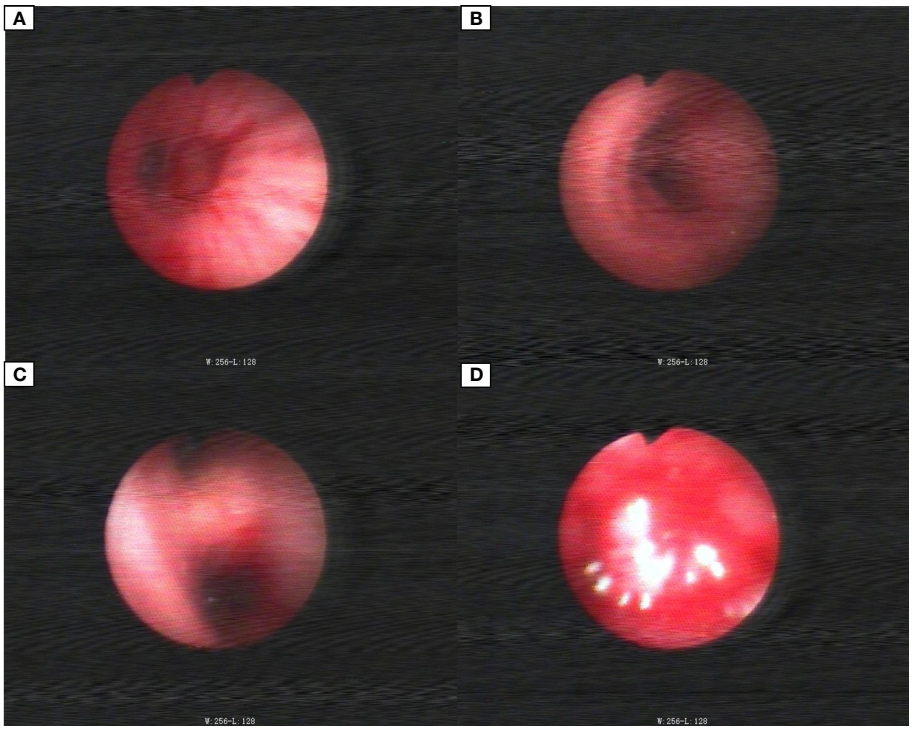

FIGURE 3
Bronchoscopic images. **(A)** Middle bronchial tubes. **(B)** Right main stem bronchi. **(C)** Right middle lobe bronchial. **(D)** Right lower lobe bronchial tube.

approximately 3.0 × 2.3 cm, and distinct patchy edematous foci were observed in surrounding areas. The patient was then given bevacizumab (7.5 mg/kg) to relieve the cerebral edema every 3 weeks. The patient's symptoms persisted for another month and then became aggravated, and right limb dyskinesia was observed. The repeat cranial MR on May 11, 2020, showed that the left frontoparietal metastatic lesions rapidly increased to a size of approximately 4.5 × 2.5 cm, with significant surrounding edema. The patient still did not agree to surgical treatment and continued to be treated with bevacizumab. He died of intracranial hypertension more than 2 months later.

Discussion

MFH is a type of soft tissue sarcoma originating from mesenchymal cells, accounting for 20% of all sarcomas, approximately one-fourth of which are radiation-related

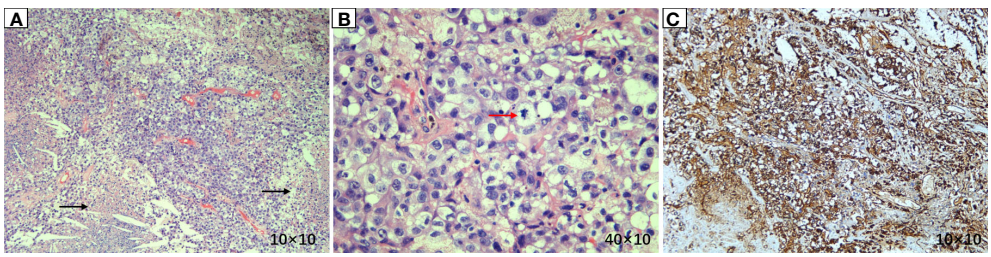

FIGURE 4
Pathological results of lung lesion biopsy. **(A)** (Hematoxylin and eosin (HE) × 100) Atypical tumor cells were arranged in a sheet-like manner, with vascular proliferation and necrosis. **(B)** (HE × 400) Atypical tumor cells showed large nuclei, hyperchromatic nuclei, prominent nucleoli, two or more nucleoli, eosinophilic or translucent cytoplasm, and pathological mitosis. **(C)** (IHC × 100) Vimentin was diffusely expressed, suggesting tumors derived from mesenchymal tissues.

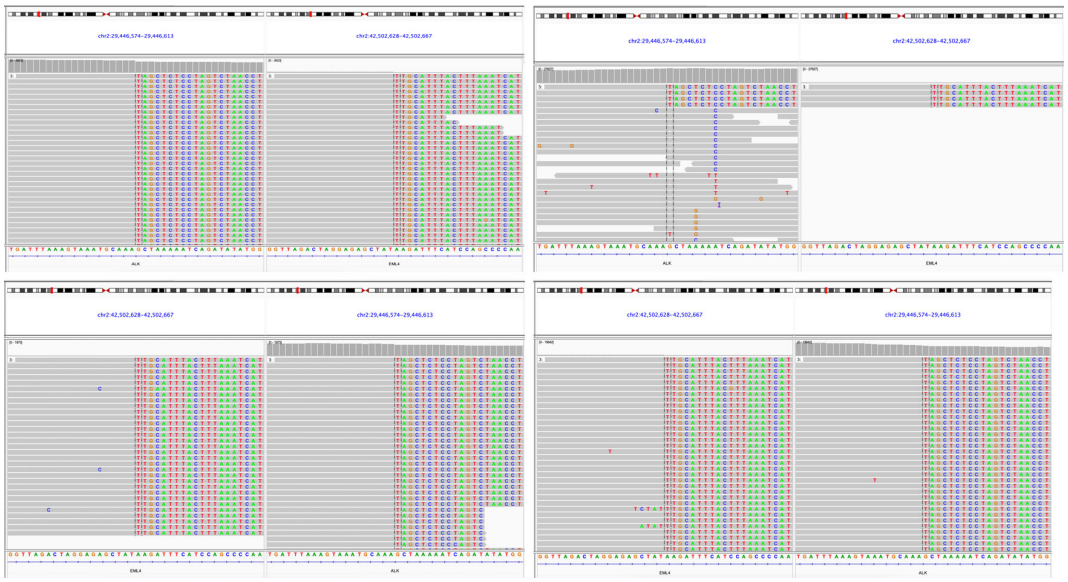

FIGURE 5
Genomic map derived from the biopsied tissue samples of four lung lesions.

tumors with multidirectional differentiation abilities. First described by O'Brien and Stout (1) in 1964, MFH was originally named malignant fibrous xanthoma. In general, superficial MFH is mostly moderately malignant, while deep histiocytoma is mostly highly malignant. PMFHL is more common in males and in the right lung at older ages. Cancer cells are not easy to detect on sputum examination. Because the tumors grow outside the tracheal lumen, they are difficult to detect by fiberoptic bronchoscopy. The symptoms mainly include cough, blood in sputum, chest pain, dyspnea, fatigue, and weight loss. Rare symptoms include hypertrophic pulmonary osteoarthropathy, hypoglycemia, and neutrophilia, and some patients may be asymptomatic (4). Lymph node metastasis is rare in this disease, hematogenous metastasis is common, and the common metastatic sites are the brain and bone. In this case, chest X-ray showed that PMFHL manifested as a large noncavitary mass with a round shadow, uniform density, generally smooth edges, and inconspicuous lobulation. CT showed that the central density was low and the edges had increased density, and the surrounding shadow was irregular. Cystic degeneration and cavity formation, which are rare in MFH, were not observed.

The molecular mechanism of PMFHL occurrence and progression is still unclear. Some scholars have performed

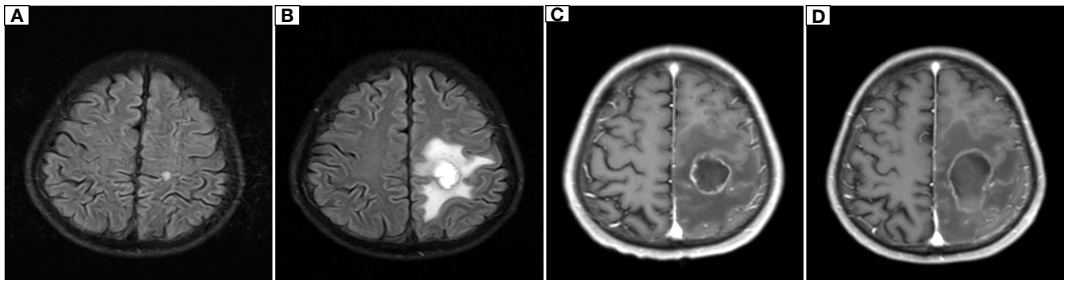

FIGURE 6
Dynamic changes on cranial MR. **(A)** The initial cranial MR on January 28, 2019, showed a nodular lesion in the left parietal lobe with a diameter of approximately 0.6 cm and a clear margin. **(B)** On December 6, 2019, cranial MR showed that the left parietal lobe nodule was enlarged to 2.1 cm × 2.3 cm, with blurred edges and patchy surrounding edema. **(C)** On March 23, 2020, cranial MR showed that the left parietal lobe nodule had grown to 3.0 cm × 2.3 cm and had blurred edges and visible patchy edematous lesions around it. **(D)** Cranial MR showed that the left parietal nodular lesion had grown to 4.5 cmx2.5 cm, with blurred edges and patchy edematous lesions.

next-generation sequencing of tumor tissues, and the results showed that the *TSC2*, *ARID1B*, *CDK8*, *KDM5C*, and *CASP8* genes had mutations. Among them, the *TSC2* gene had the highest mutation frequency (15.64%), and an M280V missense mutation was found. Therefore, *TSC2* gene mutations are hypothesized to activate the mTOR pathway, resulting in abnormal cell growth and proliferation, which may be related to the occurrence and progression of this disease (5).

Diagnosing PMFHL is a multistep process. The most important step is to confirm that the lesions originate in the lungs. PET-CT can accurately exclude other parts of the body as the origin, especially the retroperitoneal region. Due to the low incidence of this disease, the small number of cases, and radiotherapy insensitivity, no standard chemotherapy regimen is currently available. Generally, MFH chemotherapy drugs are preferred. Commonly used drugs include ifosfamide and doxorubicin, which have low effective rates (6). Due to the presence of the *EML4-ALK* (E6:A20) rearrangement (fusion), which has not been reported in PMFHL, we can only explore this disease based on our experience in non-small cell lung cancer. A phase II study evaluated the efficacy of the PD-L1 inhibitor durvalumab for third-line treatment of advanced *EGFR*-mutated *ALK*-rearranged non-small cell lung cancer but reported no response in 15 non-small cell lung cancer patients with *ALK* fusion following durvalumab treatment (7). Alectinib is a second-generation *ALK*-positive lung cancer-targeting drug with a high penetration rate of the blood–brain barrier (63% to 94%). Therefore, the efficacy of alectinib in the treatment of brain metastases from lung cancer is markedly better than that of crizotinib. For patients with brain metastases from lung cancer, the median progression-free survival period after alectinib treatment is 27.7 months, while that of crizotinib is only 7.4 months (8).

Considering that traditional chemotherapy regimens and immunotherapy drugs were not very effective, we comprehensively considered the choice of alectinib and indeed achieved good efficacy, with an overall survival time of 19 months. The cause of death of the patient was intracranial hypertension caused by progression of the intracranial lesions and compression edema. Because PMFHL was less sensitive to radiotherapy and the diameter of the left parietal lobe metastasis was >2 cm, internal manifestations of complete liquefaction and necrosis were found, with few solid components. Surgical resection was the first choice of treatment. Although the X-Knife at 12 Gy was used for three segmentations, the symptom relief duration after radiotherapy was less than 4 months. Even when we used alectinib in combination with bevacizumab, there was no significant improvement in brain edema and tumor shrinkage, resulting in improved prognosis. The patient should have achieved better overall survival, but the patient refused surgical removal of the intracranial metastases. At the same time, PD-L1 expression was high, and the TPS was 80%. It was very regretful that immune checkpoint inhibitors were not used. Because tumor progression was due to oligoprogression of a single intracranial lesion, and local therapy should have been performed, including surgery and radiotherapy. If subsequent systemic progression occurs, then immunotherapy should be considered. Pembrolizumab application in PMFHL can achieve good outcomes (9).

Conclusions

PMFHL is characterized by high malignancy, high recurrence and metastasis rates, a poor prognosis, and poor sensitivity to radiotherapy and chemotherapy. We recommend routine genetic testing of patients with PMFHL. Selecting targeted drugs with high sensitivity for possible mutation sites can often achieve better effective rates and longer survival times. Simultaneously, local treatment methods, including surgery and radiotherapy, are very important treatments when the disease progresses less. We first applied alectinib to a PMFHL patient with advanced EML4-ALK gene rearrangement (fusion) accompanied by brain metastasis. The treatment was effective. These findings need to be supported by further studies.

Data availability statement

The original contributions presented in the study are included in the article/supplementary material. Further inquiries can be directed to the corresponding author.

Author contributions

SZ collected, sorted, and analyzed the data and drafted the manuscript. XL collected and sorted the data. JC reviewed and revised the manuscript. All authors contributed to the article and approved the submitted version.

Conflict of interest

The authors declare that the research was conducted in the absence of any commercial or financial relationships that could be construed as a potential conflict of interest.

Publisher's note

References

1. O'Brien JE, Stout AP. Malignant fibrous xanthomas. *Cancer* (1964) 17:1445–55. doi: 10.(SICI)1097-0142(19961215)78/1097-0142(196411)17:11<1445::aid-cncr2820171112>3.0.co;2-g

2. Weiss SW, Enzinger FM. Malignant fibrous histiocytoma: an analysis of 200 cases. *Cancer* (1978) 41:2250–66. doi: 10.(SICI)1097-0142(19961215)78/1097-0142(197806)41:6<2250::aid-cncr2820410626>3.0.co;2-w

3. Ismailer I, Khan A, Leonidas JC, Wind E, Herman P. Computed tomography of primary malignant fibrohistiocytoma of the lung. *Comput Radiol* (1987) 11:37–40. doi: 10.1016/0730-4862(87)90027-8

4. Casey MT, Peddle LM. Primary pulmonary fibrous histiocytoma: report of three cases. *Can J Surg* (1988) 31:251–3.

5. Li X, Liu R, Shi T, Dong S, Ren F, Yang F, et al. Primary pulmonary malignant fibrous histiocytoma: case report and literature review. *J Thorac Dis* (2017) 9:E702–8. doi: 10.21037/jtd.2017.07.59

6. Halyard MY, Camoriano JK, Culligan JA, Weiland LH, Allen MS, Pluth JR, et al. Malignant fibrous histiocytoma of the lung. *Rep four cases Rev literature. Cancer* (1996) 78:2492–7. doi: 10.(SICI)1097-0142(19961215)78/(SICI)1097-0142(19961215)78:12<2492::AID-CNCR7>3.0.CO;2-M

7. Garassino MC, Cho BC, Kim JH, Mazières J, Vansteenkiste J, Lena H, et al. Durvalumab as third-line or later treatment for advanced non-small-cell lung cancer (ATLANTIC): an open-label, single-arm, phase 2 study. *Lancet Oncol* (2018) 19:521–36. doi: 10.1016/s1470-2045(18)30144-x

8. Camidge DR, Dziadziuszko R, Peters S, Mok T, Noe J, Nowicka M, et al. Updated efficacy and safety data and impact of the EML4-ALK fusion variant on the efficacy of alectinib in untreated ALK-positive advanced non-small cell lung cancer in the global phase III ALEX study. *J Thorac Oncol* (2019) 14:1233–43. doi: 10.1016/j.jtho.2019.03.007

9. Xu Z, Qu W, Yu Y. Primary giant cell malignant fibrous histiocytoma of the lung: a rare case report and literature review. *Transl Cancer Res* (2020) 9:7350–8. doi: 10.21037/tcr-20-2297

frontiers | Frontiers in Oncology

TYPE Case Report
PUBLISHED 14 September 2022
DOI 10.3389/fonc.2022.979462

OPEN ACCESS

EDITED BY
Kohei Fujita,
National Hospital Organization Kyoto Medical Center, Japan

REVIEWED BY
Chengbo Han,
ShengJing Hospital of China Medical University, China
Nanyuan Fang,
Nanjing University of Chinese Medicine, China

*CORRESPONDENCE
Hong Cheng
chenghong@znhospital.cn

SPECIALTY SECTION
This article was submitted to Thoracic Oncology, a section of the journal Frontiers in Oncology

RECEIVED 27 June 2022
ACCEPTED 22 August 2022
PUBLISHED 14 September 2022

CITATION
Wang X, Huang A, Lu Y, Gao S, Hu W and Cheng H (2022) Drug-induced liver injury associated with dacomitinib: A case report. *Front. Oncol.* 12:979462. doi: 10.3389/fonc.2022.979462

Drug-induced liver injury associated with dacomitinib: A case report

Xuanxuan Wang, Anqi Huang, Yun Lu, Suyu Gao, Wen Hu and Hong Cheng*

Department of Pharmacy, Zhongnan Hospital of Wuhan University, Wuhan, China

Dacomitinib, the second-generation epidermal growth factor receptor tyrosine kinase inhibitor (EGFR-TKI), has been used as a first-line treatment in non-small cell lung cancer (NSCLC) patients harboring EGFR mutation. In this case, we report a patient with drug-induced liver injury (DILI) associated with the use of dacomitinib. A 59-year-old man with stage IV NSCLC was prescribed with dacomitinib; 37 days after dacomitinib administration, he was admitted to our hospital because of jaundice. Laboratory examinations revealed elevated serum levels of liver enzymes and bilirubin. Following the immediate discontinuation of dacomitinib, liver enzymes decreased but bilirubin continued to rise. Total bilirubin reached the peak (18-fold) on day 26 after dacomitinib termination and normalized on day 146 after dacomitinib discontinuation. A "probable" cause of DILI by dacomitinib was determined based on the Roussel Uclaf Causality Assessment Method. The severity of DILI was assessed as acute liver failure. To our knowledge, this is the first case of DILI caused by dacomitinib monotherapy in a real-world setting. Clinicians should pay particular attention to the possibility of DILI during dacomitinib treatment.

KEYWORDS

dacomitinib, drug-induced liver injury, non-small cell lung cancer, Roussel Uclaf Causality Assessment Method, case report

Introduction

Lung cancer remains the leading cause of cancer incidence and mortality worldwide. Non-small cell lung cancer (NSCLC) accounts for 80%–90% of lung cancers (1). In addition, epidermal growth factor receptor (EGFR) gene mutations occur in 10%–44% of lung adenocarcinomas, a common type of NSCLC (2).

To date, epidermal growth factor receptor tyrosine kinase inhibitors (EGFR-TKIs) have been playing irreplaceable roles in the treatment of NSCLC patients harboring EGFR mutation (3, 4). Dacomitinib, the second-generation EGFR-TKI, is an oral, small-molecule irreversible inhibitor of the EGFR family. Available in 2018, dacomitinib is

approved for use in locally advanced or metastatic NSCLC patients harboring EGFR exon 19 deletion or exon 21 L858R substitution by the FDA. There have been no reports of drug-induced liver injury (DILI) caused by dacomitinib monotherapy in real-world environments to date.

In this study, we describe the first case of DILI associated with dacomitinib monotherapy in a real-world setting, marked by an 18-fold increase in bilirubin levels.

Case presentation

On 1 December 2021, a previously healthy 59-year-old man was diagnosed with stage IV lung adenocarcinoma harboring L858R mutation. He denied a history of hypertension, diabetes, coronary heart disease, liver diseases, or infectious diseases such as tuberculosis. A 40 × 33 × 46 mm mass in the paramediastinal of the upper lobe of the left lung is shown in Figure 1A. The patient had no family history of cancer and other diseases and no history of drugs or food allergies. He had a long history of smoking (15–25 cigarettes/day) and drinking (150–200 ml/day) for more than 30 years and quit smoking and drinking after his diagnosis of lung cancer. At the time, he had normal liver function with laboratory indicators as follows: alanine aminotransferase (ALT) at 10 U/L (normal range, 9–50 U/L), aspartate aminotransferase (AST) at 14 U/L (normal range, 15–40 U/L), alkaline phosphatase (ALP) at 73 U/L (normal range, 30–120 U/L), γ-glutamyltransferase (GGT) at 14 U/L (normal value, 8–57 U/L), total bilirubin (TBil) at 9.8 μmol/L (normal value, 5–21 μmol/L), direct bilirubin (DBil) at 2.1 μmol/L (normal value, 0–7 μmol/L), indirect bilirubin (IBil) at 7.7 μmol/L (normal value, 1.5–18 μmol/L), prothrombin time activity (PTA) at 84% (normal value, 80–130%), and international normalized ratio (INR) at 1.11 (normal value, 0.85–1.15). Five days later, he received one dose of cisplatin (40 mg, intrapleural perfusion) and initiated targeted therapy with dacomitinib (45 mg daily, oral). He was then discharged on day 16.

On the 37th day of dacomitinib administration, the patient was readmitted with jaundice. As shown in Figure 1B, the tumor size was significantly reduced compared with pre-treatment (Figure 1A). He had no other symptoms except for obvious yellowing of the skin and sclera. Laboratory examinations indicated liver injury: ALT at 324 U/L, AST at 176 U/L, ALP at 739 U/L, GGT at 523 U/L, TBil at 160.2 μmol/L, DBil at 95.8 μmol/L, IBil at 64.4 μmol/L, and bilirubin detected in urine. The patient tested negative for hepatitis A virus antibody (anti-HAV-IgM), hepatitis B virus antigen and DNA (HBsAg, HBV DNA),

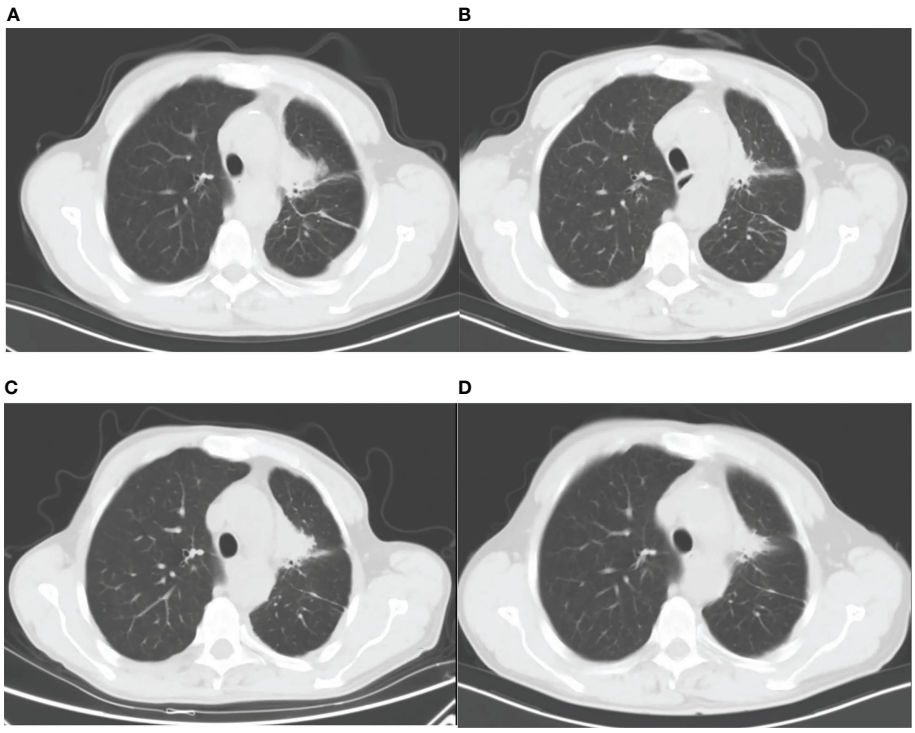

FIGURE 1
Lung CT images: **(A)** before dacomitinib administration; **(B)** 37 days after dacomitinib administration; **(C)** 50 days after dacomitinib termination; and **(D)** 95 days after afatinib administration.

hepatitis C virus antigen and RNA (HCV cAg, HCV RNA), hepatitis E virus antibody (anti-HEV-IgM/IgG), and autoantibodies (including antinuclear antibodies, smooth muscle antibodies, antibodies to the liver–kidney microsome type 1, antimitochondrial antibodies, antibodies to liver cytosol type 1, and antibodies to soluble liver antigen). With 4.27 ng/ml of alpha-fetoprotein (AFP) in the normal range (0.89–8.78 ng/ml), abdominal ultrasound and computed tomography (CT), liver magnetic resonance imaging (MRI), and magnetic resonance cholangiopancreatography (MRCP) show no abnormality.

The Naranjo score for dacomitinib-induced liver injury was 5, indicating probable adverse drug reactions. It was determined that dacomitinib was a "probable" cause of DILI based on a Roussel Uclaf Causality Assessment Method (RUCAM) score of 8 (5). In addition, the cholestatic type of DILI caused by dacomitinib was diagnosed according to DILI guidelines (6, 7). A liver biopsy was not performed due to the poor general condition of the patient.

The timeline is shown in Figure 2. Dacomitinib was discontinued on the first day of readmission. The patient then received drug and non-drug therapy, including magnesium isoglycyrrhizinate at 100 mg daily, S-adenosylmethionine at 1 g daily, and ursodeoxycholic acid at 250 mg three times daily throughout the hospital stay; *N*-acetylcysteine at 8 g daily between the 12th and 17th hospital days and infusion of plasma on the 16th hospital day because of a sudden deterioration of coagulation function; and once artificial liver therapy on the 26th hospital day due to high levels of bilirubin. The patient was discharged on the 29th hospital day (29 days after dacomitinib termination) and continued ursodeoxycholic acid treatment outside the hospital. He was followed up for 4 months.

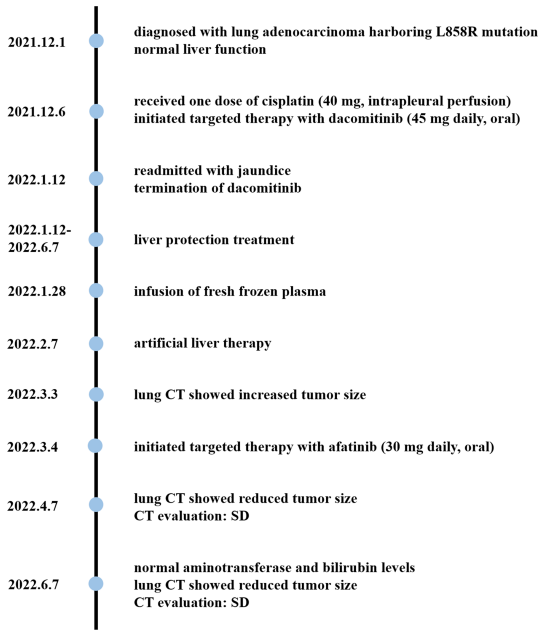

FIGURE 2
Timeline of interventions and outcomes.

During hospitalization, the patient remained sane without signs of hepatic encephalopathy. However, he developed a change in taste, poor appetite, abdominal distension, generalized itching, aggravated yellowing of the skin and sclera, yellow urine, and white stool. The serum levels of the laboratory parameters in the patient are shown in Figure 3. After the discontinuation of dacomitinib, the liver enzyme (ALT, AST, ALP, GGT) levels decreased obviously. However, bilirubin (TBil, DBil, IBil) levels showed an upward trend, reaching the highest (18-fold) level on day 26 after dacomitinib termination. It subsequently decreased partly after artificial liver therapy, followed by a gradual downward trend, and finally normalized on day 146 after dacomitinib discontinuation. Coagulation function (PTA) was relatively stable initially, decreased significantly (PTA<30%) on day 15 after dacomitinib termination, recovered, and remained in the normal range after an infusion of fresh frozen plasma (350 ml) on day 16 after dacomitinib termination. The severity of DILI was assessed as acute liver failure (ALF) based on DILI guidelines (6, 7).

Fifty days after dacomitinib termination, a lung CT image showed an increased tumor size (Figure 1C), and the patient received afatinib 30 mg daily the next day. 34 and 95 days after afatinib administration, lung CT showed a reduced tumor size without tumor progression and metastasis (Figure 1D). The patient achieved stable disease (SD) based on imaging assessment and continued to receive afatinib treatment. The patient showed agreement on the risk, medication, and treatment plan with the clinician throughout the entire treatment.

Discussion

DILI is a diagnosis of exclusion and requires careful assessment. In this case, as mentioned above, the patient reported no family history. He remained sane and developed a change in taste, poor appetite, abdominal distension, generalized itching, jaundice with elevated liver enzymes and bilirubin levels during hospitalization. Liver imaging showed no abnormality. The patient presented no symptoms of fever or lymphadenopathy, and extrahepatic manifestations of HEV infection, especially neurological injury, were not observed during hospitalization (8). Laboratory parameters for viral hepatitis and autoantibodies were all negative. Significantly elevated ALP levels were not consistent with a typical pattern of autoimmune liver diseases. These lead to an unsupported diagnosis of viral hepatitis and autoimmune hepatitis (9). Although the patient had a long history of drinking, abnormal indicators of alcoholic hepatitis, such as AST/ALT >1.5, were not

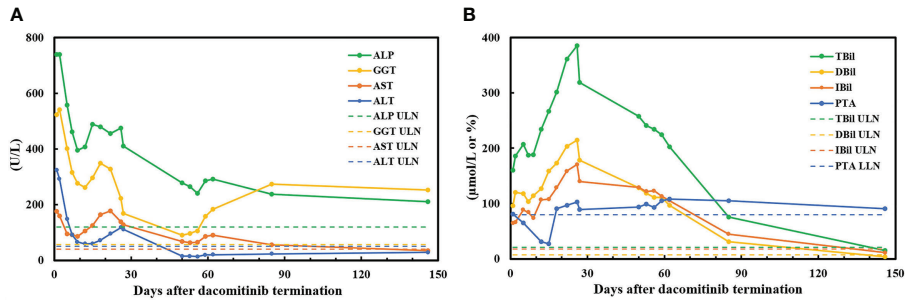

FIGURE 3
Serum levels of laboratory parameters in the patient. **(A)** Alanine aminotransferase (ALT), aspartate aminotransferase (AST), alkaline phosphatase (ALP), and γ-glutamyltransferase (GGT); **(B)** total bilirubin (TBil), direct bilirubin (DBil), indirect bilirubin (IBil), and prothrombin time activity (PTA). ULN, upper limit of normal; LLN, lower limit of normal.

observed. Steatosis and cirrhosis were also not found in the liver imaging. The diagnosis of alcohol-associated liver diseases and nonalcoholic steatohepatitis was then excluded (10). The patient presented no Kayser–Fleischer rings and neuropsychiatric disturbances, the most common presentations of Wilson disease, and reported no family history, so Wilson disease could be excluded (11). The dacomitinib-induced liver injury was finally established based on the Naranjo score of 5 and the RUCAM score of 8. However, Epstein–Barr virus, cytomegalovirus, and further examinations for HEV were not tested after the clinician empirically established the high possibility of DILI, which also made the RUCAM and Naranjo scores not higher.

Several studies have demonstrated the efficacy of dacomitinib in EGRF-mutated NSCLC patients. In the ARCHER 1050 study (NCT01774721), compared with the first-generation EGRF-TKI gefitinib, dacomitinib showed significant improvement in progression-free survival and overall survival (12, 13). The better efficacy in Asians and patients with EGFR exon 21 L858R mutation was also proven (14, 15).

However, growing evidence shown the toxicities of dacomitinib may limit its use in clinical practice (16). Adverse events (including laboratory abnormalities) are assessed and graded using the National Cancer Institute Common Terminology Criteria for Adverse Events (CTCAE) version 4.0. Adverse events (of any cause) occurred in almost all patients given dacomitinib. The most common adverse events (of any grade) of dacomitinib are diarrhea, paronychia, dermatitis acneiform, and stomatitis. Among them, the most commonly reported adverse events in grades 3–5 are dermatitis acneiform and diarrhea (12). Treatment-related serious adverse events may lead to permanent discontinuation. In patients with dacomitinib, they are gastrointestinal disorders and skin and subcutaneous disorders.

Liver injury is not a major adverse event of dacomitinib. In the ARCHER 1050 study, when taking adverse events of any cause into consideration, 19% of patients experienced grades 1–2 adverse events with elevated liver enzymes (ALT, AST), and only two patients (1%) developed a grade 3 adverse event of ALT elevation. In terms of treatment-related serious adverse events, no patients suffered liver injury such as elevated liver enzymes and bilirubin (12). The incidence of hepatotoxicity associated with dacomitinib was less frequent than with the first-generation EGFR-TKI gefitinib (12, 17). Overall, the frequency of severe aminotransferase abnormalities and DILI with dacomitinib showed a lower risk. Hepatotoxic events potentially related to dacomitinib reported in clinical trials were mostly transient increased aminotransferase levels (18). A network meta-analysis of hepatotoxicity with EGFR-TKIs revealed an uncertain association between dacomitinib and the risk of liver enzyme elevation in patients diagnosed with NSCLC (19). After consulting the literature, only one Chinese case report was involved, which was about DILI marked by elevated liver enzymes owing to the combined use of dacomitinib and metoprolol (20).

Dacomitinib is mainly metabolized by the liver through oxidative and conjugative metabolism (21). In this study, dacomitinib-induced liver injury was a near-certainty diagnosis after assessing with RUCAM, Naranjo's adverse drug reaction probability scale, and analyzing clinical, laboratory, and imaging features. The DILI case was mainly marked as an 18-fold increase in bilirubin levels accompanied by an increase in liver enzymes, which was defined as a grade 3 adverse event. Since severe DILI is a very rare complication of dacomitinib therapy, the monitoring of liver function received little attention. The occurrence of liver injury was not detected until the patient was readmitted because of jaundice a month later. Therefore, the surveillance of liver function during treatment is necessary for the early detection of hepatotoxicity.

Actually, dacomitinib-associated adverse events are manageable with treatment interruption, dose reduction, and/or adjuvant drug therapy (12). In the ARCHER 1050 study, dose

reduction did not reduce the efficacy of dacomitinib despite a prolonged overall treatment time. Also, the incidence and severity of adverse events were effectively decreased (13). This suggests that dosage reduction may be the best solution for relieving adverse events induced by dacomitinib (17). Nearly two-thirds of patients taking dacomitinib required at least one dose modification (22). However, in this study, dacomitinib-induced grade 3 hepatotoxicity and disease progression revealed by tumor imaging assessments (CT), led to the permanent withdrawal of dacomitinib and switch to afatinib. In some cases, patients who have suffered hepatotoxicity due to EGFR-TKIs were successfully switched from one EGFR-TKI to another (23, 24).

It is worth mentioning how to rule out the possibility of cisplatin-induced liver injury. First, cisplatin is metabolized by the kidneys, generally showing nephrotoxic, bone marrow toxicity, and rarely hepatotoxicity. Secondly, patients received cisplatin *via* local chemotherapy of intrapleural perfusion, reducing the influence on the liver in the abdominal. Finally, adverse reactions to cisplatin are commonly immediate. As cholestatic-type DILI, the liver injury occurred 37 days after the withdrawal of cisplatin, which was assessed as "no correlation" according to the RUCAM scale.

Furthermore, possible increased toxicity due to drug interactions is of concern. Dacomitinib is mainly metabolized in liver microsomes by CYP2D6 with a major metabolite as *O*-desmethyl dacomitinib (25). For patients taking dacomitinib, concomitant use of CYP2D6 inhibitors (such as paroxetine) or CYP2D6 substrates (such as trazodone) should be avoided to prevent an increased risk of drug toxicity (26, 27). Meanwhile, dacomitinib is a substrate/an inhibitor of adenosine triphosphate (ATP)-binding cassette (ABC) transporters including P-glycoprotein (P-gp) and breast cancer resistance protein (BCRP) on the cell membrane surface, which are related to tumor multidrug resistance (MDR) (28). In addition, concomitant use of acid-suppressing drugs possibly reduces dacomitinib exposure through reducing the solubility of dacomitinib. In this case, from receiving chemotherapy for the first time (including dacomitinib and one dose of cisplatin by intrapleural infusion) and discharging with normal liver function to readmitting with jaundice, the patient only took dacomitinib outside the hospital because of the absence of other underlying diseases. Cisplatin is metabolized *via* nonenzymatic mechanisms, not involving the CYP2D6 pathway. Therefore, the use of cisplatin is less likely to cause increased drug toxicity. Dacomitinib, on the other hand, has been shown to improve cisplatin chemosensitivity and generate synergistic antitumor effects by inhibiting the function of P-gp and BCRP (29). Cisplatin can increase the expression of ABC transporters, including P-gp and BCRP. The overexpression of P-gp and BCRP is one of the mechanisms of cisplatin resistance. Downregulating the expression of P-gp and BCRP may be a promising strategy to overcome cisplatin resistance and enhance antitumor activity (30).

There are still some limitations to this study. The lack of pathological examination and serological tests for Epstein–Barr virus, cytomegalovirus, and reverified HEV infection makes the diagnosis of DILI still challenging. The association between drug metabolism genotype and liver injury is not fully explored owing to the lack of genetic testing, and the mechanism of dacomitinib-induced liver injury remains unclear.

Conclusions

To our knowledge, this is the first case report of DILI caused by dacomitinib monotherapy in a real-world setting. Clinicians should pay particular attention to the possibility of DILI during dacomitinib treatment.

Data availability statement

The original contributions presented in the study are included in the article/supplementary material. Further inquiries can be directed to the corresponding author.

Ethics statement

Written informed consent was obtained from the individual (s) for the publication of any potentially identifiable images or data included in this article.

Author contributions

XW conceived of the design and wrote the manuscript. AH, YL, SG, and WH revised the manuscript. HC reviewed the manuscript and assumed responsibility for data completeness and accuracy. All authors contributed to the article and approved the submitted version.

Conflict of interest

The authors declare that the research was conducted in the absence of any commercial or financial relationships that could be construed as a potential conflict of interest.

Publisher's note

References

1. Bray F, Ferlay J, Soerjomataram I, Siegel RL, Torre LA, Jemal A. Global cancer statistics 2018: Globocan estimates of incidence and mortality worldwide for 36 cancers in 185 countries. *CA-Cancer J Clin* (2018) 68(6):394–424. doi: 10.3322/caac.21492

2. Paez JG, Jänne PA, Lee JC, Tracy S, Greulich H, Gabriel S, et al. Egfr mutations in lung cancer: Correlation with clinical response to gefitinib therapy. *Science* (2004) 304(5676):1497–500. doi: 10.1126/science.1099314

3. Planchard D, Popat S, Kerr K, Novello S, Smit EF, Faivre-Finn C, et al. Metastatic non-small cell lung cancer: Esmo clinical practice guidelines for diagnosis, treatment and follow-up. *Ann Oncol* (2018) 29:192–237. doi: 10.1093/annonc/mdy275

4. Zhang C, Leighl NB, Wu Y-L, Zhong W-Z. Emerging therapies for non-small cell lung cancer. *J Hematol Oncol* (2019) 12(1):1–24. doi: 10.1186/s13045-019-0731-8

5. Danan G, Benichou C. Causality assessment of adverse reactions to drugs–i. a novel method based on the conclusions of international consensus meetings: Application to drug-induced liver injuries. *J Clin Epidemiol* (1993) 46(11):1323–30. doi: 10.1016/0895-4356(93)90101-6

6. Andrade RJ, Aithal GP, Bjornsson ES, Kaplowitz N, Kullak-Ublick GA, Karlsen TH. Easl clinical practice guidelines: Drug-induced liver injury. *J Hepatol* (2019) 70(6):1222–61. doi: 10.1016/j.jhep.2019.02.014

7. Yu Y-C, Mao Y-M, Chen C-W, Chen J-J, Chen J, Cong W-M, et al. Csh guidelines for the diagnosis and treatment of drug-induced liver injury. *Hepatol Int* (2017) 11(3):221–41. doi: 10.1007/s12072-017-9793-2

8. European Assoc Study L. Easl clinical practice guidelines on hepatitis e virus infection. *J Hepatol* (2018) 68(6):1256–71. doi: 10.1016/j.jhep.2018.03.005

9. Wang G, Tanaka A, Zhao H, Jia J, Ma X, Harada K, et al. The Asian pacific association for the study of the liver clinical practice guidance: The diagnosis and management of patients with autoimmune hepatitis. *Hepatol Int* (2021) 15(2):223–57. doi: 10.1007/s12072-021-10170-1

10. Crabb DW, Im GY, Szabo G, Mellinger JL, Lucey MR. Diagnosis and treatment of alcohol-associated liver diseases: 2019 practice guidance from the American association for the study of liver diseases. *Hepatology* (2020) 71(1):306–33. doi: 10.1002/hep.30866

11. Ferenci P, Czlonkowska A, Stremmel W, Houwen R, Rosenberg W, Schilsky M, et al. Easl clinical practice guidelines: Wilson's disease. *J Hepatol* (2012) 56 (3):671–85. doi: 10.1016/j.jhep.2011.11.007

12. Wu Y-L, Cheng Y, Zhou X, Lee KH, Nakagawa K, Niho S, et al. Dacomitinib versus gefitinib as first-line treatment for patients with egfr-Mutation-Positive non-Small-Cell lung cancer (Archer 1050): A randomised, open-label, phase 3 trial. *Lancet Oncol* (2017) 18(11):1454–66. doi: 10.1016/s1470-2045(17)30608-3

13. Mok TS, Cheng Y, Zhou X, Lee KH, Nakagawa K, Niho S, et al. Improvement in overall survival in a randomized study that compared dacomitinib with gefitinib in patients with advanced non-Small-Cell lung cancer and egfr-activating mutations. *J Clin Oncol* (2018) 36(22):2244–50. doi: 10.1200/jco.2018.78.7994

14. Mok TSK, Cheng Y, Zhou X, Lee KH, Nakagawa K, Niho S, et al. Safety and efficacy of dacomitinib for egfr plus nsclc in the subgroup of Asian patients from archer 1050. *Ann Oncol* (2019) 30:ix160–1. doi: 10.1093/annonc/mdz437.006

15. Nishio M, Kato T, Niho S, Yamamoto N, Takahashi T, Nogami N, et al. Safety and efficacy of first-line dacomitinib in Japanese patients with advanced non-small cell lung cancer. *Cancer Sci* (2020) 111(5):1724–38. doi: 10.1111/cas.14384

16. Huang L, Jiang S, Shi Y. Tyrosine kinase inhibitors for solid tumors in the past 20 years (2001-2020). *J Hematol Oncol* (2020) 13(1):1–23. doi: 10.1186/s13045-020-00977-0

17. Zhou J-Y, Liu S-Y, Wu Y-L. Safety of egfr-tkis for egfr mutation-positive non-small cell lung cancer. *Expert Opin Drug Saf* (2020) 19(5):589–99. doi: 10.1080/14740338.2020.1753697

18. Houron C, Danielou M, Mir O, Fromenty B, Perlemuter G, Voican CS. Multikinase inhibitor-induced liver injury in patients with cancer: A review for clinicians. *Crit Rev Oncol Hemat* (2021) 157:103127. doi: 10.1016/j.critrevonc.2020.103127

19. Wu Z, Chen S, Du X, Wu Y, Xie X. Hepatotoxicity with epidermal growth factor receptor tyrosine kinase inhibitors in non-Small-Cell lung cancer patients: A network meta-analysis. *J Clin Pharm Ther* (2021) 46(2):310–8. doi: 10.1111/jcpt.13281

20. Guo Y, Huang L, Wei L, Tian L. A case of acute drug-induced liver injury caused by the combination use of dacomitinib and metoprolol. *Chin J Pharmacoepidemiol* (2021) 30(12):847–8. doi: 10.19960/j.cnki.issn1005-0698.2021.12.012

21. Giri N, Masters JC, Plotka A, Liang Y, Boutros T, Pardo P, et al. Investigation of the impact of hepatic impairment on the pharmacokinetics of dacomitinib. *Invest New Drug* (2015) 33(4):931–41. doi: 10.1007/s10637-015-0256-0

22. Sun H, Wu Y-L. Dacomitinib in non-Small-Cell lung cancer: A comprehensive review for clinical application. *Future Oncol* (2019) 15(23):2769–77. doi: 10.2217/fon-2018-0535

23. Ueda H, Hayashi H, Kudo K, Takeda M, Nakagawa K. Successful treatment with afatinib after gefitinib- and erlotinib-induced hepatotoxicity. *Invest New Drug* (2016) 34(6):797–9. doi: 10.1007/s10637-016-0384-1

24. Zenke Y, Umemura S, Sugiyama E, Kirita K, Matsumoto S, Yoh K, et al. Successful treatment with afatinib after grade 3 hepatotoxicity induced by both gefitinib and erlotinib in egfr mutation-positive non-small cell lung cancer. *Lung Cancer* (2016) 99:1–3. doi: 10.1016/j.lungcan.2016.05.002

25. Shirley M. Dacomitinib: First global approval. *Drugs* (2018) 78(18):1947–53. doi: 10.1007/s40265-018-1028-x

26. Ruiz-Garcia A, Giri N, LaBadie RR, Ni G, Boutros T, Richie N, et al. A phase I open-label study to investigate the potential drug-drug interaction between single-dose dacomitinib and steady- state paroxetine in healthy volunteers. *J Clin Pharmacol* (2014) 54(5):555–62. doi: 10.1002/jcph.243

27. Han M, Zhang X, Ye Z, Wang J, Kong Q, Hu X, et al. Effects of Cyp2d6 genetic polymorphism and drug interaction on the metabolism of dacomitinib. *Chem Res Toxicol* (2022) 35(2):265–74. doi: 10.1021/acs.chemrestox.1c00327

28. Fan Y-F, Zhang W, Zeng L, Lei Z-N, Cai C-Y, Gupta P, et al. Dacomitinib antagonizes multidrug resistance (Mdr) in cancer cells by inhibiting the efflux activity of abcbi and Abcg2 transporters. *Cancer Lett* (2018) 421:186–98. doi: 10.1016/j.canlet.2018.01.021

29. Xu L, Xu Y, Zheng J, Zhao Y, Wang H, Qi Y. Dacomitinib improves chemosensitivity of cisplatin-resistant human ovarian cancer cells. *Oncol Lett* (2021) 22(1):1–8. doi: 10.3892/ol.2021.12830

30. Zhao L, Zhang W, Zhang F. Poncirin downregulatesatp-binding cassette transporters to enhance cisplatin sensitivity in cisplatin-resistant osteosarcoma cells. *Phytother Res* (2021) 35(1):278–88. doi: 10.1002/ptr.6798

frontiers | Frontiers in Oncology

TYPE Case Report
PUBLISHED 23 September 2022
DOI 10.3389/fonc.2022.988625

OPEN ACCESS

EDITED BY
Wenyi Shen,
Nanjing Medical University, China

REVIEWED BY
Javier De Castro,
Hospital Universitario
La Paz-IdiPAZ, Spain
Valeria Internò,
University of Bari Aldo Moro, Italy

*CORRESPONDENCE
Qi Wang
wangqixlp@163.com

SPECIALTY SECTION
This article was submitted to Thoracic Oncology, a section of the journal Frontiers in Oncology

RECEIVED 07 July 2022
ACCEPTED 24 August 2022
PUBLISHED 23 September 2022

CITATION
Xu X, Chen D, Wu X and Wang Q (2022) A pulmonary enteric adenocarcinoma patient harboring a rare EGFR exon 19 P753S mutation: Case report and review.
Front. Oncol. 12:988625.
doi: 10.3389/fonc.2022.988625

A pulmonary enteric adenocarcinoma patient harboring a rare EGFR exon 19 P753S mutation: Case report and review

Xiaohu Xu[1], Dong Chen[2], Xiao Wu[1] and Qi Wang[1]*

[1]Department of Integrated Traditional Chinese and Western Medicine, Tongji Hospital, Tongji Medical College, Huazhong University of Science and Technology, Wuhan, China,
[2]Department of Pathology, Tongji Hospital, Tongji Medical College, Huazhong University of Science and Technology, Wuhan, China

Pulmonary enteric adenocarcinoma (PEAC) is a rare subtype of non–small cell lung cancer (NSCLC), accounting for about 0.6% of all primary lung adenocarcinoma. Although epidermal growth factor receptor (EGFR) mutation is common in primary lung adenocarcinoma, it is rarely reported in PEAC. This case report describes a PEAC patient with co-mutations of EGFR, Kirsten rat sarcoma viral oncogene (KRAS), and TP53, being treated with immunotherapy combined with chemotherapy. A 69-year-old man complained of cough and expectoration with bloody sputum for 2 weeks. The lung-enhanced CT scan showed a massive soft tissue shadow, about 46 × 35 mm in the lower lobe of the right lung. The neoplasm sample in the lower lobe of the right lung was obtained using CT-guided fine-needle aspiration (FNA). Immunohistochemical assays showed that the tumor was positive for CK7, CDX-2, C-MET, and villin. Gastroscopy and rectal colonoscopy had been performed respectively to exclude a diagnosis of colorectal adenocarcinoma. The patient was finally diagnosed with pulmonary intestinal adenocarcinoma. Next-generation sequencing (NGS) analysis showed a rare EGFR exon 19 missense mutation (c.2257C>T, p.P753S), KRAS exon 2 missense mutation (c.35G>T, p.G12V), and TP53 exon 5 missense mutation (c.401T>C, p.F134S). The lung-enhanced CT scan showed that the tumor shrank after four cycles of chemotherapy combined with immunotherapy. We hope that this case report can increase the understanding of this rare type of tumor and provide new molecular indications for diagnosis and individualized treatment. Furthermore, the combination of chemotherapy and immunotherapy seems to be an effective therapy for PEAC. Whether the use of immunotherapy can provide clinical benefits needs to be further explored with more samples in future studies.

KEYWORDS

pulmonary enteric adenocarcinoma, EGFR mutation, case report, KRAS, TP53

Introduction

Pulmonary enteric adenocarcinoma (PEAC) is a rare subtype of non–small cell lung cancer (NSCLC), which is defined as a morphological enteric cell differentiation involving more than 50% of tumor cells, without evidence of a primary digestive tract tumor (1). It is pointed out that PEAC accounts for 0.6% of all primary lung adenocarcinoma (2). The first case was reported as 'intestinal type of lung adenocarcinoma' by Tsao and Fraser in 1991 (3). PEAC was officially listed as a variant subtype of pulmonary invasive adenocarcinoma by the World Health Organization (WHO) in 2015 (4). According to a review, there are no more than 300 cases have been reported as case reports or small case studies in the literature (5). To date, differences between PEAC and conventional lung adenocarcinoma in pathogenesis, lung location type, clinical course, and radiographic features cannot be fully characterized. However, immunohistochemistry (IHC) is still a powerful tool for the diagnosis of PEAC. The rarity of PEAC makes it impossible to provide more information to evaluate the efficacy of different therapeutic methods and prognoses. With the application of next-generation sequencing (NGS) analysis technology in recent years, new perspectives have emerged in delineating new molecular profiles and therapeutic sensitivity of PEAC (6).

The present study reports a case of PEAC with a rare epidermal growth factor receptor (EGFR) exon 19 missense mutation (c.2257C>T, p.P753S), who was initially treated with chemotherapy plus an immune checkpoint inhibitor with satisfactory efficacy. In addition, it reviews PEAC pathological features, gene mutations, and treatments according to the published literature to improve the understanding of this disease. This present study was approved by the Clinical Trial Ethics Committee of Tongji Hospital, Tongji Medical College, Huazhong University of Science and Technology, Wuhan, China. Informed consent was obtained from the patient.

Case report

A 69-year-old non-smoker man was admitted to Tongji Hospital, Tongji Medical College, Huazhong University of Science and Technology (Wuhan, China) on 11 April 2022 and complained of cough and expectoration with bloody sputum for 2 weeks. In March 2022, he visited a local hospital due to cough and expectoration with bloody sputum, but there were no chills, fever, fatigue, or gastrointestinal complaints. A chest computed tomography (CT) scan in the local hospital on 1 April showed a patchy shadow in the right lower lobe. Physicians at the local hospital recommended that the patient should be transferred to the higher-level hospital for further diagnosis and treatment. The patient had a history of kidney calculi disease and denied the history of malignant tumor, other diseases, and surgery. Physical examination at admission showed no obvious positive signs. On 13 April, the lung-enhanced CT scan in Tongji Hospital showed a massive soft tissue shadow, about 46 × 35 mm in the lower lobe of the right lung (Figure 1A). To further confirm the diagnosis, the neoplasm samples in the lower lobe of the right lung were obtained using CT-guided fine-needle aspiration (FNA).

Immunohistochemical assays showed that the tumor was positive for CK7, CDX-2, C-MET, and villin; focally positive for P40, CD10, MUC6, ROS1, and mesothelin; and negative for thyroid transcription factor-1 (TTF-1), ALK, SATB2(-), MUC2 (-), MUC5AC(-), PAX8(-), GATA3(-), PSA(-), NKX3.1(-), napsin A, and CK20 (Figure 2). Further pathological

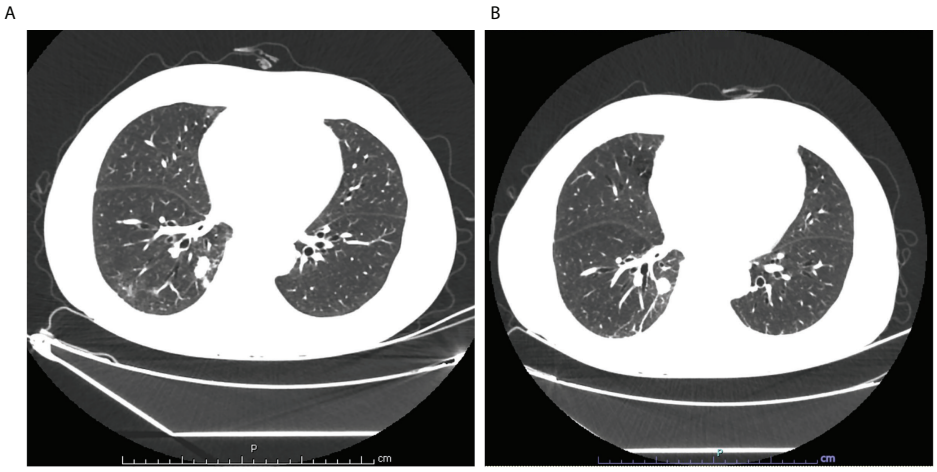

FIGURE 1
(A) Lung enhanced CT scan showed a massive soft tissue shadow, about 46×35mm in the lower lobe of the right lung on April 13; **(B)** Lung enhanced CT scan showed a massive soft tissue shadow, about 44×30mm in the lower lobe of the right lung on July 4.

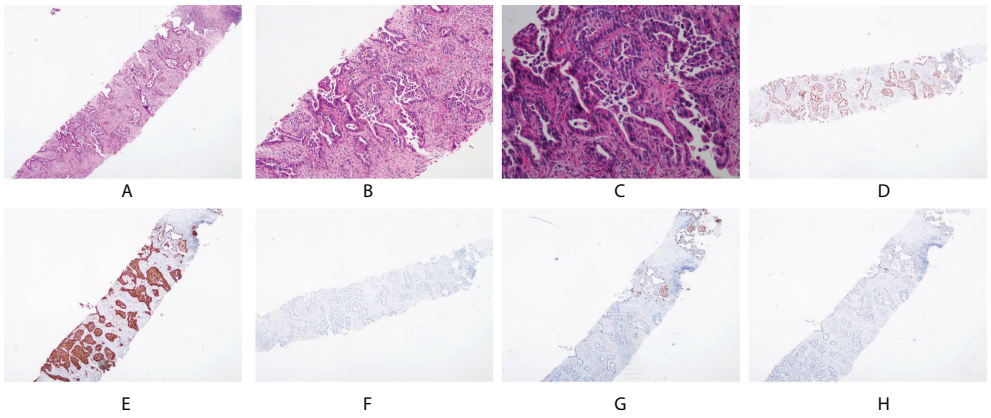

FIGURE 2
Pathological and immunohistochemical examination results. **(A)** hematoxylin-eosin staining (HE), magnification×40; **(B)** HE, magnification×100; **(C)** HE, magnification×200; **(D)** CDX-2 positivity, magnification×40; **(E)** CK7 positivity, magnification×40; **(F)** CK20 negativity, magnification×40; **(G)** NapsinA negativity, magnification×40; **(H)** TTF-1 negativity, magnification×40.

examination resulted in a diagnosis of intestinal-type adenocarcinoma of the right lung.

The laboratory data showed that cytokeratin-19 fragment antigen21-1 (CYFRA21-1, 9.57 μg/L) and carbohydrate antigen 19-9 (CA19-9, 106.60 U/ml) levels were increased compared with normal levels. To exclude a diagnosis of colorectal adenocarcinoma, gastroscopy and rectal colonoscopy had been performed respectively. Gastroscopy showed chronic hemorrhagic gastritis and gastric body polyp. Histological examination of the gastric body polyp showed gastric fundus gland polyp. Rectal colonoscopy showed multiple polyps of the sigmoid colon, which was determined as tubular adenoma by histological examination. These pathological and immunohistochemical findings excluded lung metastases of intestinal adenocarcinoma, and the patient was finally diagnosed with pulmonary intestinal adenocarcinoma.

In order to investigate the mutation profile of the neoplasm samples, we obtained the permission of patients to use NGS for gene analysis, which is designed to identify somatic variations of 32 cancer-related genes, including EGFR, KRAS, NRAS, BRAF, RET, PIK3CA, and TP53. Gene analysis of the neoplasm samples was undertaken by GREENIKON Medical Laboratory Co., Ltd (Shanghai, China) using Illumina NovaSeq 6000 platform (Illumina, San Diego, CA). Among the 32 genes examined by this assay, only the EGFR, KRAS, and TP53 genes were mutated. EGFR showed a missense mutation (c.2257C>T, p.P753S) of exon 19. KRAS showed a missense mutation (c.35G>T, p.G12V) of exon 2. TP53 showed a missense mutation (c.401T>C, p.F134S) of exon 5 (Table 1). In addition, the expression level of PD-L1 in tumor tissues of patients was detected, and IHC staining results of tissue sections showed that the tumor proportion score (TPS) of PD-L1 was 0%, indicating negative expression. From 30 April, the patient received four cycles of chemotherapy (pemetrexed + cisplatin) combined with immunotherapy (penpulimab). On 4 July, the lung-enhanced CT scan showed that the tumor was smaller than that on 13 April (Figure 1).

Discussion

As a rare subtype of NSCLC, PEAC has similar clinical manifestations to typical lung cancer, including dry cough, fever, chest/back pain, and hemoptysis. Solid lung masses can be found by CT or PET/CT imaging, and some may be accompanied by speculation, pleural effusion, or indentation radiological findings.

Smoking may be a potential risk factor for lung-intestinal adenocarcinoma, which is reported that 76.9% of PEAC patients had a history of smoking (7). However, another study showed that 46.1% of patients had a history of smoking, and it seemed that there was no significant correlation between PECA

TABLE 1 Gene mutation result.

Gene	Exon	Nucleotide variation	Amino acid variation	Mutation abundance
TP53	exon5	c.401T > C	p.F134S	19.72%
KRAS	exon2	c.35G > T	p.G12V	15.25%
EGFR	exon19	c.2257C > T	p.P753S	42.80%

and smoking (8, 9). Moreover, a study indicated that PEAC affected more men, but other studies concluded a similar or opposite incidence between men and women (8–10). These controversies may be explained by the limited number of cases reported currently. Nevertheless, there is a general consensus that most PEAC patients are elderly (7–10).

Circulating tumor markers are highly sensitive to distinguish different tumors, but it seems that it is difficult to distinguish PEAC from other tumors. A study found that 68.2% (45/66) patients had elevated carcinoembryonic antigen (CEA) levels, whereas the positive rates of CA125 and CA19-9 were relatively low, with 50% (5/10) and 48.4% (15/31) respectively (9). Another article has suggested that PEAC is associated with increases in serum CEA and CA19-9 (10). Therefore, it is necessary to exclude digestive system tumors by CT, especially gastrointestinal endoscopy.

Although there is no consensus on the characteristics of PEAC, IHC is a great significant tool for the diagnosis. PEAC has similar pathological morphology and IHC features to those of metastatic colorectal adenocarcinoma (MCRC). That is, it has at least one positive enteric differentiation marker including colorectal cancer markers such as caudal-type homeobox 2 (CDX-2), cytokeratin-20 (CK 20), mucin 2 (MUC-2), and villin, whereas lung cancer markers including CK7, napsin A, and TTF-1 can be expressed simultaneously. One study retrieved 33 articles with a total of 170 PEAC patients included in PubMed from 31 January 1991 to 1 August 2020 and found that the positive rate of CK7, CDX2, CK20, and TTF1 was 88.2% (149/169), 78.1% (132/169), 48.2% (82/170), and 38.8% (66/170), respectively (11). Another study reported that the positive expression rates of CK7 and CDX2 were 100%, whereas the positive rates of TTF1, CK20, and MUC2 were 45.6%, 32.6%, and 32.6%, respectively (12). Therefore, CK7 combined with CDX2 was considered to be an important marker for the diagnosis of PEAC.

The present patient was a 69-year-old non-smoker man who complained of cough and expectoration with bloody sputum for 2 weeks. He found a massive soft tissue shadow in the lower lobe of the right lung by a lung-enhanced CT scan. The pathological examination of the tumor tissue obtained by CT-guided FNA revealed a diagnosis of intestinal-type adenocarcinoma of the right lung. Gastrointestinal endoscopy showed that the present patient had multiple polyps, but the pathological examination results ruled out gastric cancer or colon cancer. In the present case study, IHC assays showed that the tumor was positive for colorectal cancer markers (CDX-2, villin) and lung cancer markers (CK7), but negative for TTF-1, CK20, and MUC-2. We also detected the negative expression of SATB 2, because some studies reported that SATB 2 can be used as a negative marker of lung-intestinal adenocarcinoma, so as to differentiate it from lung metastasis of colorectal cancer (13). Based on the above pathological and immunohistochemical results, the present case was diagnosed as PEAC after the primary gastrointestinal tumor was excluded.

Further genetic analysis of PEAC is helpful to provide more information for diagnosis and treatment. At present, most studies believe that the predominant mutations associated with PEAC include KRAS (G12V, G12D, G12C, and G13D) and ALK, whereas EGFR was mostly wild type (8, 10, 12–15). Nottegar et al. found that KRAS was the most common mutation in PEAC, and the mutation rates were 60.9% and 50.0% after analyzing 46 and 8 cases of PEAC, respectively (12). However, KRAS G12V is also common in colonic adenocarcinoma, so KRAS mutation cannot be used to distinguish PEAC from MCRC (13). In these cases, KRAS 12 codon is the most common mutation site, and only one case has KRAS exon 2 mutation and EGFR exon 19 deletion mutation (p.E746_S752). This is also the first report of EGFR mutation in PEAC (12). Since then, many studies have shown that the positive rate of EGFR mutations is about 16.7%, much lower than that of KRAS, and these EGFR mutations are all deletion mutations (8, 10, 12, 13, 16).

Different from what was reported by Nottegar et al., EGFR showed a missense mutation (c.2257C>T, p.P753S) of exon 19 in the present case study. This mutation will result in a change from C to T at base 2,257 of exon 19 of the EGFR gene, resulting in a change from proline (P) to serine (S) at amino acid 753 of the translated protein, which was only reported in a patient with cutaneous squamous cell carcinoma (17). It is speculated that this mutation may lead to exon jumping or protein truncation, thus activating the EGFR kinase domain and increasing the sensitivity to monoclonal antibody inhibition (17). As far as we know, this is the first case report for PEAC with EGFR-p.P753S mutation, although the role of P753 mutation in lung cancer is unclear.

EGFR mutation mainly occurs between exon 18 and exon 21 in NSCLC. The most common mutations include exon 19 deletion and L858R exon 21, which have a convincing response to EGFR tyrosine kinase inhibitors (TKIs). It is reported that 10% of patients with EGFR mutation in NSCLC have uncommon mutations, which include exon 18 mutations, exon 20 insertion mutations, and other rare variants (18). Such as exon 20 insertions and duplications are generally resistant to targeted therapy with TKIs due to the inaccessibility of the binding site for this mutation (19). Although new molecules recently have been approved as subsequent targeted therapies, chemotherapy remains the first-line regimen. In another case, p.E746-A750del and p.delL747-P753insS are the common exon 19 deletion subtypes, which could disrupt inactive conformation of EGFR kinase domain and enhance the effectiveness of EGFR TKIs (20). However, it is not enough to evaluate and determine the survival difference of the exon 19 deletion type as the number of TKI-treated patients was very few. Overall, uncommon mutations are insensitive or have a low response to EGFR-TKIs.

Additionally, we also found KRAS missense mutation (c.35G>T, p.G12V) of exon 2 in this case. KRAS gene is a proto-oncogene in the RAS family, and its most frequent mutation sites are almost all concentrated in codon 12 of exon 2, accounting for about 90% (21). The KRAS gene is a downstream factor of the EGFR signaling pathway. The continuous activation mutation of KRAS may affect the therapeutic effect of EGFR-TKIs in NSCLC patients. Pan analyzed the results of 41 global studies and found that the overall prognosis of NSCLC patients would be worse when KRAS mutation was found, and KRAS mutation was closely related to EGFR-TKIs resistance (22). In addition, TP53 showed a missense mutation (c.401T>C, p.F134S) of exon 5. TP53 is an important tumor suppressor gene in cells. It has the highest mutation frequency (>50%) in many different types of tumors. It is a negative regulator in the cell growth cycle, which is related to important biological functions such as cell cycle regulation, cell apoptosis, cell differentiation, DNA repair, and angiogenesis (23, 24). Most of the TP53 mutations are missense mutations, accounting for more than 75% of the total mutations, and exons 5–8 are the most common mutation sites (25, 26). As the most common type of co-mutation in advanced NSCLC, studies have shown that EGFR-TP53 co-mutation may weaken the therapeutic effect of TKIs (27). Because mutations of EGFR are rare in PEAC, there have been no reported cases of TKIs. Therefore, the co-mutations of EGFR, KRAS, and TP53 present in this case suggest that this patient is not suitable for targeted drug therapy.

For the treatment of this PEAC patient, we chose PP chemotherapy because it was reported that one stage IV PEAC patient was treated with four times pemetrexed + cisplatin, and tumor evaluation was PR (28). Another patient was treated with six times pemetrexed + carboplatin, and tumor evaluation was SD (29). Based on the above exploration of chemotherapy, this study case was treated with pemetrexed and carboplatin, and the fourth cycle of chemotherapy has been completed. Immunotherapy is a breakthrough in tumor therapy in recent years, and its efficacy has been confirmed in various tumors. Studies have shown that PD-1 is highly expressed in PEAC, and compared with ordinary lung adenocarcinomas, non-synonymous tumor mutational burden (TMB) is significantly higher in patients with PEAC, indicating that patients with PEAC may benefit from immune checkpoint inhibitors (10). Therefore, it is very important to determine whether PEAC patients may benefit from immunotherapy. After informing the benefits and possible side effects of immunotherapy, the patient agreed to PP chemotherapy combined with penpulimab immunotherapy (30). The lung-enhanced CT scan showed that the tumor shrank after four cycles of chemotherapy combined with immunotherapy. At the time of drafting the present article, the patient is still alive and about to undergo the next cycle of treatment.

In conclusion, the present study reports the first case of PEAC with a rare EGFR exon 19 missense mutation (c.2257C>T, p.P753S), KRAS exon 2 missense mutation (c.35G>T, p.G12V), and TP53 exon 5 missense mutation (c.401T>C, p.F134S). Immunohistochemical targets and gene mutations observed in this patient may be helpful in the diagnosis, treatment, and prognosis of patients with PEAC. Furthermore, the combination of chemotherapy and immunotherapy seems to be an effective therapy for PEAC. Whether the use of immunotherapy can provide clinical benefits needs to be further explored with more samples in future studies.

Data availability statement

The datasets for this article are not publicly available due to concerns regarding participant/patient anonymity. Requests to access the datasets should be directed to the corresponding author.

Ethics statement

The studies involving human participants were reviewed and approved by the Clinical Trial Ethics Committee of Tongji Hospital, Tongji Medical College, Huazhong University of Science and Technology, Wuhan, China. The patients/participants provided their written informed consent to participate in this study. Written informed consent was obtained from the individual(s) for the publication of any potentially identifiable images or data included in this article.

Author contributions

QW designed the idea. DC performed the pathological imaging. XXH and XW collected the data and wrote the manuscript. All authors read and approved to submit the report for publication.

Funding

This work was supported by the 6th Young Talent Lifting Project of China Association For Science and Technology (No.YESS20200255).

Acknowledgments

The authors would like to thank the patient and obtain the written informed consent provided by the patient for publishing the report.

Conflict of interest

The authors declare that the research was conducted in the absence of any commercial or financial relationships that could be construed as a potential conflict of interest.

Publisher's note

References

1. Travis WD, Brambilla E, Noguchi M, Nicholson AG, Geisinger KR, Yatabe Y, et al. International association for the study of lung cancer/American thoracic society/european respiratory society international multidisciplinary classification of lung adenocarcinoma. *J Thorac Oncol* (2011) 6(2):244–85. doi: 10.1097/JTO.0b013e318206a221

2. Inamura K, Satoh Y, Okumura S, Nakagawa K, Tsuchiya E, Fukayama M, et al. Pulmonary adenocarcinomas with enteric differentiation: histologic and immunohistochemical characteristics compared with metastatic colorectal cancers and usual pulmonary adenocarcinomas. *Am J Surg Pathol* (2005) 29 (5):660–5. doi: 10.1097/01.pas.0000160438.00652.8b

3. Tsao MS, Fraser RS. Primary pulmonary adenocarcinoma with enteric differentiation. *Cancer.* (1991) 68(8):1754–7. doi: 10.1002/1097-0142(19911015)68:8<1754::AID-CNCR2820680818>3.0.CO;2-E

4. Travis WD, Brambilla E, Burke AP, Marx A, Nicholson AG. Introduction to the 2015 world health organization classification of tumors of the lung, pleura, thymus, and heart. *J Thorac Oncol* (2015) 10(9):1240–2. doi: 10.1097/JTO.0000000000000663

5. Palmirotta R, Lovero D, D'Oronzo S, Todisco A, Internò V, Mele F, et al. Pulmonary enteric adenocarcinoma: an overview. *Expert Rev Mol Med* (2020) 22: e1. doi: 10.1017/erm.2020.2

6. Todisco A, Internò V, Stucci LS, Ostuni C, Lovero D, D'Oronzo S, et al. Cutaneous metastasis as a primary presentation of a pulmonary enteric adenocarcinoma. *Int J Biol Markers* (2019) 34(4):421–6. doi: 10.1177/1724600819877190

7. Bian T, Zhao J, Feng J, Zhang Q, Qian L, Liu J, et al. Combination of cadherin-17 and SATB homeobox 2 serves as potential optimal makers for the differential diagnosis of pulmonary enteric adenocarcinoma and metastatic colorectal adenocarcinoma. *Oncotarget.* (2017) 8(38):63442–52. doi: 10.18632/oncotarget.18828

8. Zhao L, Huang S, Liu J, Zhao J, Li Q, Wang HQ. Clinicopathological, radiographic, and oncogenic features of primary pulmonary enteric adenocarcinoma in comparison with invasive adenocarcinoma in resection specimens. *Med (Baltimore)* (2017) 96(39):e8153. doi: 10.1097/MD.0000000000008153

9. Li H, Cao W. Pulmonary enteric adenocarcinoma: a literature review. *J Thorac Dis* (2020) 12(6):3217–26. doi: 10.21037/jtd-19-4171

10. Chen M, Liu P, Yan F, Xu S, Jiang Q, Pan J, et al. Distinctive features of immunostaining and mutational load in primary pulmonary enteric adenocarcinoma: implications for differential diagnosis and immunotherapy. *J Transl Med* (2018) 16(1):81. doi: 10.1186/s12967-018-1449-z

11. Zuo Y, Bai H, Ying JM, Wang J. Progress in pulmonary enteric adenocarcinoma. *Zhonghua Zhong Liu Za Zhi* (2022) 44(4):321–5. doi: 10.3760/cma.j.cn112152-20200818-00753

12. Nottegar A, Tabbò F, Luchini C, Brunelli M, Bria E, Veronese N, et al. Pulmonary adenocarcinoma with enteric differentiation: Immunohistochemistry and molecular morphology. *Appl Immunohistochem Mol Morphol* (2018) 26 (6):383–7. doi: 10.1097/PAI.0000000000000440

13. Matsushima J, Yazawa T, Suzuki M, Takahashi Y, Ota S, Nakajima T, et al. Clinicopathological, immunohistochemical, and mutational analyses of pulmonary enteric adenocarcinoma: usefulness of SATB2 and β-catenin immunostaining for differentiation from metastatic colorectal carcinoma. *Hum Pathol* (2017) 64:179–85. doi: 10.1016/j.humpath.2017.04.006

14. Xie M, Chen D, Li Y, Liu X, Kuang D, Li X. Genetic mutation profiles and immune microenvironment analysis of pulmonary enteric adenocarcinoma. *Diagn Pathol* (2022) 17(1):30. doi: 10.1186/s13000-022-01206-7

15. Jurmeister P, Schöler A, Arnold A, Klauschen F, Lenze D, Hummel M, et al. DNA Methylation profiling reliably distinguishes pulmonary enteric adenocarcinoma from metastatic colorectal cancer. *Mod Pathol* (2019) 32 (6):855–65. doi: 10.1038/s41379-019-0207-y

16. Zhang J, Xiang C, Han Y, Teng H, Li X, Shao J, et al. Differential diagnosis of pulmonary enteric adenocarcinoma and metastatic colorectal carcinoma with the assistance of next-generation sequencing and immunohistochemistry. *J Cancer Res Clin Oncol* (2019) 145(1):269–79. doi: 10.1007/s00432-018-2788-0

17. Ganesan P, Ali SM, Wang K, Blumenschein GR, Esmaeli B, Wolff RA, et al. Epidermal growth factor receptor P753S mutation in cutaneous squamous cell carcinoma responsive to cetuximab-based therapy. *J Clin Oncol* (2016) 34(5):e34–7. doi: 10.1200/JCO.2013.50.3516

18. Ullas B, Shrinidhi N, Mansi S, Narayan S, Parveen J, Surender D, et al. All EGFR mutations are (not) created equal: focus on uncommon EGFR mutations. *J Cancer Res Clin Oncol* (2022). doi: 10.1007/s00432-022-04033-x

19. Prelaj A, Bottiglieri A, Bhat G, Washington R, Calareso G, Greco GF, et al. Case report: Exceptional response to poziotinib in patient with metastatic non-small cell lung cancer with EGFR exon 20 insertion mutation. *Front Oncol* (2022) 12:902967. doi: 10.3389/fonc.2022.902967

20. Mehta A, Vasudevan S. Rare epidermal growth factor receptor gene alterations in non-small cell lung cancer patients, tyrosine kinase inhibitor response and outcome analysis. *Cancer Treat Res Commun* (2021) 28:100398. doi: 10.1016/j.ctarc.2021.100398

21. Ludovini V, Ricciuti B, Tofanetti FR, Mencaroni C, Giannarelli D, Sidoni A, et al. *KRAS* mutation and DNA repair and synthesis genes in non-small-cell lung cancer. *Mol Clin Oncol* (2018) 9(6):689–96. doi: 10.3892/mco.2018.1731

22. Pan W, Yang Y, Zhu H, Zhang Y, Zhou R, Sun X. KRAS mutation is a weak, but valid predictor for poor prognosis and treatment outcomes in NSCLC: A meta-analysis of 41 studies. *Oncotarget.* (2016) 7(7):8373–88. doi: 10.18632/oncotarget.7080

23. Hainaut P, Hollstein M. p53 and human cancer: the first ten thousand mutations. *Adv Cancer Res* (2000) 77:81–137. doi: 10.1016/S0065-230X(08)60785-X

24. Liu Y, Tavana O, Gu W. p53 modifications: exquisite decorations of the powerful guardian. *J Mol Cell Biol* (2019) 11(7):564–77. doi: 10.1093/jmcb/mjz060

25. Baugh EH, Ke H, Levine AJ, Bonneau RA, Chan CS. Why are there hotspot mutations in the TP53 gene in human cancers? *Cell Death Differ* (2018) 25(1):154–60. doi: 10.1038/cdd.2017.180

26. Canale M, Petracci E, Delmonte A, Chiadini E, Dazzi C, Papi M, et al. Impact of *TP53* mutations on outcome in *EGFR*-mutated patients treated with first-line tyrosine kinase inhibitors. *Clin Cancer Res* (2017) 23(9):2195–202. doi: 10.1158/1078-0432.CCR-16-0966

27. Hong S, Gao F, Fu S, Wang Y, Fang W, Huang Y, et al. Concomitant genetic alterations with response to treatment and epidermal growth factor receptor tyrosine kinase inhibitors in patients with EGFR-mutant advanced non-small cell lung cancer. *JAMA Oncol* (2018) 4(5):739–42. doi: 10.1001/jamaoncol.2018.0049

28. Qureshi A, Furrukh M. Enteric adenocarcinoma lung: a rare presentation in an omani woman. *BMJ Case Rep* (2013) 2013:bcr2012007667. doi: 10.1136/bcr-2012-007667

29. Li HC, Schmidt L, Greenson JK, Chang AC, Myers JL. Primary pulmonary adenocarcinoma with intestinal differentiation mimicking metastatic colorectal carcinoma: case report and review of literature. *Am J Clin Pathol* (2009) 131 (1):129–33. doi: 10.1309/AJCPB04XWICTFERL

30. Han C, Ye S, Hu C, Shen L, Qin Q, Bai Y, et al. Clinical activity and safety of penpulimab (Anti-PD-1) with anlotinib as first-line therapy for unresectable hepatocellular carcinoma: An open-label, multicenter, phase Ib/II trial (AK105-203). *Front Oncol* (2021) 11:684867. doi: 10.3389/fonc.2021.684867

10.3389/fonc.2022.988625

Glossary

PEAC	Pulmonary enteric adenocarcinoma
NSCLC	Non–small cell lung cancer
EGFR	Epidermal growth factor receptor
KRAS	Kirsten rat sarcoma viral oncogene
TP53	Tumor protein p53
CT	Computer Tomography
FNA	Fine-needle aspiration
CK7	Cytokeratin-7
CDX2	Caudal-type homeobox 2
C-MET	Mesenchymal-epithelial transition factor
NGS	Next-generation sequencing
WHO	World Health Organization
CD10	Lymphocyte antigen 10
ROS1	Receptor tyrosine kinase
TTF-1	Thyroid transcription factor-1
ALK	Anaplastic lymphoma kinase
SATB2	Special AT-rich sequence binding protein 2
MUC2	Mucin 2
MUC6	Mucin 6
MUC5AC	Mucin 5AC
PAX8	Paired Box 8
GATA3	GATA binding protein 3
PSA	Prostate-specific antigen
NKX3.1	NK3 homeobox 1
CK20	Cytokeratin-20
CYFRA21-1	Cytokeratin-19 fragment antigen21-1
CA19-9	Carbohydrate antigen 19-9
ECT	Emission Computed Tomography
TPS	Tumor proportion score
PD-L1	Programmed death ligand 1
CA12-5	Carbohydrate antigen 12-5
TKIs	Tyrosine kinase inhibitors
PR	Partial response
SD	Stable disease
PFS	Progression-free survival
OS	Overall survival

frontiers | Frontiers in Oncology

TYPE Original Research
PUBLISHED 29 September 2022
DOI 10.3389/fonc.2022.1002155

OPEN ACCESS

EDITED BY
Kohei Fujita,
National Hospital Organization Kyoto Medical Center, Japan

REVIEWED BY
Qingjun Pan,
Affiliated Hospital of Guangdong Medical University, China
Liqiang Meng,
First Hospital, Peking University, China

*CORRESPONDENCE
Wenge Li
wenge_lee2002@126.com

SPECIALTY SECTION
This article was submitted to Thoracic Oncology, a section of the journal Frontiers in Oncology

RECEIVED 24 July 2022
ACCEPTED 13 September 2022
PUBLISHED 29 September 2022

CITATION
Xu Q, Zou G, Zhuo L, Gao H and Li W (2022) Lung cancer patients with nephropathy as the first manifestation: Literature review and clinical study report.
Front. Oncol. 12:1002155.
doi: 10.3389/fonc.2022.1002155

Lung cancer patients with nephropathy as the first manifestation: Literature review and clinical study report

Qianqian Xu, Guming Zou, Li Zhuo, Hongmei Gao and Wenge Li*

Department of Nephrology, China-Japan Friendship Hospital, Beijing, China

Background: To investigate the relationship between membranous nephropathy (MN) and lung cancer.

Methods: To report patients with lung cancer detected by follow-up after the diagnosis of MN by renal biopsy in China-Japan Friendship Hospital from January 2010 to December 2019, and to study the prognosis of lung cancer-associated MN and have a review of the literature.

Results: Lung cancer was detected in six patients followed for 1–27 months (median 8 months) after the diagnosis of MN: including four cases of lung adenocarcinoma, one case of carcinoma *in situ*, and one case of small cell lung cancer with multiple metastases. Five cases were in remission after surgical resection, and one case was remitted after chemotherapy. Six patients were negative for serum anti-PLA2R antibodies, and glomerular IgG subclass deposition detected by immunofluorescence was positive for IgG1 and IgG2. Glomerular PLA2R, THSD7A, and NELL-1 stainings were assessed in all six patients; one patient was positive for glomerular PLA2R staining, two patients were positive for glomerular THSD7A staining, and all patients were negative for NELL-1 staining. A literature review of the relationship between MN and lung cancer was performed: seven articles about cancer-associated MN were searched, reporting 32 cases of MN associated with lung cancer, among which 14 cases had nephropathy as the first manifestation and only five patients had remission of MN after treatment of lung cancer.

Conclusions: A few lung cancer patients have nephropathy as the first clinical manifestation, and MN can also be remitted after treatment of lung cancer.

KEYWORDS

lung cancer, membranous nephropathy, anti-phospholipase A2 receptor antibody, thrombospondin type-1 domain-containing 7A, NELL-1

Introduction

Membranous nephropathy (MN) is a common pathological type leading to nephrotic syndrome (NS) in adults, accounting for 9.83% to 30% of primary glomerulonephritis (1, 2). MN is a pathologic entity characterized by the formation of immune complexes under the epithelial cells and diffuse thickening of the glomerular basement membrane observed by light microscopy (3). However, 75% of MN cases are idiopathic, whereas the remainder are associated with infections, malignancies, autoimmune diseases, and drug toxicity (4).

In recent years, there have been more reports of malignancy-associated MN. In this paper, we summarized and analyzed the literature of cancer-associated MN in the past 20 years and searched seven domestic and foreign articles, totaling 113 patients with cancer-associated MN. Lung cancer was the most common type of tumor, accounting for 32 cases (28.3%), and among them, nephropathy was the first manifestation in 14 cases (12.4%). We also reported six cases of lung cancer patients who were followed up after the diagnosis of MN by kidney biopsy in China-Japan Friendship Hospital from January 2010 to December 2019 and analyzed their clinical characteristics and prognosis to explore the relationship between lung cancer and MN.

Materials and methods

Data sources and searches

We searched literature about cancer-associated MN in the past 20 years, and a total of seven articles were selected to summarize the relationship between lung cancer and MN. We also reported the clinical data and pathological characteristics of patients who were followed up and found to have lung cancer after diagnosis of MN by renal biopsy in China-Japan Friendship Hospital from January 2010 to December 2019.

This study was approved by the Ethics Committee of China-Japan Friendship Hospital (approval number: 2019-17-K12).

Patient selection

The inclusion criteria for patients with lung cancer-associated MN were as follows: (1) renal histological and immunopathological changes consistent with secondary membranous nephropathy (SMN) (5); (2) lung cancer was detected at the same time or within several years after the diagnosis of MN, and MN was in remission after treatment of lung cancer, or MN recurred when lung cancer recurred; (3) secondary causes such as systemic lupus erythematosus, hepatitis B, and hepatitis C infection were excluded, as well as no use of non-steroidal anti-inflammatory drugs, gold agents, penicillamine, and other drugs and no history of exposure to organic solvents and mercury.

Clinical and biological data

Patients with lung cancer-associated MN were counted for the following aspects of clinical data: (1) age, gender ratio, 24-h urine protein quantification, serum albumin, blood creatinine, eGFR, and anti-PLA2R antibodies; (2) the main clinical manifestations of the patients, time of diagnosis of MN and lung cancer; (3) type and treatment of lung cancer, the prognosis of lung cancer, and remission of MN after treatment of lung cancer.

The estimated glomerular filtration rate (eGFR) was estimated using the EPI formula (6).

Analysis of renal biopsies

Percutaneous renal puncture was performed, and kidney tissue specimens were obtained in three parts in all cases for light microscopy, immunofluorescence, and electron microscopy. (1) Light microscopy: light microscopic specimens all contained more than 10 glomeruli, were paraffin-embedded, sectioned 2 μm thick, and stained with HE, PAS, PASM, and MASSON, respectively. (2) Immunofluorescence: Frozen sections were used to detect IgG, IgA, IgM, C3, C1q, FRA, and IgG subclasses (IgG1, IgG2, IgG3, and IgG4) by direct immunofluorescence. (3) Electron microscopy: All kidney biopsy specimens were sent to the electron microscopy laboratory of China-Japan Friendship Hospital for examination. Renal pathological typing and diagnosis were referred to our pathological standards for renal biopsies.

Study reagents

Serum anti-PLA2R antibody assay: Patients after August 2016 were tested using the human anti-phospholipase A2 receptor antibody enzyme immunoassay kit (Shanghai Lianshuo Biological), and each step was performed according to the instructions, and finally the expression of serum anti-PLA2R to be tested was calculated according to the standard curve. Serum anti-PLA2R antibody ≥20 IU/ml was considered positive.

Paraffin-embedded sections of formalin-fixed renal tissue were utilized for immunohistochemistry (IHC) using rabbit polyclonal anti-PLA2R (1:500; Sigma-Aldrich, Germany), rabbit polyclonal anti-THSD7A (1:400; Sigma-Aldrich), and rabbit polyclonal anti–NELL-1 antibody (1:800; Sigma-Aldrich) as the primary antibodies. The glomerular expressions of PLA2R, THSD7A, and NELL-1 were detected according to the same protocol as reported previously.

Results

Literature review

We searched and summarized the literature on cancer-associated MN from 2000 to the present, and seven domestic and foreign articles were selected (7–13), totaling 113 patients, and the most common tumor was lung cancer in 32 cases (28.3%). Among the lung cancer patients, 14 cases (12.4%) had nephropathy as the first manifestation; a summary of the literature on cancer-associated MN is shown in Table 1. Among them, 12 patients with detailed information of the type of lung cancer, treatment and prognosis of lung cancer, and remission of MN are shown in Table 2.

As seen in Table 2, all patients with lung cancer-associated MN had pathology characterized by secondary membranous nephropathy, and only two patients were positive for serum anti-PLA2R antibody. Six patients with unremitting lung cancer had unremitting MN as well, one relapsed, and five patients had remission of MN after treatment and remission of lung cancer. However, the specifics of remission of MN after lung cancer treatment were not documented in these patients.

Clinical manifestations of lung cancer patients with nephropathy as the first manifestation in our center

In the follow-up of our center, we found that the pathology of six lung cancer patients with nephropathy as the first manifestation was secondary MN, and the patients were found to have lung cancer at 1–27 months (median 8 months) after the diagnosis of MN. Among them, there were three men and 3 women, the age of onset was 47–70 years, and the median age was 63 years. The histology of lung cancer included four cases of adenocarcinoma, one case of carcinoma *in situ*, and one case of small cell lung cancer with multiple metastases. Case 1 was found to have an occupying lesion in the lower left lung by chest CT without respiratory symptoms 27 months after diagnosis of MN. Adenocarcinoma was diagnosed through puncture pathology, and surgery was performed. Case 2 developed edema of both lower extremities without obvious incentives; chest CT was performed, and pulmonary nodules were found at the same time of diagnosis of MN. One month later, puncture pathology showed adenocarcinoma of the right lower lobe of the lung, and surgery was performed. Case 3 was mainly manifested with edema of both lower extremities and had no respiratory symptoms. One month after the diagnosis of MN, a mass in the lower lobe of the left lung was found during chest CT examination. The puncture pathology showed adenocarcinoma, and surgery was performed. Case 4 was found to have an occupying lesion in the left lower lobe of the lung 7 months after diagnosis of MN without respiratory symptoms. The puncture pathology showed adenocarcinoma of the lung, and surgery was performed. Case 5 was admitted to the hospital with increased foamy urine and was found to have a right lower lung nodule by chest CT 9 months after the diagnosis of MN, and the pathology showed carcinoma *in situ*, which was treated surgically. Case 6 was admitted to the hospital due to edema of both lower extremities, and after 13 months of diagnosis of MN, he consulted the respiratory department due to "cough and hemoptysis for 2 months". Chest CT showed central lung cancer in the upper lobe of the left lung with pulmonary atelectasis and puncture pathology, and PET-CT showed small cell lung cancer with multiple metastases, which were inoperable and treated with chemotherapy. The detailed information of the six patients are shown in Table 3.

TABLE 1 Summary of the literature on lung cancer-associated MN.

	Li et al. (7)	Bjørneklett et al. (8)	Qu et al. (9)	Zhang et al. (10)	Ohtani et al. (11)	Lönnbro-Widgren et al. (12)	Lefaucheur et al. (13)	Total
Follow-up period	2005-2008	1988-2003	1997-2009	2001-2017	1985-2002	2000-2012	1994-2001	
Mean age, years	53.6 ± 6.7	65 ± 11	64.4 ± 8.7	63.4 ± 7.9	64 (54, 80)	68 ± 10	73 (65, 78)	
Total number, n	10	33	8	12	10	16	24	113
Patients with lung cancer, n (%)	5 (50)	6 (18.2)	3 (37.5)	5 (41.7)	2 (20)	3 (18.7)	8 (33.3)	32 (28.3)
Diagnosed with cancer before the diagnosis of MN, n (%)	1 (10)	NA	3 (37.5)	0	0	0	NA	4 (3.5)
Diagnosed with cancer at the same time or following the diagnosis of MN, n (%)	4 (40)	NA	0	5 (41.7)	2 (20)	3 (18.7)	NA	14 (12.4)
Remission of MN after treatment of lung cancer, n (%)	1 (10)	NA	NA	2 (16.7)	0	1 (6.2)	4 (16.7)	8 (7.1)
Number of deaths during lung cancer follow-up, n (%)	1 (10)	NA	NA	2 (16.7)	2(20)	2 (12.5)	NA	7 (6.2)

NA, Not available.

TABLE 2 Review of the literature on lung cancer patients with nephropathy as the first manifestation.

Case no.	Pathology and markers of MN			Histology of lung cancer	Treatment of lung cancer		Remission of lung cancer	Remission of MN
	Pathological type	Glomerular PLA2R	PLA2R-Ab (RU/ml)		S	C/R		
1 (7)	Secondary MN	NA	+	Squamous cell carcinoma	S	C	Relapse	NR
2 (7)	Secondary MN	NA	–	Adenocarcinoma		C	No	NR
3 (7)	Secondary MN	NA	–	Squamous cell carcinoma	S	C	Yes	CR
4 (7)	Secondary MN	NA	–	Squamous cell carcinoma		C	No	NR
5 (10)	Secondary MN	–	–	Adenocarcinoma	S		Yes	PR
6 (10)	Secondary MN	–	–	Adenocarcinoma	S	C	No	NR
7 (10)	Secondary MN	–	–	Carcinoma *in situ*	S		Yes	CR
8 (10)	Secondary MN	–	–	Squamous cell carcinoma	S	C	No	NR
9 (10)	Secondary MN	+	+	Carcinoma *in situ*	S		Yes	PR
10 (12)	Secondary MN	–	NA	Lung cancer	S	R	No	NR
11 (12)	Secondary MN	–	NA	Lung cancer	No		No	NR
12 (12)	Secondary MN	–	NA	Lung cancer	S		Yes	CR

R, radiotherapy; S, surgery; C, chemotherapy; CR, complete remission; NR, no remission; PR, partial remission; NA, Not available.

All six patients had "bilateral lower limb edema" as the main manifestation, and five patients had massive proteinuria, showing nephrotic syndrome. One patient had mildly elevated blood creatinine at the beginning of the disease, and serum anti-PLA2R antibody was negative in six patients.

Renal pathology

Light microscopy

Glomerular basement membrane thickening, mild mesangial cell hyperplasia, and mesangial matrix increases were seen in all patients under light microscope, and no glomerular segmental loop necrosis, crescent, and other lesions were found. Two patients had mild interstitial fibrosis, and one had ischemic injury.

Electron microscopy

All patients had electron-dense deposits on the epithelial side, four patients had a small amount of electron dense deposition in the mesangial area, and two patients had a small amount of electron dense deposition in the subendothelial area.

Immunofluorescence

Five patients showed full bright features (IgG, IgM, IgA, C3, C1q, and FRA were deposited), and one patient had IgG, IgM, C3, and FRA deposited. Glomerular IgG subclass deposition was detected by immunofluorescence: six patients were positive for IgG1 and IgG2, only one case was positive for IgG3, and three cases were positive for IgG4 (Table 4).

Immunohistochemistry

Glomerular PLA2R, THSD7A, and NELL-1 staining was performed on formalin-fixed, paraffin-embedded (FFPE) sections using immunohistochemistry (IHC) procedure as previously described. Subepithelial granular pattern staining was considered positive, while faintly appreciable staining of the tubular brush border and along the capillary walls was considered negative (shown in Figure 1).

Treatment and prognosis

Six patients were found to have lung cancer 27, 1, 1, 7, 9, and 13 months after the diagnosis of MN. All patients had remission of MN after surgical resection of tumor or chemotherapy, and there was no significant change in renal function before and after treatment. The manifestations of MN before and after lung cancer treatment are shown in Table 5.

Discussion

Since Lee et al. (14) first proposed the existence of a relationship between NS and malignancy in 1996, the relationship between nephropathy and malignancy has been widely concerned by clinicians. In clinical practice, cancer-associated nephropathy is on the rise, mostly with proteinuria or NS as the main first symptom (8). The malignant tumors that cause kidney disease are mainly divided into two categories: solid tumors and non-solid tumors. Solid tumors include lung cancer,

10.3389/fonc.2022.1002155

TABLE 3 Clinical and pathological features of lung cancer patients with nephropathy as the first manifestation.

Case no.	Pathology and markers of MN					Histology of lung cancer	Treatment of lung cancer		Remission of lung cancer	Remission of MN
	Pathological type	PLA2R-Ab (RU/ml)	Glomerular PLA2R	Glomerular NELL-1	Glomerular THSD7A		S	C/R		
1	Secondary MN	–	–	–	–	Infiltrative adenocarcinoma	S		Yes	CR
2	Secondary MN	–	–	–	–	Infiltrative adenocarcinoma	S	C	Yes	CR
3	Secondary MN	–	–	–	–	Infiltrative adenocarcinoma	S		Yes	PR
4	Secondary MN	–	–	–	–	Mucinous adenocarcinoma	S		Yes	CR
5	Secondary MN	–	+	–	+	Carcinoma *in situ*	S		Yes	CR
6	Secondary MN	–	–	–	+	Small cell lung cancer with multiple metastases		C	Yes	CR

R, radiotherapy; S, surgery; C, chemotherapy; CR, complete remission; NR, no remission; PR, partial remission.

colon cancer, and renal cell carcinoma. Non-solid tumors include non-Hodgkin's lymphoma and multiple myeloma. Among them, MN is more closely related to solid tumors. Clinically, the pathological types of cancer-associated nephropathy are not typical and the pathogenesis is not clear.

Napat et al. (15) performed a meta-analysis on the incidence and characteristics of cancer and MN and showed that the incidence of cancer-associated MN was around 10% and the mean age of cancer in patients with MN was (67 ± 7) years, with lung cancer being the most common, followed by gastric, intestinal, prostate, and breast cancers. We summarized all the seven articles on "cancer-associated MN" from 2000 to the present: there were 113 patients, 78 men, and the most common was lung cancer in 32 cases (18 adenocarcinoma, 12 squamous cell carcinoma, and 2 *in situ* carcinoma), accounting for 28.3%. Among them, 14 cases (12.4%) had nephropathy as the first manifestation. Six patients with unremitting lung cancer had unremitting MN as well, one relapsed, and five patients had remission of MN after treatment and remission of lung cancer.

Our follow-up analysis of six cases of lung cancer patients with nephropathy as the first manifestation found in China-Japan Friendship Hospital in the past 10 years revealed that the median age was 63 years, NS was the main manifestation, and all renal pathology showed features of secondary MN, with clinical exclusion of MN due to secondary causes such as hepatitis B, hepatitis C infection, and SLE. Among them, there were four cases of lung adenocarcinoma, one case of carcinoma *in situ*, and one case of small cell lung cancer with multiple metastases. Moreover, most of these patients had bilateral lower limb edema as the main manifestation at the time of discovery of MN, without clinical manifestations related to lung cancer and elevated specific tumor markers. Therefore, for elderly patients with MN, we cannot rely solely on clinical manifestations and positive tumor markers to rank for the presence of cancer, and routine chest CT is required to screen for lung cancer if necessary. During the follow-up of elderly patients with MN, it is necessary to pay close attention to the changes of the disease, and for patients who are not in remission with conventional treatment, regular systemic examinations should be performed to exclude the presence of tumors.

In the present study, the pathological manifestation of lung cancer-associated MN was mainly characterized by secondary MN, consistent with previous reports (9). Further analysis of IgG subclass in the renal tissue in our patients revealed that IgG subclasses were predominantly IgG1 and IgG2 deposition. It has been shown that IgG4 deficiency and IgG1 and IgG2 deposition in renal biopsy tissues are associated with malignancy-associated MN (11, 12). Ohtani et al.'s study also found that the glomerular IgG subclass deposition of cancer-associated MN was dominated by IgG1 and IgG2, which was different from the glomerular IgG4 deposition of IMN (11).

In 2009, Beck et al. (16) first detected M-type PLA2R antibodies in the blood circulation of patients with IMN, which are present in the serum of approximately 70%–80% of patients with IMN and are strongly associated with disease activity and prognosis (17–19), facilitating the differential diagnosis of IMN and SMN. In our literature review, only one patient was positive for the anti-PLA2R antibody, while the six patients we followed up were all negative for serum anti-PLA2R antibodies. Therefore, MN patients with a negative anti-PLA2R antibody need to be alert for the development of malignancy (20).

In recent years, a novel autoantigen of MN, THSD7A (platelet-reactive protein type 1 domain 7A), has also been identified, which accounts for 2%–3% of the prevalence of MN in adults and is the second autoantibody in MN (21). THSD7A is

10.3389/fonc.2022.1002155

TABLE 4 Pathological and immunofluorescent features of lung cancer patients with nephropathy as the first manifestation.

Case no.	Mesangial proliferation	IgG	IgM	IgA	C3	C1q	IgG1	IgG2	IgG3	IgG4
1	1+	3+	2+	2+	2+	2+	3+	2+	0	0
2	2+	3+	2+	2+	3+	2+	3+	2+	0	2+
3	3+	4+	1+	2+	2+	2+	3+	2+	0	2+
4	2+	3+	2+	2+	2+	2+	3+	2+	0	3+
5	1+	2+	1+	0	3+	0	2+	1+	1+	0
6	2+	3+	2+	2+	2+	2+	3+	2+	0	0

detected in approximately 10% of PLA2R-negative patients, and THSD7A-associated MN is associated with the development of malignancies. It has been shown that the positivity rate of THSD7A in malignant tumors is 15%–20% (22), and the messenger RNA of THSD7A was detected in some tumor tissues (gallbladder cancer) and THSD7A protein was detected in dendritic cells of tumor-infiltrating lymph node germinal centers (23, 24). One case with lung squamous cell cancer had positive THSD7A staining in both glomeruli and cancer cells. Additionally, remission of MN was observed after surgical resection of lung cancer, supporting a mechanistic role for THSD7A in the association between cancer and MN (25). In our study, two of the six patients had positive THSD7A staining in renal tissue, and one of them had double-positive staining for PLA2R and THSD7A, suggesting that patients with positive THSD7A staining were more likely to develop tumors. In other studies, THSD7A is differentially expressed in different solid tumors, including lung, breast, kidney, and colorectal cancers, which are of value for the prognosis of the disease (26). Therefore, the detection of THSD7A provides some clues for the identification of cancer-associated nephropathy.

Autoantibodies to the neural epidermal growth factor-like 1 (NELL-1) are a recent addition to the MN disease spectrum and may be more prevalent than anti-THSD7A antibodies (27). NELL-1-associated MN was identified in approximately 16% of PLA2R-negative MN cases, representing an approximate 2.5% prevalence across the entire spectrum of MN (28). There are some reports of a connection between NELL-1-associated MN and malignancy, while NELL-1 staining in renal tissue was negative in all of our six cases, so more research is needed to explore the relationship between NELL-1 and malignancy.

Previous studies have found that the remission of cancer-associated nephropathy is closely related to the effectiveness of treatment of the tumor. Lefaucheur et al. (13) reported 24 cases of cancer-associated MN, and six of 12 patients with tumor remission achieved NS remission, none of the 12 patients whose tumors did not resolve had NS remission. In this study, six patients with lung cancer had remission of MN with resection of

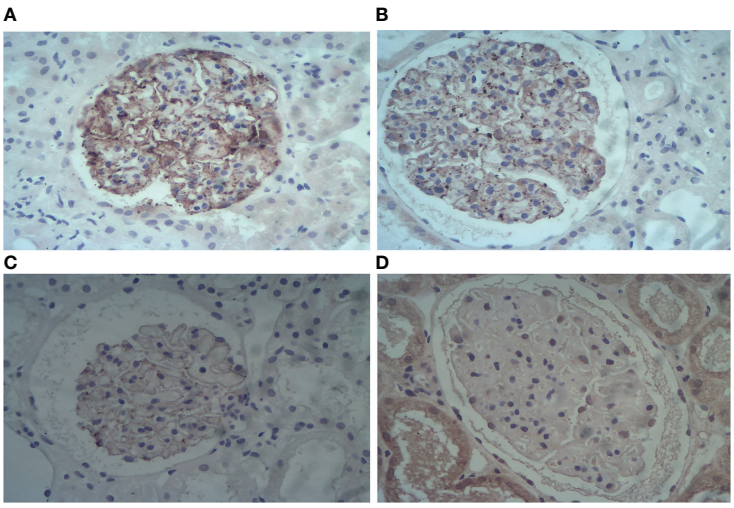

FIGURE 1
Representative images of positive glomerular PLA2R staining in case 5 **(A)** and positive THSD7A staining in case 5 **(B)** and case 6 **(C)** as determined by immunohistochemistry. Negative glomerular NELL-1 staining in case 2 **(D)**. (Immunohistochemistry staining, magnification ×400).

TABLE 5 Prognosis of lung cancer patients with nephropathy as the first manifestation.

Case no.	Gender	Age	Time from biopsy to identification of malignancy (months)	Manifestation of MN before lung cancer treatment			Manifestation of MN after lung cancer treatment		
				Proteinuria (g/day)	ALB (g/L)	Scr (μmol/L)	Proteinuria (g/day)	ALB (g/L)	Scr (μmol/L)
1	M	66	27	6.62	30.5	65.2	0.52	35.2	87.5
2	M	63	1	8.37	28.4	119.3	0.32	39.4	109.4
3	F	70	1	8.81	22.6	61.9	1.52	32.5	77.6
4	F	58	7	4.85	30.4	58.3	0.58	34.6	56.4
5	F	47	9	2.7	36.2	44.6	0.24	38.6	45.9
6	M	63	13	14.67	24.5	65.4	0.28	35.3	59.1

tumor lesions and systemic chemotherapy. The above cases further illustrate that whether malignancy-associated MN can be remitted is related to the stage of tumor development and the thoroughness of treatment. If the malignant tumor is detected early and has no metastasis and is surgically removed, NS may be in complete remission. NS cannot be relieved in most cases if the tumor lesions are not resected or have metastasized. However, NS may still be relieved by effective radiotherapy and/or chemotherapy.

Conclusions

In summary, cancer-associated MN is most common in lung cancer, and some patients with lung cancer have nephropathy as the first manifestation without lung cancer-related clinical symptoms and elevated specific tumor markers. For elderly patients with MN, especially those with negative anti-PLA2R antibodies and positive THSD7A staining by immunohistochemistry or anti-THSD7A antibodies, follow-up observation should be strengthened to be alert for tumorigenic lesions. The mechanisms involved in the etiology of MN and cancer need further study.

Data availability statement

The original contributions presented in the study are included in the article/supplementary material. Further inquiries can be directed to the corresponding author.

Ethics statement

The studies involving human participants were reviewed and approved by Ethics Committee of China-Japan Friendship Hospital (approval number: 2019-17-K12). The patients/participants provided their written informed consent to participate in this study.

Author contributions

QX and WL conceptualized and designed this retrospective study. QX performed most of the statistical analyses and wrote the draft manuscript. GZ, LZ, and HG assisted with the renal pathology sectioning and staining. All authors read and approved the final manuscript.

Funding

This work was supported by college-level projects in China-Japan Friendship Hospital (2017-2-QN-19).

Acknowledgments

This work was supported by grants from college-level projects in China-Japan Friendship Hospital, and we thank GZ and HG for renal pathology sectioning and staining.

Conflict of interest

The authors declare that the research was conducted in the absence of any commercial or financial relationships that could be construed as a potential conflict of interest.

Publisher's note

References

1. Wu YQ, Wang Z, Xu HF, Jin XM, Zhou HZ. Frequency of primary glomerular disease in northeastern China. *Braz J Med Biol Res* (2011) 44(8):810–3. doi: 10.1590/s0100-879x2011007500089

2. Li LS, Liu ZH. Epidemiologic data of renal diseases from a single unit in China: Analysis based on 13, 519 renal biopsies. *Kidney Int* (2004) 66(3):920–3. doi: 10.1111/j.1523-1755.2004.00837.x

3. Beck LH, Salant DJ. Membranous nephropathy: recent travels and new roads ahead. *Kidney Int* (2010) 77(9):765–70. doi: 10.1038/ki.2010.34

4. Ponticelli C, Glassock RJ. Glomerular diseases: membranous nephropathy-a modern view. *Clin J Am Soc Nephrol* (2014) 9(3):609–16. doi: 10.2215/CJN.04160413

5. Glassock RJ. Secondary membranous glomerulonephritis. *Nephrol Dial Transplant* (1992) 7(Suppl 1):64–71.

6. Stevens LA, Claybon MA, Schmid CH, Chen J, Horio M, Imai E, et al. Evaluation of the chronic kidney disease epidemiology collaboration equation for estimating the glomerular filtration rate in multiple ethnicities. *Kidney Int* (2011) 79(5):555–62. doi: 10.1038/ki.2010.462

7. Li SJ, Qin WS, Zhang MC, Zheng CX, Zuo K, Chen HP, et al. Tumor associated membranous nephropathy:analysis of anti-PLA2R autoantibodies and IgG subclass depositions on glomeruli. *J Nephrol Dialy Transplant* (2011) 20(1):12–7. doi: 10.3969/j.issn.1006-298X.2011.01.004

8. Bjørneklett R, Vikse BE, Svarstad E, Aasarød K, Bostad L, Langmark F, et al. Long-term risk of cancer in membranous nephropathy patients. *Am J Kidney Dis* (2007) 50(3):396–403. doi: 10.1053/j.ajkd.2007.06.003

9. Qu Z, Liu G, Li J, Wu LH, Tan Y, Zheng X, et al. Absence of glomerular IgG4 deposition in patients with membranous nephropathy may indicate malignancy. *Nephrol Dial Transplant* (2012) 27(5):1931–7. doi: 10.1093/ndt/gfr534

10. Zhang D, Zhang C, Bian F, Zhang WZ, Jiang GR, Zou J. Clinicopathological features in membranous nephropathy with cancer: A retrospective single-center study and literature review. *Int J Biol Markers* (2019) 34(4):406–13. doi: 10.1177/1724600819882698

11. Ohtani H, Wakui H, Komatsuda A, Okuyama S, Masai R, Maki N, et al. Distribution of glomerular IgG subclass deposits in malignancy-associated membranous nephropathy. *Nephrol Dial Transplant* (2004) 19(3):574– 9. doi: 10.1093/ndt/gfg616

12. Lönnbro-Widgren J, Ebefors K, Mölne J, Nyström J, Haraldsson B. Glomerular IgG subclasses in idiopathic and malignancy-associated membranous nephropathy. *Clin Kidney J* (2015) 8(4):433–9. doi: 10.1093/ckj/sfv049

13. Lefaucheur C, Stengel B, Nochy D, Martel P, Hill GS, Jacquot C, et al. Membranous nephropathy and cancer: Epidemiological evidence and determinants of high-risk cancer association.. *Kidney Int* (2006) 70(8):1510–7. doi: 10.1038/sj.ki.5001790

14. Lee JC, Yamauchi H, Hopper JJr. The association of cancer and the nephrotic syndrome. *Ann Intern Med* (1966) 64(1):41–51. doi: 10.7326/0003-4819-64-1-41

15. Leeaphorn N, KueA-Pai P, Thamcharoen N, Ungprasert P, Stokes MB, Knight EL. Prevalance of cancer in membranous nephropathy A systematic review and mete-analysis of observational studies. *Am J Nephrol* (2014) 40(1):29–35. doi: 10.1159/000364782

16. Beck LH, Bonegio RG, Lambeau G, Beck DM, Powell DW, Cummins TD, et al. M-type phospholipase A2 receptor as target antigen in idiopathic membranous nephropathy. *N Engl J Med* (2009) 361(1):11–21. doi: 10.1056/NEJMoa0810457

17. Dettmar AK, Wiech T, Kemper MJ, Soave A, Rink M, Oh J, et al. Immunohistochemical and serological characterization of membranous nephropathy in children and adolescents. *Pediatr Nephrol* (2018) 33(3):463–72. doi: 10.1007/s00467-017-3817-y

18. De Vriese AS, Glassock RJ, Nath KA, Sethi S, Fervenza FC. A proposal for a serology-based approach to membranous nephropathy. *J Am Soc Nephrol* (2017) 28(2):421–30. doi: 10.1681/ASN.2016070776

19. Kanda S, Horita S, Yanagihara T, Shimizu A, Hattori M. M-type phospholipase A2 receptor (PLA2R) glomerular staining in pediatric idiopathic membranous nephropathy. *Pediatr Nephrol* (2017) 32(4):713–7. doi: 10.1007/s00467-016-3552-9

20. Timmermans SA, Ayalon R, van Paassen P, Beck LHJr, van Rie H, Wirtz JM, et al. Anti-phospholipase A2 receptor antibodies and malignancy in membranous nephropathy. *Am J Kidney Dis* (2013) 62(6):1223–5. doi: 10.1053/j.ajkd.2013.07.019

21. Tomas NM, Beck LH, Meyer-Schwesinger C, Seitz-Polski B, Ma H, Zahner G, et al. Thrombospondin type-1 domain-containing 7A in idiopathic membranous nephropathy. *N Engl J Med* (2014) 371(24):2277–87. doi: 10.1056/nejmoa1409354

22. Ren S, Wu CW, Zhang Y, Wang AY, Li GS, Wang L, et al. An update on clinical significance of use of THSD7A in diagnosing idiopathic membranous nephropathy: A systematic review and meta-analysis of THSD7A in IMN. *Renal Failure* (2018) 40(1):306–13. doi: 10.1080/0886022X.2018.1456457

23. Hoxha E, Wiech T, Stahl PR, Zahner G, Tomas NM, Meyer-Schwesinger C, et al. A mechanism for cancer associated membranous nephropathy. *N Engl J Med* (2016) 374(20):1995–6. doi: 10.1056/NEJMc1511702

24. Hoxha E, Beck LHJr, Wiech T, Tomas NM, Probst C, Mindorf S, et al. An indirect immunofluorescence method facilitates detection of thrombospondin type 1 domain containing 7A-specific antibodies in membranous nephropathy. *J Am Soc Nephrol* (2017) 28(2):520–31. doi: 10.1681/ASN.2016010050

25. Zhang CM, Zhang MC, Chen DC, Ren Q, Xu WW, Zeng CH, et al. Features of phospholipase A2 receptor and thrombospondin type-1 domain-containing 7A in malignancy-associated membranous nephropathy. *J Clin Pathol* (2019) 0:1–7. doi: 10.1136/jclinpath-2019-205852

26. Stahl PR, Hoxha E, Wiech T, Schröder C, Simon R, Stahl RAK. THSD7A expression in human cancer. *Genes Chromosomes Cancer* (2017) 56(4):314–27. doi: 10.1002/gcc.22440

27. Alsharhan L, Beck LHJr. Membranous nephropathy: Core curriculum 2021. *Am J Kidney Dis* (2021) 77(3):440–53. doi: 10.1053/j.ajkd.2020.10.009

28. Sethi S, Debiec H, Madden B, Charlesworth MC, Morelle J, Gross L, et al. The neural tissue associated protein NELL-1 is associated with membranous nephropathy. *Kidney Int* (2020) 97(1):163–74. doi: 10.1016/j.kint.2019.09.014

frontiers | Frontiers in Oncology

TYPE Case Report
PUBLISHED 04 October 2022
DOI 10.3389/fonc.2022.1019624

OPEN ACCESS

EDITED BY
Kohei Fujita,
National Hospital Organization Kyoto Medical Center, Japan

REVIEWED BY
Junichi Shimizu,
Aichi Cancer Center, Japan
Chiao-En Wu,
Linkou Chang Gung Memorial Hospital, Taiwan

*CORRESPONDENCE
Lin Zhu
doctor_zl0301@163.com

SPECIALTY SECTION
This article was submitted to Thoracic Oncology, a section of the journal Frontiers in Oncology

RECEIVED 17 August 2022
ACCEPTED 20 September 2022
PUBLISHED 04 October 2022

CITATION
Xue F, Xu S, Jiang C, Kang M, Usman M and Zhu L (2022) Case report: Novel *junctional sarcoplasmic reticulum protein 1* intergenic region–*anaplastic lymphoma kinase* fusion in a patient with lung adenocarcinoma responds to alectinib. *Front. Oncol.* 12:1019624. doi: 10.3389/fonc.2022.1019624

Case report: Novel *junctional sarcoplasmic reticulum protein 1* intergenic region–*anaplastic lymphoma kinase* fusion in a patient with lung adenocarcinoma responds to alectinib

Feng Xue[1], Shengyuan Xu[1], Cailing Jiang[1], Mafei Kang[1], Muhammad Usman[2] and Lin Zhu[3]*

[1]Department of Oncology, Affiliated Hospital of Guilin Medical University, Guilin, China, [2]College of International Education of Guilin Medical University, Guilin, China, [3]Department of Radiotherapy, Affiliated Hospital of Guilin Medical University, Guilin, China

Novel *anaplastic lymphoma kinase* (*ALK*) fusions are still being discovered in non-small cell lung cancer (NSCLC). Most patients with *ALK*+ NSCLC respond favorably to *ALK* tyrosine kinase inhibitors. In this case report, we identified a novel nonreciprocal *ALK* fusion, namely, *junctional sarcoplasmic reticulum protein 1* (*JSRP1*) intergenic region–*ALK* fusion (Jintergenic: A20) *via* next-generation sequencing in a female patient initially diagnosed with stage IV B lung adenocarcinoma. Further examination of biopsy specimen and analysis of clinical samples by a multidisciplinary team confirmed the diagnosis of *ALK*+ NSCLC. At the 2- and 4-months follow-up after receiving alectinib, the patient responded rapidly, implying that alectinib had a remarkable therapeutic effect. We identified a novel JSRP1 intergenic region–*ALK* fusion as a carcinogenic mutation that responds to alectinib, thereby expanding the spectrum of *ALK* fusion partners in *ALK* + NSCLC. This study may help clinicians detect oncogenic mutations and provide timely treatment to patients with *ALK*+ NSCLC.

KEYWORDS

intergenic region-ALK fusion, non-small cell lung cancer, alectinib, targeted therapy, case report

Introduction

Lung cancer remains the leading cause of cancer-related deaths globally, accounting for 18% of all cancer-related deaths (1). In addition, 4–8% of patients with non-small cell lung cancer (NSCLC) harbor anaplastic lymphoma kinase (*ALK*) gene fusions, which are associated with diagnosis at a young age (2, 3). *ALK* tyrosine kinase inhibitors (TKIs) have shown remarkable effects on patients with *ALK*-rearranged NSCLC (4, 5). More than 90 distinct fusion partners have been found. Furthermore, 28 potential fusion partners due to intergenic *ALK* rearrangements have been discovered (6). *ALK* fusion is a heterogeneous biomarker that may vary in expression depending on its type (7, 8).

Case description

In December 2021, a 40-year-old Chinese woman, without a family history of cancer as well as no smoking history, presented in a community hospital with upper abdominal pain for 3 months. Computed tomography (CT) scans of her abdomen revealed multiple lesions of the liver, pancreas, and bilateral adrenal gland. Chest X-ray examination revealed a lung mass in the right lower lobe. A chest CT scan revealed multiple nodules, with the largest diameter measuring 27 mm and multiple lymph node involvement around the right hilum (Figure 1A). The patient visited our hospital for further examination on December 22, 2021. The Eastern Cooperative Oncology Group performance status was one, and physical examination revealed no abnormal signs. Enhanced magnetic resonance imaging of the brain showed no abnormalities. Emission CT revealed abnormal radioactive concentrations in the bone, which were then diagnosed as multiple bone metastases (Figure 1B). At the patient's request, ultrasound-guided liver tumor biopsy was performed on December 23, 2021. A cytologic examination of the biopsy specimen showed adenocarcinoma cells (Figure 2A), which tested positive for cytokeratin 7 and thyroid transcription factor-1 and negative for Hepa in immunohistochemistry (IHC) (Figure 2B–D). Lung adenocarcinoma with stage IV (T1bN2M1c) was confirmed by a multidisciplinary team composed of a pathologist, a thoracic radiologist, and an oncologist.

Next-generation sequencing (NGS) analysis of liver biopsy tissue was assessed by performing capture-based targeted deep sequencing using the Lung Core Panel (NextSeq 500 system, Illumina, Inc), covering the exons of 16 lung cancer-related genes (*EGFR, ALK, RET, ROS1, MET, ERBB2, KRAS, BRAF, NTRK1, NTRK2, NTRK3, CDK4, CDK6, NRAS, PIK3CA*, and *TP53*) (Guangxi Medical University REXPLO Medical Laboratory, Nanning, China). NGS revealed a novel *ALK* fusion, namely, *junctional sarcoplasmic reticulum protein 1* (*JSRP1*) intergenic region–*ALK* fusion (Jintergenic: A20) (abundance: 37.2%). The microsatellite status was microsatellite instability-stable, and the tumor proportion score of PD-L1 (antibody: 28-8) was greater than 50% (Figure 2E). IHC (Ventana D5F3) and fluorescence *in situ* hybridization (FISH) of the biopsy specimen were performed, which confirmed a marked *ALK* fusion at the protein and DNA levels (Figures 2F, G).

Most *ALK* rearrangements are sensitive to *ALK*-TKI (6). The patient was orally administered 600 mg of alectinib twice daily in January 2022. The patient complained of significant fatigue and nausea 3 days after receiving alectinib. A week after initiation, alectinib administration was reduced to 450 mg orally twice daily. The symptoms disappeared after 3 weeks of medication. At the 2- and 4-months follow-up, a CT scan revealed a remarkable reduction of the tumors in the chest, liver, pancreas, adrenal gland, and mediastinal lymph node (Figure 1A). Partial response was achieved in accordance with the Response Evaluation Criteria in Solid Tumors version 1.1.

Written informed consent for submitting this case report was obtained from the patient.

Discussion

ALK rearrangements are common driver genes in NSCLC (9). With the increasing adoption of NGS for molecular profiling of NSCLC samples, more novel fusions and their corresponding efficacy on *ALK*-TKI have been reported (6). In this report, we identified a novel *ALK* gene fusion, *JSRP1–ALK* (Jintergenic: A20), *via* NGS and confirmed its efficacy using IHC and FISH assay. Subsequently, patient harboring this novel fusion was treated with alectinib, which exerted a remarkable effect in a short period.

JSRP1 is one of the proteins constituting the junctional face membrane with an apparent molecular mass of 45 kDa. It is critical in the process of functional expression of voltage-dependent Ca^{2+} channels (10, 11). In this report, *JSRP1* intergenic region rearranged to exons 20–29 of *ALK*, retaining its intact domain (Figure 3A). Then, exons 1–19 of *ALK* rearranged to exon 2 of LINC00211 (A19: LINC00211) (Figure 3B). Based on the structure of the fusion products (Figure 3C), we speculated that the 3′-*ALK* fusion product possesses kinase activity. Ying et al. found that uncommon *ALK* fusions detected using DNA NGS are an unreliable predictor of matched targeted therapy efficacy (12). In order to exclude the discordance of NGS, FISH, and IHC results caused by the complex biological mechanisms involved in transcriptional or post-transcriptional processes, we conducted FISH and IHC to confirm the positive *ALK* gene break and the marked *ALK* fusion protein expression in the tumor specimen. As per a previous study (13), we hypothesized that the *JSRP1* intergenic region possibly generates an N-terminal-derived product that leads to the constitutive expression of *ALK*. According to the consistency of DNA NGS, FISH, and IHC results, and the good response of the patient to alectinb, we speculated that the *JSRP1–*

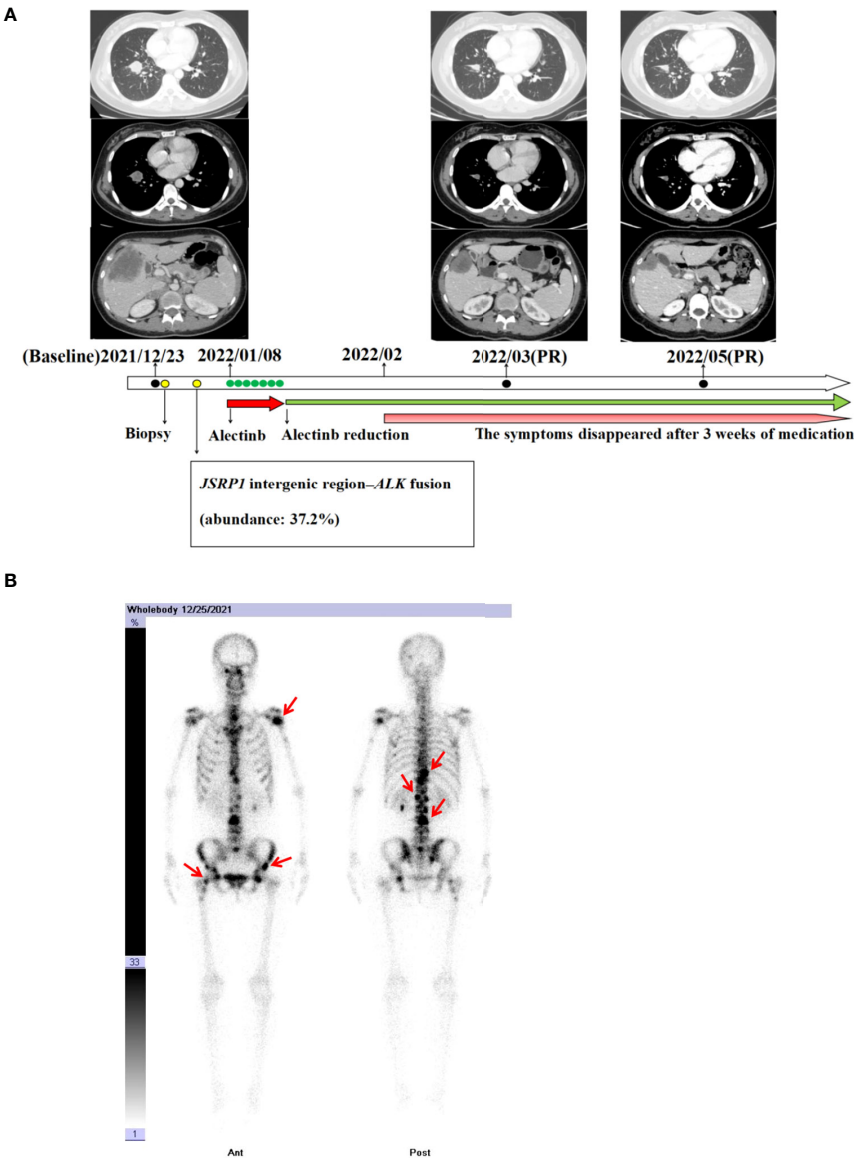

FIGURE 1
(A) Chest and abdomen computed tomography scans revealing the clinical response to alectinib. **(B)** Bone scan with technetium 99m-methyl diphosphonate prior to alectinib treatment revealing radioactive accumulation in the bones (red arrow).

ALK (Jintergenic: A20) fusion is a carcinogenic mutation in this case. Further studies should be conducted to confirm the biological function of the *JSRP1–ALK* (Jintergenic: A20) fusion in tumorigenesis. However, the biological function of 5′-*ALK* fusion translocation products remains unclear.

There are many studies and case reports on the treatment of NSCLC due to *ALK* rearrangements with crizotinib as it is the first *ALK*-TKI approved by the Food and Drug Administration for *ALK*-positive NSCLC patients. Zhang et al. reported that harboring non-reciprocal translocation is a poor predictive marker in patients with *ALK*-rearranged NSCLC treated with first-line crizotinib. Further, patients with non-reciprocal/reciprocal *ALK* translocation were reported to have a higher incidence of brain metastasis at baseline than those with classic 3′-*ALK* fusion (7). Conversely, the biopsy sample had a high level of PD-L1 expression (PD-L1 TPS of > 50%). Yang et al. revealed that positive PD-L1 expression was associated with unfavorable clinical outcomes in patients with *ALK* positive lung adenocarcinoma receiving crizotinib (14). Studies have shown that different fusion modalities may have inconsistent responses to crizotinib (7, 8). Therefore, there may have not been a long survival benefit had crizotinib been given to this patient.

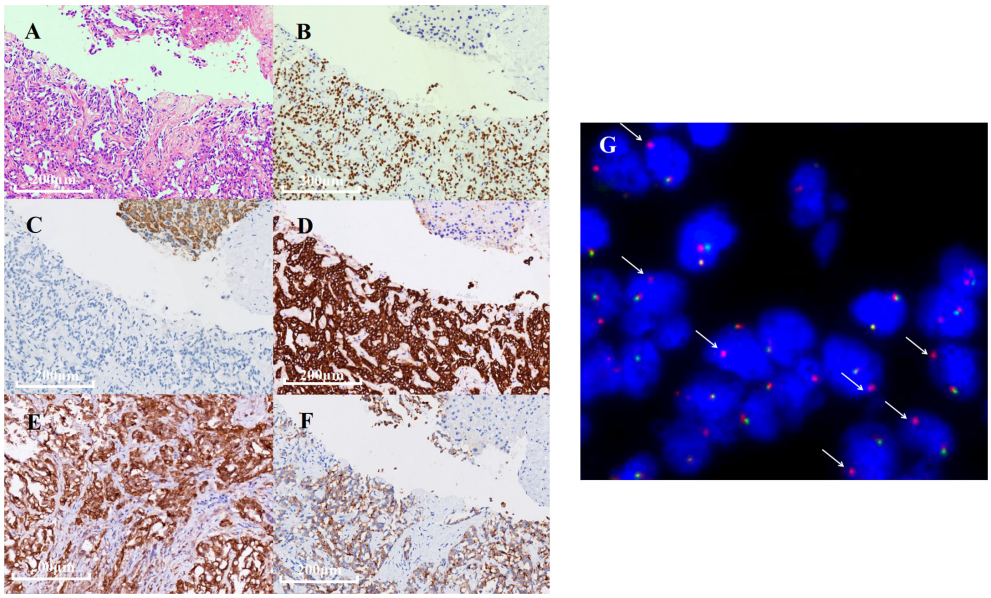

FIGURE 2
Immunohistochemistry (IHC) and fluorescence *in situ* hybridization (FISH) results of the biopsy specimen. **(A)** Hematoxylin and eosin staining revealing an adenocarcinoma. **(B–F)** IHC results of TTF-1, Hepa, CK-7, PD-L1, and ALK expression detected by D5F3 IHC assay. **(G)** FISH showed ALK gene rearrangement positive signal (one red and one yellow, indicated by white arrows).

Compared with those receiving crizotinib, patients receiving alectinib, ceritinib, brigatinib, or lorlatinib showed better response and had considerably longer progression-free survival (PFS) in advanced *ALK*-positive NSCLC (15–18). The case we presented here had PFS for more than five months till date. Whether alectinib is more effective than crizotinb in rare *ALK* rearrangements requires more research. In addition, the resistance mechanism of rare *ALK* fusion to *ALK*-TKI is rarely reported. Further clinical

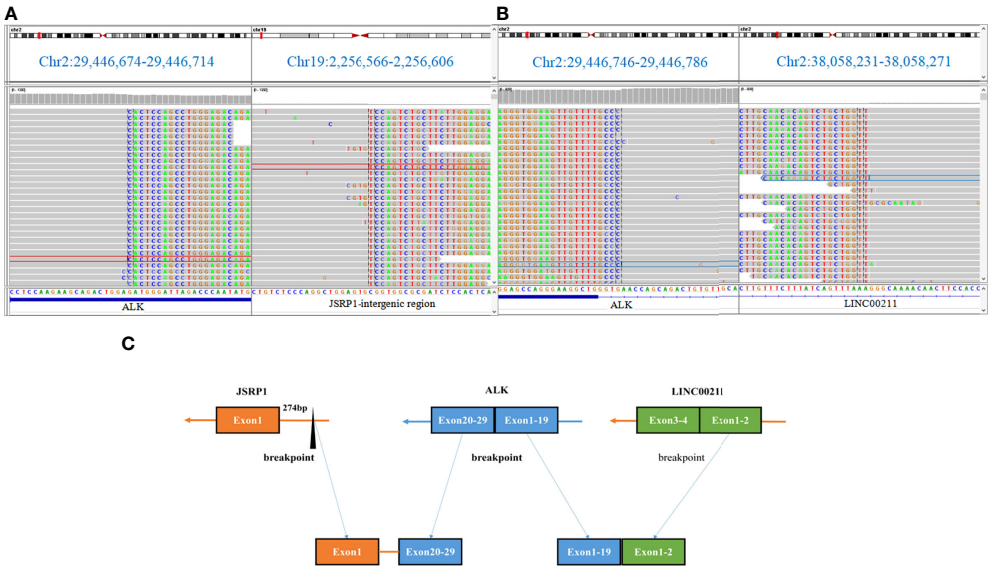

FIGURE 3
DNA-based next-generation sequencing findings for paraffin-embedded specimen of the patient. **(A, B)** The novel non-reciprocal JSRP1-ALK (Jintergenic:A20) rearrangement visualized using the Integrative Genomics Viewer.**(C)** Diagram depicting the non-reciprocal ALK fusion.

observation is required to further improve the efficacy of *ALK*-TKI in patients with novel *ALK* rearrangements.

Conclusion

We identified a novel *JSRP1* intergenic region–*ALK* fusion, expanding the spectrum of *ALK* fusion partners in patients with *ALK* + NSCLC. In addition, we found that alectinib exerted a remarkable and rapid therapeutic effect on the patient harboring this particular *ALK* fusion.

Data availability statement

The datasets presented in this article are not readily available because of ethical/privacy restrictions. Requests to access the datasets should be directed to the corresponding author.

Ethics statement

The studies involving human participants were reviewed and approved by ethics committee of Affiliated Hospital of Guilin Medical University. The patient provided her written informed consent to participate in this study. Written informed consent was obtained from the individual(s) for the publication of any potentially identifiable images or data included in this article.

Author contributions

FX: Conceptualization and writing - original draft. LZ: Supervision and data curation. SX and CJ: Validation and editing of the figures. MK and MU: Writing - review and editing. All authors contributed to the article and approved the submitted version.

Funding

This work was supported by the National Natural Science Foundation of China (Grant no. 82160471) and Beijing Xisike Clinical Oncology Research Foundation (Y-QL202101-0214).

Acknowledgments

We would like to thank the patient and her family members. We are also grateful for Jun Lu from Shanghai Yichuang Yunkang Biotechnology for their kind assistance.

Conflict of interest

The authors declare that the research was conducted in the absence of any commercial or financial relationships that could be construed as a potential conflict of interest.

Publisher's note

References

1. Sung H, Ferlay J, Siegel RL, Laversanne M, Soerjomataram I, Jemal A, et al. Global cancer statistics 2020: GLOBOCAN estimates of incidence and mortality worldwide for 36 cancers in 185 countries. *CA Cancer J Clin* (2021) 71(3):209–49. doi: 10.3322/caac.21660

2. Sacher AG, Dahlberg SE, Heng J, Mach S, Jänne PA, Oxnard GR. Association between younger age and targetable genomic alterations and prognosis in non-Small-Cell lung cancer. *JAMA Oncol* (2016) 2(3):313–20. doi: 10.1001/jamaoncol.2015.4482

3. Shimizu J, Masago K, Saito H, Nishino K, Kurata T, Itoh Y, et al. Biomarker testing for personalized, first-line therapy in advanced nonsquamous non-small cell lung cancer patients in the real world setting in Japan: a retrospective, multicenter, observational study (the BRAVE study). *Ther Adv Med Oncol* (2020) 12:1758835920904522. doi: 10.1177/1758835920904522

4. Wu YL, Lu S, Lu Y, Zhou J, Shi YK, Sriuranpong V, et al. Results of PROFILE 1029, a phase III comparison of first-line crizotinib versus chemotherapy in East Asian patients with *ALK*-positive advanced non-small cell lung cancer. *J Thorac Oncol* (2018) 13(10):1539–48. doi: 10.1016/j.jtho.2018.06.012

5. Camidge DR, Kim HR, Ahn MJ, Yang JCH, Han JY, Hochmair MJ, et al. Brigatinib versus crizotinib in *ALK* inhibitor-naive advanced *ALK*-positive NSCLC: Final results of phase 3 ALTA-1L trial. *J Thorac Oncol* (2021) 16(12):2091–108. doi: 10.1016/j.jtho.2021.07.035

6. Ou SI, Zhu VW, Nagasaka M. Catalog of 5' fusion partners in *ALK*-positive NSCLC circa 2020. *JTO Clin Res Rep* (2020) 1:100015. doi: 10.1016/j.jtocrr.2020.100015

7. Zhang Y, Zeng L, Zhou C, Li Y, Wu L, Xia C, et al. Detection of Nonreciprocal/Reciprocal *ALK* translocation as poor predictive marker in patients with first-line crizotinib-treated *ALK*-rearranged NSCLC. *J Thorac Oncol* (2020) 15:1027–36. doi: 10.1016/j.jtho.2020.02.007

8. Sun K, Nie L, Nong L, Cheng Y. Primary resistance to alectinib in a patient with STRN-*ALK*-positive non-small cell lung cancer: A case report. *Thorac Cancer* (2021) 12:1927–30. doi: 10.1111/1759-7714.13983

9. Solomon B, Varella-Garcia M, Camidge DR. ALK gene rearrangements: A new therapeutic target in a molecularly defined subset of non-small cell lung cancer. *J Thorac Oncol* (2009) 4:1450–4. doi: 10.1097/JTO.0b013e3181c4dedb

10. Zorzato F, Anderson AA, Ohlendieck K, Froemming G, Guerrini R, Treves S. Identification of a novel 45 kDa protein (JP-45) from rabbit sarcoplasmic-reticulum junctional-face membrane. *Biochem J* (2000) 351 Pt 2:537–43. doi: 10.1042/bj3510537

11. Anderson AA, Altafaj X, Zheng Z, Wang ZM, Delbono O, Ronjat M, et al. The junctional SR protein JP-45 affects the functional expression of the voltage-dependent Ca2+ channel Cav1.1. *J Cell Sci* (2006) 119:2145–55. doi: 10.1242/jcs.02935

12. Li W, Guo L, Liu Y, Dong L, Yang L, Chen L, et al. Potential unreliability of uncommon *ALK*, ROS1, and RET genomic breakpoints in predicting the efficacy of targeted therapy in NSCLC. *J Thorac Oncol* (2021) 16:404–18. doi: 10.1016/j.jtho.2020.10.156

13. Katayama R, Lovly CM, Shaw AT. Therapeutic targeting of anaplastic lymphoma kinase in lung cancer: a paradigm for precision cancer medicine. *Clin Cancer Res* (2015) 21:2227–35. doi: 10.1158/1078-0432.CCR-14-2791

14. Yang CY, Liao WY, Ho CC, Chen KY, Tsai TH, Hsu CL, et al. Association of programmed death-ligand 1 expression with fusion variants and clinical outcomes in patients with anaplastic lymphoma kinase-positive lung adenocarcinoma receiving crizotinib. *Oncologist* (2020) 25:702–11. doi: 10.1634/theoncologist.2020-0088

15. Fontana D, Ceccon M, Gambacorti-Passerini C, Mologni L. Activity of second-generation *ALK* inhibitors against crizotinib-resistant mutants in an NPM-*ALK* model compared to EML4-*ALK*. *Cancer Med* (2015) 4:953–65. doi: 10.1002/cam4.413

16. Soria JC, Tan D, Chiari R, Wu YL, Paz-Ares L, Wolf J, et al. First-line ceritinib versus platinum-based chemotherapy in advanced ALK-rearranged non-small-cell lung cancer (ASCEND-4): A randomised, open-label, phase 3 study. *Lancet* (2017) 389:917–29. doi: 10.1016/S0140-6736(17)30123-X

17. Camidge DR, Kim HR, Ahn MJ, Yang JCH, Han JY, Hochmair MJ, et al. Brigatinib versus crizotinib in advanced ALK inhibitor-naive ALK-positive non-small cell lung cancer: Second interim analysis of the phase III ALTA-1L trial. *J Clin Oncol* (2020) 38:3592–603. doi: 10.1200/JCO.20.00505

18. Shaw AT, Bauer TM, de Marinis F, Felip E, Goto Y, Liu G, et al. First-line lorlatinib or crizotinib in advanced ALK-positive lung cancer. *N Engl J Med* (2020) 383:2018–29. doi: 10.1056/NEJMoa2027187

frontiers | Frontiers in Oncology

TYPE Case Report
PUBLISHED 17 October 2022
DOI 10.3389/fonc.2022.1016320

OPEN ACCESS

EDITED BY
Mln Yu,
West China Hospital, Sichuan University, China

REVIEWED BY
Karam Khaddour,
University of Illinois at Chicago, United States
Song Xu,
Tianjin Medical University General Hospital, China

*CORRESPONDENCE
Shihong Fei
353977303@qq.com
Liling Zhang
lily-1228@hotmail.com

†These authors have contributed equally to this work

SPECIALTY SECTION
This article was submitted to Thoracic Oncology, a section of the journal Frontiers in Oncology

RECEIVED 10 August 2022
ACCEPTED 29 September 2022
PUBLISHED 17 October 2022

CITATION
Han D, Zhao K, Yang Q, Zhang L and Fei S (2022) Secondary mutant ALK-I1171s in pituitary metastases from a patient with ALK fusion-positive advanced lung adenocarcinoma: A case report and literature review. *Front. Oncol.* 12:1016320. doi: 10.3389/fonc.2022.1016320

Secondary mutant ALK-I1171s in pituitary metastases from a patient with ALK fusion-positive advanced lung adenocarcinoma: A case report and literature review

Dan Han†, Kewei Zhao†, Qin Yang, Liling Zhang* and Shihong Fei*

Cancer Center, Union Hospital, Tongji Medical College, Huazhong University of Science and Technology, Wuhan, China

Background: Pituitary metastasis accounts for a very low percentage of cases of brain metastasis from lung cancer, and there are uncertainties and challenges in diagnosis and treatment. We hope to shed some light on the diagnosis and treatment by reporting a case of ALK fusion mutation-positive lung cancer pituitary metastasis.

Case presentation: We report a 48-year-old female patient with an initial diagnosis of stage IVB lung adenocarcinoma with ALK fusion. The patient developed headache, dizziness, hypopituitarism and hyperprolactinemia one year after treatment with crizotinib. Later, the patient underwent neurosurgical resection of the pituitary tumor and then symptomatic relief. Postoperative pathology suggested pituitary metastasis, and the next-generation gene sequencing conducted on the pituitary metastasis indicated that secondary drug resistance mutation ALK-I1171s occurred after the ALK fusion gene.

Conclusion: In this article, we present a patient with suspected pituitary metastases with lung cancer. The progression to pituitary mass resection and next-generation gene sequencing of the pituitary metastasis are suggestive for further diagnosis and treatment.

KEYWORDS

pituitary metastasis, crizotinib, drug resistance, ALK, lung adenocarcinoma

Introduction

According to available reports, pituitary metastases from lung cancer are very rare, especially when compared with metastases to other endocrine glands, such as the adrenal gland and thyroid gland (1). Lung cancer (24.2%) is the second most common malignant tumor for pituitary metastases after breast cancer (37.2%), followed by prostate cancer (5%), kidney cancer (5%) and lymphoma (2). Some studies have found that the average overall survival of patients with pituitary metastases is 10-13 months (3, 4). Patients with pituitary metastases from lung cancer are usually asymptomatic at first. However, as the tumor grows to a certain size, the mass will cause central nervous system and endocrine system symptoms. The most common symptoms are visual impairment, followed by hypopituitarism, hyperprolactinemia, and diabetes insipidus (5). Clinical symptoms and imaging examination cannot effectively differentiate pituitary metastases from benign pituitary tumors. Chemotherapy, radiation therapy, hormonal therapy and surgery are the available treatment options, but there is no conclusive evidence that these treatments can prolong the survival of patients (6). This paper reports an ALK fusion mutation-positive lung adenocarcinoma patient with pituitary metastasis. After surgical treatment, the symptoms of dizziness, headache, hypopituitarism and hyperprolactinemia were significantly relieved. Meanwhile, our team also conducted next-generation gene sequencing of the pituitary metastasis, and the results indicated that secondary drug resistance mutation ALK-I1171s occurred in the ALK fusion gene.

Case presentation

A 48-year-old Chinese woman with no smoking history presented to the Union Hospital of Tongji Medical College of Huazhong University of Science and Technology in October 2020 for chest tightness and chest pain. The ^{18}F-fluorodeoxyglucose positron emission tomography/computed tomography (^{18}F-FDG PET/CT) revealed a soft tissue density shadow in the right lower lobe with a size of 3.4*2.4 cm; enlarged bilateral supraclavicular and mediastinal lymph nodes, thickened bilateral pleura and increased pericardial effusion were metabolism increased; the metabolism in thoracic vertebrae T4, lumbar vertebrae L1, L5, and right ilium were also increased (Figure 1). Baseline lung enhanced CT images are shown in Figure 2A. Brain MRI showed no abnormalities (Figure 2F). In October 2020, the patient

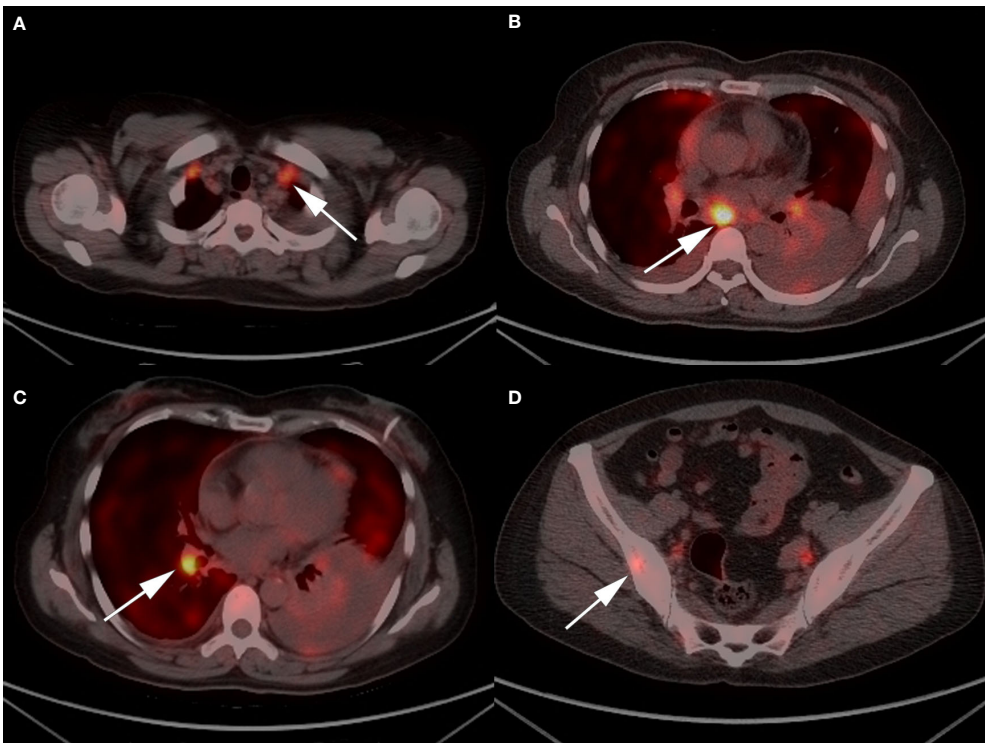

FIGURE 1
Representative ^{18}F/FDG PET-CT images of the patient: **(A)** enlarged bilateral supraclavicular and **(B)** mediastinal lymph nodes; **(C)** a 3.4*2.4 cm soft tissue density mass in the right lower lobe; and **(D)** increased metabolism in right ilium.

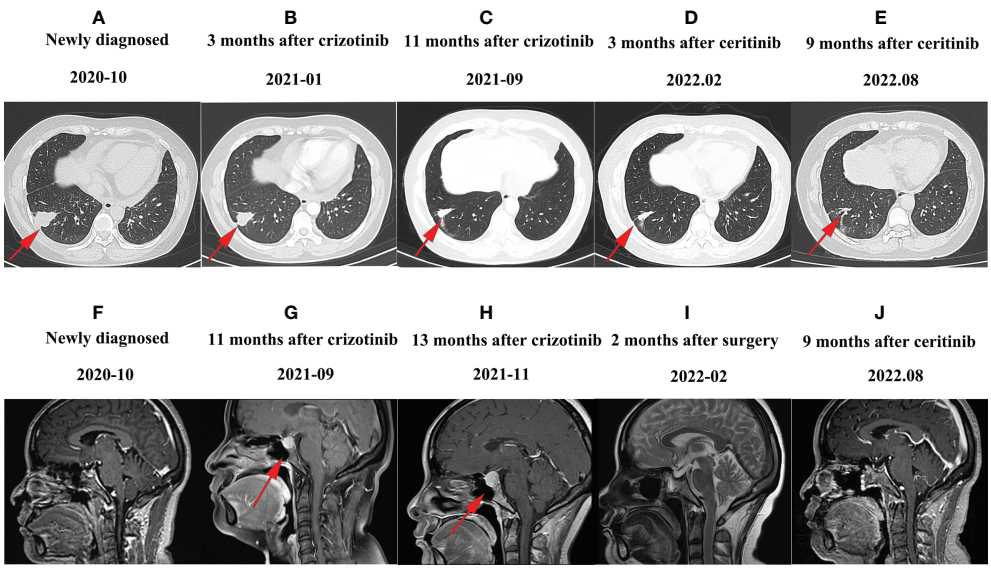

FIGURE 2
Representative CT or MRI images of the patient: **(A)** CT image of October 2020 before the treatment. **(B)** CT image of January 2021 after treatment with crizotinib. The therapeutic effect of the patients was evaluated as partial response. **(C)** CT image of September 2021 after pituitary metastases; the lung lesion was stable. **(D)** CT image of February 2022 after treatment with ceritinib; the lung lesions shrank further. **(E)** CT image of August 2022 after treatment with ceritinib; the lung lesion is still shrinking. **(F)** MRI image obtained in October 2020 before treatment; brain MRI showed no abnormalities. **(G)** MRI image of September 2021 after finding pituitary metastases. **(H)** MRI image after 1 month of supplemental hormone therapy. The pituitary gland was enlarged. **(I)** MRI image after sphenoid sinus exploration and nasal endoscopic saddle area tumor excision, and the brain MRI showed no mass. **(J)** Follow-up MRI images 9 months after tumor resection and 9 months after ceritinib administration.

underwent ultrasound-guided pericardiocentesis of pericardial effusion. Upon pathological examination of the pericardial effusion, cancer cells were detected, which was consistent with lung adenocarcinoma (Figure 3). Immunohistochemistry yielded the following: PCK (+), TTF-1(+), i+), CK5/6 (–), EGFR (–), C-met (–), Ros-1 (–), ALK (+). Next-generation genetic sequencing (whole-exome sequencing by company of gloriousmed) suggested the ALK EML4 (7, 8) - ALK (9, 10) fusion. Variant allele frequency (VAF) was 3.81%. Another driver mutation was CUX1 (mutation region: chr7: 101821924, 11 exon c.1004delA, p. Asn335fsTer20, VAF 1:00%), and others were somatic mutations of no clinical value, such as INPP4A, MED12, CDC73, CIC, SACS, NOTCH3, ARID2, RPS2, IRS2, INHA. Therefore, the patient was initially diagnosed with lung adenocarcinoma stage

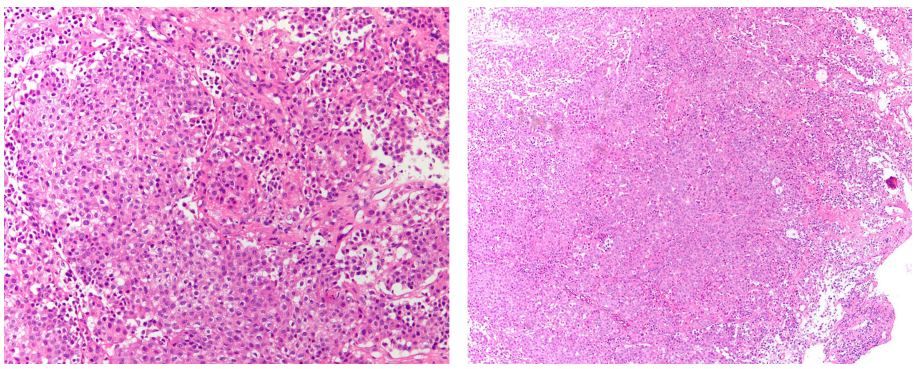

FIGURE 3
Histopathological findings of pericardial effusion by paraffin embedding of cell sediment. IHC yielded the following: PCK (+), Claudin-4(+), TTF-1 (+), NapsinA(+), Calretinin (–), CK5/6 (–), P40 (–), EGFR (–), C-met (–), Ros-1 (–), ALK(+).

cT2N3M1c IVB with EML4-ALK gene fusion (AJCC 8th Edition). She started treatment with crizotinib (p.o. 250 mg bid) in October 2020 for financial reasons. In January 2021, the patient's lung CT showed that the lesion in the lower lobe of the right lung was 2.2*1.7 cm, and the pericardial effusion was significantly reduced (Figure 2B. According to the criteria of resist1.1, the therapeutic effect was evaluated as partial response (PR). The patient started to have headache and dizziness in September 2021, and brain MRI showed that the pituitary gland was full in shape on September 7, 2021, approximately 1.4*1.4*1.3 cm in size, and the lung lesion was stable (Figures 2C, G). Then, a lumbar puncture was performed, and no significant abnormalities were seen in the cerebrospinal fluid panel, cerebrospinal fluid biochemistry or cerebrospinal fluid cytology. ACTH (0 am): 5.83 pg/ml, ACTH (8 am): 10.20 pg/ml, ACTH (4 pm): 7.03 pg/ml (normal value: 7-64 pg/ml); cortisol (0 am):7.0μg/L, cortisol (8 am):3.0μg/L, cortisol (4 pm): 1.0μg/L (normal values: 37.0-194 μg/L); prolactin: 113.35 ng/ml (normal values: 1.2-29.9 ng/ml). No abnormalities were seen in sex hormones, thyroid hormone, growth hormone, or insulin-like growth factor. Afterward, our team conducted a multidisciplinary consultation with neurology, neurosurgery, and endocrinology and recommended a follow-up MRI after 1 month of supplemental hormone therapy. However, one month later, the patient's symptoms of headache and dizziness worsened, and the brain MRI re-examination showed that the pituitary gland was enlarged with a size of approximately 1.8*1.4*1.6 cm. On November 15, 2021 (Figure 2H), the patient underwent sphenoid sinus exploration and nasal endoscopic saddle area tumor excision in our neurosurgery department. During the operation, the neurosurgery team found an occupying lesion in the sellar area with high dural tension, approximately 2*1.5 cm in size, pink in color, and tightly adherent to the surrounding tissues. The postoperative pathology showed that it was consistent with metastatic adenocarcinoma with neuroendocrine marker expression in some areas of pulmonary origin. Immunohistochemistry yielded the following: PCK (+), TTF-1 (+), Napsin A (+), ACTH (–), GH (–), PRL (–), FSH (–), LH (–), TSH (–), Ki67 (Li: 5%) (Figure 4). The next-generation sequencing (whole-exome sequencing by company of gloriousmed) conducted on the pituitary metastasis suggested EML4 (6)-ALK (10) fusion with VAF of 2.63%. Interestingly, the ALK gene then revealed a missense mutation (mutation region: chr2: 29445213, 22 exon p. Ile1171Ser, VAF: 29.2%). Four non-clinically relevant somatic gene variants (missense mutations) were also detected, namely INPP4A, MAGI2, AMER1, MED12.The patient's postoperative headache and dizziness were significantly relieved compared to before. The patient's hormone levels were reviewed on November 29, 2021, and most of the abnormal hormone levels returned to normal. On December 01, 2021, the pituitary gland MRI was reviewed and showed that the pituitary tumor was significantly smaller than before. Based on the patient's gene sequencing results, we recommended that the patient replace crizotinib with ceritinib. On February 7, 2022, the patient's lung CT showed that the lesion in the lower lobe of the right lung had shrunk further with a size of 1.8*1.4 cm, and the brain MRI re-examination showed no abnormalities (Figures 2D, I). The patient was reexamined every two months by brain MRI and lung CT. The latest reexamination was on August 7, 2022, and no progression was observed (Figures 2E, J).

Discussion

The incidence of pituitary metastases accounts for 1% of the total incidence of pituitary lesions (7), making clinical differentiation of pituitary tumors from pituitary metastases very challenging. Patients with pituitary metastases from lung cancer are often asymptomatic at the initial stage, and many patients are found to have pituitary occupancy at the time of MRI examination (8). Several studies have confirmed that visual impairment, hypopituitarism, and high prolactin levels are the

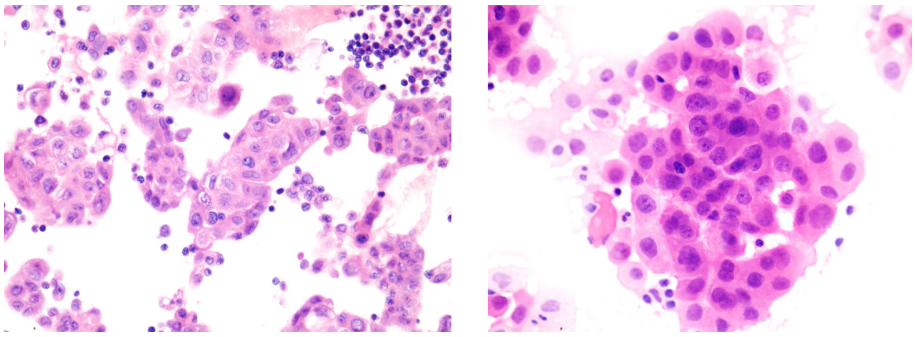

FIGURE 4
Histopathological findings of pituitary metastases. IHC yielded the following: PCK (+), TTF-1 (+), NapsinA (+), EMA (+), Syn (partial +), CgA (focal +), GFAP (–), S1001 (-), CD68 (-), CD34 (-), ACTH (-), GH (-), PRL (-), FSH (-), LH (-), TSH (-), Ki67 (Li:5%).

most common clinical manifestations of pituitary metastases (5, 11). Some studies have shown no significant difference in the overall survival of patients between surgical and nonsurgical treatment of pituitary metastases from lung cancer (12). Aida Javanbakht et al. surveyed 289 patients with pituitary metastases at Dewart Medical Center from 1984-2018 and found that 178 (61.6%) patients opted for surgery for treatment (4). The main surgical option currently available is transsphenoidal surgery, but surrounding tissue adhesions and abundant blood supply often make surgery difficult, and the performance of pituitary metastasectomy requires multidisciplinary cooperation and an experienced neurosurgical team (13). Patients undergoing surgery can suffer from secondary hypopituitarism, which requires lifelong hormone replacement therapy (14). In this case, the patient had a remarkable clinical presentation and underwent surgery after multidisciplinary collaboration between the medical oncology team and the neurosurgery team.

The ALK gene has been identified in a variety of solid tumors and is a potent oncogenic driver gene (15). ALK protein is located on the cell membrane with an extracellular receptor region and an intracellular kinase region. Under normal conditions, two ALK proteins are coupled by extracellular ligands to activate signaling pathways and promote cell growth (16). There are three types of mutations in the ALK gene: 1. ALK fusion mutations are the most common, especially EML4-ALK fusion mutations, and the protein can be activated without ligand; 2. Point mutations are less common and occur mainly in the intracellular kinase region; and after the mutation, they continue downstream conveyance of cell growth signals; 3. Amplification mutations are even less common (17). ALK fusion gene mutation frequency accounts for 2-5% of all non-small cell lung cancers worldwide (16, 17). Patients with ALK fusion mutation non-small cell lung cancer can benefit from crizotinib with an objective response rate of 60% and progression-free survival of 8-10 months, but drug resistance occurs within 1-2 years, with central nervous system relapse being the most common reversal (18, 19). However, alectinib has been shown to have longer PFS than crizotinib in multiple phase III clinical trials, and alectinib is now widely used as a first-line therapy, especially in cases of brain metastasis (20). Since the patient had stable lesions elsewhere, our team decided to perform pituitary occupancy resection to clarify the nature of the lesions and to perform next-generation sequencing if the pathology suggested metastatic adenocarcinoma. Thirty-seven percent of crizotinib resistance cases occur due to ALK secondary resistance mutations, which can be classified as ALK kinase region mutations (28%) and ALK fusion gene copy number amplification (9%) (9). In addition, mechanisms associated with crizotinib resistance also include driver gene conversion as well as tumor heterogeneity (10). This patient showed ALK missense mutations after the development of pituitary metastases, and pituitary tissue genetic sequencing suggested the presence of ALK-I1171S. I1171S refers to the conversion of the second nucleotide (3512 nucleotides of full-length ALK) encoding isoleucine ATC to AGC (serine [S]). Similarly, I1171 includes I1171N (isoleucine ATC converts to AAC (asparagine [N])) and I1171T (isoleucine ATC converts to ACC threonine [T]), etc. Currently, it is unclear why this mutation lead to resistance to crizotinib. Further basic and clinical analyses are required to investigate the biology and clinical significance of the I1171 mutation. However, the I1171 mutation was more frequently reported in secondary resistance mutations after alectinib failure than with crizotinib (21–23). In 2014, Ou SH et al. reported that two NSCLC patients with the EML4-ALK variant initially responded to crizotinib and then alectinib but developed acquired resistance with the presence of a mutation in amino acid residue 1171 (I1171N and I1171S, respectively) located in the hydrophobic regulatory spine of ALK kinase (24). I1171 mutations are believed to decrease the stability of the inhibitor through autophosphorylation (25). Gainor et al. found that ceritinib was effective when patients developed the secondary ALK-1171S mutation (26). Importantly, many researchers found that ALK-I1171 mutations mediate resistance to alectinib while generating sensitivity to ceritinib. ALK-I1171 mutations were found to be the second-most common resistance mutations in post-alectinib therapy (12%). Based on the above evidence, we recommended that our patient switch to ceritinib instead of alectinib, and to date, progression-free survival has been 8 months (22, 26).

Conclusion

Pituitary metastasis from lung cancer is very rare, and surgical treatment could be a positive option. Although crizotinib was chosen for financial reasons in this patient, alectinib has been shown to have longer PFS than crizotinib in multiple phase III clinical trials, and alectinib is now widely used as first-line therapy, especially in brain metastasis. This patient developed pituitary metastasis after crizotinib resistance, and next-generation sequencing suggested the presence of the ALK I1171S mutation. The ALK I1171S mutation has been shown to result in secondary resistance to crizotinib, and ceritinib has proved effective when patients develop the secondary ALK 1171S mutation.

Data availability statement

The original contributions presented in the study are included in the article/supplementary material. Further inquiries can be directed to the corresponding authors.

Ethics statement

Written informed consent was obtained from the individual(s) for the publication of any potentially identifiable images or data included in this article.

Author contributions

SF and DH had the original idea for the article and guided the treatment and management of the patient. DH and KZ wrote the article incorporating the comments from LZ. All authors reviewed and approved the final draft of the article. All authors contributed to the article and approved the submitted version.

Funding

This work was funded by the National Natural Science Foundation of China (82002825 to DH).

Conflict of interest

The authors declare that the research was conducted in the absence of any commercial or financial relationships that could be construed as a potential conflict of interest.

Publisher's note

All claims expressed in this article are solely those of the authors and do not necessarily represent those of their affiliated organizations, or those of the publisher, the editors and the reviewers. Any product that may be evaluated in this article, or claim that may be made by its manufacturer, is not guaranteed or endorsed by the publisher.

References

1. Bailey D, Mau C, Zacharia B. Pituitary metastasis from urothelial carcinoma: A case report and review of the diagnosis and treatment of pituitary metastases. *Cureus* (2021) 13(8):e17574. doi: 10.7759/cureus.17574

2. Komninos J, Vlassopoulou V, Protopapa D, Korfias S, Kontogeorgos G, Sakas DE, et al. Tumors metastatic to the pituitary gland: Case report and literature review. *J Clin Endocrinol Metab* (2004) 89(2):574–80. doi: 10.1210/jc.2003-030395

3. Henry A, Nugent A, Wallace IR, Oladipo B, Sheehy O, Johnston PC. Pituitary metastasis: a clinical overview. *Ulster Med J* (2021) 90(3):146–50.

4. Javanbakht A, D'Apuzzo M, Badie B, Salehian B. Pituitary metastasis: a rare condition. *Endocrine connections.* (2018) 7(10):1049–57. doi: 10.1530/ec-18-0338

5. Al-Aridi R, El Sibai K, Fu P, Khan M, Selman WR, Arafah BM. Clinical and biochemical characteristic features of metastatic cancer to the sella turcica: an analytical review. *Pituitary* (2014) 17(6):575–87. doi: 10.1007/s11102-013-0542-9

6. Lithgow K, Siqueira I, Senthil L, Chew HS, Chavda SV, Ayuk J, et al. Pituitary metastases: presentation and outcomes from a pituitary center over the last decade. *Pituitary* (2020) 23(3):258–65. doi: 10.1007/s11102-020-01034-2

7. He W, Chen F, Dalm B, Kirby PA, Greenlee JD. Metastatic involvement of the pituitary gland: a systematic review with pooled individual patient data analysis. *Pituitary* (2015) 18(1):159–68. doi: 10.1007/s11102-014-0552-2

8. Hwang JM, Kim YH, Kim TM, Park SH. Differential diagnosis and management of a pituitary mass with renal cell carcinoma. *J Korean Neurosurgical Society.* (2013) 54(2):132–5. doi: 10.3340/jkns.2013.54.2.132

9. Recondo G, Facchinetti F, Olaussen KA, Besse B, Friboulet L. Making the first move in EGFR-driven or ALK-driven NSCLC: first-generation or next-generation TKI? *Nat Rev Clin Oncol* (2018) 15(11):694–708. doi: 10.1038/s41571-018-0081-4

10. Pan Y, Deng C, Qiu Z, Cao C, Wu F. The resistance mechanisms and treatment strategies for ALK-rearranged non-small cell lung cancer. *Front Oncol* (2021) 11:713530. doi: 10.3389/fonc.2021.713530

11. Vasilev V, Rostomyan L, Daly AF, Potorac I, Zacharieva S, Bonneville JF, et al. MANAGEMENT OF ENDOCRINE DISEASE: Pituitary 'incidentaloma': neuroradiological assessment and differential diagnosis. *Eur J Endocrinol* (2016) 175(4):R171–84. doi: 10.1530/eje-15-1272

12. Zoli M, Mazzatenta D, Faustini-Fustini M, Pasquini E, Frank G. Pituitary metastases: role of surgery. *World Neurosurg* (2013) 79(2):327–30. doi: 10.1016/j.wneu.2012.03.018

13. Habu M, Tokimura H, Hirano H, Yasuda S, Nagatomo Y, Iwai Y, et al. Pituitary metastases: Current practice in Japan. *J Neurosurg* (2015) 123(4):998–1007. doi: 10.3171/2014.12.Jns14870

14. Shah KK, Anderson RJ. Acute secondary adrenal insufficiency as the presenting manifestation of small-cell lung carcinoma. *BMJ Case Rep* (2014) 2014. doi: 10.1136/bcr-2013-203224

15. Altorki NK, Markowitz GJ, Gao D, Port JL, Saxena A, Stiles B, et al. The lung microenvironment: An important regulator of tumour growth and metastasis. *Nat Rev Cancer* (2019) 19(1):9–31. doi: 10.1038/s41568-018-0081-9

16. Wu J, Savooji J, Liu D. Second- and third-generation ALK inhibitors for non-small cell lung cancer. *J Hematol Oncol* (2016) 9:19. doi: 10.1186/s13045-016-0251-8

17. Du X, Shao Y, Qin HF, Tai YH, Gao HJ. ALK-rearrangement in non-small-cell lung cancer (NSCLC). *Thorac Cancer* (2018) 9(4):423–30. doi: 10.1111/1759-7714.12613

18. Nishio M, Kim DW, Wu YL, Nakagawa K, Solomon BJ, Shaw AT, et al. Crizotinib versus chemotherapy in Asian patients with ALK-positive advanced non-small cell lung cancer. *Cancer Res Treat* (2018) 50(3):691–700. doi: 10.4143/crt.2017.280

19. Yoshida T, Oya Y, Tanaka K, Shimizu J, Horio Y, Kuroda H, et al. Differential crizotinib response duration among ALK fusion variants in ALK-positive non-Small-Cell lung cancer. *J Clin oncology: Off J Am Soc Clin Oncol* (2016) 34(28):3383–9. doi: 10.1200/jco.2015.65.8732

20. Hida T, Nokihara H, Kondo M, Kim YH, Azuma K, Seto T, et al. Alectinib versus crizotinib in patients with ALK-positive non-small-cell lung cancer (J-ALEX): an open-label, randomised phase 3 trial. *Lancet (London England)* (2017) 390(10089):29–39. doi: 10.1016/s0140-6736(17)30565-2

21. Noé J, Lovejoy A, Ou SI, Yaung SJ, Bordogna W, Klass DM, et al. ALK mutation status before and after alectinib treatment in locally advanced or metastatic ALK-positive NSCLC: Pooled analysis of two prospective trials. *J Thorac Oncol: Off Publ Int Assoc Study Lung Cancer* (2020) 15(4):601–8. doi: 10.1016/j.jtho.2019.10.015

22. Ou SH, Milliken JC, Azada MC, Miller VA, Ali SM, Klempner SJ. ALK F1174V mutation confers sensitivity while ALK I1171 mutation confers resistance to alectinib. *importance serial biopsy post progression. Lung Cancer (Amsterdam Netherlands)* (2016) 91:70–2. doi: 10.1016/j.lungcan.2015.09.006

23. Ou SH, Greenbowe J, Khan ZU, Azada MC, Ross JS, Stevens PJ, et al. I1171 missense mutation (particularly I1171N) is a common resistance mutation in ALK-positive NSCLC patients who have progressive disease while on alectinib and is sensitive to ceritinib. *Lung Cancer (Amsterdam Netherlands)* (2015) 88(2):231–4. doi: 10.1016/j.lungcan.2015.02.005

24. Ou SH, Klempner SJ, Greenbowe JR, Azada M, Schrock AB, Ali SM, et al. Identification of a novel HIP1-ALK fusion variant in non-Small-Cell lung cancer (NSCLC) and discovery of ALK I1171 (I1171N/S) mutations in two ALK-rearranged NSCLC patients with resistance to alectinib. *J Thorac oncology: Off Publ Int Assoc Study Lung Cancer* (2014) 9(12):1821–5. doi: 10.1097/jto.0000000000000368

25. Bresler SC, Weiser DA, Huwe PJ, Park JH, Krytska K, Ryles H, et al. ALK mutations confer differential oncogenic activation and sensitivity to ALK inhibition therapy in neuroblastoma. *Cancer Cell* (2014) 26(5):682–94. doi: 10.1016/j.ccell.2014.09.019

26. Gainor JF, Dardaei L, Yoda S, Friboulet L, Leshchiner I, Katayama R, et al. Molecular mechanisms of resistance to first- and second-generation ALK inhibitors in ALK-rearranged lung cancer. *Cancer Discov* (2016) 6(10):1118–33. doi: 10.1158/2159-8290.Cd-16-0596

frontiers | Frontiers in Oncology

TYPE Case Report
PUBLISHED 17 October 2022
DOI 10.3389/fonc.2022.1001627

OPEN ACCESS

EDITED BY
Kohei Fujita,
National Hospital Organization Kyoto Medical Center, Japan

REVIEWED BY
Etienne Marbaix,
Université Catholique de Louvain, Belgium
Lawrence Hsu Lin,
Department of Pathology, New York University, United States

*CORRESPONDENCE
Filipa Ferreira da Silva
Filipa.silva@fundacaochampalimaud.pt

SPECIALTY SECTION
This article was submitted to Thoracic Oncology, a section of the journal Frontiers in Oncology

RECEIVED 23 July 2022
ACCEPTED 03 October 2022
PUBLISHED 17 October 2022

CITATION
da Silva FF, Barata R, Rolim I, Carvalheiro C, Gil N and Pantarotto M (2022) Case report: Using DNA short tandem repeats to confirm nongestational origin of pulmonary choriocarcinoma. *Front. Oncol.* 12:1001627. doi: 10.3389/fonc.2022.1001627

Case report: Using DNA short tandem repeats to confirm nongestational origin of pulmonary choriocarcinoma

Filipa Ferreira da Silva[1]*, Rita Barata[2], Inês Rolim[3], Catarina Carvalheiro[2], Nuno Gil[4] and Marcos Pantarotto[4]

[1]Gynaecology Unit, Medical Oncology Department, Champalimaud Foundation, Lisbon, Portugal, [2]Thoracic Tumors Group, Surgery Department, Champalimaud Foundation, Lisbon, Portugal, [3]Thoracic Tumors Group, Pathology Department, Champalimaud Foundation, Lisbon, Portugal, [4]Thoracic Tumors Group, Medical Oncology Department, Champalimaud Foundation, Lisbon, Portugal

Gestational trophoblastic neoplasias (GTN) are malignant neoplasms that occur in pregnant or recently pregnant women. Choriocarcinoma (CCA) is a highly aggressive and rare GTN, and cases outside the female genital tract are commonly seen as secondary manifestations of gynecologic disease. In this paper, we describe the case of a 40 years-old female patient with a primary pulmonary CCA who was surgically treated and for whom the confirmation of the primary origin of the tumor was possible using a DNA short tandem repeat genotyping. Distinction between gestational and non-gestational trophoblastic neoplasia is crucial as they require different therapeutic approach and have different prognoses.

KEYWORDS

choriocarcinoma, lung neoplasms, primary tumor, non-gestational trophoblastic disease, human chorionic gonadotropin

Introduction

Gestational trophoblastic neoplasias (GTN) are malignant neoplasms that occur in pregnant or recently pregnant women. Gestational choriocarcinoma (CCA) is a highly aggressive, malignant GTN consisting of cytotrophoblastic and syncytiotrophoblastic cells, distinct from other forms of malignancy for containing genetic material from the male partner. CCA can arise from any type of normal or abnormal pregnancy, and although its diagnosis generally occurs within months of pregnancy, it can be exceptionally present during gestation (1). The tumor typically secretes beta-human chorionic gonadotropin (β-hCG) (2).

CCA may have an exceedingly rare non-gestational origin in women. Extra-gonadal non-gestational CCA usually arises in midline structures such as the mediastinum, retroperitoneum, and central nervous system. Non-midline CCA is uncommon and mainly affects the lungs, gastrointestinal tract, or breast (3).

Few Primary Pulmonary CCA (PPC) cases are reported in the literature. They are generally metastatic and with poor prognosis. Here we report the case of a localized PPC, initially assumed as gestational CCA, where a DNA test confirmed the tumor's non-gestational origin and ultimately guided our choices for the patient's treatment.

Case report

A 40-years-old female patient presented in our clinic in May 2021 for evaluation. She reported active smoking (20 packs-year) and had a history of secondary hypothyroidism. She had one uneventful vaginal delivery at age 31 and, since then, has been under continuous oral contraceptive.

In November 2020, she had a pregnancy diagnosis after a period of persistent nausea. One week later, she presented in the emergency room with spontaneous vaginal bleeding associated with pelvic pain. Physical examination was unremarkable. The analytic panel showed a β-hCG of 175U/mL (ref. value: <7.0U/mL), but pelvic ultrasonography (US) wasn't compatible with pregnancy, suggestive of spontaneous abortion. In early December 2020, due to continuing complaints of pelvic pain and bleeding, she resorted to the ER again. Pelvic US suggested a right ectopic pregnancy and β-hCG was 200U/mL. A multidisciplinary decision was made for two courses of single-dose methotrexate (MTX) to be administered one month apart, with an initial reduction of β-hCG (nadir: 140U/mL) but subsequent elevation.

Due to failure of MTX therapy, surgical treatment was carried out with laparoscopy, bilateral salpingectomy, dilation and curettage procedures that showed no ectopic pregnancy, pelvic tumor, or pregnancy in the uterus. Her endometrium was in the proliferative phase, and biopsies from both salpinges showed no evidence of malignancy or scarring.

A whole-body ^{18}F-FDG PET/CT scan showed a single hypermetabolic lesion (SUVmax 10.8) in the right upper lung lobe, measuring 24x32mm. A transthoracic needle biopsy of the lung lesion was consistent with CCA. No other lesions were identified after performing MRI of the brain, abdomen and pelvis, and thoracic CT scan.

According to the WHO/FIGO criteria (4) we assumed a low-risk GTN (4) with a single lung metastatic lesion with 3.2cm, who had not been treated with an appropriate MTX scheme. She started first-line chemotherapy (CTX) with MTX according to the 8-day Charing Cross regimen (5, 6), with persistent increase in β-hCG levels (maximum 1633U/mL). A CT scan performed after the second cycle of CTX revealed stability of the pulmonary lesion.

Considering the persistent elevation of the β-hCG despite the CTX, the absence of other foci of disease except for the lung and the fact that ectopic pregnancy has not been confirmed, a decision was made to treat the pulmonary lesion surgically.

In June 2021, or 8 months after the first symptoms, the patient had a thoracoscopic right upper lobectomy with systematic mediastinal lymphadenectomy. The postoperative course was uneventful, with the return of β-hCG titers to normal levels within three weeks. Histologic findings were consistent with CCA; immunochemistry showed positivity for β-hCG, Inhibin A, GATA3, SALL4, and negativity for TTF-1. Pathologic staging was pT2a pN0 R0 (stage IB, AJCC 8th ed) (Figure 1).

As a) there was no further evidence of more metastatic sites on the PET scan, b) the laparoscopy failed to reveal the initially supposed ectopic pregnancy in the absence of a molar pregnancy, and c) with the normalization of hCG hormone level after surgery according to the expected half-life of 24-36 hours, we considered the diagnosis of a non-metastatic PPC.

Being so rare, to confirm a non-metastatic PPC, we decided to analyze the genetic material of the tumor. A previously published case series used DNA's short tandem repeats (STR) to investigate the non-gestational origin of CCA (7). For short tandem repeat genotyping a formalin-fixed paraffin-embedded block containing tumor was selected, and patient and partner peripheral blood samples. By comparing STR from the tumor and peripheral blood samples from the patient and her husband, we observed a tumor DNA profile consisting exclusively of the patient's genetic pool, with no other donor contribution (Figure 2). Based on these findings, PPC was the final diagnosis.

No adjuvant treatment was offered, and after thirteen months (Figure 3), the patient is alive and asymptomatic, with normal β-hCG levels and no evidence of disease.

Discussion

PPC is a very rare condition with a challenging diagnosis and management. The optimal therapy for PPC, especially in the early stages, is yet to be defined. The addition of chemotherapy after surgery has been suggested to improve survival, based on the aggressive nature of this rare cancer, and supported by a small series of patients (8). Nevertheless, in contrast to gestational CCA, PPCs are generally considered resistant to chemotherapy and carry a much poorer prognosis.

Differentiation between gestational choriocarcinoma and non-gestational choriocarcinoma can be very difficult since the clinical presentation and histology of these two diseases are identical. This differentiation is essential in order to establish the best therapeutic strategy.

10.3389/fonc.2022.1001627

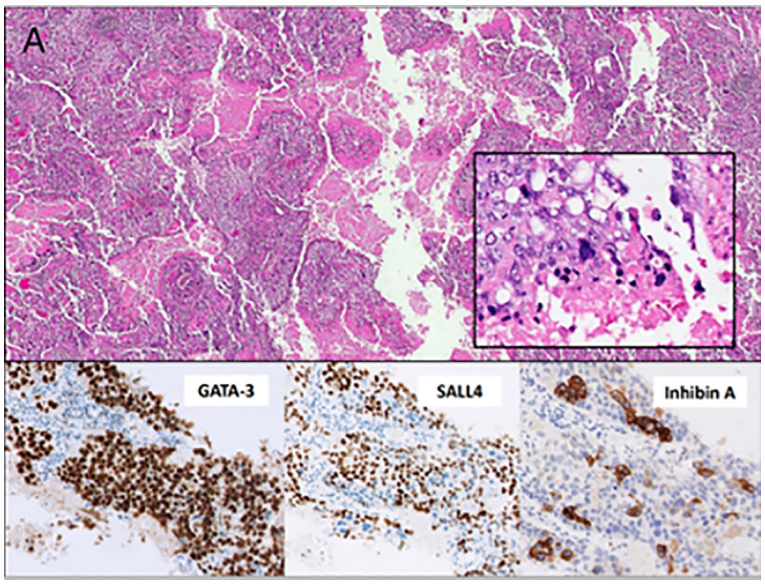

FIGURE 1
(A) The microscopic evaluation shows an extensively necrotic and hemorrhagic tumor with a distinctive biphasic appearance consisting of cytotrophoblasts, clear to light pink cytoplasm, distinct cell borders, irregular nuclei, and prominent nucleoli. Immunostaining of GATA-3 and SALL4, in close association with and capped by multinucleated syncytiotrophoblasts with abundant deeply eosinophilic cytoplasm, one or more nuclei, dark smudgy chromatin, and immunostaining of inhibin A and β-hCG (not shown). The neoplasm shows no immunostaining of TTF-1 (not shown).

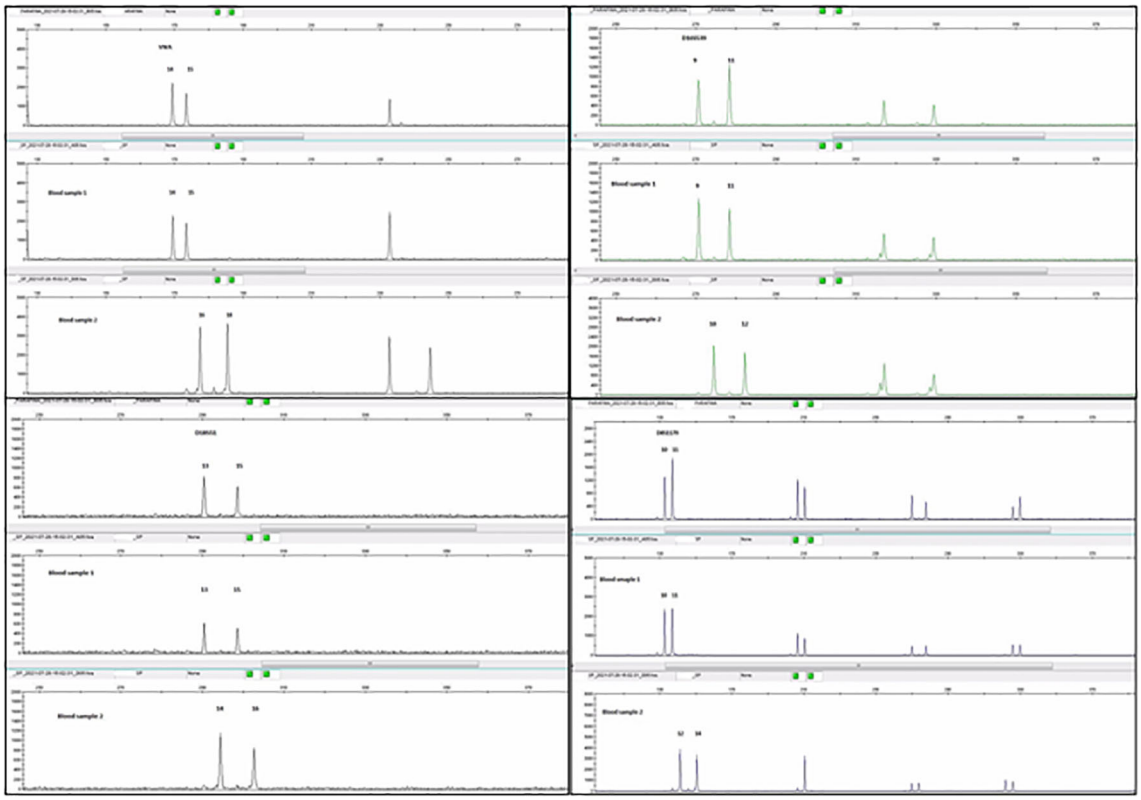

FIGURE 2
Comparative analysis of polymorphic markers (AmpFLSTR™ Identifiler™ Plus PCR Amplification Kit) in the tumor sample, patient (blood sample1) and partner (blood sample 2) blood samples. The profile of tumor´s and patient´s DNA are coincident, with no contribution from the partner`s DNA (in the case of informative markers) (image courtesy of Margarida Reis-Lima, MD, Elsa Garcia, MSc, Natália Salgueiro, MSc from Synlab laboratories, Porto, Portugal).

10.3389/fonc.2022.1001627

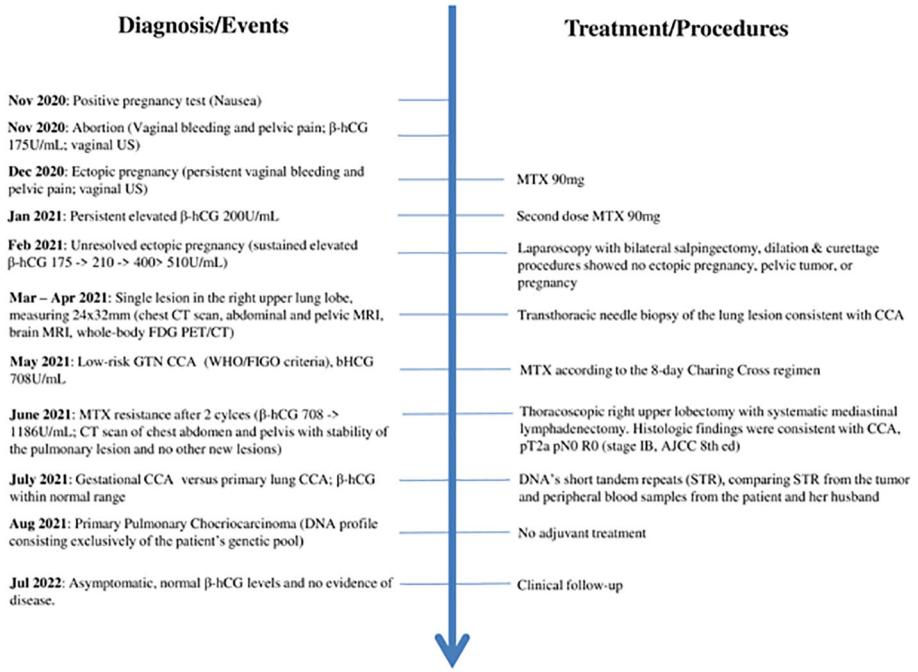

FIGURE 3
Timeline with relevant data from the episode of care. US – Ultrasound; MTX – methotrexate; GTN - Gestational trophoblastic neoplasia; CCA - choriocarcinoma.

In the case presented, with the initial suspicion of a recent abortion and subsequently of an ectopic pregnancy (refuted by laparoscopic examination), we considered the hypothesis of a metastatic lung lesion from gestational CCA as a more probable diagnosis. In addition, we know that this disease has very good prognosis and a high cure rate with chemotherapy. In order to define treatment, we applied the FIGO staging and the WHO risk score (4), resulting in a low-risk GTN (FIGO III: score <7). Assuming that the previous MTX scheme for ectopic pregnancy was not the standard regimen to treat this disease, we offered the 8-day Charing Cross MTX regimen (5, 6). The patient did not respond to CTX, with rising β-hCG levels, but fortunately maintaining radiological stable disease. In the face of resistance to CTX and the possibility of being a PPC case and not a metastatic CCA, we recommended the surgical treatment with radical intent. Histologic findings were consistent with CCA, and once again we were faced with doubt, whether it was really a PPC or metastatic gestational CCA.

The critical step for subsequent clinical decisions, such as adjuvant treatment, was determining the relation of the tumor with a gestational event or its primary origin. Molecular analysis of tumor tissue to identify unique paternal genetic contribution from a prior gestational event provides a definitive diagnostic distinction between tumors of gestational and non-gestational origin. Short tandem repeats (STR) genotyping is currently the most applicable method of identity testing, including diagnosis of gestational trophoblastic disease (9).

As reported above the tumor's DNA fully matched to the patient's, with no contribution from her partner's DNA. This established the diagnosis of PPC. There are no clear prognostic features nor guidelines to assist in clinical decisions of PPC treatment. PPC tends to grow rapidly and has high propensity to metastasize to other organs such as bone, liver, brain, spleen and contralateral lung (10). Most reported cases refer to treatment of early stages with surgery followed by adjuvant chemotherapy with BEP (bleomycin, methotrexate and cisplatin) or EMA-CO (etoposide, methotrexate, actinomycin D, cyclophospamide and vincristine).

In contrast to previously published cases, the clinical course of this patient's tumor was indolent, with stable disease for about 8 months until surgery was performed. We discussed with the patient the possibility of adjuvant CTX but ended up adopting a follow-up strategy instead.

Looking at the patient's trajectory, the gynecological symptoms presented by the patient contributed to the delay in the diagnosis of PPC. When in doubt, we emphasize the possibility of performing STR genotyping to establish the diagnosis.

Given the current availability of STR DNA analysis and the possible benefits for patients with cases like the one presented here,

we suggest that an STR DNA analysis from the tumor, the patient and partner should be used to support the diagnosis of PPC (1, 11).

Data availability statement

The original contributions presented in the study are included in the article/Supplementary Material. Further inquiries can be directed to the corresponding author.

Ethics statement

The studies involving human participants were reviewed and approved by Champalimaud Foundation's local ethics committee. The patients/participants provided their written informed consent to participate in this study. Written informed consent was obtained from the individual(s) for the publication of any potentially identifiable images or data included in this article.

Author contributions

All authors listed have made a substantial, direct, and intellectual contribution to the work, and approved it for publication.

Acknowledgments

The authors want to thank Margarida Reis-Lima, MD, Elsa Garcia, MD, and the Synlab laboratories in Lisbon, Portugal, for their help and collaboration in this case.

Conflict of interest

The authors declare that the research was conducted in the absence of any commercial or financial relationships that could be construed as a potential conflict of interest.

Publisher's note

References

1. Aranake-Chrisinger J, Huettner PC, Hagemann AR, Pfeifer JD. Use of short tandem repeat analysis in unusual presentations of trophoblastic tumors and their mimics. *Hum Pathol* (2016) 52:92–100. doi: 10.1016/j.humpath.2016.01.005

2. Wu P-S. Primary choriocarcinoma of the lung: a case report and literature review. *Int J Clin Exp Pathol* (2020) 13:2352–5.

3. Payne T, Di Palma S, Walker D, Dakin J, Thompson LDR. Extragonadal non-gestational choriocarcinoma with tonsillar presentation. *Head Neck Pathol* (2021) 15:1047–53. doi: 10.1007/s12105-020-01245-w

4. Ngan HYS, Seckl MJ, Berkowitz RS, Xiang Y, Golfier F, Sekharan PK, et al. Update on the diagnosis and management of gestational trophoblastic disease. *Int J Gynaecol Obstet Off Organ Int Fed Gynaecol Obstet* (2018) 143 Suppl 2:79–85. doi: 10.1002/ijgo.12615

5. Bagshawe KD, Dent J, Newlands ES, Begent RH, Rustin GJ. The role of low-dose methotrexate and folinic acid in gestational trophoblastic tumours (GTT). *Br J Obstet Gynaecol* (1989) 96:795–802. doi: 10.1111/j.1471-0528.1989.tb03318.x

6. McNeish IA, Strickland S, Holden L, Rustin GJS, Foskett M, Seckl MJ, et al. Low-risk persistent gestational trophoblastic disease: outcome after initial treatment with low-dose methotrexate and folinic acid from 1992 to 2000. *J Clin Oncol Off J Am Soc Clin Oncol* (2002) 20:1838–44. doi: 10.1200/JCO.2002.07.166

7. Zhang X, Yan K, Chen J, Xie X. Using short tandem repeat analysis for choriocarcinoma diagnosis: a case series. *Diagn Pathol* (2019) 14:93. doi: 10.1186/s13000-019-0866-5

8. Umemori Y, Hiraki A, Aoe K, Murakami T, Maeda T, Matsuda E, et al. Primary choriocarcinoma of the lung. *Anticancer Res* (2004) 24:1905–10.

9. Baine I, Hui P. Practical applications of DNA genotyping in diagnostic pathology. *Expert Rev Mol Diagn* (2019) 19:175–88. doi: 10.1080/14737159.2019.1568874

10. Snoj Z, Kocijancic I, Skof E. Primary pulmonary choriocarcinoma. *Radiol Oncol* (2017) 51:1–7. doi: 10.1515/raon-2016-0038

11. Nishino K, Yamamoto E, Oda Y, Watanabe E, Niimi K, Yamamoto T, et al. Short tandem repeat analysis to identify the causative pregnancy of high-risk gestational trophoblastic neoplasia: Molar versus nonmolar pregnancy and its relation to the outcome. *Placenta* (2021) 112:28–35. doi: 10.1016/j.placenta.2021.06.015

frontiers | Frontiers in Oncology

TYPE Case Report
PUBLISHED 18 October 2022
DOI 10.3389/fonc.2022.1029679

OPEN ACCESS

EDITED BY
Kohei Fujita,
National Hospital Organization Kyoto Medical Center, Japan

REVIEWED BY
Xiaoqun Ye,
Second Affiliated Hospital of Nanchang University, China
Jelena Stojsic,
University of Belgrade, Serbia

*CORRESPONDENCE
Sun Li-zhe
710815slz@163.com

†These authors share first authorship

SPECIALTY SECTION
This article was submitted to Thoracic Oncology, a section of the journal Frontiers in Oncology

RECEIVED 27 August 2022
ACCEPTED 30 September 2022
PUBLISHED 18 October 2022

CITATION
Ge-ge L, Cuicui G, Leiqiang L, Yongcang T, Jiangang M, Yiwen O and Li-zhe S (2022) Case report: A case report and literature review about Pathological transformation of lung adenosquamous cell carcinoma. *Front. Oncol.* 12:1029679. doi: 10.3389/fonc.2022.1029679

Case report: A case report and literature review about Pathological transformation of lung adenosquamous cell carcinoma

Liang Ge-ge†, Geng Cuicui†, Li Leiqiang, Tian Yongcang, Ma Jiangang, Ou Yiwen and Sun Li-zhe*

Department of Oncology, The Second Affiliated Hospital of Shaanxi University of Traditional Chinese Medicine, Xianyang, China

Background: Lung adenosquamous carcinoma is a relatively rare pathological type in lung cancer. The incidence of gene mutation is lower than that of lung adenocarcinoma. However, the cases of pathological transformation after targeted treatment of EGFR gene mutation are more rare.

Case introduction: A 55 year old female was diagnosed with lung cancer and underwent surgical treatment.The pathology suggested adenosquamous cell carcinoma. Genetic test was EGFR-L858R. After surgery, she was treated with gefitinib targeted therapy. After 2 years of surgery, she developed brain metastasis. surgery was performed again. The pathology suggested squamous cell carcinoma. She continued to take gefitinib targeted therapy orally. After one month later since brain metastasis, she was found to have heart cavity metastasis and surgery was performed for the third time. Besides, the pathology suggested adenosquamous cell carcinoma. Genetic test was EGFR-p E746_ A750del, T790M (-), and we replaced with the second-generation EGFR-TKI afatinib targeted therapy. Up to now, no recurrence or metastasis has been found.

Conclusion: We now report a rare case of lung adenosquamous carcinoma with pathological transformation during targeted therapy, which is intended to provide therapeutic ideas for the treatment of lung adenosquamous carcinoma in clinical practice. In addition, we reviewed previously reported tumor heterogeneity in the literature.

KEYWORDS

cardiac metastasis, lung cancer, pathological transformation, case report, EGFR-TKI

Introduction

Lung cancer is one of the most common malignant tumors, has distinct pathologic subtypes with diverse biological characteristics. Adenosquamous carcinoma is a rare subtype, and its malignancy and prognosis are higher and worse than those of adenocarcinoma or squamous cell carcinoma. As an important factor affecting prognosis, metastasis plays an important role in tumor staging and treatment strategies. In terms of treatment, surgery, chemotherapy and radiotherapy are still the main methods. Some patients with epidermal growth factor receptor (EGFR) gene mutations can benefit from tyrosine kinase inhibitor (TKI) treatment (1). This study collected the pathological transformation of metastatic lesions in a case of lung adenosquamous cell carcinoma after TKI treatment.

Case description

The patient, a 55 year old female, no previous disease history, no bad habits of personal history. And no history of tumor, infection or genetic disease in the family, visited our hospital on July 17, 2021 with the chief complaint of "two and a half years after lung cancer surgery and one month after brain metastasis surgery". On January 13, 2019, she went to Tangdu Hospital of the Fourth Military Medical University with "intermittent cough and expectoration for more than 20 days, and lung cancer was diagnosed for 2 days". Before admission, she performed chest CT in the First Affiliated Hospital of Xi'an Jiaotong University (Figure 1) showed left hilar space occupying lesions, more central lung cancer, obstructive pneumonia and left lower lobe atelectasis were considered. After admission, blood routine test, liver and kidney function, electrolyte, blood glucose, blood coagulation and infection were checked. Bronchoscopic biopsy was that (lower lobe of left lung) the submitted lung tissue was chronic inflammation with fibrous tissue hyperplasia, and a few atypical cells were found locally. The histological characteristics suggested that the possibility of canceration in a few washbars could not be completely excluded. PET/CT:1. Left lower lobe space occupying, left hilar enlarged lymph nodes, increased glucose metabolism, consistent with "left lung cancer" with left hilar lymph node metastasis; 2. No obvious abnormal metabolic signs are found in other parts. The clinical stage was cT2bN1M0, phase IIB. There was no surgical contraindication. On January 21, 2019, under general anesthesia, thoracoscopic radical resection of lung cancer (left lower lobe resection+regional lymph node dissection) was performed successfully. Postoperative pathology (Figure 2): specimens of left lower lobe resection: (left) central adenosquamous carcinoma of the lung (lower) lobe, mainly squamous cell carcinoma, with no invasion of the pleura; No cancer tissue was found in the bronchial stump; Metastatic cancer was found in hilar lymph nodes, and no cancer tissue was found in para bronchial lymph nodes and lymph nodes in groups 5, 7 and 9/11; In addition, 6 groups of lymph nodes were sent as fibrous adipose tissue, and no cancer tissue was found. Gene detection showed EGFR-L858R and TP53 mutations. After surgery, gefitinib(250mg Qd) was taken orally for targeted treatment, and the condition was stable without discomfort.

On June 8, 2021, the patient presented with intermittent headache, nausea, vomiting, and hallucination. She was admitted to the 215 Hospital of Shaanxi Nuclear Industry. Physical examination: lethargy, lack of cooperation, no abnormality was found in the heart, lungs, and abdomen. The muscle strength of the left lower limb was Grade 4, and that of the other limbs was Grade 5. Muscle tension was normal. The superficial and deep reflexes were normal, and the pathological signs were negative. The ranges of blood routine test, liver and kidney function, electrolyte, blood sugar, blood coagulation and infection were normal. Head MRI: The right temporal lobe had a cystic solid space occupying lesion. The lesion was mainly cystic, surrounded by large areas of edema, involving the right basal ganglia, thalamus and brain stem, and brain hernia. It was recommended that MR enhancement be further examined. Enhanced head MRI (Figure 3): cystic space occupying lesion in the right temporal lobe, with significantly enhanced uneven rosette wall, surrounding moderate brain edema area, the midline was compressed and moved to the left about 1.1cm.

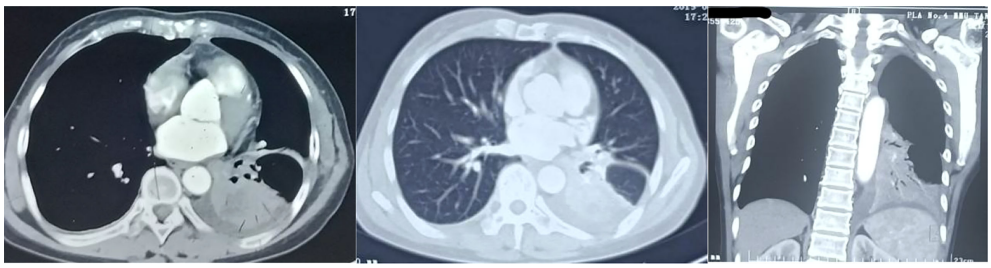

FIGURE 1
Chest CT.

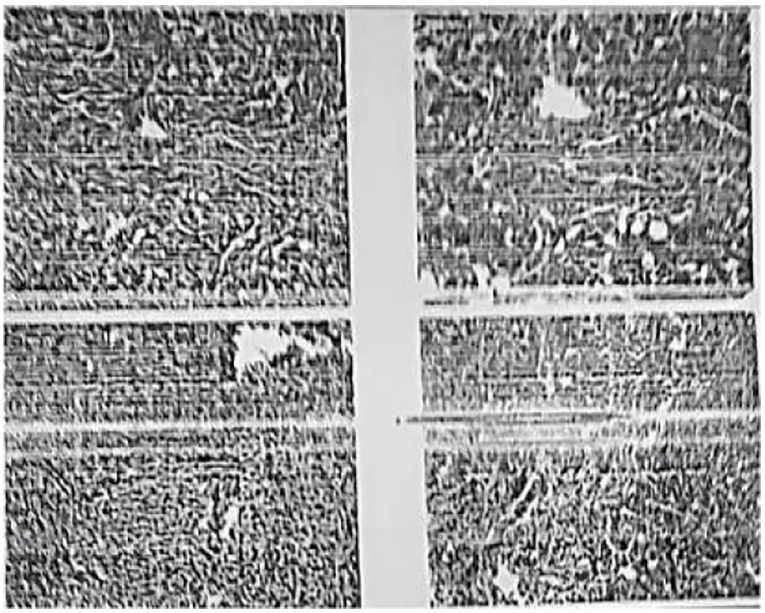

FIGURE 2
Postoperative pathology (Lung).

Considering malignant tumor, the possibility of brain metastasis was high. Chest and abdomen CT: 1. Changes after left lower lobe resection, left upper lobe and right middle and lower lobe cord foci; 2. Pleural hypertrophy on both sides with a small amount of pleural effusion; 3. Low density focus of liver, considering hemangioma. Dehydration and lowering intracranial pressure were given. Subsequently, the family members agreed to the surgical treatment. On June 13, 2021, supratentorial craniotomy was performed to remove the right frontal lobe space occupying lesion. The surgical procedure was Successful. Postoperative pathology (Figure 4): (right temporal part) poorly metastatic carcinoma with massive hemorrhage and necrosis, which combined with immunophenotype conforms to poorly differentiated squamous cell carcinoma. After the operation, gefitinib (250mg Qd)was taken orally for targeted treatment without complaints of discomfort.

On July 17, 2021, she came our department for continuing treatment with occasional headache, acupuncture-like, which can relief itself. Physical examination: The general condition was good, no abnormality in the heart, lungs and abdomen, and no swelling of both lower extremities. And echocardiography (outside hospital on 2021-7-15): hypoechoic left atrial cavity, consider: space-occupying lesion. After admission, the blood routine, urine routine, liver and kidney function, tumor markers

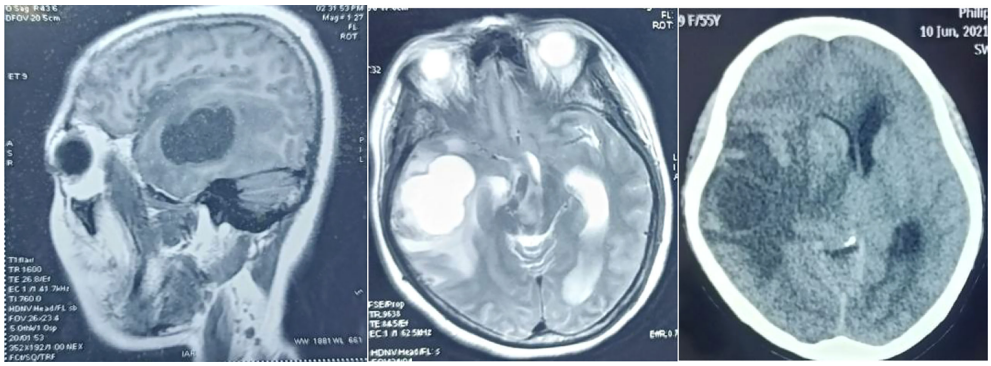

FIGURE 3
Head MRI.

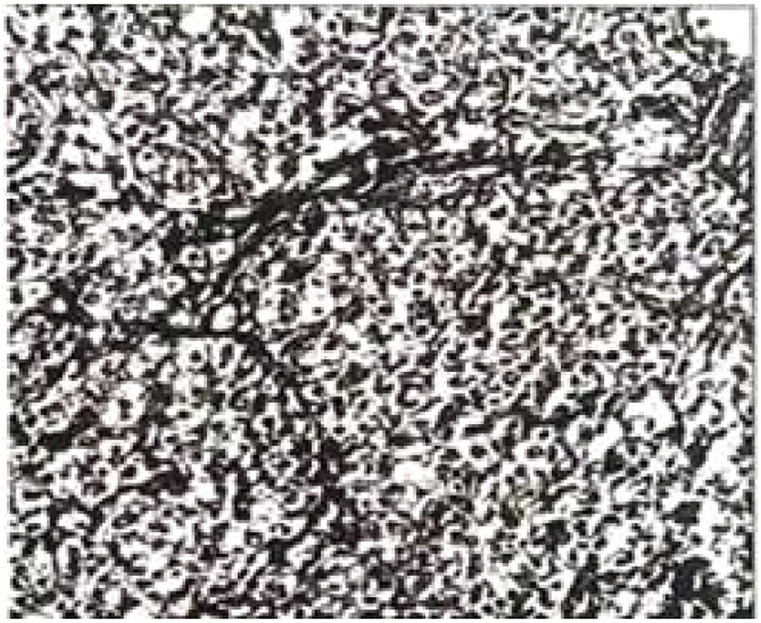

FIGURE 4
Postoperative pathology (head).

were within the normal range, and the electrocardiogram was generally normal. Cranial MRI,Chest and whole abdominal CT: no recurrence and metastasis were found, and repeated echocardiography: medium echogenic mass in the left atrium (about 1.8cm×2.9cm in size), see Figure 5. The patient developed chest tightness and palpitation, and the electrocardiogram showed atrial fibrillation. After symptomatic treatment, sinus rhythm was restored. On 2021-07-23, left atrial tumor resection

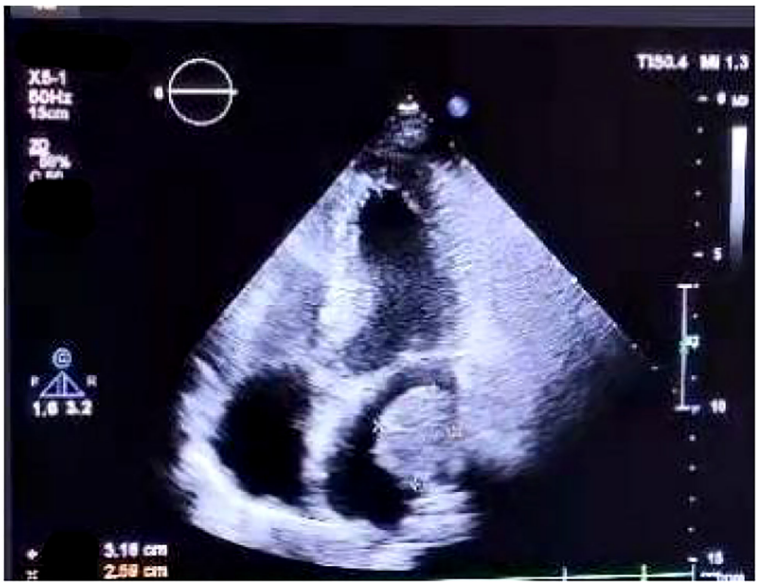

FIGURE 5
Echocardiography.

was performed under general anesthesia and low-temperature cardiopulmonary bypass. Postoperative pathology (Figure 6) suggests (left atrium) malignancy, tending to poorly differentiated adenosquamous carcinomamalignant tumors,. Gene detection: EGFR-p.E746_A750del, T790M(-).Therapy was replaced with afatinib(40mg Qd). Since the operation, the general state is good, and no recurrence (Figure 7).

Discuss

According to the current epidemiological survey, the incidence and mortality of lung cancer are now at the forefront (2). Lung adenosquamous carcinoma (ASC) is a rare subtype of non-small cell lung cancer, accounting for only 0.4% to 4% of lung cancer patients (3, 4), but research on changes in the spectrum of rare lung tumors suggests: The proportion of adenosquamous carcinoma increased slowly, from 0.84% in 2004 to 1.25% in 2015, and surpassed large cell carcinoma after 2011, becoming the most common tumor among rare lung cancers (5). Its composition includes lung adenocarcinoma (LUAD) and lung squamous cell carcinoma (LUSC) components, and in terms of morphological characteristics, it has the characteristics of classic LUAD and LUSC, but the behavior is more aggressive. The diagnostic criteria is that any component of squamous cell carcinoma and adenocarcinoma accounts for at least 10% of all tumors. Therefore, it is easy to miss diagnosis due to the limitations of biopsy specimens in clinical work.

The different pathology of metastatic lesions and primary lesions in cases reflects a major feature of tumors—heterogeneity. Tumor heterogeneity exists between patients, within tumors, and between tumors, and between-tumor heterogeneity is considered to be the diversity between the primary tumor and its metastases (6–8), which is common in patients with malignant tumors. Moreover,it plays a key role in diagnosis and treatment.

In lung cancer, its heterogeneity is related to different genetic, epigenetic, and non-genetic mechanisms (9, 10). Lung cancer development represents the initiation of a multistep process involving genetic alterations, the most important feature of which is extensive genomic aberrations, including abnormalities, gain and loss of large chromosomal regions, gene rearrangements, copy number gain, amplification (11), and the essence of these molecular-level abnormalities reflects genomic instability. Regardless of risk factors such as tumor stage, age, and gender, genomic instability is often associated with poor prognosis (12, 13), and even genomic diversity contributes to the adaptation of cancer cell populations in the tumor microenvironment, leading to tumor progression and poor prognosis.

Mutant allele-specific imbalance (MASI) is another genetic mechanism that promotes heterogeneity and affects tumor initiation, progression, metastasis, prognosis, and potential therapeutic response. MASI is common in some major oncogenes, such as EGFR, KRAS, PIK3CA, and BRAF (14), and epigenetic modifications induce variability in gene expression, determining a significant diversity according to previous studies. Furthermore, variable pressures in the lung tumor environment can generate inter-and intra-tumor heterogeneity, which affects sensitivity to targeted therapy and immunotherapy response (15).

Given the heterogeneity of lung cancer, the genomic background of ASC has been still poorly understood. They found

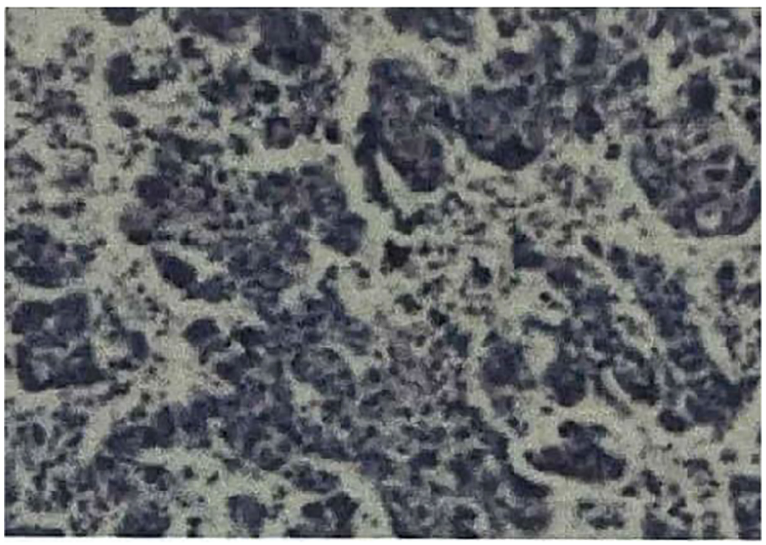

FIGURE 6
Postoperative pathology (Heart)HE × 100.

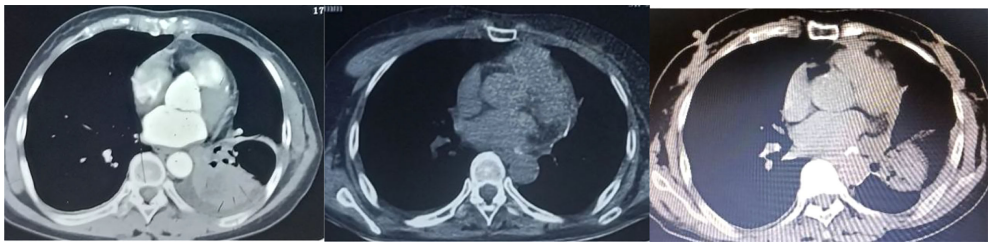

FIGURE 7
Chest CT contrast (From left to right:2019.1-2021.6-2022.4).

that there were not only TP53 mutations, but also EGFR, met and BRAF mutations in adenosquamous cell carcinoma in the project by Arthur Krause et al, who applied whole genome exon sequencing technology to interpret the clonal relationship between adenocarcinoma and squamous cell carcinoma in ASC (16). According to statistics, EGFR mutations were at least as common in ASC as in classical LUAD, with mutation rates of 15% ~ 50%, while only about 2% mutations were reported in LUSC (17–19).

With the advent of new drugs, targeted therapy has become a hotspot in the research and treatment of lung cancer. The most representative is targeted therapy for EGFR mutations in lung denocarcinoma, studies such as LUX-LUNG 7, ARCHER 1050, FLAURA and EVOLUTION (20–25) have confirmed significant benefits for those with EGFR mutations, whether in the first-line, second-line or postoperative adjuvant therapy; Iwanaga et al (26, 27) report that ASC patients after surgery with EGFR sensitive mutation receive gefitinib as a second-line treatment,and achieve a 3-year progression free survival. A study published in the journal ANNALS OF ONCOLOGY further confirmed that EGFR-TKI is effective in treating ASC patients with EGFR mutation positive (1).For oligometastatic lesions during the period of first-line EGFR-TKI treatment, EGFR-TKI treatment can be continued and combined with local treatment. For patients of lung cancer with cardiac metastasis, through literature searching, local treatment, such as surgical resection or radiotherapy, has also got good outcome (28–31).

When lung cancer was found in this patient, surgery was performed. Pathology suggested adenosquamous cell carcinoma. After surgery, gefitinib targeted therapy was performed. Brain metastasis occurred after 2 years, and surgery was performed again. Pathology suggested squamous cell carcinoma. The number of materials was sufficient and the accuracy was high. ASC was basically ruled out. After TKI targeted drug treatment, the patient induced ASC to transform into squamous cell carcinoma. It was speculated that TKI had therapeutic advantages on adenocarcinoma components, which directly leaded to the withering of adenocarcinoma component cells, while squamous cell carcinoma cells gain a quantitative advantage. Cardiac cavity metastasis was found after 1 month of brain metastasis. Postoperative pathology showed adenosquamous cell carcinoma, suggesting the existence of drug resistance and heterogeneity between metastatic lesions. It was replaced with second-generation EGFR-TKI afatinib targeted therapy.

Conclusion

ASC can have pathological transformation during the treatment process, which should be fully considered when making treatment plans; ASC patients with EGFR sensitive mutations can benefit from TKI treatment. Routine EGFR gene testing is recommended for ASC patients; When disease progression occurs in the established treatment plan, the existence of secondary biopsy and gene testing is necessary. We has followed the paitient all the time since she accepted the heart surgery and want to provide treatment ideas for ASC patients by this case. The only inadequacy is that the early treatment of patients is not carried out in our hospital, and some data in particular of figures are not provided clearly.

Data availability statement

The datasets presented in this article are not readily available because of ethical/privacy restrictions. Requests to access the datasets should be directed to the corresponding author.

Ethics statement

The studies involving human participants were reviewed and approved by the Ethics Committee of Drug Clinical Trials of the Second Affiliated Hospital of Shaanxi University of Traditional Chinese Medicine. The patients/participants provided their written informed consent to participate in this study. Written informed consent was obtained from the individual(s) for the publication of any potentially identifiable images or data included in this article.

Author contributions

LG-G was responsible for the clinical design and conceptualization. MJ, OY and TY were involved in the acquisition of the clinical data. SL and GC conducted the clinical diagnosis. LL analyzed and interpreted the data. LG-G and GC wrote the manuscript. All authors contributed to the article and approved the submitted version.

Funding

This study was funded by a grant from Natural Science Foundation of Shaanxi Province(Grant Number: S2020-JC-YB-0123).

Conflict of interest

The authors declare that the research was conducted in the absence of any commercial or financial relationships that could be construed as a potential conflict of interest.

Publisher's note

References

1. Lin G, Li C, Li PS, Fang WZ, Xu HP, Gong YH. Genomic origin and EGFR-TKI treatments of pulmonary adenosquamous carcinoma. *Ann Oncol* (2020) 31 (4):517–24. doi: 10.1016/j.annonc.2020.01.014

2. Zijie C, Qiang L. Understanding the global cancer statistics 2018: implications for cancer control. *Sci China(Life Sciences)* (2021) 64(06):1017–20. doi: 10.1007/s11427-019-9816-1

3. Shimoji M, Nakajima T, Yamatani C, Yamamoto M, Saishou S, Isaka M. A clinicopathological and immunohistological re-evaluation of adenosquamous carcinoma of the lung. *Pathol Int* (2011) 61(12):717–22. doi: 10.1111/j.1440-1827.2011.02730.x

4. Zhu L, Jiang L, Yang J, Gu W, He J. Clinical characteristics and prognosis of patients with lung adenosquamous carcinoma after surgical resection: results from two institutes. *J Thorac Dis* (2018) 10(4):2397–402. doi: 10.21037/jtd.2018.03.186

5. Xie Y, Li S. Spectrum changes and prognosis of rare lung tumors. *Res tumor Prev Treat* (2020) 47(06):432–6.

6. Jamal-Hanjani M, Quezada SA, Larkin J, Swanton C. Translational implications of tumor heterogeneity. *Clin Cancer Res* (2015) 21:1258–66. doi: 10.1158/1078-0432.CCR-14-1429

7. Rich JN. Cancer stem cells: understanding tumor hierarchy and heterogeneity. *Med (Baltimore).* (2016) 95(1 Suppl 1):S2–7. doi: 10.1097/MD.0000000000004764

8. Burrell RA, McGranahan N, Bartek J, Swanton C. The causes and consequences of genetic heterogeneity in cancer evolution. *Nature* (2013) 501:338–45. doi: 10.1038/nature12625

9. Neelakantan D, Drasin DJ, Ford HL. Intratumoral heterogeneity: Clonal cooperation in epithelial-to-mesenchymal transition and metastasis. *Cell Adh Migr.* (2015) 9:265–76. doi: 10.4161/19336918.2014.972761

10. McGranahan N, Swanton C. Clonal heterogeneity and tumor evolution: Past, present, and the future. *Cell* (2017) 168:613–28. doi: 10.1016/j.cell.2017.01.018

11. Mettu RKR, Wan YW, Habermann JK, Ried T, Guo NL. A 12-gene genomic instability signature predicts clinical outcomes in multiple cancer types. *Int J Biol Markers.* (2010) 25:219–28. doi: 10.5301/JBM.2010.6079

12. Yoo JW, Seo KW, Jang SJ, Oh YM, Shim TS, W, Kim S, et al. The relationship between the presence of chromosomal instability and prognosis of squamous cell carcinoma of the lung: fluorescence *in situ* hybridization analysis of paraffin-embedded tissue from 47 Korean patients. *J Korean Med Sci* (2010) 25:863–7. doi: 10.3346/jkms.2010.25.6.863

13. Lee AJ, Endesfelder D, Rowan AJ, Walther A, Birkbak NJ, Futreal PA, et al. Chromosomal instability confers intrinsic multidrug resistance. *Cancer Res* (2011) 71:1858–70. doi: 10.1158/0008-5472.CAN-10-3604

14. Soh J, Okumura N, Lockwood WW, Yamamoto H, Shigematsu H, Zhang W, et al. Oncogene mutations, copy number gains and mutant allele specific imbalance (MASI) frequently occur together in tumor cells. *PloS One* (2009) 7464: 1–13. doi: 10.1371/journal.pone.0007464

15. Marino FZ, Ascierto PA, Rossi G, Staibano S, Montella M, Russo D, et al. Are tumor-infiltrating lymphocytes protagonists or background actors in patient selection for cancer immunotherapy? *Expert Opin Biol Ther* (2017) 17:735–46. doi: 10.1080/14712598.2017.1309387

16. Krause A, Roma L, Lorber T, Habicht J, Lardinois D, de Filippo MR, et al. Deciphering the clonal relationship between glandular and squamous components in adenosquamous carcinoma of the lung using whole exome sequencing. *Lung Cancer* (2020) 150: 132–138. doi: 10.1016/j.lungcan.2020.10.013

17. Shi X, Wu H, Lu J, Duan H, Liu X, Liang Z, et al. Screening for major driver oncogene alterations in adenosquamous lung carcinoma using PCR coupled with next-generation and Sanger sequencing methods. *Sci Rep* (2016) 22297:1–9. doi: 10.1038/srep22297

18. Hsu K-H, Ho C-C, HsiaTC, TsengJS, SuKY, WuMF. Identification of five driver gene mutations in patients with treatment-naïve lung adenocarcinoma in Taiwan. *PloS One* (2015) 10(3):e0120852. doi: 10.1371/journal.pone.0120852

19. Network T.C.G.A.R. The cancer genome atlas research network. *Compr Mol profiling Lung adenocarcinoma Nat* (2014) 511:543–50.

20. Wu YL, Cheng Y, Zhou X, Lee HK, Nakagawa K, Niho S, et al. Dacomitinib versus gefitinib as firstline treatment for patients with, EGFR -mutation-positive non-smallcell lung cancer (ARCHER 1050): a randomised, openlabel, phase 3 trial. *Lancet Oncol* (2017) 18(11):1454–66. doi: 10.1016/S1470-2045(17)30608-3

21. He J, Su C, Liang W, Xu S, Wu L, Fu X, et al. Icotinib versus chemotherapy as adjuvant treatment for stage II–IIIA EGFR-mutant NSCLC (EVIDENCE): A randomized, open-label, phase 3 study. *Lancet Respir Med* (2021) 9(9):1021–1029. doi: 10.1016/j.jtho.2021.01.154

22. Pennell NA, Neal JW, Chaft JE, Azzoli CG, Jänne PA, Govindan R, et al. SELECT: a phase II trial of adjuvant erlotinib in patients with resected epidermal growth factor receptor–mutant non–small-cell lung cancer. *J Clin Oncol* (2019) 37 (2):97. doi: 10.1200/JCO.18.00131

23. Zhong W-Z, Wang Q, Mao W-M, Xu S-T, Wu L, Wei Y-C, et al. Gefitinib versus vinorelbine plus cisplatin as adjuvant treatment for stage II-IIIA (N1-N2) EGFR-mutant NSCLC: Final overall survival analysis of CTONG1104 phase III trial. *J Clin Oncol* (2021) 39(7):713–22. doi: 10.1200/JCO.20.01820

24. Planchard D. Adjuvant osimertinib in EGFR-mutated non–Small-Cell lung cancer. *New Engl J Med* (2020) 383(18):1780–2. doi: 10.1056/NEJMe2029532

25. Yue D, Xu S, Wang Q, Li X, Shen Y, Zhao H, et al. Erlotinib versus vinorelbine plus cisplatin as adjuvant therapy in Chinese patients with stage IIIA EGFR mutation-positive non-small-cell lung cancer (EVAN): a randomised, open-label, phase 2 trial. *Lancet Respir Med* (2018) 6(11):863–73. doi: 10.1016/S2213-2600(18)30277-7

26. Iwanaga K, Sueoka-Aragane N, Nakamura T, Mori D, Kimura S. The long-term survival of a patient with adenosquamous lung carcinoma harboring EGFR-activating mutations who was treated with gefitinib. *Int Medi* (2012) 51(19):2771–4. doi: 10.2169/internalmedicine.51.7428

27. Song Z, Lin B, Shao L, Zhang Y. Therapeutic efficacy of ge-fitinib and erlotinib in patients with advanced lung ade-nosquamous carcinoma. *J Chin Medi Associ (JCMA)* (2013) 76(9):481–5. doi: 10.1016/j.jcma.2013.05.007

28. Spiliopoulos K, Engels P, Kimpouri K, Floudas I, Salemis NS, Schmid FX, et al. The current role of surgery in the treatment of cardiac metastases from malignant melanoma: an educational presentation. *Braz J Cardiovasc Surg* (2021) 36(1): 112–115. doi: 10.21470/1678-9741-2020-0379

29. Sim AJ, Palm RF, DeLozier KB, Feygelman V, Latifi K, Redler G, et al. MR-guided stereotactic body radiation therapy for intracardiac and pericardial metastases. *Clin Trans Radiat Oncol* (2020) 25.

30. Tamura Y, Kawaoka T, Aikata H, Namba M, Fujii Y, Morio K, et al. Isolated cardiac metastases of hepatocellular carcinoma after resection: a case report. *Clin J Gastroenterol* (2020) 13(3): 421–427. doi: 10.1007/s12328-019-01075-6

31. Maebayashi A, Nagaishi M, Nakajima T, Hata M, Xiaoyan T, Kawana K, et al. Successful surgical treatment of cardiac metastasis from uterine leiomyosarcoma: A case report and literature review. *J obstetrics gynaecol. Res* (2020) 46(5): 795–800. doi: 10.1111/jog.14231

frontiers | Frontiers in Oncology

TYPE Case Report
PUBLISHED 19 October 2022
DOI 10.3389/fonc.2022.1008932

OPEN ACCESS

EDITED BY
Kohei Fujita,
National Hospital Organization Kyoto Medical Center, Japan

REVIEWED BY
Jin Kang,
Guangdong Provincial People's Hospital, China
Song Xu,
Tianjin Medical University General Hospital, China

*CORRESPONDENCE
Zheng Ma
drmar2021@163.com

SPECIALTY SECTION
This article was submitted to Thoracic Oncology, a section of the journal Frontiers in Oncology

RECEIVED 03 August 2022
ACCEPTED 27 September 2022
PUBLISHED 19 October 2022

CITATION
Xu X, Shi Z, Fu D, Huang D and Ma Z (2022) *EGFR* mutations and high PD-L1 expression of lung squamous cell carcinoma patients achieving pCR following neoadjuvant immuno-chemotherapy: Case report. *Front. Oncol.* 12:1008932. doi: 10.3389/fonc.2022.1008932

EGFR mutations and high PD-L1 expression of lung squamous cell carcinoma patients achieving pCR following neoadjuvant immuno-chemotherapy: Case report

Xiangyu Xu[1], Zixia Shi[1], Dan Fu[2], Depei Huang[2] and Zheng Ma[1]*

[1]Department of Thoracic Surgery, Chongqing General Hospital, Chongqing, China, [2]The Medical Department, 3D Medicines Inc., Shanghai, China

The treatment of lung cancer has fully entered the era of immunotherapy, which has significantly elevated the survival rate of patients with advanced non-small cell lung cancer (NSCLC), thus shedding light on resectable NSCLC. Previous clinical trial data suggested that neoadjuvant immuno-chemotherapy obtained a significant objective response rate (ORR) and disease control rate (DCR). Here, a case that achieved an excellent outcome following neoadjuvant immuno-chemotherapy was reported. The patient admitted to our hospital was 58 years old, female, with a rare case of stage IB lung squamous cell carcinoma (LUSC) harboring both epidermal growth factor receptor (*EGFR*) p.L858R mutations and high expression of programmed death ligand-1 (PD-L1) (tumor proportion score (TPS)=80%). Her tumor substantially shrunk following two cycles of neoadjuvant immuno-chemotherapy. The patient successively received single-port right upper thoracoscopic lobectomy + mediastinal lymph node dissection, which attained pathologic complete response (pCR). Additionally, the patient had grade 2 myelosuppression during the two cycles, which was treated with polyethylene glycol recombinant human granulocyte colony-stimulating factor (rhG-CSF). The patient was discharged uneventfully without any procedure-related complications. Two courses of adjuvant immuno-chemotherapy were administered postoperatively, leaving the patient in good physical condition at the 5-month follow-up visit. This case provided evidence for the feasibility and effectiveness of neoadjuvant immuno-chemotherapy in treating early-stage LUSC with *EGFR* mutations and high expression of PD-L1. However, randomized and multi-center controlled trials are required to validate the findings.

KEYWORDS

neoadjuvant immunotherapy, lung squamous cell carcinoma, epidermal growth factor receptor (EGFR), mutations, pembrolizumab, programmed death ligand-1 (PD-L1)

Introduction

As the molecular biology of lung cancer advances, immunotherapy and targeted therapy have become standard treatment protocols for advanced lung cancer in clinical practices with their application in early-stage lung cancer explored as well. Several clinical trials have proved the safety and efficacy of programmed death-1 (PD-1)/programmed death ligand-1 (PD-L1) inhibitors of neoadjuvant therapy in resectable non-small cell lung cancer (NSCLC) (1). The Checkmate 816 trial (2) was the first phase III randomized clinical trial to substantiate that neoadjuvant immuno-chemotherapy can significantly raise the percentage of pathologic complete response (pCR) in patients with resectable NSCLC, which was also the first and only preoperative neoadjuvant therapy protocol for lung cancer approved by the Food and Drug Administration (FDA). Moreover, identical to NEOSTAR (3) and NADIM (4) studies, patients with epidermal growth factor receptor (*EGFR*) +/anaplastic lymphoma kinase (*ALK*)+ were excluded and protein expression of PD-LI in baseline tumors was assessed in the Checkmate 816 trial, which revealed the association between up-regulated expression of *PD-L1* and patient's response to neoadjuvant immunotherapy. The targeted therapy exhibited prominent efficacy in treating NSCLC with *EGFR* mutations, especially the third generation of EGFR-tyrosine kinase inhibitors (EGFR-TKIs), which played essential roles in first/later line treatment and postoperative adjuvant therapy. However, only a few studies concerning neoadjuvant targeted therapy in lung cancer are available. NeoADAURA (5) and CTONG1103 (6) trials confirmed the efficacy and safety of neoadjuvant targeted therapy in patients with *EGFR* mutations, presenting superior clinical outcomes than neoadjuvant chemotherapy, while the effectiveness and safety of *EGFR*-TKIs of the neoadjuvant therapy for NSCLC remain undetermined. Hence, the optimal neoadjuvant therapy protocol is still undefined for NSCLC patients harboring both *EGFR*-sensitive mutations and *PD-L1* positive. Here, we reported a case of stage IB LUSC with *EGFR* mutation, *PD-L1* TPS=80%, and poor preoperative immune microenvironment who achieved pCR following neoadjuvant immuno-chemotherapy.

Case description

The 58-year-old patient was female and visited our hospital for one-month hemoptysis with no history of chronic diseases, smoking, and alcohol use (Figure 1). The X-ray and enhanced computed tomography (CT) demonstrated a mass in the upper lobe of the right lung (about 3.7 cm × 3.4 cm × 3.5 cm) with lobulated border and burrs, partially-occluded bronchial branches, and there were no obvious enlargement of mediastinal and bilateral hilar lymph nodes, and partial calcification. Central lung cancer was considered (Figures 2A–D). Carcinoembryonic antigen (CEA) was 86.98 ng/ml and the cytokeratin 19 fragment (CY21-1) was 4.06 ng/ml. Fiberoptic bronchoscopy indicated neoplasms in the posterior segment of the right upper lung, endoscopic biopsy suggested NSCLC (Figures 2G, H), and immunohistochemistry showed P40(+) and TTF-1 (–), suggestive of squamous cell carcinoma (Figures 3A, B). A few dyskaryotic cells were detected in bronchoalveolar lavage fluid (BALF). No significant metastasis was identified *via* upper abdominal enhanced CT scan, contrast-enhanced magnetic resonance imaging (MRI) of the head, and whole-body bone emission CT (ECT) scan. Taken together, the patient was classified as cT2aN0M0, stage IB. The patient's tumor was closely related to the right upper pulmonary artery branch (Figure 2C), and the possibility of angioplasty during direct surgery was high, increasing the risk of surgery. There is also the possibility of conversion to thoracotomy, which would be more traumatic for the patient. Considering that the patient

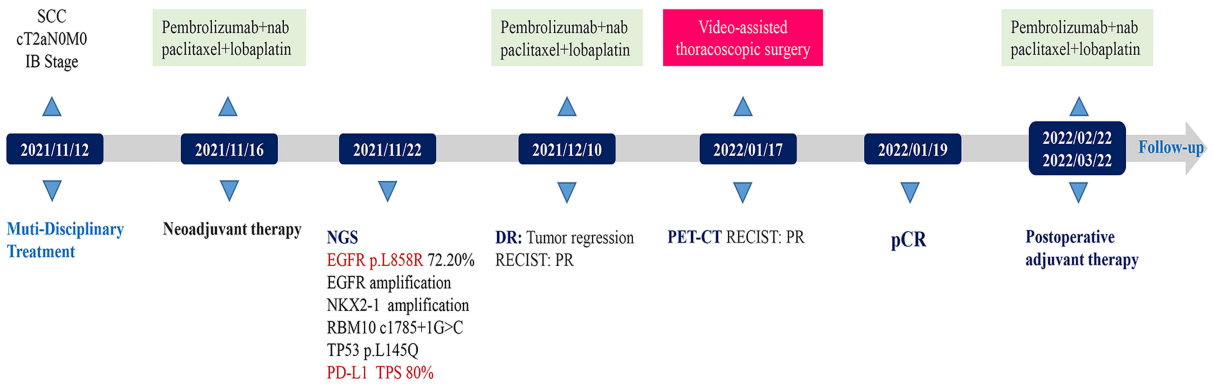

FIGURE 1
Treatment timeline of the patient.

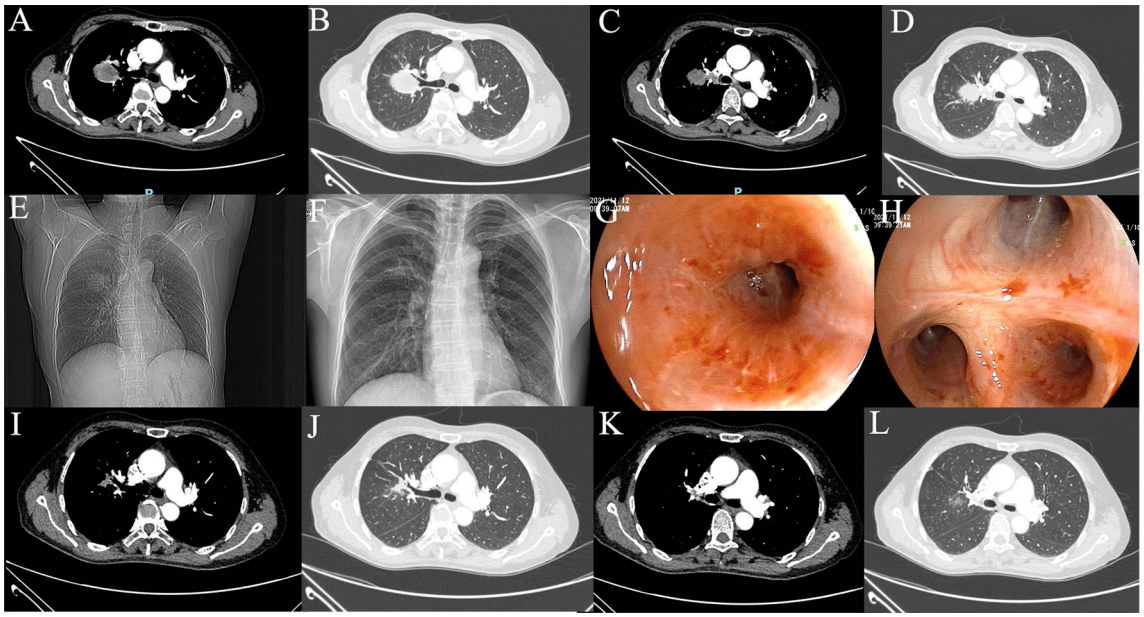

FIGURE 2
Imaging examination. **(A–D)** Preoperative CT scan; **(E)** Preoperative DR image; **(F)** DR image after one cycle of neoadjuvant therapy; **(G, H)** Preoperative fiberoptic bronchoscopy image; **(I–L)** CT image after 2 cycles of neoadjuvant therapy.

was a squamous carcinoma with a low possibility of having driver mutations, the multidisciplinary consultation recommended that neoadjuvant immune combination chemotherapy treatment should be performed first followed by surgery while waiting for NGS test and immunohistochemistry results. After signing the informed consent, the patient received anti-PD-1 therapy plus platinum-based neoadjuvant therapy (intravenous injection of 200 mg Pembrolizumab, 30 mg/m^2 lobaplatin + 260 mg/m^2 nab-paclitaxel, D1, q3w). The patient developed grade 2 myelosuppression during therapy, which was treated with an injection of polyethylene glycol recombinant human granulocyte colony-stimulating factor (rhG-CSF) with no grade 3-5 adverse events (AEs) observed. In the meantime, next-generation sequencing (NGS) and immunohistochemical (IHC) detected *EGFR* p.L858R mutations (abundance 72.2%), PD-L1 expression (TPS=80%, CPS(Combined Positive Score)

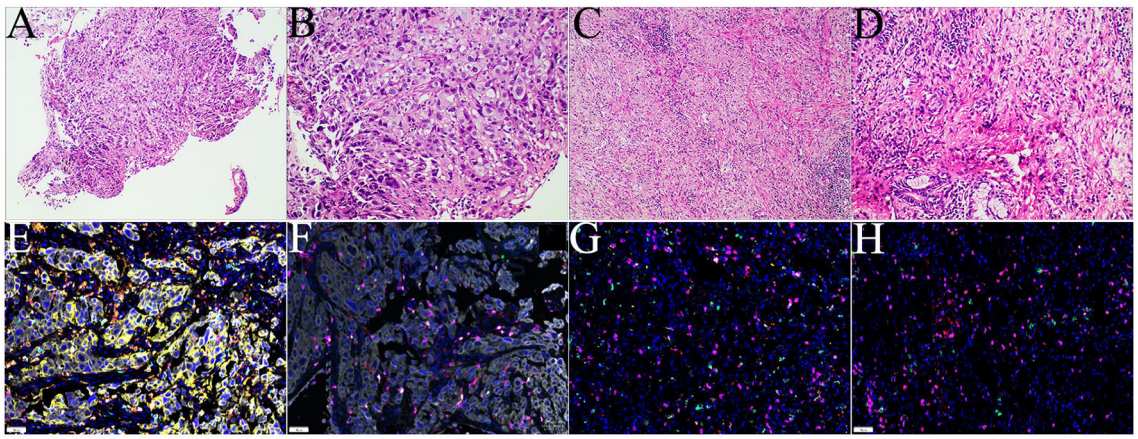

FIGURE 3
Examinations of pathology and mIHC. **(A, B)**. Histology of biopsies samples (CT guided biopsy);**(C, D)** histology of surgical tissue sample; **(E, F)** mIHC staining of tumor microenvironment of puncture tissue; **(G, H)** mIHC staining of tumor microenvironment after operation.

=80), and tumor mutational burden (TMB, 5.03Mut/Mb), accompanied by EGFR copy-number amplification as well as multiple gene mutations, such as *NKX2-1* and *TP53*. Considering the occurrence of *EGFR* mutation, the followed therapy was dilemma, which dependent on the outcome of the first treatment session as informed before. After one course of neoadjuvant immunochemotherpy, CEA and CY21-1 were 23.17 ng/ml and 2.43 ng/ml, respectively, significantly lower than the pre-treatment levels. In the meantime, chest digital radiography (DR) showed a reduction of the right upper lung occupancy (Figures 2E, F), implying partial radiographical response. So, the second cycle immunochemotherapy was perfomed as plan. Three weeks later, subsequent to the application of the second course of neoadjuvant therapy, a chest X-ray and enhanced CT scan were performed, indicating a marked reduction of the lesion in the right upper lung(about 1.9 cm × 1.4 cm) with partially bronchial stricture. At this point, CEA and CY21-1 were 3.06 ng/ml and 1.81 ng/ml respectively. Besides, positron emission tomography-computed tomography (PET-CT) illustrated an irregular patchy hyperdense shadow (2.76 cm × 2.18 cm × 1.59 cm) near the hilum of the right lung upper lobe and a mild increase in radioactivity uptake (maximum SUV = 2.57, mean SUV = 2.37), indicating that the tumor activity was remarkably suppressed (Figures 2I-L). Partial response (PR) was assessed according to the Response Evaluation Criteria in Solid Tumors (RECIST) version 1.1. In the fifth week after the neoadjuvant therapy, the single-port right upper thoracoscopic lobectomy + mediastinal lymph node dissection was successfully performed, during which the blood loss was approximately 50 ml. Postoperative pathology (Figures 3C, D)showed that the mass was 2.5 cm × 2 cm × 1.5 cm and that the fibrous tissue of the tumor bed exhibited hyperplasia with degeneration. Lymphocytes infiltrated the areas containing multinucleated giant cells and foam cells without residual disease; the bronchial mucosa manifested chronic inflammation without residualdisease. Efficacy assessment of neoadjuvant therapy showed that pCR was achieved. The lymph nodes of 2R (0/2), 3A (0/2), 4R (0/1), group 7 (0/1), group 10 (0/1), group 11 (0/7), and group 12 (0/1) were disease-free. The bronchial stump of the right upper lung was also free of cancer cells. The patient recovered well and was discharged without any operation-related complications. Biopsy tissues and surgical samples were examined using multiplex immunohistochemistry (mIHC) to reveal the alterations of the tumor microenvironment (TME) after the application of neoadjuvant therapy, especially the inflammatory and immune cells. mIHC of biopsy tissues (Figures 3E, F) illustrated intratumoral presence of CD8+ T cells (111/mm2), and high infiltration of FoxP3 (244/mm^2) and CD68 + CD163 + M2 macrophages (139/mm^2). In the surgical samples (Figures 3G, H), large amounts of CD8+ T cells (511/mm^2) and tertiary lymphoid structures were observed, while the number of CD68 + CD163 + M2 macrophages (32/mm^2) and FoxP3+ (60/mm^2) were substantially decreased. No genetic mutation was detected in the ctDNA of peripheral blood at the fourth postoperative week. The patient started receiving two cycles of adjuvant immuno-chemotherapy (intravenous injection of 200 mg Pembrolizumab, 30 mg/m^2 lobaplatin + 260 mg/m^2 nab-paclitaxel, D1, q3w) at the fifth week after surgery. The patient was in good physical condition at the 5-month follow-up visit and refused to accept the one-year single-agent immunotherapy due to financial factors.

Discussion

Multiple clinical studies (7) proved that neoadjuvant immune monotherapy or combined treatment played a crucial part in the treatment of early-stage NSCLC. The major pathologic response (MPR) rate of neoadjuvant immune monotherapy was 17% - 45% and the pCR was unsatisfactory (0%-16%), while the immuno-chemotherapy resulted in higher MPR (36.9%-83%) and pCR (24%-63%) with manageable AEs and no delay of the surgical schedule. Nevertheless, most of these studies excluded patients with *EGFR+/ALK+*. For advanced NSCLC patients with PD-L1 TPS >50%, immune checkpoint inhibitors(ICIs) prolonged the overall survival(OS) of patients with greater safety, as compared to the platinum-based doublet chemotherapy (8). Under neoadjuvant therapy, patients with high PD-L1 expression also tended to exhibit a higher response rate to immunotherapy. In the Checkmate 816 trial (2), neoadjuvant immuno-chemotherapy was confirmed to be effective in treating stage IB lung cancer, in which the pCR reached 40% and the event-free survival (EFS) risk was lowered by 76% in patients with PD-L1>50%.

EGFR or *ALK* gene alterations occur in patients with LUSC, especially non-smoking females, in which TKI treatments present clinical benefits in disease control with a considerably shorter drug-resistant duration in LUSC patients than in lung adenocarcinoma (LUAD) patients (9). A previous study (10) reported that the first-line pembrolizumab treatment was superior to conventional chemotherapy for lung cancer patients with high PD-L1 expression, and the subgroup analysis showed that pembrolizumab was more effective in treating LUSC than non-LUSC. Besides, the subgroup analysis conducted in the Checkmate 816 trial demonstrated the efficacy of preoperative neoadjuvant immono-chemotherapy in both LUAD and LUSC, while the efficacy was more significant in LUAD (HR: 0.5 vs HR: 0.77); this therapy also reduced the risk of recurrence or mortality by 23% (HR = 0.77) among LUSC patients versus chemotherapy alone, exhibiting therapeutic advantage (2). A cell experiment performed by Zhang et al. (11) revealed that higher PD-L1 expression was associated with lower sensitivity to EGFR-TKI of *EGFR*-mutant NSCLC cell lines, which leads to epithelial-to-mesenchymal transition (EMT) induced by the upregulation of Smad3 phosphorylation, potentially contributing to primary drug resistance.

Previous studies have reported that the efficacy of ICIs among NSCLC patients with EGFR mutations was minimal, and even *EGFR* alteration was considered to be related to the hyperprogression induced by ICIs, especially-monotherapy. In a single-center retrospective study (12), the objective response rate (ORR) yielded by immunotherapy of driver mutation-positive lung cancer was only 3.8%; while in another phase 2 clinical trial (NCT02879994), the ORR yielded by first-line pembrolizumab monotherapy was 0% among seven advanced NSCLC patients with *EGFR* mutations and strong PD-L1 expression (13). However, in the trials of IMPOWER 150, KEYNOTE-789, and CheckMate-722 (14–16), the advanced NSCLC patients with high *PD-L1* expression and EGFR mutations responded well to immunotherapy combined with chemotherapy or anti-vascular endothelial growth factor (VEGF)agents. Collectively, ICIs should not be completely excluded in the treatment of *EGFR*-mutated NSCLC.

Several clinical trials also investigated the safety and efficacy of ICIs plus EGFR-TKIs. Jänne et al. (17) revealed that in advanced *EGFR*-mutated NSCLC patients administered with first-line osimertinib plus durvalumab, ORR was 82% (48–98), the median duration of response (DOR) was 7.1 months and median progression-free survival (PFS) was 9.0 months. However, the enrollment in this patient cohort was terminated due to the potential risk of interstitial lung disease (ILD)-related AEs. Considering the increased risk of treatment-related AEs as well as limited efficacy and benefits, the treatment strategy of ICIs plus EGFR-TKIs is possibly unacceptable.

A preclinical study (18) discovered that the activation of the EGFR pathway up-regulated the expression of PD-1, PD-L1, cytotoxic T lymphocyte antigen-4 (CTLA-4), and proinflammatory cytokines, rendering the feature of immunosuppression. This suggested that oncogenic *EGFR* signaling triggered immune escape by remodeling the TME. In the present case, the patient's postoperative TME showed a significant increase of CD8 + T cells and an evident decrease of FoxP3 and CD68+CD163+ M2 macrophages(Supplementary Figure), together with the occurrence of tertiary lymphoid structure. T cells suppressed the anti-tumor functions of immune effector cells and were involved in tumor immune escape (19); M2 macrophages secreted anti-inflammatory cytokines and modulated wound healing to exert the immunosuppressive effects (20), and the tertiary lymphoid structure was associated with a promising prognosis immunotherapy response (21). Immuno-chemotherapy can directly kill cancer cells and regulate immune response to improve the tumor-immune microenvironment (TIME), thereby achieving better efficacy (22).

The ORR of neoadjuvant EGFR- TKI in the EGFR-sensitive mutation population is 48% and early stage NSCLC may reduce the ORR of neoadjuvant EGFR-TKIs (23), and the MPR of neoadjuvant Osimertinib was 15% (5). However the evidence for neoadjuvant targeted therapy especially in these subgroups of EGFR mutation status, PD-L1 expression is still not sufficient. In our case, ICIs were administered prior to EGFR-TKIs, given the low occurrence of driver gene mutation in LUSC, and the limited benefits of EGFR-TKIs. Besides, ICIs were more effective for LUSC, and their combination with chemotherapy might exhibit better efficacy with unknown expression of PD-L1. Due to the imaging remission, the treatment protocol was kept unchanged when the NGS- and IHC suggested high PD-L1 expression and *EGFR* p.L858R mutations accompanied by variation in multiple genes such as *EGFR* amplification. Finally, the patient underwent complete tumor resection and achieved pCR without grade 3-5 AEs during the treatment.

It was reported (24) that after receiving the first-line immuno-monotherapy, an elderly patient with metastatic squamous cell lung cancer harboring both *EGFR* mutation and high PD-L1 expression presented with continuously aggravated conditions and died 6 months later. Additionally, Oguri T et al. (25) reported that atezolizumab monotherapy led to immunotherapy-related hyperprogression in a patient with *EGFR* p.L858R-mutated pulmonary pleomorphic carcinoma. Similar to the above two cases, our case also involved high PD-L1 expression and *EGFR* p.L858R mutations with FOXP3 and M2 macrophages in the preoperative immune microenvironment, which was associated with the development of hyper progressive diseases (HPDs). Yet the tumor was obviously diminished without signs of HPD following the neoadjuvant immuno-chemotherapy, which may be attributed to the effects of immuno-chemotherapy on TIME and the good prognosis the therapy yielded. Still, HPD requires further exploration. Furthermore, Li et al. (26) reported an NSCLC patient with high PD-L1 expression, *EGFR* mutations, and cold tumors who experienced disease progression 3 weeks after neoadjuvant immuno-chemotherapy with LUAD different from LUSC in our case. Huang et al. (27) revealed that the squamous cell carcinoma components of lung adenosquamous adenocarcinoma were likely transformed from adenocarcinoma components and that EGFR-TKIs were effective for advanced *EGFR*-mutant lung adenosquamous carcinoma. Nevertheless, further researches on the immune microenvironment and immunotherapy of lung adenosquamous carcinoma need to be carried out.

Some limitations are present in this case. On the one hand, only one individual case was reported, thus it is tricky to promote this treatment protocol. On the other hand, due to the heterogeneity of tumor tissues, initial findings in pathologic biopsy were potentially inconsistent with the final ones, which means that adenosquamous carcinoma or inconsistent gene expression were probable, posing a potential risk for the selection of optimal neoadjuvant therapy modality.

Taken together, we reported a patient with stage IB NSCLC and LUSC harboring high PD-L1 expression and *EGFR* mutations who achieved pCR after two courses of neoadjuvant therapy of platinum-based chemotherapy plus pembrolizumab. This case illustrated the feasibility and effectiveness of neoadjuvant immuno-chemotherapy in treating early LUSC with *EGFR* mutations and high PD-L1 expression. Nonetheless, the conclusion requires validation in more patient samples. Moreover, therapeutic genes and biomarkers need to be further explored to select the optimal

treatment protocol for clinical scenarios with co-existing PD-L1 upregulation and *EGFR* sensitivity mutation.

Data availability statement

The datasets presented in this article are not readily available because of ethical/privacy restrictions. Requests to access the datasets should be directed to the corresponding author.

Ethics statement

The studies involving human participants were reviewed and approved by Chongqing General Hospital of ethics committee. The patients/participants provided their written informed consent to participate in this study.

Author contributions

ZM was responsible for the organization and coordination of the case. XX was the attending physician. XX, ZS, and DH contributed to data collection. XX and DF were responsible for original draft preparation. All authors contributed to the article and approved the submitted version.

Conflict of interest

DF and DH were employed by the 3D Medicines Inc.

The remaining authors declare that the research was conducted in the absence of any commercial or financial relationships that could be construed as a potential conflict of interest.

Publisher's note

All claims expressed in this article are solely those of the authors and do not necessarily represent those of their affiliated organizations, or those of the publisher, the editors and the reviewers. Any product that may be evaluated in this article, or claim that may be made by its manufacturer, is not guaranteed or endorsed by the publisher.

Supplementary material

The Supplementary Material for this article can be found online at: https://www.frontiersin.org/articles/10.3389/fonc.2022.1008932/full#supplementary-material

References

1. Provencio M, Calvo V, Romero A, Spicer JD, Cruz-Bermudez A. Treatment sequencing in resectable lung cancer: The good and the bad of adjuvant versus neoadjuvant therapy. *Am Soc Clin Oncol Educ Book* (2022) 42:1–18. doi: 10.1200/EDBK_358995

2. Forde PM, Spicer J, Lu S, Provencio M, Mitsudomi T, Awad MM, et al. Neoadjuvant nivolumab plus chemotherapy in resectable lung cancer. *N Engl J Med* (2022) 386(21):1973–85. doi: 10.1056/NEJMoa2202170

3. Cascone T, William WNJr., Weissferdt A, Leung CH, Lin HY, Pataer A, et al. Neoadjuvant nivolumab or nivolumab plus ipilimumab in operable non-small cell lung cancer: the phase 2 randomized NEOSTAR trial. *Nat Med* (2021) 27(3):504–14. doi: 10.1038/s41591-020-01224-2

4. Provencio M, Nadal E, Insa A, García-Campelo MR, Casal-Rubio J, Dómine M, et al. Neoadjuvant chemotherapy and nivolumab in resectable non-small-cell lung cancer (NADIM): an open-label, multicentre, single-arm, phase 2 trial. *Lancet Oncol* (2020) 21(11):1413–22. doi: 10.1016/S1470-2045(20)30453-8

5. Tsuboi M, Weder W, Escriu C, Blakely C, He J, Dacic S, et al. Neoadjuvant osimertinib with/without chemotherapy versus chemotherapy alone for EGFR-mutated resectable non-small-cell lung cancer: NeoADAURA. *Future Oncol* (2021) 17(31):4045–55. doi: 10.2217/fon-2021-0549

6. Zhong WZ, Chen KN, Chen C, Gu CD, Wang J, Yang XN, et al. Erlotinib versus gemcitabine plus cisplatin as neoadjuvant treatment of stage IIIA-N2 EGFR-mutant non-Small-Cell lung cancer (EMERGING-CTONG 1103): A randomized phase II study. *J Clin Oncol* (2019) 37(25):2235–45. doi: 10.1200/JCO.19.00075

7. Chen S, Zhao Z, Long H. Application of neoadjuvant immuno-chemotherapy in NSCLC. *Zhongguo Fei Ai Za Zhi* (2021) 24(4):284–92. doi: 10.3779/j.issn.1009-3419.2021.102.10

8. Mok TSK, Wu Y-L, Kudaba I, Kowalski DM, Cho BC, Turna HZ, et al. Pembrolizumab versus chemotherapy for previously untreated, PD-L1-expressing, locally advanced or metastatic non-small-cell lung cancer (KEYNOTE-042): a randomised, open-label, controlled, phase 3 trial. *Lancet* (2019) 393(10183):1819–30. doi: 10.1016/S0140-6736(18)32409-7

9. Lewis WE, Hong L, Mott FE, Simon G, Wu CC, Rinsurongkawong W, et al. Efficacy of targeted inhibitors in metastatic lung squamous cell carcinoma with EGFR or ALK alterations. *JTO Clin Res Rep* (2021) 2(11):100237. doi: 10.1016/j.jtocrr.2021.100237

10. Reck M, Rodriguez-Abreu D, Robinson AG, Hui R, Csoszi T, Fulop A, et al. Pembrolizumab versus chemotherapy for PD-L1-Positive non-Small-Cell lung cancer. *N Engl J Med* (2016) 375(19):1823–33. doi: 10.1056/NEJMoa1606774

11. Zhang Y, Zeng Y, Liu T, Du W, Zhu J, Liu Z, et al. The canonical TGF-beta/Smad signalling pathway is involved in PD-L1-induced primary resistance to EGFR-TKIs in EGFR-mutant non-small-cell lung cancer. *Respir Res* (2019) 20(1):164. doi: 10.1186/s12931-019-1137-4

12. Gainor JF, Shaw AT, Sequist LV, Fu X, Azzoli CG, Piotrowska Z, et al. EGFR mutations and ALK rearrangements are associated with low response rates to PD-1 pathway blockade in non-small cell lung cancer: A retrospective analysis. *Clin Cancer Res* (2016) 22(18):4585–93. doi: 10.1158/1078-0432.CCR-15-3101

13. Lisberg A, Cummings A, Goldman JW, Bornazyan K, Reese N, Wang T, et al. A phase II study of pembrolizumab in EGFR-mutant, PD-L1+, tyrosine kinase inhibitor naive patients with advanced NSCLC. *J Thorac Oncol* (2018) 13(8):1138–45. doi: 10.1016/j.jtho.2018.03.035

14. Reck M, Mok TSK, Nishio M, Jotte RM, Cappuzzo F, Orlandi F, et al. Atezolizumab plus bevacizumab and chemotherapy in non-small-cell lung cancer (IMpower150): key subgroup analyses of patients with EGFR mutations or baseline liver metastases in a randomised, open-label phase 3 trial. *Lancet Respir Med* (2019) 7(5):387–401. doi: 10.1016/S2213-2600(19)30084-0

15. Riely G, Hui R, Carbone D, Park K, Carrigan M, Xu X, et al. P1.01-81 phase 3 study of pemetrexed-platinum with or without pembrolizumab for TKI-Resistant/EGFR-Mutated advanced NSCLC: KEYNOTE-789. *J Thorac Oncol* (2018) 13(10):S494. doi: 10.1016/j.jtho.2018.08.637

16. Park K, Yang JC-H, Girard N, Mok T, Gainor J, Nakagawa K, et al. Nivolumab + chemotherapy vs chemotherapy in EGFR-mutated NSCLC after 1L or 2L EGFR-TKIs (CheckMate 722). *Ann Oncol* (2019) 30:vi126. doi: 10.1093/annonc/mdz343.039

17. Ahn MJ, Cho BC, Ou X, Walding A, Dymond AW, Ren S, et al. Osimertinib plus durvalumab in patients with EGFR-mutated, advanced NSCLC: A phase 1b, open-label, multicenter trial. *J Thorac Oncol* (2022) 17(5):718–23. doi: 10.1016/j.jtho.2022.01.012

18. Akbay EA, Koyama S, Carretero J, Altabef A, Tchaicha JH, Christensen CL, et al. Activation of the PD-1 pathway contributes to immune escape in EGFR-driven lung tumors. *Cancer Discov* (2013) 3(12):1355–63. doi: 10.1158/2159-8290.CD-13-0310

19. Toker A, Ohashi PS. Expression of costimulatory and inhibitory receptors in FoxP3(+) regulatory T cells within the tumor microenvironment: Implications for combination immunotherapy approaches. *Adv Cancer Res* (2019) 144:193–261. doi: 10.1016/bs.acr.2019.05.001

20. Fang P, Li X, Dai J, Cole L, Camacho JA, Zhang Y, et al. Immune cell subset differentiation and tissue inflammation. *J Hematol Oncol* (2018) 11(1):97. doi: 10.1186/s13045-018-0637-x

21. Lauss M, Donia M, Svane IM, Jönsson G. B cells and tertiary lymphoid structures: Friends or foes in cancer immunotherapy? *Clin Cancer Res* (2022) 28 (9):1751–8. doi: 10.1158/1078-0432.CCR-21-1130

22. Gandhi L, Rodriguez-Abreu D, Gadgeel S, Esteban E, Felip E, De Angelis F, et al. Pembrolizumab plus chemotherapy in metastatic non-Small-Cell lung cancer. *N Engl J Med* (2018) 378(22):2078–92. doi: 10.1056/NEJMoa1801005

23. Shi X, Dong X, Zhai J, Liu X, Lu D, Ni Z, et al. Current evidence of the efficacy and safety of neoadjuvant EGFR-TKIs for patients with non-small cell lung cancer. *Front Oncol* (2021) 11:608608. doi: 10.3389/fonc.2021.608608

24. Hamai K, Tanahashi H, Ueno S, Konishi H, Matsumura M, Nomura A, et al. First-line immune checkpoint therapy in metastatic squamous cell lung cancer harboring both EGFR mutation and high expression of PD-L1: A case report. *Thorac Cancer* (2020) 11(6):1716–9. doi: 10.1111/1759-7714.13436

25. Oguri T, Sasada S, Seki S, Murata S, Tsuchiya Y, Ishioka K, et al. A case of hyperprogressive disease following atezolizumab therapy for pulmonary pleomorphic carcinoma with epidermal growth factor receptor mutation. *Respir Med Case Rep* (2021) 33:101405. doi: 10.1016/j.rmcr.2021.101405

26. Zhao Q, Zhang X, Ma Q, Luo N, Liu Z, Wang R, et al. Case report: An "Immune-cold" EGFR mutant NSCLC with strong PD-L1 expression shows resistance to chemo-immunotherapy. *Front Oncol* (2022) 12:765997. doi: 10.3389/fonc.2022.765997

27. Lin G, Li C, Li PS, Fang WZ, Xu HP, Gong YH, et al. Genomic origin and EGFR-TKI treatments of pulmonary adenosquamous carcinoma. *Ann Oncol* (2020) 31(4):517–24. doi: 10.1016/j.annonc.2020.01.014

frontiers | Frontiers in Oncology

TYPE Case Report
PUBLISHED 20 October 2022
DOI 10.3389/fonc.2022.1026524

OPEN ACCESS

EDITED BY
Yaron Perry,
University at Buffalo, United States

REVIEWED BY
Pietro Bertoglio,
IRCCS Azienda Ospedaliero Universitaria di Bologna, Italy
Angelo Carretta,
Vita-Salute San Raffaele University, Italy

*CORRESPONDENCE
Feng Yao
yaofeng@shsmu.edu.cn
Jianxin Shi
shijx_sch@126.com

†These authors have contributed equally to this work

SPECIALTY SECTION
This article was submitted to Thoracic Oncology, a section of the journal Frontiers in Oncology

RECEIVED 24 August 2022
ACCEPTED 03 October 2022
PUBLISHED 20 October 2022

CITATION
Zhang X, Chen L, Zhou W, Wang Z, Wang C, Shi J and Yao F (2022) Case report: Complete resection of invasive thymoma invading the superior vena cava and right atrium under cardiopulmonary bypass support. *Front. Oncol.* 12:1026524. doi: 10.3389/fonc.2022.1026524

Case report: Complete resection of invasive thymoma invading the superior vena cava and right atrium under cardiopulmonary bypass support

Xiangxin Zhang[1,2,3,4,5†], Liang Chen[1†], Wenyong Zhou[1†], Zhexin Wang[1], Chong Wang[1], Jianxin Shi[1*] and Feng Yao[1*]

[1]Department of Thoracic Surgery, Shanghai Chest Hospital, Shanghai Jiao Tong University School of Medicine, Shanghai, China, [2]Department of Emergency Medicine, Qilu Hospital of Shandong University, Jinan, China, [3]Shandong Provincial Clinical Research Center for Emergency and Critical Care Medicine, Institute of Emergency and Critical Care Medicine of Shandong University, Chest Pain Center; Qilu Hospital of Shandong University, Jinan, China, [4]Key Laboratory of Emergency and Critical Care Medicine of Shandong Province, Key Laboratory of Cardiopulmonary Cerebral Resuscitation Research of Shandong Province, Shandong Provincial Engineering Laboratory for Emergency and Critical Care Medicine, Qilu Hospital of Shandong University, Jinan, China, [5]The Key Laboratory of Cardiovascular Remodeling and Function Research, Chinese Ministry of Education, Chinese Ministry of Health and Chinese Academy of Medical Sciences, The State and Shandong Province Joint Key Laboratory of Translational Cardiovascular Medicine, Qilu Hospital of Shandong University, Jinan, China

Here we describe an uncommon case of a 48-year-old male patient with an invasive thymoma invading the superior vena cava, bilateral innominate veins, right internal jugular vein, right subclavian vein, right atrium, azygos vein, and part of the lung tissues. The tumor was resected entirely under cardiopulmonary bypass support, and the venous bypass using a vascular graft was successfully established between the left innominate vein and the right atrium. The postoperative course was uneventful, and the patient was discharged 15 days after surgery without complications.

KEYWORDS

thymoma, invading the right atrium, cardiopulmonary bypass, surgery, case report

Introduction

Thymoma is the most common primary anterior mediastinal tumor in adults (1), which can be further classified into the invasive or non-invasive type according to its extracapsular extension (2). For invasive thymoma, the surgical treatment often involves adjacent resectioning structures, such as either of the innominate veins, superior vena

cava (SVC), pericardium, pleura, and the lung. The resection and reconstruction of the SVC system are considered feasible (3, 4), but it remains unclear when the SVC system and the right atrium are involved.

Here, we report a case of an invasive thymoma completely resected under cardiopulmonary bypass (CPB) support, which invades the SVC and the right atrium together with the bilateral innominate veins, the right internal jugular vein, the right subclavian vein, the azygos vein, and part of lung tissues.

Case report

A 48-year-old male patient was admitted to our center with the complaint of chest tightness. Computed tomography demonstrated a mass in the anterior mediastinum, measuring 13 cm × 7 cm, which was suspected of invading the SVC and the right atrium (Figure 1). Positron emission tomography/computed tomography scan showed no distant metastasis but mediastinal lymph node metastasis. According to the fine-needle aspiration biopsy results, the mass was considered to be type B2 thymoma. As the multidisciplinary team suggested, the patient was treated with three-cycle chemotherapy with cisplatin, cyclophosphamide, and epirubicin hydrochloride, followed by oral prednisolone for 1 month. However, the response was finally assessed as a stable disease by the Response Evaluation Criteria in Solid Tumors (version 1.1) (5). The patient had no myasthenia gravis but had mild SVC syndrome (6), so surgical treatment was decided.

Through a median sternotomy, the tumor in the anterior mediastinum was observed to invade the SVC and the right atrium together with the bilateral innominate veins, the right internal jugular vein, the right subclavian vein, the azygos vein, and the lung (Figure 2A). The left innominate vein was transected near the left venous angle and then anastomosed with the vascular prosthesis. To establish the CPB, the arterial cannula was inserted into the right femoral artery, whereas the venous cannulas in a bicaval fashion were respectively inserted into the right femoral vein and the vascular prosthesis. After that, the right internal jugular vein, the right subclavian vein, and the azygos vein were all ligated and cut off, and wedge resection for part of the lung tissues was performed using the linear staplers. Then, the mass was separated from the aorta arch and right hilum. Through a longitudinal incision of the anterior wall of the right atrium, the tumor was detected to invade part of the right atrium around the entrance of the SVC. Therefore, the right atrium was partially resected, and the tumor was removed entirely, followed by the venous bypass reconstruction between the left innominate vein and the right atrium (Figures 2B, C). During the operation, the sinus node and the left phrenic nerve were both preserved, whereas the right phrenic nerve was also

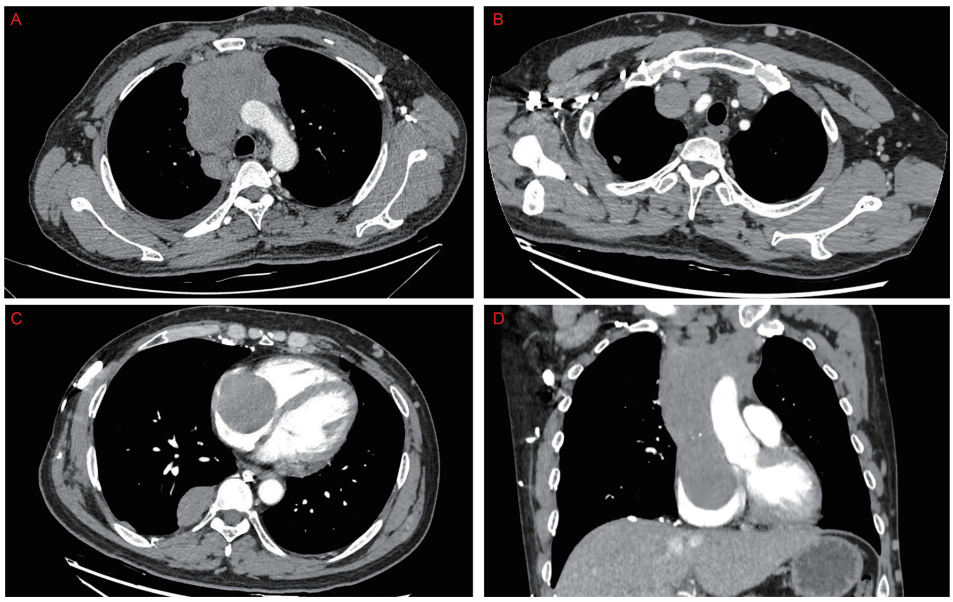

FIGURE 1
Preoperative computed tomography showed that the thymoma located in the anterior mediastinum **(A)** invaded the bilateral innominate veins, the superior vena cava, and the right atrium **(B–D)**.

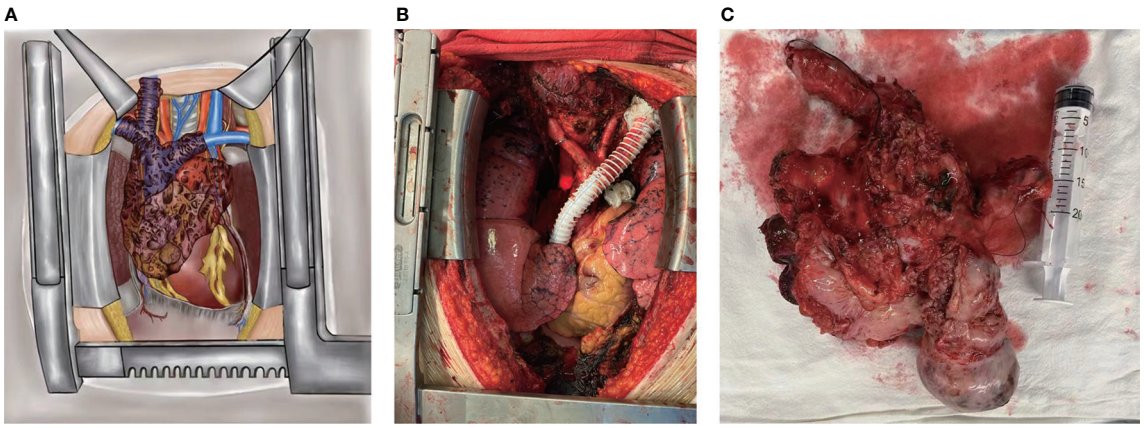

FIGURE 2
During the operation, the tumor was observed to invade the superior vena cava and the right atrium together with the bilateral innominate veins, the right internal jugular vein, the right subclavian vein, the azygos vein, and the lung **(A)**. The tumor was completely resected, and the venous bypass was established between the left innominate vein and the right atrium **(B)**. Tumor specimen **(C)**.

resected due to tumor invasion. At the end of the surgery, the CPB was safely weaned off. The internal jugular vein pressure was below 20 cmH_2O, and the patient was successfully extubated in the operating room.

The final histopathological examination confirmed the type B2/B3 mixed-type thymoma (2021 WHO Classification) and negative resected margins (Masaoka–Koga stage IIIB, T4N0M0) (7–9). The postoperative course was uneventful, and the patient was discharged 15 days after surgery without any complications (Figure 3). In order to detect the patient's blood coagulation status and physical condition, the current follow-up interval is 1 month. The patient will be treated with adjuvant chemotherapy after surgery.

Discussion

Thymoma invading the great mediastinal vessels and the right atrium simultaneously is extremely rare. Several cases have potentially revealed the promising prognoses of patients receiving surgical resection for invasive thymomas compared with those who underwent the non-surgical treatment (10–13).

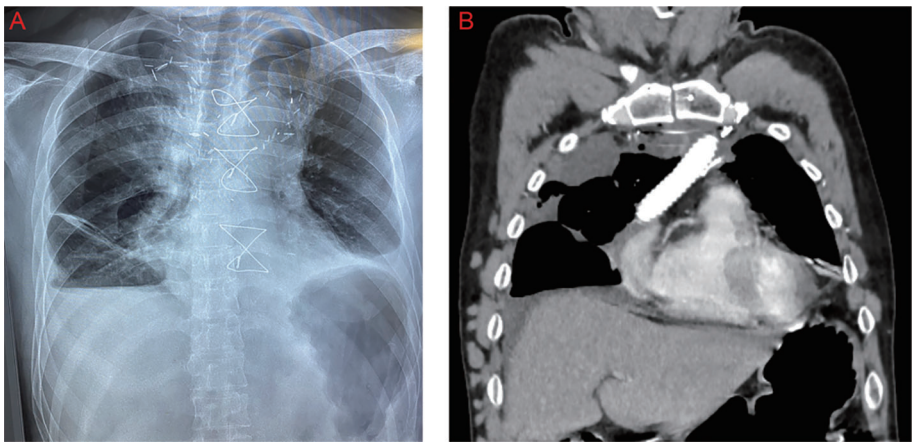

FIGURE 3
Postoperative X-ray **(A)** and computed tomography **(B)** imaging of the patient.

Kumar et al. reported the survival outcomes in 12 patients receiving surgical resection for locally advanced thymoma with SVC invasion. The 1-, 3-, and 5-year overall survival rates were 100%, 91.6%, and 83.3% in their cohort, respectively (14). After the literature review, Kurata et al. summarized the survival outcomes in 23 cases of thymoma invading the atrium. Among 20 patients receiving surgical treatment, three died within 1 month, at 2 months, and 1 year after surgery. The average survival time of the other 17 patients was 30.1 months, and the longest follow-up period was 8.5 years. However, all three remaining non-surgical treatment patients died during follow-up (15).

According to previous literatures, CBP has often been used in thoracic malignant tumors invading the heart or great vessels, trachea, or carina (16). Studies have shown that using CPB does not appear to increase the risk of tumor dissemination. For patients with locally advanced cancers, CBP can safely help remove the tumor and improve the survival to a certain extent (17, 18).

Complete resection of invasive thymoma and the involved structures (such as the great mediastinal vessels) would benefit the oncological prognosis (19). Traditionally, when the tumor invades SVC and the confluence of bilateral innominate veins, the "Y-graft" or "two separate grafts" is usually selected to reconstruct the venous drainage. When both SVC and the long segment of a single innominate vein are resected, a single straight graft between the uninvolved innominate vein and the right atrium is applied (14). In the present case, the SVC, bilateral innominate veins, the azygos vein, and part of the right atrium were all resected to perform complete resection. Meanwhile, the right internal jugular and right subclavian valves were also ligated at a high level, wherein establishing venous bypass between these vessels and the right atrium would be quite difficult (Figure 2A). Therefore, the venous drainage was only reconstructed between the left innominate vein and the right atrium. Even so, due to the development of the venous collateral circuits after the long-term occlusion of SVC, there were no clinical signs of SVC syndrome or elevated internal jugular vein pressure. Furthermore, the patient's symptoms were relieved to a great extent in this case. It was also previously reported that the symptomatic patients who suffered thoracic malignancies invading the heart or great vessels had immediate and sustained palliation of their symptoms after surgical treatment (20).

In conclusion, radical resection for such an invasive thymoma may be safely attempted in selected patients under CPB support, which may help achieve prolonged survival.

Data availability statement

The original contributions presented in the study are included in the article/supplementary material. Further inquiries can be directed to the corresponding authors.

Ethics statement

The studies involving human participants were reviewed and approved by the ethical committee of the Shanghai Chest Hospital. The patients provided their written informed consent to participate in this study. Written informed consent was obtained from the individual(s) for the publication of any potentially identifiable images or data included in this article.

Author contributions

FY, JS, WZ, CW and ZW performed the surgery together. XZ and LC wrote the manuscript. All authors contributed to the article and approved the submitted version.

Acknowledgments

We are very grateful to the anesthesiology, surgical nursing, and intensive care unit team at Shanghai Chest Hospital for their efforts.

Conflict of interest

The authors declare that the research was conducted in the absence of any commercial or financial relationships that could be construed as a potential conflict of interest.

Publisher's note

References

1. Duwe BV, Sterman DH, Musani AI. Tumors of the mediastinum. *Chest* (2005) 128(4):2893–909. doi: 10.1378/chest.128.4.2893

2. Marx A, Ströbel P, Badve SS, Chalabreysse L, Chan CKJ, Chen G, et al. ITMIG consensus statement on the use of the WHO histological classification of thymoma and thymic carcinoma: Refined definitions, histological criteria, and reporting. *J Thorac Oncol* (2014) 9(5):596–611. doi: 10.1097/JTO.0000000000000154

3. Yokoi K, Miyazawa N, Mori K, Saito Y, Tominaga K, Lmura G, et al. Invasive thymoma with intracaval growth into the right atrium. *Ann Thorac Surg* (1992) 53 (3):507–9. doi: 10.1016/0003-4975(92)90281-8

4. Amirghofran AA, Emaminia A, Rayatpisheh S, Malek-Hosseini SA, Attaran Y. Intracardiac invasive thymoma presenting as superior vena cava syndrome. *Ann Thorac Surg* (2009) 87(5):1616–8. doi: 10.1016/j.athoracsur.2008.09.052

5. Schwartz LH, Litière S, De Vries E, Ford R, Gwyther S, Mandrekar S, et al. RECIST 1.1-update and clarification: From the RECIST committee. *Eur J Cancer* (2016) 62:132–7. doi: 10.1016/j.ejca.2016.03.081

6. Friedman T, Quencer KB, Kishore SA, Winokur RS, Madoff DC. Malignant venous obstruction: Superior vena cava syndrome and beyond. *Semin Intervent Radiol* (2017) 34(4):398–408. doi: 10.1055/s-0037-1608863

7. Marx A, Chan JKC, Chalabreysse L, Dacic S, Detterbeck F, French CA, et al. The 2021 WHO classification of tumors of the thymus and mediastinum: What is new in thymic epithelial, germ cell, and mesenchymal tumors? *J Thorac Oncol* (2022) 17(2):200–13. doi: 10.1016/j.jtho.2021.10.010

8. Koga K, Matsuno Y, Noguchi M, Mukai K, Asamura H, Goya T, et al. A review of 79 thymomas: Modification of staging system and reappraisal of conventional division into invasive and non-invasive thymoma. *Pathol Int* (1994) 44(5):359–67. doi: 10.1111/j.1440-1827.1994.tb02936.x

9. Detterbeck FC, Stratton K, Giroux D, Asamura H, Crowley J, Falkson C, et al. The IASLC/ITMIG thymic epithelial tumors staging project: Proposal for an evidence-based stage classification system for the forthcoming (8th) edition of the TNM classification of malignant tumors. *J Thorac Oncol* (2014) 9(9 Suppl 2): S65–72. doi: 10.1097/JTO.0000000000000290

10. Shen W, Cao Y, Wang X, Zhang P, Zhou Q. Invasive thymoma with intravascular growth into the great veins and right atrium: A case report. *Thorac Cancer* (2020) 11(5):1326–9. doi: 10.1111/1759-7714.13242

11. Dong YQ, Liang JS, Zhang XM, Zhu SB, Xu JH, Ji T, et al. Surgical treatment of an invasive thymoma extending into the superior vena cava and right atrium. *World J Surg Oncol* (2014) 12:6. doi: 10.1186/1477-7819-12-6

12. Pastorino U, Yang XN, Francese M, Durkovic S, Biglioli P. Long-term survival after salvage surgery for invasive thymoma with intracardiac extension. *Tumori* (2008) 94(5):772–6. doi: 10.1177/030089160809400526

13. Asami-Noyama M, Furuya-Kondo T, Suetake R, Matsuda K, Oishi K, Yamaji Y, et al. Invasive thymoma extending to the right atrium with superior vena cava syndrome presenting massive intracardiac thrombosis immediately after the start of chemotherapy: an autopsy case report. *Int Cancer Conf J* (2022) 11 (2):158–63. doi: 10.1007/s13691-022-00541-2

14. Kumar A, Pulle MV, Asaf BB, Shivnani G, Maheshwari A, Kodaganur SG, et al. Superior vena cava resection in locally advanced thymoma-surgical and survival outcomes. *Indian J Surg Oncol* (2020) 11(4):711–9. doi: 10.1007/s13193-020-01204-5

15. Kurata A, Saji H, Ikeda N, Kuroda M. Intracaval and intracardiac extension of invasive thymoma complicated by superior and inferior vena cava syndrome. *Pathol Int* (2013) 63(1):56–62. doi: 10.1111/pin.12023

16. De Perrot M, Fadel E, Mussot S, De Palma A, Chapelier A, Dartevelle P. Resection of locally advanced (T4) non-small cell lung cancer with cardiopulmonary bypass. *Ann Thorac Surg* (2005) 79(5):1691–1696;discussion 1697. doi: 10.1016/j.athoracsur.2004.10.028

17. Chen L, Zhu X, Zhu R, Jin X, Tan L, Chen Y, et al. Cardiopulmonary bypass does not consequentially contribute to postoperative distant metastasis of giant refractory thoracic tumors: A retrospective study with long-term follow-up. *Thorac Cancer* (2021) 12(22):2990–5. doi: 10.1111/1759-7714.14162

18. Langer NB, Mercier O, Fabre D, Lawton J, Mussot S, Dartevelle P, et al. Outcomes after resection of T4 non-small cell lung cancer using cardiopulmonary bypass. *Ann Thorac Surg* (2016) 102(3):902–10. doi: 10.1016/j.athoracsur.2016.03.044

19. Yagi K, Hirata T, Fukuse T, Yokomise H, Inui K, Ike O, et al. Surgical treatment for invasive thymoma, especially when the superior vena cava is invaded. *Ann Thorac Surg* (1996) 61(2):521–4. doi: 10.1016/0003-4975(95)00983-3

20. Park BJ, Bacchetta M, Bains MS, Downey RJ, Flores R, Rusch VW, et al. Surgical management of thoracic malignancies invading the heart or great vessels. *Ann Thorac Surg* (2004) 78(3):1024–30. doi: 10.1016/j.athoracsur.2004.02.043

frontiers | Frontiers in Oncology

TYPE Case Report
PUBLISHED 27 October 2022
DOI 10.3389/fonc.2022.995744

OPEN ACCESS

EDITED BY
Giuseppe Cardillo,
Thoracic Surgery, Italy

REVIEWED BY
Stefanie Keymel,
University Hospital of Düsseldorf, Germany
Chong Bai,
Naval Medical University (Second Military Medical University), China

*CORRESPONDENCE
Linus D. Kloker
linus.kloker@uni-tuebingen.de

SPECIALTY SECTION
This article was submitted to Thoracic Oncology, a section of the journal Frontiers in Oncology

RECEIVED 16 July 2022
ACCEPTED 10 October 2022
PUBLISHED 27 October 2022

CITATION
Kloker LD, Calukovic B, Benzler K, Golf A, Böhm S, Günther S, Horger M, Haas S, Berchtold S, Beil J, Carter ME, Ganzenmueller T, Singer S, Agaimy A, Stöhr R, Hartmann A, Duell T, Mairhofer S, Fohrer F, Reinmuth N, Zender L and Lauer UM (2022) Case report: Immunovirotherapy as a novel add-on treatment in a patient with thoracic NUT carcinoma. *Front. Oncol.* 12:995744. doi: 10.3389/fonc.2022.995744

Case report: Immunovirotherapy as a novel add-on treatment in a patient with thoracic NUT carcinoma

Linus D. Kloker[1]*, Branko Calukovic[1], Katrin Benzler[1], Alexander Golf[1], Sebastian Böhm[1], Sven Günther[1], Marius Horger[2], Simone Haas[1,3], Susanne Berchtold[1], Julia Beil[1,4], Mary E. Carter[1], Tina Ganzenmueller[5], Stephan Singer[6], Abbas Agaimy[7], Robert Stöhr[7], Arndt Hartmann[7], Thomas Duell[8], Sandra Mairhofer[8], Fabian Fohrer[8], Niels Reinmuth[8], Lars Zender[1,9] and Ulrich M. Lauer[1,4]

[1]Department of Medical Oncology and Pneumology, Virotherapy Center Tübingen (VCT), Medical University Hospital, Tübingen, Germany, [2]Diagnostic and Interventional Radiology, University Hospital Tübingen, Tübingen, Germany, [3]Max-Planck-Institute of Biochemistry, Department of Molecular Medicine, Martinsried, Germany, [4]German Cancer Consortium (DKTK), German Cancer Research Center (DKFZ), Tübingen, Germany, [5]Institute for Medical Virology and Epidemiology of Viral Diseases, University Hospital Tübingen, Tübingen, Germany, [6]Department of Pathology, University Hospital Tübingen, Tübingen, Germany, [7]Department of Pathology, University Hospital Erlangen, Erlangen, Germany, [8]Asklepios Lung Clinic, Munich-Gauting, Munich, Germany, [9]DFG Cluster of Excellence 2180 'Image-guided and Functional Instructed Tumor Therapy', University of Tübingen, Tübingen, Germany

NUT carcinoma (NC) is a rare and extremely aggressive form of cancer, usually presenting with intrathoracic or neck manifestations in adolescents and young adults. With no established standard therapy regimen and a median overall survival of only 6.5 months, there is a huge need for innovative treatment options. As NC is genetically driven by a single aberrant fusion oncoprotein, it is generally characterized by a low tumor mutational burden, thus making it immunologically cold and insusceptible to conventional immunotherapy. Recently, we have demonstrated that oncolytic viruses (OVs) are able to specifically infect and lyse NC cells, thereby turning an immunologically cold tumor microenvironment into a hot one. Here, we report an intensive multimodal treatment approach employing for the first time an OV (talimogene laherparepvec (T-VEC); IMLYGIC®) together with the immune checkpoint inhibitor pembrolizumab as an add-on to a basic NC therapy (cytostatic chemotherapy, radiation therapy, epigenetic therapy) in a patient suffering from a large thoracic NC tumor which exhibits an aberrant, unique *BRD3:NUTM1* fusion. This case demonstrates for the first time the feasibility of this innovative add-on immunovirotherapy regimen with a profound, repetitive

and durable replication of T-VEC that is instrumental in achieving tumor stabilization and improvement in the patient´s quality of life. Further, a previously unknown *BRD3:NUTM1* fusion gene was discovered that lacks the extraterminal domain of *BRD3*.

KEYWORDS

NUT carcinoma, virotherapy, immunotherapy, T-VEC, chemotherapy, NUTM1, BRD3

Introduction

NUT carcinoma

NUT carcinoma (nuclear protein in testis carcinoma, NC), formerly known as NUT midline carcinoma, is a poorly differentiated and highly aggressive tumor which is molecularly defined by an aberrant *NUTM1* fusion gene (1).

This neoplasm can arise in all age groups, but mostly adolescents and young adults are affected with a median onset of disease at 23.6 years (2).

Very rarely, when the diagnosis can be made in a still localized state, surgery and adjuvant radiation can achieve long-term survival (3, 4), particularly when resection achieves tumor-free margins (5). Unfortunately, patients usually present in an advanced metastatic and therefore inoperable condition, facing a fatal prognosis with a median overall survival (OS) of 6.5 months only. Three different prognostic subgroups have been described depending on tumor localization and type of fusion gene, with (i) the best median OS in patients with non-thoracic non-*BRD4:NUTM1* fusion carcinoma (36.5 months from initial cancer diagnosis), (ii) a median prognosis for non-thoracic disease with *BRD4::NUTM1* fusion (10 months) and (iii) the worst prognosis (4.4 months) in patients with thoracic disease onset, independent of the fusion gene partner (2).

The foremost common fusion partner gene is *BRD4* (75%), followed by *BRD3*, *NSD3* and *ZNF532* (6). Frequently, NC is initially misdiagnosed as a poorly differentiated squamous cell carcinoma (SCC), but simple immunostaining for NUT allows a straightforward diagnosis (7). Fluorescence *in situ* hybridization or next generation sequencing approaches, including panel or exome sequencing, can reveal the corresponding fusion partner gene.

So far, there is no standard treatment regimen for palliation of metastatic disease stages. However, ifosfamide-based regimens and additional radiation therapy have shown some promising results, with published cases of some very rare partial or complete responses in non-thoracic NC (6, 8–11). The combination of carboplatin and paclitaxel is frequently used in thoracic NC, but with only limited success and progression free survival rates below 3 months (12–14).

Oncolytic virotherapy

Oncolytic virotherapy employs oncolytic viruses (OVs) to specifically infect, replicate in and lyse tumor cells whilst sparing healthy cells. Such OVs are specifically selected based on their natural tumor tropism and/or are genetically modified for improved and even more selective tumor tropism. During intratumoral (i.t.) virus replication and subsequent direct virus-mediated oncolysis, tumor neo-antigens as well as pathogen and damage associated molecular patterns (PAMPs and DAMPs) are released, thereby inducing a highly inflamed tumor microenvironment as well as an additional indirect (immunogenic) tumor cell death associated with a powerful systemic anti-tumor immune response (15). Of note, the anti-tumoral efficacy of ICIs was shown to be augmented by intratumoral application of the virotherapeutic compound T-VEC (16, 17). OVs are thought to elicit a response particularly in tumors that have an immunosuppressive tumor microenvironment and a low tumor mutation burden, and thus show very low response rates to immune checkpoint inhibition as monotherapy (18).

The oncolytic virus T-VEC

T-VEC (talimogene laherparepvec; IMLYGIC®) is a genetically engineered oncolytic herpes simplex virus type 1 (HSV-1), modified for specific tumor replication and enhanced immunostimulation, while being attenuated in healthy and especially in brain tissue (19). In 2015, T-VEC was the first and only OV to be approved by the US Food and Drug Administration (FDA), as it showed a significant benefit for treatment of advanced stages of metastatic melanoma (20). However, a recent phase III study (Masterkey-265, NCT02263508) failed to show significant benefits of the combined treatment with T-VEC and the ICI pembrolizumab in melanoma, despite indicating positive trends in the combination group. Currently, this regimen is being evaluated for treatment of melanoma in a neoadjuvant setting (NCT04330430, NCT04427306) as well as for other tumor entities such as sarcomas, triple-negative breast cancer or peritoneal surface malignancies.

For melanoma, T-VEC was already demonstrated to increase the number of tumor infiltrating CD4- and CD8-lymphocytes as well as activated CD8-lympho-cytes in the circulation and to rise expression of PD-L1 and IFNγ in virus-injected tumors (16, 17). Preclinical data suggest an alteration of the tumor microenvironment by increased neutrophils, monocytes and chemokines and the induction of tumor specific T-lymphocytes (21). These features enable T-VEC to turn immunologically cold tumors into a hot ones (22).

Immunotherapy in NUT carcinoma

So far, virotherapeutics, such as T-VEC, have not been employed in the treatment of NC. Moreover, there are only a few reported cases and no clinical trials for NC treatment with ICIs. Nevertheless, off-label treatment with ICIs is a frequent practice. In a case report, Davis et al. described a patient with thoracic NC for whom treatment with initial surgery, adjuvant chemotherapy and the anti-PD-1 agent nivolumab resulted in long-term survival of 7.5 years. Nivolumab was administered for 3.5 years, starting at disease recurrence three years after initial diagnosis (23). Previous work suggests a low PD-L1 expression and TMB in the majority of NCs (24), which generally predicts a rather poor response rate to sole PD-1 blockade.

In another case series of five NC patients treated with ICIs, the response rate to immunotherapy could be improved by previous radiation therapy, whereas one patient with high TMB did not respond to immunotherapy (12). A further case analysis of twelve patients also supported the hypothesis that radiotherapy followed by immunotherapy results in beneficial outcomes. Regarding the usage of distinct ICIs, best outcomes were seen with pembrolizumab, whereas atezolizumab so far showed no benefit (25).

It remains unclear if TMB and PD-L1 expression as predictive biomarkers are also applicable to NC, since individual differences in NC location and stage at diagnosis might overshadow reliable evidence with the reported small sample sizes. Nevertheless, infiltration of neutrophils and T-cells into NC tissues have been described (24, 26, 27). An additional strong stimulus for attracting more T-cells to the tumor sites, e.g. oncolytic virotherapy may be required and thus is a prerequisite for any effective anti-tumoral immune activation.

Case highlights

In this patient case, T-VEC is employed for treatment of NC for the first time by sequential intratumoral injections. It is combined with a multimodal treatment approach including chemotherapy, radiotherapy, an HDAC inhibitor and an ICI (pembrolizumab). This patient case demonstrates a treatment response to this multimodal approach as well as repetitively high replication yields of T-VEC when applied intratumorally into different NC locations. Moreover, a previously undescribed *BRD3::NUTM1* fusion gene was discovered.

Case report

Patient history

A 57-year-old woman with no past medical history and no history of smoking initially was evaluated for a worsening cough and dyspnea by her local specialist for internal medicine. Serial testing for COVID-19 remained negative. With a suspected pulmonary embolism, she was referred to a radiologist, who performed the initial CT scan of the chest. The CT scan revealed a large pulmonary mass (12 x 11.8 x 11 cm) in the right upper lobe with compression of the right upper lobe artery and bronchus, right-sided malignant pleural effusion with pleural metastases, enlarged ipsilateral mediastinal lymph nodes and a mediastinal shift to the left side (Figure 1A). Initial TNM staging for lung carcinoma was cT4 cN2 cM1a (pleural).

Diagnosis

The patient was subsequently hospitalized in a specialized lung clinic, where pleural drainage, biopsy *via* bronchoscopy and initiation of a standard chemotherapy with carboplatin (AUC5) and paclitaxel (175 mg/m^2) were conducted (based on a bronchoscopy guided biopsy revealing a poorly differentiated SCC, being positive for p63 and negative for TTF-1, CD56 and synaptophysin).

Shortly after the first cycle of chemotherapy, she was rehospitalized with aggravated dyspnea. Subsequently, a video assisted thoracoscopy (VATS) was performed to obtain serial biopsies and to achieve a surgical pleurodesis. Reference pathology performed at the University of Erlangen, Germany, reported an undifferentiated highly malignant tumor with spindle and polygonal cells and diffuse expression of p63 and pancytokeratin, which supported the diagnosis of a non-keratinizing SCC (Figure S1). Additional immunostaining showed only low positivity for p40 and cytokeratin 5. The final diagnosis of NC was made *via* immunostaining with an anti-NUT antibody showing a strong nuclear signal and an additional fusion panel RNA sequencing, which revealed a *BRD3::NUTM1* gene fusion (Figure 2 and Figure S1). A DNA sequencing panel for 749 genes, including standard lung-cancer diagnostics, showed no relevant alterations. At diagnosis, there was only a scattered and CD4-dominated T lymphocyte infiltration within NC tumor sites (Figure S1). Staining for PD-L1 showed a TPS (tumor proportion score) and CPS (combined positive score) <1% (Figure S1).

About three months after symptom onset, the patient was referred to the University Hospital of Tübingen, a German

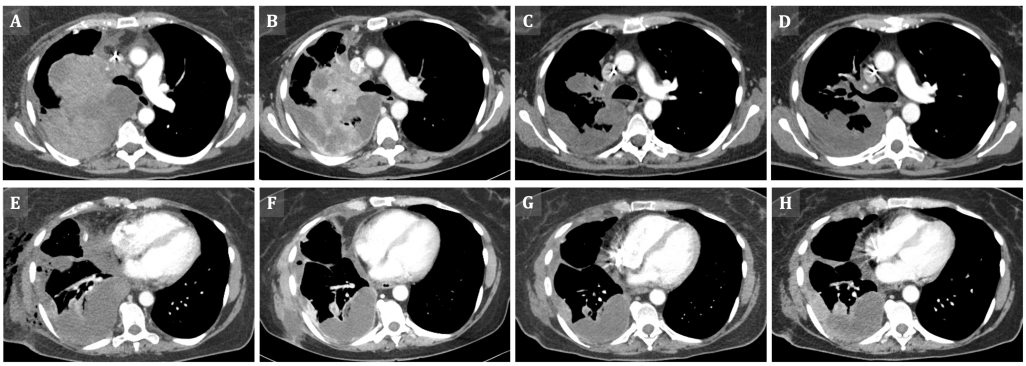

FIGURE 1
Tumor regression on sequential contrast enhanced CT scans (CECT) of the chest. **(A)** Axial chest CECT (performed on day 0, i.e. before the onset of the multimodal NUT therapy regimen) - large, highly attenuated lung mass occupying the entire right upper lung lobe with invasion of the mediastinum as well as tumoral spread to the hilar and pre-tracheal lymph nodes. **(B)** First follow-up (FU) (day 20) - increasingly heterogeneous tumor attenuation and slight shrinkage. **(C)** Second FU (day 55) - further loss in tumor attenuation (vascular supply) as well as strong volume reduction on chest CECT. **(D)** Third FU (day 77) - stable situation with respect to the residual tumor manifestations in the right lung and mediastinum. **(E)** Axial chest CECT (day 0) – right sided pleural metastases and epiphrenic tumor mass. **(F)** First FU (day 20) – volume reduction of the pleural and epiphrenic tumor manifestations. **(G)** Second FU (day 55) – stable situation. **(H)** Third FU (day 77) – slowly progredient epiphrenic and pleural tumor with increased marginal attenuation.

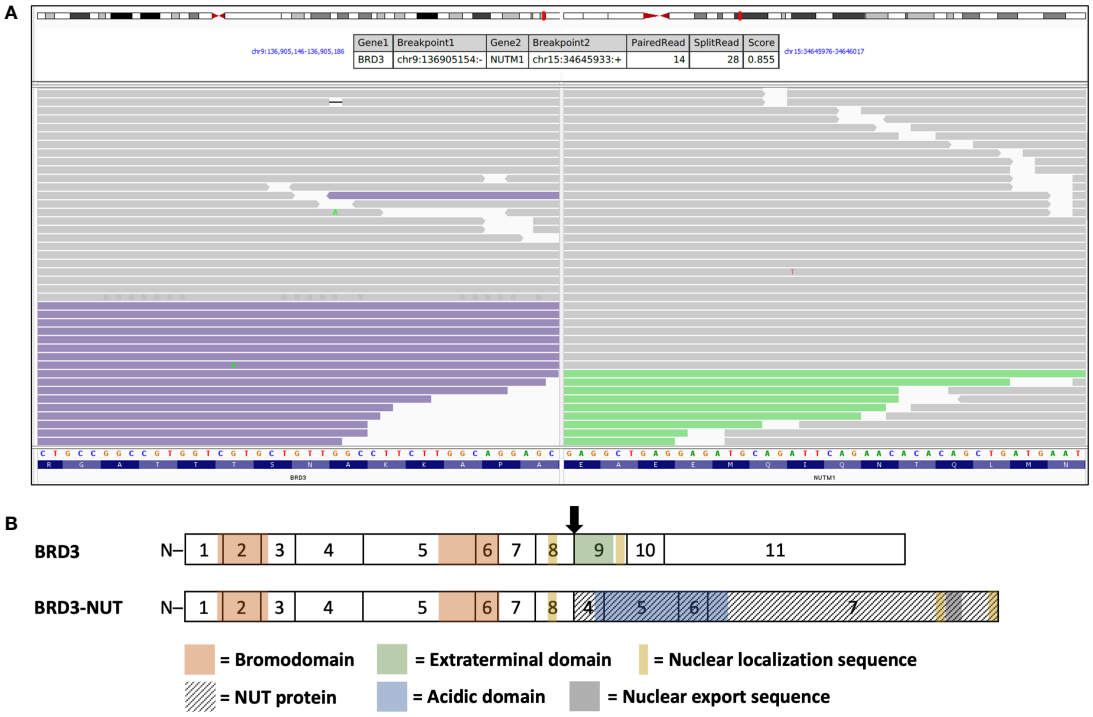

FIGURE 2
BRD3::NUTM1 gene translocation being found in fusion RNA panel sequencing of tumor tissue. **(A)** TruSight RNA fusion panel sequencing (Illumina) revealed *BRD3* as *NUTM1* fusion partner. Integrated genome viewer split-screen view of the breakpoint regions on chromosomes 9 (left) and 15 (right). Read alignments of paired-end RNA sequencing of the identified *BRD3::NUTM1* fusion event are shown. Mate pairs mapped to the fusion reads in the *BRD3* (purple color) and *NUTM1* (green color) locus are shown. **(B)** Estimated BRD3::NUT fusion protein with breakpoints after coding exon 8 of *BRD3* (arrow; chr9:136,905,154, amino acid G549) and before exon 4 of *NUTM1* (chr15:34,645,933), resulting in the respective fusion oncoprotein. Interestingly, the extraterminal domain (BRD3, amino acids 564-641) and the second nuclear localization sequence coded on exon 9 of *BRD3* are not contained in the fusion oncoprotein.

Comprehensive Cancer Center specialized in NC tumors, for further treatment. Here, an immediate CT scan displayed further progressive disease (PD) with additional involvement of the pleura, the diaphragm, the pericardium as well as mediastinal lymph nodes (Figure 1E). An additional lesion in the lateral upper region of the left mamma was identified as a NC metastasis *via* biopsy.

Mutlimodal treatment with immunovirotherapy

Shortly after admission, an intensive multimodal therapy was initiated (Figure 3). The patient received a second cycle of chemotherapy, now with ifosfamide (2.8 g/m^2) and etoposide (100 mg/m^2) followed by 11 days of radiotherapy with 3 Gy fractions each. Additionally, an oral HDAC inhibitor (suberoylanilide hydroxamic acid (SAHA), 270 mg/d) was started, but had to be discontinued shortly thereafter (before the next cycle of chemotherapy) due to a severe leukopenia and thrombopenia.

As part of our novel add-on immunovirotherapeutic concept, the first dose of T-VEC (108 PFU/ml) was administered intratumorally under ultrasound guidance on day six after the first admission (Figure 3, 4D). The patient experienced only minor expected side effects (well known for any type of oncolytic virotherapy) including a slightly elevated body temperature, glazed eyes, transient fatigue and loss of appetite. The application of pembrolizumab was omitted after the first T-VEC injection to prevent enhanced initial immune clearance of the virus.

Three weeks later she received the second dose of T-VEC and a modified cycle of chemotherapy (since ifosfamide had caused severe confusion and hallucinations), following a modified VIDE protocol with a dose reduction to 75% (VCDE: vincristine 2 mg, cyclophosphamide 1.5 g/m2, doxorubicin 20 mg/m2, etoposide 150 mg/m2). Afterwards, the patient subsequently received the first dose of intravenous pembrolizumab (200 mg) as the second part of immunovirotherapy,

A CT scan after the second therapy cycle showed a partial response (PR) of the primary tumor and of pleural and pulmonal metastases as well as shrinking mediastinal lymph nodes (Figure 1G). These findings were accompanied by a significant clinical improvement of dyspnea and coughing with no further need for any oxygen supply.

On day 56, treatment was continued with a third intratumoral dose of T-VEC again followed by pembrolizumab. Due to prolonged pancytopenia after the second chemotherapy cycle, a further dose reduction to 50% (VCDE) was necessary. A follow-up CT scan demonstrated a generally stable disease (SD), but with a slowly progressive epiphrenic tumor mass (Figure 1).

After another four weeks, the fourth intratumoral T-VEC injection was administered into a highly vital right epiphrenic tumor mass, because a previous CT-Scan had revealed a necrotic primary tumor in the right upper lobe of the lung (Figure 1D), though slowly progressive right epiphrenic tumor manifestations (Figure 1). This resulted again in high serum viral loads as detected by quantitative real-time PCR for HSV-1 DNA (HSV1&2, VZV R-GENE® Kit, Biomerieux) comparable with the level obtained after the first T-VEC injection in the initial right pulmonary tumor mass (Figure 4). Virotherapy was again accompanied by chemotherapy (VCDE; 50%) and pembrolizumab.

Today, six months after the initial diagnosis, the patient has a stable quality of life and no need for additional oxygen supply. Therapy is still ongoing with manageable side effects.

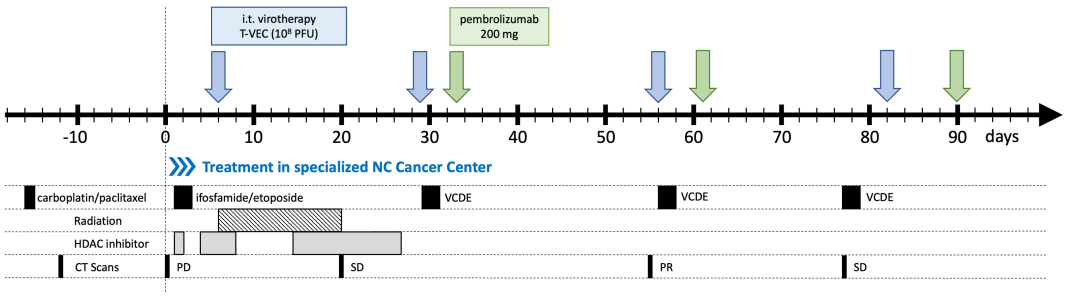

FIGURE 3
Multimodal NUT carcinoma (NC) therapy regimen, including Immunovirotherapy as a novel add-on therapy. Multimodal treatment plan. Days since first admission at specialized NC Cancer Center at University Hospital Tuebingen are shown. Mutlimodal treatment was performed with three-weekly cycles of T-VEC followed by pembrolizumab and accompanied by chemotherapy. Immunovirotherapy: T-VEC (10^8 PFU) blue arrwos, pembrolizumab (200 mg) green arrows. Chemotherapy: CTx #1 Carboplatin/Paclitaxel (performed before referral to UKT), CTx #2 Ifosfamide/Etoposide, CTx #3 Vincristin/Cyclophosphamid/Doxorubicin/Etoposide 75%, CTx #4/#5 Vincristin/Cyclophosphamid/Doxorubicin/Etoposide 50%. Radiation: 11 x 3 Gy = 33 Gy. HDAC inhibitor: oral suberoylanilide hydroxamic acid (SAHA). PD: progressive disease, SD: stable disease, PR: partial response according to RECIST 1.1.

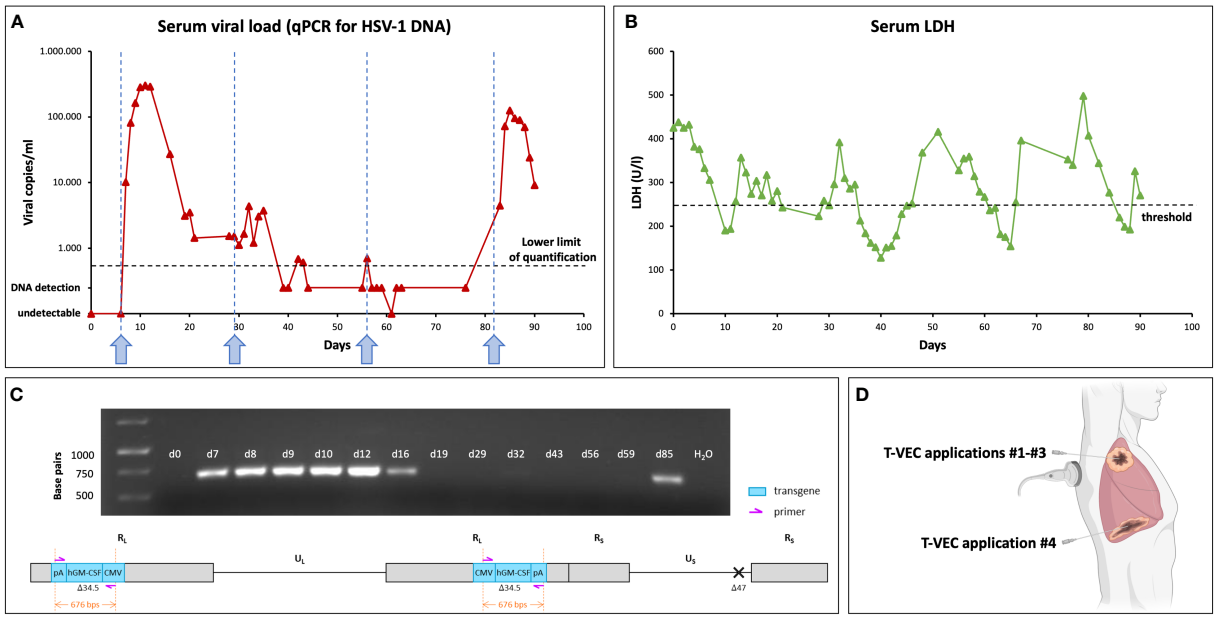

FIGURE 4
Evidence for highly efficient replication of T-VEC in NC tumor cells. **(A)** Serum viral loads over time determined by standard HSV-1 DNA real-time PCR from patient blood samples (blue arrows indicate time points of intratumoral (i.t.) injections of T-VEC). The first three times, T-VEC was administered into the right pulmonary mass identified as the primary tumor. At the time of the third i.t. injection of T-VEC, CT revealed necrosis of this pulmonary mass; as a consequence, the third injection applied again to this area no longer resulted in the production of relevant amounts of T-VEC DNA (days 56-77). Hence, injection site was changed for the fourth application of T-VEC to a highly vital and progressive epiphrenic tumor mass, now resulting again in the production of relatively high loads of HSV-1 DNA. **(B)** Serum LDH serves as a surrogate proliferation marker for NC (high levels are supposed to indicate a highly proliferative state). Each treatment cycle of the multimodal therapy regimen led to the reduction of serum LDH values below the upper normal level of 250 U/l after 5 to 10 days. However, shortly after completion of each cycle, LDH levels increased again in a highly regular manner. **(C)** Agarose gel electrophoresis of a PCR from serum samples employing T-VEC specific primers. Upper panel: Band intensities correlated well with results of standard HSV-1 qPCR **(A)**. Highest intensities were found after the first (d7-d12) and fourth (d85) T-VEC administration. Lower panel: A schematic overview of the T-VEC genome; primers (purple) bind to the flanking regions of the hGM-CSF transgene (blue) located within the terminal repeats (RL) of the unique long region (UL), being highly specific for the T-VEC genome. **(D)** The first three doses of T-VEC were administered into a tumor mass in the right upper pulmonary lobe of the lung *via* dorsal fine needle injection in the scapular line, whereas the fourth dose was injected into a right sided highly vital epiphrenic tumor manifestation at the midaxillary line. Created with BioRender.com.

Discussion

This case illustrates characteristic features of the challenge to timely and correctly diagnose NC. The patient had never smoked, had no relevant past medical history and no family history of cancer. Initially, she was diagnosed with SCC of the lung. Only after the first round of SCC-oriented chemotherapy did not exhibit a proper response, immunostaining for the NUT protein was used as crucial diagnostic tool. Of note, this patient is unusual old for a NC patient, as NC is mostly diagnosed in adolescents and young adults. Suffering from thoracic NC, she is classified in the worst prognostic NC subgroup with an estimated median OS from initial cancer diagnosis of only 4.4 months.

Immunohistochemical staining with an anti-NUT antibody showed strong staining intensity which enabled correct diagnosis (Figure S1). Additional fusion panel RNA sequencing revealed a BRD3::NUTM1 fusion gene, generally responsible for around 15% of NC cases (Figure 2). Interestingly, analysis of the gene breakpoints indicated a breakpoint of BRD3 after coding exon 8 and of NUTM1 before exon 4. Accordingly, the extraterminal domain (ET) and a second nuclear localization sequence in exon 9 of the BRD3 gene are not retained in the fusion gene (Figure 2). Previously described fusion genes of NC with either BRD3 or *BRD4* fusions contained both bromodomains and the ET of *BRD3* or *BRD4*, thus making this the first reported case with a *BRD3::NUTM1* fusion without the ET of *BRD3* (28, 29). The ET of the BET (bromodomain and extraterminal domain) proteins is strongly conserved throughout the human BET protein family and even between different species, thus indicating an important evolutionary function. It plays a major role in recruiting transcriptional regulators such as NSD1-3 and JMJD6 (30). Our findings suggest that the protein recruiting ET is not essential for the oncogenic function of the NUT fusion protein and supports recent *in vitro* studies suggesting that the two bromodomains of BRD4 in a fusion protein with NUT are sufficient for the formation of the pathological hyperacetylated megadomains

(31). However, a fully intact wild-type BRD4 protein seems to be crucial for the formation of the oncogenic nuclear complex and the pathogenesis of non-BRD4-NUT fusion NC (32–34). Importantly, the acidic domain of NUT, which is essential for downstream p300 activation, is retained in this *BRD3::NUTM1* fusion gene (35).

After no initial response to carboplatin/paclitaxel, we initiated an induction chemotherapy based on the standard VIDE protocol for Ewing Sarcoma, as these agents so far have demonstrated the best pre-clinical and case-based evidence in NC so far (6, 8, 10, 11, 36). Because of intolerable side effects (severe confusion, hallucinations) ifosfamide was exchanged with cyclophosphamide, which was shown to be non-inferior in this treatment protocol in the therapy of Ewing sarcomas (37).

The oncolytic virus T-VEC has already shown promising anti-tumoral effects in advanced sarcomas, particularly in a combinatorial treatment with the ICI pembrolizumab (38). Recently, we presented highly promising *in vitro* results exhibiting a very profound direct oncolysis in NC cell lines when being infected by T-VEC (39). Based on these results, we initiated for the first time an immunovirotherapy as a novel add-on treatment in a patient with thoracic NUT carcinoma.

Employing T-VEC, three ultrasound-guided injections into the primary tumor site were followed by a fourth injection into a metastatic epiphrenic tumor mass (Figure 4). Very high levels of serum viral HSV-1 DNA (up to 300,000 copies/ml) after T-VEC injection into previously untreated lesions (first and fourth injection) prove the clinical permissivness of NC for T-VEC as well as a highly efficient replication of T-VEC in NC tumors (Figure 4), while exhibiting only modest and easily manageable side effects. Serum HSV-1 DNA levels steeply increased after the injections and peaked 3 to 5 days after injection. Compared with experiences from melanoma treatment, higher serum viral DNA levels and a longer lasting increase in serum HSV-1 DNA after intratumoral T-VEC applications show the high susceptibility of NC to T-VEC infection and replication (40). A T-VEC-specific PCR confirmed the presence of T-VEC in serum samples and correlated with the results of standard HSV-1 qPCR (Figure 4).

Since replication of T-VEC in the addressed tumor sites is accompanied by a continuous release of immunostimulatory GM-CSF (being encoded in T-VEC as a transgene (39)) notable changes in the composition of the respective tumor micro-environments are triggered. A post treatment tumor specimen obtained from our NC patient at day 98 revealed (i) a partial necrosis, (ii) a switch from a CD3+CD4+ dominant to a CD3 +CD8+ dominant lymphocyte infiltrate as well as (iii) an increased number of tumor infiltrating macrophages (Figure S1 and S2). This indicates remarkable immunologic changes in the tumor microenvironment. Beyond that a particularly enhanced density of CD3+CD8+ lymphocytes has been found previously to be correlated with improved tumor responses to T-VEC (41).

Interestingly, lower HSV-1 serum loads were detected after injections two and three into the primary tumor site in the right upper lobe of the lung. A finding which might indicate unintended administration into mostly necrotic parts of this tumor site. Accordingly, a significant part of the injected volume of T-VEC could not induce repetitive infections of vital NC cells, ultimately causing a significantly reduced production of viral progeny. However, sequential CT scans confirmed regression and necrosis of the primary tumor site (Figure 1) and a stable situation in distant metastases. In summary, this implies a strong replication capacity and local anti-tumor efficacy of T-VEC in this case of thoracic NC. Further investigations are required to evaluate the effects of multimodal approaches, including such diverse treatments as chemotherapy, radiation, pleurodesis, HDAC inhibition, BET inhibition, immune checkpoint inhibition, virotherapy and possibly also other modalities.

For the fourth treatment cycle, the injection site was changed to a viable, slowly progressive epiphrenic tumor mass, which again resulted in the shedding of very high HSV-1 load levels into the patient´s circulation and pathologically confirmed necrosis (Figure 4; peak viral loads depicted after the fourth arrow in blue; Figure S2).

Additional pembrolizumab infusions were administered shortly after virotherapy to enhance the systemic anti-tumoral immune response primarily generated by T-VEC (16) (Figure 3). On purpose, application of pembrolizumab was not initiated right away (i.e., simultaneously with the first T-VEC injection, in order to allow unhindered T-VEC replication at this early time point and thereby induced changes in the tumor microenvironment. In this case, a clear-cut evaluation and dissection of the extent of any additional effects contributed by pembrolizumab is not possible.

During treatment, serum lactate dehydrogenase (LDH) served as a surrogate proliferation marker for NC; high levels are supposed to indicate a highly proliferative state (Figure 4). Each treatment cycle of the multimodal therapy regimen led to the reduction of serum LDH values below the upper normal level of 250 U/l. However, shortly after completion of each cycle, LDH levels increased again in a highly regular manner. Notably, the multimodal treatment approach employed here kept serum LDH levels in a range between 100 and 500 U/l during the whole treatment period; however, the contribution of immunovirotherapy to this aspect of disease stabilization cannot be clearly defined in this report of a single case and needs a broader investigation. This can be regarded as a therapeutic success, especially when looking at the very poor prognosis of NC cases exhibiting thoracic NC.

Conclusion

In summary, this case demonstrates for the first time the feasibility of virotherapy in a NC patient. Treatment was well tolerated and signs of tumor response to administration of T-VEC were noted in the context of a multimodal regime. Further, tumor stabilization and improvement of the patient's quality of

life could be achieved. Furthermore, a previously unknown variant of the *BRD3::NUTM1* fusion gene was described.

Data availability statement

The original contributions presented in the study are included in the article/Supplementary Material. Further inquiries can be directed to the corresponding author.

Ethics statement

Ethical review and approval was not required for the study on human participants in accordance with the local legislation and institutional requirements. The patients/participants provided their written informed consent to participate in this study. Written informed consent was obtained from the individual(s) for the publication of any potentially identifiable images or data included in this article.

Author contributions

LK: Conceptualization, investigation, methodology, data interpretation, writing – original draft. BC, KB, AG, SB, SG: Implementation of treatment, writing – review and editing. MH: Data interpretation, writing – original draft. SH: Investigation, methodology, data interpretation, writing – original draft. SB, JB, MC: Data interpretation, writing – review and editing. TG, SS: Implementation of treatment, writing – review and editing. AA, RS: Investigation, methodology, writing – review and editing. AH, TD, SM, FF, MR: Implementation of treatment, writing – review and editing. LZ: Supervision, writing – review and editing. UL: Supervision, conceptualization, investigation, data interpretation, implementation of treatment, writing – original draft. All authors contributed to the article and approved the submitted version.

Funding

LK is funded by the intramural *f*ortüne program of the Faculty of Medicine, University of Tuebingen (proposal number 3007-0-0).

Acknowledgments

We would like to thank our patient and her family. We further acknowledge support by the Open Access Publishing Fund of the University of Tübingen.

Conflict of interest

The authors declare that the research was conducted in the absence of any commercial or financial relationships that could be construed as a potential conflict of interest.

Publisher's note

Supplementary material

The Supplementary Material for this article can be found online at: https://www.frontiersin.org/articles/10.3389/fonc.2022.995744/full#supplementary-material

References

1. French CA. NUT midline carcinoma. *Cancer Genet Cytogenet* (2010) 203 (1):16–20. doi: 10.1016/j.cancergencyto.2010.06.007

2. Chau NG, Ma C, Danga K, Al-Sayegh H, Nardi V, Barrette R, et al. An anatomical site and genetic-based prognostic model for patients with nuclear protein in testis (NUT) midline carcinoma: Analysis of 124 patients. *JNCI Cancer Spectr* (2020) 4(2):pkz094. doi: 10.1093/jncics/pkz094

3. Moreno V, French CA, Guo T, Zhu H, Zhang S, Duncan D, et al. NUT carcinoma of the submandibular gland: A case at this uncommon site with review of the literature. *Head Neck Pathol* (2021) 16:881–92. doi: 10.1007/s12105-021-01400-x

4. Bauer DE, Mitchell CM, Strait KM, Lathan CS, Stelow EB, Luer SC, et al. Clinicopathologic features and long-term outcomes of NUT midline carcinoma. *Clin Cancer Res* (2012) 18(20):5773–9. doi: 10.1158/1078-0432.CCR-12-1153

5. Chau NG, Hurwitz S, Mitchell CM, Aserlind A, Grunfeld N, Kaplan L, et al. Intensive treatment and survival outcomes in NUT midline carcinoma of the head and neck. *Cancer* (2016) 122(23):3632–40. doi: 10.1002/cncr.30242

6. French CA, Cheng ML, Hanna GJ, DuBois SG, Chau NG, Hann CL, et al. Report of the first international symposium on NUT carcinoma. *Clin Cancer Res* (2022) 28(12):2493–505. doi: 10.1158/1078-0432.CCR-22-0591

7. Haack H, Johnson LA, Fry CJ, Crosby K, Polakiewicz RD, Stelow EB, et al. Diagnosis of NUT midline carcinoma using a NUT-specific monoclonal antibody. *Am J Surg Pathol* (2009) 33(7):984–91. doi: 10.1097/PAS.0b013e318198d666

8. Storck S, Kennedy AL, Marcus KJ, Teot L, Vaughn J, Gnekow AK, et al. Pediatric NUT-midline carcinoma: Therapeutic success employing a sarcoma based multimodal approach. *Pediatr Hematol Oncol* (2017) 34(4):231–7. doi: 10.1080/08880018.2017.1363839

9. Mertens F, Wiebe T, Adlercreutz C, Mandahl N, French CA. Successful treatment of a child with t (15,19)-positive tumor. *Pediatr Blood Cancer* (2007) 49 (7):1015–7. doi: 10.1002/pbc.20755

10. Leeman R, Pinkney K, Bradley JA, Ruiz R, DuBois SG, French C, et al. NUT carcinoma without upfront surgical resection: A case report. *J Pediatr Hematol Oncol* (2021) 43(5):e707–e10. doi: 10.1097/MPH.0000000000001865

11. Muramatsu J, Takada K, Sugita S, Tsuchiya T, Yamamoto K, Takagi M, et al. Complete response induced by concurrent chemoradiotherapy in a patient with NUT carcinoma. *Intern Med* (2022) 61(8):1299–304. doi: 10.2169/internalmedicine.7741-21

12. Xie XH, Wang LQ, Qin YY, Lin XQ, Xie ZH, Liu M, et al. Clinical features, treatment, and survival outcome of primary pulmonary NUT midline carcinoma. *Orphanet J Rare Dis* (2020) 15(1):183. doi: 10.1186/s13023-020-01449-x

13. Joel S, Weschenfelder F, Schleussner E, Hofmann GO, Weschenfelder W. NUT midline carcinoma in a young pregnant female: A case report. *World J Surg Oncol* (2020) 18(1):290. doi: 10.1186/s12957-020-02065-6

14. Zhao R, Hua Z, Hu X, Zhang Q, Zhang J, Wang J. NUT carcinoma of the LungA case report and literature analysis. *Front Oncol* (2022) 12:890338. doi: 10.3389/fonc.2022.890338

15. Lauer UM, Beil J. Oncolytic viruses: challenges and considerations in an evolving clinical landscape. *Future Oncol* (2022) 18(24):2713–32. doi: 10.2217/fon-2022-0440

16. Ribas A, Dummer R, Puzanov I, VanderWalde A, Andtbacka RHI, Michielin O, et al. Oncolytic virotherapy promotes intratumoral T cell infiltration and improves anti-PD-1 immunotherapy. *Cell* (2017) 170(6):1109–19 e10. doi: 10.1016/j.cell.2017.08.027

17. Puzanov I, Milhem MM, Minor D, Hamid O, Li A, Chen L, et al. Talimogene laherparepvec in combination with ipilimumab in previously untreated, unresectable stage IIIB-IV melanoma. *J Clin Oncol* (2016) 34 (22):2619–26. doi: 10.1200/JCO.2016.67.1529

18. Teijeira Crespo A, Burnell S, Capitani L, Bayliss R, Moses E, Mason GH, et al. Pouring petrol on the flames: Using oncolytic virotherapies to enhance tumour immunogenicity. *Immunology* (2021) 163(4):389–98. doi: 10.1111/imm.13323

19. Liu BL, Robinson M, Han ZQ, Branston RH, English C, Reay P, et al. ICP34.5 deleted herpes simplex virus with enhanced oncolytic, immune stimulating, and anti-tumour properties. *Gene Ther* (2003) 10(4):292–303. doi: 10.1038/sj.gt.3301885

20. Andtbacka RH, Kaufman HL, Collichio F, Amatruda T, Senzer N, Chesney J, et al. Talimogene laherparepvec improves durable response rate in patients with advanced melanoma. *J Clin Oncol* (2015) 33(25):2780–8. doi: 10.1200/JCO.2014.58.3377

21. Moesta AK, Cooke K, Piasecki J, Mitchell P, Rottman JB, Fitzgerald K, et al. Local delivery of OncoVEX(mGM-CSF) generates systemic antitumor immune responses enhanced by cytotoxic T-Lymphocyte-Associated protein blockade. *Clin Cancer Res* (2017) 23(20):6190–202. doi: 10.1158/1078-0432.CCR-17-0681

22. Bonaventura P, Shekarian T, Alcazer V, Valladeau-Guilemond J, Valsesia-Wittmann S, Amigorena S, et al. Cold tumors: A therapeutic challenge for immunotherapy. *Front Immunol* (2019) 10:168. doi: 10.3389/fimmu.2019.00168

23. Davis A, Mahar A, Wong K, Barnet M, Kao S. Prolonged disease control on nivolumab for primary pulmonary NUT carcinoma. *Clin Lung Cancer* (2021) 22 (5):e665–e7. doi: 10.1016/j.cllc.2020.10.016

24. He M, Chernock R, Zhou S, Gondim M, Dehner LP, Pfeifer JD. Tumor mutation burden and checkpoint immunotherapy markers in NUT midline carcinoma. *Appl Immunohistochem Mol Morphol* (2020) 28(7):495–500. doi: 10.1097/PAI.0000000000000781

25. Li X, Shi H, Zhang W, Bai C, He M, Ta N, et al. Immunotherapy and targeting the tumor microenvironment: Current place and new insights in primary pulmonary NUT carcinoma. *Front Oncol* (2021) 11:690115. doi: 10.3389/fonc.2021.690115

26. Cho YA, Choi YL, Hwang I, Lee K, Cho JH, Han J. Clinicopathological characteristics of primary lung nuclear protein in testis carcinoma: A single-institute experience of 10 cases. *Thorac Cancer* (2020) 11(11):3205–12. doi: 10.1111/1759-7714.13648

27. Lee T, Choi S, Han J, Choi YL, Lee K. Abrupt dyskeratotic and squamoid cells in poorly differentiated carcinoma: Case study of two thoracic NUT midline carcinomas with cytohistologic correlation. *J Pathol Transl Med* (2018) 52(5):349–53. doi: 10.4132/jptm.2018.07.16

28. French CA, Ramirez CL, Kolmakova J, Hickman TT, Cameron MJ, Thyne ME, et al. BRD-NUT oncoproteins: A family of closely related nuclear proteins that block epithelial differentiation and maintain the growth of carcinoma cells. *Oncogene* (2008) 27(15):2237–42. doi: 10.1038/sj.onc.1210852

29. Dickson BC, Sung YS, Rosenblum MK, Reuter VE, Harb M, Wunder JS, et al. NUTM1 gene fusions characterize a subset of undifferentiated soft tissue and visceral tumors. *Am J Surg Pathol* (2018) 42(5):636–45. doi: 10.1097/PAS.0000000000001021

30. Rahman S, Sowa ME, Ottinger M, Smith JA, Shi Y, Harper JW, et al. The Brd4 extraterminal domain confers transcription activation independent of pTEFb by recruiting multiple proteins, including NSD3. *Mol Cell Biol* (2011) 31(13):2641–52. doi: 10.1128/MCB.01341-10

31. Ibrahim Z, Wang T, Destaing O, Salvi N, Hoghoughi N, Chabert C, et al. Structural insights into p300 regulation and acetylation-dependent genome organisation. *bioRxiv* (2022), 484228. doi: 10.1101/2022.03.14.484228

32. Shiota H, Elya JE, Alekseyenko AA, Chou PM, Gorman SA, Barbash O, et al. "Z4" complex member fusions in NUT carcinoma: Implications for a novel oncogenic mechanism. *Mol Cancer Res* (2018) 16(12):1826–33. doi: 10.1158/1541-7786.MCR-18-0474

33. Alekseyenko AA, Walsh EM, Zee BM, Pakozdi T, Hsi P, Lemieux ME, et al. Ectopic protein interactions within BRD4-chromatin complexes drive oncogenic megadomain formation in NUT midline carcinoma. *Proc Natl Acad Sci U.S.A.* (2017) 114(21):E4184–E92. doi: 10.1073/pnas.1702086114

34. French CA, Rahman S, Walsh EM, Kuhnle S, Grayson AR, Lemieux ME, et al. NSD3-NUT fusion oncoprotein in NUT midline carcinoma: implications for a novel oncogenic mechanism. *Cancer Discovery* (2014) 4(8):928–41. doi: 10.1158/2159-8290.CD-14-0014

35. Reynoird N, Schwartz BE, Delvecchio M, Sadoul K, Meyers D, Mukherjee C, et al. Oncogenesis by sequestration of CBP/p300 in transcriptionally inactive hyperacetylated chromatin domains. *EMBO J* (2010) 29(17):2943–52. doi: 10.1038/emboj.2010.176

36. Beesley AH, Stirnweiss A, Ferrari E, Endersby R, Howlett M, Failes TW, et al. Comparative drug screening in NUT midline carcinoma. *Br J Cancer* (2014) 110(5):1189–98. doi: 10.1038/bjc.2014.54

37. Le Deley MC, Paulussen M, Lewis I, Brennan B, Ranft A, Whelan J, et al. Cyclophosphamide compared with ifosfamide in consolidation treatment of standard-risk Ewing sarcoma: results of the randomized noninferiority Euro-EWING99-R1 trial. *J Clin Oncol* (2014) 32(23):2440–8. doi: 10.1200/JCO.2013.54.4833

38. Kelly CM, Antonescu CR, Bowler T, Munhoz R, Chi P, Dickson MA, et al. Objective response rate among patients with locally advanced or metastatic sarcoma treated with talimogene laherparepvec in combination with pembrolizumab: A phase 2 clinical trial. *JAMA Oncol* (2020) 6(3):402–8. doi: 10.1001/jamaoncol.2019.6152

39. Ohnesorge PV, Berchtold S, Beil J, Haas SA, Smirnow I, Schenk A, et al. Efficacy of oncolytic herpes simplex virus T-VEC combined with BET inhibitors as an innovative therapy approach for NUT carcinoma. *Cancers (Basel)* (2022) 14 (11):2761–79. doi: 10.3390/cancers14112761

40. Andtbacka RHI, Amatruda T, Nemunaitis J, Zager JS, Walker J, Chesney JA, et al. Biodistribution, shedding, and transmissibility of the oncolytic virus talimogene laherparepvec in patients with melanoma. *EBioMedicine* (2019) 47:89–97. doi: 10.1016/j.ebiom.2019.07.066

41. Dummer R, Gyorki DE, Hyngstrom J, Berger AC, Conry R, Demidov L, et al. Neoadjuvant talimogene laherparepvec plus surgery versus surgery alone for resectable stage IIIB-IVM1a melanoma: A randomized, open-label, phase 2 trial. *Nat Med* (2021) 27(10):1789–96. doi: 10.1038/s41591-021-01510-7

frontiers | Frontiers in Oncology

TYPE Case Report
PUBLISHED 01 November 2022
DOI 10.3389/fonc.2022.1020875

OPEN ACCESS

EDITED BY
Kohei Fujita,
National Hospital Organization Kyoto Medical Center, Japan

REVIEWED BY
Dongsheng Chen,
Simcere, China
Aruna Nambirajan,
All India Institute of Medical Sciences, India

*CORRESPONDENCE
Xiaoyang Chen
1073356693@qq.com

SPECIALTY SECTION
This article was submitted to Thoracic Oncology, a section of the journal Frontiers in Oncology

RECEIVED 16 August 2022
ACCEPTED 13 October 2022
PUBLISHED 01 November 2022

CITATION
Shi L, Lin L, Ding Y, Zeng Y and Chen X (2022) Case report: A rapid response to immunotherapy in a thoracic SMARCA4-deficient undifferentiated tumor with respiratory failure. *Front. Oncol.* 12:1020875. doi: 10.3389/fonc.2022.1020875

Case report: A rapid response to immunotherapy in a thoracic SMARCA4-deficient undifferentiated tumor with respiratory failure

Liyong Shi, Lianshun Lin, Yin Ding, Yiming Zeng and Xiaoyang Chen*

Department of Respiratory and Critical Care Medicine, The Second Affiliated Hospital of Fujian Medical University, Quanzhou, China

Thoracic SMARCA4-deficient undifferentiated tumor (SMARCA4-UT) is an extremely rare and poor-prognosis malignancy, which has recently been noted as a subtype of lung tumors. We presented a case of SMARCA4-UT in a 50-year-old man with progressively worsening respiratory failure. The tumor was the first reported to involve pulmonary artery, and 90% of tumor cells expressed programmed cell death ligand 1 (PD-L1). High tumor mutational burden (TMB, 23.93/Mb) and mutations in SMARCA4 were detected. It is the first reported case to receive Tislelizumab monotherapy with considerable improvement in clinical condition and no adverse events. As a result of our case, we highlight the importance of recognizing SMARCA4-UT as an individual entity, as well as the efficacy of immune checkpoint inhibitor therapy, particularly in patients with high levels of TMB and PD-L1 expression.

KEYWORDS

SMARCA4-UT, immunotherapy, tislelizumab, PD-L1 expression, immune checkpoint inhibitor

Introduction

Thoracic SMARCA4-deficient undifferentiated tumor (SMARCA4-UT), an aggressive and rare malignancy, is characterized by SMARCA4 gene inactivating mutation and presents with rapidly progressive masses involving the mediastinum, lung, and pleura. It has been established as a new histomorphological and molecular entity of thoracic tumors (1). Since the first report by Sauter et al. in 2015 up to now, no more than 100 cases have been reported in the literature (2).

There are no treatment guidelines for SMARCA4-UT. It was previously classified as a sarcoma subtype and treated with chemotherapy, which was often ineffective. Despite

operable cases, recurrence occurs and systemic chemotherapy is required (2, 3). Recently, a few patients with SMARCA4-UT have been reported to be successfully treated with anti-PD-1 and PD-L1 antibodies (4–8).

We herein report a rapid response to Tislelizumab as the first-line treatment in a SMARCA4-UT with PD-L1 overexpression.

Case presentation

A 50-year-old man presented to our hospital complaining of increasingly worsening dyspnea, hemoptysis, and thoracic pain for 2 weeks with a weight loss of nearly 10 kg. He had a 36-pack-year smoking history and is a current smoker. There was no significant past medical history. His premorbid level of function was poor, with an Eastern Cooperative Oncology Group (ECOG) performance status (PS) of 3. His consciousness was clear; temperature was 36.2°C, blood pressure 136/88 mmHg, pulse 124/min, respiratory rate 26/min, and peripheral oxygen saturation 90% (room air). Following an examination of the respiratory system, decreased left-sided breath sounds were noted. Laboratory investigations revealed a normal white blood cell count of 6500/mm^3 and a normal neutrophil count (71%; reference range, 40%–75%). Arterial blood gas showed a pH of 7.42, pCO_2 of 32.8 mm Hg, and pO_2 of 58 mm Hg. Assessment of serum tumor markers revealed a high neuron-specific enolase (NSE, 29.34 ng/ml; reference range ≤16.3), whereas carcinoembryonic antigen (CEA), cytokeratin 19 fragment (Cyfra 21-1), alpha-fetoprotein (AFP), and carbohydrate antigen 125 (CA125) were within the reference range. D-Dimer was elevated, 1.05 μg/ml (reference range, 0–0.5), and the evaluation of the cardiac function including B-type natriuretic peptide (BNP), Troponin I, and electrocardiogram was normal. A CT scan revealed a large mass of 11.46 cm × 11.19 cm in the left upper lobe of the lung (Figure 1A) involving the pulmonary artery and without enlargement of the hilar and mediastinal lymph nodes. Furthermore, thoracic and cardiac color Doppler ultrasound revealed a small amount of pleural and pericardial effusion. Cerebral, abdominal, and radionuclide bone scan examinations detected no abnormalities.

We performed a color Doppler ultrasound-guided percutaneous needle biopsy for the mass. The following clinicopathological examination revealed sheets of homogenous large tumor cells with a moderate amount of eosinophilic cytoplasm, eccentrically positioned vesicular nuclei, and prominent nucleoli (Figure 2A). On immunohistochemistry, the mass was completely SMARCA4-negative and partly positive for SMARCA2 (Figures 2B, C). These tumor cells were focally positive for cytokeratin (CK), CK7, CKpan, CK8/18, and Syn (Figures 2D–G) and diffusely positive for vimentin. They were negative for Claudin-4, Napsin-A, TTF-1, S-100, CK5/6, and CgA. In addition, Ki-67 staining was positive (60%). A 520-gene panel next-generation sequencing (NGS) was performed, which showed a somatic *SMARCA4* c.797C>T (p. Ser266*) mutation and no abnormal SMARCB1 gene. The tumor exhibited microsatellite stability (MSS), tumor mutational burden (TMB) of 23.93 muts/Mb, and high PD-L1 expression (tumor proportion score more than 90%) (Figure 2H) with concurrent mutations in *KEAP1*, *TP53*, and *TERT*. According to the diagnostic criteria of the WHO (1), all evidence resulted in a definitive diagnosis of stage IVa SMARCA4-UT (ECOG PS 3) involving the pulmonary artery, pericardium, and pleura.

The patient was treated with Tislelizumab. After one dose of Tislelizumab (200 mg) infusion, the patient's dyspnea, thoracic pain, and hemoptysis were rapidly relieved the next day, suggesting a notable clinical benefit. ECOG PS reduced from 3 to 1 with stable vital signs, and peripheral oxygen saturation rose to 96% (room air). Arterial blood gas showed a pH of 7.45, a pCO_2 of 37.2 mm Hg, and a pO_2 of 76 mm Hg. Regular CT scans revealed significant improvement in pulmonary artery compression and a partial response (PR; Figures 1B, C) after 20 days. A CT scan after six cycles of Tislelizumab demonstrated

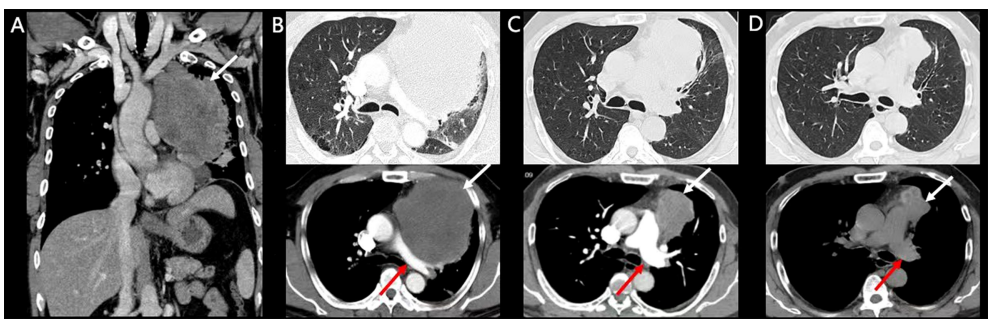

FIGURE 1
Enhanced CT and follow-up CT images. White arrows indicate tumors and red arrows indicate the pulmonary artery. **(A, B)** Pretreatment CT scan of the patient. **(C)** CT scan after two doses of Tislelizumab. **(D)** CT scan after six doses of Tislelizumab.

a sustained durable PR response [51% tumor size compared with baseline pretreatment according to RECIST version 1.1 (9)] with no adverse events (Figure 1D). The treatment timeline and therapeutic response are shown in Figure 3.

Discussion

In recent years, SMARCA4-UT has become increasingly recognized as a progressive malignant disease. There has been an important change in terminology since the 'sarcoma' classification was dropped in favor of 'thoracic SMARCA4-deficient undifferentiated tumor (SMARCA4-UT)', which is newly classified in the fifth edition of the WHO classification of thoracic tumors (2021) (1). It was classified as a subtype of undifferentiated lung cancer of pulmonary epithelial origin (10). These tumors mostly occur in the fourth and fifth decades of life; moreover, there is a strong connection with smoking history (only 10% of the cases are reported in non-smokers). It often occurs in advanced stages, presenting a poor prognosis, with a median survival of 4–7 months (1, 4, 11). The clinical features of most cases present with non-specific symptoms such as cough, dyspnea, and hemoptysis (11). Some cases present with related signs like the superior vena cava syndrome (12) and distant metastasis; in particular, skeletal metastases are common (13). Recurrent pleural effusions or empyema can accompany pleural masses (14). Only one asymptomatic case has been reported, in a smoker during a routine chest X-ray (15).

Among thoracic SMARCA4-UTs, the involvement of the mediastinum, pulmonary hilum, lung, cervical-subclavian lymph nodes, and/or pleura is common with or without chest wall invasion. The common imaging findings of SMARCA4-UT

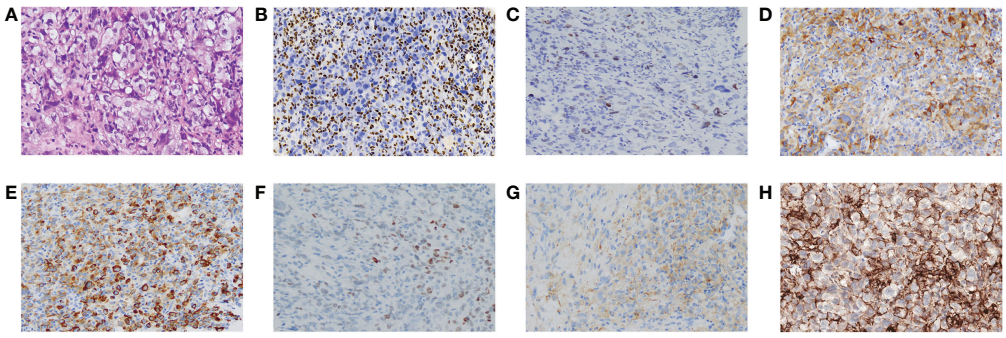

FIGURE 2
Pathological features of SMARCA4-UT. **(A)** Stained with hematoxylin and eosin. Immunostaining was negative for SMARCA4 **(B)**, and partly or focally positive for SMARCA2 **(C)**, CK8/18 **(D)**, CKpan **(E)**, SOX **(F)**, and Syn **(G)**. Programmed cell death ligand 1 (PD-L1) staining **(H)**. Magnification, 100×.

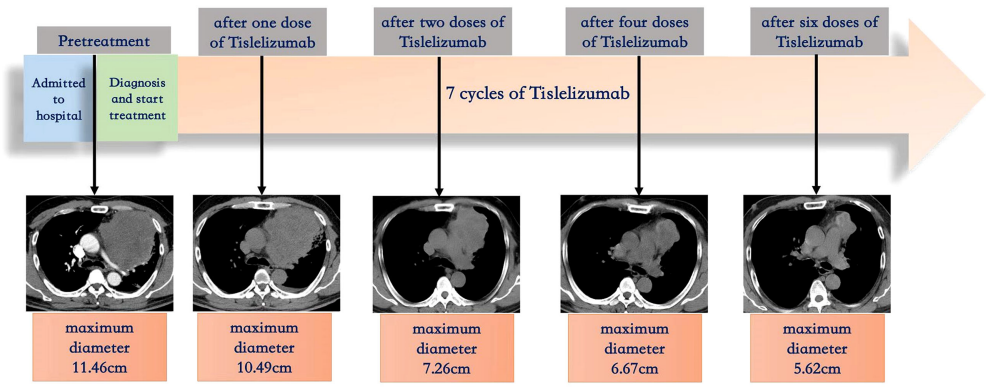

FIGURE 3
Treatment timeline and therapeutic response.

presented as ill-defined, large, and compressive masses, especially in the mediastinum, but the primary lung tumor may rarely be small (1). Metastases are frequent at presentation with adrenal, bone, and brain involvement (16). In rare cases, there are unilateral, multifocal, or single masses involving the visceral and parietal pleura, occasionally extending to the soft tissue of the chest wall. An isolated chest wall tumor (14) and axillary lymphadenopathy (17) are rare conditions. In our present case, metastases were present in the pericardium and the pleura, and it is the first reported case to show the involvement of the pulmonary artery. As a result, we suggest that imaging findings of an infiltrative, compressive, heterogeneous, ill-defined, large thoracic mass should be suspicious for SMARCA4-UT.

Histologically, SMARCA4-UT consists of undifferentiated sheets of relatively homogenous, incohesive tumor cells with prominent nuclei and vesicular nucleoli. There may be uniformly epithelioid and rhabdoid cells with abundant eosinophilic cytoplasm and high mitotic rates in tumor cells. The complete loss of Brahma-related gene-1 (*BRG1*), which is encoded by the *SMARCA4* gene, is typical, and 25% of the cases show a severe reduction of expression (11, 17, 18). Most cases show loss of *SMARCA2* (*BRM*) staining (19). A variety of low-molecular-weight cytokeratins, epithelial membrane antigens, and neuroendocrine markers are also present in the tumors. CD34, SOX2, and/or SALL4 are also expressed in many cases. Across all cases, *SMARCA4* mutations are homozygous with loss of heterozygosity (10). The ATPase subunits of the *SWI/SNF* complex are encoded by the *SMARCA4* gene (17). A loss of *BRG1* leads to a failure of the ATPase-dependent eviction of polycomb recessive complexes, resulting in chromatin reorganization, as well as changes in the levels of gene expression that likely contribute to tumorigenesis. *BRM* deficiency may potentiate sarcomatoid transformation and epidermal mesenchymal transition (20). In general, the clinical presentation and radiological features of SMARCA4-UT are non-specific. It is essentially a clinicopathological diagnosis.

The current study on therapy for a new and challenging tumor entity is fragmented (21). Most cases present are generally resistant to chemotherapy and radiotherapy (19). In some surgically resectable cases, radical surgical excision has led to remission (5, 15). Novel treatment strategies are awaited, including immune checkpoint inhibitions (ICIs). ICIs had shown promising effects in some cases. Our literature review indicated that seven other cases have used immunotherapy for the treatment of SMRACA4-UT (4, 6–8, 15). In both low and high PD-L1 expression and effector T-cell signatures, immunotherapy has been shown to improve progression-free survival (PFS). The clinical data of patients under the treatment of immunotherapy are summarized in Table 1. The patients' age ranged from 41 to 73 years, and the data exhibited a female-to-male ratio of nearly 1:1. All the patients had advanced-stage diseases. The longest PFS exhibited was more than 17 months, which was with ABCP treatment (7). In one case, renal dysfunction and respiratory failure progressively worsened in the patient, who died 25 months after the initial diagnosis (8). Six of seven cases combined immunotherapy with other treatments such as chemotherapy, radiotherapy, and even surgery (4, 7, 8, 15). A combination of pembrolizumab and ipilimumab produced mixed results in one study, which is the first case to use dual ICI combination therapy for SMARCA4-UT with PD-L1 overexpression (100%) (8). Only one case was given pembrolizumab monotherapy as a first-line treatment and demonstrated a sustained durable PR response after eight cycles (6).

The mechanisms that determine the efficacy of immunotherapy are yet to be fully elucidated. A growing body of evidence suggests that PD-L1 and TMB expression play a role in this disease (10, 22). Three studies on respective patients showed improvement after treatment of PD-1 antibody (pembrolizumab) or PD-L1 antibody (atezolizumab) in patients with high PD-L1 expression (>50%) (6–8). Of note, three cases that did not express PD-L1 exhibited PFS longer than 10 months (4, 5, 7), and a sustained PR response with no adverse events was demonstrated. These cases suggest that there may be therapeutic effect regardless of the expression of PD-L1 and TMB. However, due to the limited number of cases, TMB and PD-L1 expression cannot yet be used as independent predictors of prognosis, and, therefore, further studies and exploration are required.

In one of these cases, although TMB and PD-L1 TPS were high, PFS was still the shortest with a combination therapy of ABCP and radiotherapy (8). Schoenfeld et al. (22) have evaluated the genomic context of *SMARCA4* alterations, which showed that *SMARCA4* alterations often co-occur with *TP53*(56%), *KEAP1*(41%), *STK11*(39%), and *KRAS* (36%) alterations in lung cancer. Co-occurrence of *STK11* and *KEAP1* mutations in SMARCA4-mutant NSCLC was associated with decreased survival. Further evaluation of factors that predict outcomes to ICIs revealed that *SMARCA4*-mutant tumors with *STK11* and *KEAP1* mutations have a poor prognosis and lack of response to ICIs in *KRAS*-mutant tumors. Further research by Marinelli et al. (23) has indicated the *KEAP1* mutation is associated with resistance to immunotherapy in lung adenocarcinoma despite the high TMB. This may suggest that the poor efficacy of immunotherapy in cases with high tumor mutational burden and PD-L1 expression may be related to *KEAP1* mutation. In contradiction, in our case, response was rapid despite *KEAP1* mutation detection. Overall, the role of *KEAP1* mutation in SMARCA4-UT remains unclear.

In our case, the tumor presented as a large compressive mass and is the first reported case to involve the pulmonary

10.3389/fonc.2022.1020875

TABLE 1 Clinical data for patients with SMARCA4-UT on the therapy of immunotherapy.

	No.	Age (Y)/ gender	Smoking status	Lesion location	TMN	PD-L1 TPS (%)	TMB (/Mb)	Mutation	Treatment	Outcome (follow-up)
Henon et al. (4)	1	58/F	Unknown	Mediastinal, hilar and paratracheal involvement, along with pleural and peritoneal metastases	IV	0	Remarkably low	Unknown	Radiotherapy+ chemotherapy+ pembrolizumab	11 months PR to March 2019
Kunimass et al. (5)	2	51/M	22.5 pack-years	Right lung upper lobe with soft tissue, vertebral invasion and pleural	IVA	0	10.2	*SMARCA4* (L1161fs), *TP53* (V157L)	ABCP + surgery	9 months PR after surgery to August 2021
Kohichi et al. (6)	3	69/F	Unknown	Left mediastinal tumor, peritoneal and retroperitoneal dissemination and multiple cutaneous metastases	IV	60	Unknown	Unknown	Pembrolizumab	8 cycles of PR to September 2019
Kawachi et al. (7)	4	73/F	53 pack-years	Left upper lobe, mediastinal lymphadenopathy and osteolytic metastasis in the fifth cervical vertebra	IVB	40	11	*SMARCA4* (c.1119-1G>T), *TP53, SPTA1, CHD2*	ABCP	Progressed after 17 months of PR to 2021
Kawachi et al. (7)	5	59/M	39 pack-years	Left lower lobe, an oropharyngeal mass, left adrenal gland mass, left cervical lymphadenopathy, left hilar lymphadenopathy and multiple abdominal lymphadenopathies	IVB	0	11.8	*SMARCA4* (K755Nfs), *TP53*, *TSC2*	ABCP	Progressed after 10 months of PR to 2021
Kawachi et al. (7)	6	64/F	44 pack-years	Left upper lung lobe, mediastinal lymphadenopathy and a brain mass in the left parietal lobe	IVB	80	14.9	*SMARCA4* (H103Mfs), *TP53, SPTA1, TSC2, KEAP1*	ABCP+ Radiotherapy	Progressed after 7 cycles of PR and 2 months maintenance therapy to 2021
Anžiča et al. (8)	7	41/M	Current smoker	Upper anterior mediastinum encompassing infracarinal and hilar lymph nodes.	IV	100	674SNV and 47 indels	*CDKN2A* (p.T18fs), *SMARCA4* (p.K1334fs)	Pembrolizumab + ipilimumab + chemotherapy + radiotherapy	25 months to death

ABCP, atezolizumab, bevacizumab, paclitaxel, and carboplatins.

artery, pericardium, and pleura without extrathoracic metastasis. This case also showed overexpressed PD-L1 TPS of 90% and remarkably high TMB (29.93/Mb). It is the first reported case to receive Tislelizumab monotherapy with considerable and rapid improvement in clinical condition. Following seven courses of PD-1 inhibitor therapy, a CT scan demonstrated a sustained durable partial response with no adverse events.

In conclusion, the diagnosis of SMARCA4-UT is sometimes challenging. A multidisciplinary approach to diagnosis is essential, including clinical, radiologic, pathologic, and genetic factors. Our findings support the fact that ICIs may be beneficial, especially in patients with high PD-L1 expression and TMB. It is necessary to conduct further studies to optimize novel therapeutic approaches and to clarify whether ICI monotherapy or combination therapy is appropriate.

Data availability statement

The raw data supporting the conclusions of this article will be made available by the authors, without undue reservation.

Ethics statement

The studies involving human participants were reviewed and approved by Committee of the 2nd Affiliated Hospital of Fujian Medical University in China (ethical code B2021-315).

The patients/participants provided their written informed consent to participate in this study. Written informed consent was obtained from the individual for the publication of any potentially identifiable images or data included in this article.

Author contributions

LS and XC made accurate diagnosis and contributed to the care of this patient, the analysis of the clinical data and the literature review. LL and YD provided technical help or writing assistance. YZ was the departmental chair and provided general support. All authors contributed to the article and approved the submitted version.

Funding

National Key Research and Development Program of China (2019YFC0121705); Quanzhou City Science and Technology Program (Award number(s): 2020N034S, 2019C025R, 2018N008S); Bethune Charitable Foundation (Award number (s):SCZ134DS); Startup Fund for Scientific Research, Fujian Medical University (Grant number: 2021QH1111).

Conflict of interest

The authors declare that the research was conducted in the absence of any commercial or financial relationships that could be construed as a potential conflict of interest.

Publisher's note

References

1. WHO Classification of Tumours Editorial Board. *WHO classification of tumours. thoracic tumours [M]. 5th ed.* Lyon: IARC Press (2021).

2. Le Loarer F, Watson S, Pierron G, de Montpreville VT, Ballet S, Firmin N, et al. SMARCA4 inactivation defines a group of undifferentiated thoracic malignancies transcriptionally related to BAF-deficient sarcomas. *Nat Genet* (2015) 47(10):1200–5. doi: 10.1038/ng.3399

3. Kunimasa K, Nakamura H, Sakai K, Tamiya M, Kimura M, Nishino K, et al. Patients with SMARCA4-defificient thoracic sarcoma and severe skeletal-related events. *Lung Cancer* (2019) 132:59–64. doi: 10.1016/j.lungcan.2019.03.029

4. Henon C, Blay JY, Massard C, Mir O, Bahleda R, Dumont S, et al. Long lasting major response to pembrolizumab in a thoracic malignant rhabdoid-like SMARCA4-defificient tumor. *Ann Oncol* (2019) 30(8):1401–3. doi: 10.1093/annonc/mdz160

5. Kunimasa K, Kunimasa K, Takenaka S, Honma K, Kukita Y, Nagata S, et al. Conversion surgery for advanced thoracic SMARCA4-deficient undifferentiated tumor with atezolizumab in combination with bevacizumab, paclitaxel, and carboplatin treatment: A case report. *JTO Clin Res Rep* (2021) 2:100235. doi: 10.1016/j.jtocrr.2021.100235

6. Takada K, Sugita S, Murase K, Kikuchi T, Oomori G, Ito R, et al. Exceptionally rapid response to pembrolizumab in a SMARCA4-defificient thoracic sarcoma overexpressing PD-L1: a case report. *Thorac Cancer* (2019) 10(12):2312–5. doi: 10.1111/1759-7714.13215

7. Kawachi H, Kunimasa K, Kukita Y, Nakamura H, Honma K, Kawamura T, et al. Atezolizumab with bevacizumab, paclitaxel and carboplatin was effective for patients with SMARCA4-deficient thoracic sarcoma. *Immunotherapy* (2021) 13(10):799–806. doi: 10.2217/imt-2020-0311

8. Anžič N, Krasniqi F, Eberhardt AL, Tzankov A, Haslbauer JD. Ipilimumab and pembrolizumab mixed response in a 41-Year-Old patient with SMARCA4-deficient thoracic sarcoma: An interdisciplinary case study. *Case Rep Oncol* (2021) 14:706–15. doi: 10.1159/000515416

9. Eisenhauer EA, Therasse P, Bogaerts J, Schwartz LH, Sargent D, Ford R, et al. New response evaluation criteria in solid tumours: revised RECIST guideline (version 1.1). *Eur J Cancer* (2009) 45(2):0–247. doi: 10.1016/j.ejca.2008.10.026

10. Nambirajan A, Jain D. Recent updates in thoracic SMARCA4-deficient undifferentiated tumorx. *Semin Diagn Pathol* (2021) 38:83–9. doi: 10.1053/j.semdp.2021.06.001

11. Rekhtman N, Montecalvo J, Chang JC, Alex D, Ptashkin RN, Ai N, et al. SMARCA4-deficient thoracic sarcomatoid tumors represent primarily smoking-related undifferentiated carcinomas rather than primary thoracic sarcomas. *J Thorac Oncol* (2020) 15(2):231–47. doi: 10.1016/j.jtho.2019.10.023

12. Sesboue C, Le Loarer F. SWI/SNF-deficient thoraco-pulmonary neoplasms. *Semin Diagn Pathol* (2021) 38:183–94. doi: 10.1053/j.semdp.2020.12.002

13. Kunimasa K, Nakamura H, Sakai K. Patients with SMARCA4-deficient thoracic sarcoma and severe skeletal-related events. *Lung Canc* (2019) 132:59–64. doi: 10.1016/j.lungcan.2019.03.029

14. Nambirajan A, Parshad R, Goyal A, Mithun NKM, Jain D. Innocuous clinical presentation of a SMARCA4-deficient thoracic sarcoma arising in a patient with chronic empyema thoracis. *Pathology*. (2019) 51:657–9. doi: 10.1016/j.pathol.2019.05.011

15. Stewart BD, Kaye F, Machuca T, Mehta HJ, Mohammed TL, Newsom KJ, et al. SMARCA4-deficient thoracic sarcoma: A case report and review of literature. *Int J Surg Pathol* (2020) 28:102–8. doi: 10.1177/1066896919865944

16. Crombé A, Alberti N, Villard N. Imaging features of SMARCA4-deficient thoracic sarcomas: a multi-centric study of 21 patients. *Eur Radiol* (2019) 29:4730–41. doi: 10.1007/s00330-019-06017-x

17. Yoshida A, Kobayashi E, Kubo T, Kodaira M, Motoi N, Yonemori K, et al. Clinicopathological and molecular characterization of SMARCA4-deficient thoracic sarcomas with comparison to potentially related entities. *Mod Pathol* (2017) 30(6):797–809. doi: 10.1038/modpathol.2017.11

18. Takeda M, Tani Y, Saijo N, Shimizu S, Taniguchi Y, Otsuka K, et al. Cytopathological features of SMARCA4-deficient thoracic sarcoma: Report of 2 cases and review of the literature. *Int J Surg Pathol* (2020) 28(1):109–14. doi: 10.1177/1066896919870866

19. Perret R, Chalabreysse L, Watson S, Serre l, Garcia S, Forest F, et al. SMARCA4-deficient thoracic sarcomas: Clinicopathologic study of 30 cases with an emphasis on their nosology and differential diagnoses. *Am J Surg Pathol* (2019) 43(4):455–65. doi: 10.1097/PAS.0000000000001188

20. Nambirajan A, Singh V, Bhardwaj N, Mittal S, Kumar S, Jain D, et al. SMARCA4/BRG1-deficient non-small cell lung carcinomas: A case series and review of the literature. *Arch Pathol Lab Med* (2021) 145:90–8. doi: 10.5858/arpa.2019-0633-OA

21. Palmieri G, Tortora M, Parola S, Picozzi F, Ottaviano M. Mediastinal soft tissue sarcoma: dark sides and future lights. *Mediastinum* (2020) 4:9. doi: 10.21037/med.2020.03.02

22. Schoenfeld AJ, Bandlamudi C, Lavery JA, Montecalvo J, Namakydoust A, Rizvi H, et al. The genomic landscape of SMARCA4 alterations and associations with outcomes in patients with lung cancer. *Clin Cancer Res* (2020) 26(21):5701–8. doi: 10.1158/1078-0432.CCR-20-1825

23. Marinelli D, Mazzotta M, Scalera S, Terrenato l, Sperati F, D'Ambrosio L, et al. KEAP1-driven co-mutations in lung adenocarcinoma unresponsive to immunotherapy despite high tumor mutational burden. *Ann Oncol* (2020) 31 (12):1746–54. doi: 10.1016/j.annonc.2020.08.2105

frontiers | Frontiers in Oncology

TYPE Case Report
PUBLISHED 07 November 2022
DOI 10.3389/fonc.2022.1038774

OPEN ACCESS

EDITED BY
Kohei Fujita,
National Hospital Organization Kyoto Medical Center, Japan

REVIEWED BY
Laveniya Satgunaseelan,
Royal Prince Alfred Hospital, Australia
Yoshiyuki Suehara,
Juntendo University, Japan

*CORRESPONDENCE
Vanesa Gregorc
vanesa.gregorc@ircc.it

†These authors have contributed equally to this work and share first authorship

SPECIALTY SECTION
This article was submitted to Thoracic Oncology, a section of the journal Frontiers in Oncology

RECEIVED 07 September 2022
ACCEPTED 07 October 2022
PUBLISHED 07 November 2022

CITATION
Lazzari C, Pecciarini L, Doglioni C, Pedica F, Gajate AMS, Bulotta A, Gregorc V and Cangi MG (2022) Case report: *EML4::NTRK3* gene fusion in a patient with metastatic lung adenocarcinoma successfully treated with entrectinib.
Front. Oncol. 12:1038774.
doi: 10.3389/fonc.2022.1038774

Case report: *EML4::NTRK3* gene fusion in a patient with metastatic lung adenocarcinoma successfully treated with entrectinib

Chiara Lazzari[1†], Lorenza Pecciarini[2†], Claudio Doglioni[2], Federica Pedica[2], Ana Maria Samanes Gajate[3], Alessandra Bulotta[4], Vanesa Gregorc[1*] and Maria Giulia Cangi[2]

[1]Candiolo Cancer Institute, Fondazione del Piemonte per l'Oncologia (FPO)-IRCCS, Turin, Italy, [2]Department of Pathology, IRCCS San Raffaele Scientific Institute, Milan, Italy, [3]Department of Nuclear Medicine, IRCCS San Raffaele Scientific Institute, Milan, Italy, [4]Department of Oncology, IRCCS San Raffaele Scientific Institute, Milan, Italy

Rearrangements involving the neurotrophin kinase (*NTRK*) genes *NTRK1*, *NTRK2* and *NTRK3* with different fusion partners have been observed in both adult and pediatric solid tumors. Larotrectinib and entrectinib have been the first tumor-agnostic compounds approved for the treatment of NTRK fusion-positive tumors. Here, we report the first case of a female patient with a diagnosis of stage IV lung adenocarcinoma harboring the *EML4::NTRK3* gene fusion, and successfully treated with entrectinib.

KEYWORDS

NSCLC, NTRK, EML4::NTRK3 fusion, entrectinib, NGS

Introduction

Lung cancer is the leading cause of cancer deaths worldwide (1). Non-small cell lung cancer (NSCLC) accounts for approximately 80% of cases. In the last decade, the growing knowledge of NSCLC tumor biology and the identification of targetable molecular alterations provided new tools to develop tailored medicine and improve significantly patients' prognosis (2). Different molecular alterations, which are susceptible to targeted inhibition, have been identified in patients with NSCLC, especially in the subgroup with adenocarcinoma (2). These efforts have been translated into overall survival (OS) prolongation.

Rearrangements involving the neurotrophin kinase (*NTRK*) genes *NTRK1*, *NTRK2* and *NTRK3* with different fusion partners have been observed in adult and pediatric solid

tumors. Larotrectinib and entrectinib have been the first tumor-agnostic compounds (i.e. drugs targeting molecular alterations regardless of the tumor histotype and localization) approved for the treatment of *NTRK* fusion-positive tumors (3). Due to the low frequency of *NTRK* rearrangements, both compounds have been evaluated in phase I and phase II basket trials.

Here, we report the first case of a female patient with a diagnosis of stage IV lung adenocarcinoma harboring the *EML4::NTRK3* gene fusion, and successfully treated with entrectinib.

Case details

A 45-year-old non-smoking female patient received a diagnosis of stage IV lung adenocarcinoma on March 2021 with pleural, bilateral lung lesions and the involvement of mediastinal lymph nodes, the sternum and the right pubic symphysis (Figure 1A). The magnetic resonance (MR) of the column showed the presence of metastases in the vertebral body of T9, from T6-T7 up to T9-T10, and dural enhancement anteriorly to the spinal cord of T8. The brain MR showed at least 12 lesions at sub and supratentorial sites (Figure 1B). To obtain a diagnosis, the patient underwent video-assisted thoracoscopic surgery with the identification of multiple alterations in the parietal, diaphragmatic, mediastinal, and visceral pleura. Histologic diagnosis described multiple localizations of acinar and solid adenocarcinoma (grade 2) of the lung (Figure 2A). Targeted next-generation sequencing (NGS) analysis across 161 of the most relevant genes implicated in cancer was performed using the Oncomine™ Comprehensive Assay v3 panel (Thermo Fisher Scientific) as previously described (4). The *EML4::NTRK3* gene fusion was identified (*EML4* exon2-*NTRK3* exon14), and confirmed by both fluorescence *in situ* hybridization (FISH) analysis, using ZytoLight SPEC *NTRK3* Dual Color Break Apart and ZytoLight SPEC *EML4* Dual Color Break Apart (Figures 2B, C, and immunohistochemistry staining with panTRK antibody (Roche) (Figure 2D). The same OCAv3 NGS analysis performed on matched normal tissue of the patient did not detect germline alterations.

Based on such findings, entrectinib was started.

Whole brain radiotherapy was avoided because the patient had no neurological symptoms, there was no evidence of edema in the brain MR, the number of brain lesions did not support the use of stereotactic radiosurgery and data from literature suggested the efficacy of entrectinib to cross the blood-brain barrier.

The PET scan (Figure 3) and the brain MR performed two months following the beginning of treatment showed a partial response. Treatment is currently ongoing. The brain MR and the PET scan performed recently documented a complete radiologic regression. In Figure 4, a summary of the patient's clinical history.

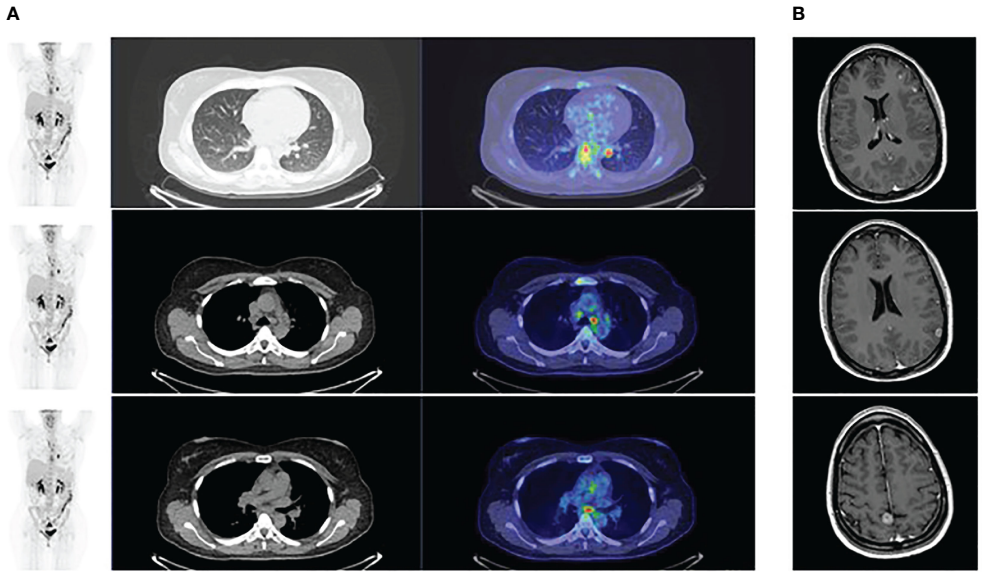

FIGURE 1
(A) PET scan at baseline showing the presence of lesions at the lung and the and mediastinal lymph nodes; **(B)** Magnetic brain resonance at baseline showing the presence of multiple brain metastases.

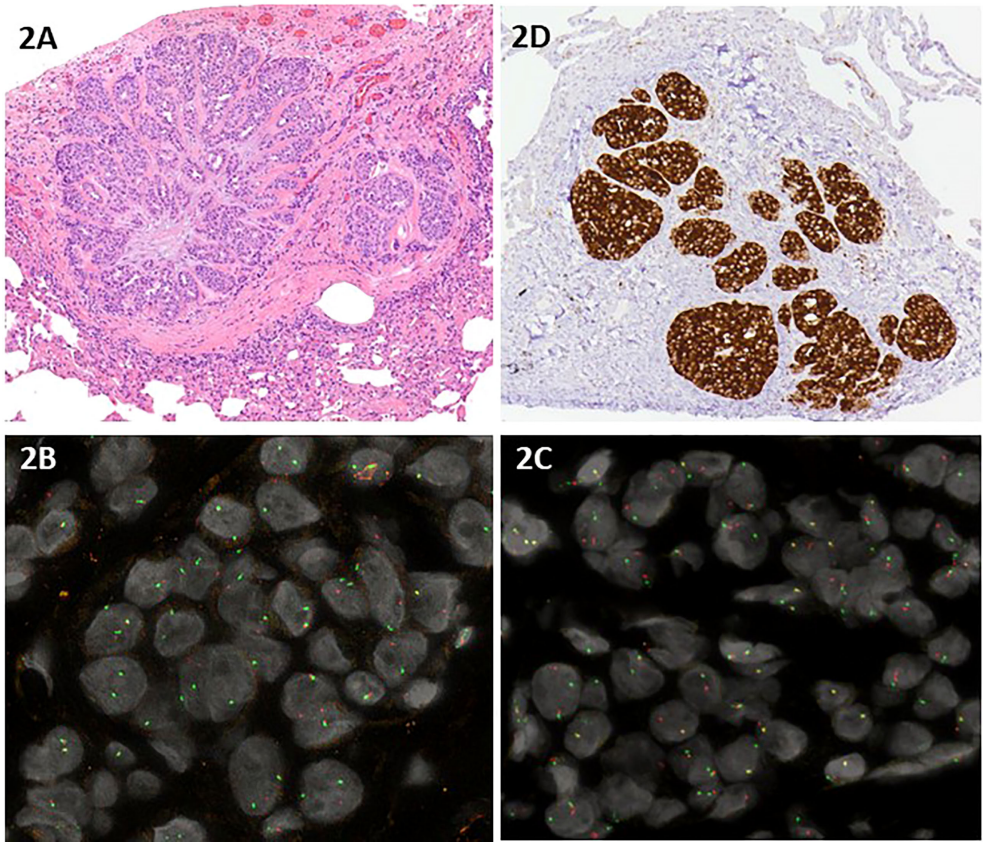

FIGURE 2
(A) Hematoxylin and eosin staining of acinar and solid adenocarcinoma grade 2 of the lung; **(B, C)** Interphase dual color break apart FISH using a NTRK3 probe **(B)** and a EML4 probe **(C)** displayed one normal orange/green fusion signal and one single orange signal and one single green signal in the majority of the neoplastic nuclei, indicating a rearrangement of both NTRK3 and EML4; **(D)** Immunohistochemistry staining with panTRK antibody (Roche).

Discussion

NTRK gene rearrangements are observed in different types of solid malignancies. They are the result of intrachromosomal or interchromosomal rearrangements between the 3' portion of *NTRK1*, *2*, *3*, which includes the tyrosine kinase domain, and the 5' portion of multiple different genes. *NTRK* rearrangements are considered agnostic tumor markers, observed in less than 1% of patients with solid malignancies. They are identified at a high frequency in rare tumors, including congenital infantile fibrosarcoma, congenital mesoblastic nephroma, secretory breast carcinoma, and mammary analog secretory carcinoma the salivary gland, and at very low frequency, in more common cancers, including NSCLC, melanoma, thyroid, esophagus, gastric or colorectal tumors (5, 6).

Retrospective data from 295676 adult and pediatric patients identified *NTRK* rearrangements in 45 tumor types and 134 different histologies (7). At least 88 rearrangements with different fusion partners have been described, being *ETV6::NTRK3* the most common, accounting for 60% of the cases (6). In NSCLC, *NTRK* rearrangements are found in less than 1% of patients, mainly in those with adenocarcinoma, but also in squamous carcinoma and large cell neuroendocrine tumors, with a variable smoking history. Here we describe for the first time the identification and characterization of an *EML4::NTRK3* fusion in a patient with lung adenocarcinoma. *NTRK3* fusions are highly enriched in patients with congenital mesoblastic nephroma, congenital fibrosarcoma, and secretory breast carcinoma. The fusion *EML4::NTRK3* has been described in two cases of infantile fibrosarcoma, one case of congenital mesoblastic nephroma (8), one patient with thyroid carcinoma (9) one 9-month old boy with congenital fibrosarcoma (10) one patient with uterus fibrosarcoma (11), two cases with colon cancer (12) and one patient with dermatofibrosarcoma protuberans (13). In carcinomas, *EML4::NTRK3* has been observed in two colon adenocarcinoma (12), and two thyroid carcinomas (9).

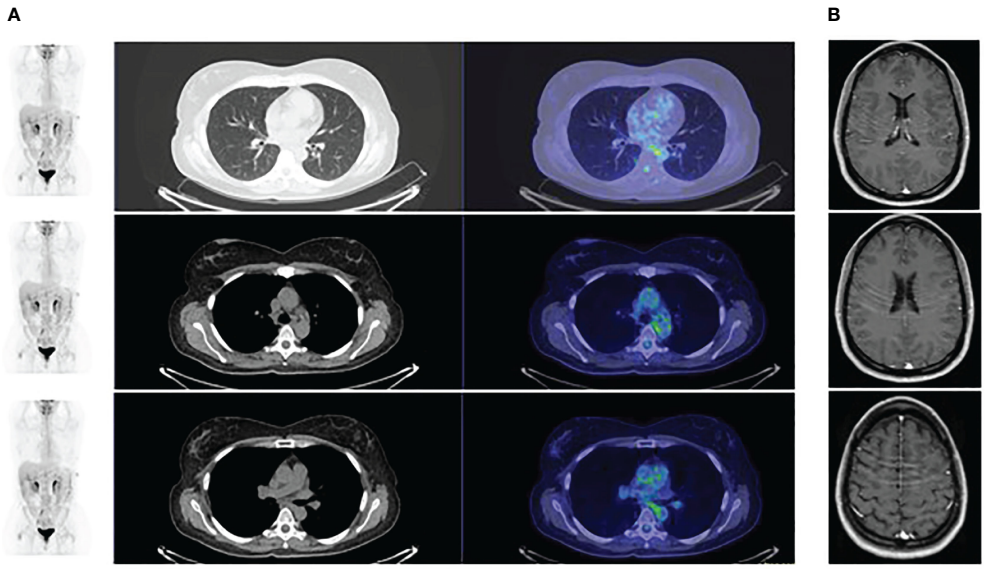

FIGURE 3
PET scan showing a partial response following 2 months of therapy.

Larotrectinib and entrectinib have been the first compounds approved for the treatment of *NTRK* positive patients irrespective of the histology (14–16).

Larotrectinib is the first-in class NTRK inhibitor. Its safety and efficacy were initially explored in a phase I dose escalation study, enrolling 70 patients with metastatic solid tumors (15). The presence of NTRK fusions was not an inclusion criterion to enter the trial, and eight patients only carried NTRK fusions. Among these, one patient had a diagnosis of lung adenocarcinoma. Objective responses (ORR) were observed in seven out of eight patients harboring NTRK fusions and in one case with NTRK1 gene amplification. Larotrectinib was further investigated in another phase I study, including 55 NTRK fusion–positive patients. Among these, four had a diagnosis of NSCLC (17). An ORR of 75% was registered. A pooled analysis included data from three phase I/II clinical trials, enrolling 159 patients with solid tumors and NTRK fusions (15). Twelve of these had a diagnosis of NSCLC, and 13 had brain lesions. Six of the patients with NSCLC had brain metastases. Twenty-two percent of the patients enrolled were naive from previous therapy, 30% had received at least one line of chemotherapy, and 47% at least two lines of previous treatments. An ORR of

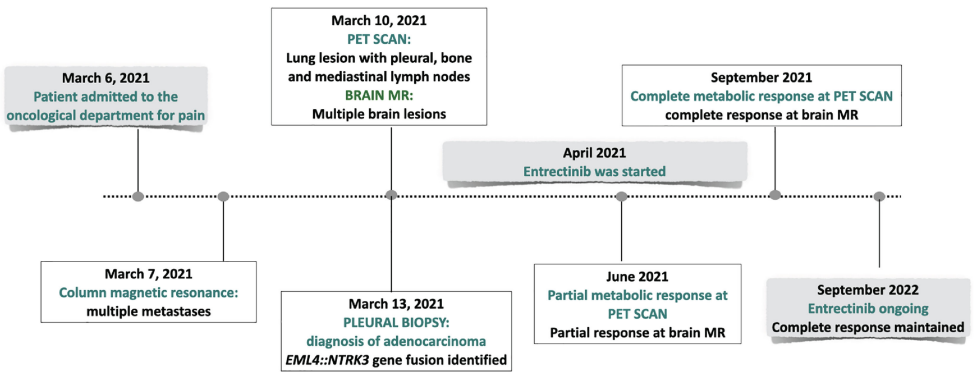

FIGURE 4
Timeline showing the clinical history of the patient.

79% was observed. Among the patients with brain lesions, three cases had measurable intracranial disease. Larotrectinib determined a complete response in one patient, in the other two a partial response (46% reduction in target tumor size) and a stable disease (14% reduction in target tumor size). Similarly to larotrectinib, the more recent FDA/EMA approved entrectinib was investigated in phase I and II studies. Entrectinib inhibits *TRKA, TRKB, TRKC, ROS1* and *ALK*, and was specifically designed to cross the blood brain barrier. Its safety has been initially evaluated in two phase I trials, the ALKA-372 -001 and the STARTK-1, which showed the good tolerability of the drug. Among the patients enrolled, four carried *NTRK*-fusions. Based on the dramatic radiologic response observed in this subgroup of patients, the phase II basket STARTRK-2 study was designed to include a cohort of patients harboring *NTRK*-fusions. A pooled analysis, from the ALKA-372–001, the STARTRK-1, and the STARTRK-2 trials, enrolling 54 patients with metastatic solid tumors carrying *NTRK* fusions was subsequently published (18). Co-primary endpoints were ORR, intracranial ORR and the duration of response. Secondary endpoints included progression free survival (PFS), overall survival (OS), clinical benefit rate, time to central nervous system progression and safety. Among the patients enrolled, ten had a diagnosis of NSCLC. Thirty-seven percent were naive from previous treatment, 20% had received one line of therapy, 42% more than two lines. An ORR rate of 57% with a median duration of response of 10.4 months and a median PFS of 11.2 months were registered. In patients with NSCLC, an ORR of 70% was observed. An updated analysis, including 121 patients with 14 tumor histologies, was recently published (19). Among these, 40% had received ≥2 prior lines of therapy, 30% were naive from previous treatments, 20% had brain lesions, and 18% had a diagnosis of NSCLC. An ORR of 81% and 61% was evidenced in naive and pre-treated patients, respectively. A comparable percentage of ORR was observed in patients with *NTRK1* and *NTRK3* gene fusions (54.2% and 70.2%, respectively), while tumor reduction was shown only in one patient carrying *NTRK2* fusion. A median duration of response of 20 months was observed, with a median PFS of 13.8 months and a median OS of 33.8 months. In the subgroup of 22 patients with NSCLC, an ORR of 63.6, with a median duration of response of 19.9 months and a median PFS of 4.9 months was evidenced. Treatment was well tolerated. The majority of the adverse events registered were of grade 1, the most common being dysgeusia, diarrhea, fatigue and weight increase. Among grade≥3 adverse events, weight gain (8.3%), anemia (5.2%) and fatigue (4.7%) were those more frequently observed. Serious adverse events were reported in 12.4% of the patients, including dizziness and cognitive disorder. Five deaths, potentially related to entrectinib, were registered. All the events were of cardiovascular nature. In approximately 20% of the patients, a dose reduction occurred.

Data from *in vitro* studies comparing entrectinib to larotrectinib showed that entrectinib is a weak P-gp substrate, thus suggesting its increased efficacy in terms of central nervous system exposure (20). Entrectinib determined an intracranial ORR of 63.6% with a median intracranial duration of response of 22.1 months and a median intracranial PFS of 19.9 months in patients with measurable brain lesions included in the pooled analysis (19). The median time to central nervous system progression was 30.2 months.

These findings have opened new questions, whether withholding brain radiation in patients with brain lesions carrying targetable alterations amenable to inhibition with agents that penetrate the blood-brain barrier and result in significant control of brain disease. This represents a significant challenge, especially considering that whole brain radiotherapy might decrease cognitive function and reduce memory in patients who have a high probability of extended survival despite the diagnosis of brain metastases. Furthermore, the use of more effective therapies and the extended survival we have observed in patients with NSCLC thanks to the introduction of molecularly targeted therapies may increase the probability of CNS metastases, thus highlighting the need to design compounds able to cross the blood brain barrier and reduce the risk of brain progression. The deeper understanding of tumor biology, the introduction of next generation sequencing as a tool to molecularly classify patients, and the up-coming of next generation targeted agents, designed to penetrate the blood brain barrier, prevent brain progression, and better control disease at brain sites, will impact on the therapeutic strategy of patients with stage IV NSCLC. Patients with unstable brain lesions should be admitted to clinical trials exploring the efficacy of next generation drugs, even if not treated with radiation.

The presented case highlights the importance of obtaining a comprehensive characterization of each neoplasia, investigating also uncommon biomarkers, such as *NTRK* genes, especially in non-smokers and young (<50yrs) NSCLC patients, as they can provide useful targets for personalized therapy. Therefore, it is mandatory to utilize a reliable diagnostic methodology with high sensitivity and specificity (21, 22). Given the key therapeutical implication of *NTRK* rearrangements, it is crucial to use the best approach for the detection of tumors harboring *NTRK1/2/3* fusions. The most recognized techniques for *NTRK* fusion gene detection are immunohistochemistry, FISH, RT-PCR, and both RNA-based and DNA-based NGS. Importantly, the assay choice should take into account the type of tumor, the laboratory resources and clinical context: in tumors where *NTRK* fusions are highly recurrent, the ESMO recommendations (23) suggest the use of FISH, RT-PCR or RNA NGS panels as confirmatory techniques, whereas in testing an unselected population where *NTRK1/2/3* fusions are uncommon, either front-line NGS sequencing, when available, or screening by immunohistochemistry followed by sequencing of positive cases should be performed.

Despite formalin-fixed paraffin-embedded (FFPE) specimens being routinely used in clinical practice for both morphological evaluation and molecular characterization, it is well known that formalin fixation negatively affects nucleic acids

quality by inducing fragmentation and sequence artifacts that may impact the downstream assay performance and therefore the possibility to obtain useful molecular data (24). Particular attention should be paid to obtaining adequate tissue samples and to applying standard protocols of fixation and tissue histologic processing (25), especially when RNA analysis for gene fusion detection is requested (26).

Nevertheless, tumor molecular characterization may be challenging because of the lack of adequate tumor cellularity in the tissue sample. To overcome this issue, it is necessary to implement in clinical practice the sequencing of circulating tumor nucleic acids to detect the druggable molecular alterations (27–29)

In conclusion, the *EML4::NTRK3* fusion, a rare alteration and not fully characterized in patients with NSCLC, proved to be a key target for therapy selection. This report about the efficacy of entrectinib in our patient, who obtained a complete radiologic response, is of major relevance as the literature is still very scarce about the clinical use of this drug, and moreover as it confirms the importance of molecular classification to guide the therapeutic strategy and to prolong patients' survival.

Data availability statement

The datasets presented in this article are not readily available because of ethical/privacy restrictions. Requests to access the datasets should be directed to the corresponding author.

Ethics statement

The studies involving human participants were reviewed and approved by IRCCS San Raffaele Hospital, Milano (Italy). The patients/participants provided their written informed consent to participate in this study. Written informed consent was obtained from the individual(s) for the publication of any potentially identifiable images or data included in this article.

Author contributions

VG, CL, MC, and LP contributed to the conception of the study and helped perform the analysis with constructive discussions. VG and CL contributed to manage and treat the patient. MC and LP were responsible for molecular genetic analysis and data interpretation. CD were responsible for histopathological evaluation. VG, CL, MC, and LP wrote the manuscript. All authors contributed to the article and approved the submitted version.

Funding

This study was supported by FPRC 5X1000 2020 Ministero della Salute progetto PRO-ACTIVEMinistero della Salute Ricerca Corrente 2022.

Conflict of interest

The authors declare that the research was conducted in the absence of any commercial or financial relationships that could be construed as a potential conflict of interest.

Publisher's note

References

1. Ganti AK, Klein AB, Cotarla I, Seal B, Chou E. Update of incidence, prevalence, survival, and initial treatment in patients with non–small cell lung cancer in the US. *JAMA Oncol* (2021) 7(12):1824–32. doi: 10.1001/jamaoncol.2021.4932

2. Rosell R, Karachaliou N. Large-Scale screening for somatic mutations in lung cancer. *Lancet.* (2016) 387(10026):1354–6. doi: 10.1016/S0140-6736(15)01125-3

3. Harada D, Takigawa N. Oligoprogression in non-small cell lung cancer. *Cancers.* (2021) 13(22):5823. doi: 10.3390/cancers13225823

4. Schiavo Lena M, Cangi MG, Pecciarini L, Francaviglia I, Grassini G, Maire R, et al. Evidence of a common cell origin in a case of pancreatic mixed intraductal papillary mucinous neoplasm-neuroendocrine tumor. *Virchows Arch* (2021) 478 (6):1215–9. doi: 10.1007/s00428-020-02942-1

5. Solomon JP, Linkov I, Rosado A, Mullaney K, Rosen EY, Frosina D, et al. NTRK fusion detection across multiple assays and 33,997 cases: Diagnostic implications and pitfalls. *Mod Pathol* (2020) 33(1):38–46. doi: 10.1038/s41379-019-0324-7

6. Rosen T, Lebwohl MG. Prevalence and awareness of actinic keratosis: barriers and opportunities. *J Am Acad Dermatol* (2013) 68(1 Suppl 1):S2–9. doi: 10.1016/j.jaad.2012.09.052

7. Westphalen CB, Krebs MG, Le Tourneau C, Sokol ES, Maund SL, Wilson TR, et al. Genomic context of NTRK1/2/3 fusion-positive tumours from a large real-world population. *NPJ Precis Oncol* (2021) 5(1):69. doi: 10.1038/s41698-021-00206-y

8. Church AJ, Calicchio ML, Nardi V, Skalova A, Pinto A, Dillon DA, et al. Recurrent EML4-NTRK3 fusions in infantile fibrosarcoma and congenital mesoblastic nephroma suggest a revised testing strategy. *Mod Pathol* (2018) 31 (3):463–73. doi: 10.1038/modpathol.2017.127

9. Chu YH, Dias-Santagata D, Farahani AA, Boyraz B, Faquin WC, Nosé V, et al. Clinicopathologic and molecular characterization of NTRK-rearranged thyroid carcinoma (NRTC). *Mod Pathol* (2020) 33(11):2186–97. doi: 10.1038/s41379-020-0574-4

10. Tannenbaum-Dvir S, Glade Bender JL, Church AJ, Janeway KA, Harris MH, Mansukhani MM, et al. Characterization of a novel fusion gene EML4-NTRK3 in a case of recurrent congenital fibrosarcoma. *Cold Spring Harb Mol Case Stud* (2015) 1(1):a000471. doi: 10.1101/mcs.a000471

11. Croce S, Hostein I, Longacre TA, Mills AM, Pérot G, Devouassoux-Shisheboran M, et al. Uterine and vaginal sarcomas resembling fibrosarcoma: A clinicopathological and molecular analysis of 13 cases showing common NTRK-

rearrangements and the description of a COL1A1-PDGFB fusion novel to uterine neoplasms. *Mod Pathol* (2019) 32(7):1008–22. doi: 10.1038/s41379-018-0184-6

12. Lasota J, Chłopek M, Lamoureux J, Christiansen J, Kowalik A, Wasąg B, et al. Colonic adenocarcinomas harboring NTRK fusion genes: A clinicopathologic and molecular genetic study of 16 cases and review of the literature. *Am J Surg Pathol* (2020) 44(2):162–73. doi: 10.1097/PAS.0000000000001377

13. Nicholson AG, Chansky K, Crowley J, Beyruti R, Kubota K, Turrisi A, et al. The international association for the study of lung cancer lung cancer staging project: Proposals for the revision of the clinical and pathologic staging of small cell lung cancer in the forthcoming eighth edition of the TNM classification for lung cancer. *J Thorac Oncol* (2016) 11(3):300–11. doi: 10.1016/j.jtho.2015.10.008

14. Doebele RC, Pilling AB, Aisner DL, Kutateladze TG, Le AT, Weickhardt AJ, et al. Mechanisms of resistance to crizotinib in patients with ALK gene rearranged non-small cell lung cancer. *Clin Cancer Res* (2012) 18(5):1472–82. doi: 10.1158/1078-0432.CCR-11-2906

15. Hong DS, DuBois SG, Kummar S, Farago AF, Albert CM, Rohrberg KS, et al. Larotrectinib in patients with TRK fusion-positive solid tumours: a pooled analysis of three phase 1/2 clinical trials. *Lancet Oncol* (2020) 21(4):531–40. doi: 10.1016/S1470-2045(19)30856-3

16. Drilon A, Somwar R, Wagner JP, Vellore NA, Eide CA, Zabriskie MS, et al. A novel crizotinib-resistant solvent-front mutation responsive to cabozantinib therapy in a patient with ROS1-rearranged lung cancer. *Clin Cancer Res* (2016) 22 (10):2351–8. doi: 10.1158/1078-0432.CCR-15-2013

17. Drilon A, Laetsch TW, Kummar S, DuBois SG, Lassen UN, Demetri GD, et al. Efficacy of larotrectinib in TRK fusion–positive cancers in adults and children. *New Engl J Med* (2018) 378(8):731–9. doi: 10.1056/NEJMoa1714448

18. Doebele RC, Drilon A, Paz-Ares L, Siena S, Shaw AT, Farago AF, et al. Entrectinib in patients with advanced or metastatic NTRK fusion-positive solid tumours: integrated analysis of three phase 1-2 trials. *Lancet Oncol* (2020) 21 (2):271–82. doi: 10.1016/S1470-2045(19)30691-6

19. Demetri GD, De Braud F, Drilon A, Siena S, Patel MR, Cho BC, et al. Updated integrated analysis of the efficacy and safety of entrectinib in patients with NTRK fusion-positive solid tumors. *Clin Cancer Res* (2022) 28(7):1302–12. doi: 10.1158/1078-0432.CCR-21-3597

20. Fischer H, Ullah M, de la Cruz CC, Hunsaker T, Senn C, Wirz T, et al. Entrectinib, a TRK/ROS1 inhibitor with anti-CNS tumor activity: Differentiation from other inhibitors in its class due to weak interaction with p-glycoprotein. *Neuro-Oncology.* (2020) 22(6):819–29. doi: 10.1093/neuonc/noaa052

21. Gregorc V, Mazzarella L, Lazzari C, Graziano P, Vigneri P, Genova C, et al. Prospective validation of the Italian alliance against cancer lung panel in patients with advanced non-Small-Cell lung cancer. *Clin Lung Cancer.* (2021) 22(4):e637–41. doi: 10.1016/j.cllc.2020.12.007

22. Lazzari C, Bulotta A, Cangi MG, Bucci G, Pecciarini L, Bonfiglio S, et al. Next generation sequencing in non-small cell lung cancer: Pitfalls and opportunities. *Diagnostics (Basel).* (2020) 10(12):E1092. doi: 10.3390/diagnostics10121092

23. Marchiò C, Scaltriti M, Ladanyi M, Iafrate AJ, Bibeau F, Dietel M, et al. ESMO recommendations on the standard methods to detect NTRK fusions in daily practice and clinical research. *Ann Oncol* (2019) 30(9):1417–27. doi: 10.1093/annonc/mdz204

24. Magliacane G, Grassini G, Bartocci P, Francaviglia I, Dal Cin E, Barbieri G, et al. Rapid targeted somatic mutation analysis of solid tumors in routine clinical diagnostics. *Oncotarget.* (2015) 6(31):30592–603. doi: 10.18632/oncotarget.5190

25. Einaga N, Yoshida A, Noda H, Suemitsu M, Nakayama Y, Sakurada A, et al. Assessment of the quality of DNA from various formalin-fixed paraffin-embedded (FFPE) tissues and the use of this DNA for next-generation sequencing (NGS) with no artifactual mutation. *PloS One* (2017) 12(5):e0176280. doi: 10.1371/journal.pone.0176280

26. Ramani NS, Patel KP, Routbort MJ, Alvarez H, Broaddus R, Chen H, et al. Factors impacting clinically relevant RNA fusion assays using next-generation sequencing. *Arch Pathol Lab Med* (2021) 145(11):1405–12. doi: 10.5858/arpa.2020-0415-OA

27. Francaviglia I, Magliacane G, Lazzari C, Grassini G, Brunetto E, Dal Cin E, et al. Identification and monitoring of somatic mutations in circulating cell-free tumor DNA in lung cancer patients. *Lung Cancer.* (2019) 134:225–32. doi: 10.1016/j.lungcan.2019.06.010

28. Lazzari C, Gregorc V, Cangi MG, Giovannetti E, Bulotta A, Santarpia M. Combined exosomal RNA and circulating tumor DNA for epidermal growth factor mutation detection in non-small cell lung cancer. *J Thorac Dis* (2018) 10(Suppl 33): S4023–7. doi: 10.21037/jtd.2018.10.17

29. Pascual J, Attard G, Bidard FC, Curigliano G, De Mattos-Arruda L, Diehn M, et al. ESMO recommendations on the use of circulating tumour DNA assays for patients with cancer: a report from the ESMO precision medicine working group. *Ann Oncol* (2022) 750–768. doi: 10.1016/j.annonc.2022.05.520

frontiers | Frontiers in Oncology

TYPE Case Report
PUBLISHED 07 November 2022
DOI 10.3389/fonc.2022.985446

OPEN ACCESS

EDITED BY
Kohei Fujita,
National Hospital Organization Kyoto Medical Center, Japan

REVIEWED BY
Yang Xu,
Geneseeq Technology Inc., Canada
Hongbin Wang,
California Northstate University, United States

*CORRESPONDENCE
Sebahat Ocak
sebahat.ocak@chuuclnamur.uclouvain.be

SPECIALTY SECTION
This article was submitted to Thoracic Oncology, a section of the journal Frontiers in Oncology

RECEIVED 03 July 2022
ACCEPTED 10 October 2022
PUBLISHED 07 November 2022

CITATION
Pasau T, Wauters E, Wauters I, Duplaquet F, Pirard L, Pop-Stanciu C, D'Haene N, Dupont M, Vander Borght T, Rondelet B and Ocak S (2022) Case report: BRAF A598-T599insV mutation as a potential resistance mechanism to alectinib in ALK-rearranged lung adenocarcinoma.
Front. Oncol. 12:985446.
doi: 10.3389/fonc.2022.985446

Case report: BRAF A598-T599insV mutation as a potential resistance mechanism to alectinib in ALK-rearranged lung adenocarcinoma

Thomas Pasau[1], Els Wauters[2,3], Isabelle Wauters[2,3], Fabrice Duplaquet[1], Lionel Pirard[1], Claudia Pop-Stanciu[4], Nicky D'Haene[5], Michael Dupont[6], Thierry Vander Borght[7], Benoît Rondelet[8] and Sebahat Ocak[1,9]*

[1]Division of Pulmonology, Centre Hospitalier Universitaire de l'Université Catholique de Louvain (CHU UCL) Namur (Godinne Site), Université Catholique de Louvain, Yvoir, Belgium, [2]Respiratory Oncology Unit (Pulmonology), University Hospitals Katholieke Universiteit Leuven, Leuven, Belgium, [3]Laboratory of Respiratory Diseases and Thoracic Surgery (BREATHE), Department of Chronic Diseases and Metabolism, Katholieke Universiteit Leuven, Leuven, Belgium, [4]Division of Pathology, Centre Hospitalier Universitaire de l'Université Catholique de Louvain (CHU UCL) Namur (Godinne Site), Université Catholique de Louvain, Yvoir, Belgium, [5]Department of Pathology, Hôpital Erasme, Université Libre de Bruxelles, Brussels, Belgium, [6]Division of Radiology, Centre Hospitalier Universitaire de l'Université Catholique de Louvain (CHU UCL) Namur (Godinne Site), Université Catholique de Louvain, Yvoir, Belgium, [7]Division of Nuclear Medicine, Centre Hospitalier Universitaire de l'Université Catholique de Louvain (CHU UCL) Namur (Godinne Site), Université Catholique de Louvain, Yvoir, Belgium, [8]Division of Thoracic Surgery, Centre Hospitalier Universitaire de l'Université Catholique de Louvain (CHU UCL) Namur (Godinne Site), Université Catholique de Louvain, Yvoir, Belgium, [9]Pole of Pulmonology, Institut de Recherche Expérimentale et Clinique, Université Catholique de Louvain, Brussels, Belgium

Anaplastic lymphoma kinase (ALK) tyrosine kinase inhibitors (TKIs) have improved the prognosis of advanced-stage non-small cell lung cancer (NSCLC) with ALK rearrangement, but resistance mechanisms limit their efficacy. We describe the case of a 63-year-old man with a stage cIVA *ALK*-rearranged lung adenocarcinoma who developed a *BRAF* A598-T599insV mutation as a potential resistance mechanism to alectinib, a second-generation ALK TKI. He was treated with an association of BRAF and MEK inhibitors but death occurred two months after treatment initiation in a context of tumor progression and toxicity. Based on this first report of *BRAF* A598-T599insV mutation occurring in lung cancer, we discuss resistance mechanisms to ALK TKIs, implications of *BRAF* mutation in NSCLC, and *BRAF* A598-T599insV mutation in other cancers.

KEYWORDS

***ALK* rearrangement, *BRAF* A598-T599insV mutation, lung adenocarcinoma, resistance to alectinib, non-small cell lung cancer**

Introduction

Lung cancer is the leading cause of cancer-related mortality worldwide, responsible for 1.5 million deaths per year (1). There are two histological types: non-small cell lung cancer (NSCLC) and small cell lung cancer (SCLC), representing ≃85% and ≃15% of cases respectively (2). NSCLC is further divided into three histological subtypes: adenocarcinoma, squamous cell carcinoma, and large cell carcinoma, representing ≃40-50%, ≃30%, and ≃10% of cases respectively. In NSCLC, oncogenic drivers such as *EGFR*, *BRAF* V600E, *MET* exon14, *KRAS* G12C mutations, and Anaplastic lymphoma kinase (*ALK)*, *ROS*-1, *RET*, and *NTRK* rearrangements have been identified and led to personalized medicine after clinical trials showed that targeted therapies against these abnormalities improved outcomes as compared to chemotherapy (3, 4).

ALK rearrangement was discovered in NSCLC in 2007. It results from an interchromosomal inversion within chromosome 2's short arm, leading to *ALK*'s 3' end fusion with Echinoderm microtubule-associated protein-like 4 (*EML4*)'s 5' end or, less frequently, another gene (e.g.: *KIF5B*, *HIP1*, *TPR*, *BIRC6*). The resulting protein is activated and leads to cancer development through the activation of downstream signaling pathways such as the mitogen-activated protein kinase (MAPK), phosphatidylinositol 3-kinase (PI3K)/protein kinase B (AKT), and Janus kinase (JAK)/signal transducer and activator of transcription (STAT) pathways. *ALK* rearrangement, observed in 2-7% of NSCLCs, is more frequent in patients with adenocarcinoma, never/light-smoking history, and younger age (5, 6).

Crizotinib was the first ALK tyrosine kinase inhibitor (TKI) evaluated in *ALK*-rearranged NSCLC. Randomized trials showed that overall response rate (ORR) and progression-free survival (PFS) were better with crizotinib than chemotherapy in first- and further-line treatment of advanced-stage *ALK*-rearranged NSCLC. However, resistance mechanisms occur inevitably, responsible for tumor progression. Second-generation (alectinib, ceritinib, brigatinib, and ensartinib) and third-generation (lorlatinib) ALK TKIs have therefore been developed, but also face resistance issues. ALK-dependent resistance mechanisms consist mainly of mutations in *ALK* tyrosine kinase domain (altering kinase conformation and/or ATP binding affinity and preventing TKI binding) and less frequently of *ALK* amplification. ALK-independent mechanisms include bypass and downstream signaling activation (6–11).

In this report, we present a *BRAF* A598-T599insV mutation as a new potential ALK-independent resistance mechanism to alectinib in a patient with metastatic *ALK*-rearranged lung adenocarcinoma. We also discuss literature related to resistance to ALK TKIs, *BRAF* mutation in NSCLC, and *BRAF* A598-T599insV mutation in other cancers.

Case presentation

In 2016, a 63-year-old never-smoking male patient, with a history of resected prostatic adenocarcinoma in 2006, was diagnosed with a left lower lobe lung adenocarcinoma, stage cIVA (UICC 7th edition) (cT2a cN3 cM1a (metastases in the contralateral lung)). While there was no oncogenic driver found by a DNA Next Generation Sequencing (NGS) panel (Ion Torrent, ThermoFisher) targeting 22 genes (Supplementary Table 1), further molecular analyses revealed an *ALK* rearrangement (score 2+ ALK expression by immunohistochemistry, confirmation by fluorescent *in situ* hybridization (FISH) (38% of analyzed tumor cells were positive) and by RNA NGS (11.115 reads), which revealed an Echinoderm microtubule-associated protein-like 4 (*EML4*) (12)-*ALK* (12) fusion) (Figure 1).

In 2016 in Belgium, ALK TKIs were not reimbursed in first-line and so, the patient initially received cisplatin-pemetrexed chemotherapy, with partial tumor response observed after three (Figures 2A, B) and five cycles. Then, pemetrexed maintenance was initiated but stopped after seven cycles despite stable disease because of a grade 2 asthenia and a grade 1 renal failure. He experienced tumor progression 2.5 months after stopping pemetrexed (Figure 2C).

Crizotinib was initiated in second-line, with partial response achieved after two months (Figure 2D) and disease progression observed in the left lung after 5.5 months (Figure 2E). Tumor re-biopsies showed persistence of an *ALK* rearrangement (30% of analyzed tumor cells positive by FISH and 15.431 reads by RNA NGS) but no resistance mechanism to crizotinib (screening with a DNA NGS panel (Ion Torrent, ThermoFisher) targeting 22 genes, including *ALK* exons 22, 23, and 25).

In third-line, the patient received alectinib. Partial response was observed after two months (Figure 2F), followed by stabilization until tumor progression after 15 months (increase of the lesions in the left lower lobe and occurrence of a left

Abbreviations: AKT, protein kinase B; ALK, anaplastic lymphoma kinase; BIRC6, Baculoviral IAP Repeat Containing 6; BRAF, v-raf murine sarcoma viral oncogene homolog B1; EGFR, epidermal growth factor receptor; EML4, echinoderm microtubule-associated protein-like; FISH, fluorescent *in situ* hybridization; HIP1, Huntingtin Interacting Protein 1; JAK , Janus kinase; KIF5B, Kinesin Family Member 5B; KRAS, Kirsten rat sarcoma viral oncogene homolog; MAPK, mitogen-activated protein kinase; MEK, Mitogen-Activated Protein Kinase Kinase 1; MET, hepatocyte growth factor receptor; NGS, Next Generation Sequencing; NSCLC, non-small cell lung cancer; NTRK, neurotrophic receptor tyrosine kinase; ORR, overall response rate; PFS, progression-free survival; PI3K, phosphatidylinositol 3-kinase; RET, rearranged during transfection; ROS-1, c-Ros oncogene 1; SCLC, small cell lung cancer; STAT, signal transducer and activator of transcription; TKI, tyrosine kinase inhibitor; TPR, Translocated Promoter Region, Nuclear Basket Protein.

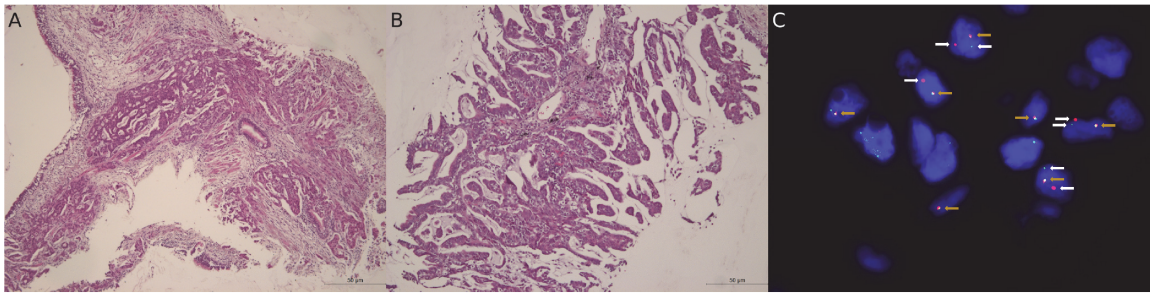

FIGURE 1
Pathological and molecular analysis of tumor samples. **(A, B)**. Hematoxylin and eosin (HE) staining shows neoplastic cells with morphological characteristics of lung adenocarcinoma. **(A)** *Picture magnification: 5x; scale bar: 50 µm.* **(B)** *Picture magnification: 10x; scale bar: 50 µm.* **(C)** Fluorescent *in situ* hybridization (FISH) reveals an *ALK* rearrangement (IQFISH break apart DAKO (Omnis)). ALK break-apart FISH utilizes DNA probes that hybridize to the 3' (red signal) and 5' (green signal) regions of the common fusion breakpoint in ALK gene. *ALK* rearrangement is identified by splitting of the red and green signals in the nuclei (white arrows) or isolated red signals, as opposed to fused adjacent red and green signals (yellow arrows). *Picture magnification: 1000x*.

pleural carcinomatosis) (Figure 2G). Tumor re-biopsies revealed persistence of an *ALK* rearrangement (24% of analyzed tumor cells positive by FISH and 16.286 reads by RNA NGS) and detected a *BRAF* A598_T599insV mutation (allelic frequency of 11%, screening with a DNA NGS panel (Ion Torrent, ThermoFisher) targeting 25 genes [the same 22 genes than in the panels used at diagnosis and at progression on crizotinib, plus three other genes (Supplementary Table 2)], while there was no *ALK* mutation.

Therefore, we did not propose a third-generation ALK TKI in fourth-line but an experimental treatment associating BRAF and MEK kinase inhibitors. Unfortunately, the patient died two months later in a context of tumor progression (Figure 2H) and toxicity (grade 3 skin rash and amylase elevation). The timeline of patient clinical history, with tumor evolution and treatments, is represented in Figure 3.

Discussion

We report here the *BRAF* A598_T599insV mutation as a potential new resistance mechanism to alectinib in metastatic *ALK*-rearranged lung adenocarcinoma.

After platinum-based chemotherapy, the patient was treated with crizotinib. Progression under crizotinib was observed after only 5.5 months and re-biopsies did not reveal any molecular resistance mechanism. Resistance to crizotinib is usually acquired (93-95%) and secondary to ALK-dependent or, more frequently, ALK-independent mechanisms (2/3 cases) (7). ALK-dependent resistance mechanisms include *ALK* mutations (the most frequent ones being L1196M (7%) and G1269A (4%), the less frequent ones C1156Y/T, L1152P/R, I1151Tins, F1174C/L/V, G1128A), *ALK* amplification (7-18%), and loss of *ALK* rearrangement (8, 11). ALK-independent resistance mechanisms include activation of bypass signaling pathways (e.g.: *EGFR* mutation and/or amplification, *KRAS* mutation, *KIT* amplification, *IGF-1R* activation, *RAS/MEK* activation), histological transformation to SCLC, and epithelial to mesenchymal transition (EMT) (11).

To overcome these resistance mechanisms to crizotinib, second-generation ALK TKIs have been developed. Randomized trials demonstrated their superiority over chemotherapy after progression on crizotinib, even in the absence of *ALK* mutations, which occur only in a minority of cases (~20%) in this setting (7). Patients progressing on crizotinib generally remain ALK-dependent despite the absence of ALK mutations probably because of the low potency of crizotinib against ALK. However, it is possible that sequencing panels do not adequately capture low frequency variants or previously undescribed ALK resistance mutations. In this context of tumor progression on crizotinib and absence of a specific resistance mechanism, our patient was treated with second-generation alectinib. Progression was observed after 15 months. ALK-dependent resistance mechanisms are more frequent with second-generation (1/2 cases) than first-generation TKIs and seem to increase with each successive generation of ALK TKI. The most frequent *ALK* mutation of resistance to second-generation TKIs is G1202R (21% post-ceritinib, 29% post-alectinib, and 43% post-brigatinib). Less frequent secondary *ALK* mutations are F1174C/L (17%), C1156Y (8%), G1202del (8%) post-ceritinib, I1171T/S (12%), V1180L (6%), and L1196M (6%) post-alectinib, and E1210K (29%), D1203N (14%), S1206Y/C (14%) post-brigatinib (11). ALK-independent resistance mechanisms to second-generation ALK TKIs include alterations in bypass activating pathways (such as *RET* fusion, *MET* amplification, mutation, or rearrangement, *PIK3CA*, *FGRFR2*, *MEK*, and *NRAS* mutations), SCLC transformation, and EMT (11). Similarly,

10.3389/fonc.2022.985446

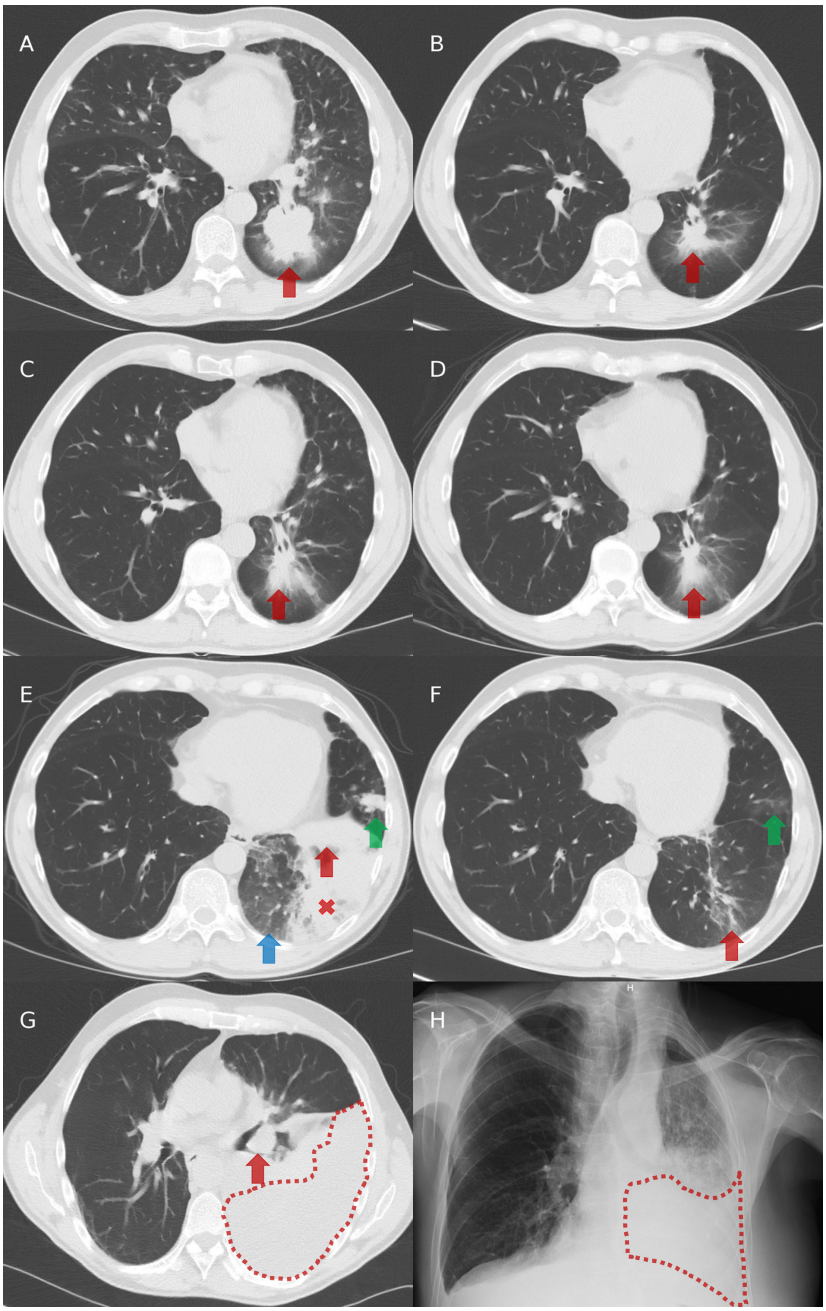

FIGURE 2
Chest imaging evolution. **(A)** Computed tomography (CT) at diagnosis: presence of a left-lower lobe primary tumor (red arrow). **(B)** CT after three cycles of cisplatin and pemetrexed in first-line: partial tumor response with decreased size of the primary tumor (red arrow). **(C)** CT after 7 cycles of pemetrexed in maintenance and then 2.5 months without systemic treatment: tumor progression with increased size of the primary tumor (red arrow). **(D)** CT after two months on crizotinib in second-line: partial tumor response with decreased size of the primary tumor (red arrow). **(E)** CT after 5.5 months on crizotinib in second-line: progression of the primary tumor (red arrow), appearance of ground glass opacities (blue arrow), a retro-obstructive condensation in the left lower lobe (red cross), and a nodular lesion in the lingula (green arrow). **(F)** CT after two months on alectinib in third-line: partial tumor response with decreased size of the left lower lobe primary tumor (red arrow) and of the lingular nodule (green arrow). **(G)** CT after 15 months on alectinib: tumor progression with increased size of the primary tumor (red arrow) and appearance of a left pleural effusion (area under red dots). **(H)** Radiography after two months on BRAF/MEK inhibitors in fourth-line: left pleural effusion (area under red dots).

10.3389/fonc.2022.985446

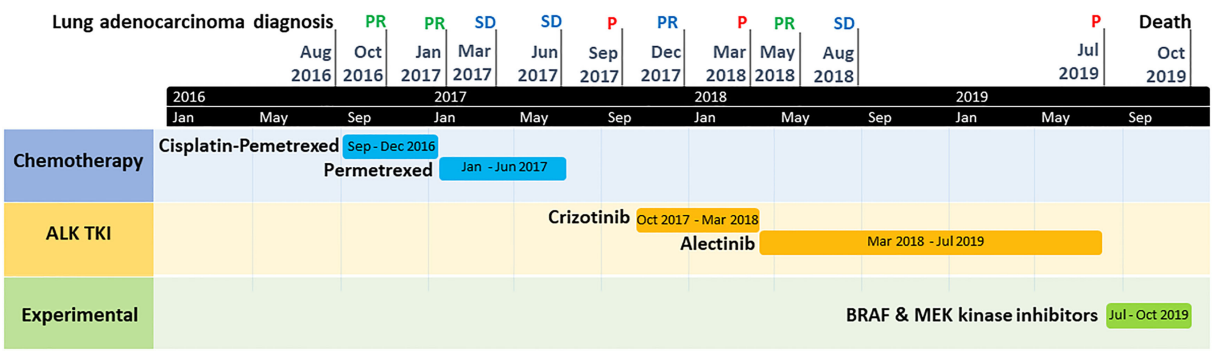

FIGURE 3
Timeline graph of patient clinical history, with tumor evolution and treatments. P, tumor progression; PR, tumor partial response; SD, tumor stable disease; TKI, tyrosine kinase inhibitor.

third-generation TKI lorlatinib has been developed to overcome these resistance mechanisms to second-generation ALK TKIs. In a phase 2 trial with lorlatinib, analysis of plasma and tissues from 198 *ALK*-rearranged NSCLC patients showed that those with *ALK* mutations post-second-generation TKI had higher ORR than those without (62% vs 32% in plasma and 69% vs 27% in tissue) (13). While ALK-independent resistance mechanisms remain sensitive to ALK inhibition post-crizotinib due to crizotinib's lower potency, this is no longer the case post-second/third-generation TKI's (11).

In our patient, in the absence of an *ALK* mutation but presence of a *BRAF* A598_T599insV mutation at progression on alectinib, we proposed participation in a phase 1b clinical trial evaluating a BRAF and a MEK inhibitor in BRAF- and KRAS-mutated NSCLC and NRAS-mutated melanoma instead of a treatment with lorlatinib. *BRAF* mutations are found in 1.5-3.5% of NSCLCs at diagnosis, almost exclusively in adenocarcinoma, and are responsible for the MAPK/ERK pathway activation leading to tumor development and progression (14). Half of *BRAF*-mutated NSCLCs have a *BRAF* V600E mutation, which is more frequent in light/never-smokers and, at diagnosis, is mutually exclusive with other oncogenic drivers such as ALK rearrangement. *BRAF* V600E-mutated NSCLC's treatment consists of a BRAF inhibitor (vemurafenib or dabrafenib) in association with a MEK inhibitor (trametinib). The response to BRAF/MEK inhibitors in presence of *BRAF* non-V600E mutations is less consistent, some of them being sensitive to BRAF/MEK inhibitors (e.g.: *BRAF* L597 and K601 mutations), while others not (e.g.: *BRAF* G464 and G469 mutations) (15). *BRAF* mutations can also occur as an acquired resistance to other targeted therapies. and have only recently been reported as a resistance mechanism to ALK TKIs. *BRAF* G15V mutation was first observed in one among 27 NSCLC patients progressing on second-generation ALK TKI (3.7%) (7). *BRAF* mutations were then reported in circulating tumor cells of 3/14 patients progressing on crizotinib (D587A in one, E586K and I592M in a second, and E586K in a third patient) (10). *BRAF* V600E mutation was observed in a patient with *ALK*-rearranged lung adenocarcinoma previously treated with crizotinib and pemetrexed (16). Because BRAF and/or MEK inhibitors were not available, the patient was treated with alectinib, but experienced tumor progression after three months. At time of progression on alectinib, rebiopsies showed persistence of the *BRAF* V600E mutation. *BRAF* V600E mutation was also found, with an *ALK* I1171T mutation, in a patient with *ALK*-rearranged lung adenocarcinoma progressing on alectinib after crizotinib (17). The patient died three months after lorlatinib was initiated. Finally, *BRAF* V600 mutation was found in a patient-derived xenograft (PDX) model from a patient progressing on alectinib (18). Triple combination of alectinib, dabrafenib, and trametinib effectively and safely suppressed tumor growth in this PDX model. To the best of our knowledge, the *BRAF* A598_T599insV mutation has never been described in lung cancer before, while only once in papillary thyroid carcinoma (19) and twice in melanoma (12, 20). Due to the rarity of non-V600E *BRAF* mutations in cancer, their clinical significance remains to be established. In this rare subset of non-V600E *BRAF* mutations, the *BRAF* A598-T599insV mutation is even rarer and its importance in cancer is unknown. In melanoma, response to BRAF/MEK inhibitors has been reported, one transient (12) and the other one complete and durable (20), suggesting that this *BRAF* A598_T599insV has an oncogenic role such as the *BRAF* V600E mutation through the activation of the MAPK/ERK pathway. In our patient, we hypothesized that the *BRAF* A598_T599insV mutation was a resistance mechanism to alectinib because it was not present at diagnosis and at progression on crizotinib but appeared at progression on alectinib. We therefore treated our patient, after stopping alectinib, with BRAF and MEK inhibitors instead of lorlatinib. However, the patient died only two months after this treatment's initiation. Failure of the BRAF/MEK inhibitors

may be explained by the fact that the *ALK* rearrangement was still present in the tumor biopsies obtained at progression on alectinib, in addition to the *BRAF* A598-T599insVmutation, these two genetic abnormalities activating different signaling pathways leading to tumor progression. Therefore, as BRAF and MEK inhibitors do not inhibit ALK and all its downstream signaling pathways, cells with *ALK* rearrangement were probably not controlled by the BRAF/MEK inhibitors targeting only the *BRAF*-mutated cells. This is often an issue in the context of acquired resistance mechanisms to oncogenic drivers, encouraging the association of multiple targeted therapies, as previously reported for instance in presence of an *EGFR* mutation and a *BRAF* V600 mutation as resistance mechanism to the third-generation EGFR TKI osimertinib (21). Even though this kind of association is interesting from a theoretical point of view, toxicity may be a problem and is the reason why we did not consider it in our patient and preferred to propose him participation in a clinical trial. In the absence of response to BRAF/MEK inhibitors, it is difficult to confirm that this *BRAF* A598-T599insV mutation was a resistance mechanism to alectinib in our patient. It is indeed possible that the *BRAF* mutation was the selection of a preexisting BRAF-clone by alectinib, even though not identified before.

Conclusion

In a patient with *ALK*-rearranged lung adenocarcinoma progressing on alectinib, we detected a *BRAF* A598-T599insV mutation, suggesting it as a resistance mechanism to alectinib. To our best knowledge, the *BRAF* A598-T599insV mutation has never been described before in lung cancer. Further research is needed to determine whether this mutation is a resistance mechanism to alectinib in lung cancer and what is the best treatment in this setting.

Data availability statement

The datasets for this article are not publicly available due to concerns regarding participant/patient anonymity. Requests to access the datasets should be directed to the corresponding author.

Ethics statement

This study was reviewed and approved by Ethical Committee of CHU UCL Namur (Godinne Site). Written informed consent was not provided because the patient deceased before the writing of the manuscript and the family has not been contacted to avoid painful memories. Ethical Committee of CHU UCL Namur provided the authorization to publish this case report without written informed consent.

Author contributions

SO made the conceptualization and supervision of the article. TP and SO wrote the original draft. EW, IW, FD, LP, CP-S, ND'H, TVB and BR reviewed the articles and gave correction. All authors contributed to the article and approved the submitted version.

Funding

This research did not receive any specific grant from funding agencies in the public, commercial, or not-for-profit sectors.

Conflict of interest

The authors declare that the research was conducted in the absence of any commercial or financial relationships that could be construed as a potential conflict of interest.

Publisher's note

All claims expressed in this article are solely those of the authors and do not necessarily represent those of their affiliated organizations, or those of the publisher, the editors and the reviewers. Any product that may be evaluated in this article, or claim that may be made by its manufacturer, is not guaranteed or endorsed by the publisher.

Supplementary material

The Supplementary Material for this article can be found online at: https://www.frontiersin.org/articles/10.3389/fonc.2022.985446/full#supplementary-material

References

1. Sung H, Ferlay J, Siegel RL, Laversanne M, Soerjomataram I, Jemal A, et al. Global cancer statistics 2020: GLOBOCAN estimates of incidence and mortality worldwide for 36 cancers in 185 countries. *CA Cancer J Clin* (2021) 71(3):209–49. doi: 10.3322/caac.21660

2. Houston KA, Henley SJ, Li J, White MC, Richards TB. Patterns in lung cancer incidence rates and trends by histologic type in the united states, 2004-2009. *Lung Cancer* (2014) 86(1):22–8. doi: 10.1016/j.lungcan.2014.08.001

3. Barlesi F, Mazieres J, Merlio JP, Debieuvre D, Mosser J, Lena H, et al. Routine molecular profiling of patients with advanced non-small-cell lung cancer: Results of a 1-year nationwide programme of the French cooperative thoracic intergroup (IFCT). *Lancet* (2016) 387(10026):1415–26. doi: 10.1016/S0140-6736(16)00004-0

4. Couraud S, Souquet PJ, Paris C, Dô P, Doubre H, Pichon E, et al. BioCAST/IFCT-1002: Epidemiological and molecular features of lung cancer in never-smokers. *Eur Respir J* (2015) 45(5):1403–14. doi: 10.1183/09031936.00097214

5. Camidge DR, Doebele RC. Treating ALK-positive lung cancer–early successes and future challenges. *Nat Rev Clin Oncol* (2012) 9(5):268–77. doi: 10.1038/nrclinonc.2012.43

6. Peng L, Zhu L, Sun Y, Stebbing J, Selvaggi G, Zhang Y, et al. Targeting ALK rearrangements in NSCLC: Current state of the art. *Front Oncol* (2022) 12:863461. doi: 10.3389/fonc.2022.863461

7. Gainor JF, Dardaei L, Yoda S, Friboulet L, Leshchiner I, Katayama R, et al. Molecular mechanisms of resistance to first- and second-generation ALK inhibitors in ALK-rearranged lung cancer. *Cancer Discovery* (2016) 6(10):1118–33. doi: 10.1158/2159-8290.CD-16-0596

8. Isozaki H, Takigawa N, Kiura K. Mechanisms of acquired resistance to ALK inhibitors and the rationale for treating ALK-positive lung cancer. *Cancers (Basel)* (2015) 7(2):763–83. doi: 10.3390/cancers7020763

9. Lin JJ, Riely GJ, Shaw AT. Targeting ALK: Precision medicine takes on drug resistance. *Cancer Discovery* (2017) 7(2):137–55. doi: 10.1158/2159-8290.CD-16-1123

10. Pailler E, Faugeroux V, Oulhen M, Mezquita L, Laporte M, Honoré A, et al. Acquired resistance mutations to ALK inhibitors identified by single circulating tumor cell sequencing in ALK-rearranged non-Small-Cell lung cancer. *Clin Cancer Res* (2019) 25(22):6671–82. doi: 10.1158/1078-0432.CCR-19-1176

11. Tabbò F, Reale ML, Bironzo P, Scagliotti GV. Resistance to anaplastic lymphoma kinase inhibitors: Knowing the enemy is half the battle won. *Transl Lung Cancer Res* (2020) 9(6):2545–56. doi: 10.21037/tlcr-20-372

12. Rogiers A, Vander Borght S, Tuand K, Wolter P, Stas M, Boecxstaens V, et al. Response to targeted therapy in two patients with metastatic melanoma carrying rare BRAF exon 15 mutations: A598_T599insV and V600_K601delinsE. *Melanoma Res* (2017) 27(5):507–10. doi: 10.1097/CMR.0000000000000376

13. Solomon BJ, Besse B, Bauer TM, Felip E, Soo RA, Camidge DR, et al. Lorlatinib in patients with ALK-positive non-small-cell lung cancer: Results from a global phase 2 study. *Lancet Oncol* (2018) 19(12):1654–67. doi: 10.1016/S1470-2045(18)30649-1

14. Zhang L, Zheng L, Yang Q, Sun J. The evolution of BRAF activation in non-Small-Cell lung cancer. *Front Oncol* (2022) 12:882940. doi: 10.3389/fonc.2022.882940

15. Dagogo-Jack I, Martinez P, Yeap BY, Ambrogio C, Ferris LA, Lydon C, et al. Impact of BRAF mutation class on disease characteristics and clinical outcomes in BRAF-mutant lung cancer. *Clin Cancer Res* (2019) 25(1):158–65. doi: 10.1158/1078-0432.CCR-18-2062

16. Urbanska EM, Sørensen JB, Melchior LC, Costa JC, Santoni-Rugiu E. Changing ALK-TKI-Resistance mechanisms in rebiopsies of ALK-rearranged NSCLC: ALK- and BRAF-mutations followed by epithelial-mesenchymal transition. *Int J Mol Sci* (2020) 21(8):2847. doi: 10.3390/ijms21082847

17. Sui A, Song H, Li Y, Guo L, Wang K, Yuan M, et al. BRAF V600E mutation as a novel mechanism of acquired resistance to ALK inhibition in ALK-rearranged lung adenocarcinoma: A case report. *Med (Baltimore)* (2021) 100(8):e24917. doi: 10.1097/MD.0000000000024917

18. Shi R, Filho SNM, Li M, Fares A, Weiss J, Pham NA, et al. BRAF V600E mutation and MET amplification as resistance pathways of the second-generation anaplastic lymphoma kinase (ALK) inhibitor alectinib in lung cancer. *Lung Cancer* (2020) 146:78–85. doi: 10.1016/j.lungcan.2020.05.018

19. Torregrossa L, Viola D, Sensi E, Giordano M, Piaggi P, Romei C, et al. Papillary thyroid carcinoma with rare exon 15 BRAF mutation has indolent behavior: A single-institution experience. *J Clin Endocrinol Metab* (2016) 101(11):4413–20. doi: 10.1210/jc.2016-1775

20. Bjursten S, Vannas C, Filges S, Puls F, Pandita A, Fagman H, et al. Response to BRAF/MEK inhibition in A598_T599insV BRAF mutated melanoma. *Case Rep Oncol* (2019) 12(3):872–9. doi: 10.1159/000504291

21. Aboubakar Nana F, Ocak S. Targeting BRAF activation as acquired resistance mechanism to EGFR tyrosine kinase inhibitors in EGFR-mutant non-Small-Cell lung cancer. *Pharmaceutics* (2021) 13(9):1478. doi: 10.3390/pharmaceutics13091478

frontiers | Frontiers in Oncology

TYPE Case Report
PUBLISHED 10 November 2022
DOI 10.3389/fonc.2022.926121

OPEN ACCESS

EDITED BY
Kohei Fujita,
National Hospital Organization Kyoto Medical Center, Japan

REVIEWED BY
Tetsuo Nakata,
Kyoto Pharmaceutical University, Japan
Tadashi Mio,
National Hospital Organization Kyoto Medical Center, Japan

*CORRESPONDENCE
Minjing Zuo
minjingzuo@163.com

†These authors have contributed equally to this work and share first authorship

SPECIALTY SECTION
This article was submitted to Thoracic Oncology, a section of the journal Frontiers in Oncology

RECEIVED 22 April 2022
ACCEPTED 26 October 2022
PUBLISHED 10 November 2022

CITATION
Peng Z, Yi L, Tao Y, Chen Z, Lin Z, He A, Jin M, Liu F and Zuo M (2022) Primary pulmonary T-cell lymphoma after operation for small intestinal stromal tumor: A case report. *Front. Oncol.* 12:926121. doi: 10.3389/fonc.2022.926121

Primary pulmonary T-cell lymphoma after operation for small intestinal stromal tumor: A case report

Zhiwei Peng[1†], Li Yi[1†], Yahong Tao[1], Zhiyong Chen[1], Ze Lin[1], Anjing He[1], Mengni Jin[1], Fanrong Liu[2] and Minjing Zuo[1*]

[1]Department of Radiology, The Second Affiliated Hospital of Nanchang University, Nanchang, China, [2]Department of Pathology, The Second Affiliated Hospital of Nanchang University, Nanchang, China

Background: The risk of gastrointestinal stromal tumor (GIST) in combination with other primary malignancies is high, which occurs before and after the diagnosis of GIST. Primary pulmonary T-cell lymphoma is a rare type of non-Hodgkin lymphoma.

Case presentation: We report a 53-year-old male patient who was admitted to our hospital with fever, cough, and expectoration for 2 weeks. Chest computed tomography (CT) showed a cavitary mass in the left lower lobe with multiple nodules in the upper lobes of both lungs. The patient had a history of surgery for small intestinal stromal tumors and was treated with oral imatinib after surgery. Lung biopsy was diagnosed as lymphomatoid granulomatosis, tending to grade 3. The pathological diagnosis was corrected by surgery and genetic testing for lung non-Hodgkin CD8-positive cytotoxic T-cell lymphoma with Epstein–Barr virus (EBV) infection in some cells. After multiple chemotherapies, the CT scan showed a better improvement than before. The patient is still under follow-up, and no tumor recurrence has been found.

Conclusion: Patients with a history of GIST should be monitored for other malignancies. The clinical symptoms and imaging examinations of primary pulmonary T-cell lymphoma are not characteristic, and the definite diagnosis still depends on pathological examination. The patient was treated with the CHOP chemotherapy regimen after the operation, the curative effect was good.

KEYWORDS

primary pulmonary T-cell lymphoma, primary pulmonary lymphoma, imatinib, gastrointestinal stromal tumors, case report

Introduction

Primary pulmonary lymphoma (PPL) refers to malignant lymphoma originating from the lymphoid tissue in the lung, originating from the bronchial mucosa-associated lymphoid tissue and/or the lymphoid tissue in the lung, and it only accounts for 0.5-1% of primary lung malignant tumors (1). The pathological types of PPL are divided into Hodgkin lymphoma (HL) and non-Hodgkin lymphoma (NHL). Low-grade B-cell lymphomas are mostly found in NHL, while T-cell lymphomas are rare (2). Other malignant tumors may occur before and after the diagnosis of GIST. We report a case of primary pulmonary T-cell lymphoma after surgery for a small intestinal stromal tumor.

Case presentation

Clinical diagnosis and treatment

The patient was a 53-year-old Chinese male with no history of cancer in his immediate family. The patient underwent small intestinal stromal tumor surgery in June 2020 and was treated with oral imatinib after surgery. The patient complained that on April 30, 2021, he had cough and sputum, yellow purulent sputum, with fever, up to 38.8°C, accompanied by chest tightness, no obvious chest pain, and no hemoptysis. After 3 days of infusion in the clinic, he went to a local hospital for treatment. Chest CT showed cavity changes in the left lung, left pleural fluid, and nodules in both lungs. The hospital was given piperacillin + etimicin + levofloxacin anti-infective treatment for 12 days. The cough and sputum were better than before, but there was still fever, and bloodshot sputum appeared. For further diagnosis and treatment, he came to the respiratory department of our hospital on May 14, 2021. Physical examination: thick breath sounds in both lungs, and weak breath sounds in the left lung. Blood routine: C-reaction protein (CRP)158 mg/L, white blood cell (WBC)3.38×10^12/L, red blood cell (RBC) 3.36×10^12/L, hemoglobin (HGB)99 g/L, lymphocyte (LYM) 0.39×10^9/L, mononuclear cell (MONO)0.74×10^9/L. Hemoglobin A1C (HbA1c) Test: 7.9%. There is no special abnormality in liver and kidney function and electrolyte examination. General bacterial, fungal sputum examination, tuberculosis and other sputum pathogenic examinations were negative. Tumor markers AFP, CEA, CA199, and PSA, were all negative. Electronic bronchoscopy showed mucosal congestion and edema in the basal segment of the left lower lobe, the lumen was narrow, and lung lavage was performed. Chest CT examination was performed on May 16, 2021 (Figures 1A–C). On May 17, 2021, a lung biopsy was performed for pathological examination. Symptomatic treatment was given, and a thoracic surgery consultation was recommended to recommend surgery. On June 19, 2021, the left lower lung mass and left lower lung were resected under thoracoscopy, and the left upper lung nodule was wedge-shaped. The surgical specimens were sent for pathological examination. They were then sent to the

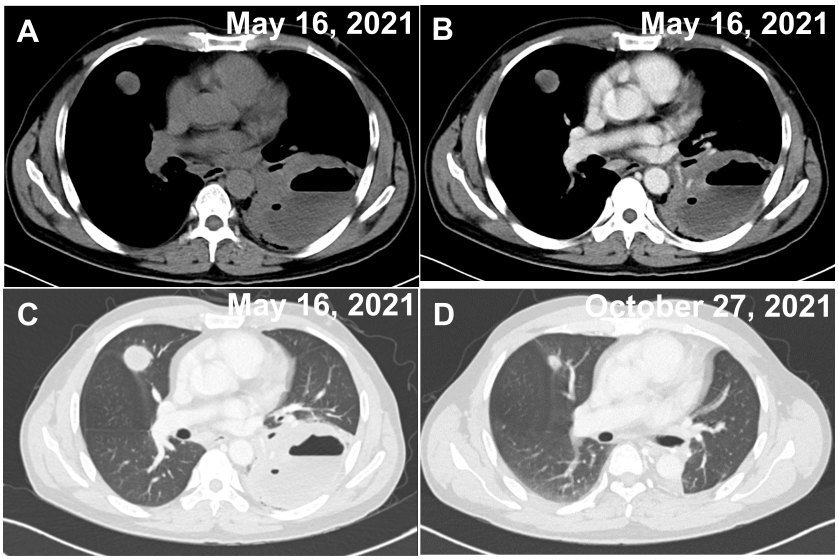

FIGURE 1
Two CT images of the chest on admission and after treatment. **(A–C)** A cavernous and fluid-flat mass in the lower lobe of the left lung and multiple nodules in the upper lobe of both lungs (the largest nodule is shown in the figure), both of which show mild circumferential enhancement on enhancement scans. **(A)** Unenhanced period. **(B)** Venous phase. **(C)** Pulmonary window. **(D)** Postoperative changes in the left lung, with significantly smaller nodules in the upper lobes of both lungs (largest nodule in the figure) than before.

Department of Pathology, Beijing Friendship Hospital, for genetic testing of T-cell clone analysis using BIOMED-2 PCR protocols. A CHOP chemotherapy regimen (ECOG score 0 points, body surface area 1.52 m^2, cyclophosphamide 1.1 g1day, pyridoxine 70 mg1day, vinorelbine 40 mg1day, prednisone 100 mg1-5day) was given on August 23, September 16, October 7, October 27, November 18, December 7, 2021, at the Department of Hematology of our hospital, and the CT scan was repeated on October 27, showing that the patient's condition improved (Figure 1D). Radiation therapy was performed in the oncology department of our hospital from January 4 to January 29, 2022. The patient is still under follow-up.

Pathological result

Pathological diagnosis on left lung biopsy on May 17, 2021, showed lymphomatoid granulomatosis, tending to grade 3.

The macroscopic examination of the surgical specimen from June 19, 2021 (Figure 2) revealed a 4x1.4x1 cm piece of lung tissue in the left upper lung and a 0.8x0.8x0.7 cm tumor seen in the lung tissue at a distance of 0.6 cm from the lung resection margin. There were many irregular tissues in the left lower lung, totaling 14x12x4 cm, of which a 9x8x4 cm gray–white, gray–yellow slightly hard area could be seen. Microscopic findings: lymphoid cells infiltrated the blood vessel wall in the tumor tissue, scattered B lymphocytes in the rich T lymphocytes background, T lymphocytes heteroplasia, mitotic figures were easy to see, and large necrosis was seen in the center of the tumor. Immunohistochemistry showed tumor tissue Vim(+), CD43, CD2, CD3, CD5, CD7, CD4, CD8 lymphocytes (+); CD56 scattered(+), TiA(+), GrB(+), CD20, CD79a and PAX5 scattered lymphocytes (+); CD10(-), bcl-6(-), Bcl-2(-), Mum(-), C-myc(-), CD21(-), CK23(-), CD30(-), CD15(-), CK(-), S-100(-), CD1a(-), langerin(-), CD68, CD163 histiocytes (+); and Ki-67 dysplastic T lymphocytes were approximately 60% (+). *In situ* hybridization: EBER focal, scattered (+). Pathological diagnosis: (left upper lung nodule) and (left lower lung) T lymphocytes heteroplasia, lymphoma cannot be excluded; genetic testing is recommended to exclude T-cell lymphoma. The 2 lymph nodes of Group 9 submitted for examination showed reactive hyperplasia.

Gene detection results: TCRβvβ+Jβ2 and DB+Jβ1/2 showed monoclonal rearrangement. Pathological diagnosis: pulmonary non-Hodgkin CD8-positive cytotoxic T-cell lymphoma with Epstein–Barr virus infection in some cells.

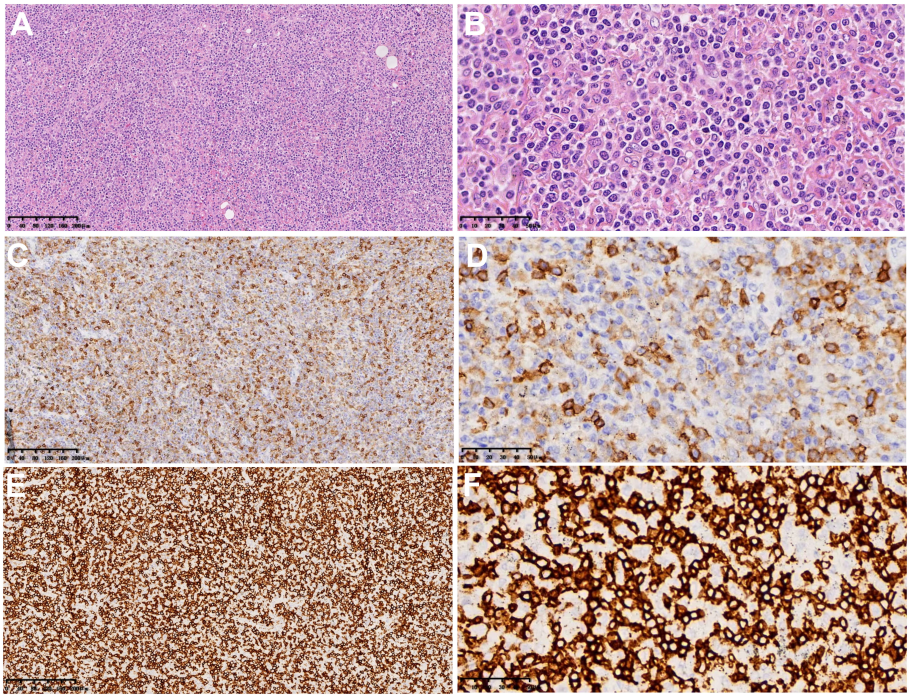

FIGURE 2
Microscopic findings and immunohistochemistry of surgical pathological specimens: lymphoid cells infiltrated the blood vessel wall in tumor tissue, B lymphocytes scattered in the background of abundant T lymphocytes, and T lymphocytes heteroplasia, with CD8-positive cells as the host. **(A, B)** Hematoxylin-eosin staining (×100 and ×400). **(C, D)** Immunohistochemical results of CD4 (×100 and ×400). **(E, F)** Immunohistochemical results of CD8 (×100 and ×400).

Discussion

There are many reports of other primary malignancies in GIST patients, ranging from 4.5% to 42.0% (3–8). Pandurengan et al. (6), in a study of 783 GIST patients, found that other malignancies were more common in GIST patients than in men and older adults. In addition, there were more patients with other malignancies before GIST diagnosis (134 patients) than patients with other malignancies after diagnosis (52 patients). Prostate cancer and breast cancer were the most common malignancies before diagnosis of GIST, and primary malignancies of the lung and kidney were the most common after diagnosis. In the study of 6112 GIST patients, Murphy et al. (7) found that the risk of other malignancies was increased in GIST patients before and after diagnosis. Esophageal cancer and bladder cancer were most common before diagnosis GIST, while ovarian cancer and small bowel cancer were most common after diagnosis GIST. Smith et al. (8) studied 1705 patients with GIST and found that colorectal cancer was the most common cancer to develop within 6 months of diagnosis GIST and that the presence of other malignancies within 6 months of diagnosis GIST was associated with poorer overall survival. In addition, GIST outside the stomach or esophagus and old age were more likely to be complicated with other malignancies.

However, it is unclear whether the presence of other malignancies in GIST patients is an incidental finding, surveillance bias or an advance in detection, or a possible causal relationship (9–13). However, it is unlikely that this is related to imatinib treatment, as other malignancies were also observed prior to the diagnosis of GIST, even at a rate comparable to the rate after diagnosis. At a time when imatinib significantly prolongs survival GIST (14), targeted surveillance and screening of patients diagnosed with GIST may be particularly important.

Primary T-cell lymphoma of the lung are rare, although the risk of GIST in combination with other primary malignancies is high. The diagnostic criteria for PPL (15) are imaging showing pulmonary and bronchial involvement without mediastinal lymph node enlargement; no evidence of lymphoma or lymphocytic leukemia at other sites outside the lungs and bronchi; no previous history of extrathoracic lymphoma diagnosis; and no signs of extrathoracic lymphoma even 3 months after presentation. The imaging presentation of PPL varies and is highly misdiagnosed. It can be classified as nodular or mass, pneumonic or alveolar, cornu, interstitial and mixed, with the nodular mass type being the most common. Most patients with primary pulmonary T-cell lymphoma present with symptoms of fever, cough and dyspnea (16).

In this case, the clinical symptoms were nonspecific. The imaging manifestations were a cavitary mass in the left lower lobe with multiple nodules in the upper lobes of both lungs. No extrapulmonary lymphoma was found during the pre- and postoperative examination of this case, so the diagnosis was made as primary pulmonary lymphoma. It can be easily misdiagnosed and need to be differentiated from a lung abscess, Wegener granulomatosis (WG), lung cancer, and pulmonary tuberculosis.

T-cell lymphoma has a poor prognosis, and the T-cell phenotype is considered an independent and significantly poor prognostic factor (17). An effective treatment strategy for primary pulmonary T-cell lymphoma has not been established, but the use of CHOP chemotherapy regimens has been reported in the literature (18). The patient, in this case, was treated with a CHOP chemotherapy regimen postoperatively with good efficacy.

Educational message

The main inspirations from this case are the following: First, patients with a history of GIST should be monitored for the possibility of other malignancies. Second, the final diagnosis of primary pulmonary T-cell lymphoma depends on pathologic examination.

Conclusion

In summary, we report a case of primary pulmonary T-cell lymphoma after operation for small intestinal stromal tumor. The clinical symptoms and imaging examination are not characteristic, so misdiagnosis can easily occur. The final diagnosis still depends on the pathological examination. In addition, patients with a history of GIST should be monitored for other malignancies. The patient, in this case, was treated with a CHOP chemotherapy regimen after surgery with good efficacy and is still being followed up.

Data availability statement

The original contributions presented in the study are included in the article/supplementary material. Further inquiries can be directed to the corresponding author.

Ethics statement

The studies involving human participants were reviewed and approved by The Second Affiliated Hospital of Nanchang University Medical Research Ethics Committee. The patients/participants provided their written informed consent to participate in this study.

Author contributions

ZP and LY wrote the article. YT and ZC collected the clinical information and images of the patients. ZL, AH, and MJ revised the article. FL interpreted the pathological findings. MZ

proofread the article. All authors contributed to the article and approved the submitted version.

Funding

This study was funded by the Key Project of Science and Technology Program of Jiangxi Provincial Department of Education (GJJ200106) and the Applied Research Cultivation Program of Jiangxi Provincial Department of Science and Technology (20212BAG70048).

Acknowledgments

We thank the Patient for his kind cooperation.

Conflict of interest

The authors declare that the research was conducted in the absence of any commercial or financial relationships that could be construed as a potential conflict of interest.

Publisher's note

References

1. Cadranel J, Wislez M, Antoine M. Primary pulmonary lymphoma. *Eur Respir J* (2002) 20(3):750–62. doi: 10.1183/09031936.02.00404102

2. Ferraro P, Trastek VF, Adlakha H, Deschamps C, Allen MS, Pairolero PC. Primary non-hodgkin's lymphoma of the lung. *Ann Thorac Surg* (2000) 69(4):993–7. doi: 10.1016/s0003-4975(99)01535-0

3. Agaimy A, Wünsch PH, Sobin LH, Lasota J, Miettinen M. Occurrence of other malignancies in patients with gastrointestinal stromal tumors. *Semin Diagn Pathol* (2006) 23(2):120–9. doi: 10.1053/j.semdp.2006.09.004

4. Kramer K, Wolf S, Mayer B, Schmidt SA, Agaimy A, Henne-Bruns D, et al. Frequence, spectrum and prognostic impact of additional malignancies in patients with gastrointestinal stromal tumors. *Neoplasia* (2015) 17(1):134–40. doi: 10.1016/j.neo.2014.12.001

5. Hechtman JF, DeMatteo R, Nafa K, Chi P, Arcila ME, Dogan S, et al. Additional primary malignancies in patients with gastrointestinal stromal tumor (gist): a clinicopathologic study of 260 patients with molecular analysis and review of the literature. *Ann Surg Oncol* (2015) 22(8):2633–9. doi: 10.1245/s10434-014-4332-z

6. Pandurengan RK, Dumont AG, Araujo DM, Ludwig JA, Ravi V, Patel S, et al. Survival of patients with multiple primary malignancies: a study of 783 patients with gastrointestinal stromal tumor. *Ann Oncol* (2010) 21(10):2107–11. doi: 10.1093/annonc/mdq078

7. Murphy JD, Ma GL, Baumgartner JM, Madlensky L, Burgoyne AM, Tang CM, et al. Increased risk of additional cancers among patients with gastrointestinal stromal tumors: a population-based study. *Cancer-Am Cancer Soc* (2015) 121 (17):2960–7. doi: 10.1002/cncr.29434

8. Smith MJ, Smith HG, Mahar AL, Law C, Ko YJ. The impact of additional malignancies in patients diagnosed with gastrointestinal stromal tumors. *Int J Cancer* (2016) 139(8):1744–51. doi: 10.1002/ijc.30231

9. Carney JA. Gastric stromal sarcoma, pulmonary chondroma, and extra-adrenal paraganglioma (carney triad): natural history, adrenocortical component, and possible familial occurrence. *Mayo Clin Proc* (1999) 74(6):543–52. doi: 10.4065/74.6.543

10. Chompret A, Kannengiesser C, Barrois M, Terrier P, Dahan P, Tursz T, et al. Pdgfra germline mutation in a family with multiple cases of gastrointestinal stromal tumor. *Gastroenterology* (2004) 126(1):318–21. doi: 10.1053/j.gastro.2003.10.079

11. Miettinen M, Fetsch JF, Sobin LH, Lasota J. Gastrointestinal stromal tumors in patients with neurofibromatosis 1: a clinicopathologic and molecular genetic study of 45 cases. *Am J Surg Pathol* (2006) 30(1):90–6. doi: 10.1097/01.pas.0000176433.81079.bd

12. Petit A, Castillo M, Santos M, Mellado B, Alcover JB, Mallofré C. Kit expression in chromophobe renal cell carcinoma: comparative immunohistochemical analysis of kit expression in different renal cell neoplasms. *Am J Surg Pathol* (2004) 28(5):676–8. doi: 10.1097/00000478-200405000-00017

13. Sengupta S, Cheville JC, Corless CL, Lohse CM, Heinrich MC, Kwon ED, et al. Rare expression of kit and absence of kit mutations in high grade renal cell carcinoma. *J Urol* (2006) 175(1):53–6. doi: 10.1016/S0022-5347(05)00059-5

14. Blanke CD, Demetri GD, von Mehren M, Heinrich MC, Eisenberg B, Fletcher JA, et al. Long-term results from a randomized phase ii trial of standard- versus higher-dose imatinib mesylate for patients with unresectable or metastatic gastrointestinal stromal tumors expressing kit. *J Clin Oncol* (2008) 26 (4):620–5. doi: 10.1200/JCO.2007.13.4403

15. Cordier JF, Chailleux E, Lauque D, Reynaud-Gaubert M, Dietemann-Molard A, Dalphin JC, et al. Primary pulmonary lymphomas. a clinical study of 70 cases in nonimmunocompromised patients. *Chest* (1993) 103(1):201–8. doi: 10.1378/chest.103.1.201

16. Yang L, Feng W, Chen C, Zhang X, Zhu Y, Lei W, et al. Primary pulmonary t-cell lymphoma mimicking pneumonia: a case report and literature review. *Exp Ther Med* (2016) 12(1):365–8. doi: 10.3892/etm.2016.3287

17. Chan JK, Sin VC, Wong KF, Ng CS, Tsang WY, Chan CH, et al. Nonnasal lymphoma expressing the natural killer cell marker cd56: a clinicopathologic study of 49 cases of an uncommon aggressive neoplasm. *Blood* (1997) 89(12):4501–13. doi: 10.1182/blood.V89.12.4501

18. Fisher RI, Gaynor ER, Dahlberg S, Oken MM, Grogan TM, Mize EM, et al. Comparison of a standard regimen (chop) with three intensive chemotherapy regimens for advanced non-hodgkin's lymphoma. *N Engl J Med* (1993) 328 (14):1002–6. doi: 10.1056/NEJM199304083281404

frontiers | Frontiers in Oncology

TYPE Case Report
PUBLISHED 14 November 2022
DOI 10.3389/fonc.2022.1019932

OPEN ACCESS

EDITED BY
Kohei Fujita,
National Hospital Organization Kyoto Medical Center, Japan

REVIEWED BY
Francesco Pepe,
University of Naples Federico II, Italy
Jan Von Der Thüsen,
Erasmus Medical Center, Netherlands

*CORRESPONDENCE
Kei Morikawa
mokke@marianna-u.ac.jp

SPECIALTY SECTION
This article was submitted to Thoracic Oncology, a section of the journal Frontiers in Oncology

RECEIVED 15 August 2022
ACCEPTED 27 October 2022
PUBLISHED 14 November 2022

CITATION
Morikawa K, Handa H, Ueno J, Tsuruoka H, Inoue T, Shimada N, Koike J, Nakamura S, Sato Y and Mineshita M (2022) *RET* fusion mutation detected by re-biopsy 7 years after initial cytotoxic chemotherapy: A case report. *Front. Oncol.* 12:1019932. doi: 10.3389/fonc.2022.1019932

RET fusion mutation detected by re-biopsy 7 years after initial cytotoxic chemotherapy: A case report

Kei Morikawa[1]*, Hiroshi Handa[1], Junko Ueno[1], Hajime Tsuruoka[1], Takeo Inoue[1], Naoki Shimada[2], Junki Koike[2], Seiji Nakamura[3], Yoshiharu Sato[3] and Masamichi Mineshita[1]

[1]Division of Respiratory Diseases, Department of Internal Medicine, St. Marianna University School of Medicine, Kawasaki, Japan, [2]Department of Pathological Diagnosis, St. Marianna University School of Medicine, Kawasaki, Japan, [3]DNA Chip Research Inc., Tokyo, Japan

Personalized medicine using molecular-targeted drugs to achieve better therapeutic response and long-term prognosis is common practice for lung cancer treatment. However, in cases before gene batch tests were available, medical treatment continued without the detection of rare mutations. We report a sixty-seven-old year man diagnosed with adenocarcinoma T1cN3M1a, stage IVA. Initial screening performed 7 years earlier using EGFR mutation and ALK immunohistochemical tests were negative. Although first-line cytotoxic combination chemotherapy was remarkably effective, a gradual regression of the primary lesion was noted. After a recent bronchoscopic re-biopsy, *RET* fusion was detected by gene panel test. In addition, we were able to confirm *RET* from FFPE specimens obtained from 7-year-old pleural effusion cell blocks. Subsequent administration of the molecular-targeted drug selpercatinib, was highly effective for the primary lesion and all metastatic lesions including brain metastases. We describe a case of *RET* fusion-positive lung cancer where molecular targeted therapy and cytotoxic drug showed a drastic response and long-term therapy was well maintained. Next generation sequencing was able to correctly diagnose *RET* fusion mutation using re-biopsy specimen after going undiagnosed for 7 years.

KEYWORDS

RET mutation detected by re-biopsy case report, gene mutation, re-biopsy, *RET* fusion lung cancer, selpercatinib

Introduction

Personalized medicine for lung cancer patients using molecular-targeted drugs and immune checkpoint inhibitors has become widespread due to their high response rates and long-term prognosis (1–3). To date, epidermal growth factor receptor (*EGFR*) mutation, anaplastic lymphoma kinase (*ALK*) fusion genes, *ROS1*, *BRAF*, *MET* exon 14 skipping mutations, *RET* fusion genes and their corresponding molecular-targeted drugs have been approved by the Food and Drug Administration (FDA). Furthermore, *KRAS* mutation, *EGFR* and *HER2* exon 20 insertion and their corresponding molecular-targeted drugs will soon be available.

However, in cases before gene batch tests were available, the patient's medical treatment would have progressed without the detection of rare mutations. It is presumed that malignancy and the therapeutic effects of cytotoxic drugs differ depending on the type of gene mutation (4, 5). Therefore, even in cases with mutation-positive advanced lung adenocarcinoma, long-term clinical courses can be maintained without the administration of molecular-targeted drugs. In particular, even in cases where the initial treatment was successful, the initial sample might not be suitable for gene panel testing due to the deterioration of nucleic acid quality over time. Furthermore, it can be difficult to select the same location for re-biopsy since the lesion might have been altered by treatment. Herein, we report a rare case in where *RET* fusion was detectable by gene panel test after re-biopsy seven years after the initial diagnosis. Sequential administration of the molecular-target drug selpercatinib showed a drastic response.

Case report

A 67-year-old male, never smoker with no remarkable medical history, was referred to our hospital with a massive left pleural effusion (Figure 1A). The cytological evaluation of the left pleural effusion was class V adenocarcinoma, consistent with the cell block pathological assessment. Pleurodesis using talc dilated the lungs well, and a 25 × 17 mm nodule at the left S^{1+2}a was presumed to be the primary lesion (Figure 1B). Clinically, he was diagnosed with adenocarcinoma T1cN3M1a, stage IVA. Initial gene mutation screening seven years earlier using Cobas® EGFR mutation and ALK immunohistochemical (IHC) tests were negative.

First-line treatment included carboplatin + pemetrexed + bevacizumab, and although a near complete response (CR) was obtained after 4 courses, nasal bleeding continued, and only pemetrexed was administered for maintenance therapy. CR was achieved over 25 courses of maintenance therapy (Figure 1C), but treatment was temporarily terminated due to a slight deterioration of renal function. One year post treatment, CT showed a slight progression in the primary lesion (Figure 1D), but the speed of regrowth was slow. One year after the progression was confirmed by CT (Figure 1E), pemetrexed monotherapy was resumed, and the primary lesion and lymph nodes decreased (Figure 1F). However, after 32 courses of maintenance therapy, a rapid systemic progression was noted. Due to the primary lesion regrowth (Figure 1G), contralateral lung metastasis, multiple liver metastases, a right adrenal metastasis, and multiple brain metastases (Figures 2A, B), adjustments to his treatment were necessary.

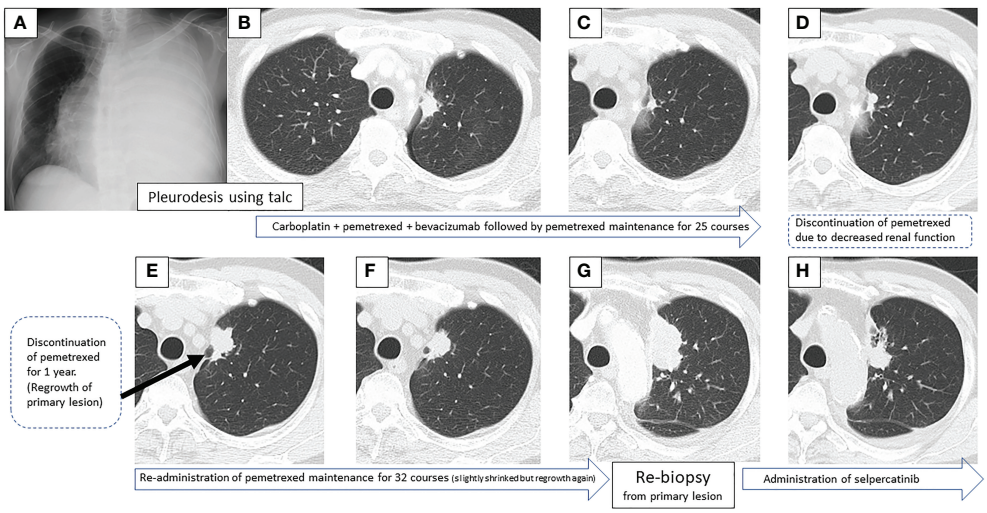

FIGURE 1
Sequential images of the primary lesion over 7 years, from the time of the first visit to the introduction of the second treatment.

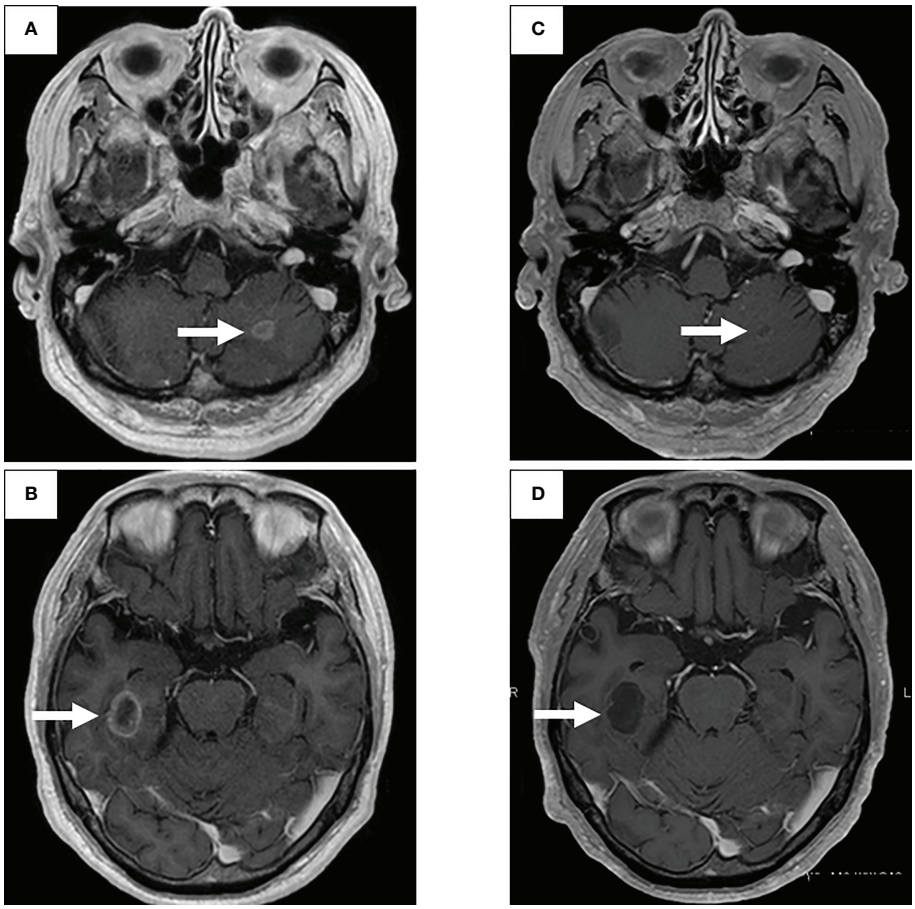

FIGURE 2
Therapeutic effect of brain metastasis using second-line treatment selpercatinib.

Bronchoscopic re-biopsy of the primary lesion revealed class V adenocarcinoma cytologically, and histological assessment confirmed this result. Oncomine™ Dx Target Test confirmed the patient was *RET* fusion gene-positive, and the RET inhibitor selpercatinib 240 mg was administered the following day. On day 13, CT revealed a good systemic response with all metastatic lesions, including brain metastases (Figures 2C, D), compared with baseline imaging (Figure 1H). Selpercatinib with a dose reduction (160 mg/day) for grade 2 elevated liver enzymes was continued. A high sensitivity next generation sequencing (NGS) panel system: lung cancer compact panel, with RNA assay using cytological brushing solution (6, 7), confirmed the fusion gene *KIF5B* exon 15; *RET* exon 12 (*K15RET12*). We could further confirm *RET* from formalin-fixed paraffin-embedded (FFPE) specimens from 7-year-old pleural effusion cell blocks (Figures 3A, B), which were morphologically similar to re-biopsy sample in terms of malignant cells with large nucleoli (Figures 3C, D). RNA (1256 ng) was collected from the initial cell block sample, with an RNA integrated number (RIN) value of 4.8. A *K15RET12* fusion peak was detected by single-plex polymerase chain reaction (PCR) (Figure 3) and NGS assay.

Finally, we provide additional information on PCR and NGS techniques. SYBR-Green real-time PCR assay with melting curve analysis was performed to detect RET fusion detection from archive cellblock sample. KOD SYBR® qPCR/RT set (Toyobo) was used for reverse transcription and real time PCR. These assays were performed according to the manufacturer's protocols. Non-tumor wild type sample was assayed in parallel as negative control. Peak call of 78 degree from melting curve chromatogram is the criteria for the detection of fusion positive. Moreover, sequence of fusion boundary was confirmed by NGS sequencing (Illumina Miseq 150 paired-end) of qPCR product.

Lung cancer compact panel assay was also performed for archive first diagnostic sample. *KIF5b-exon15_RET-exon12* fusion was also detected from this analysis. Moderate signal intensity of fusion variant was obtained from this assay (70 fusion boundary-positive reads out of 1,335 total sequencing reads). Lung cancer compact panel assay was performed

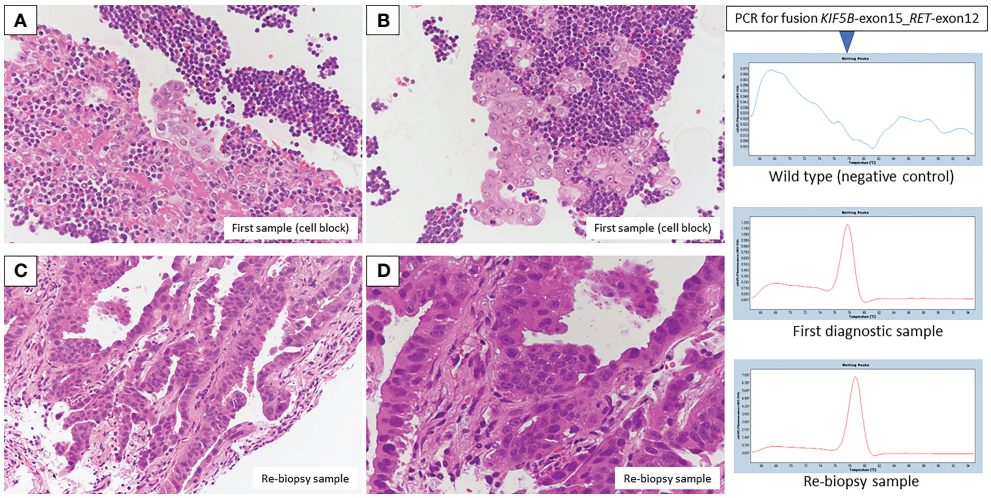

FIGURE 3
Pathologic findings from the first diagnostic cell block showed adenocarcinoma in the presence of many lymphocytes (**A, B**, H&E staining, original magnification × 400). A re-biopsy sample also showed adenocarcinoma with an alveolar, ductal structure (**C, D**, H&E staining, original magnification×200 and×400, respectively). Fusion *KIF5B*-exon 15; *RET*-exon 12 was detected by PCR/NGS assay from first diagnostic specimens, and NGS assay from re-biopsy specimens.

according to the protocol described previously (8). Limit of detection of RET fusion detection by lung cancer compact panel is no more than 1% variant allele frequency.

Discussion

Conventionally, gene mutations have been identified by the single-plex PCR method for individual gene mutations. The PCR, which has high sensitivity and specificity, a short turn-around time, and is relatively inexpensive, has become widespread mainly for the detection of EGFR. However, with the discovery of various lung cancer driver genes over the last five years, it is impractical to test single gene mutations sequentially due to time and sample consumption constraints. In 2017, the gene panel test, Oncomine Dx Target Test Multi-CDx system (Thermo Fisher Scientific, San Jose, CA, USA), which can simultaneously evaluate 46 cancer-related genes, was one of the first NGS panels for non-small cell lung cancer testing approved by the FDA (9). However, this batch test requires sufficient amounts of malignant cells in the collected tissue sample and qualified sample handling. Moreover, if a significant amount of time has passed since collection, the sample is often unsuitable for gene panel testing due to the deterioration of nucleic acid quality. Since the initial diagnosis in this case was made over 7 years ago, it was assumed that the nucleic acid quality would have deteriorated over that time. Therefore, re-biopsy of the primary lesion was performed.

This was a rare case where cytotoxic chemotherapy, and subsequent maintenance therapy, was remarkably effective for the primary lesion. Generally, progression-free survival for cytotoxic chemotherapy in advanced-stage gene mutation-positive lung adenocarcinoma is about 6 months (4, 5), and it is not often possible to continue treatment for more than one year. Even when treatment is continued beyond-progressive disease (beyond-PD), in most cases, treatment adjustments are unavoidable due to the systemic exacerbation of the disease. The prognosis for gene mutant lung adenocarcinoma without the use of molecular-targeted drugs is generally poor, but there are cases in which cancer development is observed over a very long period of time. In particular, *RET* fusion lung cancer has been reported to show a slower clinical course (10, 11). Hence, as in our patient, there are a number of cases where rare mutations have not been detected over long-term clinical courses.

Selpercatinib, similar to other molecular-targeted therapies, had sufficient systemic effects (12, 13), including brain metastases (14). In general, first-line treatment for gene mutation-positive lung adenocarcinoma is the corresponding molecular-targeted drug; however, this case suggests that the order of drugs used may be important when aiming for the longest overall survival by sequence therapy (15). In a phase 3 study of selpercatinib for *RET*-positive lung cancer, the efficacy of molecular-targeted drugs, in addition to the therapeutic effects

of cytotoxic drugs will be clarified (16). It is noteworthy that we were able to detect *RET* fusion by extracting RNA from 7-year-old pleural effusion cell blocks, which contained a low percentage of malignant cells.

Data availability statement

The original contributions presented in the study are included in the article/supplementary material. Further inquiries can be directed to the corresponding author.

Ethics statement

Written informed consent was obtained from the patient for publication of this case report and any accompanying images. The research gene analysis was with ethics approval (HREC ID 4814).

Author contributions

KM had full access to data in this case report and takes responsibility for the integrity and accuracy of data analysis. KM, HH, JU, HT and TI contributed to bronchoscopic examination and interpretation. NS, JK, SN and YS contributed to pathological evaluation and genetic analysis. KM and MM contributed to the scientific review and final approval of this manuscript. All authors contributed to the article and approved the submitted version.

Acknowledgments

The authors thank Mr. Jason Tonge from St. Marianna University School of Medicine for the linguistic review of this manuscript.

Conflict of interest

Author SN and YS was employed by DNA Chip Research Inc. The research gene analysis of this case was conducted by DNA Chip Research Inc., Tokyo, Japan.

The remaining authors declare that the research was conducted in the absence of any commercial or financial relationships that could be construed as a potential conflict of interest.

Publisher's note

References

1. Mark GK, Bruce EJ, Lynne DB, Kwiatkowski DJ, Iafrate AJ, Wistuba II, et al. Using multiplexed assays of oncogenic drivers in lung cancers to select targeted drugs. *JAMA* (2014) 311(19):1998–2006. doi: 10.1001/jama.2014.3741

2. Gambardella V, Tarazona N, Cejalvo JM, Lombardi P, Huerta M, Roselló S, et al. Personalized medicine: Recent progress in cancer therapy. *Cancers* (2020) 12 (4):1009. doi: 10.3390/cancers12041009

3. Mosele F, Remon J, Mateo J, Westphalen CB, Barlesi F, Lolkema MP, et al. Recommendations for the use of next-generation sequencing (NGS) for patients with metastatic cancers: a report from the ESMO precision medicine working group. *Ann Oncol* (2020) 31(11):1491–505. doi: 10.1016/j.annonc.2020.07.014

4. Soria JC, Tan DSW, Chiari R, Wu YL, Paz-Ares L, Wolf J, et al. First-line ceritinib versus platinum-based chemotherapy in advanced ALK-rearranged non-small-cell lung cancer (ASCEND-4): a randomised, open-label, phase 3 study. *Lancet* (2017) 389(10072):917–29. doi: 10.1016/S0140-6736(17)30123-X

5. Rosell R, Carcereny E, Gervais R, Vergnenegre A, Massuti B, Felip E, et al. Erlotinib versus standard chemotherapy as first-line treatment for European patients with advanced EGFR mutation-positive non-small-cell lung cancer (EURTAC): a multicentre, open-label, randomised phase 3 trial. *Lancet Oncol* (2012) 13(3):239–46. doi: 10.1016/S1470-2045(11)70393-X

6. Morikawa K, Kida H, Handa H, Inoue T, Saji H, Koike J, et al. A prospective validation study of lung cancer gene panel testing using cytological specimens. *Cancers* (2022) 14(15):3784. doi: 10.3390/cancers14153784

7. Morikawa K, Kinoshita K, Kida H, Inoue T, Mineshita M. Preliminary results of NGS gene panel test using NSCLC sputum cytology and therapeutic effect using corresponding molecular-targeted drugs. *Genes* (2022) 13(5):812.

8. Kato K, Okami J, Nakamura H, Honma K, Sato Y, Nakamura S, et al. Analytical performance of a highly sensitive system to detect gene variants using next-generation sequencing for lung cancer companion diagnostics. *medRxiv* (2021). doi: 10.1101/2021.10.13.21264976

9. FDA U. *Summary of safety and effectiveness data for oncomine dx target test* (2017). Available at: https://www.accessdata.fda.gov/cdrh_docs/pdf16/P160045B.pdf (Accessed 27 March 2022).

10. Drilon A, Bergagnini I, Delasos L, Sabari J, Woo KM, Plodkowski A. Clinical outcomes with pemetrexed-based systemic therapies in RET-rearranged lung cancers. *Ann Oncol* (2016) 27(7):1286–91. doi: 10.1093/annonc/mdw163

11. Shen T, Pu X, Wang L, Yu Z, Li J, Zhang Y, et al. Association between RET fusions and efficacy of pemetrexed-based chemotherapy for patients with advanced NSCLC in China: A multicenter retrospective study. *Clin Lung Cancer* (2020) 21 (5):e349–54. doi: 10.1016/j.cllc.2020.02.006

12. Illini O, Hochmair MJ, Fabikan H, Weinlinger C, Tufman A, Swalduz A, et al. Selpercatinib in RET fusion-positive non-small-cell lung cancer (SIREN): a retrospective analysis of patients treated through an access program. *Ther Adv Med Oncol* (2021) 13:17588359211019675. doi: 10.1177/17588359211019675

13. Hess LM, Han Y, Zhu YE, Bhandari NR, Sireci A. Characteristics and outcomes of patients with RET-fusion positive non-small lung cancer in real-world practice in the united states. *BMC Cancer* (2021) 21(1):28. doi: 10.1186/s12885-020-07714-3

14. Subbiah V, Gainor JF, Oxnard GR, Tan DSW, Owen DH, Cho BC, et al. Intracranial efficacy of selpercatinib in RET fusion-positive non-small cell lung cancers on the LIBRETTO-001 trial. *Clin Cancer Res* (2021) 27(15):4160–7. doi: 10.1158/1078-0432.CCR-21-0800

15. Knetki-Wróblewska M, Wojas-Krawczyk K, Kowalski DM, Krzakowski M. Non-Small-Cell lung cancer patients with coexistence of high PD-L1 expression and RET fusion-which path should we follow? case reports and literature review. *J Clin Med* (2022) 11(6):1630. doi: 10.3390/jcm11061630

16. Solomon BJ, Zhou CC, Drilon A, Park K, Wolf J, Elamin Y, et al. Phase III study of selpercatinib versus chemotherapy ± pembrolizumab in untreated RET positive non-small-cell lung cancer. *Future Oncol* (2021) 17(7):763–73. doi: 10.2217/fon-2020-0935

frontiers | Frontiers in Oncology

TYPE Case Report
PUBLISHED 15 November 2022
DOI 10.3389/fonc.2022.957661

OPEN ACCESS

EDITED BY
Hidekazu Suzuki,
Osaka Habikino Medical Center, Japan

REVIEWED BY
Waleed Kian,
Shaare Zedek Medical Center, Israel
Clelia Madeddu,
University of Cagliari, Italy
Koji Haratani,
Kindai University Hospital, Japan

*CORRESPONDENCE
Shencun Fang
fang1984@aliyun.com

†These authors have contributed equally to this work

SPECIALTY SECTION
This article was submitted to Thoracic Oncology, a section of the journal Frontiers in Oncology

RECEIVED 28 June 2022
ACCEPTED 25 October 2022
PUBLISHED 15 November 2022

CITATION
Qian C, Zhang Y, Cheng W, Zhang Q, Li M and Fang S (2022) Case report: Rechallenge with EGFR–TKIs after immunotherapy in EGFR–mutated non–small cell lung cancer with leptomeningeal metastasis. *Front. Oncol.* 12:957661. doi: 10.3389/fonc.2022.957661

Case report: Rechallenge with EGFR–TKIs after immunotherapy in EGFR–mutated non–small cell lung cancer with leptomeningeal metastasis

Chunfa Qian[1†], Yuhai Zhang[1†], Wanwan Cheng[2], Qingchao Zhang[3], Mengzhen Li[3] and Shencun Fang[2*]

[1]Department of Neurosurgery, The Affiliated Brain Hospital of Nanjing Medical University, Nanjing, China, [2]Department of Respiratory Medicine, Nanjing Chest Hospital, The Affiliated Brain Hospital of Nanjing Medical University, Nanjing, China, [3]MyGene Diagnostics Co., Ltd., Guangzhou, China

Rechallenge of epidermal growth factor receptor-tyrosine kinase inhibitors (EGFR-TKIs) after PD-1 blockade failure was an effective therapy for non-small cell lung cancer (NSCLC) patients with resistance to EGFR-TKIs. The third-generation TKIs, like osimertinib and furmonertinib, can reach higher concentration in the cerebrospinal fluid (CSF) than other TKIs, and exhibit a beneficial effect in NSCLC patients with leptomeningeal metastases (LM) harboring sensitive EGFR mutation. Here, we report that two-stage IV pulmonary adenocarcinoma patients with LM harboring an EGFR L858R mutation benefit from the third-generation EGFR-TKIs rechallenge after immune checkpoint inhibitor (ICI) and anti-angiogenic agent combination therapy. Complete response (CR) to partial response (PR) of central nervous system (CNS) response was achieved immediately after the administration of furmonertinib and osimertinib. We conducted next-generation sequencing (NGS) and IHC to elucidate the evolution of driver mutations and the immune microenvironment. In conclusion, these two cases might provide a therapeutic strategy for further clinical practice. More research was needed to elucidate the resistance mechanisms and improve current treatment strategies in EGFR-mutated patients with LM.

KEYWORDS

lung adenocarcinoma, EGFR-TKIs rechallenge, immune checkpoint inhibitor, the third generation EGFR-TKIs, leptomeningeal metastasis

Introduction

Although patients with advanced NSCLC harboring drug-sensitive EGFR mutations benefit from the use of EGFR-TKIs, most of them progress within 12 months from the start of treatment due to acquired resistance (1). In addition, approximately 40% of EGFR-mutated NSCLC patients present with disease progression in the central nervous system (CNS), either as brain metastases (BM) or leptomeningeal metastases (LM) after initial EGFR-TKI treatment failure (2). LMs are associated with poor prognosis in NSCLC patients (3). Although underdiagnosed, about 10% of EGFR-mutated NSCLC patients experience LM during systemic TKI therapy, leading to dismal outcomes with a median survival of fewer than 6 months (4, 5). In clinical practice, many physicians frequently provide a chemotherapy or immunotherapy break followed by EGFR-TKI retreatment (3, 6). However, the optimal treatment for patients with EGFR-mutated NSCLC and LM that develops after EGFR-TKI therapy failure remains unclear. It is essential to explore the effectiveness of subsequent EGFR-TKI rechallenges after initial TKI failure in patients with NSCLC and LM.

In this study, we report two cases to evaluate the effectiveness of EGFR-TKIs rechallenge in EGFR-mutated NSCLC patients with LM after TKI failure and interspersed immunotherapy.

Case report 1

A 62-year-old Chinese female without a smoking history was admitted for a cough in September 2018. A computed tomography (CT) of the patient's chest showed a mass in the right upper lung and diffuse micronodules in both lungs (Figure 1A). A needle biopsy of the mass revealed lung adenocarcinoma. Pemetrexed plus cisplatin were started as first line chemotherapy for two cycles until the disease progressed. CT examination showed that the right upper lung lesion was enlarged and the carcinoembryonic antigen (CEA) level was increased. Then docetaxel and carboplatin were chosen as the second-line treatments, and stable disease (SD) was achieved. Meanwhile, subsequent NGS of lung tissue identified the EGFR L858R mutation and the TP53 exon 8 mutation. PR was achieved after gefitinib (250 mg once daily) was added to the treatment for two cycles (Figure 1B). After 9 months, anlotinib (12 mg once daily) plus gefitinib (250 mg once daily) were initiated for pulmonary lesion progression, and no mutation was detected in plasma. PR was observed according to the CT scan (Figure 1C). Seven months later, re-examined CT suggested multiple metastases in both lungs, and the blood CEA was higher than before. Considering the progression of the disease, a pulmonary puncture was performed to search for drug-resistant genes, but the size of the puncture specimens was too small to conduct gene testing. For 1 month, empiric osimertinib was administered, but the disease still

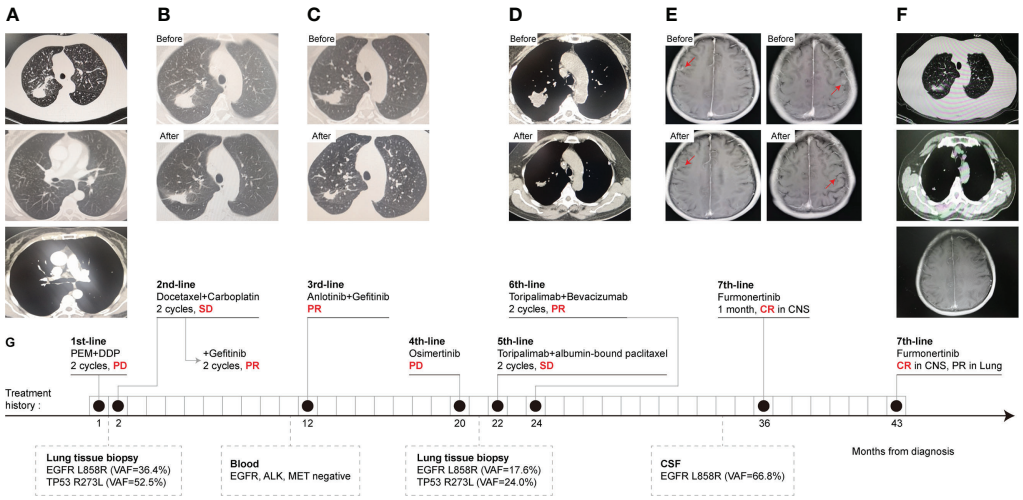

FIGURE 1
CT scans, treatment history, and gene mutation of case 1 at different clinical time points as shown. CT scans results. **(A)** Chest CT scans of right lung adenocarcinoma and lymph nodes before first-line treatment. **(B)** PR was observed after gefitinib was added to the combined chemotherapy, second-line treatment. **(C)** The change of lung lesion before and after third-line treatment, anlotinib plus gefitinib. **(D)** CT scans before and after two cycles of terriprizumab plus bevacizumab, sixth-line treatment. **(E)** MRI of the brain. CR of LM was obtained after 1 month of furmonertinib, seventh-line treatment. **(F)** The lung and CNS lesions were kept stable until recent follow-up in April 2022. **(G)** The timeline of Case 1 treatment history, follow-up diagnostic and gene test results. Numbers indicate the time from the diagnosis of NSCLC. CR, complete response; PR, partial response; SD, stable disease, PD, progressive disease; CSF, cerebrospinal fluid; CNS, central nervous system; VAF, variant allele frequency.

progressed. A lung biopsy was performed again on the right upper lung lesion and NGS was performed. The NGS results showed that EGFR L858R mutation, TP53 exon 8 missense mutation, and PD-L1 high expression (TPS = 60%), without EGFR T790M mutation. Toripalimab combined with albumin-bound paclitaxel was administered for two cycles. SD was achieved. But due to the intolerance of chemotherapy toxicity, the treatment regimen was changed to toripalimab plus bevacizumab. PR was achieved after two cycles of treatment (Figure 1D). Approximately 12 months later, she developed dizziness, headache, and vomiting and was diagnosed with LM based on cranial enhanced magnetic resonance imaging (MRI) and CSF cytological analysis. DNA sequencing of CSF and plasma specimens revealed an EGFR L858R mutation. The EGFR T790M mutation was undetectable. After 3 days of administration of furmonertinib (160 mg once daily), the neurological symptoms disappeared completely. After 1 month of EGFR-TKI rechallenge, CR of intracranial lesions was further confirmed (Figure 1E). The patient had received furmonertinib for more than 6 months, and no evidence of malignancy recurrence was found by brain MRI (Figure 1F). The treatment history and gene test results of this patient are presented in Figure 1G.

Case report 2

A 49-year-old Chinese male with a smoking history was admitted to the hospital due to left lung adenocarcinoma with multiple bone metastases in January 2019. Then two cycles of pemetrexed plus carboplatin were initiated. SD was achieved in the pulmonary lesion. However, brain metastasis at the right frontoparietal junction was found by cranial enhanced MRI, and subsequent NGS of lung tissue identified an EGFR L858R mutation, without a T790M mutation. Then, the patient received second-line osimertinib treatment and cranial SBRT local radiotherapy (DT: 50 Gy/10 F) at the same time. Progression of lung lesions was observed by chest CT after 6 months. So docetaxel plus bevacizumab was started as the third-line treatment for 6 months. Subsequently, bevacizumab therapy was maintained for another 3 months. As pulmonary metastases and bone metastases progressed, another lung biopsy NGS testing revealed an EGFR L858R mutation and high PD-L1 expression (TPS = 80%). The EGFR T790M mutation was undetectable. Therefore, the patient commenced on four-line treatment with anlotinib and durvalumab. PR was observed after two cycles (Figure 2A). But the patient developed a headache, with vomiting and a static tremor 8 months later. Metastatic adenocarcinoma cells were observed by IHC and EGFR L858R, TP53, and KRAS amplifications were obtained by NGS in CSF samples. Based on contrast-enhanced MRI, LM was indicated. The osimertinib rechallenge significantly relieved the headache after one week. Moreover, PR of LM occurred after two cycles of treatment (Figure 2B). Finally, the osimertinib rechallenge was maintained for more than 11 months and the patient was still in close follow-up (Figure 2C). The treatment history and gene test results are presented in Figure 2D.

Discussion

To the best of our knowledge, this is the first report to evaluate the efficacy of third-generation EGFR-TKI rechallenge for EGFR

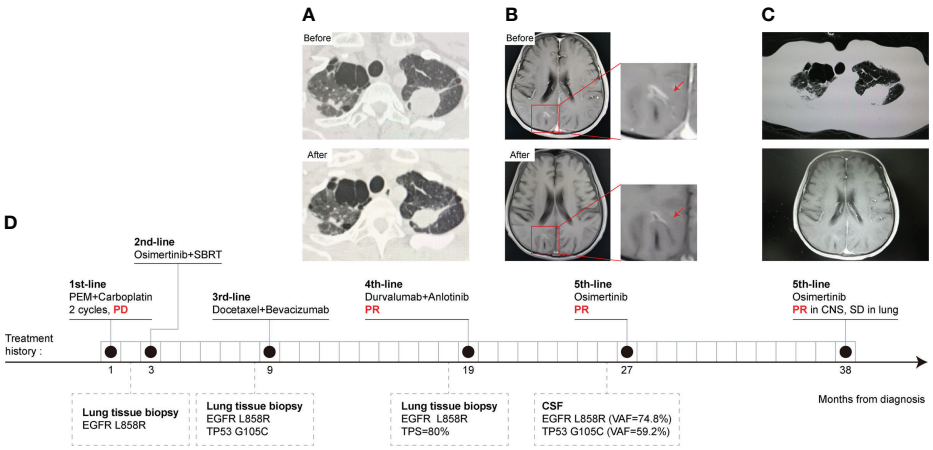

FIGURE 2
CT scans, treatment history, and gene mutation of Case 2 at different clinical time points as shown. **(A)** Chest CT scans. PR was observed after durvalumab plus anlotinib, fourth-line treatment. **(B)** MRI of the brain. A PR of LM was obtained after two cycles of osimertinib rechallenge. **(C)** The lung and CNS lesion kept stable till recent follow-up in April 2022. **(D)** The timeline of Case 2 treatment history, follow-up diagnostic and gene test results. The numbers indicate the time from the diagnosis of NSCLC.

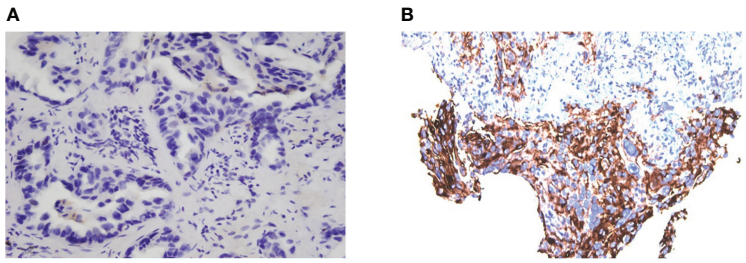

FIGURE 3
Evaluation of PD-L1 expression of tumor cells. PD-L1 expression of Case 1 in November 2018 **(A)**, TPS = 0 and July 2020 **(B)**, TPS = 60% (Dako 22C3).

L858R mutated NSCLC patients with LM after immunotherapy. This report shows that EGFR-TKI rechallenge after ICI failure provides a prolonged PR in intracranial lesions for NSCLC patients with LM. Case 2 showed that rechallenge with a previously administered EGFR-TKI after the onset of LM may be an effective treatment strategy, not just switching to an un-administered EGFR-TKI like in Case 1. Besides, the use of CSF as a liquid biopsy specimen may facilitate precise diagnosis and personalized treatment for NSCLC with LM.

In our cases, the PD-L1 expression level increased a lot after EGFR-TKI treatment resistance (Figures 3A, B), and a favorable response to subsequent immunotherapy was achieved, as reported by others (7). Because NSCLC patients with EGFR mutation naïve for EGFR-TKI cannot benefit from immunotherapy, the efficacy of immunotherapy could be influenced by tumor microenvironment (TME) changes during the EGFR-TKI treatment (8). Therefore, EGFR-TKIs and immunotherapy may have potential synergistic effects.

The mechanisms of efficacy for furmonertinib or osimertinib rechallenge may be attributed to higher penetration into the CSF (9), recovery of TKI sensitive tumor clones (10), and the histological heterogeneity of intracranial lesions.

However, the precise mechanism of EGFR-TKI rechallenge after immunotherapy failure is unclear. We speculate that two kinds of cell clones may coexist in our cases: one is the EGFR mutant clone (the abundance of clones decreased significantly after TKI treatment, the inferior clone), and the other is the PD-L1 high expression clone (the adaptive production or increase after TKI treatment, the dominant clone). After the immunotherapy, the PD-L1 high-expression clone was at a disadvantage due to its sensitivity to immunotherapy, while the EGFR mutant clone was insensitive to or resistant to immune checkpoint inhibitors. Therefore, the EGFR mutant clone became the dominant clone and then transferred to the leptomeninges (cerebrospinal fluid/blood NGS after immunotherapy resistance also confirmed a significant increase in EGFR abundance), at which time the sensitivity to EGFR-TKI may be restored. So, the EGFR-TKI rechallenge could be effective after immunotherapy failure.

Though irAE did not occur in our cases, the potential toxicity of sequential ICI followed by osimertinib should be monitored closely (11). More clinical studies are needed to explore effective therapy for advanced NSCLC with LM after multi-line treatments.

Data availability statement

The original contributions presented in the study are included in the article/supplementary material. Further inquiries can be directed to the corresponding author.

Ethics statement

The studies involving human participants were reviewed and approved by the Nanjing Chest Hospital, The Affiliated Brain Hospital of Nanjing Medical University. Written informed consent for participation was not required for this study in accordance with the national legislation and the institutional requirements. Written informed consent was obtained from the individual(s) for the publication of any potentially identifiable images or data included in this article.

Author contributions

CQ and SF designed the study. YZ collected the clinical data. QZ and ML participated in collecting the NGS data. YZ and WC analyzed the data. SF reviewed and analyzed data. CQ, YZ, and SF drafted the manuscript. SF supervised the entire study. All authors contributed to the article and approved the submitted version.

Funding

This work was supported by the “Six One Projects” in Jiangsu Province (LGY2019006). We are thankful to all

referring surgeons, pathologists, and specialists for their contributions to this study.

Acknowledgments

We would like to thank the patients and their families who gave us consent to publish these cases.

Conflict of interest

Authors QZ and ML were employed by MyGene Diagnostics Co., Ltd.

The remaining authors declare that the research was conducted in the absence of any commercial or financial relationships that could be construed as a potential conflict of interest.

Publisher's note

References

1. Cappuzzo F, Morabito A, Normanno N, Bidoli P, Del Conte A, Giannetta L, et al. Efficacy and safety of rechallenge treatment with gefitinib in patients with advanced non-small cell lung cancer. *Lung Cancer* (2016) 99:31–7. doi: 10.1016/j.lungcan.2016.06.008

2. Park S, Lee MH, Seong M, Kim ST, Kang JH, Cho BC, et al. Multicenter, two cohort study of 160 mg osimertinib in EGFR T790M-positive non-small-cell lung cancer patients with brain metastases or leptomeningeal disease who progressed on prior EGFR TKI therapy. *Ann Oncol* (2020) 31:1397–404. doi: 10.1016/j.annonc.2020.06.017

3. Kaira K, Kobayashi K, Shiono A, Yamaguchi O, Hashimoto K, Mouri A, et al. Effectiveness of EGFR-TKI rechallenge immediately after PD-1 blockade failure. *Thorac Cancer* (2021) 12:864–73. doi: 10.1111/1759-7714.13864

4. Li Y-S, Jiang B-Y, Yang J-J, Tu HY, Zhou Q, Guo WB, et al. Leptomeningeal metastases in patients with NSCLC with EGFR mutations. *J Thorac Oncol* (2016) 11:1962–9. doi: 10.1016/j.jtho.2016.06.029

5. Kuiper JL, Hendriks LE, van der Wekken AJ, de Langen AJ, Bahce I, Thunnissen E, et al. Treatment and survival of patients with EGFR-mutated non-small cell lung cancer and leptomeningeal metastasis: A retrospective cohort analysis. *Lung Cancer* (2015) 89:255–61. doi: 10.1016/j.lungcan.2015.05.023

6. Fuchs V, Kian W, Lichtenberg R, Cooper JM, Remilah AA, Levin D, et al. Next-generation sequencing liquid biopsy-guided osimertinib rechallenge in EGFR-mutated advanced non-Small-Cell lung cancer patients. *Clin Drug Investig* (2022) 42:185–92. doi: 10.1007/s40261-021-01116-4

7. Isomoto K, Haratani K, Hayashi H, Shimizu S, Tomida S, Niwa T, et al. Impact of EGFR-TKI treatment on the tumor immune microenvironment in EGFR mutation-positive non-small cell lung cancer. *Clin Cancer Res* (2020) 26:2037–46. doi: 10.1158/1078-0432.CCR-19-2027

8. Madeddu C, Donisi C, Liscia N, Lai E, Scartozzi M, Maccio A. EGFR-mutated non-small cell lung cancer and resistance to immunotherapy: Role of the tumor microenvironment. *Int J Mol Sci* (2022) 23:6489. doi: 10.3390/ijms23126489

9. Xing L, Pan Y, Shi Y, Shu Y, Feng J, Li W, et al. Biomarkers of osimertinib response in patients with refractory, EGFR-T790M-positive non-small cell lung cancer and central nervous system metastases: The APOLLO study. *Clin Cancer Res* (2020) 26:6168–75. doi: 10.1158/1078-0432.CCR-20-2081

10. Miyawaki T, Kenmotsu H, Yabe M, Kodama H, Nishioka N, Miyawaki E, et al. Rechallenge with previously administered epidermal growth factor receptor-tyrosine kinase inhibitors in EGFR-mutated non-small cell lung cancer with leptomeningeal metastasis. *Invest New Drugs* (2021) 39:1732–41. doi: 10.1007/s10637-021-01140-3

11. Schoenfeld AJ, Arbour KC, Rizvi H, Iqbal AN, Gadgeel SM, Girshman J, et al. Severe immune-related adverse events are common with sequential PD-(L)1 blockade and osimertinib. *Ann Oncol* (2019) 30:839–44. doi: 10.1093/annonc/mdz077

frontiers | Frontiers in Oncology

TYPE Case Report
PUBLISHED 18 November 2022
DOI 10.3389/fonc.2022.1059308

OPEN ACCESS

EDITED BY
Yaron Perry,
University at Buffalo, United States

REVIEWED BY
Stefan Prado Wohlwend,
University and Polytechnic Hospital La Fe, Spain
Danae Anastasia Delivanis,
Mayo Clinic, United States
Andrea M. Isidori,
Sapienza University of Rome, Italy

*CORRESPONDENCE
Yueyong Xiao
yueyongxiao@yahoo.com

†These authors share first authorship

SPECIALTY SECTION
This article was submitted to Thoracic Oncology, a section of the journal Frontiers in Oncology

RECEIVED 03 October 2022
ACCEPTED 07 November 2022
PUBLISHED 18 November 2022

CITATION
Zhang X, Meng L, Xiao Y and Chen Z (2022) Case report: Radiofrequency ablation combined with biopsy for Cushing's syndrome due to ectopic ACTH lesions in the lung. *Front. Oncol.* 12:1059308. doi: 10.3389/fonc.2022.1059308

Case report: Radiofrequency ablation combined with biopsy for Cushing's syndrome due to ectopic ACTH lesions in the lung

Xiao Zhang[1†], Liangliang Meng[1,2†], Yueyong Xiao[1*] and Zenan Chen[1]

[1]Department of Radiology, The First Medical Center, Chinese People's Liberation Army (PLA) General Hospital, Beijing, China, [2]Department of Radiology, Chinese People's Armed Police (PAP) Force Hospital of Beijing, Beijing, China

Lung carcinoid tumor is one of the major tumors causing ectopic ACTH syndrome, and the most common clinical treatment is surgical resection of the lesion. We herein report a suspected pulmonary carcinoid tumor with difficulty in surgical resection and poor response to drug therapy, which was successfully treated with radiofrequency ablation combined with intraoperative biopsy of the lesion. A 48-year-old female patient, with hypercortisolism (reddening of the face, full moon face, hirsutism, acne, and weight gain) detected three months ago. Small and high-dose dexamethasone suppression tests were not suppressed, Cushing's syndrome was under consideration. PET-CT examination suggested mild FDG uptake in two nodules in the anterior basal segment of the lower lobe of the right lung, the possibility of ectopic ACTH lesions was considered because of the clinical presentation. Due to difficult surgical approach of the lesion, high risk of surgery and the patient's anxiety, CT-guided thermal ablation combined with puncture biopsy was considered to treat the lesions. Image-guided thermal ablation can effectively inactivate ectopic ACTH lesions in the lung, rapidly improve the symptoms of high cortisol, and can be combined with biopsy for pathologic diagnosis. Therefore, this technique can be considered for treating pulmonary ACTH lesions that are difficult to resect surgically.

KEYWORDS

radiofrequency ablation, biopsy, Cushing's syndrome, ectopic, ACTH

Introduction

Adrenocorticotropic hormone(ACTH)-dependent Cushing's syndrome accounts for approximately 80-85% of Cushing's syndrome, of which approximately 20% is caused by ectopic ACTH syndrome (1). The majority of tumors in ectopic ACTH syndrome are neuroendocrine tumors, with the most common tumors being lung carcinoid tumors (21-39%), followed by small cell lung cancer (3-21%), thymic tumors (11%), pancreatic neuroendocrine tumors (8%), medullary thyroid carcinoma (2-11.6%), and pheochromocytoma (5.6%) (1–3). These lesions secrete adrenocorticotropic hormone (ACTH), which stimulates adrenal cortical hyperplasia and produces excess cortisol causing overt Cushing syndrome (4).

In patients who are clinically diagnosed with Cushing's syndrome in combination with laboratory tests, hormone experiments and the evident ectopic ACTH lesions after imaging, conventional treatments such as drug therapy and surgical resection are challenging to implement (5, 6). Some techniques can be used to target the lesions and control systemic symptoms,such as radiotherapy, chemotherapy, and radionuclides (5). Still, none of the above techniques can obtain pathological tissue for pathologic diagnosis. Imaging-guided radiofrequency ablation has been applied to the treatment of tumors in various parts of the body, which has the advantages of precise localization, exact efficacy, minimal trauma, puncture biopsy can precisely cut and take the material for small lesions (7–9). Radiofrequency ablation with simultaneous biopsy for ectopic ACTH lesions in the lung has not been reported in the literature before.

Patient description

This retrospective study was approved by the Ethics Committee of the Chinese PLA general hospital. Written informed consent was provided for this study by the patient.

The female patient, 48 years old, was found to have a reddish complexion, full moon face, increased fine hair, thin skin three months ago, weight gain of 5kg in the last month, hypertension (132/87mmHg), the presence of recurrent sleep disturbances and emotional instability in the patient.

Laboratory tests revealed hypokalemia (blood potassium 2.26-2.47 mmol/L), decreased bone metabolism (osteocalcin 9.00 ng/ml), vitamin D deficiency (Vit D 10.6 ng/ml). Then anxiety disorder was considered after the completion of relevant tests.

The patient was admitted with elevated serum cortisol (0AM:618.96 nmol/L, 8AM:637.17 nmol/L,4PM:562.20 nmol/L) and elevated ACTH levels (0AM:19.6 pmol/L, 8AM:20.7 pmol/L,4PM:19.9 pmol/L) on laboratory tests. Urine over 24 hours to measure free cortisol (2178.9 nmol), ACTH rhythms disappeared and were not suppressed by the low-dose dexamethasone suppression test (ACTH25.1 pmol/L, serum cortisol 756.42 nmol/L) or the high-dose dexamethasone suppression test (ACTH16.4 pmol/L, serum cortisol 402.35 nmol/L). The consideration of ectopic ACTH syndrome was indicated.

The patient underwent an enhanced CT chest-scan, which showed a nodular shadow in the basal segment of the right lower lobe with significant enhancement. Meanwhile, chest images showed only slight thickening of the bilateral adrenal glands without obvious signs of hyperplasia. The patient underwent ^{68}Ga- DOTATATE (Figure 1), and ^{18}F-FDG PET-CT. ^{68}Ga-DOTATATE PET-CT did not show significant uptake while ^{18}F-FDG PET-CT showed mild radiotracer uptake (standard uptake value 2.2 g/ml).

Considering laboratory tests, typical clinical symptoms and complex location that is not suitable for surgery, after multidisciplinary discussions, the decision was made to perform radiofrequency ablation and biopsy to treat the lesion and confirm whether it was an ESA.

Symptomatic treatment, potassium supplementation, and antidepressant therapy were administered according to the patient's clinical symptoms, but the clinical symptoms did not improve. Due to the complex location of the lesion, surgical resection was more traumatic, and the patient resisted; tracheoscopy was challenging to reach the location of the lesion for biopsy. Informed consent was obtained after consultation with the patient and family, CT-guided radiofrequency ablation combined with biopsy was used to treat the lesion. Because of the patient's obese body size (158 cm, 86 kg), a Big bore CT (PHILIPS, Big bore 85 CM) was used as the guiding device, along with a Medtronic radiofrequency ablation system, the matching ablation probes and Bard biopsy needle kit.

The patient was placed in a lateral position, then the needle was inserted in the posterior back. The ablation needle and needle sheath were guided to the lesion under CT guidance using a stepwise method. The ablation treatment was performed with a power of 30w after the position was satisfactory and the local temperature reached 80-110°C. After 3 min, the biopsy needle was implanted through the matched sheath for tissue cutting. The ablation situation was observed by scanning every 5 min during the ablation period. The needle was withdrawn after the ablation was satisfactory (the width of the surrounding halo sign around the lesion >the width after adequate ablation (width of the halo sign around the lesion >5 mm), the needle was withdrawn. The needle tract was ablated and blocked by injecting a mixture of snake venom hemagglutinin injection (Sounaswe, 1 ml) and an absorbable gelatin sponge (Geiloam, 100 mg) through the needle sheath (Figure 2). The patient's vital signs, such as heart rate, blood pressure, and oxygen, were closely monitored during and after surgery. A postoperative CT scan of the chest was performed to observe complications such as bleeding, pneumothorax, and air embolism.

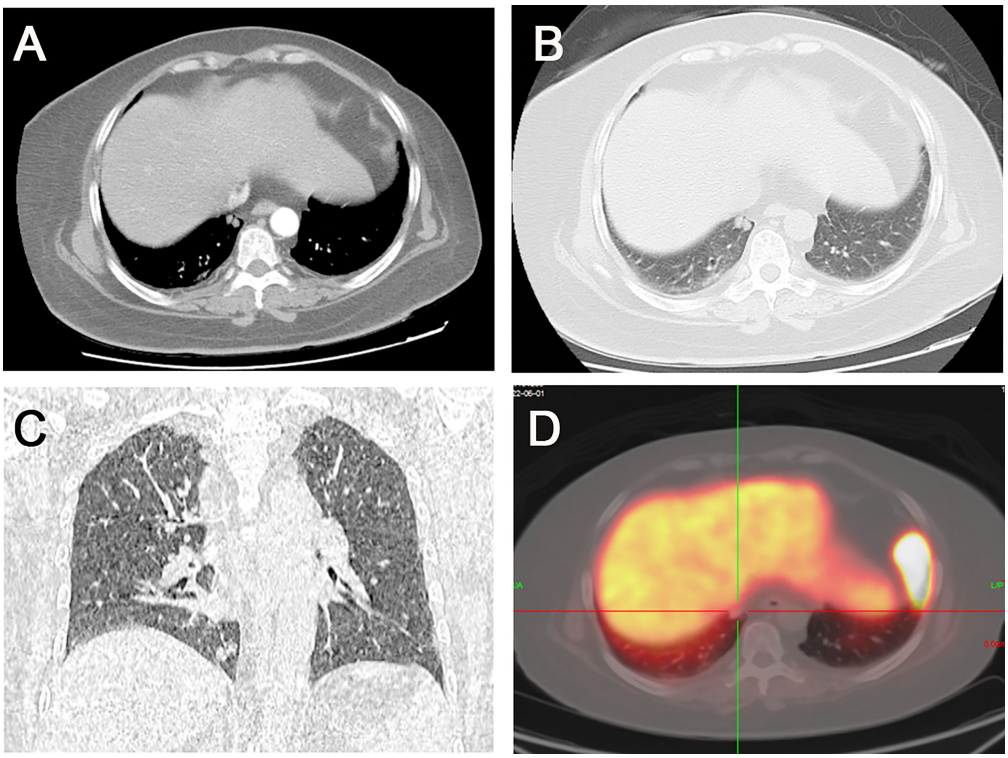

FIGURE 1
(A) Two rounded nodules in the right lower lobe of the lung, with well-defined borders and a diameter of about 6 mm. **(B)** Significant enhancement of the nodules in the arterial phase. **(C)** Coronal image showing the location of the nodules near the heart and diaphragm. **(D)** ^{68}Ga- DOTATATE PET-CT did not show significant drug uptake.

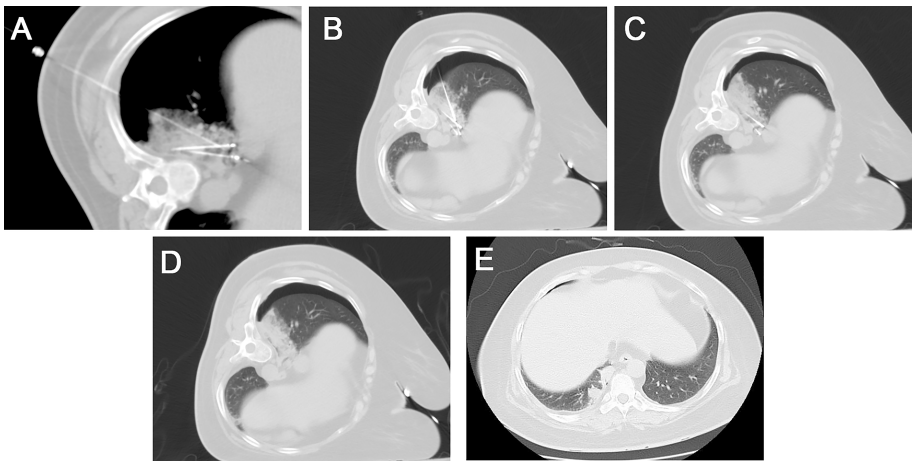

FIGURE 2
(A) Under CT guidance, the radiofrequency ablation probes (long arrow) were placed for the two lesions, and local nerve block anesthesia (short arrow) was performed using a 21G Chiba needle to the diaphragm. **(B)** A semi-automatic biopsy was used to obtain the tumor tissue from one of the lesions. **(C)** A scan was performed after 12 min of ablation with a power of 30 w, showing the formation of a halo sign around the lesion. **(D)** After removing the needle and probes, the CT scan showed substantial localized changes in the ablation zone. A small amount of bleeding from the puncture needle tract with a small amount of pneumothorax on the right side. **(E)** A follow-up one week after the operation showed a well-defined solid area in the ablation zone.

Postoperative hemostatic drugs, analgesic and anti-inflammatory drugs were routinely used.

Postoperative blood laboratory tests performed at different time points revealed a significant decrease in cortisol and ACTH levels compared to preoperative levels (Table 1), and the patient's circadian rhythm returned; CT examinations performed at 24 h and one week postoperatively showed satisfactory ablation of the lesion, solid localized lesions and surrounding lung tissue. The puncture pathology results showed: (right lower lobe of the lung) punctured lung tissue, small focal alveolar epithelial hyperplasia significant with mild atypical hyperplasia, a few histiocytic aggregates were seen around. Immunohistochemical results: Ki-67 (+3%), ALK (Ventana) (-), NapsinA (+), CK7 (+), TTF-1 (+), CD68 (histiocytes +), ACTH (-).

Based on the patient's laboratory findings, the dosage of subsequent therapeutic drugs was gradually reduced, and the patient's clinical condition gradually improved.

The presentation of the case report is in line with CARE guidelines (10).

Results

CT-guided radiofrequency ablation and biopsy of the lesion were successfully performed. The postoperative follow-up showed good inactivation of the lesion, significant decrease in ACTH and cortisol levels, restoration of ACTH-F rhythm, and improvement of clinical symptoms. The patient has now been discharged from the hospital with recovery. The pathologic findings do not currently support the diagnosis of lung carcinoid. However, considering the clinical manifestations, laboratory tests and postoperative recovery, we still believe that this is an ESA. We also wondered if the puncture obtained less tissue in order to avoid bleeding, which may have affected the acquisition of accurate pathology.

Discussion

Ectopic ACTH syndrome (EAS) accounts for approximately 20% of ACTH-dependent Cushing's syndrome (CS) and 10% of all types of CS. There are two types in EAS. The first one develops slowly and consists mainly of carcinoid tumor. The tumor often has small size, low degree of malignancy and long-term course (11, 12). Therefore, it may clinically present with more typical Cushing syndrome (13). The second one develops rapidly and consists mainly of small cell lung cancer. The tumor has a high degree of malignancy, a short-term course and serious condition. It does not show symptoms of typical Cushing syndrome. The tumors causing ectopic ACTH syndrome generally have a good prognosis if they are diagnosed early and resected completely. So making the clinical diagnosis early is extremely critical for the guidance of the treatment of this disease (14).Pulmonary EAS accounts for approximately 45% of all ACTH ectopic origin sites with an onset. It is often sudden, severe, and rapidly progressive. If clinical symptoms and biochemical parameters strongly suggest the possibility of EAS, it is crucial to find the ectopic source by imaging (CT, MRI/PET) for the treatment.

Currently, the best clinical treatment for EAS is surgical resection of the primary tumor that produced the ACTH, with complete remission in approximately 83% of patients (15). However, surgical resection in patients with EAS is associated with higher risks, both in terms of the impact of hypercortisolism on the surgery and the trauma to the patient in areas that are difficult to resect, such as lesions adjacent to large blood vessels in the hilum and large airways. Of course, bilateral adrenal subtotal resection can be considered, supplementing the patient with corticosteroid with corticosteroid replacement therapy. Oral medications may also be considered to block adrenocortical hormone synthesis, such as aminoglutethimide (16), ketoconazole (17). But the above two methods will lower the quality of living.

Therefore, it requires a comprehensive multidisciplinary discussion of the patient when appropriate therapy such as radiotherapy, ablation, etc. is used clinically to treat ectopic EAS lesions (18). As mentioned in PATIENT DESCRIPTION, we should comprehensively consider the patient's condition and choose the appropriate treatment plan. If the lung lesion is considered to be an ordinary benign lesion after discussion, a different treatment plan may be given. In addition, the possibility of performing frozen pathology before ablation was discussed preoperatively. However, due to the small and deep location of the lesion, percutaneous puncture biopsy is more difficult and has a low positive rate, which may even lead to complications such as bleeding and pneumothorax, affecting the follow-up treatment of patients. Therefore, after multidisciplinary discussion and consultation with patients, we chose to perform biopsy during

TABLE 1 Changes in indicators related to Cushing's syndrome in patients after surgery.

	Serum cortisol (nmol/L)			ACTH (pmol/L)			UFC (nmol/24h)
	0AM	8AM	4PM	0AM	8AM	4PM	
Preoperative	618.96	637.17	562.20	19.6	20.7	19.9	3559.5
5 hours postoperatively	113.85	140.56	85.49	6.76	7.46	7.57	216.1
5 days postoperatively	152.43	441.63	264.85	9.34	10.2	10.9	1499.3

ACTH, adreno-cortico-tropic-hormone; UFC, urinary free cortisol.

the ablation process to minimize the occurrence of bleeding and other complications. In fact, there was a small amount of bleeding around the lesion during the radiofrequency ablation (RFA) needle placement, which also verified our speculation.

RFA is a procedure in which an electrode probe is precisely inserted into tumor tissues under imaging guidance (19). Electromagnetic waves are emitted through a radiofrequency transmitter to produce oscillatory friction in tumor tissue cells, resulting in coagulative necrosis of tumor tissues at a temperature of 60°C-100°C. RF ablation has been widely used in the clinical treatment of tumor lesions in many body parts, such as the lung, liver, and kidney (19–21). CT-guided RFA has the following advantages (1): Precise surgical localization. For small lesions that are difficult to localize, it is necessary to expand the resection range to ensure efficacy, which causes excessive trauma and complications to patients. In contrast, the RF electrode probe can be precisely localized under CT guidance, and the error is generally less than 2mm. (2) The diameter of the RF ablation 17G electrode probe is only 1.4mm, which can be used for multiple needle punctures during the ablation of unilateral lung lesions, which is conducive to the inactivation of tumors while maximizing the protection of lung function; (3) Real-time efficacy assessment, intermittent CT scan is used during RFA, which can judge the ablation results in real-time according to the imaging characteristics and avoid excessive ablation or incomplete ablation; (4) Compared with other parenchymal organs, RFA of parenchymal lesions can be performed in the same way. Compared with RFA of other parenchymal organs, the gas around the lung lesion can restrict the heat conduction during the ablation process, and the energy can be more easily gathered inside the lesion, which makes the ablation more efficient and effective; (5) When a biopsy is required, the biopsy needle and RF probe can be placed at the same time to avoid secondary puncture injury, and the small blood vessels damaged by the puncture cut can be closed with RF ablation heating to reduce the risk of bleeding. (6) Radiofrequency ablation as a local minimally invasive ablation treatment, combined with other therapeutic methods sometimes can improve the efficacy, such as radiotherapy, holistic therapy (depending on genetic test results, choose to use chemotherapy or molecularly targeted drug therapy) and so on.

The case report we presented helped open our minds about diagnosis and treatment about ESA.

Conclusion

In conclusion, CT-guided radiofrequency ablation can be considered for EAS patients with challenging to resect lung lesions or high surgical risk, and a biopsy can be performed at the same time to clarify the pathology; thermal ablation can also be used to treat the lesions to reduce ACTH levels and improve the safety of surgical resection. Both ablation techniques have been proven to be effective complements to surgery. In general, image-guided radiofrequency ablation combined with biopsy is an effective and safe treatment for pulmonary EAS, especially for lung lesions that conventional techniques cannot treat. It deserves the clinical promotion.

Data availability statement

The original contributions presented in the study are included in the article/supplementary material. Further inquiries can be directed to the corresponding author.

Ethics statement

This retrospective study was approved by the Ethics Committee of the Chinese PLA general hospital. Written informed consent was provided for this study by the patient. Written informed consent was obtained from the individual for the publication of any potentially identifiable images or data included in this article.

Author contributions

XZ (First Author): Conceptualization, Methodology, Investigation, Validation, Formal Analysis, Project Administration, Writing - Original Draft. LM: Data Curation, Software, Visualization, Writing - Original Draft: YX (Corresponding Author): Funding Acquisition, Resources, Supervision, Writing - Review and Editing. ZC: Validation, Writing - Review and Editing. All authors contributed to the article and approved the submitted version.

Funding

This research was supported in part by research grant from the PLA Health Care Project of China (No. 22BJZ18).

Conflict of interest

The authors declare that the research was conducted in the absence of any commercial or financial relationships that could be construed as a potential conflict of interest.

Publisher's note

References

1. Balomenaki M, Margaritopoulos D, Vassiliadi DA, Tsagarakis S. Diagnostic workup of cushing's syndrome. *J Neuroendocrinol* (2022) 34:e13111. doi: 10.1111/jne.13111

2. Boscaro M, Barzon L, Fallo F, Sonino N. Cushing's syndrome. *Lancet* (2001) 357:783–91. doi: 10.1016/S0140-6736(00)04172-6

3. Hayes AR, Grossman AB. The ectopic adrenocorticotropic hormone syndrome: Rarely easy, always challenging. *Endocrinol Metab Clin North Am* (2018) 47:409–25. doi: 10.1016/j.ecl.2018.01.005

4. Espinosa-de-Los-Monteros AL, Ramírez-Rentería C, Mercado M. Clinical heterogeneity of ectopic ACTH syndrome: A long-term follow-up study. *Endocr Pract* (2020) 26:1435–41. doi: 10.4158/EP-2020-0368

5. Lacroix A, Feelders RA, Stratakis CA, Nieman LK. Cushing's syndrome. *Lancet* (2015) 386:913–27. doi: 10.1016/S0140-6736(14)61375-1

6. Chen Y, Zhang J, Zhou M, Guo C, Li S. Real-world clinicopathological features and outcome of thymic neuroendocrine tumors: a retrospective single-institution analysis. *Orphanet J Rare Dis* (2022) 17:215. doi: 10.1186/s13023-022-02366-x

7. Lu Y, Lu C, Xu D, Huang F, He Z, Lei J, et al. Computed tomography-guided percutaneous radiofrequency ablation in older adults with early-stage peripheral lung cancer: A retrospective cohort study. *Cancer Control* (2022) 29:10732748211070702. doi: 10.1177/10732748211070702

8. Yuan C, Yuan Z, Cui X, Gao W, Zhao P, He N, et al. Efficacy of ultrasound-, computed tomography-, and magnetic resonance imaging-guided radiofrequency ablation for hepatocellular carcinoma. *J Cancer Res Ther* (2019) 15:784–92. doi: 10.4103/jcrt.JCRT_836_18

9. VanSonnenberg E, Shankar S, Morrison PR, Nair RT, Silverman SG, Jaklitsch MT, et al. Radiofrequency ablation of thoracic lesions: part 2, initial clinical experience–technical and multidisciplinary considerations in 30 patients. *AJR Am J Roentgenol* (2005) 184:381–90. doi: 10.2214/ajr.184.2.01840381

10. Gagnier JJ, Kienle G, Altman DG, Moher D, Sox H, Riley D, et al. The CARE guidelines: consensus-based clinical case reporting guideline development. *BMJ Case Rep* (2013) 2:38–43. doi: 10.7453/gahmj.2013.008

11. La Salvia A, Carletti R, Verrico M, Feola T, Puliani G, Bassi M, et al. Angioside: The role of angiogenesis and hypoxia in lung neuroendocrine tumours according to primary tumour location in left or right parenchyma. *J Clin Med* (2022) 11:5958. doi: 10.3390/jcm11195958

12. La Salvia A, Persano I, Siciliani A, Verrico M, Bassi M, Modica R, et al. Prognostic significance of laterality in lung neuroendocrine tumors. *Endocrine* (2022) 76:733–46. doi: 10.1007/s12020-022-03015-w

13. Pozza C, Graziadio C, Giannetta E, Lenzi A, Isidori AM. Management strategies for aggressive cushing's syndrome: From macroadenomas to ectopics. *J Oncol* (2012) 2012:685213. doi: 10.1155/2012/685213

14. Alexandraki KI, Grossman AB. The ectopic ACTH syndrome. *Rev Endocr Metab Disord* (2010) 11:117–26. doi: 10.1007/s11154-010-9139-z

15. Isidori AM, Kaltsas GA, Pozza C, Frajese V, Newell-Price J, Reznek RH, et al. The ectopic adrenocorticotropin syndrome: clinical features, diagnosis, management, and long-term follow-up. *J Clin Endocrinol Metab* (2006) 91:371–7. doi: 10.1210/jc.2005-1542

16. Van Gaal L, Delvigne C, Abs R, Leeuw De I, Bekaert J. Cushing's syndrome, due to ectopic ACTH-secretion, successfully treated with aminoglutethimide, radiotherapy and chemotherapy. *Acta clinica Belgica* (1981) 36:130–6. doi: 10.1080/22953337.1981.11718798

17. Schteingart DE. Drugs in the medical treatment of cushing's syndrome. *Expert Opin emerging Drugs* (2009) 14:661–71. doi: 10.1517/14728210903413522

18. Corsello SM, Senes P, Iezzi R, Rufini V, Congedo MT, Paragliola RM, et al. Cushing's syndrome due to a bronchial ACTH-secreting carcinoid successfully treated with radiofrequency ablation (RFA). *J Clin Endocrinol Metab* (2014) 99:E862–5. doi: 10.1210/jc.2013-4359

19. Abtin FG, Eradat J, Gutierrez AJ, Lee C, Fishbein MC, Suh RD, et al. Radiofrequency ablation of lung tumors: imaging features of the postablation zone. *Radiographics* (2012) 32:947–69. doi: 10.1148/rg.324105181

20. Rose SC, Thistlethwaite PA, Sewell PE, Vance RB. Lung cancer and radiofrequency ablation. *J Vasc Interv Radiol* (2006) 17:927–51. doi: 10.1097/01.RVI.0000222707.44902.66

21. Takayama T, Hasegawa K, Izumi N, Kudo M, Shimada M, Yamanaka N, et al. Surgery versus radiofrequency ablation for small hepatocellular carcinoma: A randomized controlled trial (SURF trial). *Liver Cancer* (2022) 11:209–18. doi: 10.1159/000521665

frontiers | Frontiers in Oncology

TYPE Case Report
PUBLISHED 21 November 2022
DOI 10.3389/fonc.2022.1050220

OPEN ACCESS

EDITED BY
Kohei Fujita,
National Hospital Organization Kyoto Medical Center, Japan

REVIEWED BY
Xianwen Hu,
Zunyi Medical University, China
Mona Mlika,
Tunis El Manar University, Tunisia

*CORRESPONDENCE
Lili Jiang
879876047@qq.com

SPECIALTY SECTION
This article was submitted to Thoracic Oncology, a section of the journal Frontiers in Oncology

RECEIVED 26 September 2022
ACCEPTED 28 October 2022
PUBLISHED 21 November 2022

CITATION
Yang C, Li S, Liang Z and Jiang L (2022) Case Report: The first case of primary pulmonary collision tumor comprising mixed squamous cell and glandular papilloma and glomus tumor.
Front. Oncol. 12:1050220.
doi: 10.3389/fonc.2022.1050220

Case Report: The first case of primary pulmonary collision tumor comprising mixed squamous cell and glandular papilloma and glomus tumor

Chan Yang, Shuang Li, Zuoyu Liang and Lili Jiang*

Department of Pathology, West China Hospital, Sichuan University, Chengdu, China

A collision tumor is a rare entity, particularly if occurring in the lung. We report a case of a 57-year-old woman with a primary pulmonary collision tumor comprising mixed squamous cell and glandular papilloma (MSGP) and glomus tumor (GT). An abnormal mass was discovered in the right lung by computed tomography (CT) of the chest. A right lower lobectomy with mediastinal lymph node dissection was performed. Histological examination of the surgical specimen suggested that the lung cancer was composed of two neoplastic components. To the best of our knowledge, this is the first report of a primary pulmonary collision tumor comprising two benign tumors of different origins, which were MSGP and GT.

KEYWORDS

pulmonary collision tumor, mixed squamous cell and glandular papilloma, glomus tumor, biphasic tumor, histopathology

Introduction

Collision tumors are defined as independent neoplasms comprising two or more distinct tumor compositions, coexisting in the same site and growing closely to one another, without any area of intermingling (1). Because of similar histology, collision tumors must be distinguished from other tumors containing two or more components. 1) A combined tumor, a neoplasm composed of two histologically and immunohistochemically distinct but intertwined cell populations coming from a common source, has a common driver mutation with environmental impact resulting in divergent morphology (2, 3). 2) Multiple primary tumors, including more than one separate neoplasm, arise in obviously different sites and/or occur at different times (4). 3) A biphenotypic tumor is defined as a tumor that consists of two cell populations, arising from a common stem cell, and that undergoes divergent differentiation with common

immunohistochemical properties (5). The occurrence of collision tumors in the lung is extremely rare than in other various organ systems. Pulmonary adenosquamous carcinoma is classified as a collision tumor. By contrast, combined small-cell carcinoma, combined large-cell neuroendocrine carcinoma, and carcinosarcoma are classified as combined tumors, and pulmonary blastoma is classified as a biphasic tumor.

In this study, we reported an extremely rare primary pulmonary collision tumor comprised of two benign tumors: mixed squamous cell and glandular papilloma (MSGP) standing for epithelial element and collision tumor (GT) standing for mesenchymal element. In addition, the literature about collision tumors on PubMed was retrieved with the keywords "pulmonary/lung & collision tumor" and "bronchus/bronchioles & collision tumor." With a literature review, we integrated and summarized the clinicopathological features, treatment, and outcome of various types of collision tumors.

Case report

A 57-year-old woman, a non-smoker, with a medical history of type 2 diabetes mellitus was incidentally detected with a nodulous shadow on a chest radiograph obtained as part of a routine physical examination. Follow-up observation was performed and she did not receive any treatment. Three years later, computed tomography presented a 2.6-cm × 1.8-cm mass with soft tissue density and smooth margin in the lateral basal segment of the right lower lobe (Figure 1). The distal bronchi were slightly dilated and the wall of the bronchial lumen was thickened in the right lower lung field. Physical examination showed no evidence of lymphadenopathy or pleural effusion. No significant metabolic activity can be found in a positron emission tomography (PET)-CT scan. Except for CA242 (slightly increased), most serum tumor markers were within the normal ranges. Subsequently, a right lower lobectomy with lymph node dissection *via* video-assisted thoracoscopic surgery was performed.

A gross examination of the resected specimen showed an ill-defined, solid gray-white nodule measuring 1.7 cm × 1.5 cm × 1.2 cm. The visceral pleura and the surgical margin were not involved. Microscopically, the tumor was a conspicuous endobronchiolar growth within the dilated bronchus or bronchiole (Figures 2A, B, whole slide scan). The tumor showed a well-demarcated border, which was connected to the normal bronchial walls in some areas (Figure 2B). At low magnification, the tumor was composed of two different histological components, including MSGP and GT (Figure 2C). Although the two kinds of tumor cells were close to each other, a distinct demarcation between them could still be found, there were no intertwined components, and a transitional morphology existed in the neighboring cell populations (Figure 2D). At high magnification, the component of MSGP showed a prominent papillary architecture with a fibrous vessel axis, lined with discrete foci of squamous and glandular epithelium. The glandular epithelium was composed of a mixture of ciliated or non-ciliated columnar cells, mucous columnar cells, and scattered goblet cells (Figure 2E). No significant glandular atypia, necrosis, or stromal infiltration could be found, but squamous cells showed mild atypia. The GT is composed of nests of glomus cells surrounding various vessels. The uniform tumor cells were small and round, with inconspicuous nucleoli, lightly eosinophilic cytoplasm, and sharply defined cell margins (Figure 2F). Mitotic figures were generally absent. All lymph nodes were negative. Immunohistochemically, the squamous component of MSGP was positive for CK5/6, P63, and P40, and the glandular component of MSGP was positive for CK7 (Figures 3A–D).

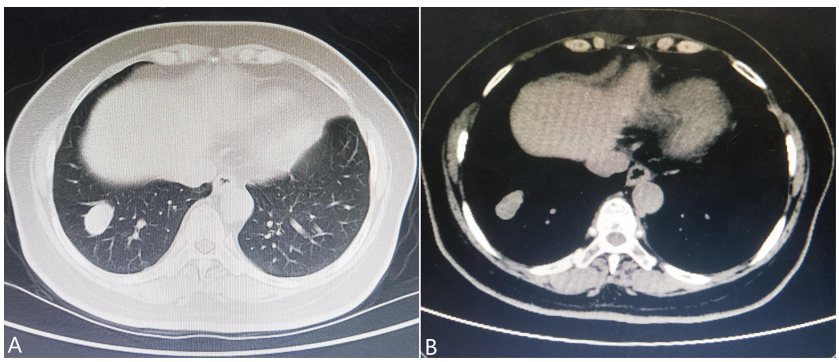

FIGURE 1
Chest computed tomography shows **(A)** a nodulous shadow located in the segmentum basale laterale of the right lower lobe measuring 2.6 cm × 1.8 cm in size with a smooth margin and **(B)** soft tissue density.

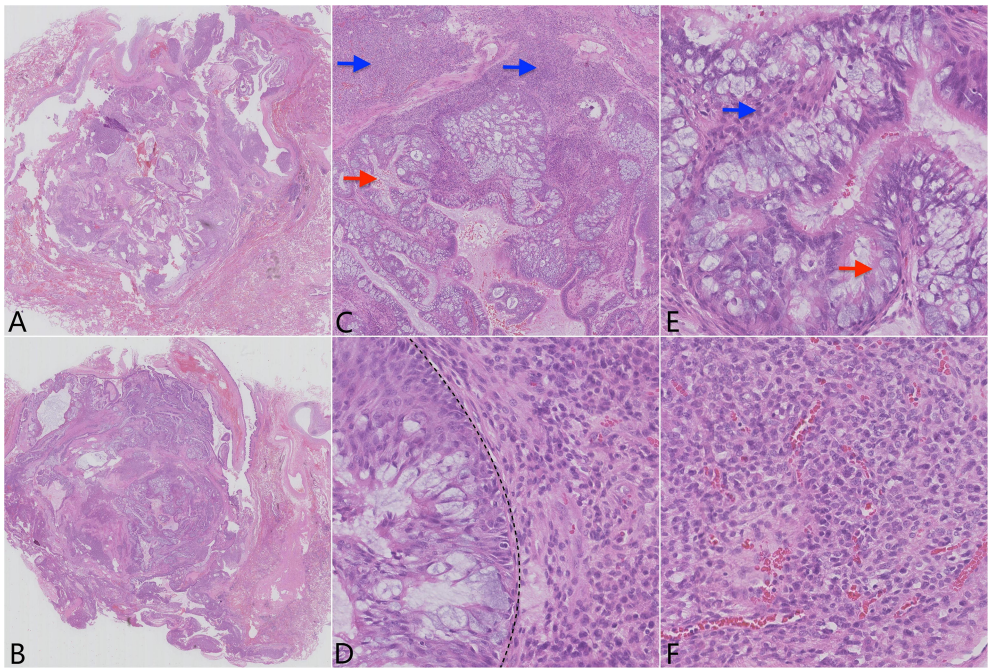

FIGURE 2
Pathological findings of the tumor show two distinct histological subtypes. **(A)** H&E of the whole slide scan showing the well-defined tumor located in the dilated bronchus or bronchiole and **(B)** focally connecting to the normal bronchial walls. **(C)** Lower power H&E (×4) reveals two distinctly demarcated tumor cell populations (red arrow: epithelial component; blue arrow: mesenchymal component). **(D)** High power H&E (×40) reveals that the two components grow closely to each other, but without a transitional zone (line). **(E)** H&E (×40) of the mixed squamous cell and glandular papilloma (red arrow: glandular component; blue arrow: squamous cell component). **(F)** H&E (×40) of the glomus tumor component.

Both components were positive for AE1/AE3 and negative for thyroid transcription factor-1 (TTF-1) (Figure 3E) and napsin A. Ki-67 was positive on the basal side of the areas of squamous epithelial (Figure 3F). GT was diffusely positive for collagen IV (Figure 3G) and muscle-specific actin (MSA) (Figure 3H), focally positive for α-smooth muscle actin (α-SMA), weakly positive for CD56, and negative for caldesmon, calponin, CD34, ERG, and STAT6. The Ki-67 index was less than 1% (Figure 3I). Two types of tumor cells were all focally positive for p53 and negative for S-100, SOX10, synaptophysin (Syn), and chromogranin A (CgA). Given all this, the tumor was diagnosed as a primary pulmonary collision tumor comprising MSGP and GT. There was no evidence of recurrence or metastasis after 6 months of follow-up.

Discussion

The 57-year-old female patient, despite having a pulmonary mass, was asymptomatic during her routine hospital visits. When making a primary diagnosis, based on clinicopathological features, two types of tumors should be considered: 1) mesenchymal cystic hamartoma and 2) collision tumor.

Mesenchymal cystic hamartoma (MCH) is a rare lung disease with an indolent clinical course. It is composed of primitive mesenchymal cells that gradually promote the formation of nodules and cysts (6). Histologically, these cystic spaces are lined with normal respiratory epithelium and surrounded by a proliferation of immature mesenchymal cells (6). On immunohistochemistry, the epithelial cells are diffusely positive for AE1/AE3 and TTF-1; the mesenchymal cells are diffusely positive for vimentin, with a low Ki-67 index of about 1%. It is noteworthy that the mesenchymal cells are negative for most specifically differentiated markers such as CD31, CD34, desmin, SMA, myoglobin, S-100, D2-40, etc. (7).

Immunohistochemistry of the tumor in our case revealed the following results: mesenchymal cells were diffusely positive for collagen IV, MSA, and CD56 and focally positive for SMA, which confirmed that the mesenchymal neoplasm is similar to GT. Meanwhile, the results excluded the possibility of MCH. On the other hand, epithelial cells were positive for AE1/AE3, CK7, CK5/6, P63, and P40, indicating MSGP, which is one of the solitary endobronchial papillomas. Negative staining of TTF-1 in epithelial cells also excluded the diagnosis of MCH.

Except for the combined tumors, multiple primary tumors, and biphenotypic tumors mentioned in the *Introduction*, only

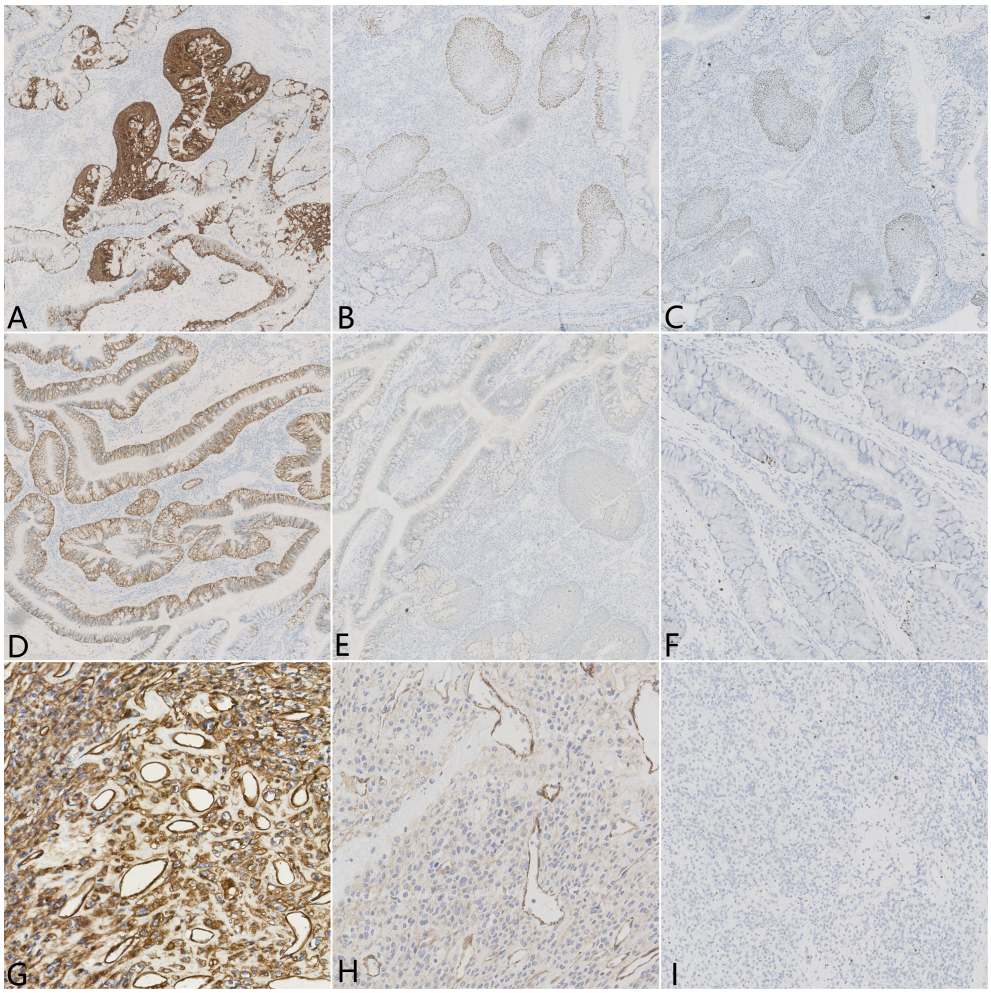

FIGURE 3
Immunohistochemical results of the pulmonary collision tumor. Epithelial element stains were positive for **(A)** CK5/6, **(B)** P63, **(C)** P40, and **(D)** CK7 but negative for **(E)** TTF-1. **(F)** Ki-67 was positive on the basal side of the areas of squamous epithelial, approximately 1%–2%. Mesenchymal element stains were diffusely positive for **(G)** collagen IV and **(H)** MSA. **(I)** The percentage of Ki-67 expression in the area of glomus tumor cells was less than 1%.

seven primary pulmonary collision tumor cases have been reported in the literature. We can further group these collision tumors according to their composition: four collision tumors, namely, malignant melanoma colliding with adenocarcinoma (8), large-cell carcinoma colliding with adenocarcinoma (9), adenocarcinoma colliding with typical carcinoid (10), and lymphoepithelioma-like carcinoma colliding with adenocarcinoma (11), are comprised of two different epithelial elements (Table 1); and three collision tumors, namely, squamous cell carcinoma colliding with T-cell lymphoma (12), epithelioid hemangioendothelioma colliding with bronchioloalveolar carcinoma (13), and carcinoid colliding with high-grade spindle-cell sarcoma (14), are comprised of epithelial and mesenchymal elements (Table 2). As we all know, a collision tumor composed of two benign entities has not been reported in the literature.

GTs are defined as benign tumors comprising neuromyoarterial glomera or glomus bodies originating from modified smooth muscle cells and surrounding arteriovenous anastomosis (15), which account for less than 2% of soft tissue tumors (16). These tumors commonly occur in subungual areas and deep dermis of the extremities where glomus bodies abound and, occasionally, in areas where glomus bodies are spare or absent, such as the gastrointestinal tract (17), bladder (18), bone (19), eyelid (20), cervix (21), ovary (22), thyroid (23), and thorax (24, 25). GTs rarely originated from the respiratory system, and the trachea is the more common site among them, with 77 cases reported to date (26). Originating from the lung is extremely uncommon, with less than 50 cases (27). Clinically, the symptoms of bronchial or tracheal GTs were commonly associated with airway irritation, but GTs occurring in the peripheral lung were generally asymptomatic (28).

TABLE 1 Summary of published pulmonary collision tumors comprising two different epithelial elements found in the literature.

Case no.	Year	Author	Age/ sex	Location	Maximum diameter (cm)	Components of pulmonary collision tumor		Imaging findings	Treatment	Outcome (follow-up time)
						Epithelial element	Epithelial element			
1	1993	T. Ueyama (8)	61/F	Left lower	4	Malignant melanoma	Adenocarcinoma	Irregular opaque shadow	Chemotherapy was performed with DTIC (dimethyl triazeno imidazole carboxamide) and interferon	Death (12 months)
2	2003	Shoji Nakata (9)	53/M	Right upper	4.2	Large cell carcinoma	Adenocarcinoma	Dumb bell-shaped mass	Right upper lobectomy with a mediastinal lymph node dissection	No evidence of recurrence (16 months)
3	2014	Kamal K. S. Abb (10)	70/F	Left upper	1.3	Typical carcinoid	Adenocarcinoma	Hazy density	Right upper and middle lobectomies with a mediastinal lymph node dissection	Not available
4	2015	Jammy Kin Iong Chan (11)	59/F	Left upper	4	Lymphoepithelioma-like carcinoma	Adenocarcinoma	Dumbbell-like mass	Left upper lung and associated hilar lymph node dissection and an EP regimen for four cycles, and then targeted therapy with an EGFR-tyrosine kinase inhibitor	Survival (12 months)

TABLE 2 Summary of published pulmonary collision tumors comprising epithelial and mesenchymal elements found in the literature.

Case no.	Year	Author	Age/ sex	Location	Maximum diameter (cm)	Components of pulmonary collision tumor		Imaging findings	Treatment	Outcome (follow-up time)
						Epithelial element	Mesenchymal element			
1	1999	Osamu Kawashima (12)	71/F	Right lower	4.5	Squamous cell carcinoma	T-cell lymphoma	Mass	Right lower lobectomy with lymph node dissection and systemic chemotherapy for malignant lymphoma	Death (7 months)
2	2003	Takahashi K (13)	59/F	Left upper	1.4	Bronchioloalveolar carcinoma	Epithelioid hemangioendothelioma	Ill-defined shadow	Complete lingulectomy	No evidence of recurrence (13 years)
3	2011	Corinne Liu (14)	54/F	Right upper	4.5	Carcinoid	High-grade spindle-cell sarcoma	Well-defined mass	Right upper lobectomy with lymph node dissection	Bone metastasis (18 months)

GTs of the respiratory tract generally occurred in middle-aged individuals (29) with no obvious sex predilection, and the maximum diameter ranged from 0.7 to 9.5 cm (15, 30). Morphological similarity may misdiagnose primary bronchopulmonary GT as carcinoid, hemangiopericytoma, paraganglioma, sugar tumor, or sclerosing pneumocytoma. Immunohistochemically, typical GTs are positive for SMA, MSA, h-caldesmon, calponin, and collagen IV. CD34 and desmin are also expressed focally in some cases, while cytokeratin, EMA, bcl–2, TTF-1, HMB45, CD117, LCA, CgA, CD31, and S-100 are invariably negative (31). Among primary lung tumors, GTs are often misdiagnosed as carcinoid for their cytomorphological features. On immunohistochemical analysis, a carcinoid shows positivity for neuroendocrine markers, such as CD56, Syn, and CgA, whereas a GT shows the opposite.

Sclerosing hemangioma is composed of cubic epithelial cells and circular stromal cells, and all these cells express TTF-1 and EMA. Paraganglioma is positive for the S-100 protein and neuroendocrine markers. A sugar tumor is diffusely positive for HMB45, which is conducive to differentiating it from GT. Occasionally, epithelioid leiomyoma can show similar histologic morphology with GT and can also express SMA. However, epithelioid leiomyoma expresses other smooth muscle markers including desmin and caldesmon.

Based on the World Health Organization's (2013) classification of soft tissue tumors, GTs are divided into benign GTs, GTs with uncertain malignant potential, and malignant GTs (32). Previous retrospective studies on primary bronchopulmonary GTs found that about 74% of cases are benign, followed by malignant cases, accounting for approximately 21%, and cases with uncertain malignant potential account for approximately 5% (15, 30). Given that malignant GTs have aggressive behavior, with up to 38% of patients developing metastasis (31) and the possibility of local recurrence for incomplete extirpation, radical surgical resection is still essential for long-term prognosis.

Solitary endobronchial papillomas are rare benign pulmonary tumors occurring in the bronchus, and they were identified in 1998, including squamous cell papilloma, glandular papilloma, and mixed squamous cell and glandular papilloma (33). The mixed entity is the rarest, showing a mixture of glandular and squamous epithelium. Each epithelial type should constitute more than one-third of the tumor (34). Occasionally, glandular epithelium can also grow with a micropapillary pattern and drop into alveolar lumens, which is easy to be misdiagnosed as micropapillary adenocarcinoma. Misdiagnosis of mucinous adenocarcinoma usually happens when mucus cell components are rich. Adenocarcinoma cells have significant atypia, without basal cells, leading to negative staining for p40 and CK5/6.

The case we presented here where GT collided with MSGP in the lung has never been reported in the literature. As with other pulmonary collision tumors that had been described, with no characteristic clinical features and imaging findings, the primary diagnosis is difficult (35), which mostly depends on the different neoplasms of the collision tumor, and the definitive diagnosis mainly relies on the pathological diagnosis.

The exact pathogenesis behind pulmonary collision tumor remains unknown. A most widely accepted theory is that each component of the collision tumor has different behavioral, histological, and genetic features, revealing their intratumoral heterogenicity and their different tumorigenesis (5, 36). Four main hypotheses have been proposed in the literature: 1) the two different types of tumors are accidentally colliding in one location (37); 2) the carcinogenic stimulus causes an increased chance of arising the simultaneous separate neoplasms at the same site (8); 3) one neoplasm induces the development of another different neoplasm through paracrine effects changing the microenvironment (38); and 4) single-cell gene mutation leads genetically homogeneous clonal cells to differentiate into histologically separate tumor cells due to the heterogeneity of the gene phenotypes (39). In our case, GT and MSGP abutted each other, but two different origins can still be recognized, and there were no mutual migration phenomena or transitional pattern histomorphologically. Furthermore, the two kinds of tumor cells of pulmonary collision tumor had different immunophenotypes demonstrating that each of them possessed different molecular properties and cytogenetics, suggesting their different tumorigenesis. Considering the clinicopathological results of our case, the case was finally diagnosed as pulmonary collision tumor consisting of MSGP and GT. With the review of CT, the density of the lesion was heterogeneous, suggesting its different cell components. Treatment and prognosis largely depend on the independent biological behavior of different histological subtypes of pulmonary collision tumor.

As the first case of primary pulmonary collision tumor comprising two benign tumors, the prognosis of this subtype has not been clearly clarified. To date, no evidence of recurrence or metastasis has been shown by the patient. We will continue to focus on the prognosis of this patient in the future. Given the rare incidence of collision tumor, the inadequate attention given to it, and the insufficient research conducted about it, further studies and in-depth research are needed to elucidate its mechanism of tumorigenesis and biological behavior.

Data availability statement

The original contributions presented in the study are included in the article/Supplementary Material. Further inquiries can be directed to the corresponding author.

Ethics statement

The studies involving human participants were reviewed and approved by Biomedical Research Ethics Committee of West China Hospital. The patient provided her written informed consent to participate in this study. Written informed consent was obtained from the individual(s) for the publication of any potentially identifiable images or data included in this article.

Author contributions

LJ contributed to the conception and design of the work. CY collected the data and wrote the original draft. SL contributed to the interpretation of data. ZL revised the manuscript. All authors approved the final version of the manuscript.

Funding

This study was funded by the Project for Disciplines of Excellence-Clinical Research Incubation Project, West China Hospital, Sichuan University (No. 2019HXFH002).

Conflict of interest

The authors declare that the research was conducted in the absence of any commercial or financial relationships that could be construed as a potential conflict of interest.

Publisher's note

References

1. Sung CT, Shetty A, Menias CO, Houshyar R, Chatterjee S, Lee TK, et al. Collision and composite tumors; radiologic and pathologic correlation. *Abdom Radiol (NY)* (2017) 42(12):2909–26. doi: 10.1007/s00261-017-1200-x

2. Aggarwal N, Amin RM, Chung D, Parwani AV. Tumor-to-tumor metastasis: case report of a pulmonary adenocarcinoma metastatic to a clear cell renal cell carcinoma. *Pathol Res Pract* (2012) 208(1):50–2. doi: 10.1016/j.prp.2011.10.003

3. Anani W, Amin M, Pantanowitz L, Parwani AV. A series of collision tumors in the genitourinary tract with a review of the literature. *Pathol Res Pract* (2014) 210 (4):217–23. doi: 10.1016/j.prp.2013.12.005

4. Zhao Z, Sun K, Yan T, Wei R, Guo W. Multiple primary tumors: a case report and review of the literature. *BMC Musculoskelet Disord* (2020) 21(1):394. doi: 10.1186/s12891-020-03426-8

5. Bulte CA, Hoegler KM, Khachemoune A. Collision tumors: A review of their types, pathogenesis, and diagnostic challenges. *Dermatol Ther* (2020) 33(6):e14236. doi: 10.1111/dth.14236

6. Mark EJ. Mesenchymal cystic hamartoma of the lung. *N Engl J Med* (1986) 315(20):1255–9. doi: 10.1056/nejm198611133152004

7. Zhu H, Huang S, Zhou X. Mesenchymal cystic hamartoma of the lung. *Ann Thorac Surg* (2012) 93(6):e145–7. doi: 10.1016/j.athoracsur.2011.12.041

8. Ueyama T, Tsuru T, Tsuneyoshi M, Sueishi K, Sibuya T, Fukuda T. Primary collision neoplasm of malignant melanoma and adenocarcinoma in the lung. a case report. *Pathol Res Pract* (1993) 189(2):178–83. doi: 10.1016/s0344-0338(11) 80089-0

9. Nakata S, Nagata Y, Sugaya M, Yasuda M, Yamashita T, Takenoyama M, et al. Primary pulmonary collision cancer consisting of large cell carcinoma and adenocarcinoma. *Ann Thorac Surg* (2005) 80(1):340–2. doi: 10.1016/j.athoracsur.2003.12.053

10. Abbi KK, Hameed MK, Jiang Y, De Las Casas LE, Schwann TA. Pulmonary collision tumor consisting of adenocarcinoma and typical carcinoid–a case report and review of literature. *Am J Ther* (2014) 21(6):e234–8. doi: 10.1097/MJT.0b013e318293b0b0

11. Chan JKI, Tai WM, Wen JM. Collision of lymphoepithelioma-like carcinoma and adenocarcinoma of the lung: a case report. *Clin Respir J* (2017) 11(6):1052–6. doi: 10.1111/crj.12404

12. Kawashima O, Sakata S, Kamiyoshihara M, Maeshima A, Ishikawa S, Morishita Y. Primary pulmonary collision tumor including squamous cell carcinoma and T-cell lymphoma. *Lung Cancer* (1999) 23(1):67–70. doi: 10.1016/s0169-5002(98)00100-7

13. Takahashi K, Nishimura M. A unique collision of epithelioid hemangioendothelioma and bronchioloalveolar carcinoma in a 54-year-old Japanese woman. *Jpn J Thorac Cardiovasc Surg* (2003) 51(7):311–3. doi: 10.1007/bf02719384

14. Liu C. Case of the season: primary pulmonary collision tumor consisting of carcinoid and high-grade spindle-cell sarcoma. *Semin Roentgenol* (2011) 46 (3):170–2. doi: 10.1053/j.ro.2011.02.001

15. Oide T, Yasufuku K, Shibuya K, Yoshino I, Nakatani Y, Hiroshima K. Primary pulmonary glomus tumor of uncertain malignant potential: A case report with literature review focusing on current concepts of malignancy grade estimation. *Respir Med Case Rep* (2016) 19:143–9. doi: 10.1016/j.rmcr.2016.10.002

16. Shugart RR, Soule EH, Johnson EWJr. GLOMUS TUMOR. *Surg Gynecol Obstet* (1963) 117:334–40.

17. Lin J, Shen J, Yue H, Li Q, Cheng Y, Zhou M. Gastric glomus tumor: A clinicopathologic and immunohistochemical study of 21 cases. *BioMed Res Int* (2020) 2020:5637893. doi: 10.1155/2020/5637893

18. Tripodi SA, Rocca BJ, Mourmouras V, Barbanti G, Colecchia M, Ambrosio MR. Benign glomus tumor of the urinary bladder. *Arch Pathol Lab Med* (2013) 137 (7):1005–8. doi: 10.5858/arpa.2012-0125-CR

19. Larsen DK, Madsen PV. Glomus tumour of the distal phalanx. *Ugeskr Laeger* (2018) 180(30):V10170807.

20. Jensen OA. Glomus tumor (Glomangioma) of eyelid. *Arch Ophthalmol* (1965) 73:511–3. doi: 10.1001/archopht.1965.00970030513012

21. Albores-Saavedra J, Gilcrease M. Glomus tumor of the uterine cervix. *Int J Gynecol Pathol* (1999) 18(1):69–72. doi: 10.1097/00004347-199901000-00010

22. Gökten N, Peterdy G, Philpott T, Maluf HM. Glomus tumor of the ovary: report of a case with immunohistochemical and ultrastructural observations. *Int J Gynecol Pathol* (2001) 20(4):390–4. doi: 10.1097/00004347-200110000-00013

23. Liu Y, Wu R, Yu T, Cao Y, Lu L. Malignant glomus tumor of the thyroid gland: a case report. *J Int Med Res* (2019) 47(6):2723–7. doi: 10.1177/0300060519844872

24. Venegas O, Newton A, Vergara N, Singhal S, Predina JD. Tracheal glomus tumor: A case report and review of the literature. *Rare Tumors* (2017) 9(1):6848. doi: 10.4081/rt.2017.6848

25. Gaertner EM, Steinberg DM, Huber M, Hayashi T, Tsuda N, Askin FB. Pulmonary and mediastinal glomus tumors–report of five cases including a pulmonary glomangiosarcoma: a clinicopathologic study with literature review. *Am J Surg Pathol* (2000) 24(8):1105–14. doi: 10.1097/00000478-200008000-00008

26. Gao M, Ye SN, Lin C, Xu YT. Tracheal glomus tumor misdiagnosed as pulmonary disease: a case report and literature review. *Braz J Otorhinolaryngol* (2021) S1808-8694(21):00107-5. doi: 10.1016/j.bjorl.2021.05.011

27. Dai SH, Tseng HY, Wu PS. A glomus tumor of the lung of uncertain malignant potential: a case report. *Int J Clin Exp Pathol* (2018) 11(12):6039–41.

28. Jin Y, Al Sawalhi S, Zhao D, Cai H, Odeh AM, Xie H. Behavior of primary tracheal glomus tumor, uncertain malignant potential subtype. *Gen Thorac Cardiovasc Surg* (2019) 67(11):991–5. doi: 10.1007/s11748-019-01085-8

29. Wang C, Ma Y, Zhao X, Sun PL, Zhang YM, Huang M. Glomus tumors of the trachea: 2 case reports and a review of the literature. *J Thorac Dis* (2017) 9(9): E815–e826. doi: 10.21037/jtd.2017.08.54

30. Fernandez-Bussy S, Labarca G, Rodriguez M, Mehta HJ, Jantz M. Concomitant tracheal and subcutaneous glomus tumor: Case report and review of the literature. *Respir Med Case Rep* (2015) 16:81–5. doi: 10.1016/j.rmcr.2015.08.001

31. Folpe AL, Fanburg-Smith JC, Miettinen M, Weiss SW. Atypical and malignant glomus tumors: analysis of 52 cases, with a proposal for the reclassification of glomus tumors. *Am J Surg Pathol* (2001) 25(1):1–12. doi: 10.1097/00000478-200101000-00001

32. Christopher DM, Julia AB, Pancras CW, Al E. *WHO classification of tumours of soft tissue and bone. 4th ed.* Lyon: IARC Press (2013).

33. Flieder DB, Koss MN, Nicholson A, Sesterhenn IA, Petras RE, Travis WD. Solitary pulmonary papillomas in adults: a clinicopathologic and in situ hybridization study of 14 cases combined with 27 cases in the literature. *Am J Surg Pathol* (1998) 22(11):1328–42. doi: 10.1097/00000478-199811000-00003

34. Travis WD, Brambilla E, Burke AP, Marx A, Nicholson AG. *World health organization classification of tumors: Pathology and genetics of tumors of the lung, pleural, thymus and heart.* Lyon: IARC (2015).

35. Weigel J, Neher M, Schrey M, Wünsch PH, Steiner HH. Collision tumor composed of meningioma and cavernoma. *J Korean Neurosurg Soc* (2017) 60 (1):102–7. doi: 10.3340/jkns.2015.0707.011

36. Satter EK, Metcalf J, Lountzis N, Elston DM. Tumors composed of malignant epithelial and melanocytic populations: a case series and review of the literature. *J Cutan Pathol* (2009) 36(2):211–9. doi: 10.1111/j.1600-0560.2008.01000.x

37. Brandwein-Gensler M, Urken M, Wang B. Collision tumor of the thyroid: a case report of metastatic liposarcoma plus papillary thyroid carcinoma. *Head Neck* (2004) 26(7):637–41. doi: 10.1002/hed.20024

38. Cornejo KM, Deng AC. Malignant melanoma within squamous cell carcinoma and basal cell carcinoma: is it a combined or collision tumor?–a case report and review of the literature. *Am J Dermatopathol* (2013) 35(2):226–34. doi: 10.1097/DAD.0b013e3182545e27

39. Fujii H, Zhu XG, Matsumoto T, Inagaki M, Tokusashi Y, Miyokawa N. Genetic classification of combined hepatocellular-cholangiocarcinoma. *Hum Pathol* (2000) 31(9):1011–7. doi: 10.1053/hupa.2000.9782

frontiers | Frontiers in Oncology

TYPE Case Report
PUBLISHED 25 November 2022
DOI 10.3389/fonc.2022.1033322

OPEN ACCESS

EDITED BY
Kohei Fujita,
National Hospital Organization Kyoto Medical Center, Japan

REVIEWED BY
Qingquan Luo,
Shanghai Jiao Tong University, China
Anello Marcello Poma,
University of Pisa, Italy

*CORRESPONDENCE
Ruijun Cai
cairjundr@163.com

SPECIALTY SECTION
This article was submitted to Thoracic Oncology, a section of the journal Frontiers in Oncology

RECEIVED 31 August 2022
ACCEPTED 07 November 2022
PUBLISHED 25 November 2022

CITATION
Liu X, Zheng Y, Mai S, Tong Y, Yang L, Huang M and Cai R (2022) Case report: an initially unresectable stage III pulmonary sarcomatoid carcinoma qith EGFR mutation achieving pathological complete response following neoadjuvant therapy with osimertinib plus chemotherapy. *Front. Oncol.* 12:1033322. doi: 10.3389/fonc.2022.1033322

Case report: an initially unresectable stage III pulmonary sarcomatoid carcinoma qith EGFR mutation achieving pathological complete response following neoadjuvant therapy with osimertinib plus chemotherapy

Xiguang Liu[1], Yating Zheng[2], Shijie Mai[1], Yu Tong[1], Lili Yang[1], Mengli Huang[2] and Ruijun Cai[1]*

[1]Nanfang Hospital, Southern Medical University, Guangzhou, China, [2]Medical Department, 3D Medicines Inc., Shanghai, China

Epidermal growth factor receptor (EGFR) tyrosine kinase inhibitors (EGFR-TKIs) provide dramatic response to patients with advanced EGFR-mutant non-small cell lung cancer (NSCLC). However, the use of neoadjuvant therapy with EGFR-TKIs in EGFR-mutant NSCLC remains controversial, especially in pulmonary sarcomatoid carcinoma (PSC). One patient with initially unresectable stage III (cT4N0M0) PSC was found to carry EGFR mutation by the next generation sequencing. After neoadjuvant therapy with osimertinib plus chemotherapy, radical resection of the right upper lung lesion was achieved, and the pathological results reached pathological complete response (pCR). To the best of our knowledge, this is the first report of an EGFR-mutant patient with initially unresectable stage III PSC achieved pCR by neoadjuvant therapy with osimertinib plus chemotherapy. Therefore, neoadjuvant therapy with EGFR-TKIs may be a viable option for EGFR-mutant PSC patients.

KEYWORDS

pulmonary sarcomatoid carcinoma, osimertinib, chemotherapy, neoadjuvant, EGFR

Introduction

Pulmonary sarcomatoid carcinoma (PSC) is a rare subclassification of non-small cell lung cancer (NSCLC), accounting for 0.5% (1). Compared with other histological subtypes of NSCLC, including lung adenocarcinoma (LUAD), lung squamous cell carcinoma (LUSC), large cell neuroendocrine carcinoma (LCNEC), and large cell carcinoma (LCC), PSC is more aggressive, has a lower response rate to conventional therapy, and a higher recurrence rate (2–4). It carries a poor prognosis (a 5-year survival of 24.5%) (4), due to early metastasis and high resistance to platinum-based chemotherapy (5, 6). It is well known that the treatment principle of PSC is similar to that of NSCLC, and radical surgery is the recommended treatment for early-stage patients (7). The treatment of stage III patients is highly individualized and guided by multidisciplinary input based on patient factors. Neoadjuvant chemotherapy can be performed in some stage III patients, and surgical resection can be performed if it is considered feasible (8, 9). Although both neoadjuvant and adjuvant chemotherapy improve survival in patients with NSCLC, the effect of perioperative chemotherapy on PSC is controversial, as is radiotherapy (10, 11). Therefore, it is critical to explore new therapeutic targets and therapeutic methods for PSC.

The mutation frequency of epidermal growth factor receptor (EGFR) in PSC is 19% (12). Currently, several EGFR tyrosine kinase inhibitors (EGFR-TKIs) have been approved by the U.S. Food and Drug Administration (FDA) as first-line therapy for advanced NSCLC with EGFR mutations (13), but there is still a lack of convincing evidence for their use as neoadjuvant therapy for stage III NSCLC. Currently, several clinical trials of EGFR-TKIs in the neoadjuvant treatment of NSCLC are underway (Supplementary Table 1). In addition, several case reports and small sample size studies have shown that EGFR-TKIs as neoadjuvant therapy for EGFR-mutant stage II-III NSCLC are acceptable in terms of efficacy, safety and surgical complications (14–19), but these reports and studies has not defined the benefit for PSC. To the best of our knowledge, we report the first case of neoadjuvant therapy with osimertinib plus chemotherapy in an initially unresectable stage III PSC.

Case presentation

An 50-year-old male was admitted to hospital on August 22th, 2021 for cough and expectoration without obvious cause. He had 35 years history of smoking a pack a day, and history of drinking 100ml/day. He had no history of infectious diseases such as dysentery, malaria, viral hepatitis or tuberculosis. His father died of esophageal cancer, denying a family history of the disease.

As the timeline of the clinical course in this patient (Supplementary Figure 1), On August 23th, 2021, a positron emission tomography-computed tomography (PET-CT) revealed a large cystic solid lesion (8.6 × 5.9 × 9.9 cm) in the lung field from the right hilum to the right upper lobe, which was considered to be a right thoracic malignant tumor. The lesion invaded mediastinum adjacent superior vena cava and main right pulmonary artery. Additionally, multiple enlarged lymph nodes were observed in both hilum, mediastinum and right supraclavicular fossa, with the largest being 1.5×1.4 cm, with mild to moderate increase in metabolism, which was considered as multiple lymph node inflammation (Figure 1A). On August 26th, 2021, an electronic bronchoscopy revealed stenosis of the right upper lobe opening and obstruction of the lumen by necrotic material (Figure 1B). An electronic bronchoscopy biopsy of the superior lobe of right lung led to a pathological diagnosis of PSC (Figure 1C). The malignancy was consistent with stage III (cT4N0M0) disease. Upon NGS analysis of the biopsy tissue sample, the patient was identified to harbor EGFR mutations (EGFR exon21 p.L861Q, EGFR exon18 p.G719C) (Supplementary Figure 2), TP53 mutation (exon8 p.R273C), BCORL1 amplification, and CCNE1 amplification. In addition, the patient was identified as having microsatellite stable (MSS) and tumor mutation burden (TMB) of 6.15Muts/Mb by NGS. In addition, immunohistochemistry (IHC) for PD-L1 was strong positive (TPS=80%).

Considering the patient's PET-CT results showed that the tumor was large and adjacent to the mediastinum and main pulmonary artery, which made it difficult to resect. The patient had no indications for surgery, and chemotherapy plus immunotherapy (albumin paclitaxel 400mg d1+ cisplatin 90mg dl+ tislelizumab 200mg dl) was subsequently started on September 4th and September 30th, 2021. After two cycles of chemotherapy plus immunotherapy, on October 27, 2021, a chest computed tomography (CT) scan showed that the size of the lesion in the lung field from the right hilum to the right upper lobe was 6.6 × 4.6 × 6.0 cm, and the largest enlarged lymph node was 1.5 × 1.3 cm, but the lesion was still close to the mediastinum and the main pulmonary artery, which was difficult to be surgically removed (Figure 2A). In addition, the patient's transaminase increased during the treatment period, indicating abnormal liver function, liver protection treatment returned to normal after a period of time. Moreover, it has been reported that immunotherapy may cause abnormal liver function in NSCLC patients, in which transaminases are increased (20–22). Considering that immunotherapy may cause liver injury, immunization was discontinued. Immediately after, the patient received chemotherapy plus EGFR-TKI (albumin paclitaxel 400mg d1+ cisplatin 50mg dl + osimertinib 30mg dl-14) on October 30th, 2021. On December 6, 2021, after one cycle of chemotherapy plus EGFR-TKI, a chest CT scan showed that the size of the lesion in the lung field from the right hilum to the right

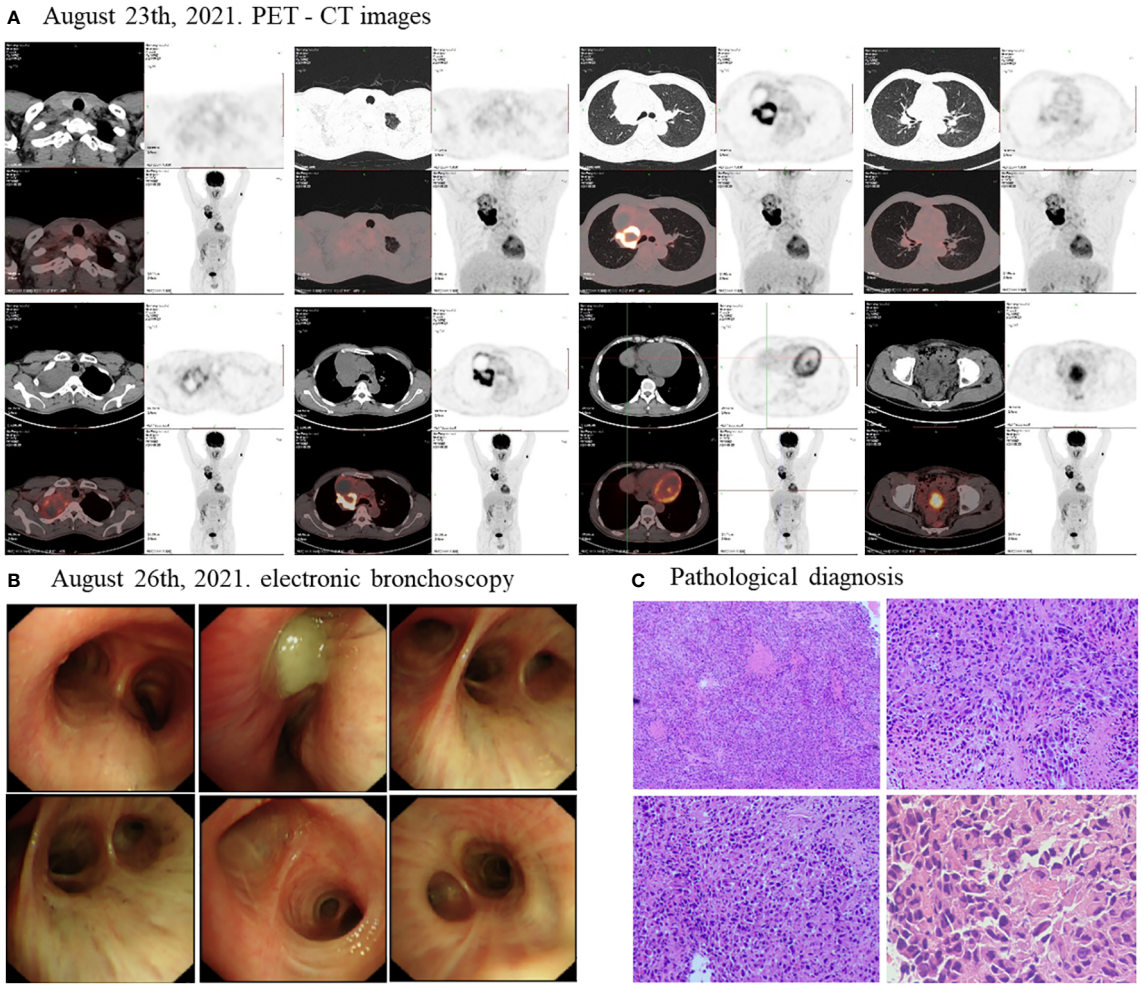

FIGURE 1
Disease status before treatment. The PET-CT scan **(A)** showed that before treatment, the size of the lung field from the right hilum to the right upper lobe of the lung large cystic solid mass was 8.6 × 5.9 × 9.9 cm. **(B)** The electronic bronchoscopy of the patient before treatment. **(C)** Pathological diagnosis of the patient before treatment.

upper lobe was 6.6 × 4.6 × 6.0 cm, and the largest enlarged lymph node was 1.7 × 0.8 cm (Figure 2B). After chemotherapy plus EGFR-TKI treatment, there was a gap between the lesion and the mediastinum, as well as between the lesion and the right pulmonary trunk, indicating that the lesion may be resected by surgery. Since no obvious contraindications were found, the patient underwent thoracoscopic radical resection of right upper lung cancer on December 15th, 2021. Postoperative pathology showed no residual tumor cells in the right upper lung lesion, no residual tumor cells in the resection margins of the trachea and blood vessels, and no tumor metastasis in the lymph nodes, reached pathological complete response (pCR) (Figure 3). On February 27th and May 23th, 2022, about 2.5 months and 5.5 months after surgical resection, chest CT scan showed no evidence of malignant tumor recurrence (Figures 4A, B).

Discussion

At present, there is no standardized treatment for managing PSC, a rare NSCLC subtype with poor prognosis, and its treatment strategy is derived from NSCLC. The use of EGFR-TKIs has revolutionized the treatment of advanced NSCLC with EGFR mutations. In the perioperative treatment of early NSCLC, ADJUVANT, EVAN and SELECT clinical trials have shown that gefitinib and erlotinib, respectively, as postoperative therapies can improve disease-free survival (DFS) in EGFR-mutant patients (23–25). Similarly, the ADAURA trial also showed that osimertinib as adjuvant therapy significantly improved DFS in patients with stage IB-IIIA EGFR-mutant NSCLC (26). In addition, there are a few case reports and small sample size studies indicating the feasibility of EGFR-TKIs (Gefitinib, Erlotinib, Afatinib, Osimertinib, Aumolertinib) in the neoadjuvant stage of EGFR-mutant NSCLC

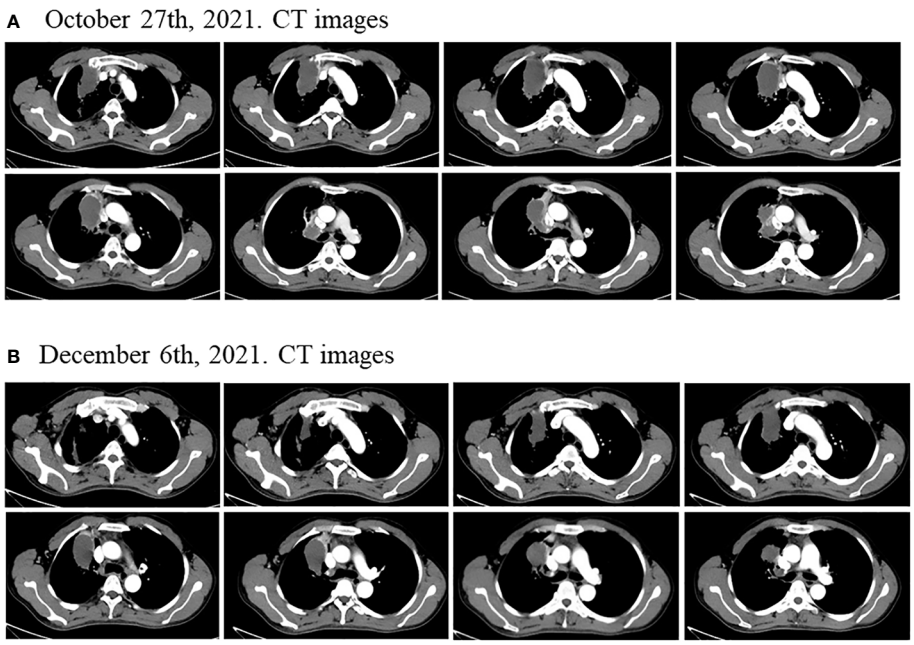

FIGURE 2
Disease status after neoadjuvant chemotherapy plus immunotherapy and chemotherapy plus EGFR-TKI. **(A)** After two cycles of neoadjuvant chemotherapy plus immunotherapy, the size of the lung field from the right hilum to the right upper lobe of the lung large cystic solid mass was 6.6 × 4.6 × 6.0 cm. **(B)** After one cycle of neoadjuvant chemotherapy plus EGFR-TKI, the size of the lung field from the right hilum to the right upper lobe of the lung large cystic solid mass was 6.2 × 3.5 × 5.5 cm.

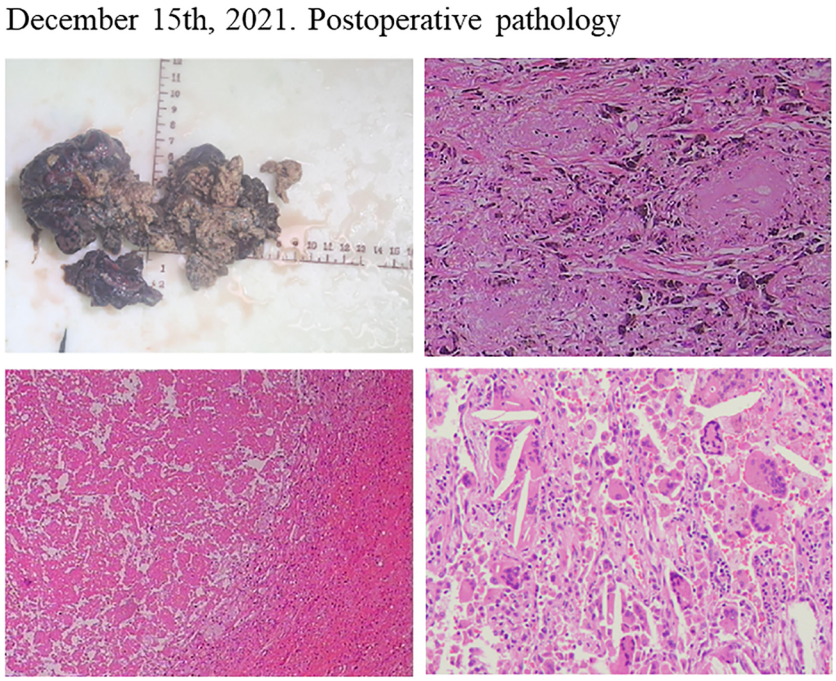

FIGURE 3
Postoperative pathology of the patient after neoadjuvant chemotherapy plus EGFR-TKI showed pathological complete response.

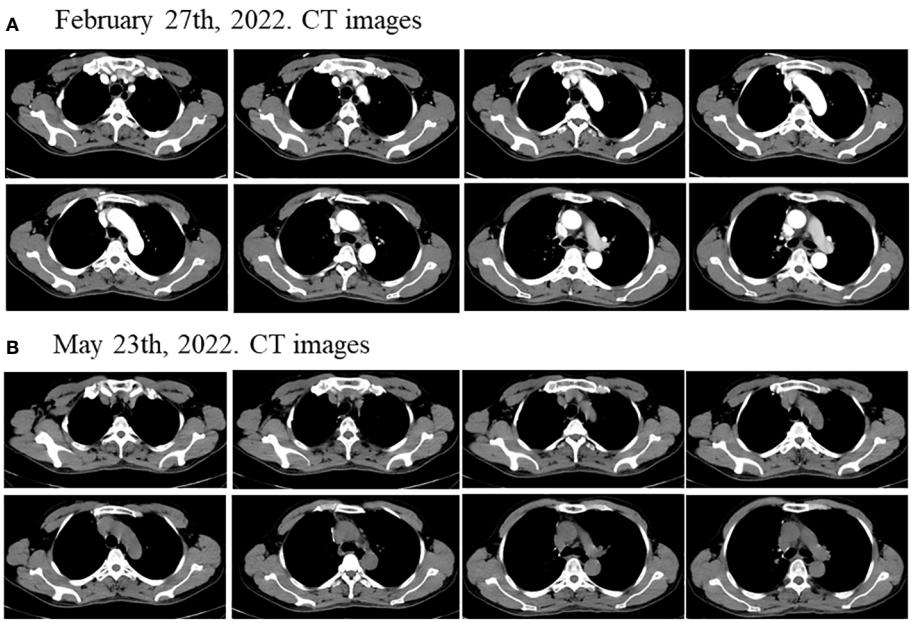

FIGURE 4
Disease status after surgical resection. The chest CT scan showed no evidence of malignant tumor recurrence about **(A)** 2.5 months and **(B)** 5.5 months after surgical resection.

patients (14–19). But these treatments have not been evaluated in PSC.

In this case, after two cycles of chemotherapy plus immunotherapy, the tumor was still inoperable, and during the treatment, the liver function of the patient was abnormal and the transaminase was elevated. After consulting the relevant literature, it was found that immunotherapy may cause liver function abnormalities in NSCLC patients, so immunotherapy was stopped after comprehensive consideration (20–22). Then the initially unresectable stage III PSC patient received osimertinib plus chemotherapy. The CT images after osimertinib plus chemotherapy treatment showed slight tumor shrinkage and the opportunity for surgery. It is difficult to determine how much of this response is due to the delayed effect of chemotherapy plus immunotherapy or to the effect of osimertinib or osimertinib plus chemotherapy. Despite this, the patient had a good treatment response, with complete resection of the primary tumor, pCR on pathological evaluation, and no disease recurrence 5.5 months after surgery. At present, there are few clinical studies on immunotherapy specifically for PSC. A retrospective study with a small sample size enrolled 37 PSC patients who received anti-PD-1 immunotherapy, and 40.5% of them achieved clinical remission, but OS was not statistically significant. In addition, we reviewed the biomarker analysis of this study and found that 19 patients tested for PD-L1 had a median PD-L1 expression of 70% and only one PD-L1-negative sample. Although the expression of PD-L1 in PSC is generally higher, the results of prognosis analysis of patients showed that there was a trend that the median OS of PD-L1+ group was higher than that of PD-L1- group, but there was no significant statistical significance. Moreover, the expression of PD-L1 in disease progression (PD), stable disease (SD) and partial response (PR) patients did not show an obvious trend of gradual increase (26). Only one patient with a detectable EGFR exon 18 mutation, TP53 mutation and low TMB (4Muts/Mb) showed early progression on immunotherapy, with a treatment duration of 0.4 months and an OS of 1.8 months (26). The patient we reported here also carried EGFR exon18 mutation, combined with TP53 mutation and low TMB (6.15Muts/Mb), which is similar to the above patient, which may imply that EGFR-mutated NSCLC patients, even PSC patients, may have a low benefit from immunotherapy. This case report suggests to some extent that that neoadjuvant therapy with osimertinib plus chemotherapy may be both effective and safe in stage III PSC and neoadjuvant therapy with EGFR-TKIs may be another viable option for patients who do not respond well to other neoadjuvant therapies.

In conclusion, although the expression of PD-L1 in PSC is generally high, and the positive rate is higher than that of other NSCLC, we cannot judge whether the expression of PD-L1 and the level of TMB are significantly positively correlated with the prognosis of immunotherapy in PSC patients based on the few clinical studies and data related to immunotherapy in PSC patients. And whether PSC patients with EGFR mutations benefit less from immunotherapy than NSCLC patients may

need more large clinical studies to explain. And there are still many problems with the use of EGFR-TKIs in the perioperative period of stage III patients. The dose and duration of neoadjuvant EGFR-TKIs therapy, as well as the optimal timing of post-treatment surgery, remain unclear. In this case, the patient received osimertinib plus chemotherapy, which responded well and was well tolerated without increased toxicity. This has been demonstrated previously in clinical studies of EGFR-TKIs plus chemotherapy for advanced NSCLC (27–29). However, large-sample clinical trials are still needed to evaluate whether the use of EGFR-TKIs plus chemotherapy in the neoadjuvant phase of stage III patients are safe and improve efficacy. In addition, few studies have explored the safety and feasibility of using EGFR-TKIs neoadjuvant therapy in initially unresectable stage III disease, and current clinical trials (Supplementary Table 1) hardly involve initially unresectable stage III disease, so more studies are needed to explore this in the future. Finally, whether to consider the use of EGFR-TKIs for adjuvant therapy is also an important exploration direction for patients who show good response to neoadjuvant therapy with EGFR-TKIs.

In brief, this is the first report of initially unresectable stage III PSC patient who harbor EGFR mutation benefiting from neoadjuvant therapy with osimertinib plus chemotherapy. This case provides new insights into the treatment in PSC patients.

Data availability statement

The datasets presented in this article are not readily available because of ethical/privacy restrictions. Requests to access the datasets should be directed to the corresponding author.

Ethics statement

The studies involving human participants were reviewed and approved by the Research Ethics Committee of the Nanfang Hospital, Southern Medical University. The patients/participants provided their written informed consent to participate in this study. Written informed consent was obtained from the individual(s) for the publication of any potentially identifiable images or data included in this article.

Author contributions

All authors contributed to the article and approved the submitted version.

Acknowledgments

The authors wish to gratefully acknowledge this patient and his family for allowing us to publish his clinical case.

Conflict of interest

Authors YZ and MH were employed by 3D Medicines Inc.

The remaining authors declare that the research was conducted in the absence of any commercial or financial relationships that could be construed as a potential conflict of interest.

Publisher's note

Supplementary material

The Supplementary Material for this article can be found online at: https://www.frontiersin.org/articles/10.3389/fonc.2022.1033322/full#supplementary-material

References

1. Steuer CE, Behera M, Liu Y, Fu C, Gillespie TW, Saba NF, et al. Pulmonary sarcomatoid carcinoma: An analysis of the national cancer data base. *Clin Lung Cancer* (2017) 18(3):286–92. doi: 10.1016/j.cllc.2016.11.016

2. Vieira T, Girard N, Ung M, Monnet I, Cazes A, Bonnette P, et al. Efficacy of first-line chemotherapy in patients with advanced lung sarcomatoid carcinoma. *J Thorac Oncol* (2013) 8(12):1574–7. doi: 10.1097/01.JTO.0000437008.00554.90

3. Yendamuri S, Caty L, Pine M, Adem S, Bogner P, Miller A, et al. Outcomes of sarcomatoid carcinoma of the lung: a surveillance, epidemiology, and end results database analysis. *Surgery* (2012) 152(3):397–402. doi: 10.1016/j.surg.2012.05.007

4. Martin LW, Correa AM, Ordonez NG, Roth JA, Swisher SG, Vaporciyan AA, et al. Sarcomatoid carcinoma of the lung: a predictor of poor prognosis. *Ann Thorac Surg* (2007) 84(3):973–80. doi: 10.1016/j.athoracsur.2007.03.099

5. Paredes Mogica JA, Reyes Sanchez E, Zaragoza Morales DA, Pierre-Louis Guillen N, Magallanes Maciel ME. Rapidly progressive lung sarcomatoid carcinoma managed with doxorubicin plus ifosfamide and pemetrexed. *Case Rep Oncol* (2021) 14(3):1677–81. doi: 10.1159/000520190

6. Giroux Leprieur E, Antoine M, Vieira T, Duruisseaux M, Poulot V, Rabbe N, et al. Clinical and molecular features in patients with advanced non-small-cell lung

carcinoma refractory to first-line platinum-based chemotherapy. *Lung Cancer* (2013) 79(2):167–72. doi: 10.1016/j.lungcan.2012.10.010

7. Zeng Q, Li J, Sun N, Xue Q, Gao Y, Zhao J, et al. Preoperative systemic immune-inflammation index predicts survival and recurrence in patients with resected primary pulmonary sarcomatoid carcinoma. *Transl Lung Cancer Res* (2021) 10(1):18–31. doi: 10.21037/tlcr-20-960

8. Hirsch FR, Scagliotti GV, Mulshine JL, Kwon R, Curran WJ, Wu Y-L, et al. Lung cancer: current therapies and new targeted treatments. *Lancet* (2017) 389 (10066):299–311. doi: 10.1016/s0140-6736(16)30958-8

9. Howington JA, Blum MG, Chang AC, Balekian AA, Murthy SC. Treatment of stage I and II non-small cell lung cancer: Diagnosis and management of lung cancer, 3rd ed: American college of chest physicians evidence-based clinical practice guidelines. *Chest* (2013) 143(5 Suppl):e278S–313S. doi: 10.1378/chest.12-2359

10. Maneenil K, Xue Z, Liu M, Boland J, Wu F, Stoddard SM, et al. Sarcomatoid carcinoma of the lung: The Mayo clinic experience in 127 patients. *Clin Lung Cancer* (2018) 19(3):e323–e33. doi: 10.1016/j.cllc.2017.12.008

11. Gang J, Yan Q, Xiang S, Zheng L, Zhao L. Clinicopathological characteristics and prognostic factors of pulmonary sarcomatoid carcinoma: a large population analysis. *Ann Transl Med* (2021) 9(2):121. doi: 10.21037/atm-20-6213

12. Liu X, Wang F, Xu C, Chen X, Hou X, Li Q, et al. Genomic origin and intratumor heterogeneity revealed by sequencing on carcinomatous and sarcomatous components of pulmonary sarcomatoid carcinoma. *Oncogene* (2021) 40(4):821–32. doi: 10.1038/s41388-020-01573-9

13. Solassol I, Pinguet F, Quantin X. FDA- and EMA-approved tyrosine kinase inhibitors in advanced EGFR-mutated non-small cell lung cancer: Safety, tolerability, plasma concentration monitoring, and management. *Biomolecules* (2019) 9(11):998. doi: 10.3390/biom9110668

14. Xiong L, Li R, Sun J, Lou Y, Zhang W, Bai H, et al. Erlotinib as neoadjuvant therapy in stage IIIA (N2) EGFR mutation-positive non-small cell lung cancer: A prospective, single-arm, phase II study. *Oncologist* (2019) 24(2):157–e64. doi: 10.1634/theoncologist.2018-0120

15. Zhang Y, Fu F, Hu H, Wang S, Li Y, Hu H, et al. Gefitinib as neoadjuvant therapy for resectable stage II-IIIA non-small cell lung cancer: A phase II study. *J Thorac Cardiovasc Surg* (2021) 161(2):434–42.e2. doi: 10.1016/j.jtcvs.2020.02.131

16. Chen CY, Fares CM, Shin DS. Osimertinib as neoadjuvant therapy in a patient with stage IIIA non-small cell lung cancer: a case report. *J Med Case Rep* (2021) 15(1):216. doi: 10.1186/s13256-021-02748-y

17. Du W, Zhao Y, Xuan Y, Qin Y, Xu R, Halmos B, et al. Different efficacy in the non-small cell lung cancer patient with bilateral synchronous lesions treated with neoadjuvant gefitinib therapy: a case report. *J Thorac Dis* (2020) 12(4):1582–7. doi: 10.21037/jtd.2020.02.60

18. Feng S, Qiang Z, Wanwan C, Zhaozhun Z, Yuewu X, Shencun F. Case report: Aumolertinib as neoadjuvant therapy for patients with unresectable stage III non-small cell lung cancer with activated EGFR mutation: Case series. *Front Oncol* (2022) 12:872225. doi: 10.3389/fonc.2022.872225

19. Mazzoni F, Petreni P, Perna M, Scotti V, Bongiolatti S, Livi L, et al. Afatinib with subsequent surgery in stage III NSCLC with EGFR mutation: Lessons learned from two clinical experiences. *Tumori* (2018) 104(6):NP5–9. doi: 10.1177/0300891618775204

20. Calderon B, Stancu A, Vanel FR, Vazquez L. Pembrolizumab treatment-induced liver toxicity. *Case Rep Gastroenterol* (2021) 15(2):742–50. doi: 10.1159/000518128

21. Wang PF, Chen Y, Song SY, Wang TJ, Ji WJ, Li SW, et al. Immune-related adverse events associated with anti-PD-1/PD-L1 treatment for malignancies: A meta-analysis. *Front Pharmacol* (2017) 8:730. doi: 10.3389/fphar.2017.00730

22. Suzman DL, Pelosof L, Rosenberg A, Avigan MI. Hepatotoxicity of immune checkpoint inhibitors: An evolving picture of risk associated with a vital class of immunotherapy agents. *Liver Int* (2018) 38(6):976–87. doi: 10.1111/liv.13746

23. Pennell NA, Neal JW, Chaft JE, Azzoli CG, Jänne PA, Govindan R, et al. SELECT: A phase II trial of adjuvant erlotinib in patients with resected epidermal growth factor receptor–mutant non–Small-Cell lung cancer. *J Clin Oncol* (2019) 37 (2):97–104. doi: 10.1200/JCO.18

24. Zhong W-Z, Wang Q, Mao W-M, Xu S-T, Wu L, Wei Y-C, et al. Gefitinib versus vinorelbine plus cisplatin as adjuvant treatment for stage II-IIIA (N1-N2) EGFR-mutant NSCLC: Final overall survival analysis of CTONG1104 phase III trial. *J Clin Oncol* (2021) 39(7):713–22. doi: 10.1200/JCO.20

25. Yue D, Xu S, Wang Q, Li X, Shen Y, Zhao H, et al. Erlotinib versus vinorelbine plus cisplatin as adjuvant therapy in Chinese patients with stage IIIA EGFR mutation-positive non-small-cell lung cancer (EVAN): a randomised, open-label, phase 2 trial. *Lancet Respir Med* (2018) 6(11):863–73. doi: 10.1016/s2213-2600(18)30277-7

26. Charlotte D, Karen L, Isabelle M, Julie M, Fabrice B, Valérie G, et al. Efficacy of immune checkpoint inhibitors in lung sarcomatoid carcinoma. *J Thorac Oncol* (2020) 15(5):860–6. doi: 10.1016/j.jtho.2020.01.014

27. Ding T, Zhou F, Chen X, Zhang S, Liu Y, Sun H, et al. Continuation of gefitinib plus chemotherapy prolongs progression-free survival in advanced non-small cell lung cancer patients who get acquired resistance to gefitinib without T790M mutations. *J Thorac Dis* (2017) 9(9):2923–34. doi: 10.21037/jtd.2017.07.107

28. Zhang Z, Zeng K, Zhao S, Zhao Y, Hou X, Luo F, et al. Pemetrexed/carboplatin plus gefitinib as a first-line treatment for EGFR-mutant advanced nonsmall cell lung cancer: a Bayesian network meta-analysis. *Ther Adv Med Oncol* (2019) 11:1758835919891652. doi: 10.1177/1758835919891652

29. Planchard D, Feng PH, Karaseva N, Kim SW, Kim TM, Lee CK, et al. Osimertinib plus platinum-pemetrexed in newly diagnosed epidermal growth factor receptor mutation-positive advanced/metastatic non-small-cell lung cancer: safety run-in results from the FLAURA2 study. *ESMO Open* (2021) 6 (5):100271. doi: 10.1016/j.esmoop.2021.100271

frontiers | Frontiers in Oncology

TYPE Case Report
PUBLISHED 01 December 2022
DOI 10.3389/fonc.2022.987484

OPEN ACCESS

EDITED BY
Francesco Pepe,
University of Naples Federico II, Italy

REVIEWED BY
Qing Song,
PLA General Hospital, China
Mingbo Zhang,
PLA General Hospital, China
Mariantonia Nacchio,
University of Naples Federico II, Italy

*CORRESPONDENCE
Qian Li
liqianlq6@outlook.com

SPECIALTY SECTION
This article was submitted to Thoracic Oncology, a section of the journal Frontiers in Oncology

RECEIVED 06 July 2022
ACCEPTED 07 November 2022
PUBLISHED 01 December 2022

CITATION
Zhai Y, Shao Y and Li Q (2022) Case Report: A case of radioactive iodine-refractory thyroid cancer accompanying cervical lymph node metastasis treated with US-guided RFA combined with ^{125}I seed implantation. *Front. Oncol.* 12:987484. doi: 10.3389/fonc.2022.987484

Case Report: A case of radioactive iodine-refractory thyroid cancer accompanying cervical lymph node metastasis treated with US-guided RFA combined with ^{125}I seed implantation

Yuanpeng Zhai, Yu Shao and Qian Li*

Department of Ultrasound, The Affiliated Cancer Hospital of Zhengzhou University & Henan Cancer Hospital, Zhengzhou, China

Background: Local control of metastases is critical to improving the life quality of patients with radioactive iodine-refractory (RAIR) thyroid cancer accompanying regional lymph node metastasis.

Case report: The reported patient suffered from RAIR thyroid cancer accompanying poorly controlled cervical lymph node metastasis. The patient's lesions were controlled through ^{125}I seed implantation combined with ultrasound-guided radio-frequency ablation (US-guided RFA). Such a combination therapy has not been reported to date.

Conclusion: This study found US-guided RFA combined with ^{125}I seed implantation to be safe and effective for the control of cervical local metastases in patients with RAIR thyroid cancer.

KEYWORDS

ultrasound- (US) guided, radiofrequency ablation (RFA), ^{125}I seed implantation, radioactive iodine-refractory (RAIR) thyroid cancer, cervical lymph node metastasis

Background

In recent years, the incidence of thyroid cancer in China has been increasing, with differentiated thyroid cancer (DTC) a dominant type. Some patients with DTC can develop radioactive iodine-refractory differentiated thyroid cancer (RAIR-DTC) as they gradually lose the capacity to uptake iodine during disease treatment and progression (1).

Patients with RAIR-DTC accompanying regional lymph node metastasis struggle with poor prognosis because they cannot benefit from ^{131}I diagnosis and treatment. Although conventional diagnosis and treatment methods employed in clinical practices, such as targeted medical therapy and surgery, can improve the prognosis of patients with RAIR-DTC to a certain extent, the overall response is not satisfactory. Some patients suffer from skin rupture caused by poorly controlled metastases, which seriously affects their quality of life. Studies have shown that ^{125}I seed implantation in the treatment of RAIR-DTC accompanying regional lymph node metastasis can safely deliver a good local control effect, making it of clinical value (2). However, the effectiveness of this treatment is usually limited to metastases of a small size. When lymph node metastases are large, with skin rupture and internal liquefactive necrosis, ^{125}I seed implantation alone has limitations. For example, in metastases of this kind, it is not easy to control the location of the implanted seeds since they are likely to fall into the liquid components, thereby reducing the therapeutic effect. New and effective methods are needed for controlling metastasis locally. As a minimally invasive treatment method, RFA has been used to treat benign thyroid nodules, papillary thyroid cancer and recurrent thyroid cancer (3–6). It is safe and feasible, especially when patients refuse surgery, have high requirements for aesthetics or have surgical contraindications, RFA as an alternative treatment can reduce patients' anxiety and improve their quality of life (7). In our case,during the operation the patients was under monitoring and questioning, the operation was sucessfull and safe.

This report presents the results achieved using ultrasound-(US) guided aspiration of metastatic liquid components, radio-frequency ablation (RFA), and ^{125}I seed implantation in the local control of metastases.

Case report

A 70-year-old woman was admitted to our hospital with "lung metastasis after papillary thyroid carcinoma surgery and new cervical masses detected over 2 years." Two years earlier, in May 2004, she had received a thyroid mass resection under local anesthesia in a local hospital to remove the cervical mass; subsequently, the postoperative pathology revealed lymph node metastasis of papillary thyroid carcinoma. With a recurrent cervical mass, the patient visited our hospital for the first time in August 2006 and underwent a radical resection of a left thyroid carcinoma under general anesthesia. The postoperative pathology indicated papillary thyroid carcinoma. The patient continued to suffer regional lymph node metastasis and received lymph node dissection twice in combination with ^{131}I therapy.

Operation history

In October 2010, the patient received a left neck dissection under general anesthesia in our hospital. Postoperative pathology indicated that one in five level-III and -IV lymph nodes had metastases of papillary thyroid carcinoma, with level VI showing the formation of a cancerous node. On March 26, 2015, the patient received a radical resection of recurrent thyroid cancer and a right recurrent laryngeal nerve anatomic exploration. The postoperative pathology indicated the infiltration of papillary thyroid carcinoma at levels IV and VI of the left neck. At levels IV and VI of the right neck, all the four lymph nodes detected were found with metastases of papillary thyroid carcinoma, accompanied by the formation of a cancerous node.

History of ^{131}iodine therapy

The patient received ^{131}I treatment in our hospital in December 2011, May and October 2012, May and October 2013, August 2014, June 2015, April 2016, and April 2017, with doses of 150, 150, 150, 100, 150, 150, 150, and 100 mCi, respectively.

According to the patient's latest physical examination, she had multiple palpable enlarged lymph nodes in the neck, with tough texture and poor mobility. In 2014, new masses were detected in the right neck, which eventually ruptured in 2019. The patient received a lymph node puncture in the right neck on November 30, 2019, in the Nuclear Medicine Department of the Shanghai Sixth People's Hospital (affiliated with Shanghai Jiao Tong University). An analysis showed papillary thyroid carcinoma due to the BRAF V600E mutation. The ruptured lesion in the right neck was not under control, and a new mass was found in the left neck, protruding through the skin. This mass had a diameter of around 30 mm and was accompanied by bruising of the local skin. The patient's quality of life was significantly affected. The patient was not provided with a therapeutic regimen after visiting upper-level hospitals several times, so she returned to our hospital. After admission, the possibility of lymph node metastasis was considered based on a contrast-enhanced computed tomography (CT) scan of the neck showing multiple nodules and tumor shadows in the thyroid region, bilateral parotid region, bilateral neck, bilateral subclavian and supraclavicular fossae, and the mediastinum. Thyroglobulin in the puncture fluid from the right cervical ruptured lesion was measured at 413 ng/ml, and the lesion was considered to be a thyroid lymph node metastasis. In recent years, the patient had undergone several surgeries, ^{131}radioiodine therapy, systemic anti-tumor therapies, and treatment with sorafenib, vemurafenib, and pembrolizumab. Unfortunately, the effects were not satisfactory, and the metastases in the cervical

lymph nodes remained uncontrolled. At that point, the patient's condition was severe, and there was no effective anti-tumor therapy.

After admission, the patient was given targeted systemic anti-tumor treatment comprising anlotinib (1 tablet/day) and Euthyrox (112.5 μg/day) as inhibition and replacement therapy. As the left cervical mass was relatively large, local cytoreductive surgery was considered for lowering the risk of skin ulceration. Given the large volume of the left cervical mass, with a diameter of approximately 30 mm, a total of 33 ^{125}I seeds were implanted one by one at an interval of 5 mm under CT scan guidance to achieve local cytoreduction for the metastases and reduce the risk of skin rupture.

Three days after ^{125}I seed implantation in the left cervical metastases, the patient reported feeling slightly better. However, the mass in her left neck remained large; it was accompanied by liquefactive necrosis, and seeds were entering the liquid components. To prevent further enlargement and development of the metastases, as well as to avoid radiation damage to adjacent tissues and organs, we proposed during multidisciplinary consultations that RFA be used to reduce the metastases in combination with other therapies for symptomatic treatment. Under the guidance of US, the size of the left cervical mass was measured to be 33 × 19 mm, which protruded through the surface of the skin. Accordingly, we aspirated the liquid components in the lesion, considering the continuous new production of fluid, seed implantation was not carried out, but RFA inactivation was performed on the solid portion at the same time as fluid extraction (Figure 1). Postoperative ultrasonography showed no obvious contrast enhancement in the metastatic lymph nodes of the left neck (Figure 2). The left lesion recover over the month following the RFA. After 23 days, the metastases no longer protruded through the skin, and all that could be seen on the cervical skin was a slight crust. Thirty days after the RFA, a contrast-enhanced CT scan of the neck revealed that the cervical anterior subcutaneous nodule could no longer be seen, which was a postoperative change. The patient's left neck completely recovered 32–35 days after the RFA.

The findings of the contrast-enhanced CT scan and the recovery of the patient's left neck provide evidence that US-guided RFA combined with ^{125}I seed implantation can deliver a complete local response for large metastases in a safe, effective manner. US-guided RFA is particularly effective in treating lymph node lesions with fluid.

As the therapeutic effect of US-guided RFA for the patient's left cervical metastases was quite considerable, we continued with RFA of a fluid-containing lymph node metastasis in the patient's right neck at a safe location. The US-guided measurements showed one of the lymph nodes in the right neck was around 21 × 11 mm, another was around 24 × 17 mm (Figures 3, 4), and there were heterogeneous internal echoes.

We aspirated the liquid components and performed RFA. According to postoperative ultrasonography, no obvious contrast enhancement was found in the cervical metastatic lymph nodes, and there was no residual ablation. The day following the right cervical lymph node RFA, there was a special location of one ulcerated lymph node on the right neck, and there was no safe entry point, so seeds were implanted in the patient's right cervical ruptured lymph node.

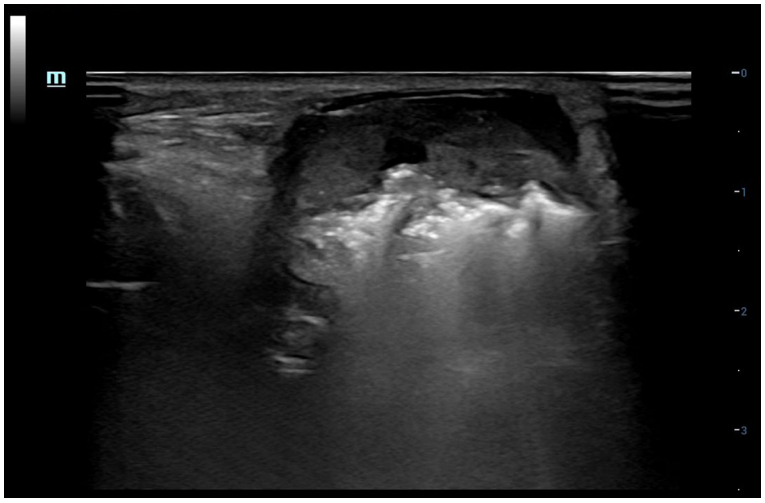

FIGURE 1
US-guided RFA for left cervical mass.

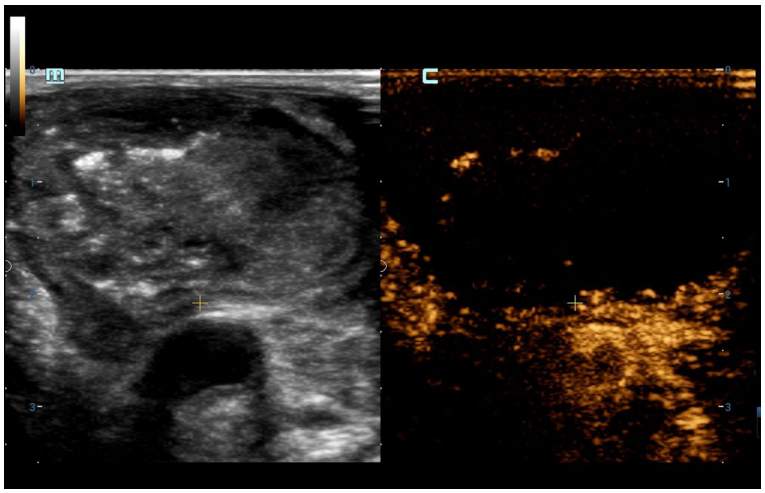

FIGURE 2
No contrast enhancement in left cervical mass according to postoperative ultrasonography.

The ruptured mass shrank following the implantation of nine ^{125}I one by one at an interval of 5 mm.

Two months later, the mass had gone. The ablated cervical mass disappeared over 40 days. Following this success, the masses of the patients in the subsequent treatment were all solid masses, and the location was deep adjacent to the important cervical nerve, so the patient had three more occasions when ^{125}I seeds were implanted into the cervical lymph nodes: 9, 16, and 9 seeds were implanted, respectively. Now, the patient is recovering well, with the local metastases in the cervical lymph nodes well under control. She was discharged from hospital and is receiving systemic targeted drug therapy.

Discussion

Most patients with DTC achieve a good prognosis after receiving surgery, ^{131}I radiotherapy, thyrotropin inhibition, and other therapies, with a 10-year survival rate of up to 90%. However, about 15% of these patients develop local recurrence

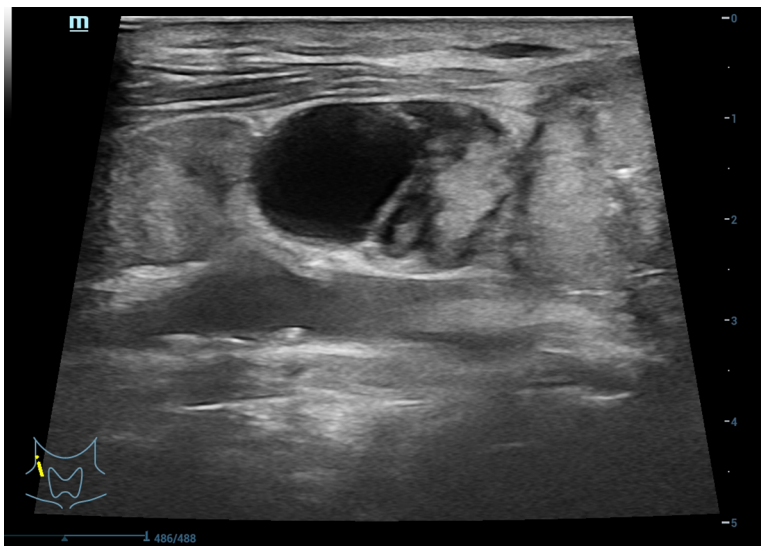

FIGURE 3
Metastatic lymph nodes accompanying internal liquefactive necrosis in right neck as shown in ultrasonography.

and/or distant metastases and have a 10-year survival rate below 10% (8). As some cases are not sensitive to radioactive iodine therapy, they may develop RAIR-DTC, which is characterized by fast progression and high mortality. It is difficult for these patients to achieve satisfactory results with the traditional methods referred to above.

Currently, the diagnosis and treatment of RAIR-DTC are controversial. According to the usual definition of RAIR-DTC, in the absence of exogenous iodine load interference when the level of thyroid-stimulating hormone is greater than 30 m IU/L, the lesion loses its iodine uptake capacity. Consequently, favorable results are not expected from ^{131}I treatment. In the case of the present study, the patient's condition was severe. Her cervical metastases could not be surgically removed, and a high dose of radioactive iodine, if allowed to accumulate around her neck, would likely have caused radiation damage to the larynx and tracheal mucosa, resulting in radiation tracheitis or radiation pneumonia. In this case, the patient was treated as RAIR-DTC because radioactive iodine therapy was not feasible for her (9). The treatment for RAIR-DTC is controversial, and cases accompanying cervical regional lymph node metastasis remain a problem to be solved (10). Surgery, chemotherapy, targeted therapy, and other related methods are now applied in clinical practices. In this case, the patient's condition was severe, and her cervical metastases could not be surgically removed. As studies in molecular biology on thyroid cancer have advanced, a large number of targeted therapeutic drugs have been developed in recent years (11–13), making targeted drug therapy a major option for patients with RAIR-DTC. However, this patient did not respond well to sorafenib, vemurafenib, pembrolizumab, and other targeted therapy drugs. Chemotherapy is mainly used for terminally ill patients with obvious invasive symptoms which are uncontrollable *via* radioactive iodine therapy or surgery. However, as most patients with RAIR-DTC are not sensitive to chemotherapy, traditional chemotherapy drugs are unsuitable (14).

For 15 years (2004–2019), the patient suffered from recurrent cervical lymph node metastases, which progressively increased in size and number and were not effectively controlled. Patients need an effective local therapy that includes surgery and external irradiation, with a focus on cytoreduction, to improve the quality of life (15). However, in this case, the patient's condition was severe, and the cervical metastases could not be surgically removed. The patient was not provided with any effective therapeutic regimen despite repeatedly visiting several hospitals. After the patient came to our hospital, we initially treated the cervical metastases with ^{125}I seed implantation and US-guided RFA.

The lymph node metastases in her left neck, which were large with liquefactive necrosis, showed a positive therapeutic effect in the early stage of ^{125}I seed implantation. Due to a short radiation distance, the ^{125}I seeds can effectively kill tumor cells in lesions with little damage to surrounding tissues, thus achieving highly conformal brachytherapy (2). Nonetheless, its effect on killing cancer cells depends on precise positioning and reasonable arrangement. Studies have shown that the larger the lesion, the lower the therapeutic effect. This has been attributed to seed displacement due to liquefactive necrosis in the large lesions, which makes it impossible to precisely position and reasonably arrange the seeds. This leads to a lower conformal index of dose distribution in the lesion, thereby weakening the therapeutic effect. Furthermore, dose deposit by

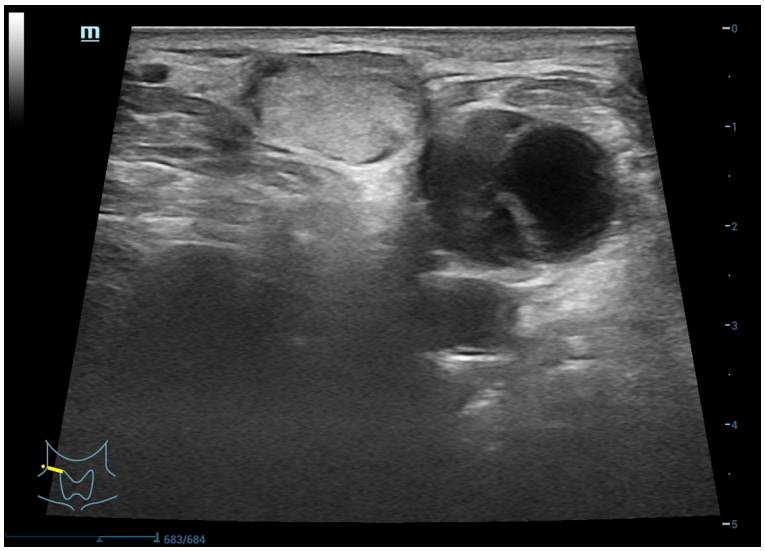

FIGURE 4
Right cervical lymph node metastasis.

seed displacement poses a greater risk of radiation damage to healthy tissues, making inflammatory reactions more likely, forming adhesions between lesions and vital organs (such as peripheral vessels), and thus making further treatment, including replantation, more difficult (16). In this case, the patient had large lymph node metastases accompanied by liquefactive necrosis, and the US showed that implanted seeds had migrated into the liquid components. Considering the unsatisfactory nature of iodine seed implantation, it is important to explore new therapies for controlling local lesions.

During multidisciplinary consultations, our department suggested that the liquid components of metastasis be treated with US-guided aspiration and metastasis be treated with RFA. The RAF can be used for patients with recurrent or metastatic lymph nodes after standard surgical resection and neck lyphnode dissection (17). The patient had undergone at least one operation before, the anatomical structure of the operation area has changed and adhesions would be severe. High risk and difficulty hindered the second operation. besides, the patient is not easy to accept the second operation. In addition, some patients may be ineffective to the iodine therapy, these patients requires further local surgery or RFA. RFA has the unique advantages of safety and simple operation, which provides a more reliable treatment option (7).

The RFA technique has been increasingly applied in clinical practice since it is minimally invasive, has a beneficial therapeutic effect, and is well tolerated. The RFA needle is inserted into lesions under the guidance of US, inducing a thermal effect *via* a high-frequency alternating current in the targeted tissues, thereby inactivating lesion cells.

In this case, the left cervical lymph node metastasis was large (33mm×19mm) and accompanied with liquefaction necrosis. 125I was not effective at first for the particles fell into the liquid components. Under the guidance of ultrasound, we aspirated the liquid components of the left cervical lesion. Considering that the liquid would be generated continuely, we did not implant the particles again, but chose to inactivate the solid parts while aspirating the liquid. RFA was then performed on metastatic tumors at safety site of the right cervical. The solid mass was deep adjacent to important cervical nerves, so 125I was selected for the following treatment.

After RFA, the metastases in the patient's left and right neck shrank. The metastases that ruptured in the upper part also shrank after the implantation of ^{125}I seeds. In summary, the patient obtained the beneficial effect of local control of the metastases through US-guided RFA combined with ^{125}I seed implantation. This is a safe method with high clinical application value.

In this case, RFA plays an important role in the safe location of fluid lymph node lesions, and seed implantation plays an important role in the subsequent treatment of lymph node lesions located deep adjacent to important cervical nerves in the right neck. The implantation of 125I seeds has good local control effect, high safety and high clinical application value for the patients with RAIR-DTC with regional lymph node metastasis. Especially, when the tumor showed liquid necrosis, the implantation position of 125I particles would be uncontrolled. If the particles fall off into the liquid components, the effectiveness will be greatly reduced. RFA has been used to treat benign thyroid nodules, papillary thyroid cancer, recurrent thyroid cancer and lymph node metastasis safely. The coagulative necrotic tissue gradually becomes smaller after the RFA operation, and the clinical symptoms caused by nodules are also significantly improved, which is safe and feasible. Besides, the solid part can be inactivated while the fluid is pumped for mixed lesions.

Conclusions

In conclusion, patients with RAIR-DTC with accompanying cervical lymph node metastases face limited therapy options and a poor prognosis. In addition to conventional therapies, such as surgery, chemotherapy, and targeted drug treatment, new local therapies are needed, particularly for lesions with large local mass accompanied by liquefactive necrosis. For such lesions, US-guided RFA is a valuable contribution to these therapies. Our patient was treated with targeted drugs and thyrotropin inhibition, combined with US-guided RFA and ^{125}I seed implantation for local control, to achieve a complete clinical response for RAIR-DTC with accompanying cervical lymph node metastases.

Data availability statement

The raw data supporting the conclusions of this article will be made available by the authors, without undue reservation.

Ethics statement

This study was conducted with approval from the Ethics Committee of the Affiliated Cancer Hospital of Zhengzhou University & Henan Cancer Hospital. The patients/participants provided their written informed consent to participate in this study.

Author contributions

Conception and design of the research: YZ, YS. Acquisition of data: QL. Analysis and interpretation of the data: YZ. Statistical analysis: YZ, YS. Obtaining financing: YZ. Writing of the manuscript: YZ, Critical revision of the manuscript for intellectual content: QL. All authors read and approved the final draft.

Funding

This study was funded by the Scientific and technological project in Henan Province (No.212102310637).

Conflict of interest

The authors declare that the research was conducted in the absence of any commercial or financial relationships that could be construed as a potential conflict of interest.

Publisher's note

References

1. Schmidt A, Iglesias L, Klain M, Pitoia F, Schlumberger MJ. Raioactive iodine –refractory differentiated thyroid cancer: An ucommon but challenging situation. *Arch Endocrinol Metab* (2017) 61:81. doi: 10.1590/2359-3997000000245

2. Ye SF, Zhou YX, Shou F, Zhang JJ, Chen Y. Clinical study on clinical study on 125I seeds implantation for colon cancer patients with liver I seeds implantation for colon cancer patients with liver metastasis. *Oncol Prog* (2018) 16:609 –612. doi: 10.11877/j.issn.1672-1535.2018.16.05.22

3. Teng D, Sui G, Liu C, Wang Y, Xia Y, Wang H. Long-term efficacy of ultrasound-guided low power microwave ablation for the treatment of primary papillary thyroid microcarcinoma: A 3-year follow-up study. *J Cancer Res Clin Oncol* (2018) 144(4):771–9. doi: 10.1007/s00432-018-2607-7

4. Zhang M, Luo Y, Zhang Y, Tang J. Efficacy and safety of ultrasound-guided radiofrequency ablation for treating low-risk papillary thyroid microcarcinoma: A prospective study. *Thyroid* (2016) 26(11):1581–7. doi: 10.1089/thy.2015.0471

5. Kim JH, Baek JH, Lim HK, Ahn HS, Baek SM, Choi YJ, et al. 2017 Thyroid radiofrequency ablation guideline: Korean society of thyroid radiology. *Korean J Radiol* (2018) 19(4):632–55. doi: 10.3348/kjr.2018.19.4.632

6. Lee GM, You JY, Kim HY, Chai YJ, Kim HK, Dionigi G, et al. Successful radiofrequency ablation strategies for benign thyroid nodules. *Endocrine* (2019) 64 (2):316–21. doi: 10.1007/s12020-018-1829-4

7. Jeon YW, Gwak HG, Lim ST, Schneider J, Suh YJ. Long-term prognosis of unilateral and multifocal papillary thyroid microcarcinoma after unilateral lobectomy versus total thyroidectomy. *Ann Surg Oncol* (2019) 26(9):2952–8. doi: 10.1245/s10434-019-07482-w

8. Liu YQ, Lin YS. [Diagnosis, treatment and prognosis of differentiated thyroid carcinoma with iodine refractory]. *Chin J Pract Surg* (2019) 39:216–20. doi: 10.3390/ijms18061292

9. Riesco-Eizaguirre G, Galofré JC, Grande E, Zafón Llopis C, Ramón y Cajal Asensio T, Navarro González E, et al. Spanish Consensus for the management of patients with advanced radioactive iodine refractory differentiated thyroid cancer. *Endocrinol Y Nutricion Organo la Sociedad Espanola Endocrinol Y Nutricion* (2016) 63:e17–24. doi: 10.1016/j.endonu.2015.08.007

10. Bray F, Ferlay J, Soerjomataram I, Siegel RL, Torre LA, Jemal A. Global cancer statistics 2018: GLOBOCAN estimates of incidence and mortality worldwide for 36 cancers in 185 countries. *CA Cancer J Clin* (2018) 68:394–424. doi: 10.3322/caac.21492

11. Brose MS, Nutting CM, Jarzab B, Elisei R, Siena S, Bastholt L, et al. Sorafenib in radioactive iodine-refractory, locally advanced or metastatic differentiated thyroid cancer: A randomised, double-blind, phase 3 trial. *Lancet* (2014) 384:319–28. doi: 10.1016/S0140-6736(14)60421-9

12. Tahara M, Schlumberger M, Elisei R, Habra MA, Kiyota N, Paschke R, et al. Exploratory analysis of biomarkers associated with clinical outcomes from the study of lenvatinib in differentiated cancer of the thyroid. *Euro J Cancer* (2017) 75:213. doi: 10.1016/j.ejca.2017.01.013

13. Brose MS, Cabanillas ME, Cohen EE, Wirth LJ, Riehl T, Yue H, et al. Vemurafenib in patients with BRAFV600E-positive metastatic or unresectable papillary thyroid cancer refractory to radioactive iodine: A non-randomised, multicentre, open-label, phase 2 trial. *Lancet Oncol* (2016) 17:1272–82. doi: 10.1016/S1470-2045(16)30166-8

14. Argiris A, Agarwala SS, Karamouzis MV, Burmeister LA, Carty SE. A phase II trial of doxorubicin and interferon alpha 2b in advanced, non-medullary thyroid cancer. *Invest New Drug* (2008) 26:183–8. doi: 10.1007/s10637-007-9091-2

15. Jarzab B, Dedecjus M, Handkiewicz-Junak D, Lange D, Lewiński A, Nasierowska-Guttmejer A, et al. Diagnostics and treatment of thyroid carcinoma. *Endokrynol Pol* (2016) 67(1):74–107. 10.5603/EP.2016.0011

16. Zeng XX, Zhang WW, Ji LQ, Li G, Wang YG, Hao SS, et al. Efficacy and safety of radioiodine-refractory differentiated thyroid cancer with regional lymph node or distant metastasis treated with 125I seed implantation. *Xian Dai Zhong Liu Yi Xue* (2020) 28:4256–61. doi: 10.3969/j.issn.1672-4992.2020.24.009

frontiers | Frontiers in Oncology

TYPE Case Report
PUBLISHED 07 December 2022
DOI 10.3389/fonc.2022.1029282

OPEN ACCESS

EDITED BY
Kohei Fujita,
National Hospital Organization Kyoto Medical Center, Japan

REVIEWED BY
Weihua Li,
Chinese Academy of Medical Sciences and Peking Union Medical College, China
Li Ma,
Beijing Chest Hospital, Capital Medical University, China

*CORRESPONDENCE
Wei Li
leewluck@gmail.com

SPECIALTY SECTION
This article was submitted to Thoracic Oncology, a section of the journal Frontiers in Oncology

RECEIVED 27 August 2022
ACCEPTED 23 November 2022
PUBLISHED 07 December 2022

CITATION
Yang MH, Yu J, Cai CL and Li W (2022) Small cell lung cancer transformation and tumor heterogeneity after sequential targeted therapy and immunotherapy in EGFR-mutant non-small cell lung cancer: A case report. *Front. Oncol.* 12:1029282. doi: 10.3389/fonc.2022.1029282

Small cell lung cancer transformation and tumor heterogeneity after sequential targeted therapy and immunotherapy in EGFR-mutant non-small cell lung cancer: A case report

Meng-Hang Yang, Jia Yu, Chen-Lei Cai and Wei Li*

Department of Oncology, Shanghai Pulmonary Hospital, School of Medicine, Tongji University, Shanghai, China

Background: Histological transformation from non-small cell lung cancer (NSCLC) to small cell lung cancer (SCLC) is one of mechanisms of the acquired resistance to epidermal growth factor receptor (EGFR)-tyrosine kinase inhibitors (TKI). However, SCLC transformation and tumor heterogeneity have never been reported in sequential targeted therapy and immunotherapy.

Case presentation: Here, we described a patient with advanced EGFR-mutant NSCLC, who received erlotinib and underwent the resistance with EGFR T790M (−). The patient then received chemotherapy plus immunotherapy of programmed cell death 1 (PD-1) inhibitor, encountered progression with pathological transformation from NSCLC to SCLC that was overcome by chemotherapy of etoposide plus carboplatin (EC) with the main lesion significantly shrinking while metastatic nodules increasing. The pathology of the metastatic nodule showed NSCLC with EGFR T790M (+). Based on the tumor heterogeneity, EC chemotherapy combined with osimertinib was used, and patients responded well. The patient experienced four lung biopsies in all, which helped to provide the patient with precise treatment.

Conclusions: This case suggested that SCLC transformation and tumor heterogeneity should be paid attention to when disease progression occurred in advanced NSCLC whether receiving targeted therapy or immunotherapy.

KEYWORDS

histologic transformation, tumor heterogeneity, immunotherapy, targeted therapy, case report

Background

Lung cancer is one of malignant tumors with highest incidence and mortality rate. Non-small cell lung cancer (NSCLC) accounts for about 80~85% of all lung cancer. In NSCLC with epidermal growth factor receptor (EGFR) mutations treated with EGFR-tyrosine kinase inhibitor (TKI), there is a rare phenomenon of drug resistance, that is pathological type transformation. The transformation to small cell lung cancer (SCLC) is one of the important mechanisms of resistance to EGFR-TKI. In fact, it is found that SCLC transformed from NSCLC has similar clinical characteristics with primary SCLC. For patients with SCLC transformation, chemotherapy is short-term effective, and the prognosis is poor with the median overall survival (OS) less than 1 year (1, 2).

With the increase of re-biopsy in clinical practice, SCLC transformation is found to be not limited to specific molecular subtypes of NSCLC, nor to specific treatment. Immunotherapy is increasingly used in advanced lung cancer. However, the transformation of NSCLC to SCLC during immunotherapy has only been reported in a few cases (3–5). Here, we described a rare case of an advanced NSCLC patient with EGFR exon 19 deletion (19del) who has received sequential targeted therapy and immunotherapy of programmed cell death 1 (PD-1) inhibitor, and undergone a pathological transformation from NSCLC to SCLC and inconsistent gene status that revealed tumor heterogeneity. We presented this case in accordance with the CARE guideline (6).

Case presentation

A 50-year-old man was admitted to our hospital on Feb 19th, 2019, complaining of recurrent dry cough for 3 weeks. He had a smoking history of half pack per day for 20 years. Physical examination discovered that one of the left supraclavicular lymph nodes was enlarged. Chest computed tomography (CT) scan showed a mass in the upper lobe of the right lung accompanied by multiple small nodules in both lungs, enlarged mediastinal and hilum lymph nodes (Figure 1A, B). Enhanced brain magnetic resonance imaging (MRI) showed a lesion in the cerebellum that tended to be tumor metastasis. Bone scan and abdomen B-ultrasound showed no active findings. We performed biopsies of both the enlarged left supraclavicular lymph node and the right upper lobe (RUL) lesion. The pathology results indicated lung adenocarcinoma (Figure 1C), and the genetic testing found EGFR 19del mutation. The patient was diagnosed with right upper lobe lung adenocarcinoma T4N3M1b-Stage IVA (brain, contralateral lung, pleura) with EGFR 19del. Erlotinib as the first-line therapy was given, and the best response was partial response (PR) (Figure 1D). The progression-free survival (PFS) of first-line therapy was 6.5 months.

Then the patient underwent progressive disease (PD) (Figure 2A). A repeat biopsy of RUL lesion revealed lung adenocarcinoma (Figure 2B) with EGFR 19del, T790M (–) and programmed death ligand 1 (PD-L1) tumor proportion score (TPS) 90% (+). The patient participated in a phase III clinical study (JS001-CT25-III-NSCLC), and received 6 cycles of PD-1 inhibitor (toripalimab) plus pemetrexed and carboplatin, followed by 2 cycles of toripalimab plus pemetrexed as maintenance treatment. PR was achieved again (Figure 2C). The PFS of second-line therapy was 6.6 months.

Then the patient experienced the second PD (Figures 3A–C), and the third biopsy of RUL lesion was performed. Unexpectedly, histologic analysis showed a transformation to SCLC (Figure 3D) with immunohistochemical staining confirmed as Syn (+) and Ki-67 (70%+). Then, the patient received the treatment of etoposide plus carboplatin (EC). After 2 cycles of EC chemotherapy (PFS 1.9 months), the main lesion located in RUL significantly shrank (Figure 3E), however, the intrapulmonary metastatic nodules increased and enlarged (Figures 3E–G).

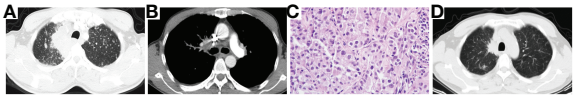

FIGURE 1
Chest CT scan of baseline **(A, B)**, pathological examination (H&E stain) showing lung adenocarcinoma **(C)** and chest CT scan of best response PR after the treatment of Erlotinib **(D)**. CT, computed tomography; PR, partial response.

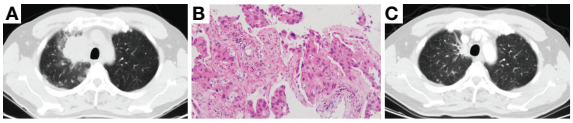

FIGURE 2
Chest CT scan of PD resistant to erlotinib **(A)**, photomicrograph of re-biopsy (H&E stain) showing lung adenocarcinoma **(B)** and chest CT scan of best response PR after the treatment of chemotherapy combined with PD-1 inhibitor **(C)**. CT, computed tomography; PD, progressive disease; PR, partial response; PD-1, programmed cell death 1.

Abbreviations: NSCLC, Non-small cell lung cancer; SCLC, Small cell lung cancer; EGFR, Epidermal growth factor receptor; TKI, Tyrosine kinase inhibitors; PD-1, Programmed cell death 1; EC, Etoposide plus carboplatin; OS, Overall survival; CT, Computed tomography; MRI, Magnetic resonance imaging; RUL, Right upper lobe; PR, Partial response; PD-L1, Programmed death ligand 1; TPS, Tumor proportion score; PD, Progressive disease; MDT, Multi-disciplinary team; RLL, Right lower lobe.

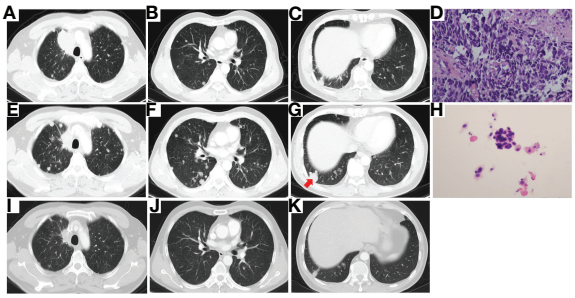

FIGURE 3
Chest CT scan of PD after 8 cycles of chemotherapy combined with PD-1 inhibitor **(A–C)**, photomicrograph of the third biopsy (H&E stain) showing SCLC transformation **(D)**, Chest CT scan after 2 cycles of EC chemotherapy showing the main lesion of RUL significantly shrank **(E)**, while intrapulmonary metastatic nodules increased and enlarged **(F, G)**, the pathology (H&E stain) of the enlarged metastatic lesion of RLL (*red arrow*) showing NSCLC **(H)**, and chest CT scan of PR after 2 cycles of combination therapy of osimertinib and EC chemotherapy **(I–K)**. CT, computed tomography; PD, progressive disease; PD-1, programmed cell death 1; SCLC, small cell lung cancer; EC, etoposide plus carboplatin; RUL, right upper lobe; RLL, right lower lobe; NSCLC, non-small cell lung cancer; PR, partial response.

To find out the reasons for the inconsistent response of different lesions to EC chemotherapy, we performed a needle aspiration of an enlarged metastatic lesion in the right lower lobe (RLL). The pathological results revealed NSCLC (Figure 3H) with the genetic testing showing EGFR 19del and T790M (+). Considering the heterogeneity of tumor, after comprehensive discussion of multi-disciplinary team (MDT), the patient began to receive EC chemotherapy combined with the 3rd-generation of EGFR-TKI, osimertinib. Encouragingly, after 2 cycles of combination therapy, the main lesion in RUL continued to shrink (Figure 3I), and the metastatic nodules in both lungs decreased significantly (Figure 3J,K). PR was achieved again. The patient well tolerated with the treatment. He then returned to the local hospital for subsequent treatment. The timeline of the treatment process is shown in Figure 4.

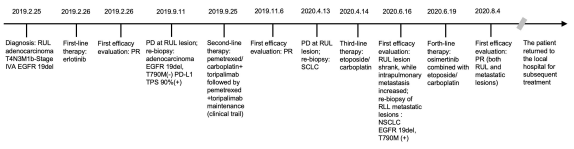

FIGURE 4
Timeline of the patient. RUL, right upper lobe; EGFR, epidermal growth factor receptor; PR, partial response; PD, progressive disease; PD-L1, programmed death ligand 1; TPS, tumor proportion score; SCLC, small cell lung cancer; RLL, right lower lobe; NSCLC, non-small cell lung cancer.

Discussion and conclusions

SCLC transformation has been recognized as one of mechanisms of resistance to EGFR-TKI in advanced lung adenocarcinoma with EGFR mutant, accounting for 5%~15% of the causes of EGFR-TKI resistance (7, 8). In contrast, transformation of NSCLC to SCLC was less reported in patients receiving immunotherapy like PD-1 inhibitors. Imakita et al. (3) reported SCLC transformation during immunotherapy with nivolumab. Abdallah et al. (4) reported two cases of potential histologic transformation of NSCLC to SCLC during the treatment of nivolumab and pembrolizumab, respectively. Iams et al. (5) described two cases of SCLC transformation as a mechanism of resistance to nivolumab in KRAS-mutant lung adenocarcinoma. However, the SCLC transformation after targeted therapy followed by immunotherapy has not been reported so far.

The precise mechanism of SCLC transformation in this case was considered from the following aspects. Firstly, it is supposed that there were two histological components of NSCLC and SCLC in the initial tumors before diagnosis, according to the heterogeneity of tumor. Approximately 5%~28% of SCLC contains NSCLC or other pathological components, which was called combined SCLC (9). Some researchers believe that tumor samples from lung biopsy when initial NSCLC diagnosis are insufficient, so the existence of a very low proportion of SCLC components cannot be detected, which is due to the limitations of the existing examination methods and technology (10). As the number of EGFR-mutant NSCLC cells decreased owing to targeted therapy of EGFR-TKI, the SCLC component of initial tumor became dominant. If the initial tumor contained both NSCLC and SCLC components, SCLC components would proliferate and reach PD rapidly after TKI effectively inhibited EGFR-mutant NSCLC components. However, the patient in this case had a relatively long remission and drug response period before SCLC transformation, the hypothesis of mixed histological components may not generalize the whole picture of this case.

Secondly, EGFR-TKI might be the cause of SCLC transformation in this case. The phenomenon of SCLC transformation was firstly described by Zakowski et al, 2006; they reported that a 45-year-old non-smoking female patient with adenocarcinoma received EGFR-TKI without gene analysis, underwent PD after 18 months and received re-biopsy suggesting a synaptophysin-positive SCLC with EGFR 19del (11). Since then, SCLC transformation was gradually recognized and was considered to be one of mechanisms of EGFR-TKI resistance. The transformation of NSCLC to SCLC often occurs 13~18 months after targeted therapy (1, 2, 12). The patients often retain the original EGFR mutation, but the expression of EGFR protein decreases and patients are no longer sensitive to the original TKI treatment (13). The biological behavior of SCLC transformation is similar to that

of primary SCLC. Genomic analysis revealed that TP53 and RB1 mutation existed in most SCLC transformation (1, 14). Compared with primary SCLC, patients with SCLC transformation are younger; the proportion of non-smokers or light smokers is higher; the incidences of men and women are similar (1). At present, there is a lack of standard treatment options for SCLC transformation, and chemotherapy of etoposide and platinum for primary SCLC is the mostly used treatment option, which is usually short-term effective. After the transformation of NSCLC to SCLC, the median PFS is around 3.5 months and the median OS is about 10 months (1, 2, 12, 15). There was no significant difference of PFS and OS after SCLC transformation between patients initially receiving the 1st- or 2nd-generation of TKI and the 3rd-generation of TKI (2). In the current case, resistance to 1st-generation TKI occurred 7 months after diagnosis; then the patients received chemotherapy and immunotherapy and SCLC transformation occurred about 7 months later. The transformation period was not consistent with the transformation after TKI resistance mentioned above. The patient in this case acquired EGFR T790M mutation after SCLC transformation, which is different from patients suffering transformation of NSCLC to SCLC after EGFR-TKI treatment retaining the original EGFR mutation.

Additionally, it is hypothesized that NSCLC in this case underwent histological transformation to SCLC owing to immunotherapy of PD-1 inhibitor. Although the mechanism for this is unclear, some theories support this hypothesis. The existence of cancer stem cells, being related to the differentiation and proliferation of cancer cells, were supposed to have ability to differentiate into either SCLC or NSCLC (16–20). Lung adenocarcinoma and SCLC were found to have the potential shared cell of origin. Alveolar type II cells were always believed to be the origin of lung adenocarcinoma. Surprisingly, it was reported that alveolar type II cells could also led to the development of SCLC when targeted disrupting of TP53 and RB1 (21, 22). In this case, it was regrettable that the patient did not undergo next-generation sequencing (NGS) tests. Although the information about TP53 and RB1 mutations at diagnosis was not collected, the possibility that immunotherapy led to alveolar type II cells induced SCLC transformation by changing the tumor microenvironment cannot be excluded.

In summary, we reported a case of a 50-year-old man with EGFR 19del advanced NSCLC, who showed a favorable response to the first-line erlotinib with PR, overcame the resistance to erlotinib with EGFR T790M (–) by a combination of pemetrexed and carboplatin plus PD-1 inhibitor and achieved PR, overcame progression and histologic transformation from NSCLC to SCLC by EC chemotherapy with the main lesion significantly shrinking while metastatic nodules increasing. The pathology of the metastatic nodule showed NSCLC with EGFR T790M (+), which revealed the heterogeneity of tumor. Finally, EC chemotherapy combined with osimertinib was used, and patients responded well. Transformation of NSCLC to SCLC is a result of tumor evolution during the anti-tumor treatment. Although SCLC transformation after immunotherapy is very rare, and its exact molecular mechanism is still under study, it should be paid attention to when disease progression occurred during immunotherapy. Chemotherapy of etoposide and platinum is the common treatment for SCLC transformation, but more effective strategies are need to be explored. What's more, re-biopsy played a key role in this case, which provided the patient with precise treatment. Therefore, this case suggested that, based on the consideration of tumor evolution and tumor heterogeneity, re-biopsy is of great significance, which could bring more benefits to patients.

Data availability statement

The original contributions presented in the study are included in the article/supplementary material. Further inquiries can be directed to the corresponding author.

Ethics statement

The studies involving human participants were reviewed and approved by Medical Ethics Committee of Shanghai Pulmonary Hospital. The patients/participants provided their written informed consent to participate in this study. Written informed consent was obtained from the individual(s) for the publication of any potentially identifiable images or data included in this article.

Author contributions

M-HY and WL was involved in the drafting and preparation of the manuscript, JY and C-LC were involved in the editing and fact checking of the manuscript. All authors contributed to the article and approved the submitted version.

Funding

This study was supported by grants from National Natural Science Foundation of China (82074065 and 81602618).

Conflict of interest

The authors declare that the research was conducted in the absence of any commercial or financial relationships that could be construed as a potential conflict of interest.

Publisher's note

References

1. Marcoux N, Gettinger SN, O'Kane G, Arbour KC, Neal JW, Husain H, et al. EGFR-mutant adenocarcinomas that transform to small-cell lung cancer and other neuroendocrine carcinomas: Clinical outcomes. *J Clin Oncol* (2019) 37(4):278–85. doi: 10.1200/JCO.18.01585

2. Wang W, Xu C, Chen H, Jia J , Wang L , Feng H, et al. Genomic alterations and clinical outcomes in patients with lung adenocarcinoma with transformation to small cell lung cancer after treatment with EGFR tyrosine kinase inhibitors: A multicenter retrospective study. *Lung Cancer* (2021) 155:20–7. doi: 10.1016/j.lungcan.2021.03.006

3. Imakita T, Fujita K, Kanai O, Terashima T, Mio T. Small cell lung cancer transformation during immunotherapy with nivolumab: A case report. *Respir Med Case Rep* (2017) 21:52–5. doi: 10.1016/j.rmcr.2017.03.019

4. Abdallah N, Nagasaka M, Abdulfatah E, Shi D , Wozniak AJ , Sukari A. Non-small cell to small cell lung cancer on PD-1 inhibitors: Two cases on potential histologic transformation. *Lung Cancer (Auckl)* (2018) 9:85–90. doi: 10.2147/LCTT.S173724

5. Iams WT, Beckermann KE, Almodovar K, Hernandez J, Vnencak-Jones C, Lim LP, et al. Small cell lung cancer transformation as a mechanism of resistance to PD-1 therapy in KRAS-mutant lung adenocarcinoma: A report of two cases. *J Thorac Oncol* (2019) 14(3):e45–8. doi: 10.1016/j.jtho.2018.11.031

6. Riley DS, Barber MS, Kienle GS, Aronson JK, von Schoen-Angerer T, Tugwell P, et al. CARE guidelines for case reports: explanation and elaboration document. *J Clin Epidemiol* (2017) 89:218–35. doi: 10.1016/j.jclinepi.2017.04.026

7. Lee JK, Lee J, Kim S, Kim S , Youk J , Park S, et al. Clonal history and genetic predictors of transformation into small-cell carcinomas from lung adenocarcinomas. *J Clin Oncol* (2017) 35:3065–74. doi: 10.1200/JCO.2016.71.9096

8. Oser MG, Niederst MJ, Sequist LV, Engelman JA. Transformation from non-small-cell lung cancer to small-cell lung cancer: Molecular drivers and cells of origin. *Lancet Oncol* (2015) 16:e165–72. doi: 10.1016/S1470-2045(14)71180-5

9. Qin J, Lu H. Combined small-cell lung carcinoma. *Onco Targets Ther* (2018) 11:3505–11. doi: 10.2147/OTT.S159057

10. Levacq D, D'Haene N, de Wind R, Remmelink M , Berghmans T. Histological transformation of ALK rearranged adenocarcinoma into small cell lung cancer: A new mechanism of resistance to ALK inhibitors. *Lung Cancer* (2016) 102:38–41. doi: 10.1016/j.lungcan.2016.10.012

11. Zakowski MF, Ladanyi M, Kris MG. Memorial Sloan-Kettering cancer center lung cancer OncoGenome group. EGFR mutations in small-cell lung cancers in patients who have never smoked. *N Engl J Med* (2006) 355(2):213–5. doi: 10.1056/NEJMc053610

12. Yu HA, Arcila ME, Rekhtman N, Sima CS, Zakowski MF, Pao W, et al. Analysis of tumor specimens at the time of acquired resistance to EGFR-TKI therapy in 155 patients with EGFR-mutant lung cancers. *Clin Cancer Res* (2013) 19 (8):2240–7. doi: 10.1158/1078-0432.CCR-12-2246

13. Niederst MJ, Sequist LV, Poirier JT, Mermel CH, Lockerman EL, Garcia AR, et al. RB loss in resistant EGFR mutant lung adenocarcinomas that transform to small-cell lung cancer. *Nat Commun* (2015) 6:6377. doi: 10.1038/ncomms7377

14. Santoni-Rugiu E, Grauslund M, Melchior LC, Costa JC, Sørensen JB, Urbanska EM. Heterogeneous resistance mechanisms in an EGFR exon 19-mutated non-small cell lung cancer patient treated with erlotinib: Persistent FGFR3-mutation, localized transformation to EGFR-mutated SCLC, and acquired T790M EGFR-mutation. *Lung Cancer* (2017) 113:14–7. doi: 10.1016/j.lungcan.2017.08.024

15. Lin JJ, Langenbucher A, Gupta P, Yoda S, Fetter IJ, Rooney M, et al. Small cell transformation of ROS1 fusion-positive lung cancer resistant to ROS1 inhibition. *NPJ Precis Oncol* (2020) 4:21. doi: 10.1038/s41698-020-0127-9

16. Mainardi S, Mijimolle N, Francoz S, Vicente-Dueñas C, Sánchez-García I, Barbacid M. Identification of cancer initiating cells in K-ras driven lung adenocarcinoma. *Proc Natl Acad Sci USA* (2014) 111:255–60. doi: 10.1073/pnas.1320383110

17. Desai TJ, Brownfield DG, Krasnow MA. Alveolar progenitor and stem cells in lung development, renewal and cancer. *Nature* (2014) 507:190–94. doi: 10.1038/nature12930

18. Chang KJ, Yin JZ, Huang H, Li B, Yang MH. Arsenic trioxide inhibits the growth of cancer stem cells derived from small cell lung cancer by downregulating stem cell-maintenance factors and inducing apoptosis *via* the hedgehog signaling blockade. *Transl Lung Cancer Res* (2020) 9(4):1379–96. doi: 10.21037/tlcr-20-467

19. Yang MH, Li B, Chang KJ. Notch pathway inhibition mediated by arsenic trioxide depletes tumor initiating cells in small cell lung cancer. *Mol Biol Rep* (2022) 49(3):2245–53. doi: 10.1007/s11033-021-07046-w

20. Sutherland KD, Song JY, Kwon MC, Proost N, Zevenhoven J, Berns A. Multiple cells-of-origin of mutant K-ras-induced mouse lung adenocarcinoma. *Proc Natl Acad Sci USA* (2014) 111:4952–57. doi: 10.1073/pnas.1319963111

21. Sutherland KD, Proost N, Brouns I, Adriaensen D, Song JY, Berns A. Cell of origin of small cell lung cancer: inactivation of Trp53 and Rb1 in distinct cell types of adult mouse lung. *Cancer Cell* (2011) 19:754–64. doi: 10.1016/j.ccr.2011.04.019

22. Park KS, Liang MC, Raiser DM, Zamponi R, Roach RR, Curtis SJ, et al. Characterization of the cell of origin for small cell lung cancer. *Cell Cycle* (2011) 10:2806–15. doi: 10.4161/cc.10.16.17012

frontiers | Frontiers in Oncology

TYPE Case Report
PUBLISHED 15 December 2022
DOI 10.3389/fonc.2022.1089108

OPEN ACCESS

EDITED BY
Kohei Fujita,
National Hospital Organization Kyoto Medical Center, Japan

REVIEWED BY
Qiaoyun Tan,
Huazhong University of Science and Technology, China
Giuseppa Scandurra,
Cannizzaro Hospital, Italy

*CORRESPONDENCE
Quentin Dominique Thomas
quentin.thomas@icm.unicancer.fr

SPECIALTY SECTION
This article was submitted to Thoracic Oncology, a section of the journal Frontiers in Oncology

RECEIVED 08 November 2022
ACCEPTED 01 December 2022
PUBLISHED 15 December 2022

CITATION
Thomas QD, Colard-Thomas J, Delansay D, Leenhardt F, Solassol J, Vendrell JA and Quantin X (2022) Case report: Liquid biopsy, the sooner the better?
Front. Oncol. 12:1089108.
doi: 10.3389/fonc.2022.1089108

Case report: Liquid biopsy, the sooner the better?

Quentin Dominique Thomas[1,2*], Julien Colard-Thomas[1], Delphine Delansay[1], Fanny Leenhardt[2,3], Jerome Solassol[4], Julie A. Vendrell[4] and Xavier Quantin[1,2]

[1]Department of Medical Oncology, Montpellier Cancer Institute (ICM), Montpellier, France, [2]Oncogenic Pathways in Lung Cancer, Montpellier Cancer Research Institute (IRCM), University of Montpellier (UM), Montpellier, France, [3]Pharmacy department, Montpellier Cancer institute (ICM), Montpellier, France, [4]Department of Pathology, Montpellier University Hospital (CHU) Montpellier, Arnaud de Villeneuve Hospital, Montpellier, France

The detection of circulating tumor DNA (ctDNA) by liquid biopsy is taking an increasing role in thoracic oncology management due to its predictive and prognostic value. For non-small cell lung cancer, it allows the detection of molecular mutations that can be targeted with tyrosine kinase inhibitors (TKIs). We report the case of a patient with life-threatening hepatocellular failure and thrombotic microangiopathy at the diagnosis. A salvage chemotherapy was attempted, resulting in a major worsening of her general condition and the decision to stop all anti-cancer treatment. The liquid biopsy performed at the time of immunohistochemical non-small cell lung cancer diagnosis revealed within 7 days the presence of an epidermal growth factor receptor (*EGFR)*^{DEL19} activating mutation with 736,400 DNA copies/ml of plasma. It was finally decided to attempt a treatment with osimertinib (third generation anti-EGFR TKI) despite the fact that the patient was in a pre-mortem situation. Osimertinib led to a significant and prompt improvement of her performance status after only one week of treatment. The tumor tissue genotyping performed by next-generation sequencing (NGS) was available 10 days after starting TKI treatment. It revealed in addition to the *EGFR*^{DEL19} mutation, a *JAK3* and *EGFR* amplification, highlighting the complex interactions between EGFR and the JAK/STAT signaling pathways. The first CT-scan performed after 2 months under osimertinib showed a tumor morphologic partial response. The biological assay showed a major decrease in the *EGFR*^{DEL19} mutation ctDNA levels (40.0 copies/ml). The liquid biopsy allowed an early implementation of a targeted therapy without which the patient would probably be dead. Testing for ctDNA should be discussed routinely at diagnosis in addition to tumor tissue genotyping for patient with metastatic non-small cell lung cancer that raise the clinical profile of oncogenic addiction.

KEYWORDS

lung cancer, ctDNA = circulating tumor DNA, liquid biopsy, EGFR, thrombotic microangiopathy (TMA), osimertinib

Introduction

Oncogenic activating mutations are common for patients with a non-small cell lung cancer (NSCLC) benefiting from treatment by targeted therapies (1). Systematic molecular and biomarker analysis is performed at diagnosis. It is recommended, when feasible, that testing be carried out *via* a broad, panel-based approach, next-generation sequencing (NGS) in clinical laboratories. Testing failure often occurs due to the small size of tissue samples obtain *via* mini-invasive technics. A second clinical limitation is the delay in the delivery of molecular results, which in most cases takes around three weeks. In most clinical situations this delay is acceptable for optimal therapeutic decision making. However, in some clinical presentations where patients are life-threatening at diagnosis, a technology that allows a faster molecular testing may be necessary. Liquid biopsy offers a solution to these both challenges allowing results for circulating tumor DNA (ctDNA) within approximately one week. Detection of ctDNA guides therapy decisions and has recently been shown, in a large prospective cohort of 1,127 patients with NSCLC, to be associated with shorter survival (hazard ratio (HR), 2.05; 95% confidence interval (CI), 1.74-2.42; $P < 0.001$) independently of clinicopathologic features and metabolic tumor volume in a large prospective cohort of 1,127 patients with NSCLC (2).

Epidermal growth factor receptor (*EGFR*) activating mutations, such as exon 19 deletion ($EGFR^{DEL19}$) or the $EGFR^{L858R}$ mutation in exon 21, occur in 10-15% of Caucasian patients with NSCLC. For these patients with metastatic disease, specific tyrosine kinase inhibitors (TKIs) are recommended. Osimertinib, a third-generation *EGFR* TKI, has become the first-line standard of care for patients with *EGFR*-mutated NSCLC (3). We report the case of a patient with a life-threatening medical situation at diagnosis of NSCLC with severe hepatocellular failure and thrombotic microangiopathy for which liquid biopsy revealed an *EGFR* activating alteration. The detection of this mutation allowed us to rapidly initiate treatment with *EGFR* TKI, without which the patient would have died from complications of her cancer at diagnosis.

Case report

A 61-year-old female patient with no personal medical history except osteoporosis and no familial history of cancer; former smoker estimated at 2 packs/year presented in May 2022 severe and rapid deterioration in general condition resulting in severe asthenia associated with complete anorexia, nausea and epigastric pain. Clinical examination revealed a painful hepatomegaly without other clinical abnormality, and hepatic sonogram showed diffuse bilobar lesions.

On June 7, a computerized tomography (CT) scan showed diffuse hepatic lesions associated with multiple sus and sub-diaphragmatic lymphadenopathies, pleural effusion, diffuse bone and pulmonary lesions.

On June 15, a liver biopsy led to the diagnosis of a CK7+; CK20-; TTF1+; SATB2-; GATA 3- mucus-secreting carcinoma leading to the diagnosis of T1aN3M1c bronchopulmonary adenocarcinoma according to the 8th version of the TNM classification. Blood tests on June 17 revealed anemia with hemoglobin at 7.5 g/dL; international normalized ratio (INR) increase at 1.51; hepatic enzymes increase with gamma-glutamyltransferase at 458 U/L; alkaline phosphatase at 703 U/L; aspartate aminotransferase at 156 U/L; alanine aminotransferase at 129 U/L; total and conjugated bilirubin increase at respectively 56.9 µmol/L and 32.6 µmol/L. The suspicion of acute liver failure led to her hospitalization. Eastern Cooperative Oncology Group Performance Status (ECOG PS) was 3, oxygen was needed at 1-2 L/min. Viral serologies were negatives (Hepatitis B, Hepatitis C, HIV, Cytomegalovirus), there were no history of alcoholic intoxication or recent introduction of new medication explaining the hepatic perturbations. Treatment was initially postponed waiting for the results of tumor molecular biology, considering the high probability of an oncogenic driver for this patient former smoker under 5 packs/year. A liquid biopsy was realized on June 21 to research ctDNA alterations.

On June 22, following to appearance of encephalopathy due to hepatic failure it was decided to initiate salvage chemotherapy with weekly paclitaxel/carboplatin regimen. After 48 hours, the patient developed a massive hematoma in front of central venous catheter associated with clinical degradation and increase of oxygen need to 4 L/min. Blood tests revealed grade 3 according to common terminology criteria for adverse events v5.0 (CTCAE v5.0) platelet count decrease leading to an initial diagnosis of disseminated intravascular coagulation. Subsequent analysis revealed anemia, negative haptoglobin, and schizocytes on blood smear, rectifying the diagnosis of paraneoplastic thrombotic microangiopathy. A new CT-scan showed massive pleural and peritoneal effusion. This dramatic clinical and biological deterioration resulted in stopping antitumor treatment and focusing on best supportive care.

However, on June 27, the results of ctDNA performed on June 21 by digital droplet PCR (ddPCR) revealed the presence of an $EGFR^{DEL19}$ mutation with very high amount of copies (736,400 per mL of plasma). A last-ditch attempt was decided by initiating a TKI treatment with osimertinib 80 mg per day, first dose received on June 28 (Figure 1).

After one week of treatment, a clinical and biological improvement was observed with decrease of oxygen requirement, edemas, lactate dehydrogenase and INR. On July 4, a control of ctDNA showed a drastic drop to 3,763 copies of mutated DNA/mL of plasma. A second control was performed on July 12, finding 6,377 copies/mL for $EGFR^{DEL19}$ and a possible $EGFR^{T790M}$ resistance mutation at 4.0 copies/mL (Figure 1).

Clinically, oxygen was stopped on July 8, after 10 days of treatment with osimertinib. Molecular alterations were also

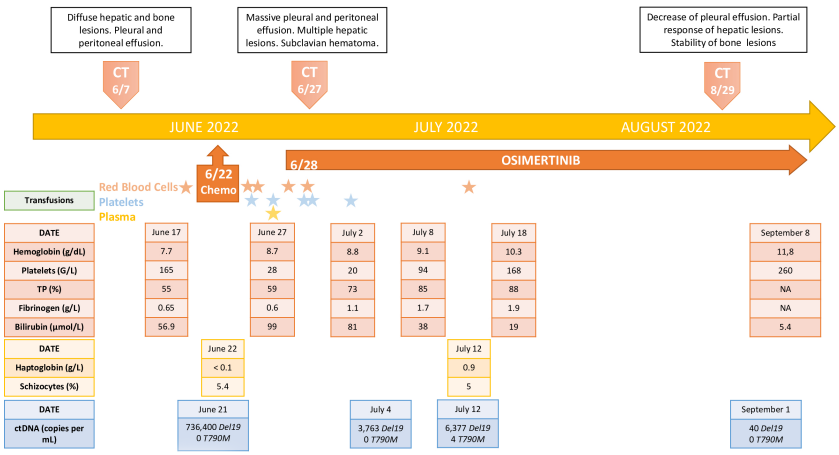

FIGURE 1
Timeline of the disease course.

investigated on the hepatic punctured tissue: the results came out on July 7. The NGS performed on tissue biopsy confirmed the presence of an *EGFR*$^{\text{DEL 19}}$ with a variant allele frequency of 88.45%. The NGS experiment also revealed the presence of an *EGFR* amplification with 10 copies of genes and a Janus Kinase 3 (*JAK3*) amplification with 14 copies of genes.

After three weeks of treatment by osimertinib associated with supportive care, the patient was able to return directly to her home without requiring a rehabilitation. After 2 months of treatment with osimertinib, the patient was clinically asymptomatic and has no side effects from the TKI. The CT-scan performed shows a partial morphological response according to RECIST1.1 criteria (Figure 2). Control of ctDNA rate revealed a residual value for the *EGFR*$^{\text{DEL19}}$ activating mutation (40.0 copies/mL) and the disappearance of the *EGFR*$^{\text{T790M}}$ mutation (Figure 1).

To date, after 5 months of full-dose treatment with osimertinib 80mg/day, the patient still has an excellent tolerance of the treatment with maintained efficacy.

Discussion

To the best of our knowledge, we present the case of a NSCLC EGFR-mutated patients with one of the highest levels of ctDNA reported in the literature (4). This patient who was ECOG PS 4 and in terminal phase of hepatocellular insufficiency and thrombotic microangiopathy improved clinically in 10 days (ECOG PS0) with a normalization of her biological results in 15 days under osimertinib. Clinical practice guidelines recommend treating patients with ECOG PS 3-4 with best supportive care. Patients with NSCLC with oncogenic addiction represent a particular population for which targeted therapies can be proposed even for ECOG PS 3-4 (5). This case report highlights the possibility of clinical improvement under TKI even in life-threatening situations. Several case series reports support this observation, showing that an invasive attitude can be beneficial for these patients. Indeed, patients intubated in intensive care units due to respiratory failure related to the disease or patients who require enteral feeding to administer TKI tablets benefit from the treatment with a clear recovery of their quality of life and a clear improvement of their survival (6) (7).

From a molecular point of view, this patient presents several characteristics that deserve to be discussed. In our center, we systematically search for gene copy number variation by NGS amplification technique performed on tumor tissue. This analysis identified in addition to the *EGFR*$^{\text{DEL 19}}$ mutation, an amplification of the *EGFR* gene as well as an amplification of the *JAK3* gene. *EGFR* amplification has been described identified as a potential mechanism of primary resistance to third generation-TKIs resistance (8). In addition, *EGFR* mutations can induce abnormal activation of the downstream JAK/STAT signaling pathway considered as one of the central communication nodes in the cell function. The JAK family consists of non-receptor tyrosine protein kinases with four main members (JAK 1-3 and TYK2). Dysregulation of the JAK/STAT pathway promote abnormal tumor proliferation, angiogenesis, invasion and metastasis (9). There are actually several clinical trials evaluating the role of JAK/STAT pathway inhibitors in NSCLC *EGFR*-mutated (Table 1).

Regarding ctDNA, complete clearance of the activating mutation under anti-*EGFR* TKI treatment has proven prognostic value. It is also a powerful tool for anticipating tumor relapse (10). Concomitant tissue detection of

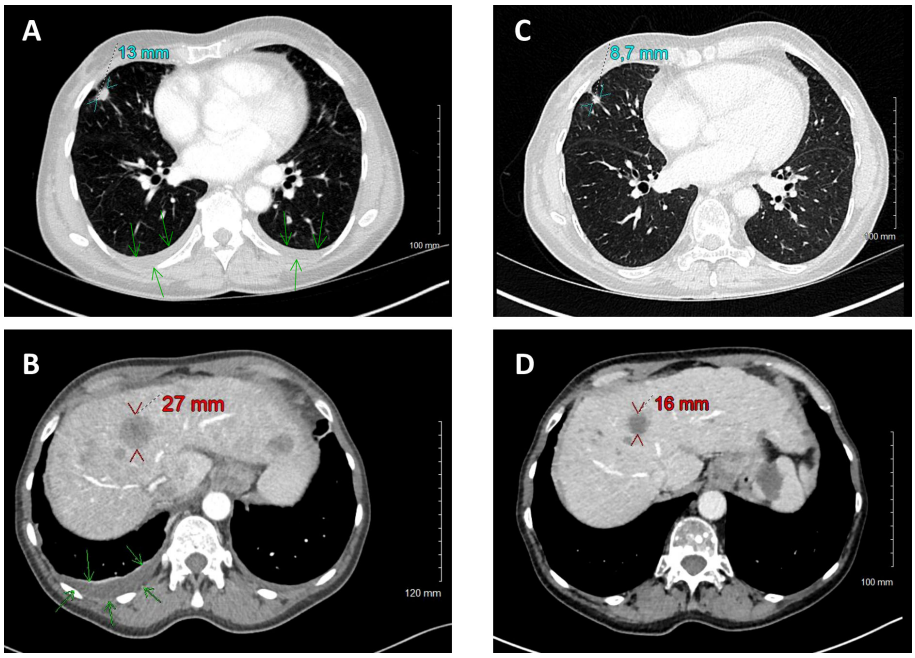

FIGURE 2
Comparison of CT scans before (June 7, **A**, **B**) and with osimertinib treatment (August 29, **C**, **D**). Size reduction of primary tumor (cyan) and target hepatic metastasis (red). Disparition of pleural effusion (green arrows).

preexisting *EGFR*^{T790M} associated with *EGFR* activating mutations is an event occurring in 1-5% of *EGFR*-NSCLC, conferring a worse prognosis value (11) (12). Liquid biopsy detection of a pre-existing *EGFR*^{T790M} mutation by ddPCR also appears to have prognostic value in the management of NSCLC patients (13). In our case, the detection of an *EGFR*^{T790M} mutation is probably a background noise inherent to the ddPCR technique. Indeed, the appearance of an *EGFR*^{T790M} mutation is not observed under osimertinib, whose mechanism of action precisely targets this mutation. This hypothesis is confirmed by the absence of detection of *EGFR*^{T790M} mutation after 2 months of treatment with osimertinib and the continued decrease in the ctDNA rate of the *EGFR*^{DEL19} mutation.

Interestingly, the number of copies of mutated ctDNA detected increased during the course of treatment by osimertinib and finally decreased secondarily. This observation led us to suspect an early resistance to osimertinib. The kinetics of the decrease of the ctDNA level after 2 months of treatment show us that this rebound of the ctDNA level is probably related to the loss of effectiveness of the chemotherapy carried out in first intention by paclitaxel/carboplatin regimen. Indeed, the chemotherapy probably had an anti-tumor activity associated with the treatment with osimertinib which contributed to the decrease of the *EGFR*^{DEL19} ctDNA level. This observation reinforces the importance of clinical trials combining chemotherapy with TKIs for NSCLC with oncogenic addiction (NCT04035486; NCT05200481).

Advantages and disadvantages of liquid biopsy in comparison to tissue biopsy for tumor genotyping in advanced or metastatic NSCLC can be summarized as follows: liquid biopsy present high concordance rate with tissue biopsy; the technique is faster repeatable over time and minimally invasive. Liquid biopsy better capture tumor heterogeneity and clonal evolution under treatment. However, liquid biopsy is less sensitive, does not allow the evaluation of non-DNA biomarkers, in particular the programmed death ligand-1 (PD-L1) status, which is fundamental in the decision of the therapeutic strategy in first metastatic line. It also increases costs if performed concurrently with tissue testing (14). Some complementary approaches of liquid biopsy including characterization of circulating tumor cells and tumor mutation burden may be a promising tool to help clinicians in therapeutic decision-making for advanced NSCLC (15). Liquid biopsy is an increasingly important tool in oncology. It provides prognostic information for curative patients (16). It is already a leading tool in the stratification of the therapeutic strategy for adjuvant chemotherapy for colorectal patients (17). One of the main challenges for liquid biopsy research in the coming years will be to optimize its use for the detection of early-stage neoplasms or tumor relapse by detecting a minimal residual disease. In this context, efforts are being made to improve the detection of smallest

TABLE 1 Published and ongoing trial evaluating inhibitors of JAK/STAT pathway for EGFR-mutated non-small cell lung cancer.

Drug regimens	ClinicalTrial.gov	Therapeutic line	Development stage	Patient included	Clinical outcomes
AZD4205 (JAK 1 inhibitor) + Osimertinib	NCT03450330	Activating EGFR mutation positive NSCLC and have failed prior EGFR TKIs treatment	Phase I/II Completed	10	Safety and tolerability
Ruxolitinib (JAK1 + JAK2 inhibitor) + Afatinib	NCT02145637	Disease progression after platinum doublet (all), EGFR TKI (if EGFR mutant), and crizotinib (if ALK positive)	Phase I Completed	30	- ORR: 23.3% (7PR/ 0CR) - DCR: 93.3% - PFS: 4.9months (95% CI, 2.4-7.5)
Itacitinib (JAK 1 inhibitor) + Osimertinib	NCT02917993	Progressed on or after treatment with an EGFR tyrosine kinase inhibitor (TKI). Additional lines of systemic therapy including investigational agents for locally advanced or metastatic NSCLC are allowed.	Phase I/II Active not recruting	59	Safety and tolerability ORR
Momelotinib (JAK1/2 and TANK-binding kinase 1 (TBK1) inhibitor) + Erlotinib	NCT02206763	Patients with EGFR TKI-naïve NSCLC	Phase I Completed	11	-ORR: 54.5% (90% CI 27.1-80.0) -PFS : 9.2 months (90% CI 6.2-12.4)
AZD1480 (JAK 2 inhibitor)	NCT01219543	Asian patients with advanced EGFR or ROS mutant NSCLC	Phase I Completed	47	Safety and tolerability

DCR, disease control rate; EGFR, Epidermal growth factor receptor; NSCLC, non-small cell lung cancer; JAK, Janus kinase; ORR, Objective response rate; PFS, Progression free survival; TKI, Tyrosine kinase inhibitor.

amounts of ctDNA in the "sea" of normal circulating free DNA. Ultrasensitives liquid biopsy technologies will probably be a prerequisite to implement liquid biopsy in these strategies (18).

We report here a rare situation of the added value of liquid biopsy. It provides faster information on molecular tumor alterations than tissue biopsy. This time saving can lead to propose earlier targeted therapy to NSCLC patients. Our opinion is that a liquid biopsy must be discussed routinely at the diagnosis of NSCLC in a complementary approach with tumor tissue genotyping.

Data availability statement

The original contributions presented in the study are included in the article/Supplementary Material. Further inquiries can be directed to the corresponding author.

Ethics statement

Written informed consent was obtained from the individual (s) for the publication of any potentially identifiable images or data included in this article.

Author contributions

QT: Conceptualization; Writing - Original Draft; Writing - Review & Editing; Visualization. JC-T: Writing - Original Draft; Writing - Review & Editing; Visualization. DD, FL, JS, JV, and XQ: Writing - Review & Editing; Supervision. All authors contributed to the article and approved the submitted version.

Conflict of interest

The authors declare that the research was conducted in the absence of any commercial or financial relationships that could be construed as a potential conflict of interest.

Publisher's note

References

1. Tan AC, Tan DSW. Targeted therapies for lung cancer patients with oncogenic driver molecular alterations. *J Clin Oncol Off J Am Soc Clin Oncol* (2022) 40(6):611–25. doi: 10.1200/JCO.21.01626

2. Jee J, Lebow ES, Yeh R, Das JP, Namakydoust A, Paik PK, et al. Overall survival with circulating tumor DNA-guided therapy in advanced non-small-cell lung cancer. *Nat Med* (2022) 28(11):2353–63. doi: 10.1038/s41591-022-02047-z

3. Soria JC, Ohe Y, Vansteenkiste J, Reungwetwattana T, Chewaskulyong B, Lee KH, et al. Osimertinib in untreated EGFR-mutated advanced non-Small-Cell lung cancer. *N Engl J Med* (2018) 378(2):113–25. doi: 10.1056/NEJMoa1713137

4. Krug AK, Enderle D, Karlovich C, Priewasser T, Bentink S, Spiel A, et al. Improved EGFR mutation detection using combined exosomal RNA and circulating tumor DNA in NSCLC patient plasma. *Ann Oncol Off J Eur Soc Med Oncol* (2018) 29 (3):700–6. doi: 10.1093/annonc/mdx765

5. Planchard D, Popat S, Kerr K, Novello S, Smit EF, Faivre-Finn C. Metastatic non-small cell lung cancer: ESMO clinical practice guidelines for diagnosis, treatment and follow-up. *Ann Oncol* (2018) 29(Suppl 4):iv192–iv237. doi: 10.1093/annonc/mdy275

6. Facchinetti F, Bordi P, Bini P, Bidin L, Camisa R, Tiseo M. Enteral administration of TKIs: Report of a response to ceritinib in an ALK-positive NSCLC patient and literature review. *Curr Drug Targets* (2018) 19(14):1649–56. doi: 10.2174/1389450119666180213102939

7. Thomas QD, Pautas M, Guilhaume MN, Fiteni F, Ge T, Girard N. Enteral administration of alectinib for ALK-positive non-small cell lung cancer in an elderly patient: A case report. *Med (Baltimore)* (2021) 100(43):e27611. doi: 10.1097/MD.0000000000027611

8. Suryavanshi M, Jaipuria J, Mattoo S, Dhandha S, Khatri M. Audit of molecular mechanisms of primary and secondary resistance to various generations of tyrosine kinase inhibitors in known epidermal growth factor receptor-mutant non-small cell lung cancer patients in a tertiary centre. *Clin Oncol R Coll Radiol G B* (2022) 34(11): e451–e462. doi: 10.1016/j.clon.2022.06.003

9. Hu X, Li J, Fu M, Zhao X, Wang W. The JAK/STAT signaling pathway: from bench to clinic. *Signal Transduct Target Ther* (2021) 6(1):402. doi: 10.1038/s41392-021-00791-1

10. Remon Masip J, Besse B, Ponce Aix S, Callejo A, Al-rabi K, Bernabe Caro R. Annals of oncology. *Ann Oncol* (2022) 33(suppl_7):S808–69. doi: 10.1016/annonc/annonc1089

11. Li H, Hu H, Wang R, Pan Y, Wang L, Li Y, et al. Primary concomitant EGFR T790M mutation predicted worse prognosis in non-small cell lung cancer patients. *OncoTargets Ther* (2014) 7:513–24. doi: 10.2147/OTT.S60122

12. Ding D, Yu Y, Li Z, Niu X, Lu S. The predictive role of pretreatment epidermal growth factor receptor T790M mutation on the progression-free survival of tyrosine-kinase inhibitor-treated non-small cell lung cancer patients: a meta-analysis. *OncoTargets Ther* (2014) 7:387–93. doi: 10.2147/OTT.S58870

13. Vendrell JA, Mazieres J, Senal R, Rouquette I, Quantin X, Pujol JL, et al. Ultra-sensitive EGFR T790M detection as an independent prognostic marker for lung cancer patients harboring EGFR del19 mutations and treated with first-generation TKIs. *Clin Cancer Res Off J Am Assoc Cancer Res* (2019) 25(14):4280–9. doi: 10.1158/1078-0432.CCR-18-2683

14. Rolfo C, Mack P, Scagliotti GV, Aggarwal C, Arcila ME, Barlesi F, et al. Liquid biopsy for advanced NSCLC: A consensus statement from the international association for the study of lung cancer. *J Thorac Oncol* (2021) 16(10):1647–62. doi: 10.1016/j.jtho.2021.06.017

15. Sinoquet L, Jacot W, Quantin X, Alix-Panabières C. Liquid biopsy and immuno-oncology for advanced nonsmall cell lung cancer. *Clin Chem* (2022), hvac166. doi: 10.1093/clinchem/hvac166

16. Pellini B, Chaudhuri AA. Circulating tumor DNA minimal residual disease detection of non-Small-Cell lung cancer treated with curative intent. *J Clin Oncol Off J Am Soc Clin Oncol* (2022) 40(6):567–75. doi: 10.1200/JCO.21.01929

17. Tie J, Cohen JD, Lahouel K, Lo SN, Wang Y, Kosmider S, et al. Circulating tumor DNA analysis guiding adjuvant therapy in stage II colon cancer. *N Engl J Med* (2022) 386(24):2261–72. doi: 10.1056/NEJMoa2200075

18. Alix-Panabières C, Klaus P. Liquid biopsy: From discovery to clinical application. *Cancer Discovery* (2021) 11(4):858–73. doi: 10.1158/2159-8290.CD-20-1311

frontiers | Frontiers in Oncology

TYPE Case Report
PUBLISHED 22 December 2022
DOI 10.3389/fonc.2022.1074821

OPEN ACCESS

EDITED BY
Kohei Fujita,
National Hospital Organization Kyoto Medical Center, Japan

REVIEWED BY
Shilpa Rao,
National Institute of Mental Health and Neurosciences (NIMHANS), India
Marcello Migliore,
University of Catania, Italy

*CORRESPONDENCE
Xiaodong Jiang
xd1981@sohu.com

SPECIALTY SECTION
This article was submitted to Thoracic Oncology, a section of the journal Frontiers in Oncology

RECEIVED 27 October 2022
ACCEPTED 08 December 2022
PUBLISHED 22 December 2022

CITATION
Gong D, Yu J and Jiang X (2022) Case report: Rare intrapulmonary malignant mesothelioma complicated with myositis. *Front. Oncol.* 12:1074821. doi: 10.3389/fonc.2022.1074821

Case report: Rare intrapulmonary malignant mesothelioma complicated with myositis

Dandan Gong, Jian Yu and Xiaodong Jiang*

Department of Critical Care Medicine, the Second Hospital of Dalian Medical University, Dalian, Liaoning, China

Malignant pleural mesothelioma is an uncommon aggressive tumor. Its incidence is even lower when the lung parenchyma is the primary site. Myositis is a common paraneoplastic syndrome, but it rarely presents with malignant pleural mesothelioma. This report presents a rare intrapulmonary malignant mesothelioma complicated by cancer-associated myositis. The patient presented with limb muscle weakness as the first symptom and was diagnosed with intrapulmonary malignant mesothelioma complicated by cancer-associated myositis on the basis of clinical, histological, immunohistochemical, and radiological findings. The patient responded poorly to conventional hormone therapy and died of respiratory failure within 2 months after the first presence of limb muscle weakness.

KEYWORDS

mesothelioma, cancer-associated myositis, oncology, lung parenchyma, primary

1 Introduction

Malignant mesothelioma is an aggressive tumor, associated with poor prognosis, which arises from the pleura, peritoneum, pericardium, or tunica vaginalis testis (1). Malignant pleural mesothelioma (MPM), which accounts for 90% of malignant mesothelioma cases (2), has proven to be a massive challenge for clinicians and scientists, with a median survival time of 9–12 months (3). MPM typically encases the lungs as a thick rind, and involvement of the lung parenchyma is rare. Here, we report a patient with myositis as a paraneoplastic syndrome with pulmonary parenchymal involvement.

2 Case description

A 66-year-old male presented to our hospital with a 1-month history of limb muscle weakness. He was an active smoker (20 cigarettes/day), had a family history of lung

cancer. He had a history of diabetes mellitus for 15 years, no history of cancer and immune checkpoint inhibitors therapy.He also had no exposure history of asbestos.

In March 2022, the patient presented with limb muscle weakness and subcutaneous edema without any apparent cause. He was admitted to Zhongshan Hospital, affiliated with Dalian Medical University, for acute ileus in April 2022. Chest computed tomography (CT) performed during hospitalization showed a space-occupying lesion in the right upper lobe. The patient was treated conservatively and discharged.

Furthermore, positron emission tomography-CT was performed in our hospital, which revealed a soft tissue density occupying the lesion and enlarged lymph nodes in the right lobe, measuring 26 mm and 18 mm in diameter, respectively. No abnormal uptake was observed at other sites, including the lungs and pleura (Figure 1). Thus, the tumor was considered a primary tumor.

The patient was admitted to our hospital for diagnosis. After admission,he was presented with progressive limb muscle weakness (lower extremities:grade 1-2,upper extremities:grade 3-4), expectorating sputum hardly and respiratory muscle weakness.And he was transferred from inpatient unit to the intensive care unit (ICU) because of acute respiration failure complicating severe pneumonia at a week after admission.

Blood cell counts were within normal ranges upon admission, but the admission laboratory tests revealed definite abnormalities: high aspartate aminotransferase (AST, 536.09 U/L), alanine aminotransferase (ALT, 11.23 U/L), creatine kinase (CK; 12919.26 U/L), and creatine kinase (CK)-MB (CK-MB, 140.12 U/L) levels. Moreover, the level of CA125 increased to 182.73 U/mL (normal, <30.2 U/ml), CYFRA21-1 to 6.11 ng/mL (normal, <3.3 ng/mL), and NSE to 82.89 (normal, <16.3 ng/mL). Without hormone therapy, the levels of ALT (102.74 U/L), AST (157.65 U/L), CK (2768.34 U/L), and CK-MB (24.07U/L) became normal after 5 days.

Percutaneous biopsy of the lung lesions guided by fusion CT was performed after admission (Figure 2). Photomicroscopy with hematoxylin and eosin staining revealed unusual epithelioid cells of the primary tumor. Immunohistochemically, the tumor cells were positive for calretinin, CK, p36, CK5/6, WT-1, and Ki-67

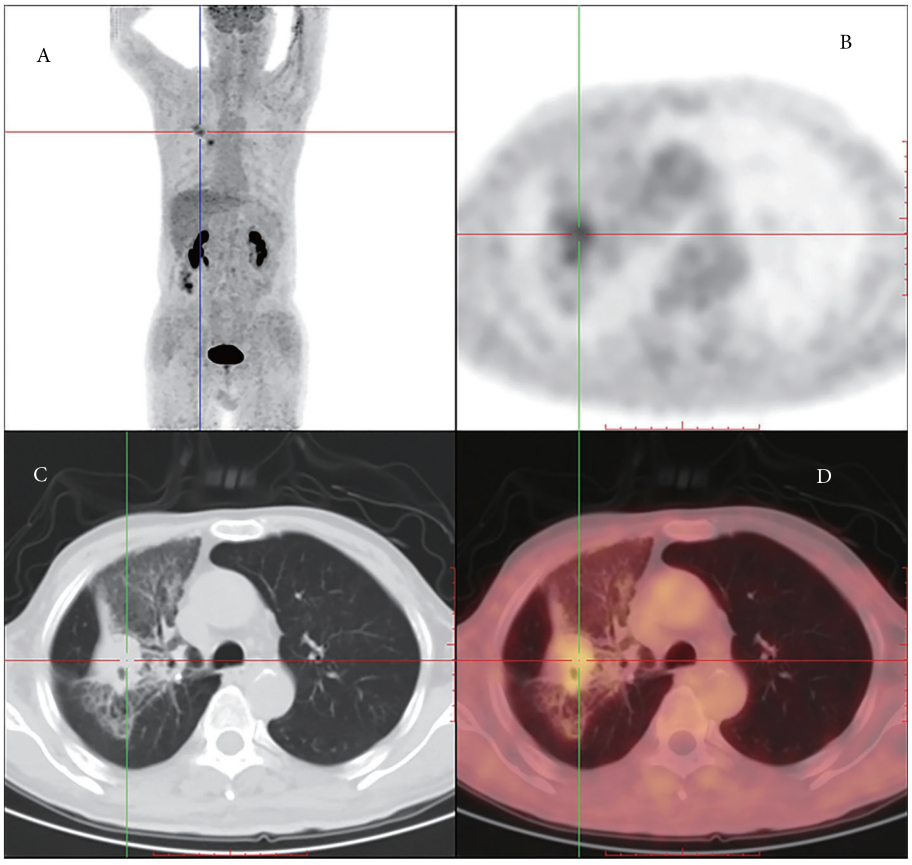

FIGURE 1
(A) Coronal PET (positron emission tomography) image shows higher FDG (fluorodeoxyglucose) uptake in the right lung and the lymph nodes on the left side. **(B)** Axial PET images. **(C)** Chest PET-CT presenting mesothelioma. **(D)** Axial PET images with higher tracer uptake.

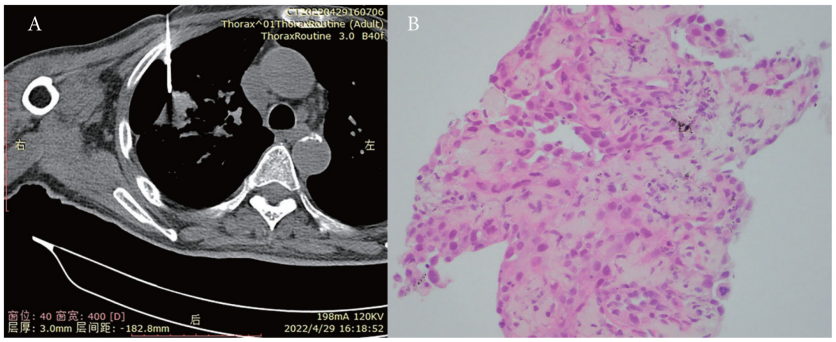

FIGURE 2
(A) Percutaneous biopsy of lung lesions guided by fusion CT. **(B)** Photomicroscopy with H&E (hematoxylin and eosin) staining presented unusual epithelioid cells.

but negative for TTF-1 and p40 (Figure 3). Sputum culture was performed and the detection of stenotrophomonas maltophilia, enterococcus faecium, and candida albicans in sputum of patients were postive.These results suggested intrapulmonary malignant mesothelioma complicated with pneumonia. As the poor performance status of the patient,surgery and radiotherapy were not suitable. Antibiotic therapy was performed with combination of cefepime,vancomycin,and caspofungin.

Cranial magnetic resonance imaging (MRI) and lumbar puncture were performed to investigate the potential causes of limb muscle weakness. However, there were no definite abnormalities in the symptoms of limb muscle weakness. Electromyography showed bilateral myogenic damage to the upper limbs, and nerve conduction tests revealed damage to the peripheral nervous system of all four limbs and delayed F-waves in the bilateral tibial nerve. Antibodies against nRNP/Sm, Sm, SSA, Ro52, SSB, Scl-70, Jo-1, and rRNP detected by enzyme-linked immunosorbent assay were all negative, whereas his auto-antibody profile showed anti-nuclear matrix protein 2 (NXP2) antibody positivity, which indicated cancer-associated myositis.

On the basis of these findings, we diagnosed the patient with intrapulmonary malignant mesothelioma complicated by myositis, which is the leading cause of limb muscle weakness. Upon diagnosis, the patient received 7 days of methylprednisolone (80 mg/day), but he had a poor response with progressive aggravation of limb muscle weakness and emergent expiratory dyspnea complicating pneumonia and died of respiratory failure. It was only 2 months from the first presence of limb muscle weakness onset to death.

3 Discussion

The 66-year-old patient presented with limb muscle weakness as the first symptom and was found a mass (2.6 cm) of the right upper lobe. He was an active smoker and had a family history of lung cancer, who had no history of asbestos exposure, cancer and immune checkpoint inhibitors therapy (ICI). According to the result of histological, immunohistochemical, and radiological findings,he was diagnosed as intrapulmonary malignant mesothelioma. Malignant mesothelioma often presents with diffuse involvement of the serous membranes, localized malignant mesotheliomas are extremely rare solitary circumscribed nodular tumors (4). Only very few cases have been reported that presented in ovary (5), liver (6), pancreatic (7) and lung (8). Diagnosing intrapulmonary malignant mesothelioma on the basis of clinical findings alone is difficult. A combination of histological, immunohistochemical, and radiological findings is needed. In our case,morphology and immunostains (positivity with calretinin,WT-1, and CK5/6; negativity with TTF-1 and p40) were consistent with an epithelioid malignant mesothelioma. For radiological investigations, European Society For Medical Oncology recommends applying CT scanning of the thorax for the localization of tumor sites and distant metastases or detecting early response to treatment. In our case,a soft tissue density occupying the lesion and enlarged lymph nodes in the right lobe were found and no abnormal uptake was observed at other sites.

Malignant mesothelioma are associated with risk factors including asbestos exposure, related minerals, simian virus 40, and nitrosamine (9). Asbestos exposure is the most important cause of malignant mesothelioma, accounting for 70–80% of cases (10). In the present case, the patient did not have any history of asbestos exposure, but he had a history of smoking and a family history of lung cancer.

Platinum-pemetrexed–based systemic therapy is a standard-of-care treatment in malignant mesothelioma (11). To early MPM,maximal tumor reduction surgery is recommended. While surgical resection for mesothelioma is always incomplete and it is not possible to cure someone with surgery alone, the multimodal approach to malignant pleural

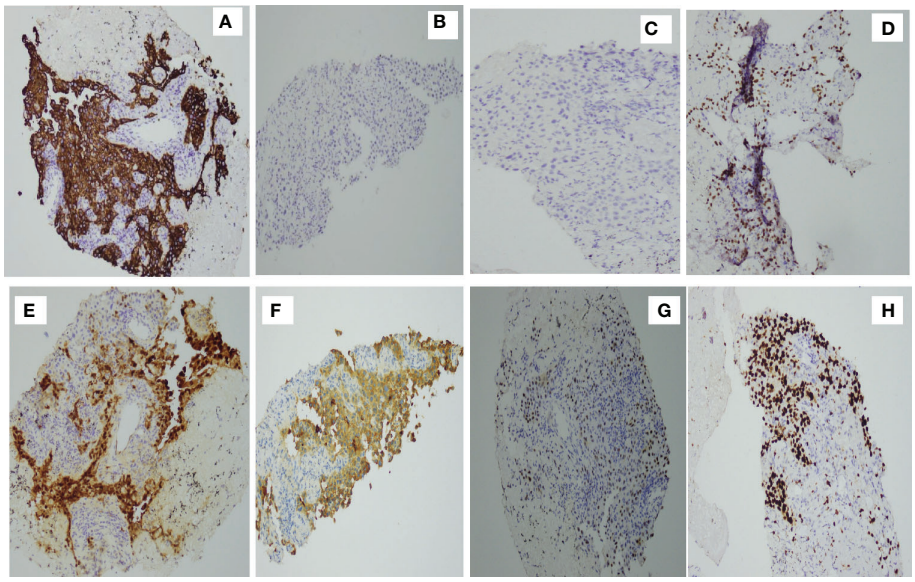

FIGURE 3
Immunohistochemical studies. Tumor cells are positive for **(A)** CK(+) **(D)** p63, **(E)** calretinin, **(F)** CK5/6, **(G)** WT-1, and **(H)** Ki-67 but negative for **(C)** p40 and **(B)** TTF-1.

mesothelioma is gradually becoming the standard of care for MPM in patients with good performance status (12, 13). For inoperable patients, radiotherapy and chemotherapy was recommended. In recent year, immunotherapy and mesothelin-targeted therapies for treatment of patients with advanced unresectable mesothelioma has been highlighted (14). In our case, the patient was in a critical condition with acute respiration failure and severe pneumonia, who was not suitable for surgery, radiotherapy or chemotherapy.Antibiotic therapy and intensive care was performed.

Cancer-associated myositis is defined as the development of a malignancy within 3 years of the diagnosis of myositis, which is one of the typical paraneoplastic syndromes. Cancer-associated myositis have been increasingly referred as being related with a variety of malignancies, including hematological and solid cancers (15). While cancer-associated myositis rarely presents with MPM (16). In our case, there was no definite abnormality for symptoms of limb muscle weakness on cranial MRI and lumbar puncture. Antibodies to related immunological markers for the diagnosis of primary rheumatic diseases were all negative, whereas the auto-antibody profile showed NXP2 antibody positively.NXP2 antibodies are reportedly associated with cancer-associated myositis (17). Although, myasthenia gravis was reported to be induced by immune checkpoint inhibitors (ICI) (18), the patient in our case had no history of ICI therapy.The result of cranial MRI, lumbar puncture, and immunological profile were inferred that the myositis in the present case was cancer-associated. Methylprednisolone was used for treatment of the myositis. While the patient poorly responsed to methylprednisolone, after receiving 7 days of methylprednisolone, he died of respiratory failure.

4 Conclusion

In conclusion, cancer-associated myositis may be present in patients with intrapulmonary malignant mesothelioma. To our knowledge, this case, in which the patient experienced limb muscle weakness as the first symptom, is the first to report intrapulmonary malignant mesothelioma complicated with cancer-associated myositis. It was a fast-progression and poor-prognosis disease, and had a poor response to methylprednisolone.

Data availability statement

The original contributions presented in the study are included in the article/supplementary material. Further inquiries can be directed to the corresponding author.

Ethics statement

The studies involving human participants were reviewed and approved by The Ethics Committee of the Second Affiliated Hospital of Dalian Medical University. The patients/participants provided their written informed consent to participate in this study. Written informed consent was obtained from the

individual(s) for the publication of any potentially identifiable images or data included in this article.

Author contributions

DG, JY and XJ conceived the idea for the article. XJ drafted the manuscript. XJ approved the final version of the manuscript. All authors contributed to the article and approved the submitted version.

Funding

This work was supported by the "1+X" Plan Clinical Technology Improvement Project of the Second Hospital of Dalian Medical University, Project No. 2022LCJSGC11.

Conflict of interest

The authors declare that the research was conducted in the absence of any commercial or financial relationships that could be construed as a potential conflict of interest.

Publisher's note

References

1. Gemba K, Fujimoto N, Aoe K, Kato K, Takeshima Y, Inai K, et al. Treatment and survival analyses of malignant mesothelioma in Japan. *Acta Oncol* (2013) 52 (4):803–8. doi: 10.3109/0284186X.2012.709948

2. Janes SM, Alrifai D, Fennell DA. Perspectives on the treatment of malignant pleural mesothelioma. *N Engl J Med* (2021) 385(13):1207–18. doi: 10.1056/NEJMra1912719

3. Pistolesi M, Rusthoven J. Malignant pleural mesothelioma: Update, current management, and newer therapeutic strategies. *Chest* (2004) 126(4):1318–29. doi: 10.1378/chest.126.4.1318

4. Allen TC, Cagle PT, Churg AM, Colby TV, Gibbs AR, Hammar SP, et al. Localized malignant mesothelioma. *Am J Surg Pathol* (2005) 29(7):866–73. doi: 10.1097/01.pas.0000165529.78945.dc

5. Ouafki I, Nouiakh L, Boujarnija R, Amarti A, Amaadour L, Oualla K, et al. Mésothéliome malin de l´ovaire: à propos d´un cas [Malignant mesothelioma of the ovary: A case report]. *Pan Afr Med J* (2021) 38:92. doi: 10.11604/pamj.2021.38.92.24462

6. Ghimire S, Regmi N, Yang T, Shah H, Srivatana U, Sarker A, et al. Primary malignant mesothelioma of the liver: Case report and review of the literature. *Eur J Case Rep Intern Med* (2020) 7(12):002128. doi: 10.12890/2020_002128

7. Espinal-Witter R, Servais EL, Klimstra DS, Lieberman MD, Yantiss RK. Localized intrapancreatic malignant mesothelioma: A rare entity that may be confused with other pancreatic neoplasms. *Virchows Arch* (2010) 456(4):455–61. doi: 10.1007/s00428-010-0885-9

8. Kumazawa M, Arakawa H, Shiobara T, Ishii Y, Nakazato Y, Kaji Y. A case of diffuse intrapulmonary malignant mesothelioma. *J Thorac Imaging* (2019) 34(6): W147–9. doi: 10.1097/RTI.0000000000000447

9. Carbone M, Emri S, Dogan AU, Steele I, Tuncer M, Pass HI, et al. A mesothelioma epidemic in cappadocia: scientific developments and unexpected social outcomes. *Nat Rev Cancer* (2007) 7(2):147–54. doi: 10.1038/nrc2068

10. Barbanti-Brodano G, Sabbioni S, Martini F, Negrini M, Corallini A, Tognon M. Simian virus 40 infection in humans and association with human diseases: results and hypotheses. *Virology* (2004) 318(1):1–9. doi: 10.1016/j.virol.2003.09.004

11. Vogelzang NJ, Rusthoven JJ, Symanowski J, Denham C, Kaukel E, Ruffie P, et al. Phase III study of pemetrexed in combination with cisplatin versus cisplatin alone in patients with malignant pleural mesothelioma. *J Clin Oncol* (2003) 21 (14):2636–44. doi: 10.1200/JCO.2003.11.136

12. Spatola C, Militello C, Tocco A, Salamone V, Luigi R, Migliore M, et al. Single-institution experience of intensity-modulated radiotherapy for malignant pleural mesothelioma at university of catania. *Future Oncol* (2018) 14(6s):17–21. doi: 10.2217/fon-2017-0280

13. Friedberg JS, Culligan MJ, Tsao AS, Rusch V, Sepesi B, Pass HI, et al. A proposed system toward standardizing surgical-based treatments for malignant pleural mesothelioma, from the joint national cancer institute-international association for the study of lung cancer-mesothelioma applied research foundation taskforce. *J Thorac Oncol* (2019) 14(8):1343–53. doi: 10.1016/j.jtho.2019.04.029

14. Hu ZI, Ghafoor A, Sengupta M, Hassan R. Malignant mesothelioma: Advances in immune checkpoint inhibitor and mesothelin-targeted therapies. *Cancer* (2021) 127(7):1010–20. doi: 10.1002/cncr.33433

15. Bosma NA, Carter E, Karim S. A case report of anorectal squamous cell carcinoma associated with overlap myositis syndrome-a possible paraneoplastic myositis syndrome. *Clin Colorectal Cancer* (2021) 20(2):148–52. doi: 10.1016/j.clcc.2021.02.004

16. Lei Y, Liu C, Wan X, Yang Y, Yao Y, Luo L, et al. Polymyositis as a paraneoplastic syndrome of a patient with primary pulmonary lymphoepithelioma-like carcinoma: A case report and literature review. *J Cardiothorac Surg* (2022) 17(1):1–7. doi: 10.1186/s13019-022-01860-4

17. Suga T, Oiwa H, Ishida M, Iwamoto Y. Clinical value of cancer-associated myositis-specific antibodies, anti-transcriptional intermediary factor 1-γ, and anti-nuclear matrix protein 2 antibodies in a retrospective cohort of dermatomyositis/polymyositis in a Japanese community hospital. *Clin Rheumatol* (2022) 41 (9):2803–8. doi: 10.1007/s10067-022-06166-3

18. Seki M, Uruha A, Ohnuki Y, Kamada S, Noda T, Onda A, et al. Inflammatory myopathy associated with PD-1 inhibitors. *J Autoimmun* (2019) 100:105–13. doi: 10.1016/j.jaut.2019.03.005

frontiers | Frontiers in Oncology

TYPE Case Report
PUBLISHED 23 December 2022
DOI 10.3389/fonc.2022.1040452

OPEN ACCESS

EDITED BY
Kohei Fujita,
National Hospital Organization Kyoto Medical Center, Japan

REVIEWED BY
Ahmed El Bastawisy,
Cairo University, Egypt
Jiaxi He,
First Affiliated Hospital of Guangzhou Medical University, China

*CORRESPONDENCE
Yosuke Fukuda
y.f.0423@med.showa-u.ac.jp

SPECIALTY SECTION
This article was submitted to Thoracic Oncology, a section of the journal Frontiers in Oncology

RECEIVED 09 September 2022
ACCEPTED 05 December 2022
PUBLISHED 23 December 2022

CITATION
Kashima A, Fukuda Y, Shimamura M, Ijichi M and Sagara H (2022) Successful treatment of extensive-stage small cell lung cancer with concurrent pleural and pericardial effusions: Case report.
Front. Oncol. 12:1040452.
doi: 10.3389/fonc.2022.1040452

Successful treatment of extensive-stage small cell lung cancer with concurrent pleural and pericardial effusions: Case report

Ayaka Kashima, Yosuke Fukuda*, Miri Shimamura, Miharu Ijichi and Hironori Sagara

Department of Medicine, Division of Respiratory Medicine and Allergology, School of Medicine, Showa Universityo, Tokyo, Japan

It is unclear whether pleural/pericardial drainage and pleurodesis/pericardiodesis should be performed before or after initiating chemotherapy in patients with chemotherapy-sensitive small-cell lung cancer. A 76-year-old woman presented to the emergency department with progressive dyspnea on exertion for a week. Chest computed tomography showed a mass shadow anterior to the left upper lobe, bilateral pleural effusions, and a circumferential pericardial effusion surrounding the heart. We diagnosed extensive-stage small-cell lung cancer based on the clinical course and pathological findings. We first performed pleurodesis and pericardial drainage and successfully initiated immune checkpoint inhibitor combined chemotherapy, with improved performance status. This case highlights the importance of aggressive drainage and pleurodesis/pericardiodesis, and suggests that drainage and pleurodesis/pericardiodesis should be considered before systemic chemotherapy in patients with concurrent pericardial or pleural effusions, even in patients with small-cell lung cancer that is sensitive to chemotherapy.

KEYWORDS

pericardial effusion, pleural effusion, pleurodesis, small-cell lung cancer, immune checkpoint inhibitor

Introduction

Small-cell lung cancer (SCLC) is rapidly progressive and is highly sensitive to chemotherapy compared to non-small-cell lung cancer. SCLC with concurrent pleural and pericardial effusions at the time of the initial presentation is rare. A retrospective observational study found that of 765 patients with SCLC, 63 had pleural effusions, 17

had pericardial effusions, and 16 had both (1). Recently, the initiation of chemotherapy with immune checkpoint inhibitors has been reported to improve the clinical outcomes of patients with SCLC (2). Although early initiation of chemotherapy with immune checkpoint inhibitors (ICIs) is desirable to improve the prognosis and symptoms of patients with SCLC, there is concern that patients with SCLC and pericardial or pleural effusions may not be able to initiate chemotherapy safely due to poor performance status (PS). Moreover, it is unclear whether pleural/pericardial drainage and pleurodesis/pericardiodesis should be performed before or after initiating chemotherapy should in patients with chemotherapy-sensitive SCLC. Here, we report a case of successful initiation of chemotherapy combined with ICI therapy in a patient with SCLC and pleural and pericardial effusions, after performing pleurodesis and pericardial drainage.

Case report

A 76-year-old woman presented to the emergency department with progressive dyspnea on exertion for a week. Her medical history included hypertension, dyslipidemia, and hyperuricemia. Her vital signs at the visit were: body temperature 36.1°C, pulse rate 68 beats/min, blood pressure 130/78 mmHg, respiratory rate 18 breaths/min, and oxygen saturation 92% breathing ambient air, and her consciousness was clear. Physical examination revealed decreased breath sounds in the lower left side of the chest and decreased cardiac sounds. Blood tests revealed white blood cell count 7,700/μL, aspartate aminotransferase 52 IU/L, alanine aminotransferase 55 IU/L, C-reactive protein 0.97 mg/dL, pro-gastrin-releasing peptide 71.9 pg/mL, and neuron specific enolase 254 ng/mL. Chest computed tomography (CT) showed a mass shadow anterior to the left upper lobe, bilateral pleural effusions (Figure 1A), and pericardial effusion circumferentially around the entire heart (Figure 1B). We performed pericardial drainage on day 2 because of concern about the possibility of the development of cardiac tamponade and for diagnosis. Pericardial fluid was exudative, but cytology of the fluid was negative for malignant cells. On day 4, the patient required oxygen therapy because of an increased left pleural effusion, and we performed pleural drainage. Pleural effusion was exudative, and cytology of the fluid was positive for small cell lung cancer. On day 8, we performed a CT-guided lung biopsy. Hematoxylin and eosin staining of the biopsy specimen revealed dense sheet-like growth of bare nucleated atypical cells with increased chromatin (Figure 2A), and immunostaining was positive for insulinoma-associated protein 1 (Figure 2B) and chromogranin A (Figure 2C) and negative for thyroid transcription factor-1, p40, and leukocyte common antigen (not shown). We diagnosed extensive-stage small cell lung cancer (ES-SCLC) based on the

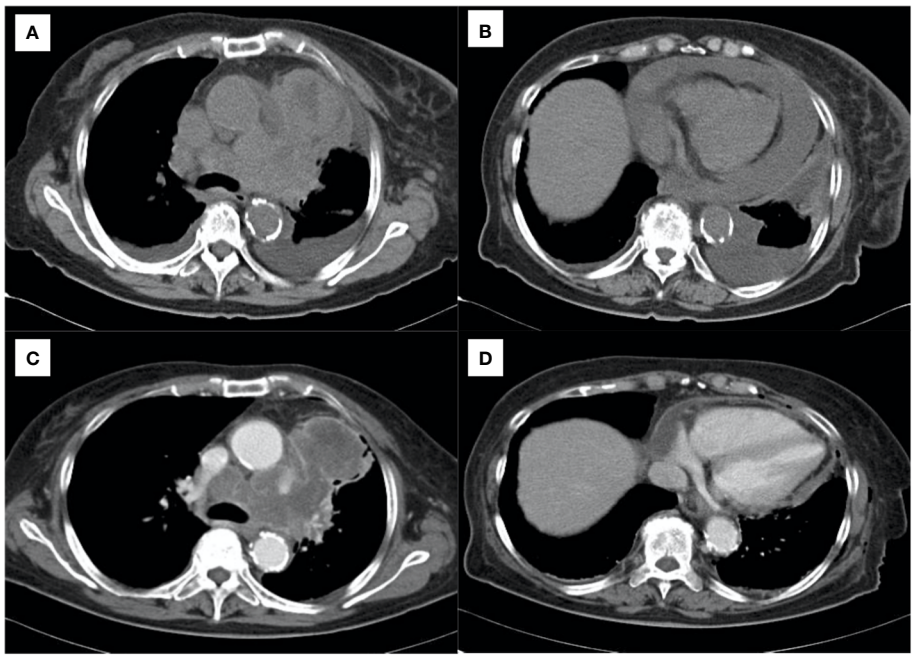

FIGURE 1
Chest computed tomography showing **(A)** primary lung cancer and bilateral pleural effusions and **(B)** pericardial effusion. **(C, D)** After drainage of the effusions and pleurodesis, showing control of the effusions before starting systemic chemotherapy.

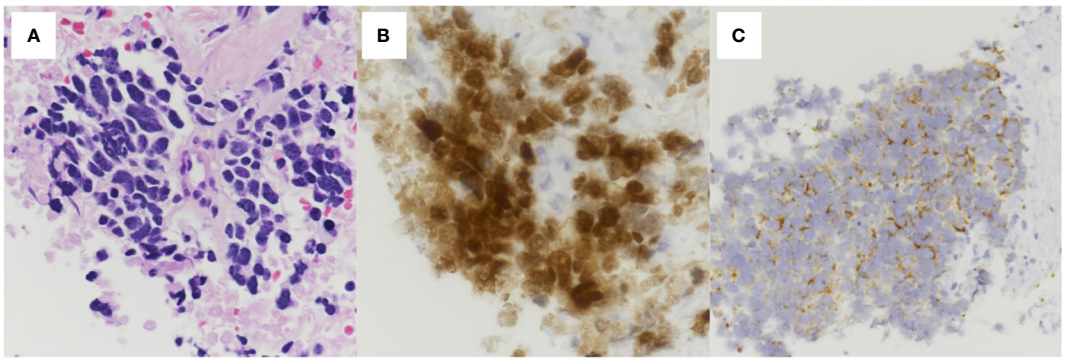

FIGURE 2
Histopathological findings of the pulmonary tumor. **(A)** Hematoxylin and eosin staining showing dense sheet-like growth of bare nucleated atypical cells with increased chromatin (400× magnification). Immunostaining showing positive **(B)** insulinoma-associated protein 1 (400× magnification) and **(C)** chromogranin A (200× magnification).

clinical course and pathological findings. The pleural fluid was drained over 5,000ml and we confirmed lung re-expansion on chest X-ray. Later, we performed talc pleurodesis to control the pleural effusion (Figures 1C, D) and improve the PS, which was 2 at the initial visit, and subsequently improved to 0. We did not perform pericardiodesis due to concern about the risk of adverse events. Instead, we administered a combination regimen of carboplatin, etoposide, and atezolizumab as first-line chemotherapy. After 4 cycles of first-line chemotherapy, we evaluated the patient to have progressive disease, so we administered amrubicin as second-line chemotherapy. However, her general condition worsened after 2 cycles, and considering her wishes, she was treated with best supportive care alone after that. The patient died approximately 9 months after diagnosis. The timeline of all relevant interventions from the initial visit to the introduction of treatment is shown in Figure 3.

Discussion

Based on the TNM classification, the 5-year survival rate for patients with SCLC with T4 lesions and pleural effusions is 3.6%, with a median overall survival of 7 months (3). Patients with ES-SCLC with pleural effusion on the same side as the primary tumor have a significantly lower overall survival rate than ES-SCLC without pleural effusion (20.9 months vs. 11.8 months, $p < 0.001$) (4). In patients with SCLC, the presence of malignant pleural effusions is an independent prognostic factor for SCLC, and reduce the median overall survival time by approximately 4 months, and are associated with lower 1-year and 2-year survival rates (17% and 6%, respectively) (5). The median overall survival of patients with SCLC and pericardial effusions is 14.2 months, which is approximately 7 months shorter than that of SCLC patients without pericardial effusions (1). In addition, metastasis of SCLC to the pericardium generally occurs at a relatively late stage in the disease (6). Therefore, the early initiation of chemotherapy is desirable in patients with SCLC patients and pleural effusions, pericardial effusions, or both.

In the IMpower133 trial, which tested the efficacy of a regimen combining atezolizumab, carboplatin, and etoposide compared to placebo, combination chemotherapy increased the overall survival by 2 months (12.3 months vs. 10.3 months, $p < 0.01$), with no increase in serious adverse events compared to standard therapy (2). In addition, ICIs, including pembrolizumab and durvalumab,

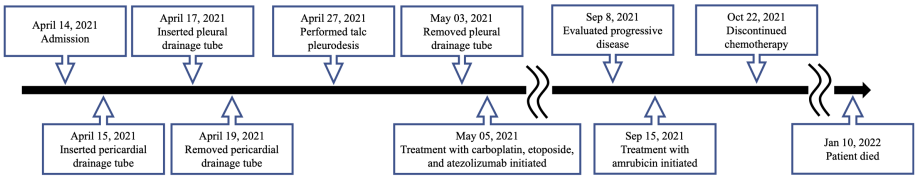

FIGURE 3
Timeline of the main interventions from the initial visit to the treatment course.

combined with cytotoxic anticancer agents improve progression-free survival and overall survival (7, 8). Thus, early initiation of chemotherapy with ICIs, especially in patients with SCLC and pleural or pericardial effusions, who generally have a poor prognosis (9), may contribute to improving the clinical outcome.

A prospective observational study with malignant pleural effusion control as an outcome, conducted in cancer patients with pharmacologically sensitive and non-pharmacologically sensitive tumors of whom 13% had SCLC, found that factor that had the greatest effect on controlling malignant pleural effusions was not whether the patients received systemic chemotherapy, but whether they underwent pleurodesis (10). Another prospective observational study of 509 patients with lung cancer and malignant pleural effusions found that compared to chemotherapy alone, early treatment of malignant pleural effusions reduced the need for future re-intervention (23.5% vs. 53.8%, $p < 0.01$) (11). In patients with non-small cell lung cancer, intrapericardial chemotherapy alone and a combination of intrapericardial chemotherapy and systemic chemotherapy improve control of cancer-related pericarditis (12–14). These results suggest that in patients with SCLC and pleural and pericardial effusions, drainage and pleurodesis/pericardiodesis prior to chemotherapy might lead to better fluid control and improved symptom control and prognosis.

In this case, we were concerned about the increased risk of adverse events with combined pleurodesis and pericardiodesis; therefore, we performed pleurodesis and pericardial drainage, without pericardiodesis. As a result, chemotherapy could be safely introduced with improved PS. However, there are several limitations in this case. First, the clinical course of chemotherapy preceded by pericardial or pleural drainage is uncertain. Randomized controlled trials of non-small cell lung cancer with pleural effusion suggested that a pleural effusion control rate of 86.9-92.9% may be achieved with chemotherapy alone without pleurodesis (15, 16). Local approaches, such as drainage to the pericardial and thoracic space, are unlikely to result in serious outcomes (12, 17) but may delay the administration of chemotherapy in about 2% of patients (18). Second, the patient's clinical response was not adequate. The patient had to stop chemotherapy during the second round of chemotherapy due to poor performance status, resulting in death 9 months after diagnosis. In other words, the clinical course could have been different if chemotherapy had been administered prior to the procedure. Third, the impact of pleurodesis on PET/CT, which may be performed to determine the efficacy of chemotherapy, needs to be considered (19). In this patient, PET/CT was not performed due to the inaccessibility and financial burden of PET/CT. We needed to plan our treatment strategy with these matters in mind carefully.

This case highlights the importance of considering aggressive drainage and pleurodesis/pericardiodesis before systemic chemotherapy in patients with SCLC and concurrent pericardial or pleural effusions, even in patients with SCLC that is sensitive to chemotherapy.

Patient perspective

I went to the hospital because I was short of breath, and had fluid drained from around my heart and lungs. This treatment was successful, and I was able to receive chemotherapy before the cancer worsened. Fortunately, I did not experience any major side effects of chemotherapy, and I am continuing to live my daily life.

Data availability statement

The raw data supporting the conclusions of this article will be made available by the authors, without undue reservation.

Ethics statement

Ethical review and approval was not required for the study on human participants in accordance with the local legislation and institutional requirements. The patients/participants provided their written informed consent to participate in this study.

Author contributions

AK, YF, MS, and MI collected and interpreted the clinical data. AK and YF drafted the manuscript. MS, MI, and HS reviewed and revised the manuscript. All authors read and approved the final version of the manuscript.

Acknowledgments

We would like to thank Editage (www.editage.jp) for English language editing.

Conflict of interest

The authors declare that the research was conducted in the absence of any commercial or financial relationships that could be construed as a potential conflict of interest.

Publisher's note

References

1. Niho S, Kubota K, Yoh K, Goto K, Ohmatsu H, Nihei K, et al. Clinical outcome of small cell lung cancer with pericardial effusion but without distant metastasis. *J Thorac Oncol* (2011) 6:796–800. doi: 10.1097/JTO.0b013e318208ec77

2. Horn L, Mansfield AS, Szczęsna A, Havel L, Krzakowski M, Hochmair MJ, et al. First-line atezolizumab plus chemotherapy in extensive-stage small-cell lung cancer. *N Engl J Med* (2018) 379:2220–9. doi: 10.1056/NEJMoa1809064

3. Ignatius Ou SH, Zell JA. The applicability of the proposed IASLC staging revisions to small cell lung cancer (SCLC) with comparison to the current UICC 6th TNM edition. *J Thorac Oncol* (2009) 4:300–10. doi: 10.1097/JTO.0b013e318194a355

4. Niho S, Kubota K, Yoh K, Goto K, Ohmatsu H, Nihei K, et al. Clinical outcome of chemoradiation therapy in patients with limited-disease small cell lung cancer with ipsilateral pleural effusion. *J Thorac Oncol* (2008) 3:723–7. doi: 10.1097/JTO.0b013e31817c606a

5. Shojaee S, Singh I, Solsky I, Nana-Sinkam P. Malignant pleural effusion at presentation in patients with small-cell lung cancer. *Respiration* (2019) 98:198–202. doi: 10.1159/000499372

6. Megyesfalvi Z, Tallosy B, Pipek O, Fillinger J, Lang C, Klikovits T, et al. The landscape of small cell lung cancer metastases: Organ specificity and timing. *Thorac Cancer* (2021) 12:914–23. doi: 10.1111/1759-7714.13854

7. Rudin CM, Awad MM, Navarro A, Gottfried M, Peters S, Csőszi T, et al. Pembrolizumab or placebo plus etoposide and platinum as first-line therapy for extensive-stage small-cell lung cancer: Randomized, double-blind, phase III KEYNOTE-604 study. *J Clin Oncol* (2020) 38:2369–79. doi: 10.1200/JCO.20.00793

8. Goldman JW, Dvorkin M, Chen Y, Reinmuth N, Hotta K, Trukhin D, et al. Durvalumab, with or without tremelimumab, plus platinum-etoposide versus platinum-etoposide alone in first-line treatment of extensive-stage small-cell lung cancer (CASPIAN): Updated results from a randomised, controlled, open-label, phase 3 trial. *Lancet Oncol* (2021) 22:51–65. doi: 10.1016/S1470-2045(20)30539-8

9. Nakazawa K, Kurishima K, Tamura T, Kagohashi K, Ishikawa H, Satoh H, et al. Specific organ metastases and survival in small cell lung cancer. *Oncol Lett* (2012) 4:617–20. doi: 10.3892/ol.2012.792

10. Holling N, Patole S, Medford ARL, Maskell NA, Bibby AC. Is systemic anticancer therapy associated with higher rates of malignant pleural effusion control in people with pharmacologically sensitive tumors?: A retrospective analysis of prospectively collected data. *Chest* (2021) 160:1915–24. doi: 10.1016/j.chest.2021.05.027

11. Chiang KY, Ho JC, Chong P, Tam TC, Lam DC, Ip MS, et al. Role of early definitive management for newly diagnosed malignant pleural effusion related to lung cancer. *Respirology* (2020) 25:1167–73. doi: 10.1111/resp.13812

12. Moriya T, Takiguchi Y, Tabeta H, Watanabe R, Kimura H, Nagao K, et al. Controlling malignant pericardial effusion by intrapericardial carboplatin administration in patients with primary non-small-cell lung cancer. *Br J Cancer* (2000) 83:858–62. doi: 10.1054/bjoc.2000.1397

13. Maruyama R, Yokoyama H, Seto T, Nagashima S, Kashiwabara K, Araki J, et al. Catheter drainage followed by the instillation of bleomycin to manage malignant pericardial effusion in non-small cell lung cancer: A multi-institutional phase II trial. *J Thorac Oncol* (2007) 2:65–8. doi: 10.1097/JTO.0b013e31802c8260

14. Lestuzzi C, Bearz A, Lafaras C, Gralec R, Cervesato E, Tomkowski W, et al. Neoplastic pericardial disease in lung cancer: Impact on outcomes of different treatment strategies. *A multicenter study. Lung Cancer* (2011) 72:340–7. doi: 10.1016/j.lungcan.2010.10.013

15. Usui K, Sugawara S, Nishitsuji M, Fujita Y, Inoue A, Mouri A, et al. A phase II study of bevacizumab with carboplatin-pemetrexed in non-squamous non-small cell lung carcinoma patients with malignant pleural effusions: North East Japan study group trial NEJ013A. *Lung Cancer* (2016) 99:131–6. doi: 10.1016/j.lungcan.2016.07.003

16. Tamiya M, Tamiya A, Yamadori T, Nakao K, Asami K, Yasue T, et al. Phase2 study of bevacizumab with carboplatin-paclitaxel for non-small cell lung cancer with malignant pleural effusion. *Med Oncol* (2013) 30:676. doi: 10.1007/s12032-013-0676-7

17. Saka H, Oki M, Kitagawa C, Kogure Y, Kojima Y, Saito A, et al. Sterilized talc pleurodesis for malignant pleural effusions: A phase II study for investigational new drug application in Japan. *Jpn J Clin Oncol* (2018) 48:376–81. doi: 10.1093/jjco/hyy020

18. Singh N, Aggarwal AN, Behera D, Jindal SK. Intercycle delays during chemotherapy of non-small cell lung cancer in a health care resource-constrained setting and their effect on overall survival. *J Thorac Oncol* (2010) 5:236–9. doi: 10.1097/JTO.0b013e3181c3f5f7

19. Ulaner GA, Lyall A. Identifying and distinguishing treatment effects and complications from malignancy at FDG PET/CT. *Radiographics* (2013) 33:1817–34. doi: 10.1148/rg.336125105

frontiers | Frontiers in Oncology

TYPE Case Report
PUBLISHED 06 January 2023
DOI 10.3389/fonc.2022.1077777

OPEN ACCESS

EDITED BY
Kohei Fujita,
National Hospital Organization Kyoto Medical Center, Japan

REVIEWED BY
Alessandro Boscarelli,
Institute for Maternal and Child Health Burlo Garofolo (IRCCS), Italy
Giovannella Palmieri,
CRCTR Rare Tumors Coordinating Center of Campania Region, Italy

*CORRESPONDENCE
Yaqing Zhao
bettertomorrow18@163.com

SPECIALTY SECTION
This article was submitted to Thoracic Oncology, a section of the journal Frontiers in Oncology

RECEIVED 23 October 2022
ACCEPTED 13 December 2022
PUBLISHED 06 January 2023

CITATION
Ren J, Fu Z and Zhao Y (2023) Case report: Imaging findings of true thymic hyperplasia at ^{18}F-FDG PET/CT in an infant.
Front. Oncol. 12:1077777.
doi: 10.3389/fonc.2022.1077777

Case report: Imaging findings of true thymic hyperplasia at ^{18}F-FDG PET/CT in an infant

Jiazhong Ren[1], Zheng Fu[1] and Yaqing Zhao[2*]

[1]Department of Medical Imaging, PET-CT Center, Shandong Cancer Hospital and Institute, Shandong First Medical University and Shandong Academy of Medical Sciences, Jinan, Shandong, China, [2]Department of General Affairs Section, The Second Affiliated Hospital of Shandong University of Traditional Chinese Medicine, Jinan, Shandong, China

True thymic hyperplasia (TTH) in children is rare and difficult to distinguish from other thymic tumors such as thymoma and thymic carcinoma. A 3-year-old girl underwent an ^{18}F-fluorodeoxyglucose (^{18}F-FDG) positron emission tomography (PET)/computed tomography (CT) scan (^{18}F-FDG PET/CT) and a chest CT scan to evaluate an anterior mediastinal mass. ^{18}F-FDG PET/CT revealed a mediastinal mass showing heterogeneously increased FDG uptake with a maximum standardized uptake value (SUVmax) of 7.1. Eventually, postoperative pathological diagnosis demonstrated TTH. So far, there are no reports of ^{18}F-FDG PET/CT imaging of this disease.

KEYWORDS

^{18}F-FDG PET/CT, CT, mediastinum, TTH, MTH

Introduction

True thymic hyperplasia (TTH) usually presents as an anterior mediastinal mass and causes significant challenges in its diagnosis and treatment (1). The enlargement of the thymus occurs most often during infancy and usually spontaneously degenerates after the age of 3 years (2). TTH is the most common benign tumor observed in pediatric patients with tumors following chemotherapy and is essentially a rebound of the thymus gland (3). However, TTH in children is rare, mostly has unknown etiology, and is usually not with any comorbidity (4). Computed tomography (CT) and magnetic resonance imaging (MRI) are mainly used to evaluate thymic lesions. ^{18}F-fluorodeoxyglucose positron emission tomography/CT (^{18}F-FDG PET/CT) has an excellent diagnostic value in thymic rebound and can differentiate between thymic hyperplasia (TH), thymoma, and thymic carcinoma (5). However, there are fewer reports on the diagnostic value of ^{18}F-FDG PET/CT in scanning children with TTH. Here, we describe the case of a child whose diagnosis of TTH was based on a pathological diagnosis after surgical resection, which was

supported by CT-enhanced imaging and an ^{18}F-FDG PET/CT scan. ^{18}F-FDG PET/CT is of great value in the preoperative evaluation of pediatric patients with TTH.

Case presentation

A 3-year-old girl was admitted to the hospital owing to a 20-day history of cough and sputum without hemoptysis. Physical examination revealed an anterior chest bulge measuring approximately 6 × 5 cm^2, firm in texture, with poor mobility, and with no sternal pressure and rubbing sensation in the chest. She had no other symptoms and no family history of TTH or other diseases. Laboratory tests showed a mildly elevated lactate dehydrogenase (LDH) at 276 U/L (reference range: 38–126 U/L), a white blood cell count of 13.76 × 10^9/L (reference range: 4–10 × 10^9/L), and a red blood cell count of 5.09 × 10^{12}/L (reference range: 4–4.5 × 10^{12}/L). However, thyroid-related laboratory test results were normal. In addition, neuron-specific enolase (NSE) and human chorionic gonadotropin levels (HCG) were normal. The chest CT scan revealed a well-defined irregular mass of 17 × 10 × 7.5 cm^3 in the right anterior mediastinum, with strip-like low-density shadows in the lesion, and a CT value of approximately −67 Hounsfield units, thereby suggesting adipose tissue (Figure 1). The arterial phase showed less vascularity and heterogeneous hypodensity within the lesion (A, white arrow; Figure 1); the venous phase showed persistent hypodensity (B, white arrow; Figure 1) with compression of the cardiac cavity, right main bronchus, and occlusion of the right main bronchus (C, red arrow; Figure 1) ; the compressed right main bronchus and corresponding lung tissue returned to normal (D, black arrow; Figure 1) one week after the patient underwent chest surgery.

After a CT scan of the chest, ^{18}F-FDG PET/CT was performed owing to concerns that the lesion may be malignant. Coronal PET/CT fusion images (A; Figure 2) show a large, heterogeneous hypermetabolic mass in the right thorax (white arrows; Figure 2), whereas the thyroid was normal and not hypermetabolic (green arrows; Figure 2), thereby suggesting a thymic origin of the mass. In axial images (B: CT; C: PET/CT fusion; D: PET; Figure 2), the uptake of FDG with an SUVmax of 7.1 (white and black arrows; Figure 2) shows that the mass has heterogeneous hyperactivity. Pathological images (E, hematoxylin–eosin stain; original magnification × 100) showed histologically normal thymic tissue consisting of lobules with well-defined cortical and medullary cells. Immunohistochemical staining was positive for CKpan, CK19, LCA, CD3, TDT, MDM2, and CD1a and negative for CK20, and Desmin. The lesion was eventually diagnosed as TTH, and the patient recovered well during the follow-up period.

Discussion

The thymus is a gland situated in the anterior mediastinum; it is embryologically derived from the pharyngeal pouch of the third and fourth branchial arch (2). Its size varies with age because thymic tissue gradually shrinks and is replaced by adipose tissues. The thymus gland gradually invaginates during the first 3–4 years of life (6).

TH is usually divided into two categories: TTH and lymphatic follicular hyperplasia (LFH) (7). TTH is characterized by a diffused thickening and enlargement of the thymus that exceeds the corresponding upper limit of size or mass in a normal child of the same age but maintains the normal thymic structure and immunohistochemical features (8). TH is often caused by chemotherapy for tumors, thermal burns, or surgery. LFH is characterized by an increase in the number of lymphoid follicles and germinal centers in the thymus, which may be normal or slightly enlarged in size. LFH is associated with several endocrine and autoimmune diseases such as Graves' disease, myasthenia gravis, and systemic lupus erythematosus (9).

TTH in children is a rare clinical condition, has unknown etiology, and often has no comorbidities. It is often referred to as massive thymic hyperplasia (MTH) because it is characterized by a relatively larger and heavier thymus than the thymus of a healthy individual. The diagnostic features of MTH are as follows: 1. radiographs show gland projection exceeding the cardiac shadow, 2. The thymus weighs several times its expected weight at a specific age, 3. the mass of the thymus is > 2% of the body mass, and 4. pathological test shows normal thymus

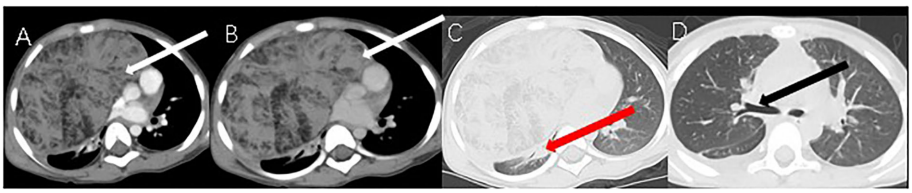

FIGURE 1
CT images.

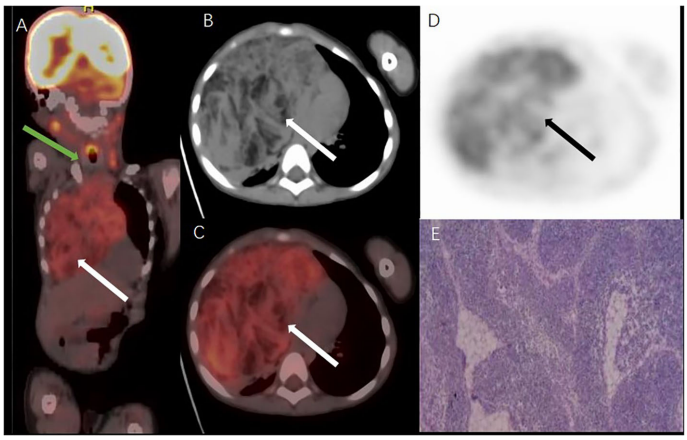

FIGURE 2
18F FDG PETCT images and pathologic picture.

structure (10). The patient in this case report largely met the above diagnostic criteria.

The most common tumors of the anterior mediastinum in children are tumors of thymic, lymphatic, or germ-cell origin (11). Tumor markers (alpha-fetoprotein (AFP), HCG, and NSE) are helpful in the differential diagnosis of some tumors such as germ cell tumors (GCTs). Mediastinal yolk sac tumor is often associated with elevated levels of serum AFP, seminoma with elevated levels of serum HCG, and lymphoma with elevated levels of LDH. MRI or CT scans are often used to evaluate thymic lesions (11, 12). Mediastinal GCTs are mostly teratomas, often containing fatty tissues and calcifications, and are easily diagnosed. Invasion of the thymus by lymphoma usually occurs in the setting of extensive systemic disease. Homogeneous enlargement of the thymus with mediastinal and/or axillary lymph node enlargement is usually diagnosed as lymphoma (13). Previous studies have reported that ^{18}F-FDG PET/CT can differentiate between benign and malignant thymic tumors but cannot distinguish between aggressive and non-aggressive thymoma and still relies on morphological examination by CT and MRI or pathological examination (8, 14, 15). In general, benign uptake of physiological thymus or chemotherapy-induced thymic rebound hyperplasia is less intense on ^{18}F-FDG PET/CT scans, where SUVmax is approximately 1.0–2.8. In comparison to thymoma and TH, thymic carcinoma shows considerably higher FDG uptake (13).

Although multimodal imaging has an excellent diagnostic value for TTH, MRI can more easily identify mediastinal masses, which are directly contiguous with and follow the same signal features as the main body of the thymus (12). Moreover, MRI is more sensitive in detecting adipose tissue in TTH, which can enable us to accurately deduce the origin and nature of the mass. Therefore, we recommend that MRI should always be preferred in diagnosing pediatric patients if feasible, specifically because it is free of ionizing radiation and is therefore safe for these patients. Unfortunately, due to our inexperience with TTH and the suspicion that the mediastinal mass was malignant as detected by enhanced CT, we selected ^{18}F-FDG PET/CT instead of MRI for further examination.

In this case report, ^{18}F-FDG PET/CT scan revealed that there was an increase in the heterogeneous hypermetabolism at the lesion with an SUVmax of 7.1, the lung tissue adjacent to the lesion was only compressed but not invaded, and the patient had no lymph node metastases and distant metastases. Although ^{18}F-FDG PET/CT has limited diagnostic value for thymic lesions (8, 12), especially in children, in this case report, it helped us to determine that the lesion was benign with no adjacent tissue invasion, which enabled subsequent surgery plans for the patient.

Most previous case reports suggest that treatment of TTH with steroids is usually ineffective; therefore, surgical resection is a better option (6, 10, 16). Finally, the patient underwent complete surgical resection of the mediastinal tumor and recovered well after surgery without any postoperative complications. Therefore, we recommend that surgical resection should be the first option for pediatric patients with TTH because this tumor is non-invasive to adjacent tissues and easily resectable, and the surgery is free of any postoperative complications.

In conclusion, ^{18}F-FDG PET/CT is of great value in the preoperative diagnosis and assessment of pediatric patients with TTH. In addition, awareness of these findings is important in the interpretation of PET/CT scans of anterior mediastinal masses in young children.

Data availability statement

The original contributions presented in the study are included in the article/supplementary material. Further inquiries can be directed to the corresponding author.

Ethics statement

The studies involving human participants were reviewed and approved by Ethics Committee of Cancer Hospital Affiliated to Shandong First Medical University. Written informed consent to participate in this study was provided by the participants' legal guardian/next of kin. Written informed consent was obtained from the minor(s)' legal guardian/next of kin for the publication of any potentially identifiable images or data included in this article.

Author contributions

JR acquisition of data, drafting of the manuscript; ZF and YZ: revision of the manuscript, supervision. All authors read and critically revised the manuscript for intellectual content and approved the final manuscript.

Acknowledgments

We thank Bullet Edits Limited for the linguistic editing and proofreading of the manuscript.

Conflict of interest

The authors declare that the research was conducted in the absence of any commercial or financial relationships that could be construed as a potential conflict of interest.

Publisher's note

References

1. Mlika M, Yaiche R, Fourti A, Braham E, Houcin Y, Marghli A, et al. Thymic hyperplasia: A study of 46 cases. *Ann Pathol* (2021) 41:544–8. doi: 10.1016/j.annpat.2021.01.003

2. Hofmann WJ, Mö ller P, Otto HF. Thymic hyperplasia. i. true thymic hyperplasia. review of the literature. *Klin Wochenschr* (1987) 65:49–52. doi: 10.1007/BF01745472

3. Smith CS, Schoder H, Yeung HW. Thymic extension in the superior mediastinum in patients with thymic hyperplasia: potential cause of false-positive findings on 18F-FDG PET/CT. *AJR Am J Roentgenol* (2007) 188:1716–21. doi: 10.2214/AJR.06.0552

4. Rice HE, Flake AW, Hori T, Galy A, Verhoogen. RH. Massive thymic hyperplasia: Characterization of a rare mediastinal mass. *J Pediatr Surg* (1994) 29(12):1561–4. doi: 10.1016/0022-3468(94)90216-x

5. Kawano T, Suzuki A, Ishida A, Takahashi N, Lee J, Tayama Y, et al. The clinical relevance of thymic fluorodeoxyglucose uptake in pediatric patients after chemotherapy. *Eur J Nucl Med Mol Imaging* (2004) 31:831–6. doi: 10.1007/s00259-004-1466-4

6. Tan Z, Ying LY, Zhang ZW, Li JH, Gao Z, Qi JC. True thymic hyperplasia in an infant. *J Pediatr Surg* (2010) 45:1711–3. doi: 10.1016/j.jpedsurg.2010.05.001

7. Weis CA, Markl B, Schuster T, Vollert K, Strobel P, Marx A. [True thymic hyperplasia: Differential diagnosis of thymic mass lesions in neonates and children]. *Pathologe* (2017) 38:286–93. doi: 10.1007/s00292-017-0283-z

8. Nguyen R, Coleman JL, Howard SC, Metzger ML. Watchful waiting for some children with a mediastinal mass: the potential role for (1)(8)F-fluorodeoxyglucose positron emission tomography: A case report and review of the literature. *BMC Pediatr* (2013) 13:103. doi: 10.1186/1471-2431-13-103

9. Kiwaki T, Tanaka H, Akiyama Y, Akaki M, Tomita M, Kataoka H. A rare association between true thymic hyperplasia and thyroid follicular tumor: A case report. *J Med Case Rep* (2020) 14:9. doi: 10.1186/s13256-019-2332-0

10. Linegar AG, Odell JA, Fennell WM, Close M, De Groot MK, Casserly DR, et al. Massive thymic hyperplasia. *Ann Thorac Surg* (1993) 55(5):1197–201. doi: 10.1016/0003-4975(93)90033-e

11. Nariman M, Willi W, Hansjörg S, Martin B, Michael G, Konrad R. Case report: True thymic hyperplasia in a 30-Day-Old boy. *Klin Padiatr* (2021) 233 (6):299–302. doi: 10.1055/a-1557-1427

12. Ka KW, Elisa F, Morand P. F-18 FDG PET/CT study showing cervical extension of thymic tissue. *Clin Nucl Med* (2008) 33(8):547–8. doi: 10.1097/RLU.0b013e31817dec53

13. Liu Y. Characterization of thymic lesions with f-18 FDG PET-CT: an emphasis on epithelial tumors. *Nucl Med Commun* (2011) 32:554–62. doi: 10.1097/MNM.0b013e328345b984

14. Tatsuro T, Satoko K, Akiko K, Motoko Y, Akihiko T, Hirohiko K, et al. First description of the role of 18F-FDG-PET/CT as compared to CT, MRI To suspect a case of thymoma in a pediatric patient. *Hell J Nucl Med* (2012) 15(1):68–9.

15. Ferdinand B, Gupta P, Kramer EL. Spectrum of thymic uptake at 18F-FDG PET. *Radiographics* (2004) 24(6):1611–6. doi: 10.1148/rg.246045701

16. Tadiotto E, Clemente M, Pecoraro L, Piacentini G, Degani D, Pietrobelli A. Massive thymic hyperplasia in a 15-month-old boy: Case report and literature review. *Clin Case Rep* (2019) 7:27–31. doi: 10.1002/ccr3.1896

frontiers | Frontiers in Oncology

TYPE Case Report
PUBLISHED 09 January 2023
DOI 10.3389/fonc.2022.1037964

OPEN ACCESS

EDITED BY
Kohei Fujita,
National Hospital Organization Kyoto Medical Center, Japan

REVIEWED BY
Nanying Che,
Beijing Chest Hospital, Capital Medical University, China
Rajesh Parmar,
University of California, Los Angeles, United States

*CORRESPONDENCE
Xialin Li
945666341@qq.com

SPECIALTY SECTION
This article was submitted to Thoracic Oncology, a section of the journal Frontiers in Oncology

RECEIVED 06 September 2022
ACCEPTED 19 December 2022
PUBLISHED 09 January 2023

CITATION
Fang Y, Zhang Q, Wang W, Tong J and Li X (2023) Successful treatment of a patient with advanced lung adenocarcinoma (EGFR-T790M and C797S cis) with lazertinib: A case report and literature review. *Front. Oncol.* 12:1037964. doi: 10.3389/fonc.2022.1037964

Successful treatment of a patient with advanced lung adenocarcinoma (EGFR-T790M and C797S cis) with lazertinib: A case report and literature review

Yue Fang, Qiankun Zhang, Weimin Wang, Juanjuan Tong and Xialin Li*

Hefei Cancer Hospital, Chinese Academy of Sciences, Hefei, China

Lazertinib has been shown to treat non-small cell lung cancer (NSCLC) patients with EGFR-T790M, Ex19del, and L858R mutations. However, there are still no studies to prove that lazertinib could be used in patients with EGFR-T790M and C797s cis mutations in NSCLC. We report a case of a patient with advanced lung adenocarcinoma with EGFR-T790M and C797s cis mutations who were treated with lazertinib and achieved satisfactory efficacy without serious side effects. And the scratch assay and colony-forming unit assay were performed using lung adenocarcinoma cells from patients, the results showed that both lazertinib and amivantamab could inhibit the proliferation and migration of lung adenocarcinoma cells to some extent, and the inhibitory effect of lazertinib was better than that of amivantamab ($p < 0.01$), while the inhibitory effect of lazertinib combined with amivantamab was not statistically different from that of lazertinib alone($p>0.05$). This finding suggests that lazertinib may be an effective treatment option for patients with lung adenocarcinoma presenting with EGFR-T790M and C797s cis mutations.

KEYWORDS

lazertinib, lung adenocarcinoma, EGFR-T790M, C797s, case report

Introduction

Lung cancer remains one of the most prevalent malignancies that damage human lives, with approximately 1.7 million deaths from lung cancer worldwide in 2020, as reported by Sung et al (1). Adenocarcinoma of the lung is the most common type of pathology in lung cancer, accounting for approximately 45% of the total number of cases. The five-year survival rate for patients with lung adenocarcinoma is only 15%, as most patients are already in the progressive stage at the time of initial diagnosis (2, 3). Lung

adenocarcinoma displays a high degree of heterogeneity, with frequent mutations in multiple genes, including epidermal growth factor receptor (EGFR), anaplastic lymphoma kinase (ALK), v-raf murine sarcoma viral oncogene homolog B1 (BRAF), and Kirsten ratsarcoma viral oncogene homolog (KRAS), which can promote the progression of this cancer. EGFR mutations are the most common gene mutation in patients with lung adenocarcinoma, present in approximately 50-60% of Asian patients; most patients with these mutations have a low survival rate (4).

EGFR-TKIs are a class of targeted drugs that target EGFR mutations, and previous studies have shown that patients are best treated when their sensitive mutation is most frequently found in exon 19 or exon 21 mutations (5). However, first-generation EGFR-TKIs, such as gefitinib, often developed resistance to the drugs after some time (6). It was found that approximately 55% of patients who developed drug resistance had a T790M mutation after first or second-generation EGFR-TKIs treatment, which severely affected survival (7).

Lazertinib, the third-generation EGFR-TKIs approved by the US Food and Drug Administration (FDA) in 2021, was found in previous studies that are effective in improving lung adenocarcinoma patients with T790M mutations (8). However, some patients with lung adenocarcinoma may develop T790M and C797s mutations after taking third-generation EGFR-TKIs, which may lead to drug resistance again. There is still no effective treatment for lung adenocarcinoma patients with both T790M and C797s cis mutations.

Here, we report a case of a patient with advanced lung adenocarcinoma with brain metastases and who had stable disease (SD) after 6 courses of treatment with lazertinib, with no significant side effects.

Methods

Primary cells culture

The lung tissue was removed by bronchoscopic puncture under general anesthesia, placed in a sterile dish and transferred to an ultra-clean table, cut into 1-2 mm^3 pieces, and digested by adding 2 ml of 0.25% trypsin (Beyotime, Shanghai) in a water bath at 37°C for 30 min. Excess digestate was discarded, followed by 3 gentle rinses in PBS (Gibco, USA) and 1 rinse in DMEM (Gibco, USA). Discard excess medium, add 5ml of 10% serum medium, disperse well with a pipette to make a cell suspension, and count under a microscope with a cell counting plate. Cells were placed in DMEM medium with 10% FBS and incubated at 37°C with 5% CO_2 (9, 10). The cells were recovered and tested by NGS to confirm that the mutation sites were unaltered, and the results showed EGFR T790M and C797s mutations with mutation frequencies of 26.65% and 20.50%, similar to the results of the third NGS test in this patient, and the cells were subsequently used in the experiment.

Cell scratch assay

Cells were spread evenly in 6-well plates ($3x10^4$/well). 3ml of cell culture medium was added and incubated in the incubator. When the cells are 90% fused, discard the medium and rinse gently with PBS twice. Discard the PBS and make vertical lines in the wells with a 200 ml sterile tip. The suspended cells were then gently washed away with PBS and 3 ml of cell culture medium was added. Photographs were taken at 0h and 24h of scratching, respectively, under a microscope (Olympus, China), and the widths were measured and calculated (11).

Colony-forming unit assay

Digest the cells with 0.25% trypsin for 5 min, add 1 ml of medium to resuspend the cells; evenly spread the mixed cells into a 6-well plate ($1×10^3$/well), continue to culture for 10 days, change the medium every 3 days and observe the cell status; After the cloning was completed, the cells were photographed under the microscope, then gently rinsed once with PBS, fixed with 1 mL of 4% paraformaldehyde per well for 30 min, and then gently rinsed with PBS once; shake the six-well plate to cover the staining solution evenly, and incubate for 10 min; then wash the cells three times with PBS, and take pictures for counting after drying (12).

Statistics

All experiments in this study were repeated three times (n = 3). GraphPad Prism software 7.0 (Beijing, China) was used to generate graphs, and SPSS 23.0 (IBM, USA) was used for the statistical analysis of the data. The *t*-test was used for comparisons between groups. The statistical significance level was set at $p < 0.05$.

Case report

The patient was a 37-year-old Chinese female. In December 2017, the patient visited Nanjing Drum Tower Hospital for "pain in the right lower limb". MRI suggested a lower limb femoral lesion. PET-CT results showed that right lung cancer has multiple metastases in the lung, brain, and bone(T3N2M1). Pathology revealed a lung adenocarcinoma lesion, and IHC assay revealed CK7(+), AE1/AE3(+), TTF-1(+), CDX2(-), PAX8(-), NapsinA(-), P63(-), GATA3(-), CK20(-) (Figures 1A, B). NSG sequencing

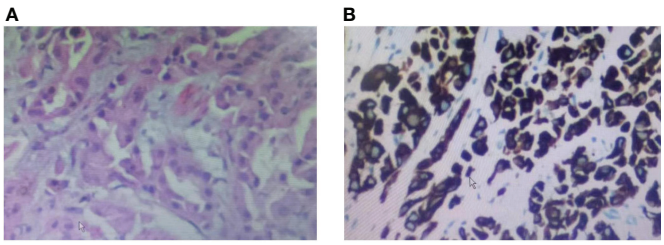

FIGURE 1
Biopsy pathology of a tumor of the lung lesion. **(A)** HE staining of the patient's lung lesion, **(B)** IHC staining of the patient's lung lesion.

suggests EGFR mutations (p.GLY719Cys (22.34%) and EGFR-p.Glu709Val (23.24%) in lung adenocarcinoma.

For further treatment, the patient was transferred to Hefei Cancer Hospital of Chinese academy of science on 11 January, 2018. The physical examination showed the patient's right lung breath sounds were lower than the left, and the right anterior chest was painful on deep inspiration. The patient denied having a family history of oncologic disease. In January 2018, she started treatment with erlotinib (150mg, QD) in combination with bevacizumab (7.5mg/kg). In November 2018, chest CT findings suggested progression of the right lung lesion. The second NGS test was performed in November 2018 and the results suggested EGFR T790M mutation (G719X (24.56%) and T790M (27.81%)) and a change of treatment to osimertinib (80mg, QD).

In November 2019, the patient had a severe headache and a cranial CT showed progression of the brain metastases. Then a change of treatment to bevacizumab + osimertinib and patient headache relief.

In May 2021, the patient was readmitted with a severe headache with vomiting. Cranial MR showed multiple abnormal signals in the left frontoparietal-occipital lobe, basal ganglia region, thalamus, and right cerebellar hemisphere (Figure 2A). The third NGS test revealed EGFR-T790M and C797s cis mutations(G719C (17.86%), T790M (24.56%) and C797S(21.37%)) and subsequent discontinuation of targeted treatment with osimertinib, which changed to temozolomide + cisplatin + bevacizumab treatment.

On May 28, the patient suffered a sudden onset of unconsciousness with paroxysmal limb twitching and dyspnoea. After tracheal intubation, cranial pressure reduction, sedation, and anti-epileptic treatment, vital signs gradually stabilized. To relieve the patient's symptoms, treatment with gammaglobulin was from April 3rd to 7th. Afterward, the patient's state of consciousness and limb weakness improved compared to before. On June 19, CT of the chest showed pulmonary atelectasis and pleural effusion (Figure 2B).

Amivantamab (350mg/d) single-drug anti-tumor therapy for 6 cycles begins on July 19, 2021. On October 9, CT of the chest showed an increase in the size and number of diffuse nodules in both lungs, suggesting progression of the disease (Figure 3A). On October 19, treatment with lazertinib in combination with amivantamab (240mg QD + 700mg d1) was started. The patient's headache subsided, and a chest CT showed a reduction in lung lesions, improved relief of atelectasis, and a reduction in lymph nodes in the lungs on December 30, 2021. The condition was disease-stable (Figure 3B). Until our last follow-up in July 2022, the patient was still living and without serious adverse effects. Statistically, the patient had an OS of 54 months Figure 4.

Discussion

Lazertinib (YH25448) is a new, highly potent third-generation EGFR-TKI with good anti-tumor effects in patients with single (Ex19del, L858R, T790M) and dual (Ex19del/T790M and L858R/T790M) EGFR mutations (13, 14).

In a phase 1-2 clinical study by Ahn (15) et al. 127 patients with non-small cell lung cancer with EGFR (L858R, exon 19 deletions, G719X, or L861Q) mutations were enrolled, and approximately 54% of these patients achieved an objective response rate after oral lazertinib.

In addition, in a subgroup analysis of 127 patients divided into 108 patients with T790M-positive mutations and 19 patients with T790M-negative mutations, the objective response rate was approximately 64% in the T790M-positive group and 37% in the negative group after treatment with lazertinib and no significant side-effects. This study confirmed that lazertinib is effective in treating patients with non-small cell lung cancer and is more efficient in patients with T790M mutations. In a study exploring the cardiac safety of lazertinib, a total of 181 patients with EGFR mutation-positive advanced NSCLC treated with lazertinib were enrolled, and the result

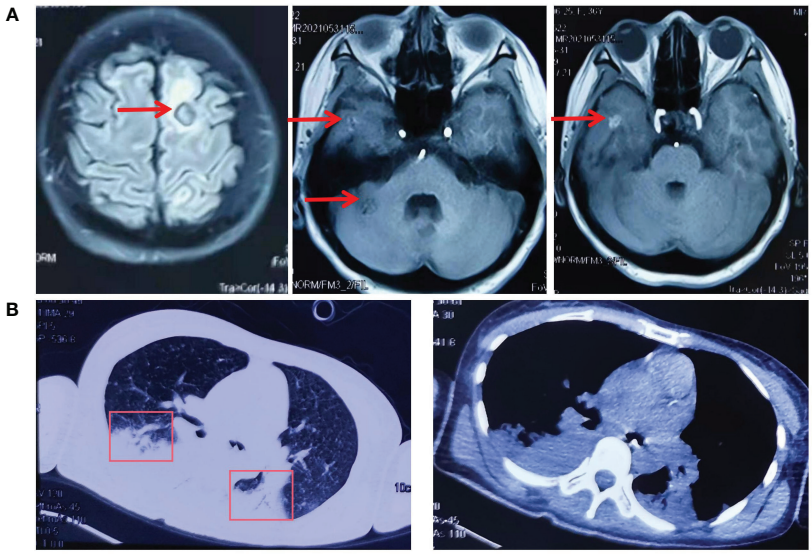

FIGURE 2
The cranial MR and CT of the chest before and after lazertinib and amivantamab treatment. **(A)** In May 2021, cranial MR showed multiple abnormal signals in the left frontoparietal-occipital lobe, basal ganglia region, thalamus, and right cerebellar hemisphere; **(B)** In July 2021, CT of the chest showed pulmonary atelectasis and pleural effusion.

showed that lazertinib did not cause serious cardiotoxicity (16). The above findings suggest that lazertinib is effective in the treatment of NSCLC patients with the T790M mutation without serious toxic effects. In addition, the previous study has also confirmed the anti-tumor effects of lazertinib *in vitro* studies. To further understand the content of previous studies related to lazertinib, we have summarized general information about patients involved in these studies in Table 1, such as race and

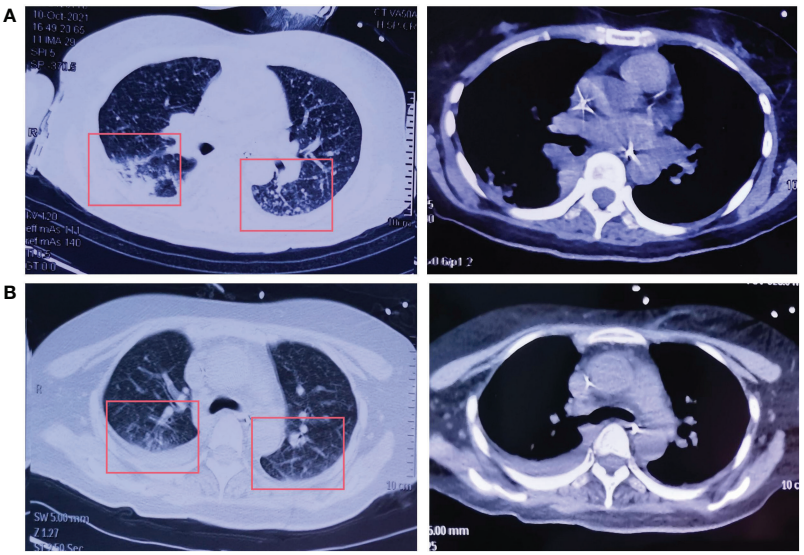

FIGURE 3
The CT of the chest after lazertinib and amivantamab treatment. **(A)** Increased size and number of diffuse nodules in both lungs on chest CT after amivantamab alone on October 9, 2021; **(B)** Decreased size and number of diffuse nodules in both lungs on chest CT after lazertinib in combination with amivantamab on December 30, 2021.

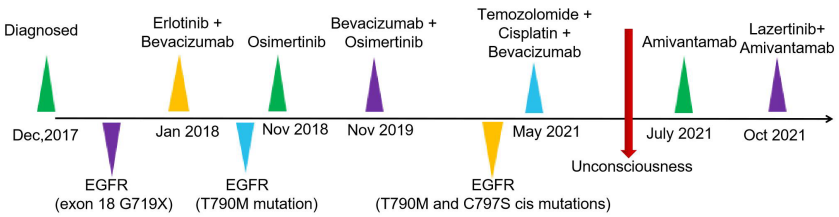

FIGURE 4
Timeline of treatment.

TABLE 1 Previous clinical studies related to lazertinib.

Authors	Year of publication	Number of participants	Race	Median age/age	Sex	Treatment regiem	Ending points
Ahn, et al (15)	2019	127	Asian	NA	Female and male	lazertinib	ORR and AEs
Jang, et al (16)	2021	181	Asian	62	Female and male	lazertinib	Cardiac-related AEs
Park, et al (17)	2020	1	Asian	38	Male	lazertinib	NA

NA, unknown.

gender . In addition, in the study by Yun (14) et al. lazertinib was found to be effective in blocking EGFR and downstream signaling pathways in lung cancer cells, and in the nude mouse transplant tumor model, lazertinib was more effective than osimertinib in anti-tumor progression by using the same concentration.

We report a case of a female patient with advanced lung adenocarcinoma who developed T790M and C797s cis mutations after gefitinib, chemotherapy, and osimertinib, and whose disease continued to progress after three months of amivantamab, while tumor progression was significantly inhibited after the combination of lazertinib. In contrast to our report, Park et al (17). reported a patient with EGFR-T790M and C797s cis mutations after treatment of lazertinib. This is contrary to the results of our report, with such a little information that the authors provided, we are unable to determine exactly what caused this patient to be resistant to lazertinib. But in cell viability assay and western blot assay, the cells drived from patient were also shown a c-MET mutation and resistence to savolitinib(c-Met inhibitor). As reported in previous studies, c-MET mutation is one of the common bypass mutations in lung adenocarcinoma patients with EGFR mutation who develop drug resistance (18). Therefore, we speculate that the patient had a T790M and C757s mutation along with a c-MET mutation, which led to stimulated resistance to lazertinib. However, this conjecture still needs to be further confirmed by extensive *in vivo* and vitro experiments.

In our report, the patient was treated with lazertinib in combination with amivantamab. To clarify which of these two drugs exerted an anti-cancer effect, we investigated the inhibitory

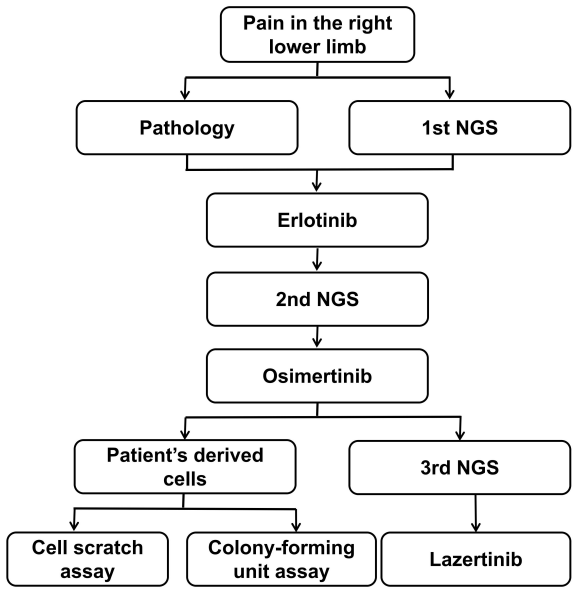

FIGURE 5
Figure of analysis process.

effects of these two drugs on cell invasion and proliferation by culturing patient-derived lung adenocarcinoma cells (T790M and C797s cis) and cell scratch assay and Colony-forming unit assay. Our analysis process is showing in Figure 5.

Con: only patient-derived lung adenocarcinoma cells (T790M and C797s cis); Laz: patient-derived lung adenocarcinoma cells (T790M and C797s cis)+ lazertinib (1 μ/mol); Ami: patient-derived lung adenocarcinoma cells (T790M and C797s cis)+ amivantamab (1 μ/mol); Laz+Ami:patient-derived lung adenocarcinoma cells (T790M and C797s cis)+ lazertinib (1 μ/mol)+amivantamab. ** and ***p< 0.01, 0.001, respectively, compared to the control group.

The results showed that both lazertinib and amivantamab could inhibit cell proliferation and migration, and the inhibitory effect of lazertinib was better than that of amivantamab (p < 0.01), while the inhibition effect of lazertinib combined with amivantamab was not statistically different from that of lazertinib alone (Figures 6A, B, p > 0.05). This result suggests that lazertinib is effective in treating lung adenocarcinoma patients with EGFR-T790M and C797s mutations, while the combination of amivantamab did not significantly improve the treatment effect.

Our study is the first to report successful treatment with lazertinib in patients with advanced lung adenocarcinoma with EGFR-T790M and C797s cis mutations and validated this conclusion with *in vitro* experiments. However, our study has some shortcomings, such as: 1. only one patient report; 2. lack of evidence from animal studies. These shortcomings will be improved in our future studies.

Conclusion

We here report a case of advanced lung adenocarcinoma (T790M and C797s cis mutations) successfully treated with lazertinib with an OS of 54 months, and confirm the therapeutic effect of lazertinib by *in vitro* experiments. This finding is expected to help patients with lung adenocarcinoma who also have T790M and C797s cis mutations choose their treatment subject.

Patients perspective

I was initially suffering from pain in the right lower limb and was diagnosed with lung cancer in another hospital. Therefore, I came here with the aim of better treatment. Doctor Li and Fang have devised a comprehensive treatment plan for me. One day in 2021, I fell into a coma and Dr Li informed my husband that I might have become drug-resistant again, which led to the non-stop progression of lesions in my lungs and brain. After another genetic test, Dr Fang told me that I had a rare mutation for which there was no targeted drug and suggested I try lazertinib or amivantamab. The doctors then treated me with amivantamab, but unfortunately my disease continued to progress. Dr Li and Dr Fang then treated me with lazertinib and my disease finally stabilized after a few treatments. I am very grateful to the doctors for helping to ease my pain and extend my life. I agreed to share my medical history and Specimens, I have already signed an informed consent form.

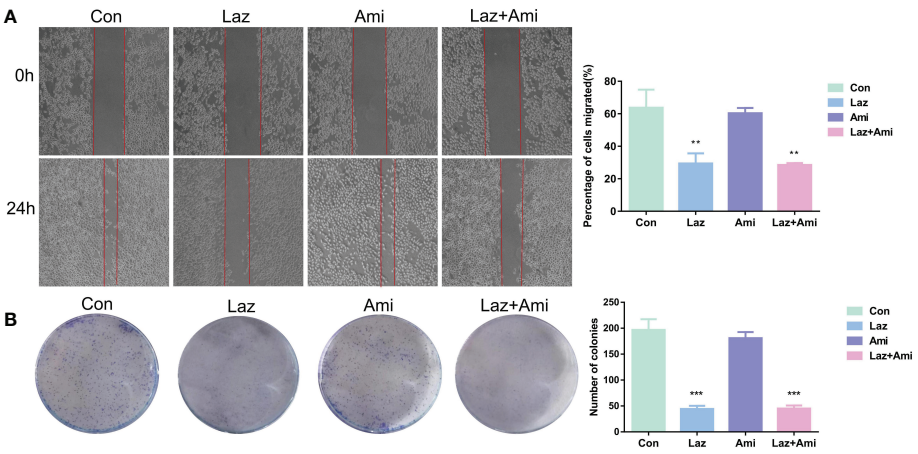

FIGURE 6
The effect of lazertinib and amivantamab on migration and proliferation of patient's lung adenocarcinoma cells. **(A)** Scratch assay shows lazertinib inhibits migration ability of lung adenocarcinoma cells better than amivantamab; **(B)** Colony-forming unit assays shows lazertinib inhibits lung adenocarcinoma cell proliferation ability more than amivantamab. *p < 01, ***p < 0.001.

Data availability statement

The raw data supporting the conclusions of this article will be made available by the authors, without undue reservation.

Ethics statement

The studies involving human participants were reviewed and approved by Medical Ethics Committee of Hefei Cancer Hospital, Chinese Academy of Sciences. The patients/participants provided their written informed consent to participate in this study. Written informed consent was obtained from the individual(s) for the publication of any potentially identifiable images or data included in this article.

Author contributions

Xl and YF participated in the conception and design of the research; YF and QZ completed the experiment and wrote the article; WW and JT helped to collect information. The final manuscript was reviewed by all authors. All authors contributed to the article and approved the submitted version.

Conflict of interest

The authors declare that the research was conducted without any commercial or financial relationships and withoutpotential conflicts of interest.

Publisher's note

All claims expressed in this article are solely those of the authors and do not necessarily represent those of their affiliated organizations, or those of the publisher, the editors and the reviewers. Any product that may be evaluated in this article, or claim that may be made by its manufacturer, is not guaranteed or endorsed by the publisher.

References

1. Sung H, Ferlay J, Siegel RL, Laversanne M, Soerjomataram I, Jemal A, et al. Global cancer statistics 2020: GLOBOCAN estimates of incidence and mortality worldwide for 36 cancers in 185 countries. *CA Cancer J Clin* (2021) 71:209–49. doi: 10.3322/caac.21660

2. Nooreldeen R, Bach H. Current and future development in lung cancer diagnosis. *Int J Mol Sci* (2021) 22(16):8661. doi: 10.3390/ijms22168661

3. Spella M, Stathopoulos GT. Immune resistance in lung adenocarcinoma. *Cancers (Basel)* (2021) 13(3):384. doi: 10.3390/cancers13030384

4. Siegel RL, Miller KD, Jemal A. Cancer statistics, 2017. *CA Cancer J Clin* (2017) 67(1):7–30. doi: 10.3322/caac.21387

5. Tan DS, Yom SS, Tsao MS, Pass HI, Kelly K, Peled N, et al. The international association for the study of lung cancer consensus statement on optimizing management of EGFR mutation-positive non-small cell lung cancer: Status in 2016. *J Thorac Oncol* (2016) 11(7):946–63. doi: 10.1016/j.jtho.2016.05.008

6. Rawluk J, Waller CF. Gefitinib. *Recent Results Cancer Res* (2018) 211:235–46. doi: 10.1007/978-3-319-91442-8_16

7. Liao BC, Griesing S, Yang JC. Second-line treatment of EGFR T790M-negative non-small cell lung cancer patients. *Ther Adv Med Oncol* (2019) 11:1758835919890286. doi: 10.1177/1758835919890286

8. Dhillon S. Lazertinib: First approval. *Drugs* (2021) 81(9):1107–13. doi: 10.1007/s40265-021-01533-x

9. Speirs V, Green AR, Walton DS, Kerin MJ, Fox JN, Carleton PJ, et al. Short-term primary culture of epithelial cells derived from human breast tumours. *Br J Cancer* (1998) 78(11):1421–9. doi: 10.1038/bjc.1998.702

10. Tiran V, Lindenmann J, Brcic L, Heitzer E, Stanzer S, Tabrizi-Wizsy NG, et al. Primary patient-derived lung adenocarcinoma cell culture challenges the association of cancer stem cells with epithelial-to-mesenchymal transition. *Sci Rep* (2017) 7(1):10040. doi: 10.1038/s41598-017-09929-0.11

11. Gao F, Yin P, Wu Y, Wen J, Su Y, Zhang X, et al. Knockdown of RhoC inhibits oral squamous cell carcinoma cell invasion and metastasis *via* regulation of HMGA2. *J Oncol* (2021) 2021:6644077. doi: 10.1155/2021/6644077

12. Sun C, Gao W, Liu J, Cheng H, Hao J. FGL1 regulates acquired resistance to gefitinib by inhibiting apoptosis in non-small cell lung cancer. *Respir Res* (2020) 21 (1):210. doi: 10.1186/s12931-020-01477-y

13. Dhillon S. Lazertinib: First Approval. Drugs. (2021) 81(9):1107–13. doi: 10.1007/s40265-021-01533-x

14. Yun J, Hong MH, Kim SY, Park CW, Kim S, Yun MR, et al. YH25448, an irreversible EGFR-TKI with potent intracranial activity in EGFR mutant non-small cell lung cancer. *Clin Cancer Res* (2019) 25(8):2575–87. doi: 10.1158/1078-0432.CCR-18-2906

15. Ahn MJ, Han JY, Lee KH, Kim SW, Kim DW, Lee YG, et al. Lazertinib in patients with EGFR mutation-positive advanced non-small-cell lung cancer: results from the dose escalation and dose expansion parts of a first-in-human, open-label, multicentre, phase 1-2 study. *Lancet Oncol* (2019) 20(12):1681–90. doi: 10.1016/S1470-2045(19)30504-2

16. Jang SB, Kim KB, Sim S, Cho BC, Ahn MJ, Han JY, et al. Cardiac2 safety assessment of lazertinib: Findings from patients with EGFR mutation-positive advanced NSCLC and preclinical studies. *JTO Clin Res Rep* (2021) 2(10):100224. doi: 10.1016/j.jtocrr.2021.100224

17. Park S, Ku BM, Jung HA, Sun JM, Ahn JS, Lee SH, et al. EGFR C797S as a resistance mechanism of lazertinib in non-small cell lung cancer with EGFR T790M mutation. *Cancer Res Treat* (2020) 52(4):1288–90. doi: 10.4143/crt.2020.278

18. Park S, Ku BM, Jung HA, Sun JM, Ahn JS, Lee SH, et al. Asian Thoracic oncology research group (ATORG) expert consensus statement on MET alterations in NSCLC: Diagnostic and therapeutic considerations. *Clin Lung Cancer* (2022) 23(8):670–85. doi: 10.1016/j.cllc.2022.07.012

frontiers | Frontiers in Oncology

TYPE Case Report
PUBLISHED 13 January 2023
DOI 10.3389/fonc.2022.1032225

OPEN ACCESS

EDITED BY
Kohei Fujita,
National Hospital Organization Kyoto Medical Center, Japan

REVIEWED BY
Dan Ma,
Affiliated Hospital of Guizhou Medical University, China
Hussain Alizadeh,
University of Pécs, Hungary

*CORRESPONDENCE
Dan Liu
liudan10965@wchscu.cn

SPECIALTY SECTION
This article was submitted to Thoracic Oncology, a section of the journal Frontiers in Oncology

RECEIVED 30 August 2022
ACCEPTED 21 December 2022
PUBLISHED 13 January 2023

CITATION
Tian H, Yang L, Hou W, Wu Y, Dai Y, Yu J and Liu D (2023) Case report: Identification of acute promyelocytic leukemia during osimertinib resistance followed by granulocyte colony-stimulating factor and pembrolizumab. *Front. Oncol.* 12:1032225. doi: 10.3389/fonc.2022.1032225

Case report: Identification of acute promyelocytic leukemia during osimertinib resistance followed by granulocyte colony-stimulating factor and pembrolizumab

Huohuan Tian[1], Linhui Yang[1], Wang Hou[1], Yu Wu[2], Yang Dai[2], Jiang Yu[3] and Dan Liu[1]*

[1]Department of Respiratory and Critical Care Medicine, West China Hospital, Sichuan University, Chengdu, Sichuan, China, [2]Department of Hematology, West China Hospital, Sichuan University, Chengdu, Sichuan, China, [3]Department of Laboratory Medicine, West China Hospital, Sichuan University, Chengdu, Sichuan, China

Background: The occurrence of acute promyelocytic leukemia (APL) during the management of lung cancer is rare and life-threatening. It was mainly reported to be secondary to chemoradiotherapy. A few studies reported an increased incidence of therapy-related acute promyelocytic leukemia (t-APL) after gefitinib became available.

Case presentation: We reported a patient who developed thrombocytopenia after receiving oral osimertinib in combination with intensity-modulated radiotherapy (IMRT). For half a year, she had an unrecoverable low platelet count, which progressed to concomitant leukopenia and the transient appearance of orthochromatic normoblasts in the peripheral blood test, indicating a dormant myeloid disorder. Due to simultaneous resistance to epidermal growth factor receptor (EGFR) tyrosine kinase inhibitors (TKI), pembrolizumab and granulocyte colony-stimulating factor (G-CSF) were administered, revealing prominent signs of hematological malignancy in a peripheral blood test that was later identified as t-APL.

Conclusion: In general, patients undergoing EGFR-TKI combined with local radiotherapy should be concerned about their hematological assessment. If patients exhibit unrecoverable abnormalities in routine blood tests, a secondary nonsolid malignancy other than myelosuppression should be considered, and further lung cancer treatment should be discontinued.

KEYWORDS

therapy-related acute promyelocytic leukemia, osimertinib, granulocyte colony-stimulating factor, pembrolizumab, lung cancer

Introduction

Therapy-related acute myeloid leukemia (t-AML) secondary to the administration of chemotherapy and radiotherapy has been considered an exceptional and serious complication with an antecedent malignancy (1). As a fatal subtype of AML, acute promyelocytic leukemia (APL) is commonly characterized by a balanced chromosomal translocation between chromosomes 15 and 17 t-(15;17) (q24; q21), which leads to promyelocytic leukemia (PML)-retinoic acid receptor-α (RARα) rearrangement (2). Comparatively, t-APL may be favored to harbor additional cytogenetic abnormalities, commonly occurring in chromosomes 5, 7, and 17 (3, 4).

According to a systematic review, therapy-related APL following breast cancer is frequent in clinical practice (5). There are scattered reports of APL secondary to lung cancer and corresponding treatment.

Chemotherapy, radiotherapy, or both for prior neoplasms are demonstrated contributors to the development of t-APL (4, 6, 7). Current therapeutic strategies for lung cancer have flourished due to the emergence of targeted agents, immunotherapy, and the transition from conventional radiotherapy to intensity-modulated radiotherapy (IMRT). However, there is scarce evidence regarding APL in these novel therapies (8, 9).

Herein, we report a case of t-APL with advanced non-small cell lung cancer (NSCLC) after targeted therapy and IMRT followed by granulocyte colony-stimulating factor (G-CSF) and immune checkpoint inhibitor (ICI) treatment. Since t-APL shows a similar remission rate to *de novo* APL (80%) but a high risk of life-threatening coagulopathy (5, 10), we delineated the details so that clinicians may timely notice and treat the complication during the management of lung cancer.

Case report

A 58-year-old woman was diagnosed with lung adenocarcinoma with an EGFR-L858R mutation and thoracic vertebral (T5 and T11) invasion in January 2021. Osimertinib was started in February 2021 at a dose of 80 mg/day. The patient received IMRT at the T5 (3,000 cGy 10 times, 2,100 cGy 7 times) and T11 (3,000 cGy 10 times, 2,100 cGy 7 times) from 3 to 17 June 2021 and 24 June to 5 July 2021, respectively. In June 2021, the patient complained of subtle ostealgia, and her laboratory tests revealed mild thrombocytopenia. While continuing osimertinib, the patient was followed up every 2 months until she achieved partial remission (PR). During that time, her platelet count was consistently 50–90 × 10^9/L (Table 1), with no signs of hemorrhage.

In March 2022, the patient reported a mildly aggravated ostealgia. A computed tomography (CT) scan in March 2022 revealed metastasis in the left humerus and sternum. Considering EGFR-TKI resistance, the clinician performed a tissue rebiopsy after withdrawing osimertinib. Peripheral blood test upon admission displayed thrombocytopenia, leukopenia, and orthochromatic normoblast appearance (Table 1), and coagulation parameters are shown in Supplementary Table S1. The pathological result of the rebiopsy is shown in Supplementary Table S2. Because spontaneous thrombocytopenia remission was predicted on 7 June 2022 (Table 2), immunotherapy combined with platinum-based chemotherapy was recommended. On the day when pembrolizumab at 200 mg/dl was administered, the patient experienced severe ostealgia all night. After receiving G-CSF and interleukin (IL)-11, myeloblasts containing Auer's body appeared in her peripheral blood. Considering the possibility of APL, we monitored her coagulation parameters (Supplementary Table S1). A bone marrow aspiration was performed after stopping G-CSF and IL-11 treatment for 3 days. The bone marrow cytology revealed 68% promyelocytes, indicating t-APL (Supplementary Figure S1). Marrow flow cytometry (FCM) confirmed the finding (Figure 1). The identification of a rare PML/RARα (Bcr 3) fusion gene suggested acute myeloid rearrangement. There was no mutation in any common AML prognostic gene, including FLT3, dupMLL, IDH1, IDH2, NPM1, KIT, NRAS, CEBPA, DNMT3A, PHF6, TET2, ASXL1, RUNX1, TP53, and WT1. Chromosome karyotypic analysis showed 46, XX, add (7, 11), t (15;17) (q24; q21) [6]/46, XX [14] (Figure 2). Subsequently, the patient underwent all-trans retinoic acid and arsenic acid induction therapy. During the induction therapy, fever, hypotension, and pleural effusion occurred. Dexamethasone and vasopressor agents were also administered. She was successfully cured eventually. In September 2022, she received chemotherapy for lung cancer after documenting the complete

TABLE 1 Peripheral blood tests during osimertinib and adjuvant IMRT.

	2,021.6.10	2,021.7.1	2,021.8.5	2,021.10.25	2,021.12.21	2,022.1.24	2,022.3.21	2,022.4.30
Hb (g/L)	130	129	112	125	127	128	119	116
WBC (10^9/L)	5.5	3.97	3.97	4.14	3.73	3.84	3.08	1.9
PLT (10^9/L)	83	58	55	66	81	86	68	37
ON (/100 cells)	0	0	0	0	0	0	0	1

Hb, hemoglobin; WBC, white blood cell; PLT, platelet; ON, orthochromatic normoblast; IMRT was started on 3 June 2021.

TABLE 2 Peripheral blood tests during usage of G-CSF and pembrolizumab.

	2,022.5.1	2,022.5.3	2,022.5.5	2,022.5.9	2,022.6.7	2,022.6.10	2,022.6.13
Hb (g/L)	103	96	104	96	96	89	94
PLT (10^9/L)	36	35	42	63	97	49	49
WBC (10^9/L)	4.64	2.77	2.91	2.15	1.49	4.13	4.74
ON (/100 cells)	0	0	0	1	0	1	0
Myeloblast (10^9/L)	0	0	0	0	0	0	2
Promyelocytes (%)	0	0	0	0	0	0	1
G-CSF	+	−	+	+	−	+	+

Hb, hemoglobin; WBC, white blood cell; PLT, platelet; ON, orthochromatic normoblast; G-CSF, granulocyte colony-stimulating factor; "+" G-CSF was injected; "−" G-CSF was not used.

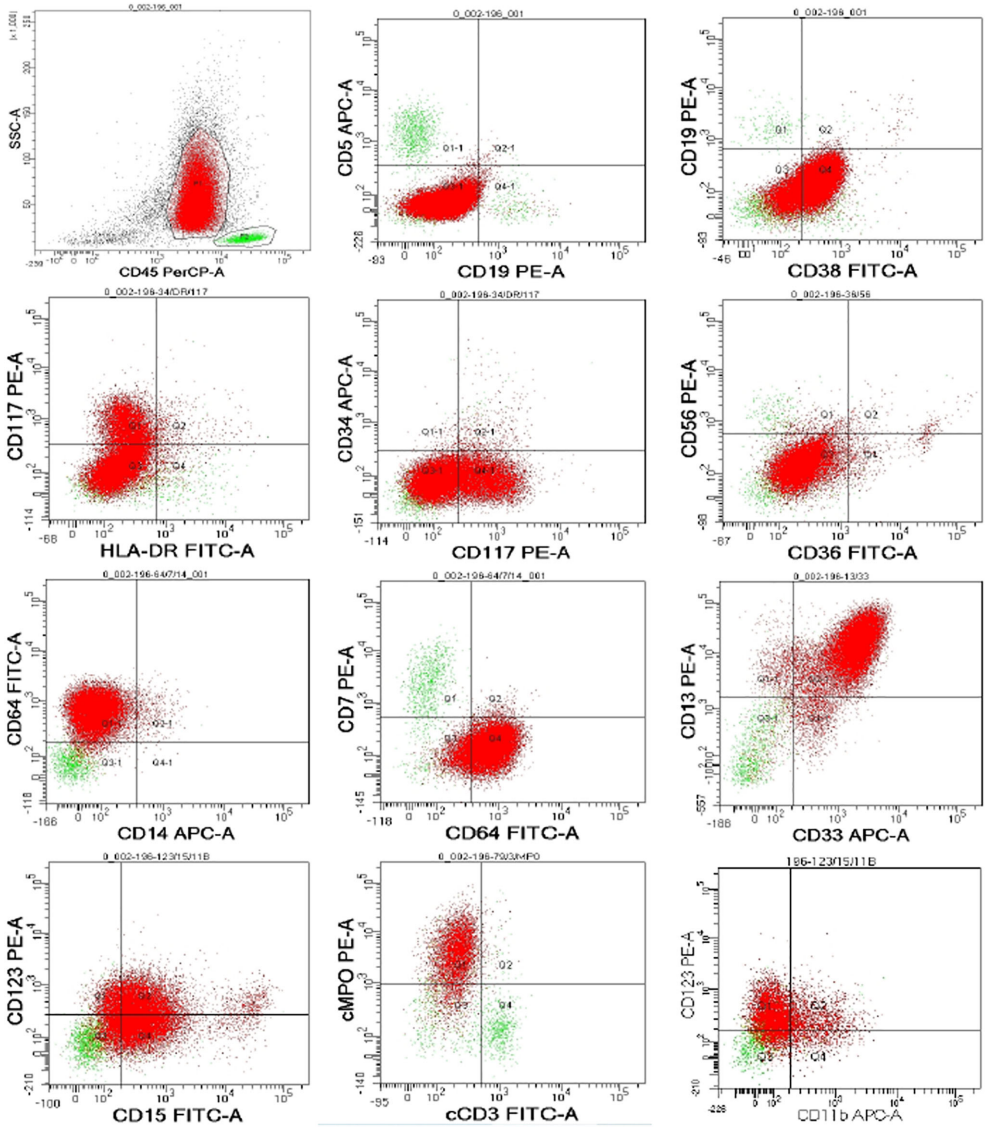

FIGURE 1
Bone marrow flow cytometry.

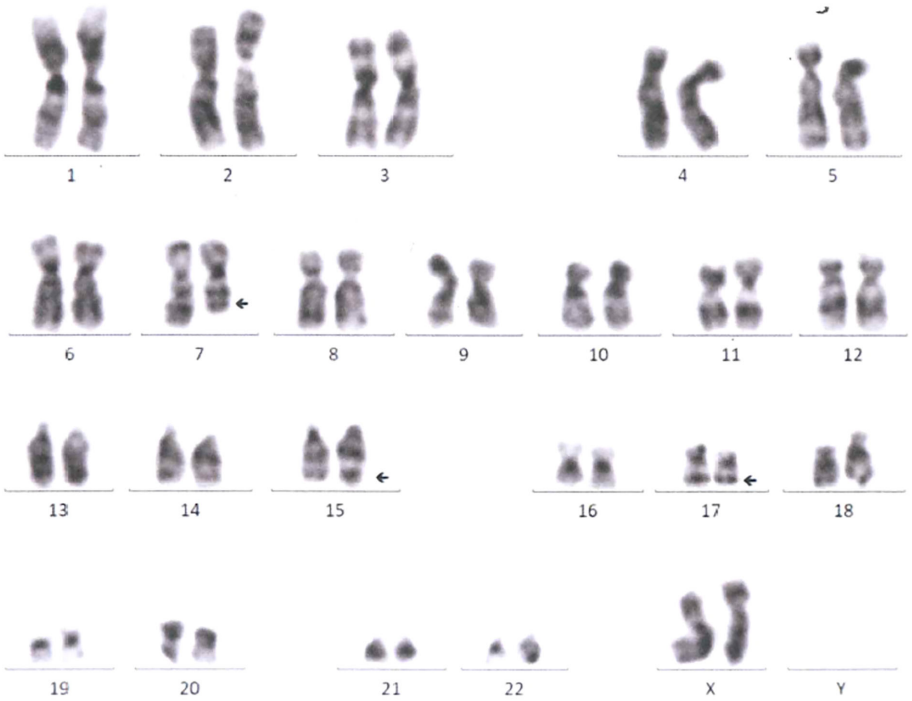

FIGURE 2
Marrow chromosomal analysis.

remission of APL. She is now being followed up by telephone every month.

The patient had no history of any hematological disease that could lead to acute leukemia, such as lymphoma, myelodysplastic syndromes (MDS), multiple myeloma, and so on. She denied any hematological disease history in her family members.

Discussion

EGFR-TKI ± radiotherapy is the first-line treatment for advanced NSCLC patients with EGFR mutation and oligometastasis (12). Studies demonstrated that radiation was the inciting factor for myeloid neoplasms, including all AML categories and MDS (5, 7, 13). Lung cancer treated with radiation showed an increased relative risk of AML/MDS over the next 1–12 years (14). Ionizing radiation may prompt reactive oxygen species, causing DNA double-strand breaks (15). However, the radiotherapy modality research involved mainly encompassed external beam therapy (EBRT) and brachytherapy. The use of IMRT increased in the past few years because of its superior safety and fewer side effects. Modulated radiation beams and sculpted radiation doses ensure precise coherence with geometric targets and enhanced therapeutic effects (16). A study revealed that secondary MDS/AML could be provoked by IMRT in prostate cancer patients (17). Hematological toxicity, such as thrombocytopenia, was also observed in malignant pleural mesothelioma patients treated with IMRT (18). However, it has not been reported as a factor for hematological malignancy or toxicity in lung cancer patients.

Patients with radiation-induced secondary malignancies tend to experience a long latency period (19, 20). Paradoxically, the intervals between initial radiotherapy and our patient's thrombocytopenia and t-APL diagnosis were 7 days and 12 months, respectively. In 2006, Keitaro et al. observed a clustered incidence of acute promyelocytic leukemia in NSCLC cases treated with first-generation EGFR-TKI gefitinib (8, 21). Notably, all the observed cases reported cytopenia, especially thrombocytopenia in the beginning. The authors suggested that the t-APL inducibility of gefitinib should be further elucidated. In 2016, clinicians from Japan found a chronic myelomonocytic leukemia blast crisis when synchronous lung adenocarcinoma was treated by EGFR-TKI (22). Another study in 2021 reported a case of thrombocytopenia with immature cells in the peripheral blood during receiving erlotinib, which turned out to be t-AML (11). To date, no report has identified hematological malignancies while the patient was receiving osimertinib treatment. We identified transient orthochromatic normoblasts in our patient's peripheral blood on 30 April 2022, during osimertinib treatment in our case. Furthermore, subsequent G-CSF and IL-11 after TKI cessation did not ameliorate her thrombocytopenia and emerging leukopenia from 30 April 2022 to 9 May 2022 (Table 2), signifying a hematopoiesis disorder such as MDS and acute myeloid

leukemia. Hence, we speculated that continuous usage of third-generation EGFR-TKI osimertinib may hasten the secondary APL. Regrettably, bone marrow aspiration was not performed when cytopenia occurred during continuous EGFR-TKI and regional radiotherapy treatment.

T-APL was not confirmed until the administration of a second-line therapy comprising pembrolizumab and chemotherapy. G-CSF is a hematopoietic glycoprotein produced by monocytes, macrophages, fibroblasts, and endothelial cells (23). It is used to accelerate neutrophil recovery after chemotherapy by regulating cell cycle activation, proliferation, and terminal maturation (23). Researchers revealed that congenital neutropenia patients on G-CSF are more susceptible to developing MDS/AML over time (24). Granulocyte colony-stimulating factor has also been shown to be a risk factor for AML/MDS in breast and lung cancer populations (25). Promyelocytes containing Auer's body indeed emerged in our patient's peripheral blood after G-CSF usage. Nevertheless, progressive thrombocytopenia, leukopenia, and orthochromatic normoblast were virtually presented in her peripheral blood before G-CSF usage, when she was still undergoing osimertinib treatment. Considering that t-APL typically occurs without the prodromal, preleukemic, and myelodysplastic phases (5), we speculated a likelihood of t-APL existence prior to the use of G-CSF.

Immunotherapy plays a critical role in NSCLC. PD-1-binding pembrolizumab disrupted its anchoring to PD-L1, impeding the inhibition of T cells and mounting its recognition to tumor cells (26). There is only one case report to date about t-APL involving the history of pembrolizumab treatment (9). According to our observation, the intravenous infusion of pembrolizumab aggravated the patient's chronic ostealgia acutely. The association between pembrolizumab and t-APL remained occult. Of interest, the refractory leukopenia was alleviated but the thrombocytopenia was exacerbated following pembrolizumab and G-CSF (Table 2). This phenomenon resembled Paola's study, which found that G-CSF injection worsened anemia in breast cancer patients receiving chemotherapy (27), and it is hypothesized that granulopoietic lineages competed with erythropoietic lineages for differentiating hematopoietic cell stems.

Altogether, our patient had been exposed to a series of predisposing factors to t-APL, making it difficult to ascertain that the third-generation EGFR-TKI osimertinib was the sole and determining cause of the complication. However, it is reasonable to conclude that the myeloid disease developed during IMRT plus continuous osimertinib. Further evaluation based on a larger sample size is warranted. Regardless, a widespread matter of osimertinib resistance gives rise to novel therapy exploration (28). KEYNOTE-789 is an ongoing trial assessing platinum-based chemotherapy combined with pembrolizumab for this entity. EGFR-TKI, radiation, G-CSF, and chemotherapy agents are all widely used, increasing the risk of a secondary hematological disease and even malignancy. Given the positive response of t-APL to all-trans retinoic acid therapy, a key problem now is determining whether we can identify those nearly asymptomatic patients early and withhold APL-facilitating interventions. Thus, after the patients achieved hematological remission, should the treatment strategy for lung cancer be persisted?

Conclusion

We first reported the identification of t-APL when the patient acquired resistance to osimertinib. Chemotherapy, radiotherapy, or both have been demonstrated to be risk factors for t-APL. Previous reports and our case supported positive concern for such complications, given the widespread usage of EGFR TKI and resistance to targeted therapy

Data availability statement

The original contributions presented in the study are included in the article/Supplementary Material. Further inquiries can be directed to the corresponding author.

Ethics statement

The studies involving human participants were reviewed and approved by Sichuan University Ethics Review Board. The patients/participants provided their written informed consent to participate in this study. Written informed consent was obtained from the individual(s) for the publication of any potentially identifiable images or data included in this article.

Author contributions

HT, LY, and WH: writing—original draft. YW, YD, and JY: writing original draft preparation. DL: administrative support and supervision. All the authors contributed to the article and approved the submitted version.

Funding

This work was supported by National Natural Science Foundation of China (Grant Number 82173182).

Acknowledgments

The authors thank the patient and her family for their persistence in comprehensive treatment and granting permission to present her medical history here. We also thank all our colleagues for the management of such an infrequent patient.

Conflict of interest

The authors declare that the research was conducted in the absence of any commercial or financial relationships that could be construed as a potential conflict of interest.

Publisher's note

All claims expressed in this article are solely those of the authors and do not necessarily represent those of their affiliated organizations, or those of the publisher, the editors and the reviewers. Any product that may be evaluated in this article, or claim that may be made by its manufacturer, is not guaranteed or endorsed by the publisher.

Supplementary material

The Supplementary Material for this article can be found online at: https://www.frontiersin.org/articles/10.3389/fonc.2022.1032225/full#supplementary-material

References

1. Leone G, Fianchi L, Pagano L, Voso MT. Incidence and susceptibility to therapy-related myeloid neoplasms. *Chemico-biological Interact* (2010) 184(1-2):39–45. doi: 10.1016/j.cbi.2009.12.013

2. Jimenez JJ, Chale RS, Abad AC, Schally AV. Acute promyelocytic leukemia (APL): a review of the literature. *Oncotarget* (2020) 11(11):992–1003. doi: 10.18632/oncotarget.27513

3. Yin CC, Glassman AB, Lin P, Valbuena JR, Jones D, Luthra R, et al. Morphologic, cytogenetic, and molecular abnormalities in therapy-related acute promyelocytic leukemia. *Am J Clin Pathol* (2005) 123(6):840–8. doi: 10.1309/tjff-k819-rpcl-fkj0

4. Beaumont M, Sanz M, Carli PM, Maloisel F, Thomas X, Detourmignies L, et al. Therapy-related acute promyelocytic leukemia. *J Clin Oncol Off J Am Soc Clin Oncol* (2003) 21(11):2123–37. doi: 10.1200/jco.2003.09.072

5. Rashidi A, Fisher SI. Therapy-related acute promyelocytic leukemia: a systematic review. *Med Oncol* (2013) 30(3):625. doi: 10.1007/s12032-013-0625-5

6. Wang H, Yin Y, Wang R, Huang J, Xue H, Cheng Y, et al. Clinicopathological features, risk and survival in lung cancer survivors with therapy-related acute myeloid leukaemia. *BMC Cancer.* (2020) 20(1):1081. doi: 10.1186/s12885-020-07603-9

7. Le Deley MC, Suzan F, Cutuli B, Delaloge S, Shamsaldin A, Linassier C, et al. Anthracyclines, mitoxantrone, radiotherapy, and granulocyte colony-stimulating factor: risk factors for leukemia and myelodysplastic syndrome after breast cancer. *J Clin Oncol Off J Am Soc Clin Oncol* (2007) 25(3):292–300. doi: 10.1200/JCO.2006.05.9048

8. Matsuo K, Kiura K, Tabata M, Uchida A, Hotta K, Niiya D, et al. Clustered incidence of acute promyelocytic leukemia during gefitinib treatment for non-small-cell lung cancer: experience at a single institution. *Am J Hematol* (2006) 81 (5):349–54. doi: 10.1002/ajh.20569

9. Suzuki R, Kawai H, Furuya D, Akashi H, Ogawa Y, Kawada H, et al. Successful treatment of therapy-related acute promyelocytic leukemia:with all-trans-retinoic acid following. *Tokai J Exp Clin Med* (2020) 45(2):92–6.

10. Tallman MS. The thrombophilic state in acute promyelocytic leukemia. *Semin Thromb hemostasis.* (1999) 25(2):209–15. doi: 10.1055/s-2007-994922

11. Koo SM, Kim KU, Kim YK, Uh ST. Therapy-related myeloid leukemia during erlotinib treatment in a non-small cell lung cancer patient: A case report. *World J Clin Cases.* (2021) 9(24):7205–11. doi: 10.12998/wjcc.v9.i24.7205

12. Ettinger DS, Wood DE, Aisner DL, Akerley W, Bauman JR, Bharat A, et al. Non-small cell lung cancer, version 3.2022, NCCN clinical practice guidelines in oncology. *J Natl Compr Canc Netw* (2022) 20(5):497–530. doi: 10.6004/jnccn.2022.0025

13. Teepen JC, Curtis RE, Dores GM, Berrington de Gonzalez A, van den Heuvel-Eibrink MM, Kremer LCM, et al. Risk of subsequent myeloid neoplasms after radiotherapy treatment for a solid cancer among adults in the united states, 2000-2014. *Leukemia* (2018) 32(12):2580–9. doi: 10.1038/s41375-018-0149-2

14. Radivoyevitch T, Sachs RK, Gale RP, Molenaar RJ, Brenner DJ, Hill BT, et al. Defining AML and MDS second cancer risk dynamics after diagnoses of first cancers treated or not with radiation. *Leukemia* (2016) 30(2):285–94. doi: 10.1038/leu.2015.258

15. Sill H, Olipitz W, Zebisch A, Schulz E, Wölfler A. Therapy-related myeloid neoplasms: pathobiology and clinical characteristics. *Br J Pharmacol* (2011) 162 (4):792–805. doi: 10.1111/j.1476-5381.2010.01100.x

16. Chun SG, Hu C, Choy H, Komaki RU, Timmerman RD, Schild SE, et al. Impact of intensity-modulated radiation therapy technique for locally advanced non-Small-Cell lung cancer: A secondary analysis of the NRG oncology RTOG 0617 randomized clinical trial. *J Clin Oncol Off J Am Soc Clin Oncol* (2017) 35 (1):56–62. doi: 10.1200/JCO.2016.69.1378

17. Wang R, Zeidan AM, Yu JB, Soulos PR, Davidoff AJ, Gore SD, et al. Myelodysplastic syndromes and acute myeloid leukemia after radiotherapy for prostate cancer: A population-based study. *Prostate* (2017) 77(5):437–45. doi: 10.1002/pros.23281

18. Matsuo Y, Shibuya K, Okubo K, Ueki N, Aoyama A, Sonobe M, et al. Long-term outcomes of intensity-modulated radiotherapy following extra-pleural pneumonectomy for malignant pleural mesothelioma. *Acta Oncologica* (2017) 56 (7):957–62. doi: 10.1080/0284186x.2017.1279749

19. Hall EJ, Wuu C-S. Radiation-induced second cancers: the impact of 3D-CRT and IMRT. *Int J Radiat OncologyBiologyPhysics.* (2003) 56(1):83–8. doi: 10.1016/s0360-3016(03)00073-7

20. Amadori S, Papa G, Anselmo AP, Fidani P, Mandelli F, Biagini C. Acute promyelocytic leukemia following ABVD (doxorubicin, bleomycin, vinblastine, and dacarbazine) and radiotherapy for hodgkin's disease. *Cancer Treat Rep* (1983) 67(6):603–4.

21. Uchida A, Matsuo K, Tanimoto M. APL during gefitinib treatment for non-small-cell lung cancer. *N Engl J Med* (2005) 352(8):843. doi: 10.1056/NEJM200502243520825

22. Ogata H, Okamoto I, Yoshimoto G, Obara T, Ijichi K, Iwama E, et al. Chronic myelomonocytic leukemia blast crisis in a patient with advanced non-small cell lung cancer treated with EGFR tyrosine kinase inhibitors. *Respir Investig* (2017) 55(2):181–3. doi: 10.1016/j.resinv.2016.12.002

23. D'Souza A, Jaiyesimi I, Trainor L, Venuturumili P. Granulocyte colony-stimulating factor administration: adverse events. *Transfus Med Rev* (2008) 22 (4):280–90. doi: 10.1016/j.tmrv.2008.05.005

24. Rosenberg PS, Alter BP, Bolyard AA, Bonilla MA, Boxer LA, Cham B, et al. The incidence of leukemia and mortality from sepsis in patients with severe congenital neutropenia receiving long-term G-CSF therapy. *Blood.* (2006) 107 (12):4628–35. doi: 10.1182/blood-2005-11-4370

25. Danese MD, Schenfeld J, Shaw J, Gawade P, Balasubramanian A, Kelsh M, et al. Association between granulocyte colony-stimulating factor (G-CSF) use and myelodysplastic syndrome (MDS) or acute myeloid leukemia (AML) among elderly patients with breast, lung, or prostate cancer. *Adv Ther* (2022) 39 (6):2778–95. doi: 10.1007/s12325-022-02141-1

26. Garon EB, Rizvi NA, Hui R, Leighl N, Balmanoukian AS, Eder JP, et al. Pembrolizumab for the treatment of non-small-cell lung cancer. *N Engl J Med* (2015) 372(21):2018–28. doi: 10.1056/NEJMoa1501824

27. Papaldo P, Ferretti G, Di Cosimo S, Giannarelli D, Marolla P, Lopez M, et al. Does granulocyte colony-stimulating factor worsen anemia in early breast cancer patients treated with epirubicin and cyclophosphamide? *J Clin Oncol Off J Am Soc Clin Oncol* (2006) 24(19):3048–55. doi: 10.1200/jco.2005.02.9488

28. Johnson M, Garassino MC, Mok T, Mitsudomi T. Treatment strategies and outcomes for patients with EGFR-mutant non-small cell lung cancer resistant to EGFR tyrosine kinase inhibitors: Focus on novel therapies. *Lung Cancer* (2022) 170:41–51. doi: 10.1016/j.lungcan.2022.05.011

frontiers | Frontiers in Oncology

TYPE Case Report
PUBLISHED 25 January 2023
DOI 10.3389/fonc.2023.1062138

OPEN ACCESS

EDITED BY
Kohei Fujita,
National Hospital Organization Kyoto Medical Center, Japan

REVIEWED BY
K. Shilo,
The Ohio State University, United States
Asli Suner,
Ege University, Türkiye

*CORRESPONDENCE
Dongdong Zhang
zhangdongdong@whu.edu.cn

SPECIALTY SECTION
This article was submitted to Thoracic Oncology, a section of the journal Frontiers in Oncology

RECEIVED 05 October 2022
ACCEPTED 13 January 2023
PUBLISHED 25 January 2023

CITATION
Liu Y, Yu H, Dong Y and Zhang D (2023) Case Report: A case of synchronous right upper lobe adenocarcinoma and left lower lobe squamous cell carcinoma treated with immune checkpoint inhibitor plus chemotherapy.
Front. Oncol. 13:1062138.
doi: 10.3389/fonc.2023.1062138

Case Report: A case of synchronous right upper lobe adenocarcinoma and left lower lobe squamous cell carcinoma treated with immune checkpoint inhibitor plus chemotherapy

Yujiao Liu[1], Han Yu[2], Youhong Dong[3] and Dongdong Zhang[3]*

[1]State Key Laboratory of Separation Membranes and Membrane Processes, School of Chemistry, Tiangong University, Tianjin, China, [2]Department of Pathology, Xiangyang No.1 People's Hospital, Hubei University of Medicine, Xiangyang, China, [3]Department of Oncology, Xiangyang No. 1 People's Hospital, Hubei University of Medicine, Xiangyang, China

Globally, lung cancer is the leading cause of cancer-related mortality. Multiple primary lung cancers (MPLC) account for a very small portion of all primary lung cancer cases. Importantly, a quick and precise differentiation between MPLC and intrapulmonary metastases is directly related to patient prognoses as treatment strategies vary according to pathological type. Synchronous MPLC are most commonly seen in the same lung. Here, we report a rare case of a patient with synchronous MPLC of both lungs. A 67-year-old man, with a 1-month cough and expectoration history, was admitted in our hospital. Computed tomography (CT) chest scan revealed a lower lobe nodule in the left lung and an upper lobe nodule in the right lung. He underwent successive fiberoptic bronchoscopy and CT-guided percutaneous pulmonary aspiration biopsy of both lungs. The pathological diagnosis was squamous cell carcinoma of the left lung and adenocarcinoma of the right lung.

KEYWORDS

multiple primary lung cancers, intrapulmonary metastases, squamous cell carcinoma, adenocarcinoma, synchronous MPLC

Introduction

An early diagnosis and the increasing effectiveness of cancer therapies have significantly prolonged overall survival times in cancer patients. However, cancer survivors had a higher risk of developing new malignancies when compared with the general population. This situation poses new problems which are manifested as soaring incidences of multiple primary tumors (1).

Globally, lung cancer is the most common cause of cancer death, with the lungs one of the most common sites in terms of multiple primary malignancy (2). Initial diagnostic criteria for "multiple primary lung cancers" (MPLC) were published in 1975 based on histology and tumor locations (3). However, these criteria could not differentiate MPLC from intrapulmonary metastases (IPM). Furthermore, special cases may be misdiagnosed as MPLC without the pathological confirmation of every lesion, such as lepidic adenocarcinoma, it displays multiple pure ground-glass opacity lesions by computed tomography (CT) (4). In 2015, the World Health Organization Classification of Tumors of the Lung redefined MPLC diagnostic criteria and recommended a multidisciplinary tumor board approach to confirm the diagnosis (5). In addition to histological subtyping, algorithms based on comprehensive clinical and imaging variables and comparative genomic hybridization array information, were also applied to differentiate MPLC from IPM (6, 7).

MPLC is subdivided into two categories depending on the time of diagnosis of each primary site; metachronous MPLC (MMPLC) and synchronous MPLC (SMPLC). MMPLC is common and generally occurs in sequence after more than a 2-year cancer-free interval, while SMPLC is relatively rare and presents simultaneously or within a six months interval (8). In this study, we present a SMPLC case with right upper lobe adenocarcinoma and left lower lobe squamous cell carcinoma.

Case presentation

On December 28th, 2020, a 67-year-old male came to our institute with a 1-month history of fever, cough and expectoration. He had smoked for 20 years. A physical examination revealed moist rales in the left lung base. From routine blood tests, the white blood cell count was 18.68×10^9/L. Inflammatory indicators, such as C-reactive protein and procalcitonin, were significantly elevated. Tumor marker detection indicated carcinoembryonic antigen serum levels were slightly elevated. Sputum cultures suggested a fungal infection. CT scan identified an infectious lesion in the left lower lobe, accompanied by pulmonary atelectasis and an upper lobe nodule in the right lung (Figure 1A). He then underwent fiberoptic bronchoscopy (FB). The pathological diagnosis from this was squamous cell carcinoma of the left lung. Hematoxylin and eosin (HE) staining showed squamous cell carcinoma (Figure 2A). Immumohistochemical staining (IHC) showed a P40, P63, and CK5/6 positive status (Figures 2B–D). Considering a fungal infection in the left lower lobe and atelectasis, he first received anti-infection therapy for approximately 1 month. The patient was then admitted and reviewed on January 23rd, 2021, a chest CT indicated that the soft tissue mass and obstructive atelectasis in the left lower lobe were absorbed (Figure 1B). Considering bilateral lung metastases before treatment, he received adjuvant chemotherapy as an initial treatment. After four cycles of docetaxel plus nedaplatin (TP) regimen, CT showed a partial response in the left lower lobe; however, the right lung nodule showed no significant change (Figure 1C). To make a definite diagnosis of the right lung lesion and inaugurate timely and responsive clinical treatment, he underwent a percutaneous right lung puncture biopsy guided by CT. Pathological examination showed changes which were completely different from the left lung (Figure 3A). IHC staining showed that CK7 and TTF-1 were strongly positive, while NapsinA was weakly positive (Figures 3B–D), therefore, the pathological diagnosis was adenocarcinoma. Genetic testing indicated a *TP53* mutation, *EGFR* was wild type, and the tumor cell proportion score was 5%. After completion of the 5th TP regimen cycle on May 14th, 2021, CT showed a very good partial response in the left lower lobe, while the right lung nodular was larger than before (Figure 1D). Considering the significant regression of the left lung lesion, the patient commenced adenocarcinoma treatment. He received stereotactic radiotherapy on June 14th, 2021, the prescribed dose was 60.0 Gy in eight fractions. He subsequently received immune checkpoint inhibitor (ICI) therapy in combination with pemetrexed and carboplatin (PP). The right lung lesion had obviously diminished after completion of the first immunochemotherapy cycle (Figure 1E) and he achieved very good remission in both lungs after three cycles of this regimen (Figure 1F). Due to the frequency of grade III-IV myelosuppression and pulmonary infection, he was given another three cycles of pemetrexed plus ICI, followed by intensity modulated radiation therapy for the left lung lesion. The prescribed pulmonary dose was 60.0 Gy, with daily fractions of 2.0 Gy. Finally, paclitaxel plus ICI was administrated every 3 weeks for maintenance treatment. Currently, the patient exhibits no evidence of disease recurrence and progression. Detailed diagnosis information and a treatment flow chart are shown (Figure 4).

Discussion

We report a patient with SMPLC who was successively diagnosed with left lung squamous cell carcinoma and right lung adenocarcinoma. SMPLC were identified in 1924 and then were widely recognized. The estimated SMPLC incidence accounts for

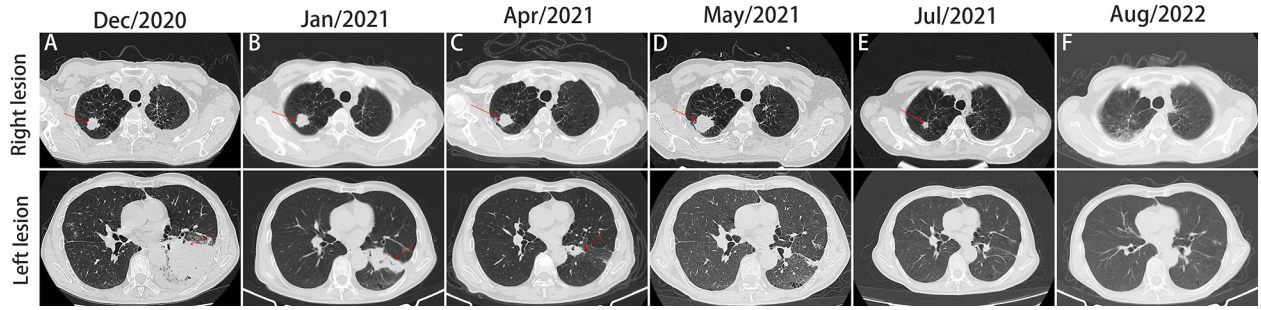

FIGURE 1
Computed tomography (CT) scan of the patient throughout the whole course of diagnosis and treatment. Figures A-E, imaging changes of chest CT (mediastinal window and pulmonary window) at different times.

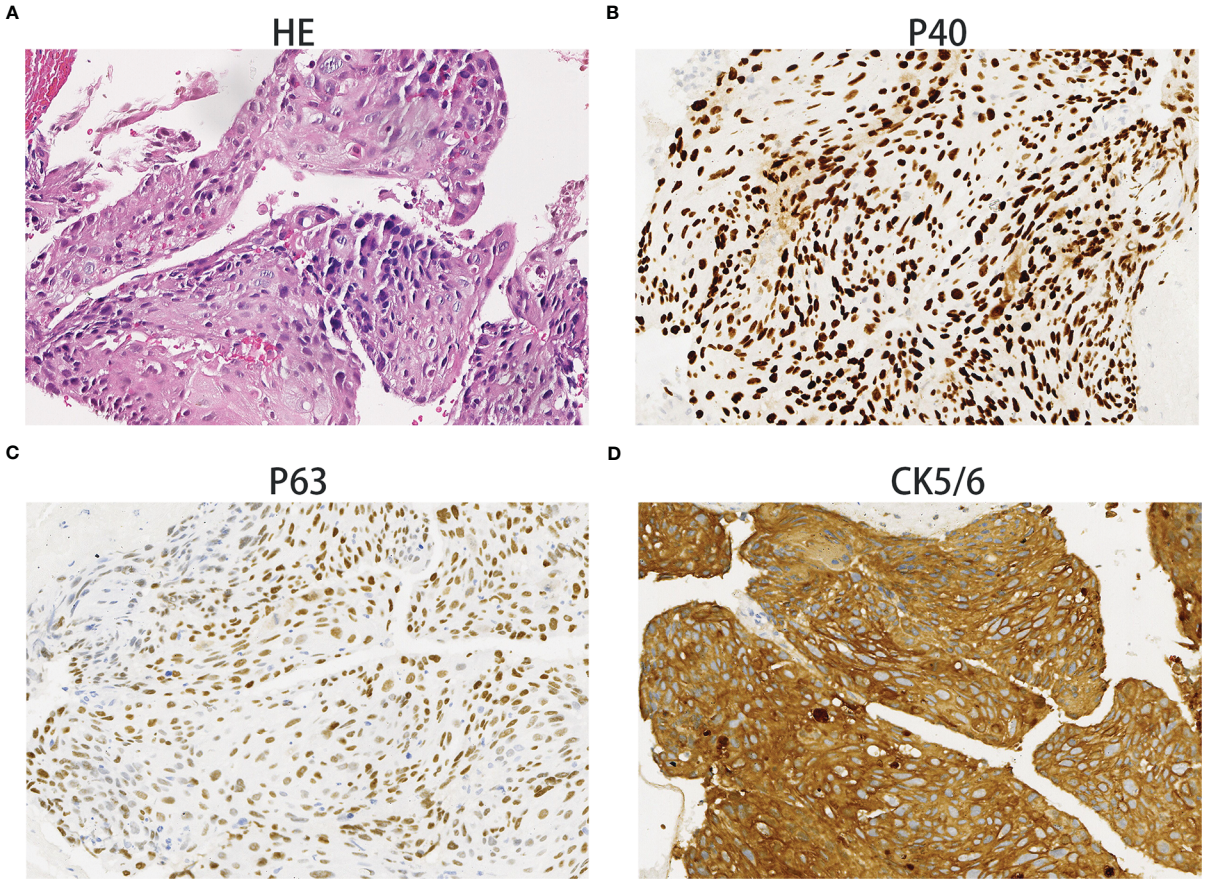

FIGURE 2
Squamous cell carcinoma. Hematoxylin and eosin staining showing squamous cell carcinoma histology **(A)**. The immunohistochemical examination indicated malignant cells immunoreactive for P40 **(B)**; positive for P63 **(C)**; strongly positive for CK5/6 **(D)**. Magnification 100×.

0.2%–8% of all lung cancers and has steadily increased over the past three decades (9).

MPLC may be caused by intrinsic and non-intrinsic cancer risk factor; intrinsic risk factors are defined as the genetic mutations caused by DNA replication errors, including *EGFR, KRAS, TP53*, or *PARP1* mutations (10). Non-intrinsic risk factors refer to modified endogenous factors, including lifestyle, radiation, and any other endogenous factors. It is accepted that smoking and the widespread use of high-resolution CT and positron emission tomography-CT contribute to MPLC occurrence (9).

Currently, no golden diagnostic criteria exist for MPLC due to the tumor heterogeneity and a poor understanding of associated clinicopathological characteristics. Therefore, a diagnosis should be considered by a multidisciplinary tumor board based on clinical manifestations, imaging features, pathological characteristics, and molecular genetic characteristics (11). MPLC stage classification is critical for patients, because staging affects initial treatment choices. For MMPLC, the second tumor should be staged as the primary according to the 7th Tumor-Node-Metastasis (TNM) classification guidelines. However, SMPLC staging is ambiguous, each tumor should be staged separately and only one TNM stage should be provided based on all combined tumors (8). In some situations, SMPLC is defined as the highest pathological stage (12).

Surgery is the cornerstone treatment for early MPLC without lymph node involvement. For surgery, the indications and contraindications must be strictly understood. Tumor's size and location, Eastern Cooperative Oncology Group performance status, and cardiopulmonary function must be considered before surgery. Operational styles are also closely related to patient quality of life and prognosis. Pneumonectomy has a high risk of postoperative respiratory failure and may herald a poor prognosis. Though segmentectomy or wedge resection has a risk of local recurrence (up to 15%), it is tolerable for patients with compromised pulmonary function who are unfit for more extensive resection (13). The Lung Study Group recommends that pneumonectomy should be avoided whenever possible, thus limited resection remains the mainstay treatment for MPLC.

Systemic chemotherapy is crucial for patients with mediastinal lymph node and distant metastasis. For patients with MMPLC, the second tumor should be treated as a primary tumor. However, the SMPLC treatment strategy is that each tumor should be staged and treated separately (14). Due to differences in chemotherapy regimens between adenocarcinoma and squamous cell carcinoma, it is often difficult for clinicians to select which regimen should be first perform for SMPLC patients with distinct tumor histology. It remains to be determined whether both effective regimen or sequential treatment for each tumor should be the first choice. In our study, the patient benefited from sequential treatments. After five TP regimen cycles, the lesion shrank and obstructive pneumonia improved significantly in this lung. Then, the right lung nodule significantly was reduced

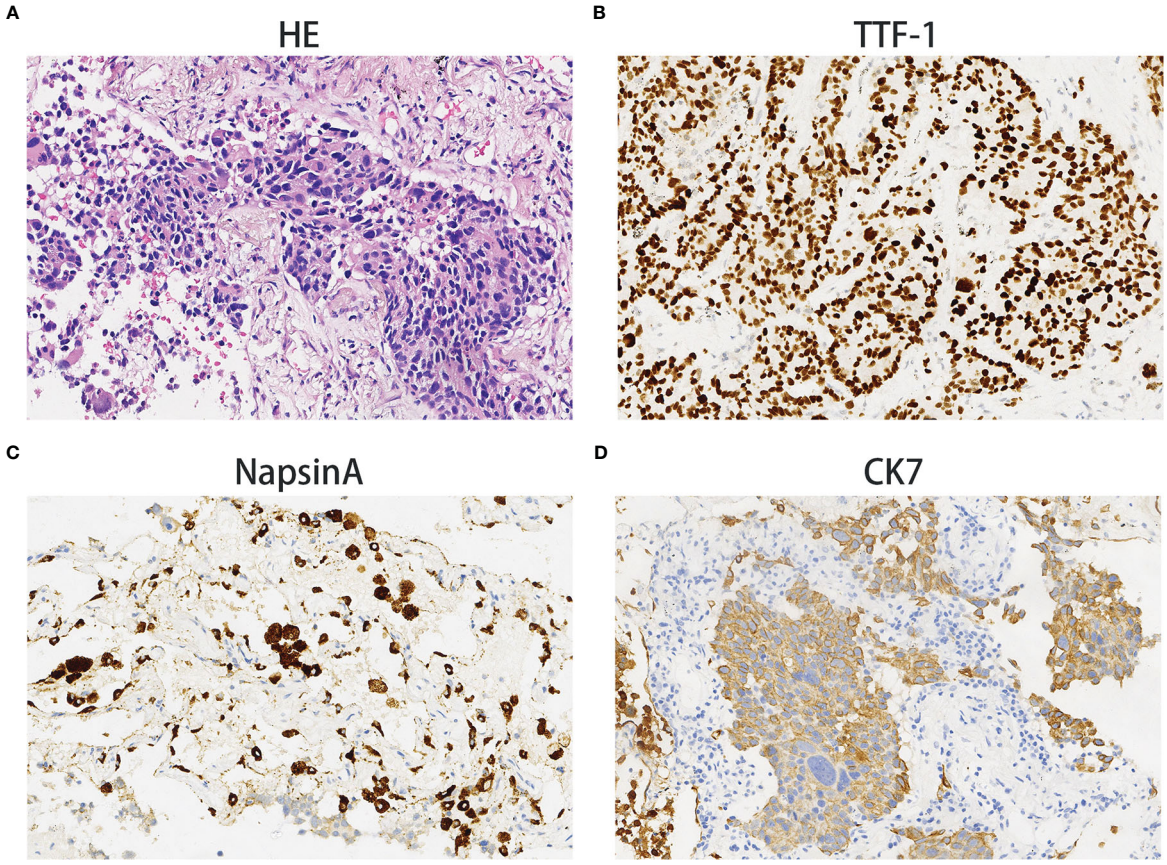

FIGURE 3
Adenocarcinoma. Hematoxylin and eosin staining showing adenocarcinoma histology **(A)**. The immunohistochemical examination indicated malignant cells immunoreactive for TTF-1 **(B)**; weakly positive for NapsinA **(C)**; strongly positive for CK7 **(D)**. Magnification 100×.

after the replacement of the PP regimen. Our strategy indicated that sequential treatment was effective for patients with SMPLC in both lungs with different pathological types, especially when the problem was more severe in one lung, such as severe pulmonary infection, obstructive pneumonia or pulmonary atelectasis.

Previous studies reported that ICI plus chemotherapy generated higher objective remission rates and superior overall survival and progression-free survival rates in patients with previously untreated, metastatic, non-small cell lung cancer (NSCLC) when compared with single chemotherapy (15, 16). Our patient benefited from combined

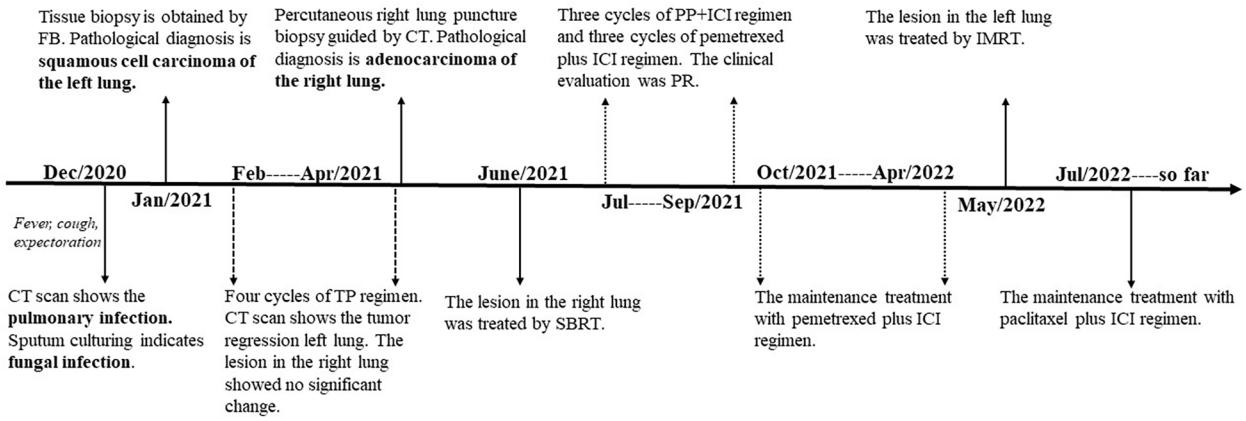

FIGURE 4
The timeline of the patient's events from diagnosis to treatment. CT, computed tomography; FB, fiberoptic bronchoscopy; TP, docetaxel plus nedaplatin; SBRT, stereotactic body radiation therapy; ICI, immune checkpoint inhibitor; PP, pemetrexed plus carboplatin; PR, partial remission; IMRT, intensity-modulated radiation therapy.

ICI and chemotherapy in adjuvant and maintenance treatment phases. Thus, ICI may be recommended for patients with advanced MPLC, but this hypothesis requires further research.

Radiotherapy improves local control rates in cancer. Intensity-modulated radiation therapy or three-dimensional conformal radiation is still an important treatment strategy for stage I–IIIB inoperable patients with lung cancers (17). Several studies reported that stereotactic body radiation therapy (SBRT) generated similar clinical outcomes in early NSCLC when compared with surgical treatment (18). Furthermore, SBRT may be a potential cure approach for early stage MPLC as it achieves promising long-term tumor control and survival (19). Given these factors, radiation is indispensable for MPLC treatment.

The 5-year overall survival for MPLC ranges from 20% to 70% (12). The prognosis is related to several clinical factors. Patients with same tumor histology are relatively favorable when compared with those with different histology (20). Patients with SMPLC or early MMPLC have lower survival rates when compared with patients with late MMPLC (21). Pneumonectomy has a higher early postoperative mortality rate and a shorter overall survival rate when compared with limited resection (21). Multivariable analyses have indicated that pathological stage and lymph node metastases are associated with prognosis (21). Therefore, the MPLC diagnosis and treatment should be determined by a multi-disciplinary team.

In conclusion, we reported the rare but interesting case of a patient with SMPLC in both lungs. The patient was first misdiagnosed with squamous cell carcinoma of the left lung, accompanied by right IPM and mediastinal lymph node metastasis. He received sequential chemotherapy plus ICI and radiotherapy without surgical resection, and is doing well under ICI maintenance. We believe this interesting case may provoke debate in the literature about the precise diagnosis and effective treatment for MPLC cases. Our result also indicated that the proper tumor subclassification (with IHC and molecular methods) was important for patients with SMPLC to receive individualize treatment and achieve better outcome.

Data availability statement

The original contributions presented in the study are included in the article/Supplementary Material. Further inquiries can be directed to the corresponding author.

Ethics statement

This study was approved by the Ethics and Scientific Committee of Hubei University of Medicine with approval number XYY2021002. The patients/participants provided their written informed consent to participate in this study. Written informed consent was obtained from the individual for the publication of any potentially identifiable images or data included in this article.

Author contributions

Conceptualization, DZ; data curation and writing, writing—review and editing, YL, YD, and HY; funding acquisition, DZ. All authors contributed to the article and approved the submitted version.

Funding

This study was supported by National Natural Science Foundation of China (Grants number: 82200214), Key Research and Development Project of Hubei (Grants number: 2022BCE028), Innovative Research Program of Xiangyang No.1 People's Hospital (Grants number: XYY2021Q02), Platform Special Fund for Scientific Research of Xiangyang No.1 People's Hospital (Grants number: XYY2022P05) and Key projects of Xiangyang Science and Technology Bureau (2021YL26).

Conflict of interest

The authors declare that the research was conducted in the absence of any commercial or financial relationships that could be construed as a potential conflict of interest.

Publisher's note

References

1. Spratt JS Jr., Hoag MG. Incidence of multiple primary cancers per man-year of follow up: 20-year review from the Ellis fischel state cancer hospital. *Ann surgery.* (1966) 164(5):775–84. doi: 10.1097/00000658-196611000-00001

2. Shoji F, Yamazaki K, Miura N, Katsura M, Oku Y, Takeo S, et al. Postoperative management of multiple primary cancers associated with non-small cell lung cancer. *Anticancer Res* (2018) 38(6):3773–8. doi: 10.21873/anticanres.12660

3. Martini N, Melamed MR. Multiple primary lung cancers. *J Thorac Cardiovasc surgery.* (1975) 70(4):606–12. doi: 10.1016/S0022-5223(19)40289-4

4. Kim HK, Choi YS, Kim J, Shim YM, Lee KS, Kim K. Management of multiple pure ground-glass opacity lesions in patients with bronchioloalveolar carcinoma. *J Thorac Oncol Off Publ Int Assoc Study Lung Cancer.* (2010) 5(2):206–10. doi: 10.1097/JTO.0b013e3181c422be

5. Travis WD, Brambilla E, Nicholson AG, Yatabe Y, Austin JHM, Beasley MB, et al. The 2015 world health organization classification of lung tumors: Impact of genetic, clinical and radiologic advances since the 2004 classification. *J Thorac Oncol Off Publ Int Assoc Study Lung Cancer.* (2015) 10(9):1243–60. doi: 10.1097/JTO.0000000000000630

6. Suh YJ, Lee HJ, Sung P, Yoen H, Kim S, Han S, et al. A novel algorithm to differentiate between multiple primary lung cancers and intrapulmonary metastasis in multiple lung cancers with multiple pulmonary sites of involvement. *J Thorac Oncol Off Publ Int Assoc Study Lung Cancer.* (2020) 15(2):203–15. doi: 10.1016/j.jtho.2019.09.221

7. Ostrovnaya I, Olshen AB, Seshan VE, Orlow I, Albertson DG, Begg CB. A metastasis or a second independent cancer? Evaluating the clonal origin of tumors using array copy number data. *Stat Med* (2010) 29(15):1608–21. doi: 10.1002/sim.3866

8. Jiang L, He J, Shi X, Shen J, Liang W, Yang C, et al. Prognosis of synchronous and metachronous multiple primary lung cancers: Systematic review and meta-analysis. *Lung Cancer (Amsterdam Netherlands).* (2015) 87(3):303–10. doi: 10.1016/j.lungcan.2014.12.013

9. Warth A, Macher-Goeppinger S, Muley T, Thomas M, Hoffmann H, Schnabel PA, et al. Clonality of multifocal nonsmall cell lung cancer: Implications for staging and therapy. *Eur Respir J* (2012) 39(6):1437–42. doi: 10.1183/09031936.00105911

10. Izumi M, Oyanagi J, Sawa K, Fukui M, Ogawa K, Matsumoto Y, et al. Mutational landscape of multiple primary lung cancers and its correlation with non-intrinsic risk factors. *Sci Rep* (2021) 11(1):5680. doi: 10.1038/s41598-021-83609-y

11. Detterbeck FC, Postmus PE, Tanoue LT. The stage classification of lung cancer: Diagnosis and management of lung cancer, 3rd ed: American college of chest physicians evidence-based clinical practice guidelines. *Chest* (2013) 143(5 Suppl):e191S–210S. doi: 10.1378/chest.12-2354

12. Liu M, He W, Yang J, Jiang G. Surgical treatment of synchronous multiple primary lung cancers: a retrospective analysis of 122 patients. *J Thorac disease.* (2016) 8(6):1197–204. doi: 10.21037/jtd.2016.04.46

13. Kocaturk CI, Gunluoglu MZ, Cansever L, Demir A, Cinar U, Dincer SI, et al. Survival and prognostic factors in surgically resected synchronous multiple primary lung cancers. *Eur J cardio-thoracic Surg Off J Eur Assoc Cardio-thoracic Surgery.* (2011) 39 (2):160–6. doi: 10.1016/j.ejcts.2010.05.037

14. Jiang L, He J, Shi X, Shen J, Liang W, et al. Prognosis of synchronous and metachronous multiple primary lung cancers: Systematic review and meta-analysis. lung cancer. *J Int Assoc Study Lung Cancer* (2015) 87(3):303-10. doi: 10.1016/j.lungcan.2014.12.013

15. Garassino MC, Gadgeel S, Esteban E, Felip E, Speranza G, Domine M, et al. Patient-reported outcomes following pembrolizumab or placebo plus pemetrexed and platinum in patients with previously untreated, metastatic, non-squamous non-small-cell lung cancer (KEYNOTE-189): A multicentre, double-blind, randomised, placebo-controlled, phase 3 trial. *Lancet Oncol* (2020) 21(3):387–97. doi: 10.1016/S1470-2045 (19)30801-0

16. Paz-Ares L, Luft A, Vicente D, Tafreshi A, Gümüş M, Mazières J, et al. Pembrolizumab plus chemotherapy for squamous non-Small-Cell lung cancer. *New Engl J Med* (2018) 379(21):2040–51. doi: 10.1056/NEJMoa1810865

17. Grills IS, Yan D, Martinez AA, Vicini FA, Wong JW, Kestin LL. Potential for reduced toxicity and dose escalation in the treatment of inoperable non-small-cell lung cancer: a comparison of intensity-modulated radiation therapy (IMRT), 3D conformal radiation, and elective nodal irradiation. *Int J Radiat oncology biology physics.* (2003) 57 (3):875–90. doi: 10.1016/S0360-3016(03)00743-0

18. Shirvani SM, Jiang J, Chang JY, Welsh JW, Gomez DR, Swisher S, et al. Comparative effectiveness of 5 treatment strategies for early-stage non-small cell lung cancer in the elderly. *Int J Radiat oncology biology physics.* (2012) 84(5):1060–70. doi: 10.1016/j.ijrobp.2012.07.2354

19. Chang JY, Liu YH, Zhu Z, Welsh JW, Gomez DR, Komaki R, et al. Stereotactic ablative radiotherapy: A potentially curable approach to early stage multiple primary lung cancer. *Cancer* (2013) 119(18):3402–10. doi: 10.1002/cncr.28217

20. Jung EJ, Lee JH, Jeon K, Koh WJ, Suh GY, Chung MP, et al. Treatment outcomes for patients with synchronous multiple primary non-small cell lung cancer. *Lung Cancer (Amsterdam Netherlands).* (2011) 73(2):237–42. doi: 10.1016/j.lungcan.2010.11.008

21. Tanjak P, Suktitipat B, Vorasan N, Juengwiwattanakitti P, Thiengtrong B, Songjang C, et al. Risks and cancer associations of metachronous and synchronous multiple primary cancers: A 25-year retrospective study. *BMC cancer.* (2021) 21(1):1045. doi: 10.1186/s12885-021-08766-9

frontiers | Frontiers in Oncology

TYPE Case Report
PUBLISHED 25 January 2023
DOI 10.3389/fonc.2023.1091459

OPEN ACCESS

EDITED BY
Kohei Fujita,
National Hospital Organization Kyoto Medical Center, Japan

REVIEWED BY
Hong Zhu,
Sichuan University, China
Ruiguang Zhang,
Huazhong University of Science and Technology, China

*CORRESPONDENCE
Qi Wang
wangqixlp@163.com

SPECIALTY SECTION
This article was submitted to Thoracic Oncology, a section of the journal Frontiers in Oncology

RECEIVED 08 November 2022
ACCEPTED 13 January 2023
PUBLISHED 25 January 2023

CITATION
Song K, Dong H, Jiang S, Xu X, Zhang C, Chen Q and Wang Q (2023) Case report: A rare case of sintilimab-induced gastric stenosis and literature review.
Front. Oncol. 13:1091459.
doi: 10.3389/fonc.2023.1091459

Case report: A rare case of sintilimab-induced gastric stenosis and literature review

Kunkun Song[1], Haoxu Dong[1], Shujun Jiang[1], Xiaohu Xu[1], Chao Zhang[2], Qian Chen[3] and Qi Wang[1]*

[1]Department of Integrated Traditional Chinese and Western Medicine, Tongji Hospital, Tongji Medical College, Huazhong University of Science and Technology, Wuhan, China, [2]Department of Pathology, Tongji Hospital, Tongji Medical College, Huazhong University of Science and Technology, Wuhan, China, [3]Department of Gastroenterology, Tongji Hospital, Tongji Medical College, Huazhong University of Science and Technology, Wuhan, China

Sintilimab is a fully human IgG4 monoclonal antibody against programmed death-1 (PD-1) used to treat classical Hodgkin's lymphoma and various solid tumors. With increasing use of sintilimab, some rare adverse reactions have been reported. Here, we report a case of a 50-year-old woman with squamous non-small cell lung cancer (NSCLC) (metastasis to pericardium and pleura) who received two cycles of 200 mg sintilimab immunotherapy combined with albumin-bound paclitaxel and carboplatin chemotherapy and one cycle of sintilimab monotherapy. She was diagnosed with Sjogren's syndrome (with symptoms of fever, dry mouth, dysphagia, and eating difficulty) after three cycles' treatment and received standard steroidal therapy. Prior to admission, the patient experienced severe stomach discomfort with vomiting and was hospitalized. Upper gastrointestinal iodine angiography showed significant gastric stenosis as well as lower esophageal stenosis. Subsequent ultrafine gastroscopy revealed ulceration at the stenotic site and an absence of normal peristalsis of the gastric wall. Pathological examination of the lesions showed reactive changes, including ulceration, fibrosis, and inflammatory cell infiltration. After multidisciplinary consultation, it was considered that the patient's gastric stenosis with inflammatory fibrosis changes was due to a sintilimab-induced immune hyperinflammatory reaction. The patient had been treated with standard steroidal therapy since suffering from Sjogren's syndrome, but the gastric stenotic changes were not relieved. The patient then received regular bouginage of esophago-cardiac stenosis under gastroscopy to physically reexpand the fibrous hyperplasia and stenotic site, enabling normal eating function. To our knowledge, this is the first case of gastric stenosis in a patient with squamous NSCLC after using sintilimab and may help clinicians better understand potential immune-related adverse events due to sintilimab and improve assessment and management.

KEYWORDS

programmed death-1, sintilimab, immune-related adverse events, gastric stenosis, non-small cell lung cancer

1 Introduction

Over the last decade, significant progress has been made in the use of anti-programmed death-1 (PD-1)/programmed death-ligand 1 (PD-L1) immunotherapy for treating cancer. Cancer cells can take advantage of PD-1 signaling to escape immune surveillance (1). By specifically blocking PD-1 on the surface of T cells, anti PD-1/PD-L1 immunotherapy can eliminate tumor-mediated immune suppression, thereby restoring the ability of T cells to recognize and destroy tumor cells. Anti PD-1 monotherapy, or its combination with other chemotherapy, has shown promising anti-tumor efficacy in clinical applications with an increased survival rate and, overall, manageable and acceptable adverse side effects. As anti PD-1/PD-L1 immunotherapy shows good tolerability and patient compliance, its clinical use is increasing. Sintilimab is a fully human IgG4 monoclonal antibody against PD-1 that is approved for treating classical Hodgkin's lymphoma and various solid tumors, including hepatocellular carcinoma, non-small cell lung cancer (NSCLC), esophageal squamous carcinoma, and gastric adenocarcinoma (2). Clinical trials for other malignancies are on-going. With increasing use, some rare adverse reactions have emerged. Thus, it is necessary that clinicians are aware of all possible side effects for early identification and successful treatment. Similar to other anti PD-1 therapies, the main side effects of sintilimab are immune-related adverse events (irAEs), which occur because blocking PD-1 on T cells can decrease the body's immune tolerance and cause autoimmune activation in some people. Reported irAEs of sintilimab include immune associated pneumonia, colonitis, hepatitis, nephritis, and myocarditis; however, sintilimab-induced gastric lesions are uncommon. Here, we describe a rare case of gastric stenosis in a patient with squamous NSCLC after using sintilimab.

2 Case presentation

A 50-year-old woman with a history of squamous NSCLC and metastasis to pericardium and pleura, who had pathological tissue samples that were ALK negative and PD-L1 positive with Tumor cell Proportion Score (TPS) of 80%, received two cycles of 200 mg sintilimab immunotherapy combined with chemotherapy of albumin-bound paclitaxel and carboplatin (from July to August 2020) and one cycle of sintilimab monotherapy (September 2020). The patient developed symptoms of fever, thirst, dysphagia, and difficulty eating, as well as severely damaged submandibular gland (no response to acid stimulation) and lacrimal gland (a tear flow rate of zero in both eyes) function after three cycles' treatment. She was diagnosed with Sjogren's syndrome through consultation with an immunologist in September 2020 and discontinued sintilimab immunotherapy. The patient was then treated with steroidal therapy (80 mg methylprednisolone). The symptoms of fever and thirst were relieved and food intake started to increase one week later. The steroid dose was gradually reduced (60 mg methylprednisolone for 10 days, 40 mg for 14 days, 20 mg for 11 weeks, and 16 mg for 2 weeks prior to admission). While treating Sjogren's syndrome, four cycles of albumin-bound paclitaxel mono-chemotherapy were administered (from October 2020 to January 2021).

For approximately 10 days prior to admission in February 2021, the patient experienced heavy stomach discomfort and irregularly vomited her stomach contents, although there was no significant abdominal pain, with regular intestinal exhaust and defecation, without symptoms of fever, diarrhea, dizziness, headache, or backache. On physical examination, there was no obvious abdominal tenderness or rebound pain. Additional relevant examinations were performed after admission. Blood tests showed red blood cells of 3.57×10^{12}/L, hemoglobin of 10^{6} g/L, D-D dimer of 1.1 μg/mL FEU, creatinine of 35 μmol/L (white blood cells count, platelet count, glutamic pyruvic transaminase, glutamic oxalacetic transaminase and urea nitrogen were normal). Fecal occult blood was weakly positive. Gastroscopy was performed under anesthesia by a gastroenterologist. Circumferential stenosis of the lower esophagus was observed approximately 34–37 cm from the esophageal incisors (Figures 1A–C), with a brittle mucous membrane and tendency to bleed while touching; the remaining esophageal mucosa was smooth with a clear vascular texture. As the endoscope could not pass through the stricture at that time, the gastric lesion was not clear. Upper gastrointestinal iodine angiography was recommended by the gastroenterologist, which showed an irregular shape of the stomach and obvious gastric stricture (Figure 2) with gastroesophageal reflux. To observe the gastric lesion, ultrafine gastroscopy was performed. The gastric cavity was obviously constricted with a peripheral ulcer and normal peristalsis was absent. The surface of the gastric wall was covered with white moss and bled easily while touching, with ulcers visible in the gastric body (Figures 1D, E). To further identify the etiology and nature of gastric and esophageal stenosis, ulcer tissue samples were taken for pathological examination. The results showed a patch of smooth muscle tissue with small foci of calcifications, and a patch of small blood vessels, nerve, and hyperplasia of fibrous tissue with inflammatory cell infiltration, which were considered to be reactive changes (Figure 3); no carcinoma was found. Positron emission tomography–computed tomography (PET/CT) examination was also performed and showed that the gastric wall the of corpus gastricum was thickened at the site of stenosis, but without obvious metabolism. Thus, cancer was not considered.

Considering the patient's history of Sjogren's syndrome after using sintilimab along with the gastroscopy and gastrointestinal iodine angiography results (obvious constriction and stiffness of the gastric cavity, absence of normal peristalsis) and pathological manifestation of inflammatory hyperplasia with fibrosis, after multidisciplinary consultation, the patient's gastric stenosis with inflammatory fibrosis changes was determined to be caused by a sintilimab-induced immune hyperinflammatory reaction.

The patient had been treated with steroidal therapy since suffering from Sjogren's syndrome. As the gastric stenotic changes were not relieved, this complication was not sensitive to steroidal therapy. To relieve vomiting and increase the patient's energy level, gastroscopic nasointestinal tube placement was performed. Five months later (July 2021), when the patient's nutritional status improved, laser incision of the stenosis site under gastroscopy was performed (Figures 4A–C). Seven days later, a metal rack was placed to expand the stenosis site. The patient could eat normally after these procedures. In February 2022, the metal rack fell off in the stomach and was removed under gastroscopy. Bouginage of the esophago-cardiac stenosis was performed (Figures 4D–F); 5 mm, 7 mm, 9 mm, and 11 mm zebra

10.3389/fonc.2023.1091459

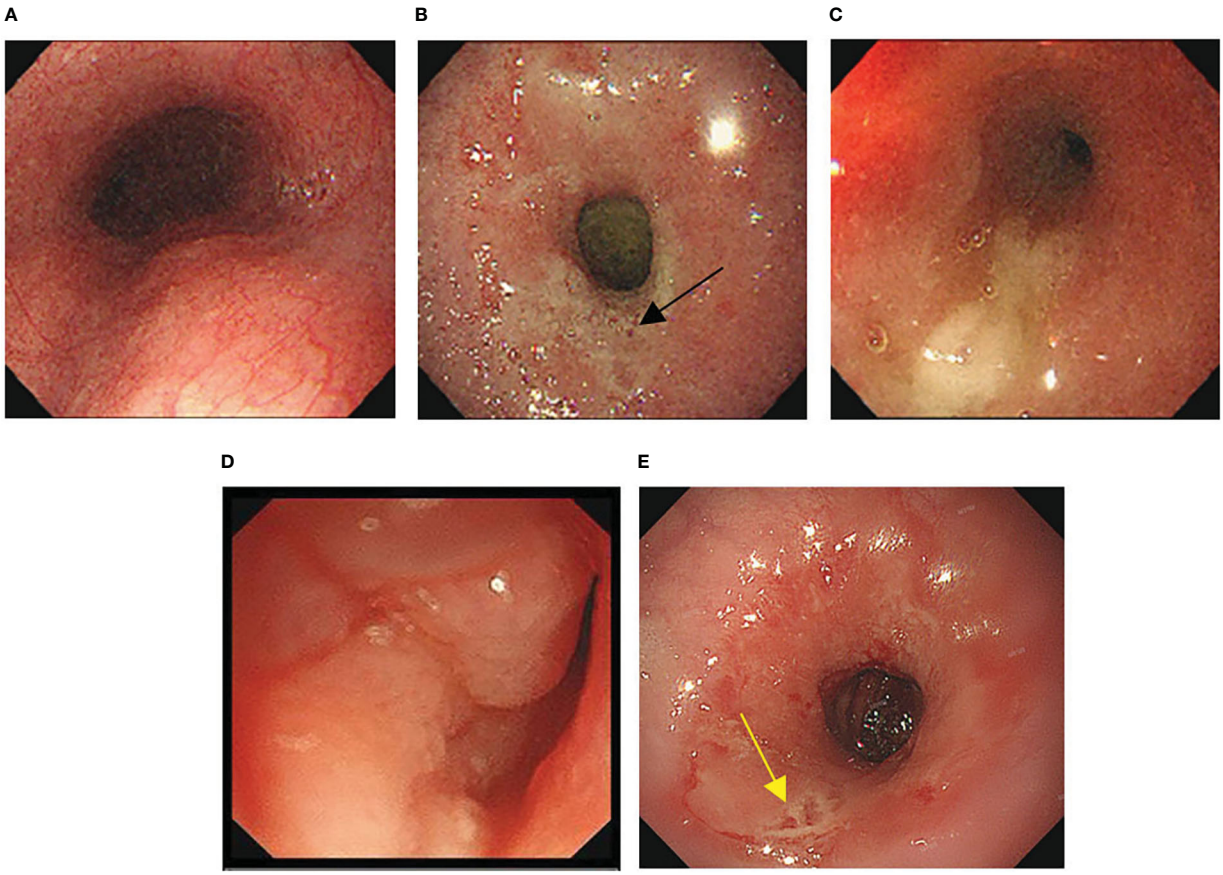

FIGURE 1
(A-C) Morphology of esophagus under gastroscopy. **(A)** The upper esophagus was morphologically normal. **(B)** Circumferential stenosis was observed 34cm from the esophageal incisor (black arrow indicates lower esophageal ulcers). **(C)** Extreme stenosis was observed 37cm from the esophageal incisor so that the endoscope could not pass through. **(D, E)** Gastric morphology under ultrafine endoscopy. **(D)** The gastric body was covered with white moss, and easy to bleed while touching. **(E)** Normal peristalsis was absent and ulcers were seen in the gastric body (yellow arrow indicates gastric body ulcers).

guidewires were used for continuous expansion for 1 min each, with an interval of 1 min. After the operation, the mucosa was obviously torn without active bleeding. An attempt to insert another metal rack failed because the front end of the rack could not pass through the stenosis. Although the metal rack was not implanted, the patient was able to eat normally after bouginage. Subsequently, the patient underwent regular bouginage of esophago-cardiac stenosis approximately every 2–3 months (second time in May 2022, third time in July 2022, and fourth time in October 2022). The patient was able to eat normally during this period.

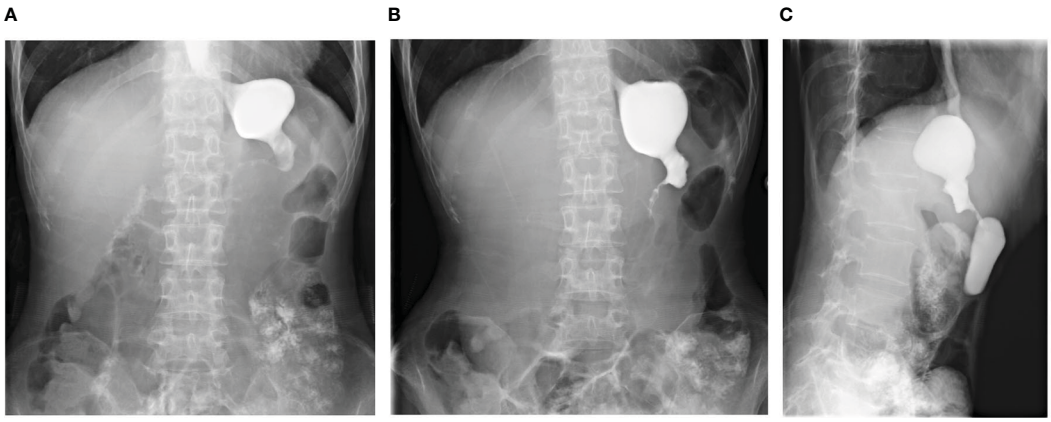

FIGURE 2
Upper gastrointestinal iodine angiography showed significant stenosis of the gastric cavity. **(A, B)** Anteroposterior views of the upper gastrointestinal iodine angiography. **(C)** Lateral views of the upper gastrointestinal iodine angiography.

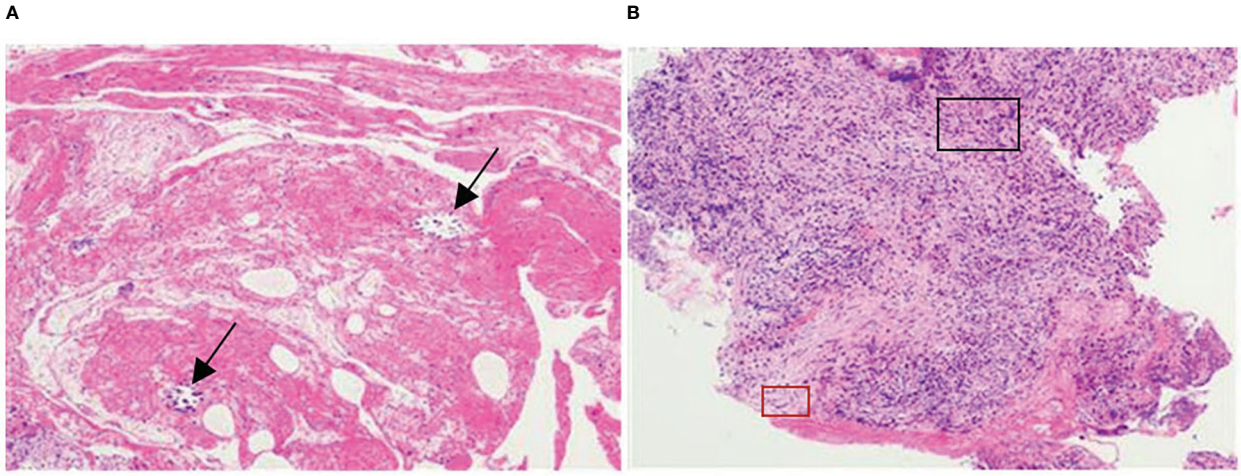

FIGURE 3
Pathological manifestation at the site of stenosis. **(A)** A patch of smooth muscle tissue with small foci of calcifications (arrows indicate the calcifications). **(B)** A patch of small blood vessels, nerve and hyperplasia of fibrous tissue with inflammatory cell infiltration (inflammatory and fibrous cells were scattered, black andred rectangles indicate relatively obvious inflammatory and fibrous cell aggregates, respectively).

3 Discussion

At present, lung cancer accounts for 11.4% of new cancers, second only to breast cancer (11.7%), and results in 18% of cancer-associated fatalities globally, making it the leading cause among all cancer types (3). More than 85% of lung cancers are the NSCLC type, of which approximately 33% are the squamous subtype (4). For patients with unresectable NSCLC who do not have targeted gene mutations, platinum-based doublet chemotherapy was once the first-line treatment option. However, in the last decade, the development of

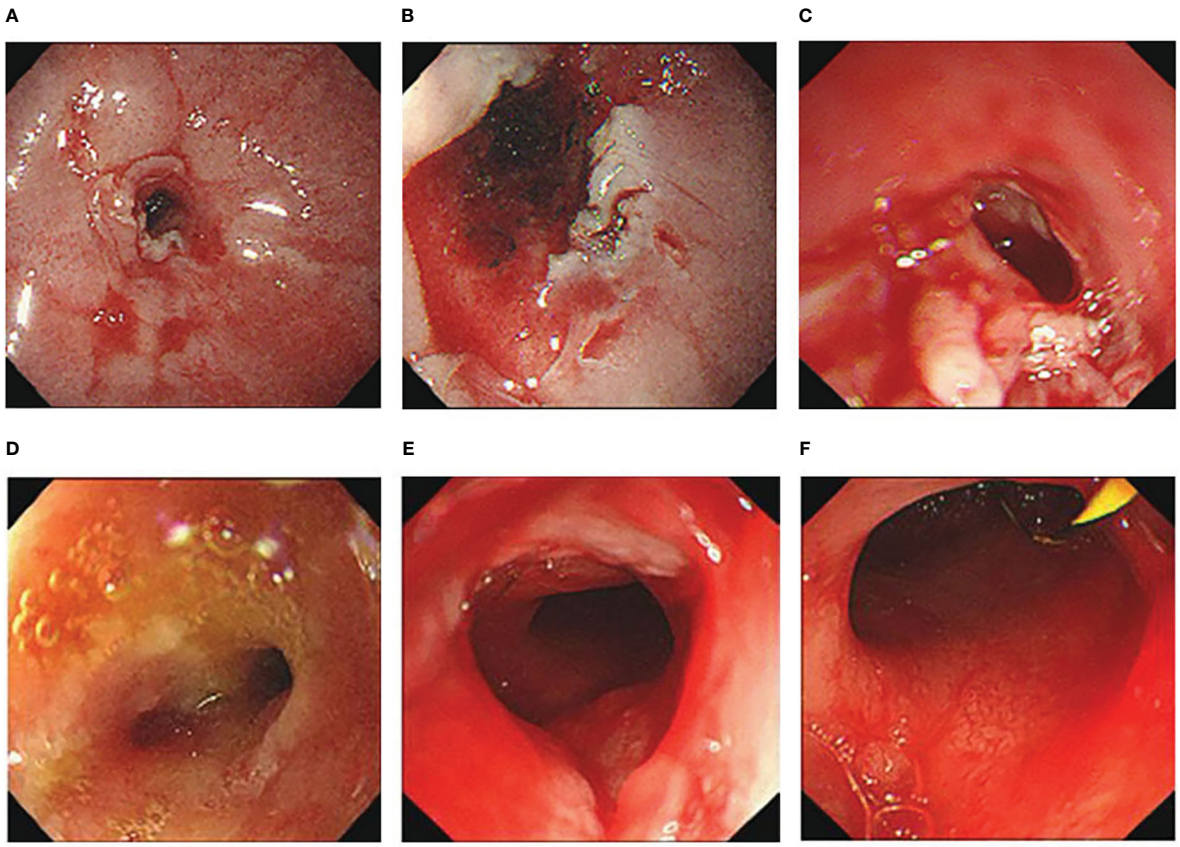

FIGURE 4
(A–C) Cardiac morphology before **(A)**, during **(B)** and after **(C)** laser incision. **(D–F)** Cardiac morphology before **(D)**, during **(E)** and after **(F)** bouginage.

immune checkpoint inhibitors (ICIs) has greatly changed this situation. Among all ICIs, anti PD-1/PD-L1 immunotherapy is the most mature method. Sintilimab is a Chinese domestic monoclonal antibody against PD-1 that was initially approved by the National Medical Products Administration (NMPA) to treat patients with classical Hodgkin's lymphoma who had already received more than two lines of systematic chemotherapies but the disease was still progressive (5, 6). With ongoing clinical trials, the use of sintilimab has gradually expanded to other solid tumors. For NSCLC, sintilimab immunotherapy combined with chemotherapy has been approved by NMPA as the first-line treatment (7). Specifically, sintilimab combined with gemcitabine and platinum is approved for squamous NSCLC, while sintilimab combined with pemetrexed and platinum is approved for EGFR-negative and ALK-negative non-squamous NSCLC.

Although immunotherapy has achieved great success, there are increasing reports of treatment-related adverse events (TRAE) induced by ICIs. Thus, this issue cannot be ignored (8). A meta-analysis of 36 phase II/III trials showed a pooled incidence of TRAEs of 54%–76% (9). Another study assessed the lethal toxicity spectrum associated with ICIs, finding that the incidence of lethal TRAEs was 0.361% for PD-1 inhibitors and 0.63% for PD-L1 inhibitors (10). For sintilimab, the pooled incidences of TRAEs and lethal TRAEs are 16.7%–100% and 1%–6.25%, respectively (2). TRAEs caused by ICIs are mainly irAEs. By enhancing the ability of T cells to destroy tumors cells, ICIs can promote cancer patients' immune function; however, if activation of the immune system is aggressive, irAEs may occur (11). Common sintilimab-induced irAEs include debilitation, fever, pneumonia, hypothyroidism, skin eruptions, and thrombocytopenia. Less common sintilimab-induced irAEs include hypoadrenocorticism, cardiotoxicity and myocarditis, paraneoplastic syndrome, and rhabdomyolysis (2). However, immune-induced gastric lesions are uncommon. Thus, this case of sintilimab-induced irAEs of gastric stenosis with inflammatory fibrosis changes is rare.

Follow-up of PD-1 monotherapy in patients with neoadjuvant resectable NSCLC showed that patients with high PD-L1 expression (TPS ≥ 50%) tended to have a higher two-year disease-free survival rate (12). PD-L1 immunochemical staining and targeted DNA sequencing of tumor samples from 29 NSCLC patients before immunotherapy revealed a positive correlation between TPS and the degree of pathological regression. In addition, a higher TPS (≥ 50%) was significantly associated with major pathological response (13). The patient in the present case had high PD-L1 expression (TPS = 80%), suggesting that anti PD-1 immunotherapy has a high response rate and sintilimab is in accordance with the indications for its application.

The patient developed Sjogren's syndrome after three cycles of sintilimab treatment, and obvious gastric stenosis was found five months later. Due to the long time since sintilimab was discontinued, gastroscope pathological examination and PET/CT examination was performed; tumor-associated lesions of the stenosis area were not considered.

In addition to sintilimab, the patient had also received chemotherapy of albumin-bound paclitaxel and carboplatin. However, the main adverse reactions of albumin-bound paclitaxel are leukopenia, neutropenia, neuropathy, fatigue, and infection (14), and that of carboplatin are myelosuppression, anaphylaxis, hepatotoxicity, ototoxicity, and cardiotoxicity (15). The pathological manifestation of inflammatory hyperplasia with fibrosis of this patient were more consistent with the characteristic of hyperimmunity, which was the main side effect of ICIs. Considering the fact that the patient had a history of irAEs (Sjogren's syndrome), it was thought that the patient's gastric stenosis with inflammatory fibrosis changes was caused by a sintilimab-induced immune hyperinflammatory reaction.

This patient had suffered from dry mouth and swallowing and eating discomfort since Sjogren's syndrome was diagnosed and these symptoms were relieved by steroidal therapy. Thus, the symptom of eating discomfort was always considered to be related to Sjogren's syndrome. Gastroscope examination was not performed until 5 months later because of increasingly discomfort after eating accompanied by vomiting, which finally revealed obvious gastric stenosis with ulcer and fibrosis. Our experience suggests that if patients experience stomach discomfort or difficulty eating after using sintilimab, gastroscopy should be performed as soon as possible to detect any gastric lesions and allow adjustment of the dose or discontinuation.

Glucocorticoids remain the first-line treatment for irAEs. Patients with severe reactions or reactions involving important organs might also require biological immunomodulators. Individualized treatment is recommended for irAEs of different organs caused by ICIs (16). Although our patient was treated with standardized steroidal therapy due to Sjogren's syndrome for 5 months (80 mg methylprednisolone for 7 days, 60 mg for 10 days, 40 mg for 14 days, 20 mg for 11 weeks, and 16 mg for 2 weeks prior to admission), the lesion of gastric stenosis was not reversed. This result suggests that immune-related gastric stenosis might not respond well to steroidal therapy, or that the dose of glucocorticoid used in this case was insufficient or not applied early enough. Regular bouginage of esophago-cardiac stenosis was performed under gastroscopy to physically reexpand the fibrous hyperplasia and stenotic site, which enabled normal eating function for the patient. This case suggests one approach for the treatment of gastric stenosis secondary to immunotherapy, although more research is still needed.

4 Conclusion

This is the first reported case of gastric stenosis caused by sintilimab. Since sintilimab monotherapy or combination therapy is widely used for various malignant tumors, it is essential to understand the potential irAEs and conduct adequate evaluation and management.

Data availability statement

The original contributions presented in the study are included in the article/supplementary material. Further inquiries can be directed to the corresponding author.

Ethics statement

The studies involving human participants were reviewed and approved by Tongji Hospital, Tongji Medical College, Huazhong University of Science and Technology. The patients/participants provided their written informed consent to participate in this study. Written informed consent was obtained from the individual(s) for the publication of any potentially identifiable images or data included in this article.

Author contributions

KS: Designed the case report and wrote the manuscript. HD: Collected the patient's data. SJ: Edited the image. XX: Collated and verified the data. QW: Revised and reviewed the manuscript. CZ: Analyzed the pathological results. QC: Edited and Analyze the digestive endoscopy images. All authors contributed to the article and approved the submitted version.

Funding

This work was supported by the National Natural Science Foundation of China (Grant no. 81904008).

Conflict of interest

The authors declare that the research was conducted in the absence of any commercial or financial relationships that could be construed as a potential conflict of interest.

Publisher's note

References

1. Yi M, Zheng X, Niu M, Zhu S, Ge H, Wu K. Combination strategies with PD-1/PD-L1 blockade: Current advances and future directions. *Mol cancer* (2022) 21(1):28. doi: 10.1186/s12943-021-01489-2

2. Liu X, Yi Y. Recent updates on sintilimab in solid tumor immunotherapy. *biomark Res* (2020) 8(1):69. doi: 10.1186/s40364-020-00250-z

3. Sung H, Ferlay J, Siegel RL, Laversanne M, Soerjomataram I, Jemal A, et al. Global cancer statistics 2020: GLOBOCAN estimates of incidence and mortality worldwide for 36 cancers in 185 countries. *CA: Cancer J Clin* (2021) 71(3):209–49. doi: 10.3322/caac.21660

4. Shi Y, Chen W, Li C, Zhang Y, Bo M, Qi S, et al. Efficacy and safety of first-line treatments with immune checkpoint inhibitors plus chemotherapy for non-squamous non-small cell lung cancer: A meta-analysis and indirect comparison. *Ann palliative Med* (2021) 10(3):2766–75. doi: 10.21037/apm-20-1498

5. Hoy SM. Sintilimab: First global approval. *Drugs.* (2019) 79(3):341–6. doi: 10.1007/s40265-019-1066-z

6. Zhang L, Mai W, Jiang W, Geng Q. Sintilimab: A promising anti-tumor PD-1 antibody. *Front Oncol* (2020) 10:594558. doi: 10.3389/fonc.2020.594558

7. Zhang L, Lin W, Tan F, Li N, Xue Q, Gao S, et al. Sintilimab for the treatment of non-small cell lung cancer. *Biomark Res* (2022) 10(1):23. doi: 10.1186/s40364-022-00363-7

8. Ramos-Casals M, Brahmer JR, Callahan MK, Flores-Chávez A, Keegan N, Khamashta MA, et al. Immune-related adverse events of checkpoint inhibitors. *Nat Rev Dis primers* (2020) 6(1):38. doi: 10.1038/s41572-020-0160-6

9. Xu C, Chen YP, Du XJ, Liu JQ, Huang CL, Chen L, et al. Comparative safety of immune checkpoint inhibitors in cancer: Systematic review and network meta-analysis. *BMJ* (2018) 363:k4226. doi: 10.1136/bmj.k4226

10. Wang DY, Salem JE, Cohen JV, Chandra S, Menzer C, Ye F, et al. Fatal toxic effects associated with immune checkpoint inhibitors: A systematic review and meta-analysis. *JAMA Oncol* (2018) 4(12):1721–8. doi: 10.1001/jamaoncol.2018.3923

11. Naidoo J, Page DB, Li BT, Connell LC, Schindler K, Lacouture ME, et al. Toxicities of the anti-PD-1 and anti-PD-L1 immune checkpoint antibodies. *Ann oncol: Off J Eur Soc Med Oncol* (2015) 26(12):2375–91. doi: 10.1093/annonc/mdv383

12. Gao S, Li N, Gao S, Xue Q, Wang S, Lv F, et al. Two-year follow-up of single PD-1 blockade in neoadjuvant resectable NSCLC. *J Clin Oncol.* (2021) 39(15_suppl):8522. doi: 10.1200/JCO.2021.39.15_suppl.8522

13. Wang S, Yuan P, Mao B, Li N, Ying J, Tao X, et al. Genomic features and tumor immune microenvironment alteration in NSCLC treated with neoadjuvant PD-1 blockade. *NPJ Precis Oncol* (2022) 6(1):2. doi: 10.1038/s41698-021-00244-6

14. Nakao M, Fujita K, Suzuki Y, Arakawa S, Sakai Y, Sato H, et al. Nab-paclitaxel monotherapy for relapsed small cell lung cancer: Retrospective analysis and review. *Anticancer Res* (2020) 40(3):1579–85. doi: 10.21873/anticanres.14105

15. Oun R, Moussa YE, Wheate NJ. The side effects of platinum-based chemotherapy drugs: a review for chemists. *Dalton Trans* (2018) 47(19):6645–53. doi: 10.1039/C8DT00838H

16. Esfahani K, Elkrief A, Calabrese C, Lapointe R, Hudson M, Routy B, et al. Moving towards personalized treatments of immune-related adverse events. *Nat Rev Clin Oncol* (2020) 17(8):504–15. doi: 10.1038/s41571-020-0352-8

frontiers | Frontiers in Oncology

TYPE Case Report
PUBLISHED 26 January 2023
DOI 10.3389/fonc.2023.1074378

OPEN ACCESS

EDITED BY
Kohei Fujita,
National Hospital Organization Kyoto Medical Center, Japan

REVIEWED BY
Alberto Bongiovanni,
Istituto Romagnolo per lo Studio dei Tumori (IRST) "Dino Amadori"(IRCCS), Italy
Katerina Kopeckova,
University Hospital in Motol, Czechia

*CORRESPONDENCE
Mario Giuliano
m.giuliano@unina.it

†These authors have contributed equally to this work and share first authorship

SPECIALTY SECTION
This article was submitted to Thoracic Oncology, a section of the journal Frontiers in Oncology

RECEIVED 19 October 2022
ACCEPTED 05 January 2023
PUBLISHED 26 January 2023

CITATION
Caltavituro A, Buonaiuto R, Salomone F, Morra R, Pietroluongo E, De Placido P, Tortora M, Peddio A, Picozzi F, Ottaviano M, Marino M, De Placido S, Palmieri G and Giuliano M (2023) Extraskeletal Ewing's sarcoma of the mediastinum: Case report. *Front. Oncol.* 13:1074378. doi: 10.3389/fonc.2023.1074378

Extraskeletal Ewing's sarcoma of the mediastinum: Case report

Aldo Caltavituro[1†], Roberto Buonaiuto[1†], Fabio Salomone[1], Rocco Morra[1], Erica Pietroluongo[1], Pietro De Placido[1], Marianna Tortora[2], Annarita Peddio[1], Fernanda Picozzi[3], Margaret Ottaviano[4], Mirella Marino[5], Sabino De Placido[1,2], Giovannella Palmieri[2] and Mario Giuliano[1,2*]

[1]CRCTR Coordinating Rare Tumors Reference Center of Campania Region, Naples, Italy, [2]Rare Tumors Coordinating Center of Campania Region (CRCTR) Coordinating Rare Tumors Reference Center of Campania Region, Naples, Italy, [3]Division of Medical Oncology, Azienda Ospedaliera di Rilievo Nazionale (A.O.R.N.) dei COLLI "Ospedali Monaldi-Cotugno-Centro Traumatologico Ortopedico (CTO)", Naples, Italy, [4]Unit of Melanoma, Cancer Immunotherapy and Development Therapeutics, Istituto Nazionale Tumori IRCCS Fondazione Pascale, Napoli, Italy, [5]Department of Pathology, Regina Elena National Cancer Institute, Rome, Italy

Background: Ewing sarcoma (ES) represents the second most common malignant bone tumor in children and young adults. ES is not a frequent finding in sites different from the skeletal. Common sites of appearance of ES are lower extremities, the pelvis, paravertebral spaces and head and neck. Primary extraskeletal ES located in the anterior mediastinum are very rare. These neoplasms should be discussed in specialized contests with a high volume of patients treated. Here, we present an uncommon mediastinal mass challenging in its characterization and management.

Case description: A thirty-year-old woman performed a thoracic CT scan for dyspnea and persistent cough. Imaging showed a solid mass of 14 x 11 cm involving the left thorax with mediastinal deviation to the right side. Patient underwent an en bloc resection of the mass. Initial histological examination was suggestive for B3 thymoma/thymic carcinoma. Patient was then referred to our rare tumor reference center where a histological review excluded the diagnosis of thymic/thymoma neoplasms meanwhile a third revision assessed a diagnosis of ES. Patient refused adjuvant chemotherapy due to her desire of maternity and radiation therapy was not indicated because surgery was performed too many months earlier. A close follow-up was considered. After a few months the patient relapsed and first line chemotherapy was proposed. She reached a complete response at the first evaluation maintained also at the end of the protocol. In order to consolidate the obtained response, high dose chemotherapy followed by autologous stem cell transplantation (HDCT/ASCT) was suggested and the patient agreed.

Conclusions: This case underlined that, potentially, ES can arise from any soft tissue site in the body, even in rare sites such as mediastinum. The evaluation of

expert centers was critical to establish a correct diagnosis and therapeutic approach in this complex case. Taking into account the time lasting from the diagnosis and the aggressiveness of this kind of neoplasm, frequently relapsing, the patient after a multidisciplinary discussion was a candidate for a multimodal treatment.

KEYWORDS

case report, Ewing sarcoma, multidisciplinary management, thoracic oncology, misdiagnosis cancer

Introduction

Adult soft tissue and visceral sarcomas are rare tumors, with an estimated incidence averaging of 4– 5/100.000/year in Europe that account for less than 1% of all tumors (1). They include over 80 different histological subtypes that differ one from another in terms of incidence, treatment and prognosis (2).

Although they can arise from different sites, extremities and abdomen are most commonly involved (3).

Sarcomas can origin also from the mediastinum even if this location is not the most frequent one (4– 5).

The diagnosis of these types of tumors can be very challenging and a multidisciplinary approach is required in order to figure out the most appropriate management.

A lot of professional figures are involved in this field: pathologists, radiologists, thoracic surgeons, oncologists and many more.

ES is a high-grade round cell sarcoma (RCS) that generally affects bones and soft tissues, particularly in children and young adults. Ewing sarcoma family is a group of neoplasms containing but not limited to ES, also peripheral primitive neuroectodermal tumors belong to this group. Principles applied for bone ES are also extended to primary extraskeletal locations. The discovery of an ES in the mediastinum is not very common. Here we described a case of primary extraskeletal mediastinal ES.

This article aimed to show an uncommon finding of ES of the mediastinum and its complex and multidisciplinary management.

We present the following case in accordance with the CARE reporting checklist.

Case presentation

A thirty-years old woman, fifteen cigarettes/die smoker, without relevant medical history, referred to the emergency service complaining of persistent cough and unusual dyspnea.

During the physical exam a silent auscultatory area in the left upper hemithorax was found.

A chest X-Ray showed, in the anterior mediastinum, a huge mass (19 cm x 11 cm x 12 cm) with defined margins expanding in the superior and medium left hemithorax consistent with the auscultatory abnormality. The mass induced a contralateral dislocation of mediastinal structures and upper airways compression.

Computed tomography (CT) scan confirmed a solid mass characterized by dishomogeneous contrast enhancement, bordering to the costal pleura on the lateral side and to mediastinal great vessels, which compressed the superior lung lobe (Figure 1).

18- Fluorodeoxyglucose-Positron Emission Tomography/ Computed Tomography scan (18F-FDG PET/CT scan), performed later, did not reveal any sign of metabolic or morphological suspicion of distant disease.

The patient was a candidate for up-front surgery.

Despite the major surgery, the patient did not experienced remarkable post-operative complications and achieved a complete recovery. In addition, neither functional nor aesthetical impairment occurred.

The lesion was removed en bloc with the thoracic wall and the intercostal muscles; during surgery the anterior arches of the third, fourth and fifth ribs were excised and a segmental resection of the lingula and the anterior segment of the superior lobe of the left lung was performed.

Pathological examination was performed and, macroscopically, the excised lesion appeared as a spongy and gray encapsulated mass (16.5 x 14 x 8 cm) with white subcapsular areas and blood spots; microscopically, small size neoplastic cells with vesicular nucleus, poor cytoplasm and lobular growth were described.

The immunohistochemical analysis revealed a positivity for P63, CD99, CD117 and vimentina with poor lymphatic infiltrations (CD45+) and negativity to: MPO, TdT, CD3, CD4, CD5, CD30, CD34, CD43, CD68, AFP, HGG, Inhibin A, CK AE1/ AE3, CK7, CK20, EMA, PLAP, Calretinin, SMA, Desmine, Synaptophysin, S100, P53. Ki-67 proliferative index was 40%.

All these features were suggestive for a well differentiated thymic carcinoma, also known as B3 thymoma, according to the WHO classification (6). AJCC/UICC TNM 8th edition classified this neoplasm as pT1b (Stage 1 Masaoka modified staging) and according to the last guidelines she underwent a close clinical and radiological follow up (7).

The patient was referred to the Coordinating Rare Tumors Reference Center of Campania (CRCTR) where an immunochemical and histological revision of the material was requested (Figures 2, 3).

A second opinion from a center with high expertise in thymic malignancies was requested.

The negativity to different types of cytokeratins, the elevated mitotic index, the rare presence of classical thymic markers led

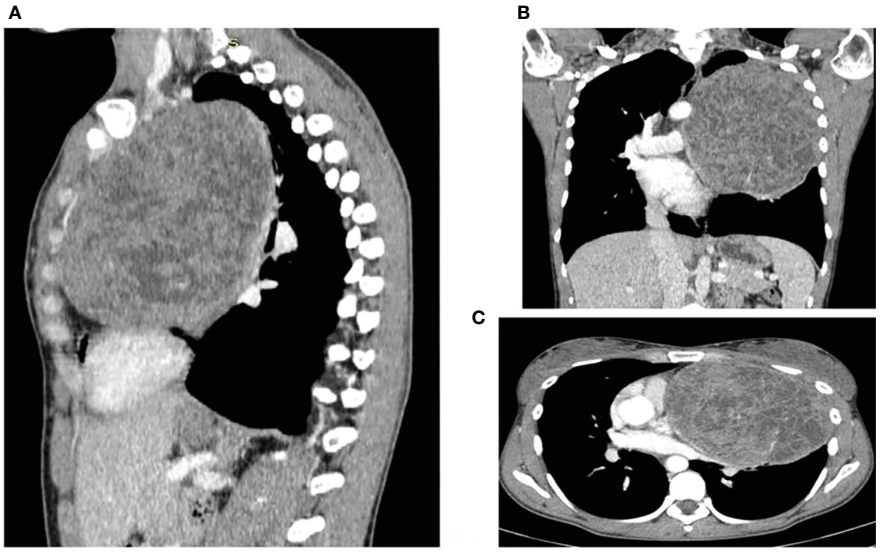

FIGURE 1
CT scans showing the presence and anatomical relation of the heteroplastic mass. **(A)** sagittal plane **(B)** coronal plane **(C)** transverse plane.

to the exclusion of a diagnosis of thymoma or thymic carcinoma. The occasional positivity to P63 was not specific for an epithelial neoplasm, instead the morphological pattern and the only positivity for CD99 were actually consistent with a diagnosis of undifferentiated sarcoma.

Genetic analyses, conducted using next generation sequencing (NGS) technology did not reveal any relevant mutations suitable for diagnostic characterization or therapeutic strategies; in fact no mutations were found in c-KIT gene nor in other candidate genes such as: PDGFR, IDH1, IDH2, PTEN, HRAS, NRAS, GNAQ, BRAF, CTNNB1, TP53, H3F3A, RET, MAP2K1, NF1, GNAS, GNA11.

Furthermore, the transcriptome was analyzed for the following 26 genes: ALK, CAMTA1, CCNB3, CIC, EPC1, EWSR1, FOXO1, FUS, GLI1, HMGA2, JAZF1, MEAF6, MKL2, NCOA2, NTRK3, PDGFB, PLAG1, ROS1, SS18, STAT6, TAF15, TCF12, TFE3, TFG, USP6, YWHAE.

RNA quality was not sufficient for NGS testing with the Archer FusionPlex Sarcoma genes by IonTorrent S5 Prime, an assay that is available for fusion gene detection.

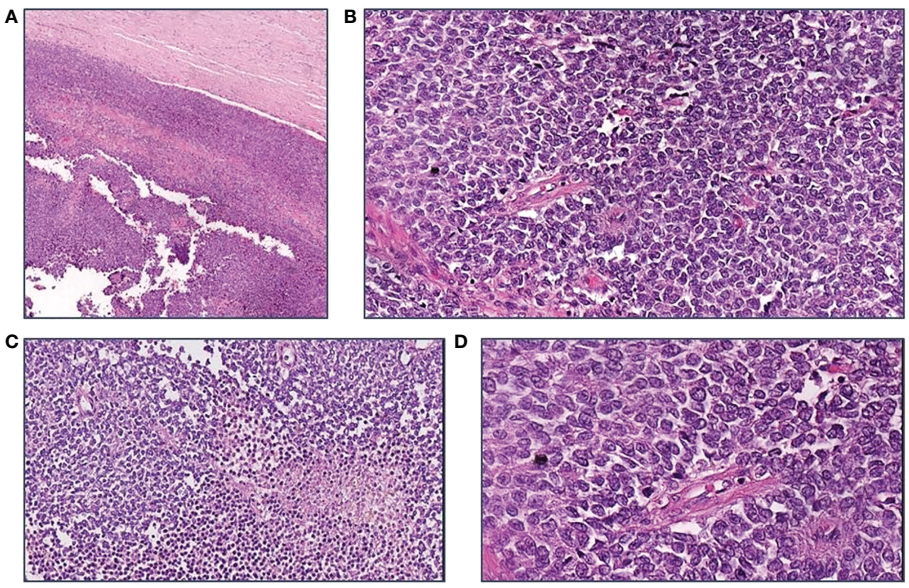

FIGURE 2
Morphological features of the tumor. **(A)** H$E, 40x: A thick fibrous capsule surrounds the large tumor; **(B)** H$E, 200X; Richly cellular sheets. Cells have scant cytoplasm and vesicular irregular nuclei; frequent mitoses are seen; no lymphocytes are found; **(C)** H$E, 200X: Necrotic foci are scattered; **(D)** H$E, 400X: The cells, rather small, form sheets with a sort of palisading around vessels.

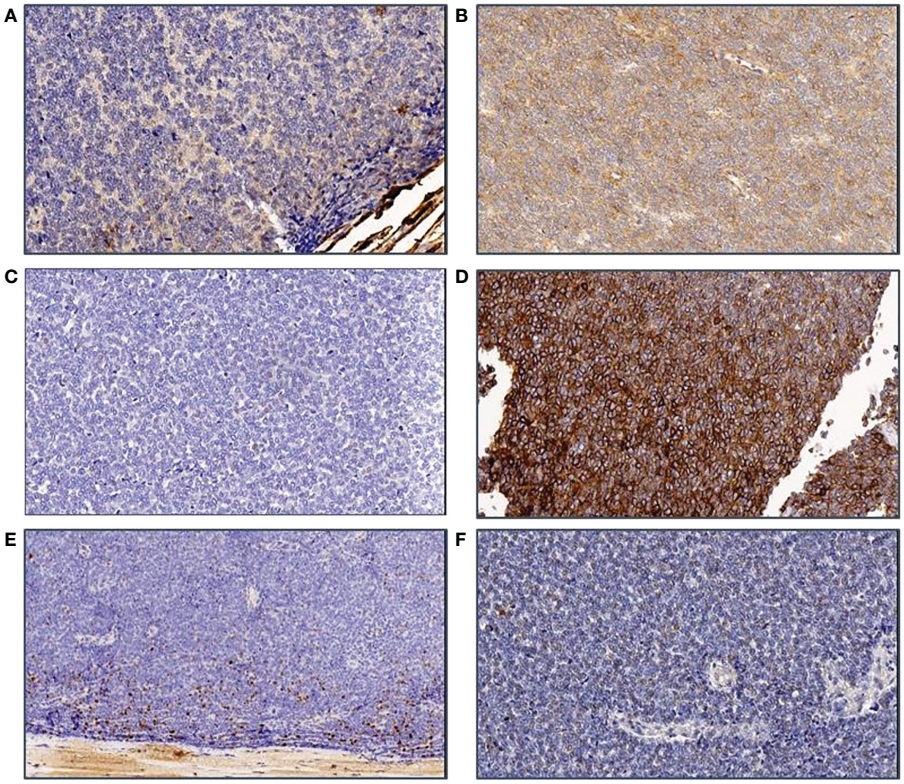

FIGURE 3
Immunohistochemical features of the tumor. **(A)** ker AE1/3 staining: The tumor cells are negative; **(B)** CD117: A slight unspecific staining is observed; **(C)** ker MNF116 is also neagtive in tumor cells; **(D)** CD99 membrane staining is clearly seen in all cells; **(E)** The Ki-67 staining shows that only the peripheral part of the tumor is marked, probably because of preanalytical damage of tumor tissue; **(F)** Synaptophysin marking is negative in tumor cells.

The number of reads was not sufficient for an adequate test interpretation.

Considering the unusual behavior of this neoplasm and the uncertainty of its histology, we requested another revision of the tissue samples from a center with high expertise in sarcoma neoplasms. According to this last analysis, the thoracic mass was suggestive of a malignant, round-cell, high- grade mesenchymal neoplasm whose morphological and immunophenotypic characteristics were consistent with the diagnosis of ES. The sample's cells were characterized by CD99 +; NKX2.2 +; cytokeratin AE1/AE3 -; desmin -; myogenin -; ETV4 -; S100 -.

The case was discussed in a national multidisciplinary tumor board specialized on sarcomas and, according to a sharing decision, the patient was candidate to an adjuvant chemotherapy.

The optimal therapeutic approach, suggested by the board, was an adjuvant chemotherapy with Vincristine, Doxorubicin and Cyclophosphamide (VDC) alternated to Ifosfamide and Etoposide (IE). Due to the fact that this intense regimen frequently leads to permanent infertility, a cryopreservation course was proposed to the young patient.

The treatment choice was communicated to the patient in order to share with her the benefit and the risks of the same. She expressed a strong childbearing desire so we also discussed the risks and benefits of postponing chemotherapy.

She decided to delay chemotherapy and the cryopreservation course in order to have a natural pregnancy.

Unfortunately, the patients relapsed after a few months. In fact, a CT scan performed during a close follow-up revealed a voluminous breast-like tissue of pathological significance in correspondence of the left lung apex with an inhomogeneous structure and areas of contextual necrosis of 68x50 mm in its maximum axial diameter. This tissue spread superiorly into the structures of the thoracic inlet contiguous to the first two costal arches and with the vascular structures of the left upper limb; posteriorly it invaded the costal pleura and medially infiltrated the smooth tissue of the anterior- superior mediastinum.

There were confluent multiple pathological swellings with necrotic appearance extended caudally in the para-aortic region, whose largest diameter measured 51x30 mm. Solid hypervascular nodulations were found along the pericardial sheet, the largest nodulation measured 16x10 mm and was associated with reactive fluid flap. Pathological tissue of 47x23 mm was also detected along the left costo- vertebral pleura with contextual pleural effusion flap. All these findings were consistent with a locoregional disease recurrence (Figure 4).

The patient started the chemotherapeutic protocol VDC-IE. After four cycles of VDC-IE a radiological evaluation was performed with a CT scan. Fortunately, the voluminous solid breast-like tissue, previously described at the level of the left apex, the multiple pathological swellings of necrotic appearance, the solid nodulations along the pericardial leaflet and the pathological tissue along the left costo-vertebral pleura were no longer evident. This was considered a complete response and the patients continued her protocol with the last five cycles.

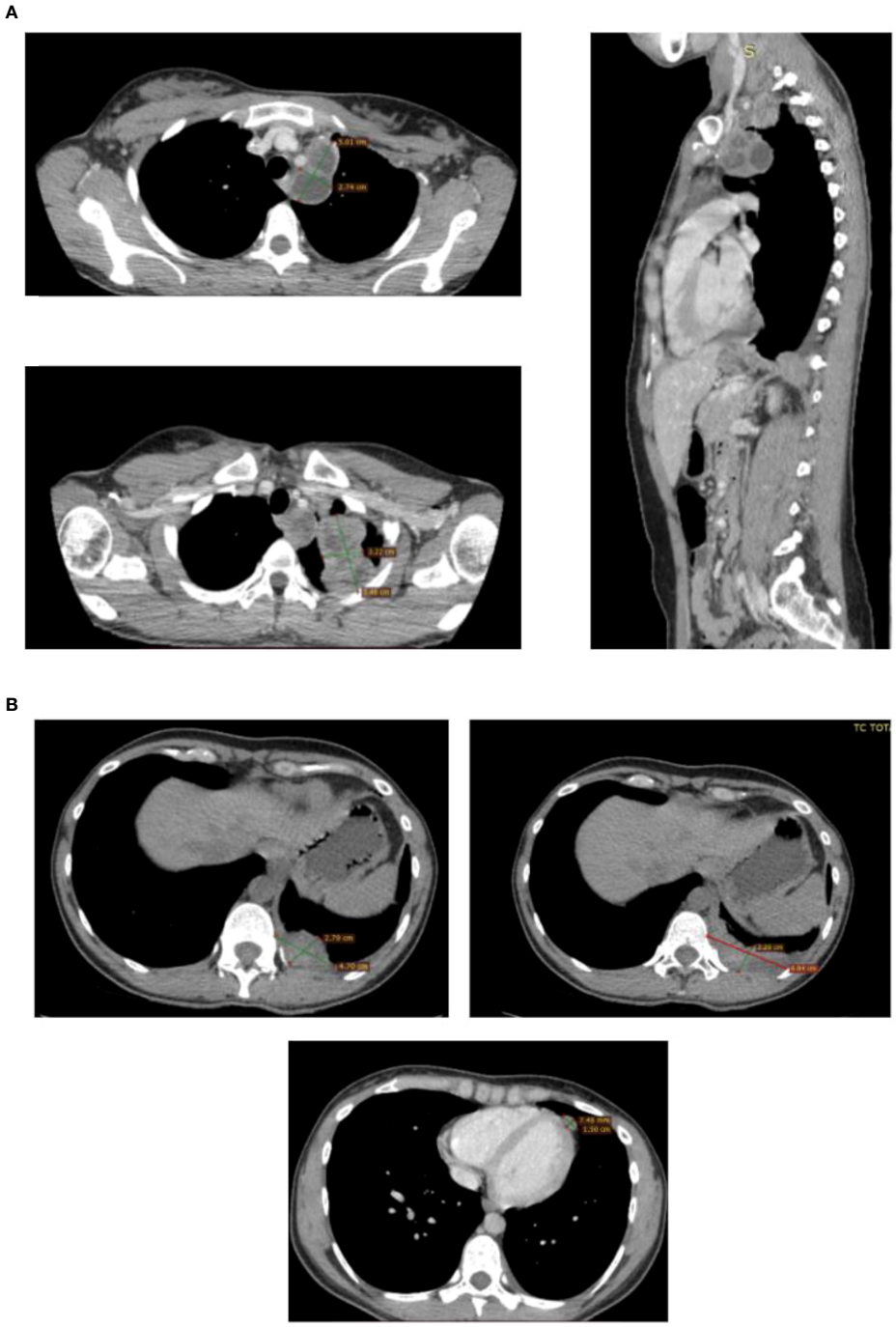

FIGURE 4
CT scans showing the presence and anatomical relation of the heteroplastic mass. CT scan detecting locoregional recurrence. **(A)** Necrotic pathological swelling in para-aortic region and breast-like pathological tissue in the left lung apex, axial and sagittal plane. **(B)** Solid nodulation along the pericardial sheet with reactive fluid flap and pathological mass along the left costo-vertebral pleura with pleural effusion flap.

At the end of the ninth cycle the previously achieved complete response was maintained. The patient had experienced mild neutropenia and anemia, graded as G1, that did not lead to treatment discontinuation.

The case was discussed in the multidisciplinary board once again to evaluate the most suitable options to minimize the risk of a second recurrence and to strengthen the achieved optimal response. Among the feasible strategies there were: local radiation therapy, consolidation chemotherapy or close follow-up.

Considering the complete response previously achieved with a chemotherapy-based approach, after relapsing to up-front surgery, we proposed her high dose chemotherapy with subsequent autologous transplant (HDCT/ASCT) as consolidation treatment. The patient agreed and underwent two courses of mobilitiation chemotherapy followed by stem cell collection.

Notably, during the mobilization phase of the HDCT/ASCT, the patient experienced mild anemia, graded as G1, and moderate neutropenia, graded as G2 that did not required any medical

interventions and did not lead to treatment interruption or discontinuation.

Overall, the treatment was well tolerated.

Finally, she received high dose chemotherapy with busulfan and melphalan and autologous transplantation.

To date, the patient is free from recurrences.

Remarkedly, the patient experienced an emotional journey through surgery chemotherapy and stem cell transplantation. Particularly, since the beginning she expressed a strong childbearing desire, unfortunately delayed by the required therapeutic interventions. Initially, the patient was prone to postpone chemotherapy adjuvant treatment to carry out a natural pregnancy. Subsequently, her perspective changed since the disease recurred and the fear of the unpredictable future forced her to a present-moment awareness. Of note, during the therapeutic iter, we offered the patient the possibility of cryopreservation to protect her desire. Nowadays, the patient is reshaping her future with more self-consciousness aiming to carry out a pregnancy and to find a renewed balance.

Discussion

Ewing sarcoma is the second most common bone tumor among children and young adults. ES arises from bones but also from extraskeletal locations, even if more rarely.

ES patients should be addressed to referred high volume centers with recognised expertise in the diagnosis and treatment of rare entities.

The optimal management of ES requires ultraspecialized knowledge and resources.

EUropean Reference Network on Rare Adult Cancer (EURACAN) represents one of the most experienced and powerful reality connecting health care centers specialized in rare cancers.

The diagnosis and the management of extraskeletal ES follow the same principles as for bone ES (8). Nowadays, the diagnosis of ES is made by histological features and immunohistochemical markers positivity, even if their accuracy is low. Cluster of differentiation 99 (CD99) and Friend leukemia integration 1 (FLI-1) are currently accepted for the diagnosis of Ewing Sarcoma but they can also be expressed in a wide range of cancer entities different from ES.

FLI-1 is a transcription factor with a specificity and sensitivities, as a diagnostic marker for ES, that can vary from 63% to 100% and from 60% to 97%, respectively (9).

CD99 is a transmembrane molecule encoded by the pseudoautosomal gene MIC2. CD99 has been reported to have a marked effect on the migration, invasion and metastasis of tumor cells (10).

The definitive diagnosis is made on biopsy.

Molecularly, it is characterized by the presence of the translocation t (11,22) (q24;q12) that involves one of the members of the FET family (FUS/EWS/TLS), mostly EWSR1 and a member of the ETS (E26 transformation-specific or E-twenty-six) gene family, FLI1 in most cases (11).

This translocation is reciprocal and involves the Ewing sarcoma breakpoint region 1 (EWSR1) gene and almost always the FLI1 gene. EWSR1 and FLI1 merge in order to create a fusion gene that codifies for a fusion protein. The most frequent rearrangement is t (11,22) (q24;q12) that accounts for about 80% of ES while another 10% is represented by the fusion of EWSR1 with ETS-related gene (ERG) in the translocation t (21,22)(q11;q12) (12).

This molecular finding is mandatory in order to differentiate ES from other RCS.

Considering the rare incidence of these tumors, the histological assessment should be performed by specialized pathologists and a second revision should be encouraged to confirm the diagnosis.

Staging can be performed with both PET/CT scans and whole body magnetic resonance imaging (WB-MRI).

The treatment of ES involves combined modality therapy with chemotherapy and local therapy, both surgery and radiotherapy.

Surgery plays an important role in the management of ES and its aim is to ensure that the entire volume of tissue involved at diagnosis, and not only the tissue that remains after induction chemotherapy, is treated to guarantee an optimal local control.

Surgery is considered the best up-front modality also because local recurrence is frequent in ES, especially if radiotherapy (RT) is performed alone.

Generally, an induction chemotherapy is performed after the biopsy and prior to the local control with surgery and radiotherapy. The most used drugs are: vincristine (V), doxorubicin (D), cyclophosphamide (C)/ifosfamide (I) and etoposide (E). They all have proven activity in ES in large collaborative trials.

RT can be performed as up-front treatment when surgery can not guarantee a complete and radical excision or as adjuvant/neoadjuvant treatment (12).

As ES eventually relapses, first line therapy includes combined chemotherapy with vincristine, adriamycin, cyclophosphamide, ifosfamide and etoposide (13).

When a response, either partial or complete, to this salvage therapy is gained a consolidation therapy with high dose chemotherapy followed by autologous transplantation can be taken into consideration (14).

This regimen is characterized by different phases: stem cells stimulation, stem cells collection, called apheresis, stem cell preservation, high dose chemotherapy, stem cells transplantation and engraftment.

In the stem cell stimulation phase, also known as mobilization, three to four cycles of chemotherapy regimen with cyclophosphamide and etoposide followed by daily injections of Granulocytes-colony stimulating factor (G-CSF) are administered. Subsequently, Peripheral blood stem cells (PBSC) are collected by continuous apheresis.once the peripheral blood CD34+ count is at least 5 cells/l.

The stem cells are frozen using liquid nitrogen in a process known as cryopreservation.

Morever, autologous transplantation is started with high dose chemotherapy with busulfan and melphalan and peripheral blood stem cells are infused on day 0.

Supportive care included: antibiotic, antiviral and antimycotic drugs are used in order to reduce the risk of opportunistic and not opportunistic infections.

Furthermore, a low-dose heparin prophylaxis given by continuous infusion at 100 U/kg can be considered to prevent a fearful consequence of HDCT/ASCT as sinusoidal obstruction

Due to the high rates of relapse of ES, there is an unmet need in finding therapeutic opportunities for patients whose disease recur after standard first line therapies. Besides, the phase III rEECur trial provided the first randomized evidence of activity between regimens in an extremely rare disease as ES. Indeed, the four most common regimen used in recurrent and primary refractory ES, irinotecan plus temozolomide (IT), gemcitabine plus docetaxel (GD), high dose ifosfamide (hd-IFO) and topotecan plus cyclophosphamide (TC) were compared one with the other.

The trial was designed to discontinue the least successful treatment arms after 50 and then 75 patients had been randomly assigned and their results evaluated, respectively, regardless of the treatment difference magnitude.

At the first and second interim analysis the two arms, GD and IT, were discontinued.

Between hd-IFO and TC, the first showed better progression free survival and overall survival in the last analysis.

Currently, the rEECur trial is recruiting patients to hd-IFO and another, recently added arm, carboplatin plus etoposide (CE). Data is still awaited, as a molecularly targeted agent arm is planned (15). Moreover, as intensive chemotherapy regimens represent the essential backbone of ES treatment, the toxicity as well as the quality of life evaluation has to be considered. In particular, whereas our patient experienced mild neutropenia, and anemia that did not lead to treatment discontinuation, commonly the chemotherapeutic protocol adopted has been associated with high toxicity rate (16). Besides, the rEECur trial showed different toxicity profiles between regimens as hd-IFO arm compared with TC arm was more likely associated with 3/4 encephalopathy and kidney impairment and patients were more likely to experience treatment discontinuation. Therefore, a multidisciplinary approach is required to better select patients according to performance status, organ functions, time relapsed since prior therapy, and to manage the related adverse events that could eventually affect treatment efficacy.

Conclusion

Although ES arising from mediastinum is extremely rare, it should be considered when a differential diagnosis of a mediastinal mass has to be made in adult patients who may benefit from an aggressive multimodality treatment.

As far as we know, only a few cases of primary mediastinal extraskeletal Ewing sarcoma have been reported and currently there is no consensus on the optimal treatment strategy to adopt. The main issue is represented by the lack of concordance in the histological diagnosis which eventually leads to a delayed diagnosis. Moreover, the sequential combination of chemotherapeutic protocols required, as well as the toxicities related to management, needs a long-established expertise and a multidisciplinary approach in order to provide the patient with the most appropriate treatment selection.

Data availability statement

The original contributions presented in the study are included in the article/supplementary material, further inquiries can be directed to the corresponding author/s.

Ethics statement

The authors are accountable for all aspects of the work in ensuring that questions related to the accuracy or integrity of any part of the work are appropriately investigated and resolved. The patient signed informed consent for the use of all the reported data. The anonymity was assured. Written informed consent was obtained from the patient for publication of this case report and accompanying images. A copy of the written consent is available for review by the editorial office of this journal. The authors are accountable for all aspects of the work in ensuring that questions related to the accuracy or integrity of any part of the work are appropriately investigated and resolved.

Author contributions

AC and RB contribute to the writing of the case report. MO, GP, SDP, and MG contribute to the idea of the case report and the supervision of the manuscript. MT, FS, AP, and FP, resources and data curation. RM, EP, and PDP revision of the manuscript and editing. MM contributes to the anatomopathological support in the writing of the case report and supply all the figures regarding this aspect. All authors contributed to the article and approved the submitted version.

Acknowledgments

This report was part of research activity of the Rare Tumors Coordinating Center of Campania Region (CRCTR), recognized as a full member of the European Reference Network (ERN-EURACAN). The authors would like to acknowledge the ERN-EURACAN as a powerful resource for transnational collaboration in rare cancers.

Conflict of interest

SDP reports consulting fees for Consulting or advisory Role: Lilly, GSK, MSD, Seagen, Daichii Sankyo, Gilead, Eisai, Bristol Myers Squibb, AstraZeneca, Novartis, Pfizer, Roche; and Speaker's Bureau: AstraZeneca, Novartis, Pfizer, Roche. MG reports consulting fees for Consulting or advisory Role: Lilly, Novartis, Pfizer, AstraZeneca; Speaker's Bureau: Lilly, Novartis, Pfizer, Eisai, Roche, AstraZeneca, Daichii Sankyo, MSD; Travel, accommodation, expenses: Novartis, Pfizer, Roche. The authors have no other conflicts of interest to declare.

The remaining authors declare that the research was conducted in the absence of any commercial or financial relationships that could be construed as a potential conflict of interest.

Publisher's note

References

1. Jemal A, Tiwari RC, Murray T, Ghafoor A, Samuels A, Ward E, et al. Cancer statistics, 2004. *CA Cancer J Clin* (2004) 54:8–29. doi: 10.3322/canjclin.54.1.8

2. Casali PG, Abecassis N, Aro HT, Bauer S, Biagini R, Bielack S, et al. Soft tissue and visceral sarcomas: ESMO– EURACAN clinical practice guidelines for diagnosis, treatment and follow- up††FootnotesApproved by the ESMO guidelines committee and EURACAN: December 2017. *Ann Oncol* (2018) 29(Supplement 4):iv51–67. doi: 10.1093/annonc/mdy096

3. Mastrangelo G, Coindre JM, Ducimetière F, Dei Tos AP, Fadda E, Blay J-Y, et al. Incidence of soft tissue sarcoma and beyond: a population-based prospective study in 3 European regions. *Cancer* (2012) 118(21):5339–48. doi: 10.1002/cncr.27555

4. Macchiarini P, Ostertag H. Uncommon primary mediastinal tumours. *Lancet Oncol* (2004) 5:107–18. doi: 10.1016/S1470-2045(04)01385-3

5. Burt M, Ihde JK, Hajdu SI, Smith JW, Bains MS, Downey R, et al. Primary sarcomas of the mediastinum: results of therapy. *J Thorac Cardiovasc Surg* (1998) 115:671–80. doi: 10.1016/S0022-5223(98)70333-2

6. Marx A, Chan JKC, Chalabreysse L, et al. The 2021 WHO classification of tumors of the thymus and mediastinum: What is new in thymic epithelial, germ cell, and mesenchymal tumors? *J Thorac Oncol* (2022) 17(2):200–213. doi: 10.1016/j.jtho.2021.10.010

7. Ahmad U. The eighth edition TNM stage classification for thymic tumors: What do I need to know? *J Thorac Cardiovasc Surg Elsevier* (2021) 161(4):1524–9. doi: 10.1016/j.jtcvs.2020.10.131

8. Strauss SJ, Frezza AM, Abecassis N, Bajpai J, Bauer S, Biagini R, et al. Bone sarcomas: ESMO-EURACAN- GENTURIS-ERNPaedCan clinical practice guidelines for diagnosis, treatment and follow- up on behalf of the ESMO guidelines committee, EURACAN, GENTURIS & ERNPaedC;Published in 2021. *Ann Oncol* (2021) 32 (12):1520–36. doi: 10.1016/j.annonc.2021.08.1995

9. Folpe AL, Chand EM, Goldblum JR, Weiss SW. Expression of fli-1, a nuclear transcription factor, distinguishes vascular neoplasms from potential mimics. *Am J Surg Pathol* (2001) 25(8):1061–6. doi: 10.1097/00000478-200108000-00011

10. Pasello M, Manara MC, Scotlandi K. CD99 at the crossroads of physiology and pathology. *J Cell Commun Signal* (2018) 12(1):55–68. doi: 10.1007/s12079-017-0445-z

11. Lessnick SL, Ladanyi M. Molecular pathogenesis of Ewing sarcoma: new therapeutic and transcriptional targets. *Annu Rev Pathol* (2012) 7:145–59. doi: 10.1146/annurev-pathol-011110-130237

12. Riggi N, Stamenkovic I. The biology of Ewing sarcoma. *Cancer Lett* (2007) 254 (1):1–10. doi: 10.1016/j.canlet.2006.12.009

13. Khanna N, Pandey A, Bajpai J. Metastatic ewing's sarcoma: Revisiting the "Evidence on the fence". *Indian J Med Paediatr Oncol* (2017) 38(2):173–81. doi: 10.4103/ijmpo.ijmpo_24_17

14. Tenneti P, Zahid U, Iftikhar A, Yun S, Sohail A, Warraich Z, et al. Role of high-dose chemotherapy and autologous hematopoietic cell transplantation for children and young adults with relapsed ewing's sarcoma: A systematic review. *Sarcoma* (2018), 2640674. doi: 10.1155/2018/2640674

15. McCabe M, Kirton L, Khan M, Fenwick N, Strauss SJ, Valverde C, et al. Phase III assessment of topotecan and cyclophosphamide and high-dose ifosfamide in rEECur: An international randomized controlled trial of chemotherapy for the treatment of recurrent and primary refractory Ewing sarcoma (RR-ES). *J Clin Oncol* (2022) 40(suppl 17; abstr LBA2). doi: 10.1200/JCO.2022.40.17_suppl.LBA2

16. Whelan J, Khan A, Sharma A, Rothermundt C, Dileo P, Michelagnoli M, et al. Interval compressed vincristine, doxorubicin, cyclophosphamide alternating with ifosfamide, etoposide in patients with advanced ewing's and other small round cell sarcomas. *Clin Sarcoma Res* (2012) 2(1):12. doi: 10.1186/2045-3329-2-12

frontiers | Frontiers in Oncology

TYPE Case Report
PUBLISHED 02 February 2023
DOI 10.3389/fonc.2023.1053497

OPEN ACCESS

EDITED BY
Kohei Fujita,
National Hospital Organization Kyoto Medical Center, Japan

REVIEWED BY
Gen Lin,
Fujian Provincial Cancer Hospital, China
Tawee Tanvetyanon,
Moffitt Cancer Center, United States

*CORRESPONDENCE
Alessandro Inno
alessandro.inno@sacrocuore.it

SPECIALTY SECTION
This article was submitted to Thoracic Oncology, a section of the journal Frontiers in Oncology

RECEIVED 25 September 2022
ACCEPTED 17 January 2023
PUBLISHED 02 February 2023

CITATION
Inno A, Lattuada E, Foti G and Gori S (2023) Chemo-immunotherapy for metastatic non-squamous NSCLC in a patient with HIV infection: A case report. *Front. Oncol.* 13:1053497. doi: 10.3389/fonc.2023.1053497

Chemo-immunotherapy for metastatic non-squamous NSCLC in a patient with HIV infection: A case report

Alessandro Inno[1]*, Emanuela Lattuada[2], Giovanni Foti[3] and Stefania Gori[1]

[1]Unità Operativa di Oncologia Medica, IRCCS Ospedale Sacro Cuore Don Calabria, Negrar di Valpolicella (VR), Italy, [2]Unità Operativa di Malattie Infettive e Tropicali, AOUI Verona, Verona, Italy, [3]Unità Operativa di Radiologia, IRCCS Ospedale Sacro Cuore Don Calabria, Negrar di Valpolicella (VR), Italy

Activity and safety data of chemo-immunotherapy for patients with metastatic NSCLC and known HIV infection are still limited, since HIV-positive patients were generally excluded from clinical trials. Here we report the case of a metastatic NSCLC patient with HIV infection and undetectable viral load treated with first-line chemo-immunotherapy (pembrolizumab, carboplatin and pemetrexed), achieving a meaningful and durable objective response, with no treatment-related adverse events and no HIV-related complications. This report suggests that NSCLC patients with virologically controlled HIV infection can be safely treated with chemo-immunotherapy and should not be excluded from this treatment based on their viral infection only.

KEYWORDS

NSCLC, HIV, chemotherapy, immunotherapy, carboplatin, pemetrexed, pembrolizumab, anti-PD1

Introduction

Immune checkpoint inhibitors (ICIs) have deeply changed the treatment landscape of non-small cell lung cancer (NSCLC) over the last decade. For metastatic, non-oncogene addicted NSCLC, monoclonal antibodies against programmed cell death protein 1 (PD-1) or programmed cell death ligand 1 (PD-L1) now represent standard of care as single-agents in the first-line treatment for patients with PD-L1 expression on ≥50% of tumor cells, or in combination with standard platinum-based chemotherapy for all patients regardless of PD-L1 expression level (1–3). However, clinical trials with ICIs, alone or in combination with chemotherapy for NSCLC, generally excluded patients living with human immunodeficiency virus (HIV) infection (PLWHI), due to the concern of viral flares and/or triggering of immune-related adverse events, therefore the benefit/risk balance of ICIs needs to be further elucidated in this special population (4).

Here we report the case of a patient with HIV infection and metastatic NSCLC treated with pembrolizumab plus chemotherapy.

Case presentation

In September, 2020 a 50-year-old current smoker male presenting with persisting cough, fatigue and dyspnea was diagnosed with non-squamous, *EGFR* wild-type, ALK negative, ROS1 negative, PDL-1 positive (tumor proportion score 5%) NSCLC. Baseline tumor assessment with head-chest-abdomen CT scan and total-body 18-FDG PET/CT scan showed a large primary tumor (10 cm in size) in the upper right pulmonary lobe with metastatic homolateral hilar, mediastinal, supraclavicular and IIa/Ib level latero-cervical lymph nodes (stage cT4 cN3 cM1a, cIVA). Relevant past medical history included: squamous cell carcinoma of the nasal wing treated with radical surgery followed by adjuvant radiotherapy with concomitant weekly cisplatin chemotherapy in 2016; recurrent breast abscesses; known HIV infection since 2008, on treatment with ART consisting of emtricitabin/rilpivirine/tenofovir at the time of NSCLC diagnosis. In addition, baseline infectious disease screening also revealed past HBV infection.

From 14th October 2020, the patient underwent first-line treatment for NSCLC with pembrolizumab (200 mg iv), carboplatin (AUC 5 mg/ml/min iv) and pemetrexed (500 mg/m2 iv) every three weeks for 4 cycles. After the first two cycles the patient achieved a dramatic clinical response with complete resolution of the cough and a meaningful improvement of dyspnea and fatigue. Tumor assessment with CT scan after 4 cycles of treatment confirmed an objective partial response with an impressive tumor shrinkage (Figure 1). After that, the patient was started on maintenance therapy with pembrolizumab and pemetrexed. until May, 2022 when pemetrexed was discontinued (after 20 maintenance courses) due to G2 protracted fatigue, not associated with significant chemotherapy-induced hematologic toxicity. Although fatigue may occur on a multifactorial basis, including as a side effect of ART as well as of immunotherapy, it was considered mainly related to prolonged pemetrexed exposure. In fact, fatigue resolved after pemetrexed discontinuation. Pembrolizumab alone was continued as maintenance therapy, with further 10 courses administered from May to December 2022, and it is still ongoing, with a ongoing progression-free survival of 27+ months so far. During cancer treatment the patient had a left breast abscess that was successfully managed with oral anti-inflammatory and antibiotic therapy and surgical drainage, and he has experienced no treatment-related adverse events (TRAEs) but the G2 fatigue leading to pemetrexed discontinuation. Particularly, there has been no HIV viral flare or significant worsening of CD4 cell count. In fact, before starting chemo-immunotherapy HIV viral load was undetectable and CD4 cell count was 531/μl (23%) with CD4/CD8 ratio of 0.67, whereas last values while on chemo-immunotherapy treatment were as it follows: viral load undetectable, CD4 cell count 474/μl (24%), CD4/CD8 ratio 0.71.

Discussion

There is some retrospective evidence on safety and activity of ICIs in PLWHI with NSCLC. A systematic review including 73 cases of cancer PLWHI treated with ICIs (5), 23 of them with NSCLC, reported grade ≥ 3 immune-related adverse events (irAEs) in only 6 out of 70 patients (8.6%). Among 25 patients with paired pre-treatment and post-treatment CD4+ cell counts, the cell counts increased. Objective response rate (RR) among patients with NSCLC was 30%. Similarly, data retrospectively collected from the French CANCERHIV database on 23 PLWHI treated with ICIs for lung cancer (n=21), melanoma (n=1) or head and neck cancer (n=1) reported only two grade 3 irAEs (6). All patients were on antiretroviral therapy (ART) when started ICIs. HIV viral load was undetectable for all the 13 patients with available data about HIV viremia, and only one patient experienced a positive HIV viral load but this occurred after antiretroviral therapy (ART) interruption. CD4+ cell counts had no major changes during treatment with ICIs. In this study, RR among NSCLC was 18%.

More recently, prospective phase 1 and 2 clinical trials also reported data on safety and activity of ICIs in PLWHI with NSCLC. A phase 1 study assessed safety of pembrolizumab as single agent among 30 patients with advanced cancer and HIV infection receiving ART, with a viral load of < 200 copies/mL, and a CD4+ cell count > 100/μl (7). Toxicity profile was acceptable with grade 3 irAEs reported in 6 (20%) patients, no meaningful variations in viral load or need for change of ART. In this study, only one patient with NSCLC was enrolled, obtaining a sustained complete response. A phase 2 study with durvalumab for the treatment of solid tumors in PLWHI enrolled 20 patients, 14 of them with NSCLC (8). According to inclusion criteria, all the patients had to be on ART with undetectable viral load, regardless of their CD4+ T-cell count. No grade ≥ 3 irAEs were observed. CD4+ and CD8+ T-cell remained stable throughout the study, with no significant increase in viral load. Four of 16 response-evaluable patients (25%) had a partial response, and all the responders were NSCLC patients. Interestingly, no correlation of clinical benefit with basal CD4+ or CD8+ T-cell counts was found. Another phase 2 study evaluated nivolumab in 16 PLWHI with NSCLC, with viral load of <200 copies/mL, and no restriction in terms of CD4+ T-cell count (9). Two patients achieved partial response (12.5%), with a disease control rate of 62.5%. Adverse events were generally mild-moderate, with only one case of severe skin toxicity. HIV viral load was stable during treatment, whereas an increase in proliferating CD8+ and CD4+ T-cells was observed after 3 nivolumab cycles in a subgroup of 9 patients.

Taken together, data from retrospective studies and prospective phase 1 and 2 clinical trials reported meaningful activity with an acceptable toxicity profile and no significant risk of viral flare among patients with NSCLC and virologically controlled HIV infection treated with single-agent ICIs. However, data about activity and safety of ICIs plus chemotherapy combinations in this special population are still lacking.

We described a patient with metastatic NSCLC and concurrent HIV infection with undetectable viral load, treated with pembrolizumab, carboplatin and pemetrexed, that achieved a meaningful and durable response, without clinically meaningful TRAEs or HIV flares. This report suggests that chemo-immunotherapy may be active and safe for selected HIV-positive patients with metastatic NSCLC receiving ART with undetectable viral load. Thus, PLWHI with NSCLC should be not excluded from chemo-immunotherapy based only on their viral infection. Data from prospective clinical trials and/or observational registries could contribute to further evaluate chemo-immunotherapy in this special population. At this regard, new clinical trials with ICIs in NSCLC allow the enrollment of patients with HIV infection. For example,

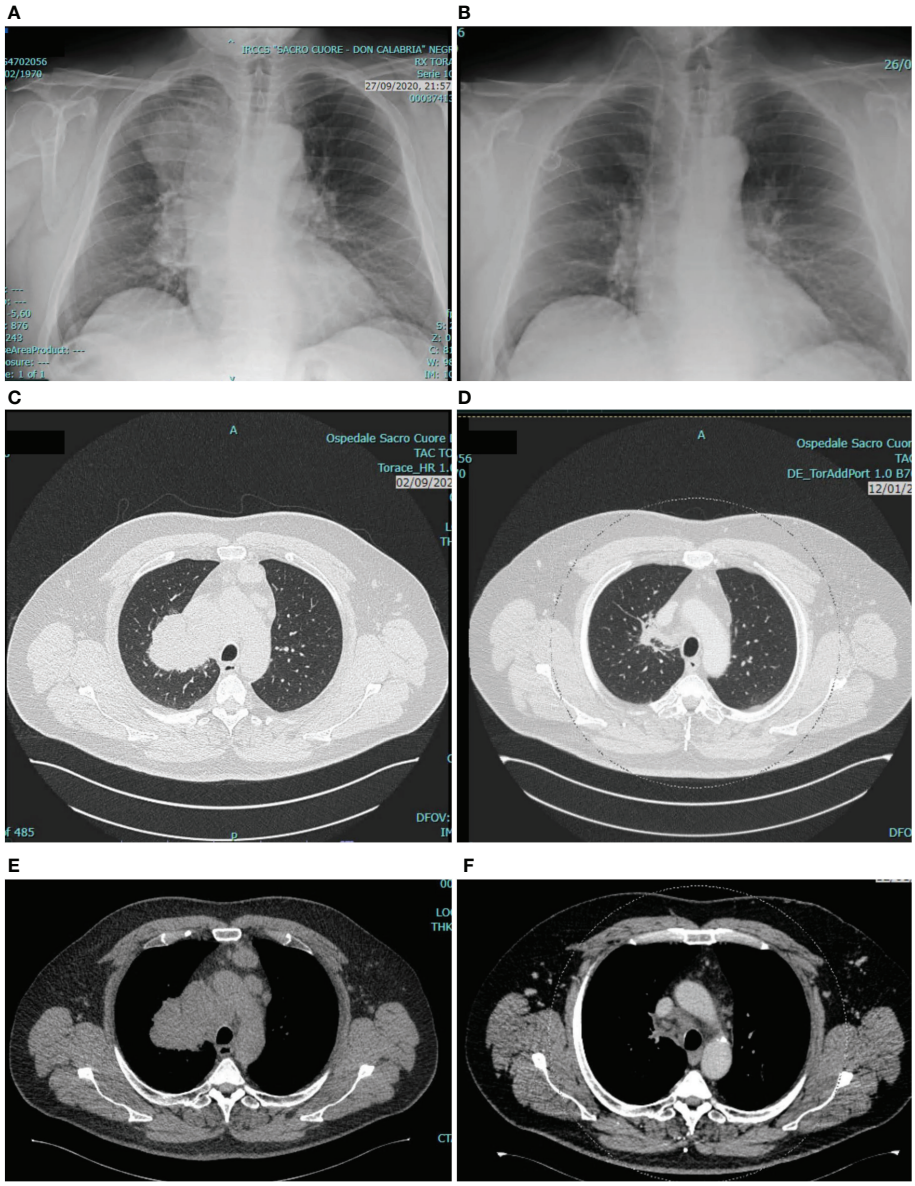

FIGURE 1
Tumor assessment at baseline and after 4 cycles of pembrolizumab/carboplatin/pemetrexed. The figure shows chest X-ray before **(A)** and after **(B)** treatment, and chest CT scan before **(C, E)** and after **(D, F)** treatment. As compared with baseline, tumor assessment after 4 cycles revealed a deep response of the primary tumor in the upper right pulmonary lobe, and a reduction of para-tracheal and pre-vascular mediastinal pathologic lymph nodes.

phase 3 randomized clinical trials with cemiplimab alone or in combination with chemotherapy for advanced NSCLC did include patients with controlled HIV infection, but results in the HIV-positive population have not been reported yet (10, 11).

Data availability statement

The raw data supporting the conclusions of this article will be made available by the authors, without undue reservation.

Ethics statement

Written informed consent was obtained from the individual(s) for the publication of any potentially identifiable images or data included in this article.

Author contributions

AI wrote the manuscript. All authors contributed to the article and approved the submitted version.

Conflict of interest

The authors declare that the research was conducted in the absence of any commercial or financial relationships that could be construed as a potential conflict of interest.

Publisher's note

All claims expressed in this article are solely those of the authors and do not necessarily represent those of their affiliated

organizations, or those of the publisher, the editors and the reviewers. Any product that may be evaluated in this article, or claim that may be made by its manufacturer, is not guaranteed or endorsed by the publisher.

References

1. Paz-Ares L, Luft A, Vicente D, Tafreshi A, Gümüş M, Mazières J, et al. Pembrolizumab plus chemotherapy for squamous non-Small-Cell lung cancer. *N Engl J Med* (2018) 379(21):2040–51. doi: 10.1056/NEJMoa1810865

2. Gandhi L, Rodríguez-Abreu D, Gadgeel S, Esteban E, Felip E, De Angelis F, et al. Pembrolizumab plus chemotherapy in metastatic non-Small-Cell lung cancer. *N Engl J Med* (2018) 378(22):2078–92. doi: 10.1056/NEJMoa1801005

3. Herbst RS, Giaccone G, de Marinis F, Reinmuth N, Vergnenegre A, Barrios CH, et al. Atezolizumab for first-line treatment of PD-L1-Selected patients with NSCLC. *N Engl J Med* (2020) 383(14):1328–39. doi: 10.1056/NEJMoa1917346

4. Vora KB, Ricciuti B, Awad MM. Exclusion of patients living with HIV from cancer immune checkpoint inhibitor trials. *Sci Rep* (2021) 11(1):6637. doi: 10.1038/s41598-021-86081-w

5. Cook MR, Kim C. Safety and efficacy of immune checkpoint inhibitor therapy in patients with HIV infection and advanced-stage cancer: A systematic review. *JAMA Oncol* (2019) 5(7):1049–54. doi: 10.1001/jamaoncol.2018.6737

6. Spano JP, Veyri M, Gobert A, Guihot A, Perré P, Kerjouan M, et al. Immunotherapy for cancer in people living with HIV: safety with an efficacy signal from the series in real life experience. *AIDS* (2019) 33(11):F13–9. doi: 10.1097/QAD.0000000000002298

7. Uldrick TS, Gonçalves PH, Abdul-Hay M, Claeys AJ, Emu B, Ernstoff MS, et al. Assessment of the safety of pembrolizumab in patients with HIV and advanced cancer-a phase 1 study. *JAMA Oncol* (2019) 5(9):1332–9. doi: 10.1001/jamaoncol.2019.2244

8. Gonzalez-Cao M, Morán T, Dalmau J, Garcia-Corbacho J, Bracht JWP, et al. Assessment of the feasibility and safety of durvalumab for treatment of solid tumors in patients with HIV-1 infection: The phase 2 DURVAST study. *JAMA Oncol* (2020) 6 (7):1063–7. doi: 10.1001/jamaoncol.2020.0465

9. Lavole A, Mazieres J, Schneider S, Brosseau S, Kiakouama L, Greillier L, et al. Assessment of nivolumab in HIV-infected patients with advanced non-small cell lung cancer after prior chemotherapy. the IFCT-1602 CHIVA2 phase 2 clinical trial. *Lung Cancer* (2021) 158:146–50. doi: 10.1016/j.lungcan.2021.05.031

10. Sezer A, Kilickap S, Gümüş M, Bondarenko I, Özgüroğlu M, Gogishvili M, et al. Cemiplimab monotherapy for first-line treatment of advanced non-small-cell lung cancer with PD-L1 of at least 50%: a multicentre, open-label, global, phase 3, randomized, controlled trial. *Lancet* (2021) 397:592–604. doi: 10.1016/S0140-6736(21)00228-2

11. Gogishvili M, Melkadze T, Makharadze T, Giorgadze D, Dvorkin M, Penkov K, et al. Cemiplimab plus chemotherapy versus chemotherapy alone in non-small cell lung cancer: a randomized, controlled, double-blind phase 3 trial. *Nat Med* (2022) 28:2374–80. doi: 10.1038/s41591-022-01977-y

frontiers | Frontiers in Oncology

TYPE Case Report
PUBLISHED 06 February 2023
DOI 10.3389/fonc.2022.1020339

OPEN ACCESS

EDITED BY
Kohei Fujita,
National Hospital Organization Kyoto Medical Center, Japan

REVIEWED BY
Alessandro Inserra,
Bambino Gesù Children's Hospital (IRCCS), Italy
Haitao Zhu,
Affiliated Hospital of Jiangsu University, China

*CORRESPONDENCE
Wu Cai
xwg608@126.com

SPECIALTY SECTION
This article was submitted to Thoracic Oncology, a section of the journal Frontiers in Oncology

RECEIVED 16 August 2022
ACCEPTED 28 December 2022
PUBLISHED 06 February 2023

CITATION
Cui M, Zhai D, Liu Y, Zhou X, Wang T, Wang L, Cai W, Fan G and Ju S (2023) Case report: Primary mediastinal Ewing's sarcoma presenting with chest tightness.
Front. Oncol. 12:1020339.
doi: 10.3389/fonc.2022.1020339

Case report: Primary mediastinal Ewing's sarcoma presenting with chest tightness

Manman Cui[1], Duchang Zhai[1], Yan Liu[1], Xiuzhi Zhou[1], Tingting Wang[1], Lihuan Wang[2], Wu Cai[1]*, Guohua Fan[1] and Shenghong Ju[3]

[1]Department of Radiology, The Second Affiliated Hospital of Soochow University, Suzhou, China, [2]Department of Radiology, The First People`s Hospital of Taicang, Taicang, China, [3]Department of Radiology, Zhongda Hospital, Medical School of Southeast University, Nanjing, China

Ewing's sarcoma is a part of a rare group of malignant neoplasms, whose pathological morphological features are small round cells. Extraskeletal Ewing's sarcoma is a more uncommon primary tumor. Herein, we report the case of a 66-year-old man who complained of chest tightness. Subsequent chest CT scans revealed an irregular and uneven density mass on the right side of the anterior mediastinum with invasion of the superior vena cava, pericardium and right lung. The patient's clinical symptoms were improved after performing excision of the mediastinal lesions under cardiopulmonary bypass. Based on histological and immunohistochemical findings, the tumor was diagnosed as extraskeletal Ewing's sarcoma.

KEYWORDS

Ewing's sarcoma, extraskeletal, oncology, mediastinum, primary, chest

Introduction

Extraskeletal Ewing's sarcoma (EES) is a small round cell malignant tumor that grows outside of bone tissue, which arises from the mediastinum is extremely rare. Compared with patients with bone tumors, patients with EES have an older average age of onset. The clinical features and imaging appearances are non-specific, and patients often present with a rapidly growing mass that causes localized pain (1). The diagnosis of this tumor mainly relies on pathological, cytogenetic, immunohistochemical and molecular genetic analysis. We report a patient who presented with chest tightness and had a mediastinal ES, which was not confirmed until postoperative pathological examination was performed.

Case report

A 66-year-old man with an anterior mediastinal tumor was admitted to the hospital for surgical treatment. He went to the emergency department of the hospital 1 day prior because of chest tightness, and plain chest CT showed a mass on the right side of the anterior mediastinum that compressed the adjacent right lung, accompanied by pleural effusion (Figures 1A, B). Laboratory examinations revealed elevated levels of troponin, cardiac enzymes, CA125, NSE and cytokeratin, which indicated myocardial injury and abnormal cancer markers. The preoperative contrast-enhanced CT scan showed a giant cystic and solid mass on the right side of the anterior mediastinum, which had moderately uneven enhancement, and the mediastinal lymph nodes were enlarged (Figures 1C, D). The mass on the right side of the anterior mediastinum with invasion of the superior vena cava, pericardium and right lung could be observed from the coronal multiplanar reconstruction images (Figures 1E, F). In summary, we initially considered that the mass was a malignant tumor arising from the thymus.

Intraoperative exploration revealed that the tumor had invaded the superior vena cava, pericardium and right middle lung, so the surgeon adopted resection of the mediastinal lesions under cardiopulmonary bypass, partial resection of the superior vena cava with artificial blood vessel replacement and lobectomy of the right middle lung with lymph node dissection. The pathological findings confirmed that it was a small round cell malignant tumor (Figure 2A). The mediastinal lymph nodes submitted for examination showed that metastasis of the tumor had already occurred. The immunohistochemical results demonstrated a Ki-67 of 90%, positivity for AE1/AE3, P16, CD 99 (Figure 2B), CD56 and synaptophysin, partial positivity for EMA, MDM2 and desmin (Figure 2C), and negativity for vimentin, CK7, CAM5.2, SMA, NSE and S-100. Based on these findings, primary mediastinal ES was diagnosed. The patient's chest tightness and overall condition improved after the operation, and he was discharged after 1 month of symptomatic and supportive treatments. One month later, the patient was admitted to the hospital again. His blood test showed a significant increase in the heart failure index score. After symptomatic treatments, the symptoms improved. Subsequently, the patient's chest tightness was not relieved, and he had orthopnea. After consultation with experts, he was considered to have postoperative cachexia of a malignant tumor. There was a risk of respiratory cardiac arrest at any time, and the prognosis was very poor. Four days later, he was transferred to the ICU for treatment. Echocardiography showed that there was a large amount of pericardial effusion, and combined with the history of the tumor invading the pericardium, the effusion was considered to be tumor tissue. Finally, pathological examination of the pericardial effusion confirmed that it had malignant tumor cells (Figure 2D).

Because the circulatory failure caused by pericardial tamponade was difficult to cure, the family members of the patient finally refused further invasive surgery for the patient; only noninvasive ventilators were used to maintain the patient's vital signs, and he had entered the end stage of clinical life.

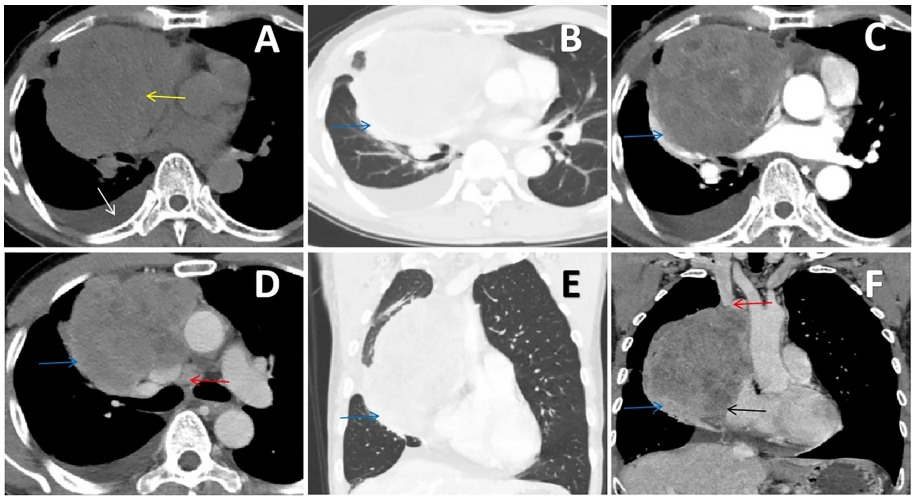

FIGURE 1
(A, B) Chest CT scan showing an irregular soft tissue density mass (yellow arrow) on the right side of the anterior mediastinum that compressed the adjacent right lung (blue arrow), accompanied by pleural effusion (white arrow). **(C, D)** Contrast-enhanced chest CT scan showing that the mass had moderately uneven enhancement, which invaded the right lung (blue arrow), and the mediastinal lymph nodes were enlarged (red arrow). **(E, F)** The coronal multiplanar reconstruction images clearly delineated the irregular and uneven density mass on the right side of the anterior mediastinum with invasion of the superior vena cava (red arrow), pericardium (black arrow) and right lung (blue arrow).

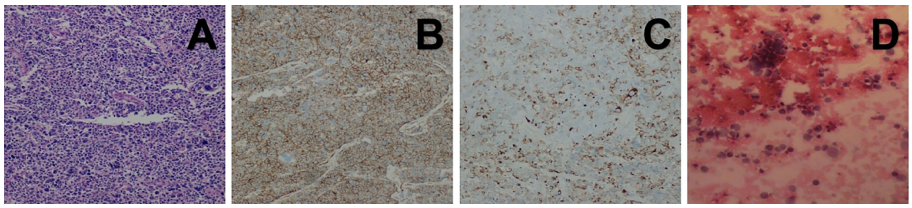

FIGURE 2
(A) Histopathological image showing tumor cells composed of primitive small round cells (H&E staining). **(B, C)** Immunohistochemical images showing positivity for CD99 and desmin. **(D)** Histopathological image showing pericardial effusion, which consisted of poor differentiation of malignant tumors.

Discussion

EES is a rare entity with high-grade malignancy that commonly involves the soft tissues of the trunk and extremities. It is more common in the lower limbs, paraspinal, retroperitoneum and chest wall and rarely occurs in solid organs. Primary mediastinal EES is extremely rare (2, 3). Therefore, the case we present can increase our understanding of this malignant tumor. Its early clinical symptoms are mostly uncharacteristic; it usually presents as a painless mass that rarely attracts attention, and the late stage manifests as a progressive enlargement of the mass accompanied by pain and the symptoms of invaded adjacent tissues. The histological pattern of EES consists of a large number of small round cells with a uniform shape, which have a high nuclear to cytoplasmic ratio (4). In immunohistochemistry, CD99, FLI-1 and vimentin are almost expressed, and NSE and synaptophysin are expressed to varying degrees. CD99, the product of the *MIC* gene, is a relatively specific antibody of the ES family. However, CD99 expression is not specific to ES, as it can be expressed by other tumors, such as ependymoma (5). To the best of our knowledge, the translocation t(11;22)(q24;q12) is an important factor for EES diagnosis as well as differential diagnosis. Delattre et al. reported that 85% of cases were associated with the translocation t(11;22)(q24;q12), which leads to the formation of the *EWS-FLI-1* fusion gene (6). The imaging findings of EES are often nonspecific, and most CT scans show that it is a soft tissue density mass in different parts. In magnetic resonance imaging (MRI), the mass shows a moderate signal on T1WI and a moderately high signal on T2WI. Sometimes the density or signal is uneven because of haemorrhage and necrosis. It is more common to see cystic degeneration and necrosis, but calcification is rarely observed, and capsules may appear. Enhanced scans can show that a mass is uneven and that the degree of enhancement is different. Since the tumor is invasive, it tends to invade surrounding tissue structures. The CT of the patient we report clearly revealed that the tumor had invaded the superior vena cava, pericardium and lung tissue. Furthermore, enhanced scanning can show the blood supplying arteries of the mass and can also be used to evaluate the feasibility of tumor surgery and determine clinical treatment plans. Since mediastinal ES is relatively rare, it needs to be differentiated from malignant thymoma, mediastinal lymphoma, teratoma, seminoma, endodermal sinus tumor and solitary fibroma. Malignant thymoma should be considered first when a large, irregular and uneven mass appears in the anterior mediastinum, which was the reason for misdiagnosis in the study. Malignant thymomas show similar radiologic findings as EWS (7). However, malignant thymomas are much less malignant than mediastinal ES, such as they usually have no lymph node metastasis and no pleural effusion. In addition, malignant thymomas are usually accompanied by myasthenia gravis. Teratomas are often accompanied by fat, calcification, and bone and soft tissue density masses. The majority of lymphomas in the mediastinum have lymphadenopathy in the neck and other areas of the mediastinum, and the clinical symptoms are more typical. If there is a homogeneous and soft tissue density solid mass with no calcification and fat accompanied by elevated β-HCG levels, then seminoma should be considered. Enhanced scans of mediastinal endodermal sinus tumors show centripetal irregular striped and reticular blood vessels, and the surrounding irregular thick-walled ring is obviously enhanced. In addition, AFP and β-HCG levels are significantly increased in most patients. Large solitary fibromas are heterogeneous, and map-like uneven enhancement and creeping blood vessels can be observed by enhanced scanning. However, the final diagnosis depends on pathology and immunohistochemistry. Adverse prognostic factors consist of large tumors, nonsurgical treatment and regional lymph node metastasis (8). Treatment of EES includes combination therapy with chemotherapy and topical therapy delivered by surgical resection, radiation, or both (9). Covelli et al. confirmed that surgical resection alone can improve the survival rate of EES patients but also proposed that surgery combined with radiotherapy and chemotherapy is the best treatment for EES (10). The patient we report underwent surgery, but he did not receive chemotherapy or radiotherapy for economic reasons. Finally, he had a poor prognosis and entered the end stage of clinical life. Liu et al. reported a case of mediastinal ES that invaded surrounding tissues and was unresectable, but after chemotherapy, the patient's disease was almost completely in remission with no serious side effects (11).

Conclusion

Most cases of primary EES in the mediastinum appear as masses upon diagnosis with no specific clinical symptoms. On imaging, these tumors are usually large, enveloped, soft tissue density masses that can compress or invade adjacent tissues and easily metastasize, and an enhanced scans can show inhomogeneous moderate or significant enhancement. Imaging can be performed as a diagnostic tool, but the final diagnosis is mainly based on pathology and immunohistochemistry. In terms of treatment, surgical resection combined with chemotherapy, radiotherapy or both is the best solution.

Data availability statement

The original contributions presented in the study are included in the article/Supplementary Material. Further inquiries can be directed to the corresponding author.

Ethics statement

Written informed consent was obtained from the participant for the publication of any potentially identifiable images or data included in this article.

Author contributions

MC, DZ, XZ, YL, TW, LW, GF, SJ, and WC conceived the idea for the article. MC drafted the manuscript. WC approved the final version of the manuscript. All authors contributed to the article and approved the submitted version.

Funding

This study was supported by the Project of State Key Laboratory of Radiation Medicine and Protection, Soochow University (GZK1202136), "National Tutor System" Training Program for Health Youth Key Talents in Suzhou (Qngg2021006、Qngg2021039), Suzhou Health Talent (GSWS2021025), "Image Medical Star" Project of Suzhou Medical Association (2022YX-M05), Pre-research Foundation of Second Affiliated Hospital of Soochow University (SDFEYBS1904), and Project of Nuclear Technology Medical Application Supported by Discipline Construction of Second Affiliated Hospital of Soochow University (XKTJ-HRC20210010). The authors declare that this study received funding from "Technological Innovation" Project of CNNC Medical Industry Co. Ltd. (ZHYLYB2021006). The funder was not involved in the study design, collection, analysis, interpretation of data, the writing of the article, or the decision to submit it for publication.

Conflict of interest

The authors declare that the research was conducted in the absence of any commercial or financial relationships that could be construed as a potential conflict of interest.

Publisher's note

References

1. Abboud A, Masrouha K, Saliba M, Haidar R, Saab R, Khoury N, et al. Extraskeletal Ewing sarcoma: Diagnosis, management and prognosis. *Oncol Lett* (2021) 21(5):354. doi: 10.3892/ol.2021.12615

2. Reali A, Mortellaro G, Allis S, Trevisiol E, Anglesio SM, Bartoncini S, et al. A case of primary me-diastinal ewing's Sarcoma/Primitive neuroectodermal tumor presenting with initial compression of superi-or vena cava. *Ann Thorac Med* (2013) 8(2):121–3. doi: 10.4103/1817-1737.109834

3. Halefoglu AM. Extraskeletal ewing's sarcoma presenting as a posterior mediastinal mass. *Arch Bronconeumol.* (2013) 49(2):82–4. doi: 10.1016/j.arbres.2012.02.020

4. Riggi N, Stamenkovic I. The biology of Ewing sarcoma. *Cancer Lett* (2007) 254(1):1–10. doi: 10.1016/j.-canlet.2006.12.009

5. Kurdi M, Eberhart C. Immunohistochemical expression of Olig2, CD99, and EMA to differentiate oli-godendroglial-like neoplasms. *Folia Neuropathol.* (2021) 59(3):284–90. doi: 10.5114/fn.2021.108526

6. Delattre O, Zucman J, Plougastel B, Desmaze C, Melot T, Peter M, et al. Gene fusion with an ETS DNA-binding domain caused by chromosome translocation in human tumours. *Nature* (1992) 359(6391):162–5. doi: 10.1038/359162a0

7. Bae SH, Hwang JH, Da Nam B, Kim HJ, Kim KU, Kim DW, et al. Multiple Ewing Sarcoma/Primiti-ve neuroectodermal tumors in the mediastinum: A case report and literature review. *Med (Baltim-ore).* (2016) 95(7):e2725. doi: 10.1097/MD.0000000000002725

8. Chen Z, Jiao Y, Liu Z, Yang J, Sun J, Wang P. Extraskeletal ewing's sarcoma: Outcomes and CT fe-atures of endoceliac lesions. *Transl Cancer Res* (2021) 10 (9):4065–75. doi: 10.21037/tcr-21-607

9. Casali PG, Bielack S, Abecassis N, Aro HT, Bauer S, Biagini R, et al. Bone sarcomas: SMO-EURAC-AN-GENTURIS-ERN PaedCan clinical practice guidelines for diagnosis, treatment and follow-up. *Ann Oncol* (2018) 29(Su-ppl 4):iv79–95. doi: 10.1093/annonc/mdy310

10. Covelli HD, Beekman JF, Kingry RL. Extraskeletal ewing's sarcoma: Prolonged survival with recurr-ence after operation. *South Med J* (1980) 73 (9):1294–5. doi: 10.1097/00007611-198009000-00053

11. Liu M, Liu B, Dong L, Han T, Zhang L. Extraskeletal ewing's Sarcoma/Primitive neuroectodermal tumor of the mediastinum: Significant response to chemoradiotherapy. *Oncol Lett* (2015) 9(2):626–8. doi: 10.3892/ol.2014.2788

frontiers | Frontiers in Oncology

TYPE Case Report
PUBLISHED 16 February 2023
DOI 10.3389/fonc.2023.1100207

OPEN ACCESS

EDITED BY
Kohei Fujita,
National Hospital Organization Kyoto Medical Center, Japan

REVIEWED BY
Ahmed I. Younes,
East Carolina University, United States
Jitendra Singh Nigam,
All India Institute of Medical Sciences, India

*CORRESPONDENCE
Qi Dang
199057020185@email.sdu.edu.cn

SPECIALTY SECTION
This article was submitted to Thoracic Oncology, a section of the journal Frontiers in Oncology

RECEIVED 17 November 2022
ACCEPTED 30 January 2023
PUBLISHED 16 February 2023

CITATION
Nie L, Wang S, Feng Z, Sun Y, Wang Z, Dang Q, Gao A and Lv Y (2023) Nonfunctional ectopic adrenocortical carcinoma in the lung: A case report and literature review.
Front. Oncol. 13:1100207.
doi: 10.3389/fonc.2023.1100207

Nonfunctional ectopic adrenocortical carcinoma in the lung: A case report and literature review

Limin Nie[1,2], Shuyun Wang[1], Zongfeng Feng[3], Yuping Sun[1], Zhen Wang[4], Qi Dang[1]*, Aiqin Gao[5] and Yajuan Lv[6]

[1]Phase I Clinical Research Center, Shandong University Cancer Center, Jinan, Shandong, China, [2]Department of Oncology, Caoxian People's Hospital, Heze, Shandong, China, [3]Department of General Surgery, Caoxian People's Hospital, Heze, Shandong, China, [4]Department of Pathology, Caoxian People's Hospital, Heze, Shandong, China, [5]Department of Radiation Oncology, Shandong University Cancer Center, Jinan, Shandong, China, [6]Department of Oncology, Shandong Key Laboratory of Rheumatic Disease and Translational Medicine, Shandong Lung Cancer Institute, the First Affiliated Hospital of Shandong First Medical University & Shandong Provincial Qianfoshan Hospital, Jinan, Shandong, China

Background: Ectopic adrenocortical tissues and neoplasms are rare and usually found in the genitourinary system and abdominal cavity. The thorax is an extremely rare ectopic site. Here, we report the first case of nonfunctional ectopic adrenocortical carcinoma (ACC) in the lung.

Case presentation: A 71-year-old Chinese man presented with vague left-sided chest pain and irritable cough for 1 month. Thoracic computed tomography revealed a heterogeneously enhancing 5.3 × 5.8 × 6.0-cm solitary mass in the left lung. Radiological findings suggested a benign tumor. The tumor was surgically excised upon detection. Histopathological examination using hematoxylin and eosin staining showed that the cytoplasm of the tumor cells was rich and eosinophilic. Immunohistochemical profiles (inhibin-a$^+$, melan-A$^+$, Syn$^+$) indicated that the tumor had an adrenocortical origin. The patient showed no symptoms of hormonal hypersecretion. The final pathological diagnosis was non-functional ectopic ACC. The patient was disease-free for 22 months and is still under follow-up.

Conclusions: Nonfunctional ectopic ACC in the lung is an extremely rare neoplasm that can be easily misdiagnosed as primary lung cancer or lung metastasis, both preoperatively and on postoperative pathological examination. This report may provide clues to clinicians and pathologists regarding the diagnosis and treatment of nonfunctional ectopic ACC.

KEYWORDS

ectopic adrenocortical carcinoma, lung, nonfunctional, case report, adrenocortical carcinoma

Introduction

Adrenocortical carcinoma (ACC) is a rare malignancy with an incidence of 1–2 cases/million persons/year and often has a poor prognosis (1). It has a predilection for the female gender (F:M; 1.5–2.5:1) and a bimodal age distribution with peaks in early childhood (under the age of 5 years) and middle-aged adulthood (40–50 years) (2, 3). Most cases of ACC are functional and usually exhibit endocrine symptomatology due to hormonal hypersecretion (4). Nonfunctional ACC is less common and lacks specific signs and symptoms (5, 6). Patients are identified incidentally or present with nonspecific complaints related to tumor overgrowth and mass effects, such as abdominal or back pain, or metastatic symptoms (5, 7–9). Nonfunctional ACC generally occurs in older adults and exhibits a rapidly worsening course (6). Ectopic ACC is a condition in which ACC appears in locations other than the adrenal glands, usually in the genitourinary system [ovary (10)] and abdominal cavity [abdominal wall (6), liver (4) and retroperitoneum (11, 12)] and occasionally in the nervous system (8). However, to the best of our knowledge, ectopic ACC has not been reported in the lungs. Here, we report an extremely rare case of nonfunctional ectopic ACC in the lung, detailing the clinical and pathological findings, treatment, and follow-up.

Case report

Clinical findings

A 71-year-old man with complaints of vague left-sided chest pain and irritable cough for 1 month was admitted to our hospital in March 2021. He had no chills, fever, hemoptysis, wheezing, or abdominal pain. He was healthy with no relevant medical or family history of diseases, such as hypertension or diabetes, and no history of smoking or alcohol consumption. The laboratory findings showed that only the prograstin-releasing peptide (ProGRP) level was elevated (198.7 pg/mL), other tests showed no abnormalities. Thoracic computed tomography (CT) revealed a 5.3 × 5.8 × 6.0-cm heterogeneously enhancing globose mass in the posterior segment of the left upper lung lobe with a smooth margin without obvious lobulation or burr (Figure 1), suggestive of a benign tumor. After adequate preparation, thoracoscopic surgery of the upper lobectomy of the left lung was performed.

Postoperatively, the pathological diagnosis was suspected to be of an extrapulmonary and adrenocortical origin. Abdominal CT showed that the bilateral adrenal glands and kidneys were normal in size and shape without abnormal mass (Figure 1). ^{18}F-fluorodeoxyglucose positron emission tomography was recommended to assess the condition of the whole body for invisible lesions. However, the patient refused.

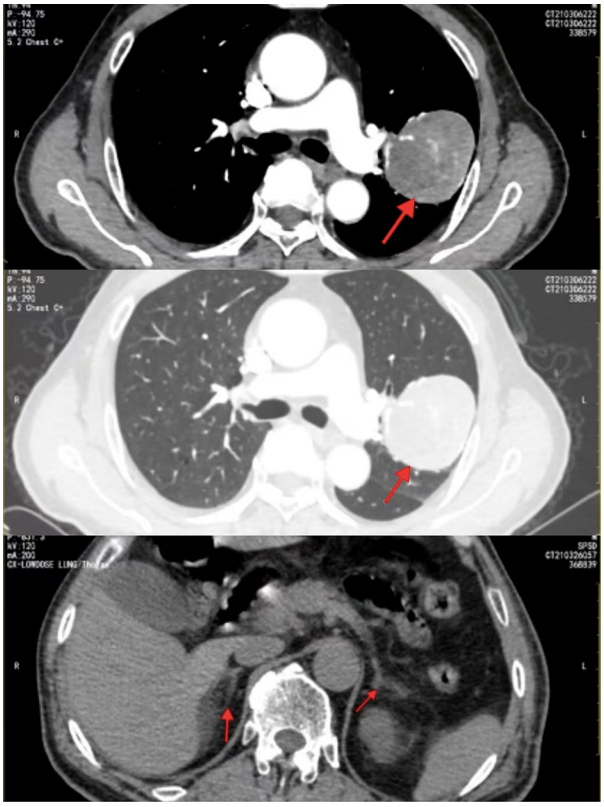

FIGURE 1
Contrast-enhanced CT revealed a heterogeneously enhancing solitary mass in the left lung;abdominal CT showed that the bilateral adrenal glands were normal in size and shape without abnormal mass.

Repeated laboratory examination revealed that the ProGRP level reduced from 198.7 to 78.5 pg/mL without any other abnormalities. We performed the Cortisol, ACTH, DHEA-S and Aldosterone tests, They're all in the normal range. As the patient had no relevant clinical symptoms of hormonal hypersecretion, estradiol or other hormone tests were not performed.

Pathological findings

Gross inspection of the lobectomy specimen revealed a mass lesion measuring 16×9×4 cm. The surface of the mass was mostly smooth, covered by the visceral pleura, and ruptured through the smooth inner capsule in an area measuring 6.7×6.5×4 cm. Capsular tissues had prolapsed at multiple sites. Sectioning revealed well-circumscribed, multilocular, tan-brown to tan-yellow cut surfaces.

Light microscopic examination of the hematoxylin and eosin-stained specimen revealed that the cytoplasm of the tumor cells was rich and eosinophilic. The tumor cells were pleomorphic and arranged in varying round blunt cell cords and cord-like structures, with transparent bodies in some cells. Interstitial blood vessels were abundant in the tumor tissue (Figure 2). The immunohistochemical results were: inhibin-α (+), melan A (+), Syn (+), CK (+), CgA (+), CD10 (+), TTF-1 (-), PAX8 (-), hepatocyte (-), and arginase-1 (-) (Figure 3). The Weiss score was 5, as the cells were pleomorphic and distributed in varying round blunt cell cords, with extensive necrosis, an irregular karyotype, and capsular invasion (13). After consultation with another pathological diagnostic center, combined with the clinical findings, morphology,

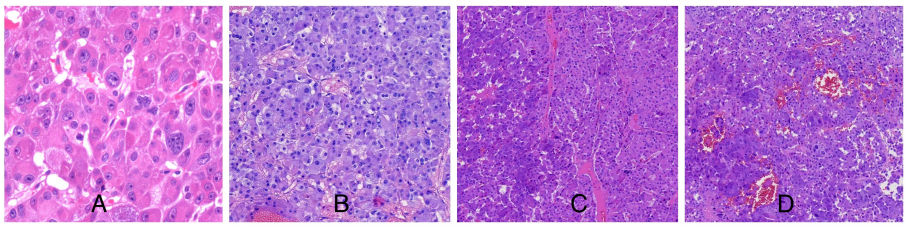

FIGURE 2
(A) The cytoplasm of the tumor cells was rich and eosinophilic and irregular karyotype; **(B)** Transparent bodies were seen in some tumor cells; **(C)** The tumor cells were pleomorphic and arranged in varying round blunt cell cords and cord-like structures; **(D)** Interstitial blood vessels were abundant in the tumor tissue.

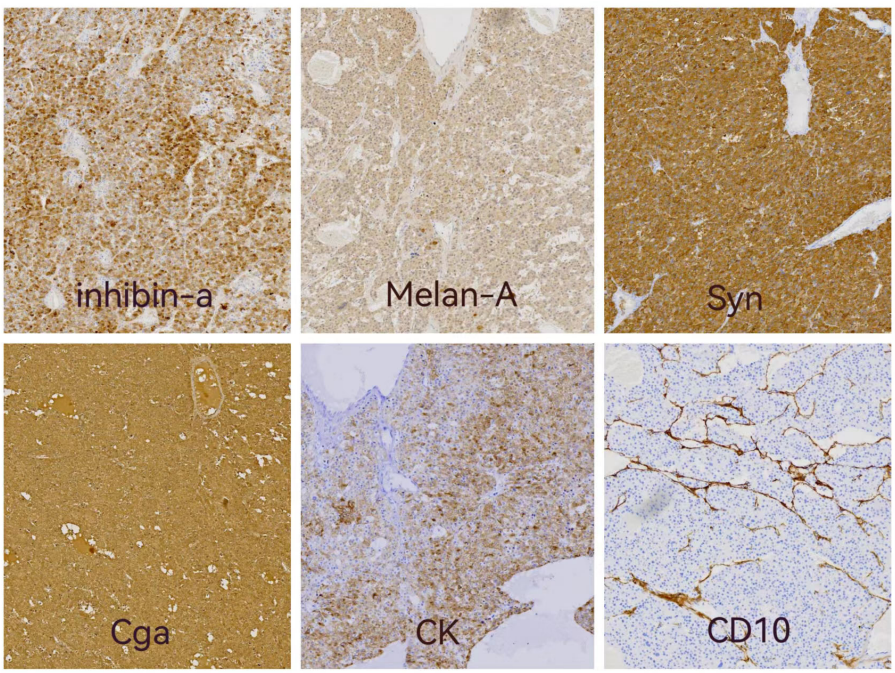

FIGURE 3
Immunohistochemistry results: immunostaining of inhibin-a, Melan A,Syn and CK showed positive in cytoplasmic. Cytoplasmic and nuclear staining were positive of Cga and CD10 showed positive in intercellular fibrous tissue.

immunohistochemistry findings, and Weiss score, primary pulmonary ectopic ACC was finally diagnosed.

Treatment and follow-up

According to the staging criteria of ectopic ACC by the American Joint Committee on Cancer and European Network for the Study of Adrenal Tumors, the final pathologic stage was pT2N0M0, i.e., stage II.

Since ectopic ACC is a rare neoplasm, no consensus has been reached for treatment recommendations (14). After multidisciplinary consultation, mitotane was selected as the first-line treatment, however, mitotane is unavailable in China. Since ProGRP is still higher than normal after surgery, we choose chemotherapy as the adjuvant treatment (15). Therefore, chemotherapy with combined etoposide and cisplatin was used as the adjuvant treatment for 4 cycles 3 weeks postoperatively. The ProGRP level continued to decline to normal after two cycles of chemotherapy, and thoracic and abdominal CT showed no obvious abnormalities after two and four cycles of chemotherapy, respectively.

The patient was followed-up every 3 months after chemotherapy for 2 years, with the latest follow-up on August 25, 2022. The patient did not complain of discomfort, and physical examination, thoracic and abdominal CT, and laboratory examination showed no obvious abnormalities. The patient had a disease-free survival (DFS) of 22 months and is still under follow-up.

Ethics statement

Ethics approval was obtained from Caoxian People's Hospital. Data was collected following patient's concent. Informed consent has been obtained from the patient for publication of the case report and accompanying images.

Discussion

ACC is a rare malignancy with an incidence of 1–2 cases/million population and often has a poor prognosis (1), with a 5-year survival rate of 38%–27% (16, 17) and a 10-year survival rate of 7% (17). Approximately 40% cases of ACC are nonfunctional (3), with nonfunctional ectopic ACC being even rarer. Ectopic ACC is usually found in the genitourinary system and abdominal cavity (5, 6, 8–10, 12, 18–20) and occasionally found in the nervous system (8). However, to the best of our knowledge, ectopic ACC has not been reported in the lungs.

Here, we reported a rare case of nonfunctional ectopic ACC in the lung of a 71-year old man who presented with nonspecific complaints of vague left-sided chest pain and irritable cough caused by an overgrowth tumor. In the pathologic examination, both macroscopic and light microscopic findings were inconsistent with common lung tumors. Immunohistochemical results were: inhibin-a (+), melan-A (+), Syn (+), CK (+), CgA (+), TTF-1 (-), PAX8 (-), hepatocyte (-), and arginase-1 (-). Immunohistochemical profiles (inhibin-a$^+$, Melan-A$^+$, Syn$^+$) indicated that the tumor had an adrenocortical but extrapulmonary origin. The Weiss score was 5, as the cells were pleomorphic and distributed in various round blunt cell cords, with extensive necrosis, and irregular karyotype, and capsular invasion (13).

Differential diagnosis of ACC and sex cord-stromal tumor, compared with ACC, first, the morphologic of sex cord-stromal tumor cells was not arranged in varying round blunt cell cords and cord-like structures, but were large, multi-shaped and densely clumped, and the cytoplasm was acidophilic or lipoid vacuolar with hematoxylin and eosin staining. Second, although the immunophenotype of sex cord-stromal tumor are also positive for inhibin and melan A, the other markers are negative for Syn, CK, CgA. The diagnosis sex cord-stromal tumor is excluded (21, 22).

Abdominal CT showed no adrenal mass in either adrenal gland, ruling out an adrenal origin. Combined with the clinical findings, tumor cell morphology, immunohistochemical results, and Weiss score, the final pathologic diagnosis was primary nonfunctional ectopic ACC of the lung. Adjuvant chemotherapy was provided for four cycles, and the patient had a DFS of 23 months.

Ectopic ACC in the lungs has not been previously reported. Representative ectopic adrenal tissues and neoplasms are located in anatomical organs, such as the urethral tract (23), kidney (9), ovary (10), abdominal wall (6), liver (20), retroperitoneum (11, 12), gastric wall (19), spinal canal (8), thorax (24), and lung (25). Although ectopic adrenocortical tissues and neoplasms may also be present at any anatomical location, they rarely originate in the lungs. PubMed search yielded only three reports of ectopic adrenal tissues located in the lung. First, Wadhwani et al. reported a case of ectopic adrenal tissue in the paratracheal region incidentally found during the autopsy of a 99-year-old woman. The tissue was composed of both cortical and medullary cells (24). Second, Armin et al. reported a case of congenital cytomegalic adrenal tissues in the lung of a 5-day-old infant found on autopsy (25). Third, Bozic et al. reported a case of ectopic adrenal cortex and cytomegaly in the lung found on the autopsy of a newborn (26). Table 1 summarizes the main features and follow-up results of representative reported cases.

In ectopic remnants of adrenal tissues, cortical tissues are usually seen alone, and medullary tissues are seen rarely. They are usually found incidentally during surgeries or autopsies (23, 24). Ectopic adrenal tissues may develop hyperplasia, adenoma, or carcinoma. These tumors are usually benign and nonfunctional (8, 9, 19, 20) and occasionally malignant and functional (6, 10, 12). They can produce glucocorticoids, androgens, or other sex hormones and cause clinical symptoms, such as Cushing's syndrome, or clinical signs of virilization (4, 27).

The etiology of ectopic adrenal tissues and neoplasms in the lungs and other organs is unclear. Nevertheless, two hypotheses have been proposed. Bozic et al. suggested that mesothelial cells are located in the primordial mesenchyme of the wall of the dorsal coelom adjacent to the dorsal mesentery and primitive genitourinary structure, where they differentiate into elements that form the fetal adrenal tissue. Because the peritoneum and pleura have the same mesodermal origin as the adrenal gland, the primitive pleural mesothelium, which lies between the ramifications of the bronchial tree buds, can differentiate into ectopic adrenal tissue of the lung (26). Another possibility is that true adrenal heterotopia arises as a failure to separate the developing

TABLE 1 Ectopic adrenocortical tissues, adenomas and carcinomas of representative reported cases.

Case No	Authors	Age/ Gender	Diameter	Location	Functional or nonfunctional	Radiological aspect	Findings of autopsy or Surgery	Pathological diagnosis	Treatment	Follow up
1	Current case	71Y/M	6.7cm	lung	nonfunctional	5.3×5.8×6.0cm	tan-brown to tan-yellow MASS NA	ectopic ACC	tumor resection	DF 22 months
2	Shigematsu et al (23)	99Y/ F	0.5 cm	paratracheal region	functional	ND	gray-brown nodule about 5 mm NA	ectopic adrenal tissues compatible with adrenal cortex and medulla.	ND	ND
3	Armin et al (24)	5D/M	ND (two nodules)	lung	functional	ND	nodule ND	ectopic cytomegalic adrenal tissues	ND	ND
4	Bozic et al (25)	2D/F	ND (one nodules)	lung	ND	ND	ND	ectopic adrenal cortex with cytomegaly	ND	ND
5	Anuk et al (20)	1-16Y/M (Total 15) +30Y/M+70Y/ F	mean 0.25 cm (range 0.2 cm -0.5 cm).	hernia sac, spermatic cord, testis, uterus	nonfunctional	ND	Yellow orange color tissues NA	ectopic adrenal cortical tissues	tumor resection	ND
6	Liu et al (8)	27Y/F	2.7 cm	renal hilum	nonfunctional	CT: a well-circumscribed, round, soft-tissue mass	ND, NA	ectopic adrenocortical adenoma	tumor resection	DF for 3 months
7	Chentli et al (7)	34Y/F	14 cm	right ovary	functional	CT: 14 cm right ovarian mass	a brown lobulated mass measuring 14.5×13.7cm	ectopic ACC	tumor resection	died on the second post-surgical day
8	Chen et al (9)	44Y/M	6cm	liver	nonfunctional	CT:7.8cm enhanced mass	Solid and yellowish-grey mass with clear margin NA	Ectopic adrenocortical oncocytic adenoma	tumor resection	ND
9	Ren et al (12)	72Y/F	3cm	gastric wall	nonfunctional	CT:15 mm × 25 mm abnormal enhanced nodule	30 mm × 30 mm mass with medium density NA	ectopic adrenal cortical adenoma	tumor resection	ND
10	Zhou et al (6)	77Y/M	30 cm	in front of the posterior peritoneum	nonfunctional	CT:30 cm × 15 cm × 8 cm tumor	a 30 cm × 15 cm × 8 cm tumor NA	ectopic ACC	tumor resection	DF for 9 months
11	Wright et al (11)	68Y/M	3.5 cm	retroperitoneal	nonfunctional	CT: a 8.3×6.0×1.6 cm mass	a tan, round, mass with nodular heterogenous borders NA	ectopic ACC	tumor resection、adjuvant radiation (5000 cGy) and adjuvant mitotane therapy	DF for 24 months
12	Konstantinov et al (13)	55Y/F	25 mm	spinal canal	nonfunctional	MRI: epidural formation18×25 mm nodule	a small knot at the base of the ponytail. NA	ectopic adrenocortical adenoma	resection	ND

Y, year; D, day; M, male; F, female; ACC, adrenocortical carcinoma; ND, not described; DF, disease-free; NA, normal adrenal.

10.3389/fonc.2023.1100207

adrenal gland from the coelomic mesothelium, thus allowing partial incorporation into the adjacent organs (28).

Ectopic adrenal tissues may develop hyperplasia, adenoma, or carcinoma, similar to normal tissues. Therefore, we speculate that ectopic ACC in the lung of this present patient was caused by dislocation or self-differentiation of mesenchymal cells in the embryonic period, which then developed into carcinoma.

In conclusion, nonfunctional ectopic ACC in the lung is an extremely rare neoplasm that can be easily misdiagnosed as primary lung cancer or lung metastasis, both preoperatively and on postoperative pathological examination. This report may provide clues to clinicians and pathologists.

Data availability statement

The original contributions presented in the study are included in the article/supplementary material. Further inquiries can be directed to the corresponding author.

Ethics statement

The studies involving human participants were reviewed and approved by Caoxian People's Hospital. The patients/participants provided their written informed consent to participate in this study.Written informed consent was obtained from the individual (s) for the publication of any potentially identifiable images or data included in this article.

Author contributions

LN collected information, wrote the manuscript and literature review; Z-FF and ZW provided figures and pathology review. AG, SW, QD, YL and YS supervised the project and reviewed the manuscript.

Funding

This work was supported by grants from the National Natural Science Foundation of China (82103340 and 81902919) and the Shandong Province Medicine and Health Science and Technology Development Plan Project (No:202009031334).

Conflict of interest

The authors declare that the research was conducted in the absence of any commercial or financial relationships that could be construed as a potential conflict of interest.

Publisher's note

References

1. Else T, Kim AC, Sabolch A, Raymond VM, Kandathil A, Caoili EM. Adrenocortical carcinoma. *Endocr Rev* (2014) 35:282–26. doi: 10.1210/er.2013-1029

2. Wajchenberg BL, Albergaria Pereira MA, Medonca BB, Latronico AC, Campos Carneiro P, Alves VA. Adrenocortical carcinoma: Clinical and laboratory observations. *Cancer* (2000) 88:711–36. doi: 10.1002/(SICI)1097-0142(20000215)88:4<711::AID-CNCR1>3.0.CO;2-W

3. Erickson LA, Rivera M, Zhang J. Adrenocortical carcinoma: Review and update. *Adv Anat Pathol* (2014) 210:151–9. doi: 10.1097/PAP.0000000000000019

4. Permana H, Darmawan G, Ritonga E, Kusumawati M, Miftahurachman M, Soetedjo NN. An interesting case of hepatic adrenocortical carcinoma. *Acta Med Indones* (2018) 50:257–9.

5. George C, Ioannis P, Dimitra-Rafailia B, Dimitrios G, Panagiotis S. Giant nonfunctioning adrenal tumors: Two case reports and review of the literature. *J Med Case Rep* (2018) 12:335. doi: 10.1186/s13256-018-1876-8

6. Zhou DK, Liu ZH, Gao BQ, Wang WL. Giant nonfunctional ectopic adrenocortical carcinoma on the anterior abdominal wall: A case report. *World J Clin cases* (2019) 7:2075–80. doi: 10.12998/wjcc.v7.i15.2075

7. Athani VS, Mulholland SG. Primary nonfunctioning adrenal tumors in adults. *Urology* (1981) 18:131–3. doi: 10.1016/0090-4295(81)90421-0

8. Konstantinov AS, Shelekhova KV. Ectopic adrenal cortical adenoma in the spinal canal: A case report and a review of the literature. *Arkh Patol* (2016) 78:44–8. doi: 10.17116/patol201678344-48

9. Liu Y, Jiang YF, Wang YL, Cao HY, Wang L, Xu HT. Ectopic adrenocortical adenoma in the renal hilum: A case report and literature review. *Diagn Pathol* (2016) 11:40. doi: 10.1186/s13000-016-0490-6

10. Chentli F, Terki N, Azzoug S. Ectopic adrenocortical carcinoma located in the ovary. *Eur J Endocrinol* (2016), 175(4):K17–23. doi: 10.1530/EJE-16-0224

11. Saygin I, Cakir E, Ercin ME, Eyuboglu I. Incidental retroperitoneal oncocytoma (Ectopic oncocytic adrenocortical adenoma): Case report and review of the literature. *Indian J Pathol Microbiol* (2019) 62:132–5. doi: 10.4103/IJPM.IJPM_58_18

12. Wright JP, Montgomery KW, Tierney J, Gilbert J, Solorzano CC, Idrees K. Ectopic retroperitoneal adrenocortical carcinoma in the setting of lynch syndrome. *Fam Cancer* (2018) 17:381–5. doi: 10.1007/s10689-017-0042-6

13. Aubert S, Wacrenier A, Leroy X, Devos P, Carnaille B, Proye C. Weiss System revisited: A clinicopathologic and immunohistochemical study of 49 adrenocortical tumors. *Am J Surg Pathol* (2002) 26:1612–9. doi: 10.1097/00000478-200212000-00009

14. Vaidya A, Nehs M, Kilbridge K. Treatment of adrenocortical carcinoma. *Surg Pathol Clin* (2019) 12:997–1006. doi: 10.1016/j.path.2019.08.010

15. Cremaschi V, Abate A, Cosentini D, Grisanti S, Rossini E, Laganà M. Advances in adrenocortical carcinoma pharmacotherapy: What is the current state of the art? *Expert Opin Pharmacother* (2022) 23(12):1413–24. doi: 10.1080/14656566.2022.2106128

16. Icard P, Goudet P, Charpenay C, Andreassian B, Carnaille B, Chapuis Y. Adrenocortical carcinomas: Surgical trends and results of a 253-patient series from the French association of endocrine surgeons study group. *World J Surg* (2001) 25:891–7. doi: 10.1007/s00268-001-0047-y

17. Tran TB, Postlewait LM, Maithel SK, Prescott JD, Wang TS, Glenn J. Actual 10-year survivors following resection of adrenocortical carcinoma. *J Surg Oncol* (2016) 114:971–6. doi: 10.1002/jso.24439

18. Wadhwani N, Mais D, Kaushik D, Kitano M. A case of adrenocortical oncocytic carcinoma arising in ectopic adrenal tissue: A multidisciplinary diagnostic challenge. *Ecancer Med Sci* (2020) 14:1135. doi: 10.3332/ecancer.2020.1135

19. Ren PT, Fu H, He XW. Ectopic adrenal cortical adenoma in the gastric wall: Case report. *World J Gastroenterol* (2013) 19:778–80. doi: 10.3748/wjg.v19.i5.778

20. Chen J, Wan X, Lu Y, Wang W, Zhao D, Lu Z. An ectopic adrenocortical oncocytic adenoma in the liver highly mimicking hepatocellular carcinoma: Case report and literature review. *Diagn Pathol* (2021) 16:58. doi: 10.1186/s13000-021-01097-0

21. Morinaga S, Aoki S, Tsuzuki T, Kanematsu K, Kawai N, Sato S, et al. Malignant testicular unclassified sex cord stromal tumor: A case report. *J Med Case Rep* (2022) 16 (1):406. doi: 10.1186/s13256-022-03640-z

22. Ye H, Ulbright TM. Difficult differential diagnoses in testicular pathology. *Arch Pathol Lab Med* (2012) 136(4):435–46. doi: 10.5858/arpa.2011-0475-RA

23. Uğur Kılınç AN, Bayramoğlu Z, Ünlü Y, Keçeli AM, Dönmez M İ. Incidental ectopic adrenal cortical tissue: Retrospective analysis of 16 patients. *J Pediatr Urol* (2021) 17:258.e1-e6. doi: 10.1016/j.jpurol.2020.12.027

24. Shigematsu K, Toriyama K, Kawai K, Takahara O. Ectopic adrenal tissue in the thorax: A case report with*in situ* hybridization and immunohistochemical studies. *Pathol Res Pract* (2007) 203:543–8. doi: 10.1016/j.prp.2007.03.006

25. Armin A, Castelli M. Congenital adrenal tissue in the lung with adrenal cytomegaly. case report and review of the literature. *Am J Clin Pathol* (1984) 82:225–8. doi: 10.1093/ajcp/82.2.225

26. Bozic C. Ectopic fetal adrenal cortex in the lung of a newborn. *Virchows Arch A Pathol Anat Histol* (1974) 363:371–4. doi: 10.1007/BF00447848

27. Tritos NA, Cushing GW, Heatley G, Libertino JA. Clinical features and prognostic factors associated with adrenocortical carcinoma: Lahey clinic medical center experience. *Am Surg* (2000) 66:73–9. doi: 10.1177/000313480006600115

28. Anderson JR, Ross AH. Ectopic adrenal tissue in adults. *Postgrad Med J* (1980) 56:806–8. doi: 10.1136/pgmj.56.661.806

frontiers | Frontiers in Oncology

TYPE Case Report
PUBLISHED 24 February 2023
DOI 10.3389/fonc.2023.1096160

OPEN ACCESS

EDITED BY
Kohei Fujita,
National Hospital Organization Kyoto Medical Center, Japan

REVIEWED BY
Wala Ben Kridis,
Habib Bourguiba University Hospital, Tunisia
Stephane Ducassou,
Centre Hospitalier Universitaire de Bordeaux, France

*CORRESPONDENCE
Konstantin Shilo
konstantin.shilo@osumc.edu

SPECIALTY SECTION
This article was submitted to Thoracic Oncology, a section of the journal Frontiers in Oncology

RECEIVED 11 November 2022
ACCEPTED 13 February 2023
PUBLISHED 24 February 2023

CITATION
Shilo K, Kneuertz PJ, Liebner D and Chen W (2023) Case report: Pulmonary synovial sarcoma in a long-term survivor of childhood Hodgkin lymphoma.
Front. Oncol. 13:1096160.
doi: 10.3389/fonc.2023.1096160

Case report: Pulmonary synovial sarcoma in a long-term survivor of childhood Hodgkin lymphoma

Konstantin Shilo[1]*, Peter J. Kneuertz[2], David Liebner[3] and Wei Chen[1]

[1]Department of Pathology, The Ohio State University Wexner Medical Center, Columbus, OH, United States, [2]Division of Thoracic Surgery, The Ohio State University Wexner Medical Center, Columbus, OH, United States, [3]Division of Medical Oncology, The Ohio State University Wexner Medical Center, Columbus, OH, United States

Solid organ malignancies have been reported in survivors of Hodgkin lymphoma treated with chemoradiation; however, to the best of our knowledge no cases of pulmonary synovial sarcoma have been documented in the literature in this cohort. We herein provide a detailed description of synovial sarcoma occurring in the lung of a long-term survivor of childhood Hodgkin lymphoma. A 29-year-old female never smoker with past medical history of Hodgkin lymphoma diagnosed at the age of 7 years and treated with chemotherapy and radiation therapy was admitted for management of pneumothorax. Wedge lung resection of an ulcerated subpleural nodule revealed a malignant spindle cell tumor that based on light microscopic and immunohistochemical features was classified as monophasic synovial sarcoma. The diagnosis was further confirmed by identification of SS18 (SYT) rearrangement by fluorescence *in situ* hybridization and SS18-SSX1 gene fusion by RNA sequencing. The case documents a rare occurrence of synovial sarcoma in a long-term survivor of childhood Hodgkin lymphoma. While comprising a typical genetic profile for synovial sarcoma, the tumor had unusual histological features such as cystic and low-grade morphology. The case suggests that synovial sarcoma falls within an expanding spectrum of secondary malignancies following prior treatment of Hodgkin lymphoma.

KEYWORDS

synovial sarcoma, SS18 (SYT) rearrangement, SS18-SSX1 fusion, second malignancy, childhood Hodgkin lymphoma, survivor

Abbreviations: SS, synovial sarcoma; HL, Hodgkin lymphoma; LAM, lymphangioleiomyomatosis; IFRT, involved field radiation therapy; CT, computed tomography; PET/CT, positron emission tomography/computed tomography; NGS, next generation sequencing; PTX, pneumothorax; VATS, video-assisted thoracoscopic surgery; MRI, magnetic resonance imaging.

Introduction

As more childhood Hodgkin lymphoma (HL) patients achieve disease free adulthood, they face increased risk of second malignancies associated with side effects of radiation and chemotherapy (1–3). Secondary solid organ malignancies have been reported in this cohort; however, to the best of our knowledge no cases of pleuropulmonary synovial sarcoma (SS) have been documented in the literature.

SS is a rare soft tissue sarcoma that also affects visceral organs including lung (4). It is associated with a specific chromosomal translocation, which most commonly fuses SS18 (SYT) in chromosome 18 and SSX1 or SSX2 in chromosome X (5). The tumor tends to occur in young adults and shows no sex predilection. The presenting symptoms are nonspecific mostly related to the site of origin. Rare occasions of SS presenting with pneumothorax have been reported (6–9).

We herein provide a detailed description of pulmonary SS in a long-term survivor of childhood Hodgkin lymphoma and highlight some unusual clinicopathological features.

Case presentation

A 29-year-old female never smoker was admitted for inpatient management of a left sided pneumothorax (PTX) that was discovered on a screening breast magnetic resonance imaging (MRI). The patient's past medical history was significant for HL diagnosed at the age of 7 years. She was treated with DBVE chemotherapy which included Doxorubicin (D), Bleomycin (B), Vincristine (V) and Etoposide (E), and involved field radiation therapy (IFRT) to cervical spine, supraclavicular area, and middle and lower mediastinum (2,550 cGy administered in 17 fractions of 150 cGy each) according to a pediatric oncology group study (POG-9426) (10). Her past medical history was also notable for hypothyroidism, migraine, and polycystic ovarian syndrome. Breast MRI showed no evidence of malignancy but was significant for a mediastinal shift with the heart shifted to the right (Figure 1A). Chest X-ray (CXR) confirmed left PTX with slight cardiac and mediastinal shift rightward suggesting underlying tension component (Figure 1B). As a chest tube placement did not produce complete resolution of the PTX (Figure 1C) and she endorsed a persistent air leak, a video assisted thoracoscopic surgery (VATS) was performed for pleurodesis. The intraoperative findings included severe pleural adhesions and a dense lung parenchyma. A focal umbilication and surface disruption of the visceral pleural surface of left upper lobe was detected, which was thought to be site of the air leak. On further palpation a subpleural ulcerated nodule was discovered. A VATS lung wedge resection of the nodule was performed with clear margins. There was no evidence of pleural seeding at thoracoscopy. Gross examination showed a 1.3 x 0.8 x 0.4 cm cystic nodular lesion abutting visceral pleura. On light microscopic examination, the lesion was represented by small cysts associated with spindle cell proliferation of variable cellularity (Figure 2A). The cystic spaces were partially lined by entrapped nonneoplastic pneumocytes and partially lined by respiratory epithelium. The spindle cells were arranged in fascicles (Figure 2B). There was variable amount of collagen, areas of fibrous scarring and microscopic calcifications. There were rare apoptotic bodies and rare mitotic figures (1 per 10 high power fields). The tumor cells were immunoreactive with CD56, BCL2 and SS18-SSX (clone E9X9V, Cell Signaling Technology, Danvers, MA) (Figures 2C, D). Rare tumor cells were weakly positive for Keratin AE1/AE3, Synaptophysin and Estrogen Receptor (ER). Immunostains for Calretinin, WT1, CD68, PLAP, Inhibin, Smooth Muscle Actin, Desmin, Myogenin, CD34, STAT6, SOX10, HMB45, CD117a, Progesterone Receptor (PR), CD10, PAX8, CK7, CK20, CDX2, p40 and TTF1 were negative. Ki67 proliferation rate was approximately 1-3%. The tumor showed SS18 rearrangement by fluorescence *in situ* hybridization (FISH). Gene rearrangement analysis from RNA sequencing (Tempus xT, targeted panel of 648 genes) reveled SS18-SSX1 gene fusion, with tumor mutation burden of 0 m/Mb, and stable microsatellite instability status. Based on the morphological and immunohistochemical and genetic findings, the tumor was classified as monophasic SS. As per a multidisciplinary conference review, no adjuvant therapy was recommended at the time. Two months following initial diagnosis, restaging computed tomography (CT) and fused positron emission tomography/computed tomography (PET/CT) showed no residual disease in the chest and no distant metastatic disease. No evidence of recurrence

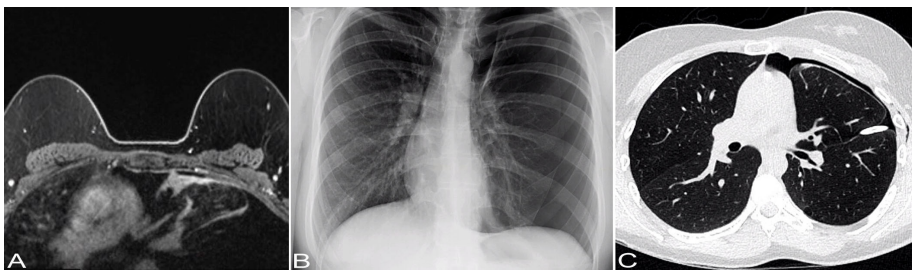

FIGURE 1
Imaging findings. **(A)** Axial non-contrast T1-weighted breast MRI image shows no evidence of malignancy. There is a mediastinal shift with the heart shifted to the right and a lack of lung markings in the upper left lung, suggesting the possibility of bulla in the upper left lung. **(B)** Chest X-ray shows a left-sided pneumothorax with cardiac and mediastinal shift rightward suggesting underlying tension component. **(C)** Chest CT shows a small left anterior pneumothorax. There is a left-sided pleural drainage catheter with its tip along the left major fissure. There are subtle patchy consolidative opacities in the subpleural aspects of the left upper lobe.

10.3389/fonc.2023.1096160

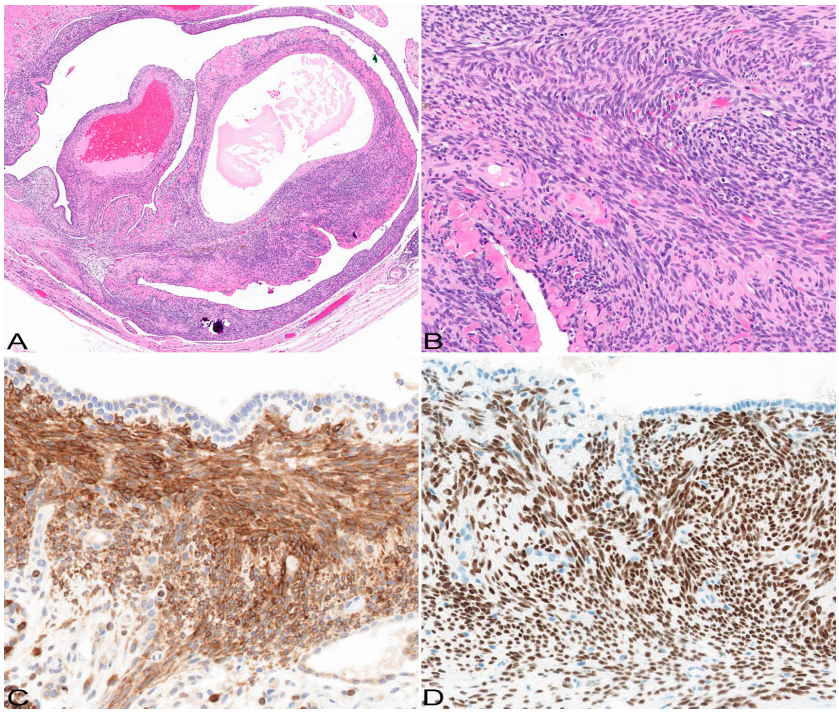

FIGURE 2
Pathological features. The tumor is represented by cystic and solid components **(A)**; HE original magnification x5. The solid component is composed of spindle cells forming fascicles **(B)**; there is variable background collagen deposition; HE original magnification x20. The tumor cells are immunoreactive with bcl2 **(C)** and SS18-SSX **(D)** antibodies; immunohistochemistry, original magnification x20 and x20.

was documented at 5-month follow-up chest CT. The patient was well without evidence of disease at 1 year following the initial diagnosis. A strategy of close radiographic surveillance with serial chest CT (or PET/CT for equivocal findings) for at least 10 years was recommended.

Discussion

HL survivors demonstrate increased risk for developing radiation-related breast cancer, lung cancer and colorectal cancer and their risk appears to be associated with the site of radiation (3). Radiation associated sarcomas with nonrecurrent complex genetic alterations following HL treatment are well documented in the literature (11, 12). They characteristically develop after a latency period of one to two decades within radiotherapy fields and majority represent malignant fibrous histiocytoma and osteosarcoma (11, 12). Sarcomas carrying specific translocations such as Ewing sarcoma are relatively rare (13–16). To the best of our knowledge only a single case report of an infraclavicular SS arising at the site of prior radiation for HL has been documented in the literature (17). In contrast to our patient, a patient reported by Van De Rijn at al developed SS in infraclavicular soft tissue, showed locally aggressive behavior with involvement of brachial plexus and based on the microscopic description had no cystic morphology.

Our patient was treated with IFRT and DBVE chemotherapy for HL according to the POG-9426 protocol and developed SS after 22 years. While it is not yet entirely certain if the risk of the development of second malignancy is associated with therapy or with genetic background of patients or both, the occurrence of SS at the site of prior radiation following latency period of about 2 decades is consistent with a notion of a possible causative association between prior chemoradiation and the development of second malignancy in our case. The lung is not intended target during mantle radiotherapy for HL and radiation dose across the lung can vary several folds (18). Nevertheless, the medial aspects of the lung including visceral and parietal pleura overlap with the mediastinal component of the radiation fields and therefore, the visceral pleura of the left upper lobe, the site of the tumor in our patient, is at the increased risk of radiation induced malignancy. Some sarcomas, such as rhabdomyosarcoma, malignant peripheral nerve sheath tumor and liposarcoma, are known to be associated with germline alterations, while others, such as Ewing sarcoma, show no known hereditary associations (19). Possibly due to its rarity, the evidences for hereditary predisposition for SS are currently lacking.

The majority of SS are highly proliferative tumor that fall within FNCLCC grade 2 and 3, however, a low percentage (up to 10%) of SS show low mitotic rate (less than 10 per 10 high power fields), as the tumor in this case (20–22). While the overall histological and genetic features of the tumor in this report fall within the spectrum of that typically seen in SS, it also showed some unusual findings including the small size (1.3 cm), cystic morphology, and low mitotic/proliferation rate. The cystic morphology of the tumor was likely responsible for the clinical presentation as PTX.

Cystic primary pulmonary SS as a small subset have been recognized to present with PTX and manifest pathologically as cystic or bullous lesions with only subtle evidence of a malignant proliferation (6, 8). The original publication reported 4 patients (ages 20 to 29) all with a monophasic variant of SS and emphasized that since these tumors manifest primarily as cystic lesions presenting as PTX, they can be confused with benign cystic lung disease and therefore in the settings of PTX a thorough examination of all resected tissue with increased cellularity should be carried out (6). As of date, 7 cases of pleuropulmonary SS with cystic morphology have been reported (6–9). As in our case, all 7 of 7 cases were monophasic SS, 3 of 7 cases were small less than 1.5 cm lesions, 2 of 7 had microscopic calcifications and 3 of 3 tested cases demonstrated the gene fusion product SS18-SSX1, similar to that in our case. None of these 7 cases specifically reported history of prior malignancy including HL.

Since the presence of specific chromosomal translocation is a requirement for the diagnosis of SS, it is the most decisive feature to help to exclude other lesions. However, at the initial work-up or if molecular testing is not available, lymphangioleiomyomatosis (LAM) and pulmonary involvement by endometriosis have to be excluded, especially in young adult female patients. PTX at presentation and the presence of spindle cell proliferation associated with parenchymal cysts are the findings that are shared between SS and LAM (23–25). However, LAM represents a diffuse cystic lung disease associated with proliferation of so called perivascular epithelioid cells that characteristically show aberrant expression of melanocytic markers (e.g. HMB45, Melan A) and therefore their use will help to exclude the diagnosis of LAM at immunohistochemical level. While uncommon, the pulmonary endometriomas can be seen in the setting of endometriosis and present with catamenial PTX. The overlapping features between endometriosis and SS include the presence of spindle cell stroma showing CD56 expression (26). However, in endometriosis expression of other markers of Müllerian origin such as ER, PR and PAX8 will help to distinguish it from SS.

Conclusion

This report documents a rare case of SS arising in a long-term survivor of childhood HL and suggests its possible association with prior therapy. The tumor's cystic morphology is likely responsible for unusual clinical presentation as PTX.

Data availability statement

The original contributions presented in the study are included in the article/supplementary material. Further inquiries can be directed to the corresponding author.

Ethics statement

Written informed consent was obtained from the individual for the publication of any potentially identifiable images or data included in this article.

Author contributions

PK and DL participated in data collection. WC and KS participated in the conception of the study. KS wrote the manuscript text. PK, DL, WC, and KS edited the manuscript. All authors contributed to the article and approved the submitted version.

Acknowledgments

The authors are thankful to Shawn Scally for excellent assistance in figures preparation.

Conflict of interest

The authors declare that the research was conducted in the absence of any commercial or financial relationships that could be construed as a potential conflict of interest.

Publisher's note

References

1. Travis LB. Therapy-associated solid tumors. *Acta Oncol* (2002) 41:323–33. doi: 10.1080/028418602760169361

2. Friedman DL, Whitton J, Leisenring W, Mertens AC, Hammond S, Stovall M, et al. Subsequent neoplasms in 5-year survivors of childhood cancer: The childhood cancer survivor study. *J Natl Cancer Inst* (2010) 102:1083–95. doi: 10.1093/jnci/djq238

3. Holmqvist AS, Chen Y, Berano Teh J, Sun C, Birch JM, van den Bos C, et al. Risk of solid subsequent malignant neoplasms after childhood Hodgkin lymphoma–identification of high-risk populations to guide surveillance: A report from the late effects study group. *Cancer* (2019) 125:1373–83. doi: 10.1002/cncr.31807

4. Travis WD, Brambilla E, Nicholson AG, Yatabe Y, Austin JHM, Beasley MB, et al. The 2015 world health organization classification of lung tumors: Impact of genetic, clinical and radiologic advances since the 2004 classification. *J Thorac Oncol* (2015) 10:1243–60. doi: 10.1097/JTO.0000000000000630

5. Fletcher CDM, Bridge JA, Hogendoorn PCW, Mertens F. The WHO Classification of Tumours Editorial Board. *WHO classification of tumours of soft tissue and bone Tumours*, 5th ed. Lyon: IARC Press; 2020.

6. Cummings NM, Desai S, Thway K, Stewart S, Hill DA, Priest JR, et al. Cystic primary pulmonary synovial sarcoma presenting as recurrent pneumothorax: Report of 4 cases. *Am J Surg Pathol* (2010) 34:1176–9. doi: 10.1097/PAS.0b013e3181e85c87

7. Guo C, Liu C, Pu Q, Lin F, Liu L. Occult primary pulmonary synovial sarcoma presenting as recurrent spontaneous pneumothorax and explosive progression. *Thorac Cancer* (2017) 8:121–3. doi: 10.1111/1759-7714.12410

8. Johnson ED, Downs-Kelly E, Bull DA, Gulbahce HE. Primary cystic pleuropulmonary synovial sarcoma presenting as recurrent pneumothorax. *CRO* (2017) 10:660–5. doi: 10.1159/000478845

9. Patel PB, Sankrith M, Cedeno-Rodriguez A. Pediatric pleuropulmonary synovial sarcoma: A case report in a recurrent spontaneous pneumothorax. *Respir Med Case Rep* (2022) 36:101622. doi: 10.1016/j.rmcr.2022.101622

10. Tebbi CK, Mendenhall NP, London WB, Williams JL, Hutchison RE, FitzGerald TJ, et al. Response-dependent and reduced treatment in lower risk Hodgkin lymphoma in children and adolescents, results of P9426: A report from the children's oncology group. *Pediatr Blood Cancer* (2012) 59:1259–65. doi: 10.1002/pbc.24279

11. Wolden SL, Lamborn KR, Cleary SF, Tate DJ, Donaldson SS. Second cancers following pediatric hodgkin's disease. *JCO* (1998) 16:536–44. doi: 10.1200/JCO.1998.16.2.536

12. Giulino-Roth L, Pei Q, Buxton A, Bush R, Wu Y, Wolden SL, et al. Subsequent malignant neoplasms among children with Hodgkin lymphoma: a report from the children's oncology group. *Blood* (2021) 137:1449–56. doi: 10.1182/blood.2020007225

13. Anselmo AP, Cartoni C, Pacchiarotti A, Pescarmona E, Cafolla A, Rendina E, et al. Peripheral neuroectodermal tumor of the chest (Askin tumor) as secondary neoplasm after hodgkin's disease: a case report. *Ann Hematol* (1994) 68:311–3. doi: 10.1007/BF01695039

14. Chaavez RD, Calvo PS, Green-Schneewiss L, Goamez ER, Martianez LQ. Peripheral neuroectodermal tumor of the chest wall in a patient treated for hodgkin's disease. *Leukemia Lymphoma* (1995) 17:509–13. doi: 10.3109/10428199509056865

15. Khadwal A, Biswas G, Arora B, Kurkure PA, Deshmukh C, Shetty V. Primitive neuroectodermal tumor (PNET) as second malignancy after treatment of hodgkin's disease. *Indian J Pediatr* (2006) 73:437–8. doi: 10.1007/BF02758571

16. Wolpert F, Grotzer MA, Niggli F, Zimmermann D, Rushing E, Bode-Lesniewska B. Ewing's sarcoma as a second malignancy in long-term survivors of childhood hematologic malignancies. *Sarcoma* (2016) 2016:5043640. doi: 10.1155/2016/5043640

17. Van De Rijn M, Barr FG, Xiong Q, Salhany KE, Fraker DL, Fisher C. Radiation-associated synovial sarcoma. *Hum Pathol* (1997) 28:1325–8. doi: 10.1016/S0046-8177(97)90213-6

18. van Leeuwen FE, Klokman WJ, Stovall M, Hagenbeek A, van den Belt-Dusebout AW, Noyon R, et al. Roles of radiotherapy and smoking in lung cancer following hodgkin's disease. *JNCI J Natl Cancer Institute* (1995) 87:1530–7. doi: 10.1093/jnci/87.20.1530

19. Vagher J, Dietz MS, Schiffman JD, Kohlmann W, Maese L. Germline predisposition to soft tissue sarcoma. *J Cancer Metastasis Treat* (2022) 8:31. doi: 10.20517/2394-4722.2022.31

20. Bégueret H, Galateau-Salle F, Guillou L, Chetaille B, Brambilla E, Vignaud J-M, et al. Primary intrathoracic synovial sarcoma: A clinicopathologic study of 40 t(X;18)-positive cases from the French sarcoma group and the mesopath group. *Am J Surg Pathol* (2005) 29:339–46. doi: 10.1097/01.pas.0000147401.95391.9a

21. Hartel PH, Fanburg-Smith JC, Frazier AA, Galvin JR, Lichy JH, Shilo K, et al. Primary pulmonary and mediastinal synovial sarcoma: a clinicopathologic study of 60 cases and comparison with five prior series. *Mod Pathol* (2007) 20:760–9. doi: 10.1038/modpathol.3800795

22. Lan T, Chen H, Xiong B, Zhou T, Peng R, Chen M, et al. Primary pleuropulmonary and mediastinal synovial sarcoma: a clinicopathologic and molecular study of 26 genetically confirmed cases in the largest institution of southwest China. *Diagn Pathol* (2016) 11:62. doi: 10.1186/s13000-016-0513-3

23. McCormack FX. Lymphangioleiomyomatosis: a clinical update. *Chest* (2008) 133:507–16. doi: 10.1378/chest.07-0898

24. Mikroulis DA, Didilis VN, Konstantinou F, Vretzakis GH, Bougioukas GI. Catamenial pneumothorax. *Thorac Cardiovasc Surg* (2008) 56:374–5. doi: 10.1055/s-2006-924707

25. McCormack FX, Travis WD, Colby TV, Henske EP, Moss J. Lymphangioleiomyomatosis. *Am J Respir Crit Care Med* (2012) 186:1210–2. doi: 10.1164/rccm.201205-0848OE

26. He H, Luthringer DJ, Hui P, Lau SK, Weiss LM, Chu PG. Expression of CD56 and WT1 in ovarian stroma and ovarian stromal tumors. *Am J Surg Pathol* (2008) 32:884–90. doi: 10.1097/PAS.0b013e3181609d59

frontiers | Frontiers in Oncology

TYPE Case Report
PUBLISHED 16 March 2023
DOI 10.3389/fonc.2023.1082115

OPEN ACCESS

EDITED BY
Kohei Fujita,
National Hospital Organization Kyoto Medical Center, Japan

REVIEWED BY
Kentaro Semba,
Waseda University, Japan
Jennifer Whisenant,
Vanderbilt University Medical Center, United States

*CORRESPONDENCE
Junhua Guo
dpkog@126.com

SPECIALTY SECTION
This article was submitted to Thoracic Oncology, a section of the journal Frontiers in Oncology

RECEIVED 27 October 2022
ACCEPTED 27 February 2023
PUBLISHED 16 March 2023

CITATION
Ye Z and Guo J (2023) Acquired ALK G1202R-, ALK I1171N-, or EML4-ALK-mediated resistance to ensartinib in lung adenocarcinoma but responded to lorlatinib: A case report.
Front. Oncol. 13:1082115.
doi: 10.3389/fonc.2023.1082115

Acquired ALK G1202R-, ALK I1171N-, or EML4-ALK-mediated resistance to ensartinib in lung adenocarcinoma but responded to lorlatinib: A case report

Zhifeng Ye and Junhua Guo*

Department of Oncology, Hangzhou Chinese Traditional Medicine Hospital, Hangzhou, China

ALK rearrangements are identified as driver mutations in non-small-cell lung cancer (NSCLC). EML4 is the most common partner of ALK rearrangements. Here, we reported a patient with lung adenocarcinoma who was identified with EML4-ALK mutations when he progressed on an immune checkpoint inhibitor. The patient was treated with alectinib and obtained a progression-free survival (PFS) of 24 months. Then, next-generation sequencing on circulating tumor DNA identified multiple ALK mutations, including ALK G1202R, I1171N, ALK-ENC1, and EML4-ALK. Ensartinib was given, and the patient achieved a PFS of 5 months. After progression, lorlatinib was administered, and the patient achieved a partial response. Now, the benefit is still ongoing with a PFS over 10 months. Our case may provide evidence for the treatment choice of multiple ALK mutations, including ALK I1171N.

KEYWORDS

lung cancer, multiple ALK mutations, I1171N, ensartinib, lorlatinib

1 Introduction

Lung cancer is one of the most common causes of cancer-related death worldwide. Anaplastic lymphoma kinase (ALK) belongs to the family of tyrosine kinases involved in the pathogenesis and development of lung cancer (1). It has been well-documented that ALK fusions play an essential role in the oncogenic process of lung cancer by activating downstream signaling cascades, such as the PI3K/mTOR pathway (2). ALK gene consists of 30 exons mapping to the long arm of chromosome 2 (2p23.2–p23.1) (3). Approximately 3%–10% of non-small cell lung cancer (NSCLC) patients have ALK fusions (1, 4–7), with EML4-ALK fusion accounting for approximately 80% (7, 8).

Many previous studies show that ALK fusions responded well to ALK inhibitors. Nevertheless, several studies report that different ALK partners responded differently to ALK inhibitors (6). Even I1171N has been proposed to resist the second-generation ALK inhibitor alectinib (8).

Herein, we presented a patient with NSCLC harboring multiple ALK fusion mutations, including I1171N, who experienced rapid disease progression after ensartinib treatment but responded well to lorlatinib. This case provides a meaningful reference for treating NSCLC patients with ALK I1171N and other ALK fusions.

2 Case presentation

A 53-year-old Asian man, who is a heavy smoker, was diagnosed with lung adenocarcinoma in December 2013 and subsequently underwent R0 resection (Figure 1). Unfortunately, recurrence occurred in March 2017. Intra-hospital detection of biopsy samples revealed negative EAR (EGFR, ALK, and ROS1). Then, bevacizumab combined with AP chemotherapy was applied, and the best response was partial response (PR). Multiple central nervous system (CNS) metastases were found after 16 months of treatment. The physical condition and the location of metastases made this patient not suitable for biopsy. Alternatively, non-invasive circulating tumor DNA (ctDNA) detection was performed using a nosocomial test and found to be negative in driver genes, such as EGFR, ALK, ROS1, and MET. Stereotactic body radiation therapy (SBRT) was applied to treat CNS metastases. In February 2019, metastases occurred in the liver, spleen, and lumbar vertebrae. Toripalimab and SBRT were started, and the best response was stable disease (SD). Then, toripalimab plus paclitaxel was initiated, achieving a PR at the first evaluation but developing into progressive disease (PD) at 3 months treatment (Figures 2A, B). Considering the rapid tumor growth and the urgent condition of the patient, we conducted the ctDNA next-generation sequencing (NGS) with a depth of 36,000× for additional treatment choices and identified the ALK-intergenic region (ALK-IR) and EML4-ALK mutations. According to the National Comprehensive Cancer Network (NCCN) guidelines, the patient received alectinib treatment in July 2019 (Figures 2C, D). Follow-up examination found an elevation of carcinoembryonic antigen (CEA) level. Meanwhile, ctDNA identified new mutations, including ALK G1202R, I1171N, ALK-ENC1, EML4-ALK, and TP53. PD was verified at follow-up on September 2021, and crizotinib treatment was started. However, severe gastrointestinal effects and hypodynamia prevented the continuation of crizotinib treatment, and ensartinib was chosen for subsequent therapy. After 5 months, he suffered from nausea, vomiting, and pain in the lower back and lower extremities. Chest CT and increased blood tumor markers revealed PD (Figure 2E). Brain magnetic resonance imaging (MRI) showed no disease progression. In February 2022, identifying the same driver genes prompted the treatment with lorlatinib, and the best response was PR. After treatment, his pain was significantly alleviated, so he refused to undergo another MRI. At the last follow-up date in December, clinical benefit is still ongoing (Figure 2F).

3 Discussion

To our knowledge, this is the first report in NSCLC that acquired ALK I1171N and G1202R co-mutation-mediated resistance to ensartinib but responded well to lorlatinib. At the first diagnosis after recurrence, NGS testing on the biopsy sample identified no mutations in EGFR, ALK, or ROS1, which promoted the application of toripalimab. However, the rapid deterioration of the condition prompted double checking of the mutation landscape,

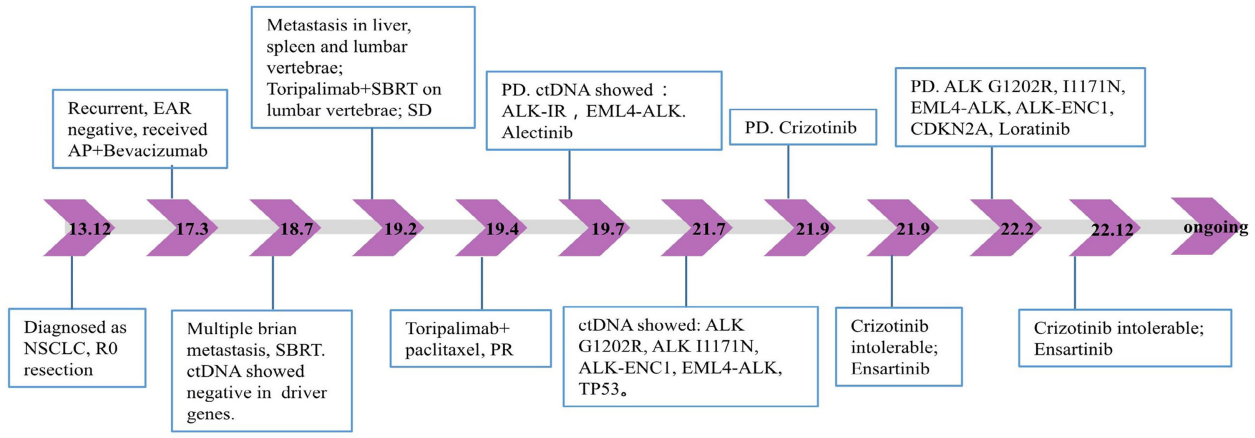

FIGURE 1
Timeline of the patient's treatment history and plasma NGS results. EAR, EGFR, ALK, and ROS1; AP, pemetrexed plus cisplatin; NSCLC, non-small-cell lung cancer; SBRT, stereotactic body radiation therapy; SD, stable disease; ctDNA, circulating tumor DNA; PR, partial response; PD, progressive disease; NGS, next-generation sequencing.

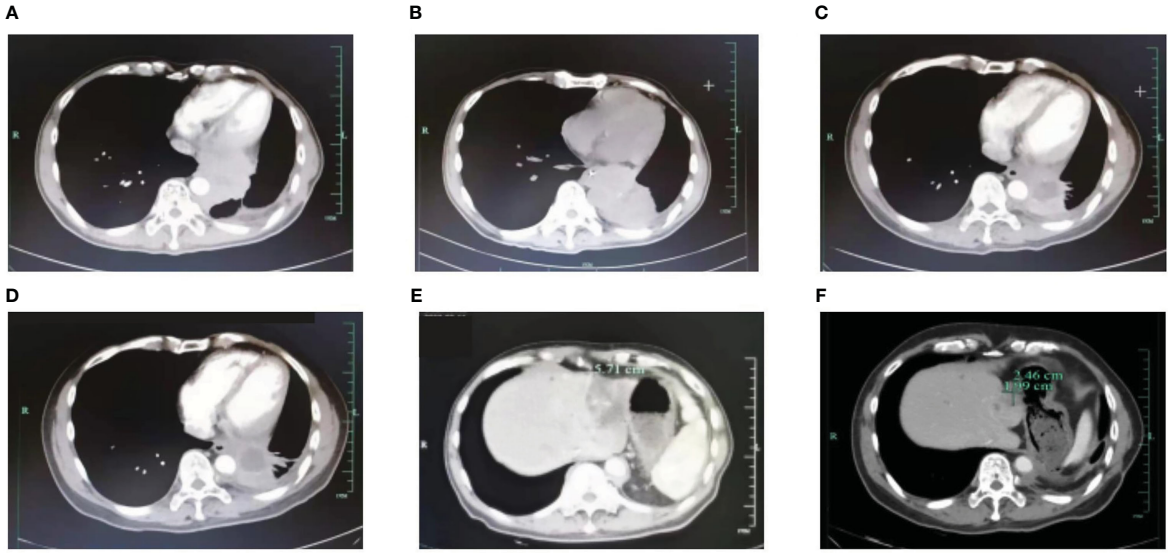

FIGURE 2
Radiographical changes. **(A)** PET/CT scan shows the failure of AP+Bevacizumab treatment in March 2019. **(B)** CT scan shows the failure of toripalimab+paclitaxel in July 2019. CT shows a durable response to alectinib in December 2019 **(C)** and 2020 **(D)**. **(E)** PD on ensartinib in February 2022. **(F)** CT shows a partial response to lorlatinib in December 2022. AP, pemetrexed plus cisplatin; PD, progressive disease; PET/CT, positron emission tomography/computed tomography.

and the acquired ALK rearrangement was found in ctDNA, which induced treatment regimen change. It has been reported that ALK-positive NSCLC has a highly aggressive clinical behavior in contrast with wild-type patients (3, 7, 9). Patients with ALK fusions tend to be not sensitive to immune checkpoint inhibitors (10). The resistance to toripalimab increased the likelihood that the driver gene existed. The clinical management of this patient highlights the importance of dynamic monitoring of ctDNA for patients, especially those whose health condition deteriorated rapidly.

Ensartinib is a second-generation ALK inhibitor, achieving a response rate (RR) of 60% and a median PFS of 9.2 months. In ALK TKI-naive patients, RR was 80%, and median PFS was 26.2 months, while in patients with prior TKI treatment, RR was 69%, and median PFS was 9.0 months (11). In this case, the patient experienced a PR and got a PFS of only 5 months. In previous studies, ALK G1202R has been shown to be resistant to ensartinib in patients with lung cancer (12, 13), while I1171N was sensitive to ensartinib in cell lines (14). Here, we found that co-mutation of ALK I1171N and G1202R was resistant to ensartinib.

Lorlatinib is a third-generation ALK inhibitor exploited to penetrate the blood–brain barrier and overcome ALK resistance mutations (15). After PD on ensartinib, lorlatinib was given because of its accessibility in mainland China. The phase 2 study of lorlatinib in patients with ALK-positive lung cancer showed that 87.0% of patients with measurable baseline CNS lesions achieved an intracranial response. It has been well-documented that acquired ALK G1202R is sensitive to lorlatinib (13, 15–17). In addition, I1171N was recently found to be more sensitive to lorlatinib than to crizotinib and alectinib in the preclinical study (18). Significantly, a case reported that the multiple ALK mutation, including I1171N, L1196M, and G1202R, mediated the resistance to lorlatinib in malignant pleural mesothelioma. However, in this case, we reported that the co-mutation of I1171N and G1202R was sensitive to lorlatinib (19). Our case with acquired multiple mutations respond differently to different ALK-TKIs, contributing to the understanding of complex ALK-TKI resistance mechanisms.

4 Conclusions

As reported in previous clinical trials, ALK fusions were sensitive to ALK inhibitors, especially EML4-ALK fusion. However, different rare ALK fusions respond differently to various generation ALK inhibitors. Here, we reported a patient harboring multiple ALK fusions, including ALK G1202R, I1171N, and EML4-ALK, who was sensitive to lorlatinib. This case provides evidence that this complex ALK fusion combination is sensitive to the third-generation ALK inhibitor.

Data availability statement

The raw data supporting the conclusions of this article will be made available by the authors, without undue reservation.

Ethics statement

The studies involving human participants were reviewed and approved by Ethics Committee of Hangzhou Traditional Chinese Medicine Hospital. The patients/participants provided their written informed consent to participate in this study. Written informed consent was obtained from the individual(s) for the publication of any potentially identifiable images or data included in this article.

Author contributions

ZY and JG followed patients and collected patient data. JG wrote the initial draft. All authors contributed to the article and approved the submitted version.

Funding

This work was sponsored by The Construction Fund of Medical Key Disciplines of Hangzhou.

Acknowledgments

We thank the patient and his family members for their participation and cooperation. ctDNA with a depth of 36,000× was performed by 3D Medicines-Shanghai Inc.

Conflict of interest

The authors declare that the research was conducted in the absence of any commercial or financial relationships that could be construed as a potential conflict of interest.

Publisher's note

References

1. Soda M, Choi YL, Enomoto M, Takada S, Yamashita Y, Ishikawa S, et al. Identification of the transforming EML4-ALK fusion gene in non-small-cell lung cancer. *Nature* (2007) 448(7153):561–6. doi: 10.1038/nature05945

2. Chiarle R, Voena C, Ambrogio C, Piva R, Inghirami G. The anaplastic lymphoma kinase in the pathogenesis of cancer. *Nat Rev Cancer* (2008) 8(1):11–23. doi: 10.1038/nrc2291

3. Inamura K, Takeuchi K, Togashi Y, Nomura K, Ninomiya H, Okui M, et al. EML4-ALK fusion is linked to histological characteristics in a subset of lung cancers. *J Thorac Oncol* (2008) 3(1):13–7. doi: 10.1097/JTO.0b013e31815e8b60

4. Devarakonda S, Morgensztern D, Govindan R. Genomic alterations in lung adenocarcinoma. *Lancet Oncol* (2015) 16(7):e342–51. doi: 10.1016/S1470-2045(15)00077-7

5. Colombino M, Paliogiannis P, Cossu A, Santeufemia DA, Sardinian Lung Cancer Study G, Sini MC, et al. EGFR, KRAS, BRAF, ALK, and cMET genetic alterations in 1440 sardinian patients with lung adenocarcinoma. *BMC Pulm Med* (2019) 19(1):209. doi: 10.1186/s12890-019-0964-x

6. Rosas G, Ruiz R, Araujo JM, Pinto JA, Mas L. ALK rearrangements: Biology, detection and opportunities of therapy in non-small cell lung cancer. *Crit Rev Oncol Hematol* (2019) 136:48–55. doi: 10.1016/j.critrevonc.2019.02.006

7. Noh KW, Lee MS, Lee SE, Song JY, Shin HT, Kim YJ, et al. Molecular breakdown: a comprehensive view of anaplastic lymphoma kinase (ALK)-rearranged non-small cell lung cancer. *J Pathol* (2017) 243(3):307–19. doi: 10.1002/path.4950

8. Mologni L, Ceccon M, Pirola A, Chiriano G, Piazza R, Scapozza L, et al. NPM/ALK mutants resistant to ASP3026 display variable sensitivity to alternative ALK inhibitors but succumb to the novel compound PF-06463922. *Oncotarget* (2015) 6(8):5720–34. doi: 10.18632/oncotarget.3122

9. Shaw AT, Yeap BY, Mino-Kenudson M, Digumarthy SR, Costa DB, Heist RS, et al. Clinical features and outcome of patients with non-small-cell lung cancer who harbor EML4-ALK. *J Clin Oncol* (2009) 27(26):4247–53. doi: 10.1200/JCO.2009.22.6993

10. Mazieres J, Drilon A, Lusque A, Mhanna L, Cortot AB, Mezquita L, et al. Immune checkpoint inhibitors for patients with advanced lung cancer and oncogenic driver alterations: results from the IMMUNOTARGET registry. *Ann Oncol* (2019) 30(8):1321–8. doi: 10.1093/annonc/mdz167

11. Horn L, Infante JR, Reckamp KL, Blumenschein GR, Leal TA, Waqar SN, et al. Ensartinib (X-396) in ALK-positive non-small cell lung cancer: Results from a first-in-Human phase I/II, multicenter study. *Clin Cancer Res* (2018) 24(12):2771–9. doi: 10.1158/1078-0432.CCR-17-2398

12. Yang Y, Huang J, Wang T, Zhou J, Zheng J, Feng J, et al. Decoding the evolutionary response to ensartinib in patients with ALK-positive NSCLC by dynamic circulating tumor DNA sequencing. *J Thorac Oncol* (2021) 16(5):827–39. doi: 10.1016/j.jtho.2021.01.1615

13. Horn L, Whisenant JG, Wakelee H, Reckamp KL, Qiao H, Leal TA, et al. Monitoring therapeutic response and resistance: Analysis of circulating tumor DNA in patients with ALK+ lung cancer. *J Thorac Oncol* (2019) 14(11):1901–11. doi: 10.1016/j.jtho.2019.08.003

14. Doi Y, Tagaya H, Noge A, Semba K. Prediction of resistance mutations against upcoming anaplastic lymphoma kinase inhibitors. *Target Oncol* (2022) 17(6):695–707. doi: 10.1007/s11523-022-00919-5

15. Solomon BJ, Besse B, Bauer TM, Felip E, Soo RA, Camidge DR, et al. Lorlatinib in patients with ALK-positive non-small-cell lung cancer: results from a global phase 2 study. *Lancet Oncol* (2018) 19(12):1654–67. doi: 10.1016/S1470-2045(18)30649-1

16. Shaw AT, Solomon BJ, Besse B, Bauer TM, Lin CC, Soo RA, et al. ALK resistance mutations and efficacy of lorlatinib in advanced anaplastic lymphoma kinase-positive non-Small-Cell lung cancer. *J Clin Oncol* (2019) 37(16):1370–9. doi: 10.1200/JCO.18.02236

17. Zou HY, Friboulet L, Kodack DP, Engstrom LD, Li Q, West M, et al. PF-06463922, an ALK/ROS1 inhibitor, overcomes resistance to first and second generation ALK inhibitors in preclinical models. *Cancer Cell* (2015) 28(1):70–81. doi: 10.1016/j.ccell.2015.05.010

18. Yoda S, Lin JJ, Lawrence MS, Burke BJ, Friboulet L, Langenbucher A, et al. Sequential ALK inhibitors can select for lorlatinib-resistant compound ALK mutations in ALK-positive lung cancer. *Cancer Discov* (2018) 8(6):714–29. doi: 10.1158/2159-8290.CD-17-1256

19. Hu J, Zhang B, Yao F, Fu Y, Chen D, Li D, et al. Acquired multiple mutations ALK I1171N, L1196M and G1202R mediate lorlatinib resistance in EML4-ALK-rearranged malignant pleural mesothelioma: A case report. *Ther Adv Respir Dis* (2020) 14:1753466620935770. doi: 10.1177/1753466620935770

frontiers | Frontiers in Oncology

TYPE Case Report
PUBLISHED 16 March 2023
DOI 10.3389/fonc.2023.1008587

OPEN ACCESS

EDITED BY
Yaron Perry,
University at Buffalo, United States

REVIEWED BY
Frits Van Rhee,
University of Arkansas for Medical Sciences, United States
David Boutboul,
Aphp Hôpital Saint Louis, France

*CORRESPONDENCE
Jian Li
lijianhouma@139.com

SPECIALTY SECTION
This article was submitted to Thoracic Oncology, a section of the journal Frontiers in Oncology

RECEIVED 01 August 2022
ACCEPTED 27 February 2023
PUBLISHED 16 March 2023

CITATION
Shi X, Liao M, Yin X, Chen Y, Huang C, Yin W and Li J (2023) Case report: The stroma-rich variant of Castleman's disease of hyaline-vascular type with atypical stromal cell proliferation and malignant potential: An exceptional rare case occurred in mediastinal lymph node. *Front. Oncol.* 13:1008587. doi: 10.3389/fonc.2023.1008587

Case report: The stroma-rich variant of Castleman's disease of hyaline-vascular type with atypical stromal cell proliferation and malignant potential: An exceptional rare case occurred in mediastinal lymph node

Xiaoxin Shi[1], Mengying Liao[1], Xiaomin Yin[1], Yaoli Chen[1], Chuqiang Huang[1], Weihua Yin[1] and Jian Li[1,2]*

[1]Department of Pathology, Peking University Shenzhen Hospital, Shenzhen, China, [2]State Key Laboratory of Chemical Oncogenomics, Peking University Shenzhen Graduate School, Shenzhen, China

The stroma-rich variant of Castleman disease of hyaline-vascular type (SR-HVCD) is characterized by interfollicular proliferation of the fibroblastic, myofibroblastic, and/or histiocytic-derived stromal cells, occurred in a background of Castleman disease of hyaline-vascular type (HVCD). It has been considered as a hyperplastic disorder by far. Herein, we presented a case of a 40-year-old male suffering from an occupation in the right middle mediastinum. Microscopically, the lesion was characterized by atretic lymphoid follicles and overgrowth of the interfollicular spindle-shaped cells. Those spindle cells were histologically bland in some areas, while exhibited notable cellular atypia and focal necrosis in other areas. SMA and CD68 were immunostained with a subset of the spindle cells in both areas, whereas p53 staining was only perceived in areas with markedly cellular atypia. In addition, indolent T-lymphoblastic proliferation (iT-LBP) was present inside the lesion. The patient developed multiple sites metastases 4 months after surgery, and succumbed to the disease at 7 months. Our case demonstrates for the first time that SR-HVCD have a tumorigenesis potential rather than a simple hyperplastic process. Such disorder should be carefully evaluated to avoid underdiagnosis.

KEYWORDS

Castleman's disease, hyaline-vascular, malignant, stromal hyperplasia, p53

Introduction

Castleman disease (CD) is an uncommon lymphoproliferative disorder and the incidence is estimated to be around 21 to 25 cases per million person-years (1, 2). According to the latest consensus of the Castleman Disease Collaborative Network (CDCN), CD encompasses a spectrum of conditions with heterogeneous etiologies, clinical manifestations, and histological characteristics (3). Clinically, it is grouped into unicentricity and multicentricity. Histologically, CD is classified into variants of hyaline-vascular (HVCD), plasma-cell, mixed type, hypervascular, and plasmablastic phenotype (3, 4).

HVCD accounts for nearly 90% of unicentric CD (2) and often manifested as a unicentric leison. The mediastinal lymph nodes is one of the most common sites of HVCD. Microscopically, HVCD is characterized by atretic follicles with hyalinized penetrating vessels and concentric onion-skin-like mantle zone. The interfollicular region generally exhibits proliferated vasculatures and unapparent lymphosinuses. In 1993, Danon et al. defined a new variant of HVCD, named as stroma-rich variant of Castleman disease of hyaline-vascular type (SR-HVCD) (5). Unlike the classical HVCD, SR-HVCD demonstrates a florid hyperplasia of actin-positive fibroblastic cells and KP1-positive histiocytic cells in the interfollicular zone. By definition, the area of interfollicular zone is required to be larger than that of follicular zone. Since then, a few studies further explored the clinicopathological features of this rare disorder (5–12). However, the etiology of SR-HVCD is still kept unknown. It is generally presumed to be a hyperplastic lesion based on the fact that all the reported cases exhibit a benign process and no associated malignancies have been recorded by far.

Interestingly, very few malignancies have been shown to be concurrently occurred with HVCD. One of them is follicular dendritic cell sarcoma (FDCS). The association between HVCD and FDCS was first unraveled by Chan et al. in 1994 (13), and was subsequently described by other researchers (13–15). Lymphoma, including Hodgkin's disease and non-Hodgkin's lymphoma, is another type of malignant tumors occasionally coexisted with HVCD (4, 16, 17). Herein, we presented an unusual case of SR-HVCD that exhibited a malignant profile, featured by dysplastic proliferation of the stromal cells and subsequent metastasis. The lesion's morphologic features and related differential diagnosis were discussed in detail.

Case presentation

The patient was a 40-year-old male with a complaint of shortness of breath after activity. The symptom had lasted for around one month. No remarkable medical history has been stated by the patient. Computed tomography scans revealed a large mass in the right middle mediastinum. The maximum diameter was about 10cm (Figure 1A). Tracheal and the superior vena cava were found to be compressed. The laboratory findings (Table 1) showed a slight increase in soluble interleukin-2 receptor (SIL-2R) and lactate dehydrogenase (LDH). C-reactive protein (CRP), aspartate transaminase (AST), alanine transaminase (ALT), and creatinine did not show obvious abnormalites. The mass was then completely removed by surgery. Operative findings revealed the mass compressed the right upper lobe bronchus and the superior vena cava.

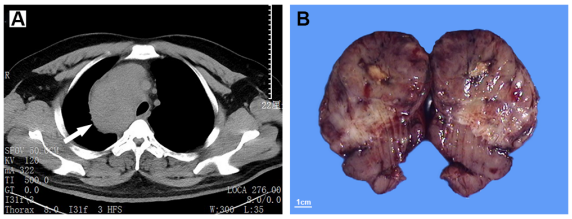

FIGURE 1
Computed tomography (CT) scans show an occupation in the right middle mediastinum (white arrow), with a CT value of 20-80 Hu **(A)**. The resected mass is well-demarcated, and exhibits a solid and lobulated appearance in cut surface **(B)**.

Pathological features

Macroscopically, the mass was 10.5cm×8.7cm×7cm in size and grey to red in color. It was solid and nodular in cut surface and tenacious to soft in texture (Figure 1B). A fibrous capsule was observed in the periphery regions of the mass. Microscopically, the lymphoid follicles were unevenly distributed under the capsule (Figure 2A). Most of them were atretic in appearance. The hyperplastic follicular dendritic cells in germinal center and concentrically-arrayed lymphocytes in mantle zone could be easily observed (Figures 2B, C). Occasionally, penetrated sclerotic blood vessels were found. Toward to the central region, the lymphoid follicles were markedly attenuated. The interfollicular fields were dominated by the compact plump spindle cells with a fascicular and storiform arrangement (Figure 2D). In some areas, the spindle cells demonstrated slender cytoplasm and indistinct cellular borders. The nuclei were oval and/or elongated, with vesicular to fine chromatin and small nucleoli. No obvious nuclear atypia or pleomorphism was presented (Figures 2E, F, 3A). By contrast, in other areas they exhibited enlarged and hyperchromatic nuclei, increased mitotic activity (5 per 10 high power fields), and atypical mitoses (Figure 3B, Supplementary Figure 1). Neoplastic necrosis was observed focally (Supplementary Figure 2). The morphologic transition could be perceived between the mild and dysplastic cellular areas (Figure 3C, Supplementary Figure 1). In addition, proliferated small vessels were found tightly intermixed with the stromal cells (Supplementary Figure 3). Moreover, small lymphocyte infiltrates were also noticed inside the lesion and distributed in a varied density. Those lymphocytes illustrated oval nuclei, darkly-stained chromatin and inconspicuous nucleoli (Figures 2E, F).

Immunohistochemically, the spindle cells were focally stained with SMA and CD68 (Figures 4A–F). Strong P53 staining and increased Ki-67 index (20%) was detected in regions with notably cellular atypia, while negative P53 staining and low Ki-67 index (10%) was presented in spindle cells with benign morphology

TABLE 1 The laboratory findings of the patient.

Laboratory findings (range)	Preoperation	At the fourth month after surgery
Hemoglobin (130-175g/L)	157	86
Red blood cell (4.3-5.8E+12/L)	5.29	3.1
White blood cell (3.5-9.5E+9/L)	7.30	17.89
Platelet (125-350E+9/L)	222	84
Aspartate transaminase (13-35U/L)	30.83	127.68
Alanine transaminase (0-50U/L)	29.75	83.43
Alkaline phosphatase (35-135U/L)	97.04	298.11
Total Bilirubin (0-26umol/L)	8.7	96
Blood urea nitrogen (2.60-8.80mmol/L)	4.79	5.28
Creatinine (41-81umol/L)	78.54	36.67
C-reactive protein (0-10mg/L)	10.60	37.69
Interleukin-6 (0-7.0pg/mL)	21.97	46.64
CA125 (0-35U/mL)	26.51	75.9
Soluble interleukin-2 receptor (180-265U/mL)	377.6	537.38
Lactate dehydrogenase (120-250U/L)	289.83	470.37

(Figures 4G–J). On the other hand, they were uniformly negative for CD21, CD23, CD35, SSTR2, D2-40, and CXCL13 (Supplementary Figure 4). Moreover, they also exhibited negative staining for CK-pan, CK5/6, CK8/18, CK19, P63, CD5, CD117, STAT-6, CD34, CD31, ERG, ALK, S-100, MDM2, CDK4, p16, TLE1, GLUT1, TRK, Muc4, and HHV-8. EBER *in situ* hybridization was negative either. FISH analysis by break-apart probes showed negative results for the rearrangements of EWSR1 and SS18 gene. The staining of CD20 highlighted B-cells in follicles. The interfollicular small lymphocytes were immunoreactive with CD3 and CD5, and some of them were positive for TdT and CD10 (Figures 5A–D). PCR analysis revealed there was no clonal rearrangement in T-cell receptor (TCR) beta and gamma gene.

Post-surgery treatment and prognosis

After the pathological diagnosis was drawn, the patient received additional physical examination and no definite symptoms correlated with HVCD, such as myasthenia gravis, erythra, paraneoplastic pemphigus, and bronchiolitis obliterans were discerned. He received combined treatments of epidoxorubicin and bevacizumab after surgery and kept well for 3 months. Then he developed chest pain and weakness of lower limbs at 4 month. Magnetic resonance imaging revealed multifocal bone and liver metastasis (Supplementary Figure 5). The level of SIL-2R, LDH, AST, ALT, total bilirubin, CRP, CA125, and interleukin-6 were variably increased (Table 1). The patient refused biopsy on the metastatistic lesions and accepted the immunotherapy of nivolumab. However, the tumor's progression persisted and the patient succumbed to to the disease 7 months later after operation.

Discussion

Mediastinum is one of the most common sites of HV-CD. In this perplexing case, we still can trace the characteristic profiles of intranodal HV-CD, e.g., the atretic follicles with proliferative dendritic cells, concentrically-arrayed lymphocytes in mantle zone, and expended interfollicular zone with abundant small vessels. However, it is challenge to explain the nature of those proliferated spindle cells, which demonstrated features varying from bland morphology to remarkable atypia.

Interestingly, Danon et al. (5) had described a florid proliferation of the interfollicular spindle cells in a few cases of HV-CD they enrolled. Those cells showed mild ovoid vesicular and plump nuclei. Their volume proportion was generally greater than 75% of the whole lesion and the follicles in between were atrophied. The spindle cells were focally immunoreactive with actin and CD68. The name of SR-HVCD was then proposed for such lesions. Subsequently, Lin et al. and Miki et al. (6, 7) respectively reported similar cases, characterized by the overgrowth of spindle cells in the interfollicular areas. Positive staining of SMA and CD68 were also found in a subset of those cells. Based on the morphologic and immunophenotypic features, the spindle cells were postulated to be derived from the fibroblastic, myofibroblastic, histiocytic cells, and/or vessel-related pericytes in the lymph node. So the angiomyoid proliferative lesion of HV-CD was alternatively used to describe such disorders (5), which particularly highlights the cellular composition inside the disorder. More importantly, all the reported cases exhibited a benign course and no recurrence was occurred after excision.

Our case was most likely conformed to the characteristics of SR-HVCD, whereas the interfollicular spindle cells exhibited

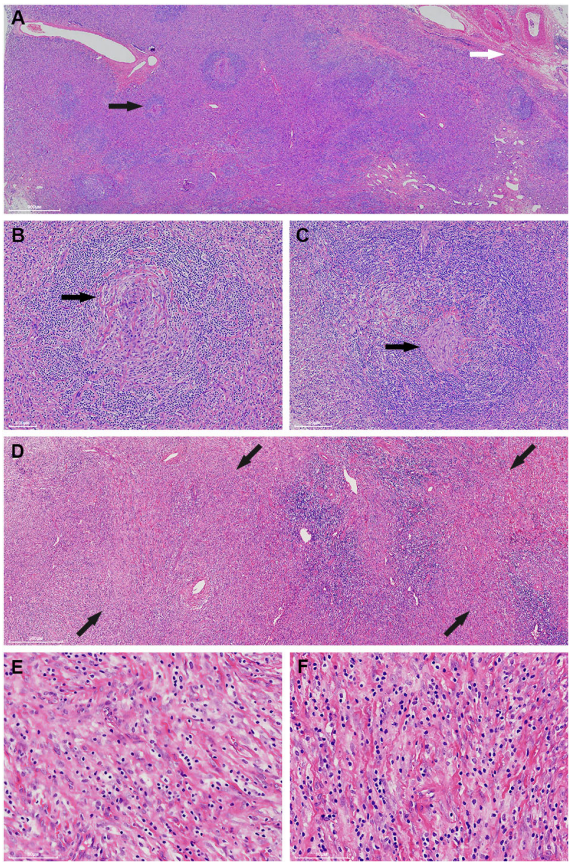

FIGURE 2
The mass generally exhibits a histologic structure of Castleman disease of hyaline-vascular type (HVCD). Beneath the capsule (white arrow), the lymphoid follicles are unevenly distributed and the follicles are generally atrophied (black arrow) **(A)**. The germinal centers are characterized by a depletion of lymphoid cells and proliferation of follicular dendritic cells (black arrow). The mantle zone lymphocytes are concentrically arranged and impart an onion-skin-like appearance **(B, C)**. Toward the central region, the interfollicular areas are widened by storiform-arranged spindle cells under low power (back arrow) **(D)**. Those spindle cells illustrate long, slender cytoplasm and vesicular to fine chromatin nuclei. No distinctive nuclear atypia is perceived in these fields **(E, F)**.

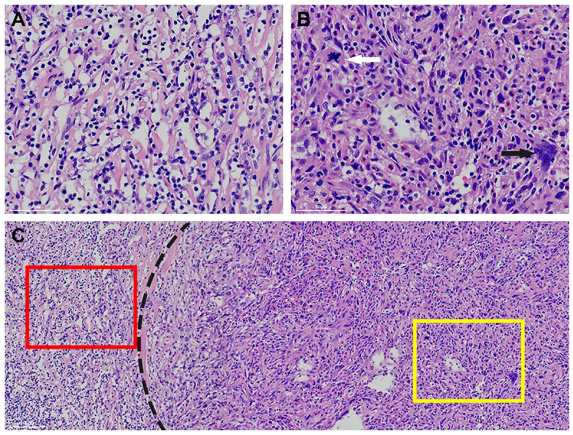

FIGURE 3
Apart from the cells with a bland appearance **(A)**, some of the spindle cells demonstrate remarkably pleomorphism. Abnormal mitoses (white arrow) and multinucleated tumor cells (black arrow) could be observed **(B)**. There exists a morphological transition between the bland (left side of the dot line) and atypical cellular regions (right side of the dot line). The high power fields of the red square and the yellow square are corresponding to **(A, B)**, respectively **(C)**.

remarkably atypia in some regions. Miki et al. specifically emphasized that their six cases of SR-HVCD were cytologically benign, lack of mitoses and necrosis. In addition, there were very low Ki-67 index and negative P53 expression (7). By contrast, the dysplastic spindle cells in our case demonstrated atypical mitoses and necrosis, and showed strong P53 expression and high Ki-67 index. Those characteristics obviously deviated from the profiles of previous reports and largely suggested it was a malignant process. The subsequent metastatic event also supported this speculation.

To clarify the nature of those interfollicular spindle cells, a substantial examination, including immunohistochemistry and FISH, was performed and showed the spindle cells, either in bland or atypical morphology, only displayed focal reaction with SMA and CD68. On the one hand, the results indicated, in consistence with earlier reports, they are probably originated from the fibroblastic, myofibroblastic, and/or histiocytic cells. On the other hand, a list of differential diagnosis was excluded: follicular dendritic cell sarcoma (CD21-, CD23-, CD35-, CXCL-13-, D2-40-, and SSTR2-), interdigitating dendritic cell sarcoma (S100-), indeterminate dendritic cell tumor (S100- and CD1a), Kaposi's sarcoma (HHV8-, CD34-, CD31-, and ERG-), solitary fibrous tumor (CD34- and STAT6-), malignant peripheral nerve sheath tumors (S100-, H3K27me3+, and SOX10-), NTRK gene fusion-positive tumors (TRK-, CD34-, and S100-), melanoma (S100-, SOX10-, HMB45-, Melanoma A-, and p16-), inflammatory myofibroblastic tumor (CK- and ALK-), poorly-differentiated/undifferentiated carcinoma (CK-pan-, CK8/18-, EMA-, E-cadherin-, and EBER-), thymic carcinoma (CK-pan-, CK19-, CD5-, and CD117-), sclerosing epithelioid fibrosarcoma (EWSR1 gene rearrangement-, MUM4-), and synovial sarcoma (SS18 gene rearrangement-).

Notably, there are two intriguing issues that remain unsettled. First, if the pleomorphic spindle cells were considered as malignancy, what type of tumor should they be classified? Undifferentiated sarcoma (UC) might be a possibility based on the cells' immunstaining features (SMA+ and CD68+). However, the atypical cellular component was generally self-limited inside the lesion, and no destruction or invasion to the adjacent structures was observed in our case. In addition, the nature of the metastatic lesion was regrettably kept unknown. So it seems insufficient to draw a diagnosis of UC based on the available evidences. Additional accumulated cases are expected to further clarify this question. Second, whether there existed a potential link between the atypical and bland stromal cells in pathogenesis. We assume the association could not be ruled out for the below reasons: (1) The two types of spindle cells were focally adjacent or intermingled inside the lesion, and a morphological transition could be perceived between them. (2) Both of them are supposed to be derived from fibroblastic, myofibroblastic, and/or histiocytic cells. Attractively, the acquired expression of p53 protein in the atypical spindle cells possibly indicated the p53 genetic alteration may trigger and/or contribute to

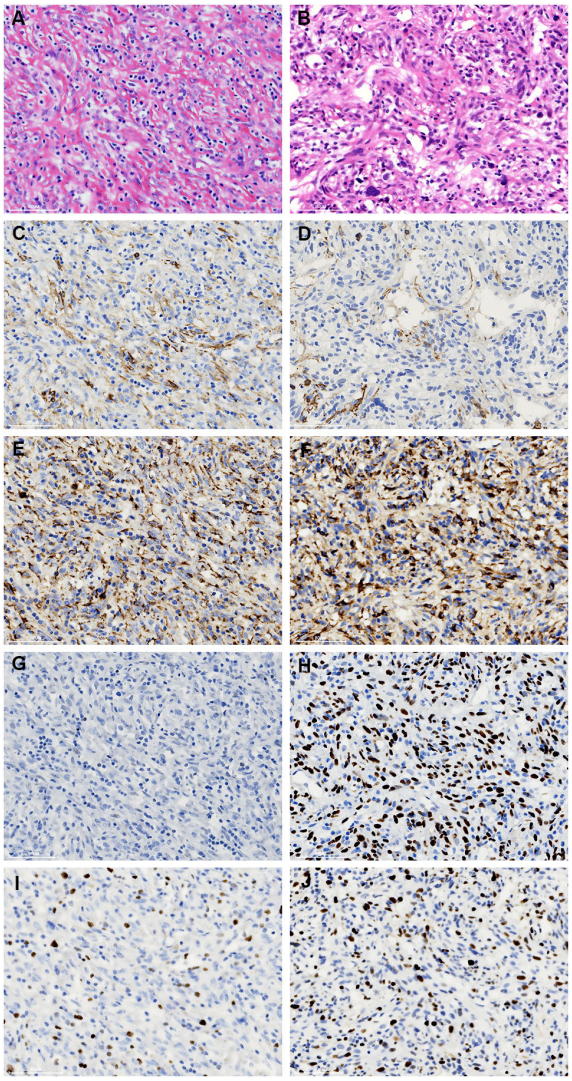

FIGURE 4
Comparison of the immunostaining features of the bland **(A, C, E, G, I)** and atypical spindle cells **(B, D, F, H, J)**. They are focally immunoreactive with SMA **(C, D)** and CD68 **(E, F)**. However, the staining of p53 is negative in the former **(G)**, while strongly expressed in the latter **(H)**. In addition, an increased ki-67 index is noticed in the atypical spindle cells **(I, J)**.

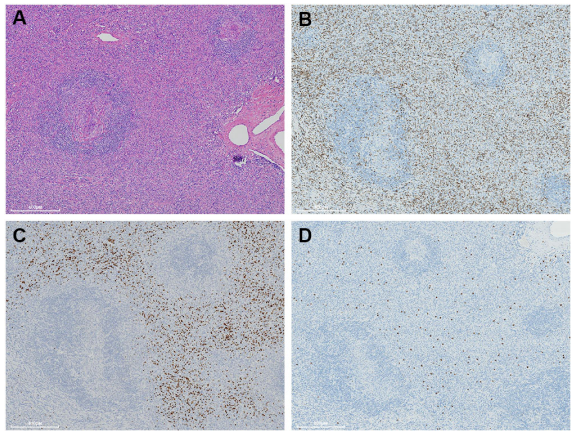

FIGURE 5
A moderate number of small lymphocytes are unevenly infiltrated inside the interfollicular regions **(A)**. They are variably immunostained with CD3 **(B)**, CD10 **(C)**, and TdT **(D)**.

their oncogenesis. In fact, p53 gene mutation has been demonstrared to play pivotal roles in the tumorigenesis of a variety of neoplasms (18, 19). A clonality analysis on the two cellular components might be helpful to fully unravel their internal relationship.

Finally, we also noticed the indolent T-lymphoblastic proliferation (iT-LBP) inside the lesion. Those T-lymphoblastic cells exhibited the phenotypes of precursor cortical thymocytes (TDT+, CD3+, CD5+, and CD10+), while presented no cytologic atypia. The TCR receptor rearrangement was not detected. Those features satisfied the diagnostic criteria of iT-LBP, as proposed by Ohgami et al. (20). It is worth noting that iT-LBP is frequently concurrent in disorders associated with the follicular dendritic cells' proliferation, such as HV-CD, FDCS, and angioimmunoblastic T-cell lymphoma. The dysfunction of follicular dendritic cells may create an extrathymic immunomilieu benefiting for the development of iT-LBP (21).

In summary, we described a rare case of SR-HVCD that was featured by the atypical hyperplasia of the stromal cells and demonstrated a malignant behaviour. The atypical stromal cells acquired aberrant P53 protein expression. Although the etiology remains to be further clarified, it is likely the first report that manifests SR-HVCD has a tumorigenesis potential and challenges the conventional viewpoint that SR-HVCD is a simple benign and hyperplastic disorder. Acquaintance with this entity would favor pathologists and clinicians to make an inerrant diagnosis and treatment in practice.

Data availability statement

The original contributions presented in the study are included in the article/Supplementary Material. Further inquiries can be directed to the corresponding author.

Ethics statement

The studies involving human participants were reviewed and approved by Peking University Shenzhen Hospital. The patients/participants provided their written informed consent to participate in this study. Written informed consent was obtained from the individual(s) for the publication of any potentially identifiable images or data included in this article.

Author contributions

XS, JL, and WY were engaged in the pathological diagnosis. XS, ML, and JL drafted the manuscript. XY, YC, and CH was involved in the immunohistochemical and molecular studies. All authors contributed to the article and approved the submitted version.

Funding

This study was supported by Open Research Fund of State Key Laboratory of Chemical Oncogenomics in 2021, Shenzhen Science and Technology Program (No. JCYJ20220531094017039), the Key Program for Clinical Research at Peking University Shenzhen Hospital (No.LCYJZD2021009), and the San-ming Project of Medicine in Shenzhen (No. SZSM20182088).

Acknowledgments

We appreciate Professor John K.C. Chan, from the Deparment of Pathology, Queen Elizabeth's Hospital, Hong Kong, for the consultation on the submitted case.

Conflict of interest

The authors declare that the research was conducted in the absence of any commercial or financial relationships that could be construed as a potential conflict of interest.

Publisher's note

All claims expressed in this article are solely those of the authors and do not necessarily represent those of their affiliated organizations, or those of the publisher, the editors and the reviewers. Any product that may be evaluated in this article, or claim that may be made by its manufacturer, is not guaranteed or endorsed by the publisher.

Supplementary material

The Supplementary Material for this article can be found online at: https://www.frontiersin.org/articles/10.3389/fonc.2023.1008587/full#supplementary-material

SUPPLEMENTARY FIGURE 1
Another field demonstrates the morphologic transition of the spindle cells from mild morphology (left side of the dot line) to marked atypia (right side of the dot line) **(A)**. In the former region (the red square), the spindle cells exhibit vesicular to fine chromatin, and inconspicuous small nucleoli **(B)**. In contrast, the cells in the latter region (the yellow square) illustrate enlarged, irregular nuclei and atypical mitosis (white arrow) **(C)**.

SUPPLEMENTARY FIGURE 2
The atypical spindle cells demonstrate the hemangiopericytoma-like arrangement (white arrow) and focal necrosis (black arrow).

SUPPLEMENTARY FIGURE 3
Hyperplastic small vessels are intermixed with the compact atypical spindle cells. They are not easily detectable on H&E section, while could be highlighted by CD34 staining.

SUPPLEMENTARY FIGURE 4
The atypical spindle cells show negative staining with CD21, CD23, CD35, SSTR2, D2-40, and CXCL13.

SUPPLEMENTARY FIGURE 5
Magnetic resonance imaging shows nodular abnormal signals (white arrow) in the liver, right paraspinal **(A)** and vertebral bodies **(B)**.

References

1. Nikhil M, Maneesha M, Helgi van de V, Avinash D, Ravi P, Jessica V. Use of a claims database to characterize and estimate the incidence rate for castleman disease. *Leuk Lymphoma* (2015) 56(5):1252–60. doi: 10.3109/10428194.2014.953145

2. David W, Megan SL, Elaine SJ. Pathology of castleman disease. *Hematol Oncol Clin North Am* (2018) 32(1):37–52. doi: 10.1016/j.hoc.2017.09.004

3. Ping L, Huaipu L, Hao L, Ang L, Guangyin Y, Weihua Y. Alkaline vascular variant of unicentric castleman disease of the tonsil: A case report. *Diagn Pathol* (2019) 29;14 (1):70. doi: 10.1186/s13000-019-0836-y

4. Claire L, Patrice C, Jean S, Eric O, Jean-Pierre C, Jean-Charles P, et al. Castleman's disease and lymphoma: report of eight cases in HIV-negative patients and literature review. *Am J Hematol* (2002) 69(2):119–26. doi: 10.1002/ajh.10022

5. Danon AD, Krishnan J, Frizzera G. Morpho-immunophenotypie diversity of castleman's disease, hyaline-vascular type: with emphasis on a stroma-rich variant and a new pathogenetic hypothesis. *Virchows Arch A Pathol Anat Histopathol* (1993) 423 (5):369–82. doi: 10.1007/BF01607150

6. Lin O, Frizzera G. Angiomyoid and follicular dendritic cell proliferative lesions in castleman's disease of hyaline-vascular type: a study of 10 cases. *Am J Surg Pathol* (1997) 21(11):1295–306. doi: 10.1097/00000478-199711000-00004

7. Miki I, Mamoru M, Masahiko K, Keiichi I, Kiyoshi M. Angiomyoid proliferative lesion: an unusual stroma-rich variant of castleman's disease of hyaline-vascular type. *Virchows Arch* (2002) 441(4):400–5. doi: 10.1007/s00428-002-0611-3

8. Yan X, Ying Z, Ying W, Jia N, Ting L. [Stroma-rich variant of hyaline-vascular castleman's disease: a clinicopathologic and histogenetic study]. *Zhonghua Bing Li Xue Za Zhi* (2010) 39(1):14–8.

9. Haifen M, Maofen J, Weihua X. A rare stroma-rich variant of hyaline-vascular castleman's disease associated with calcifying fibrous pseudotumor. *Int J Clin Exp Pathol* (2015) 8(3):3362–4.

10. Chaithra Gowthuvalli V, Hema K, Debarshi S, Sharada R, Deepa Sowkur Anandarama A, Ranjitha R, et al. Histomorphologic spectrum in hyaline vascular variant of castleman disease. *J Clin Diagn Res* (2017) 11(8):EC01–4. doi: 10.7860/JCDR/2017/29415.10326

11. Leyi W, Lin N, Furong L, Xue W, Rui W, Xixue C, et al. Predominant stroma-rich feature in hyaline vascular variant of castleman disease is associated with paraneoplastic pemphigus. *Am J Clin Pathol* (2020) ;154(3):403–13. doi: 10.1093/ajcp/aqaa053

12. Paida G, Zsombor M, Sarah J and Judit S. Paraneoplastic pemphigus caused by pre-existing stroma-rich variant of castleman disease: from a pathologist's point of view. *BMJ Case Rep* (2021) 14(5):e241374. doi: 10.1136/bcr-2020-241374

13. Chan JK, Tsang WY, Ng. Follicular dendritic cell tumor CS. And vascular neoplasm complicating hyaline-vascular castleman's disease. *Am J Surg Pathol* (1994) 18(5):517–25. doi: 10.1097/00000478-199405000-00013

14. Alexandra N, Aparna B, Nahid S, Jahanbanoo S, James LZ, Roger AW, et al. Next-generation sequencing of idiopathic multicentric and unicentric castleman disease and follicular dendritic cell sarcomas. *Blood Adv* (2018) 2(5):481–91. doi: 10.1182/bloodadvances.2017009654

15. Lei J, Liang Yu Z, Yuan L, Yun Fu Z. Castleman's disease of the neck: report of 4 cases with unusual presentations. *J Oral Maxillofac Surg* (2011) 69(4):1094–9. doi: 10.1016/j.joms.2010.03.007

16. Sergio P-O, Wei W, Erin V, John T Manning J, L Jeffrey M. Follicular lymphoma with hyaline-vascular castleman disease-like follicles and CD20 positive follicular dendritic cells. *Pathology* (2017) 49(5):544–7. doi: 10.1016/j.pathol.2017.03.006

17. Frits van R, Eric O, Gordan S, Peter V, Megan L, Angela D, et al. International evidence-based consensus diagnostic and treatment guidelines for unicentric castleman disease. *Blood Adv* (2020) 4(23):6039–50. doi: 10.1182/bloodadvances.2020003334

18. Elizabeth T, Amanda C, Tomoo I. TP53 in bone and soft tissue sarcomas. *Pharmacol Ther* (2019) 202:149–64. doi: 10.1016/j.pharmthera.2019.06.010

19. Chahat, Rohit B, Bhupinder K. p53 as a potential target for treatment of cancer: A perspective on recent advancements in small molecules with structural insights and SAR studies. *Eur J Med Chem* (2023) 247(5):115020. doi: 10.1016/j.ejmech.2022.115020

20. Ohgami RS, Arber DA, Zehnder JL, Natkunam Y, Warnke RA. Indolent T-lymphoblastic proliferation (iT-LBP): A review of clinical and pathologic features and distinction from malignant T-lymphoblastic lymphoma. *Adv Anat Pathol* (2013) 20 (3):137–40. doi: 10.1097/PAP.0b013e31828d17ec

21. Quesada AE, Young KH, Medeiros LJ, Thakral B. Indolent T-lymphoblastic proliferation associated with low grade follicular dendritic cell sarcoma and castleman disease. *Pathology* (2018) 50(3):351–2. doi: 10.1016/j.pathol.2017.09.017

frontiers | Frontiers in Oncology

TYPE Case Report
PUBLISHED 06 April 2023
DOI 10.3389/fonc.2023.1043244

OPEN ACCESS

EDITED BY
Kohei Fujita,
National Hospital Organization Kyoto Medical Center, Japan

REVIEWED BY
Xiaobo Du,
Mianyang Central Hospital, China
Tao Qin,
Sun Yat-sen Memorial Hospital, China

*CORRESPONDENCE
Lan Sun
sunlan6203@163.com
Shengwen Calvin Li
sli@choc.org

†These authors have contributed equally to this work

SPECIALTY SECTION
This article was submitted to Thoracic Oncology, a section of the journal Frontiers in Oncology

RECEIVED 13 September 2022
ACCEPTED 13 March 2023
PUBLISHED 06 April 2023

CITATION
Wang J, Li X, Zhou J, Qiu D, Zhang M, Sun L and Li SC (2023) Long-term survival with anlotinib as a front-line treatment in an elderly NSCLC patient: A case report. *Front. Oncol.* 13:1043244. doi: 10.3389/fonc.2023.1043244

Long-term survival with anlotinib as a front-line treatment in an elderly NSCLC patient: A case report

Jingyi Wang[1†], Xiaoqing Li[1†], Juan Zhou[1], Dan Qiu[1], Mengyao Zhang[1], Lan Sun[1*] and Shengwen Calvin Li[2,3*]

[1]Department of Oncology, Bishan Hospital of Chongqing Medical University, Chongqing, China, [2]Neuro-Oncology and Stem Cell Research Laboratory, Center for Neuroscience Research, CHOC Children's Research Institute, Children's Hospital of Orange County (CHOC), Orange, CA, United States, [3]Department of Neurology, University of California-Irvine School of Medicine, Orange, CA, United States

Background: Half of the population of non-small cell lung cancer (NSCLC) patients are older than 70 years and have limited therapeutic options due to poor tolerance and being excluded in most clinical trials. Anlotinib hydrochloride, a novel oral multi-target tyrosine kinase inhibitor, has been approved for the standard third-line treatment for NSCLC in China. Herein we report an elderly NSCLC patient without any driver gene mutations who was undergoing anlotinib as a front-line treatment and who achieved long-term survival.

Case summary: The 77-year-old male patient was admitted to the hospital for chest tightness after engaging in physical activity for a week. The patient has been diagnosed with stage IIIB driver gene-negative squamous cell lung carcinoma. After that, he was treated with anlotinib for 2 years and 10 months from the first diagnosis until the last disease progression. Briefly, anlotinib combined with platinum-based chemotherapy was performed as the first-line therapy over six cycles. After 6 more cycles of anlotinib monotherapy maintenance, disease progression occurred. Then, anlotinib combined with tegafur was administered as a salvage treatment, and the disease was controlled again. After 29 cycles of anlotinib combined with tegafur regimens, the disease progressed finally. The patient achieved a total of 34 months of progression-free survival after anlotinib was used as the front-line treatment. He is still alive with a good performance status now (performance status score: 1).

Conclusion: This patient achieved long-term survival using anlotinib as a front-line regimen combined with chemotherapy.

KEYWORDS

non-small cell lung cancer, anti-angiogenesis therapy, front-line treatment, elderly patients, case report, Anlotinib hydrochloride, tegafur-uracil, chemotherapy

Introduction

Lung cancer is one of the most common malignant tumors and the leading cause of global cancer mortality (1). Angiogenesis is one of the characteristics of malignant tumors, which can provide nutrition for the growth of tumor cells and secrete growth factors to promote cancer cell proliferation, thus playing an essential role in tumor growth, invasion, and metastasis (2, 3). A growing number of studies have shown that advanced non-small cell lung cancer (NSCLC) patients can benefit from anti-angiogenesis therapy with higher anti-cancer activity and fewer adverse effects than traditional chemoradiotherapy (4, 5). Anlotinib is a novel oral multitarget tyrosine kinase inhibitor which strongly inhibits vascular endothelial growth factor (VEGF), platelet-derived growth factor receptor (PDGF), fibroblast growth factor receptor (FGFR), and stem cell factor receptor (c-Kit), resulting in the inhibition of the growth of tumor blood vessels (6). On May 9, 2018, anlotinib was approved by China Food and Drug Administration as a standard third-line treatment regimen for advanced NSCLC based on the results of the ALTER-0303 study (7). However, the evidence for anlotinib as a front-line treatment for NSCLC is limited. Herein we report an elderly NSCLC patient without any driver gene mutations undergoing anlotinib as a front-line treatment.

Background

Chief complaints

A 77–year-old male patient developed chest tightness after an activity and precardiac pain in June 2018. He had an occasional cough with sputum.

History of present illness

The patient had chest tightness after an activity, precardiac pain, and occasional cough with sputum.

History of past illness

The patient had a history of chronic obstructive pulmonary disease (COPD) and diabetes mellitus type 2 (T2DM), with a smoking history of 55 years averaging 20 cigarettes per day. He had quit smoking for more than 2 years.

Personal and family history

The patient had a cancer-relative family susceptibility. His one brother and two sisters suffered from lung cancer, and another brother had liver cancer.

Physical examination

The results of the physical examination showed that the patient's body temperature was 36.3°C, the pulse rate was 70 beats per minute (bpm), the blood pressure was 128/76 mmHg, respiratory rate was 19 breaths/min, and the performance status score was 1.

Laboratory examinations

His blood count showed a WBC level of 5.75×10^9/L, Hb level of 116 g/L, and platelet count of 201×10^9/L. The serum level of carcinoembryonic antigen was 6.6 ng/ml.

Pathology and genetic testing

The histopathological analysis of the tissue biopsy samples collected from the right lung revealed poorly differentiated squamous cell carcinoma (Figure 1). The immunohistochemistry result showed the following details: CK5/6 (+), P63 (+), P40 (+), NapsinA (-), TTF1 (-), CK7(-), and CK14(+). A molecular analysis did not find any driver gene mutations of EGFR, ALK, and ROS1. Tissue samples were detected *via* next-generation sequencing with a panel consisting of 211 genes, which revealed TP53 (mutant abundance: 14.37%) and tumor mutation burden (TMB) of 21.15 Muts/Mb. The somatic mutations are shown in Table 1.

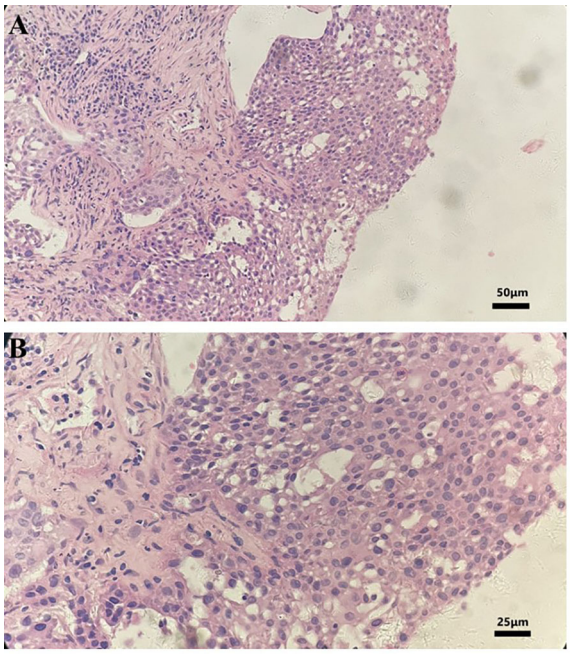

FIGURE 1
Hematoxylin and eosin staining photomicrographs of a right lung tumor tissue biopsy. **(A)** Magnification, ×200. **(B)** Magnification, ×400.

TABLE 1 List of somatic mutations.

Gene	Exon	Nucleotide variation	Amino acid change	Mutation abundance
PIK3CA	exon10	c.1624G>A	p.E542K	1.14%
TP53	exon6	c.637C>T	p.R213*	14.37%
FANCM	exon20	c.5237C>G	p.S1746*	1.18%
PTEN	exon6	c.631T>C	p.C211R	9.78%
PALB2	exon4	c.1366G>C	p.E456Q	8.04%
ATR	exon3	c.157G>C	p.V53L	4.35%
GATA3	exon3	c.388C>T	p.L130F	23.42%
HNF1A	exon2	c.331G>A	p.D111N	12.28%
JAK2	exon22	c.2951T>G	p.V984G	11.49%
NTRK3	exon14	c.1540C>A	p.P514T	10.60%
MAP3K1	exon1	c.212A>T	p.D71V	1.50%

The asterisk symbol (*) indicates the ending amino acid position during translation upon a stop codon (or termination codon) that is a codon for transcription termination signal. The single letter is for the abbrreviation of amino acids and the number is for the position of an amino acid) in the "amino acid change" column.

Imaging examinations

The chest scan first computed tomography (CT) result showed a mass which was 52 mm × 50 mm in size (Figure 2A). No metastasis was observed on enhanced CT of the skull and the abdomen. The lymph node ultrasound showed no metastasis. As per the solid tumor version 1.1 (RECIST 1.1) response evaluation criteria, the maximum lesion reduction reached 40.4% after four cycles of anlotinib with platinum-based chemotherapy (Figure 2B). After six courses of anlotinib monotherapy maintenance, the MRI results showed bilateral clavicular lymph node metastasis, and the patient's PFS_1 was 10 months. Then, after 12 cycles of anlotinib in combination with tegafur, the lesion reduction reached 13.8% compared with the previous best curative effect (Figure 2C). The disease remained stable after this, and there were no significantly enlarged lymph nodes on bilateral neck ultrasound. On May 24, 2021, the lesion enlarged by 41.4%, and the efficacy was evaluated as disease progression (Figure 2D), so the patient's PFS_2 was 24 months.

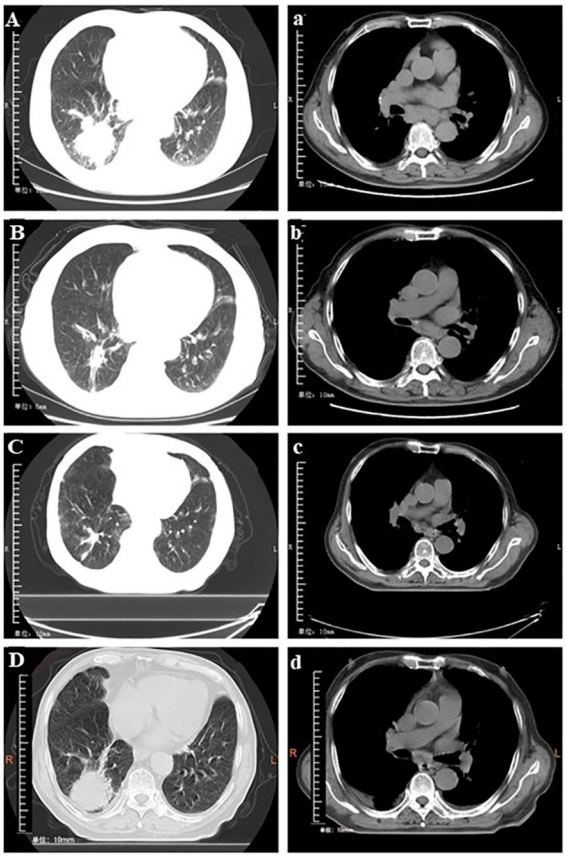

FIGURE 2
Conversion of chest computed tomography at different times. (**A** and **a**) Baseline findings on chest computed tomography (tumor size: 52 × 55 mm). (**B** and **b**) The mass shrank significantly (tumor size: 31 × 18 mm) after treatment with four cycles of anlotinib plus cisplatin. (**C** and **c**) Stable disease (tumor size: 25 × 21 mm) following 12 cycles of anlotinib + tegafur. (**D** and **d**) Progressive disease (tumor size: 41 × 34 mm) after 29 cycles of anlotinib + tegafur.

Final diagnosis

Finally, the patient was diagnosed with stage IIIB poorly differentiated driver gene-negative squamous cell lung carcinoma (cT3N2M0 in accordance with version 8 of TNM staging).

Treatment

Since July 24, 2018, the patient was treated with anlotinib (12 mg, d1–d14, q3w) and nedaplatin (85 mg/m^2, q3w) for the first-line therapy. After six courses of anlotinib combined with platinum-based chemotherapy, we used anlotinib monotherapy for maintenance treatment (12 mg, d1–d14, q3w), but the patient reduced the drug dose on his own during the last two courses of

maintenance therapy. The disease progressed after six cycles of maintenance treatment. Afterwards, the regimen was switched to anlotinib (12 mg, d1–d14, q3w) combined with tegafur (120 mg d1–d14, q3w) (Figure 3).

Outcome and follow-up

As of May 24, 2021, the patient received 2 years and 10 months of anlotinib treatment, with a progression-free survival of 34 months. The degree of adverse event was assessed according to Common Terminology Criteria Adverse Events Version 5.0. During the period of the treatment of anlotinib combined with nedaplatin, the patient experienced thrombocytopenia in the second cycle (grade 4), which was controlled with thrombopoietin therapy. Fatigue (grade 2) developed during the 11th and 12th cycles, which gradually improved during the interval between cycles. After the disease progressed, we proposed to adjust the treatment option several times, but the patient and his family refused. The last follow-up was on December 12, 2022, and the CT result showed that the lesion size was 78 mm × 59 mm, which increased from the original diagnosis of 52 mm × 50 mm in size (Figure 2A).

Discussion

In this case, the patient was diagnosed in July 2018 (cT3N2M0), and he could first be considered for surgery. However, his family adamantly refused due to his advanced age and underlying diseases. We also considered immunotherapy in combination with platinum-based chemotherapy, but PD-1 inhibitors were expensive and not financially affordable the patient and his family. Shortly before his diagnosis, anlotinib was approved by China Food and Drug Administration as a third-line treatment for advanced squamous lung cancer (the peripheral type only) based on the results of two clinical trials of anlotinib as a third-line or further treatment for NSCLC. One clinical study (ALTER0302) showed that the median progression-free survival (PFS) of the anlotinib group was significantly better than that of placebo (4.8 vs. 1.2 months) (8). The other clinical trial (ALTER0303) showed that anlotinib has extended median OS and PFS significantly, that is, 9.6 months vs. 6.3 months and 5.4 months vs. 1.4 months, respectively, compared with the placebo. Under the third-line or beyond treatment setting, the anlotinib combination therapy showed manageable toxicities and encouraging efficacy, indicating a good application prospect (9), which is one of the reasons why we administrated anlotinib as a front-line treatment. The other reasons are as follows: first, according to the National Comprehensive Cancer Network guidelines (2018 edition), radical concurrent chemo-radiotherapy is preferred for inoperable stage IIIB NSCLC patients. However, clinical studies have shown that concurrent radiotherapy is poorly tolerated in elderly patients (10), with a high possibility of discontinuing treatment. Sequential chemoradiotherapy may be considered for patients who cannot tolerate concurrent chemoradiotherapy. However, this patient had multiple underlying diseases such as COPD and T2DM; thus, the risk of uncontrollable side effects was high. Moreover, the target volume was too large to determine an appropriate radiotherapy plan ensuring antitumor efficacy and safety. Third, the toxicity of anti-angiogenesis drugs, including anlotinib, is much lower than chemotherapy, and adverse effects are controllable (9, 11). Anlotinib is reported to have the advantage of low toxicity (12). The most frequent toxicities include hypertension, hand–foot syndrome, fatigue, *etc.* Fourth, anti-angiogenesis treatment required attention to the side effect of hemoptysis. Fortunately, this patient had no symptoms of active hemorrhage, and the lesion was peripheral, so the risk of hemorrhage was evaluated as low. Fifth, the patient and his family refused to undergo radiation therapy, so we applied to the Ethics Committee for the inclusion of anlotinib as first-line treatment. The patient and his family eventually chose anlotinib as the first-line treatment and signed the informed patient's consent as approved. He achieved a total progression-free survival of 34 months using anlotinib as the front-line regimen. From the time of the patient's diagnosis to the time of the last follow-up (46 months), the maximum diameter of his tumor lesion increased by 12 mm. No uncontrollable toxic side effects were observed in this patient during the drug administration. We analyzed this patient's long-term survival for several reasons. Firstly, this patient did not develop distant metastases, and the clinical studies associated with anlotinib have validated distant metastases as an important prognosis (13). Secondly, it has been shown that inhibition of autophagy improves the efficacy of anlotinib (14), and age is one of the important reasons for the effect of autophagy (15). Given the advanced age of this patient, we consider that he may have a sustainable survival benefit due to his autophagy inhibition status. Thirdly, this patient has hypofractionated squamous carcinoma. Although hypofractionated tumor cells are conventionally more malignant, there is a complex relationship between cancer and inflammation. Hypofractionated cell proliferation may inhibit the growth of tumor cells through specialized pro-resolving mediators (16), which may also be a factor in this patient's long survival. Fourthly, the patient in this case had TP53 mutations (mutant abundance: 14.37%) with TMB: 21.15 Muts/Mb. TP53 mutations have been identified to be involved in the process of neovascularization associated with increased VEGF expression, which is one of the important targets of anlotinib. Fu et al. found that TP53 mutations are significantly associated with a favorable prognosis in patients with advanced solid malignancies (17). It has also been shown that advanced NSCLC patients with high TMB mutations (>10 Muts/Mb) can benefit from anti-angiogenesis therapy (18). Unfortunately, we could not ascertain PD-L1 expression

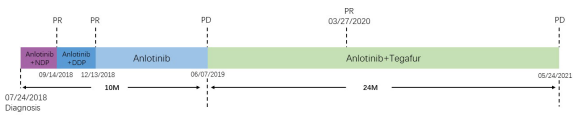

FIGURE 3
Timeline of events from diagnosis to progressive disease and summary of the administered treatments. Treatment work flow from [(anlotinib + NDP) à (anlotinib + DDP)] (6 cycles) to(anlotinib) (6 cycles) and to (anlotinib + tegafur) (29 cycles). After undergoing this treatment strategy, the patient has achieved a PFS of 34 months and an OS of 53 months. These results surpass those seen in the majority of real-world studies and clinical trials.

TABLE 2 Some clinical trials of anlotinib in non-small cell lung cancer (NSCLC) for the first line.

Line(s) of treatment	Study population	Study population	Number of patients	Median progression-free survival (months)	ORR (%)	DCR (%)	Reference
First line	Patients with EGFR wild-type stage IIIB–IV NSCLC aged more than 70 years	Anlotinib (12 mg, d1–d14/q3w)	40	3.00	17.50	67.50	(22)
First line	Patients with treatment-naïve and EGFR wild-type stage IIIB–IV NSCLC aged 18 to 75 yeas	Anlotinib (12 mg, d1–d14/q3w) + sintilimab (200 mg, d1/q3w)	22	15.00	72.70	100.00	(18)
First line	Patients with EGFR-mutated locally advanced and/or metastatic stage IIIB-IV NSCLC aged 18 to 75 years	Anlotinib (12 mg, d1–d14/q3w) + icotinib (125 mg, tid)	35	6.01	59.00	88.00	(25)

because of the insufficient volume of tissue obtained in the first biopsy and the patient's unwillingness to undergo a repeat biopsy.

This patient had disease progression after six cycles of anlotinib monotherapy maintenance. We switched to anlotinib combined with tegafur because oral tegafur treatment was more convenient and economical. The EAST study demonstrated that tegafur is equally as efficacious as docetaxel (19). In addition, anti-angiogenesis therapy can improve the local hypoxic condition of the tumor microenvironment, which is more conducive to the entry of chemotherapeutic drugs into the tumor tissue. There is a growing number of studies on anlotinib as a second-line treatment from 2018 onwards. One study showed that anlotinib combined with chemotherapy might be an effective and well-tolerated treatment for advanced NSCLC in patients who fail in first- or second-line therapy (20). Anlotinib plus camrelizumab had shown promising efficacy and manageable toxicity as a second-line or later-line therapy for NSCLC, especially in the 12 mg cohorts (21). However, another study showed that anlotinib was less effective than platinum-pemetrexed chemotherapy in T790M-negative lung adenocarcinoma, implicating that it may be more suitable for squamous cell lung carcinoma (22). Hence, anlotinib has a synergistic antitumor effect and good safety for NSCLC and may be promising for front-line treatment for NSCLC (20). There have also been more studies of anlotinib as a first-line treatment in the last 2 years, and most of these studies have adopted the combination therapy model. The latest clinical analysis of first-line therapy in elderly patients with advanced lung adenocarcinoma without driver gene mutations showed similar median PFS (3.0 m vs. 2.8 m) and OS (7.0 m *vs.* 7.0 m) in the anlotinib group and the chemotherapy group ($P > 0.05$), and there was no significant difference in ORR (17.5 vs. 15%) or DCR (67.5 vs. 65.5%) between both treatment groups (23). The other studies have shown that, for driver gene-negative NSCLC patients, the median PFS in the anlotinib combined with chemotherapy group was 1.54 months longer than that in the chemotherapy group (9.38 months vs. 7.84 months, $P < 0.05$), and the median OS in the anlotinib combined with chemotherapy group was longer as well (11.52 months vs. 10.46 months), but the difference was not statistically significant ($P > 0.05$) (24). A study on inoperable NSCLC patients indicated that the median PFS of sequential chemoradiotherapy patients was 10.8 months, but grade 3 acute esophagitis occurred in four of 78 patients (5%) (25). As shown in Table 2 (18, 23, 26), anlotinib is promising for the first-line treatment for NSCLC with its median PFS range of 3.0 to 15.0 months.

Recently, more studies focused on the first-line usage for NSCLC but less for elderly patients. To the best of our knowledge, the NSCLC patients in most clinical trials were not allowed to be older than 75 years—for example, the median age of patients with lung cancer who were treated in pivotal trials involving immunotherapy ranged from 61 and 65 years, which are lower than the median age at diagnosis. Thus, such poor representation of older patients in clinical trials makes truly evidence-based decisions on the best regimen for geriatric patients difficult. This patient was 77 years old at diagnosis and achieved a total PFS of 34 months and OS of 53 months after anlotinib treatment, which exceeded most of the results of real-world studies and clinical trials. This case report suggests that combining anlotinib with chemotherapy shows promise as a front-line treatment for elderly patients with advanced NSCLC. Further prospective studies are necessary to validate these findings.

Conclusion

As a front-line treatment, anlotinib significantly prolonged this elderly NSCLC patient's survival time and improved his quality of life.

Data availability statement

The original contributions presented in the study are included in the article/supplementary material. Further inquiries can be directed to the corresponding author.

Ethics statement

The studies involving human participants were reviewed and approved by The ethics committee of The People's Hospital of Bishan District Chongqing. The patients/participants provided their written informed consent to participate in this study. Written informed

consent was obtained from the individual(s) for the publication of any potentially identifiable images or data included in this article.

Author contributions

JW and JZ contributed significantly to analysis and manuscript preparation. JW performed the data analyses and wrote the manuscript. XL and DQ helped perform the analysis with constructive discussions. MZ assisted in joint evaluation of patients and figure design. LS contributed to the conception of the study. SCL revised the article and made important suggestions. All authors contributed to the article and approved the submitted version.

Funding

This work was supported in part by the Natural Science Foundation of Chongqing, China (cstc2020jcyjmsxmX1063) and Beijing Science and Technology Innovation Medical Development Foundation, China (KC2021-JX-0186-28). This work was also supported in part by the UCI ICTS Award #16004004 (CHOC).

Acknowledgments

We thank the patient and his family for giving permission for his inclusion in this study.

Conflict of interest

The authors declare that the research was conducted in the absence of any commercial or financial relationships that could be construed as a potential conflict of interest.

Publisher's note

References

1. Siegel RL, Miller KD, Jemal A. Cancer statistics, 2019. *CA: Cancer J Clin* (2019) 691:7–34. doi: 10.3322/caac.21551

2. Hanahan D, Weinberg RA. Hallmarks of cancer: The next generation. *Cell* (2011) 1445:646–74. doi: 10.1016/j.cell.2011.02.013

3. Alshangiti A, Chandhoke G, Ellis PM. Antiangiogenic therapies in non-small-cell lung cancer. *Curr Oncol (Toronto Ont.)* (2018) 25Suppl 1:S45–s58. doi: 10.3747/co.25.3747

4. Barlesi F, Scherpereel A, Gorbunova V, Gervais R, Vikström A, Chouaid C, et al. Maintenance bevacizumab-pemetrexed after first-line cisplatin-pemetrexed-bevacizumab for advanced nonsquamous nonsmall-cell lung cancer: Updated survival analysis of the AVAPERL (MO22089) randomized phase III trial. *Ann Oncol* (2014) 255:1044–52. doi: 10.1093/annonc/mdu098

5. Margolin K, Gordon MS, Holmgren E, Gaudreault J, Novotny W, Fyfe G, et al. Phase ib trial of intravenous recombinant humanized monoclonal antibody to vascular endothelial growth factor in combination with chemotherapy in patients with advanced cancer: Pharmacologic and long-term safety data. *J Clin Oncol* (2001) 193:851–6. doi: 10.1200/JCO.2001.19.3.851

6. Shen G, Zheng F, Ren D, Du F, Dong Q, Wang Z, et al. Anlotinib: A novel multi-targeting tyrosine kinase inhibitor in clinical development. *J Hematol Oncol* (2018) 111:120. doi: 10.1186/s13045-018-0664-7

7. Han B, Li K, Wang Q, Zhang L, Shi J, Wang Z, et al. Effect of anlotinib as a third-line or further treatment on overall survival of patients with advanced non-small cell lung cancer: The ALTER 0303 phase 3 randomized clinical trial. *JAMA Oncol* (2018) 411:1569–75. doi: 10.1001/jamaoncol.2018.3039

8. Han B, Li K, Zhao Y, Li B, Cheng Y, Zhou J, et al. Anlotinib as a third-line therapy in patients with refractory advanced non-small-cell lung cancer: A multicentre, randomised phase II trial (ALTER0302). *Br J Cancer* (2018) 1185:654–61. doi: 10.1038/bjc.2017.478

9. Wang F, Jin F, Cheng B, Zhang Y, Zhou Q, Wang S. The real-world efficacy and safety of anlotinib in advanced non-small cell lung cancer. *J Cancer Res Clin Oncol* (2021) 148(7):1721–35. doi: 10.21203/rs.3.rs-282608/v1

10. Jalal SI, Riggs HD, Melnyk A, Richards D, Agarwala A, Neubauer M, et al. Updated survival and outcomes for older adults with inoperable stage III non-small-cell lung cancer treated with cisplatin, etoposide, and concurrent chest radiation with or without consolidation docetaxel: Analysis of a phase III trial from the Hoosier oncology group (HOG) and US oncology. *Ann Oncol* (2012) 237:1730–8. doi: 10.1093/annonc/mdr565

11. Shao L, Wang W, Song Z, Zhang Y. The efficacy and safety of anlotinib treatment for advanced lung cancer. *OncoTargets Ther* (2019) 12:6549–54. doi: 10.2147/OTT.S205674

12. Sun Y, Niu W, Du F, Du C, Li S, Wang J, et al. Safety, pharmacokinetics, and antitumor properties of anlotinib, an oral multi-target tyrosine kinase inhibitor, in patients with advanced refractory solid tumors. *J Hematol Oncol* (2016) 91:105. doi: 10.1186/s13045-016-0332-8

13. Zhang K, Ma X, Gao H, Wang H, Qin H, Yang S, et al. Efficacy and safety of anlotinib in advanced non-small cell lung cancer: A real-world study. *Cancer Manage Res* (2020) 12:3409–17. doi: 10.2147/CMAR.S246000

14. Liang L, Hui K, Hu C, Wen Y, Yang S, Zhu P, et al. Autophagy inhibition potentiates the anti-angiogenic property of multikinase inhibitor anlotinib through JAK2/STAT3/VEGFA signaling in non-small cell lung cancer cells. *J Exp Clin Cancer Res* (2019) 381:71. doi: 10.1186/s13046-019-1093-3

15. Leidal AM, Levine B, Debnath J. Autophagy and the cell biology of age-related disease. *Nat Cell Biol* (2018) 2012:1338–48. doi: 10.1038/s41556-018-0235-8

16. Norling LV, Serhan CN. Profiling in resolving inflammatory exudates identifies novel anti-inflammatory and pro-resolving mediators and signals for termination. *J Internal Med* (2010) 2681:15–24. doi: 10.1111/j.1365-2796.2010.02235.x

17. Fu S, Hou MM, Naing A, Janku F, Hess K, Zinner R, et al. Phase I study of pazopanib and vorinostat: A therapeutic approach for inhibiting mutant p53-mediated angiogenesis and facilitating mutant p53 degradation. *Ann Oncol* (2015) 265:1012–8. doi: 10.1093/annonc/mdv066

18. Chu T, Zhong R, Zhong H, Zhang B, Zhang W, Shi C, et al. Phase 1b study of sintilimab plus anlotinib as first-line therapy in patients with advanced NSCLC. *J Thorac Oncol* (2021) 164:643–52. doi: 10.1016/j.jtho.2020.11.026

19. Nokihara H, Lu S, Mok TSK, Nakagawa K, Yamamoto N, Shi YK, et al. Randomized controlled trial of s-1 versus docetaxel in patients with non-small-cell lung cancer previously treated with platinum-based chemotherapy (East Asia s-1 trial in lung cancer). *Ann Oncol* (2017) 2811:2698–706. doi: 10.1093/annonc/mdx419

20. Wang HY, Chu JF, Zhao Y, Tang H, Wang LL, Zhou MQ, et al. A trial of the safety and efficacy of chemotherapy plus anlotinib vs chemotherapy alone as second- or third-line salvage treatment for advanced non-small cell lung cancer. *Cancer Manage Res* (2020) 12:3827–34. doi: 10.2147/CMAR.S249678

21. Zhou N, Jiang M, Li T, Zhu J, Liu K, Hou H, et al. Anlotinib combined with anti-PD-1 antibody, camrelizumab for advanced NSCLCs after multiple lines treatment: An open-label, dose escalation and expansion study. *Lung Cancer (Amsterdam Netherlands)* (2021) 160:111–7. doi: 10.1016/j.lungcan.2021.08.006

22. Zhong RB, Xu JL, Lou YQ, Chu TQ, Zhong H, Han BH, et al. Anlotinib or platinum-pemetrexed as second-line therapy in EGFR T790M-negative lung cancer. *Ann palliative Med* (2020) 94:1681–7. doi: 10.21037/apm-20-105

23. Zhu J, Xie Q, Zhong A, Le Y. Clinical analysis of anlotinib as first-line treatment for elderly patients with advanced lung adenocarcinoma without driver gene mutations. *Anti-cancer Drugs* (2022) 331:e584–9. doi: 10.1097/CAD.0000000000001186

24. Zhang L, Zhang Q, Jin J, Liu X, Zhao Y, Yu H, et al. Efficacy of anlotinib combined with AN regimen in first-line treatment of advanced EGFR, ALK and ROS1 wild-type lung adenocarcinoma. *Guangdong Med* (2021) 42:151–6. doi: 10.13820/j.cnki.gdyx.20200278

25. Belderbos J, Uitterhoeve L, van Zandwijk N, Belderbos H, Rodrigus P, van de Vaart P, et al. Randomised trial of sequential versus concurrent chemo-radiotherapy in patients with inoperable non-small cell lung cancer (EORTC 08972-22973). *Eur J Cancer (Oxford Engl 1990)* (2007) 431:114–21. doi: 10.1016/j.ejca.2006.09.005

26. Huang D, Zhong D, Zhang C, Zhang Y, Shang Y, Wang L, et al. Study of anlotinib combined with icotinib as the first-line treatment in NSCLC patients harboring activating EGFR mutations: Updated results of ALTER-L004.Ann. *Oncol* (2021) 32:S969–9. doi: 10.1016/j.annonc.2021.08.1824

frontiers | Frontiers in Oncology

TYPE Case Report
PUBLISHED 17 October 2023
DOI 10.3389/fonc.2023.1073938

OPEN ACCESS

EDITED BY
Kohei Fujita,
National Hospital Organization Kyoto Medical Center, Japan

REVIEWED BY
Chunxia Su,
Shanghai Pulmonary Hospital, China
Chengdi Wang,
West China Hospital, Sichuan University, China
Luis Lara-Mejía,
National Institute of Cancerology (INCAN), Mexico

*CORRESPONDENCE
Yongsheng Wang
wangys@scu.edu.cn

RECEIVED 24 October 2022
ACCEPTED 20 September 2023
PUBLISHED 17 October 2023

CITATION
Ma Q, Shu P, Zhou K and Wang Y (2023) Case Report: Termination of unplanned pregnancy led to rapid deterioration of non-small-cell lung cancer during osimertinib treatment.
Front. Oncol. 13:1073938.
doi: 10.3389/fonc.2023.1073938

Case Report: Termination of unplanned pregnancy led to rapid deterioration of non-small-cell lung cancer during osimertinib treatment

Qizhi Ma[1], Pei Shu[1], Kexun Zhou[2] and Yongsheng Wang[1]*

[1]Division of Thoracic Tumor Multimodality Treatment, Cancer Center, State Key Laboratory of Biotherapy, West China Hospital, Sichuan University, Chengdu, China, [2]Department of Medical Oncology, Cancer Center, West China Hospital, Sichuan University, Chengdu, China

We present a case of a woman with non-small-cell lung cancer (NSCLC) who experienced disease progression during treatment with the epidermal growth factor receptor (EGFR)-tyrosine kinase inhibitor (TKI) osimertinib due to an unplanned pregnancy. Given the risk of tumor progression, the patient underwent an artificial abortion. However, disease deterioration occurred shortly after termination of the pregnancy, with severe chest pain, increased dyspnea, and pleural effusion. After positive rescue measures, including emergency thoracic drainage, thoracentesis, and oxygen uptake, her symptoms improved. Considering pregnancy as an immune escape physiological process, the patient continued treatment with osimertinib, and a partial response (PR) lasting 16 months was observed. Therefore, this case highlights the importance of being vigilant about the rapid development of the tumor after delivery in pregnant patients with EGFR-mutation lung cancer and taking preventive measures to cope with various emergencies.

KEYWORDS

pregnancy, non-small-cell lung cancer, epidermal growth factor receptor, tyrosine kinase inhibitor, deterioration

Introduction

In recent decades, lung cancer has remained the most lethal type of cancer. According to the 2020 global cancer statistics (1), there were 1.8 million deaths from lung cancer, far surpassing other cancer types and posing a serious threat to people's health and lives. While lung cancer frequently occurs in individuals over the age of 60, its incidence has been gradually increasing in the younger female population in recent years (2, 3). As women delay family formation due to social and economic development, tumors and pregnancy may occur simultaneously. Although the occurrence of malignant tumors during pregnancy is relatively rare, approximately 1 case per 1,000 pregnant women is

diagnosed with malignancy (4). While lung cancer is one of the most common malignancies, it is rare during pregnancy. Non-small-cell lung cancer (NSCLC) is the most common histological type, accounting for 80%–85% of all lung cancers in pregnancy (5).

The epidermal growth factor receptor (EGFR) pathway is a crucial signaling pathway in NSCLC, and the discovery of EGFR mutations as the most significant oncogenic driver genes in NSCLC has revolutionized the treatment paradigm for patients with advanced NSCLC. The deletion of exon 19 and the L858R mutation in exon 21 are considered the "classical" EGFR mutations, accounting for approximately 85% of EGFR mutations in NSCLC (6). Several targeted EGFR tyrosine kinase inhibitors (TKI) have been developed, demonstrating promising efficacy in patients with EGFR mutations. Among them, the third generation TKI, osimertinib, has stood out (7).

The ethical dilemma of balancing the health of the mother and the fetus has garnered significant attention. If a woman decides to proceed with the pregnancy, treatment options can present a significant challenge (5, 8). A review of published literatures related to lung cancer during pregnancy has revealed more than 80 reported cases. The majority of patients had advanced or metastatic disease and experienced unfavorable outcomes. To our knowledge, few reports exist on the administration of third-generation EGFR inhibitors (osimertinib) to pregnant patients with lung cancer. The effects of osimertinib on the fetus and its efficacy in the treatment of lung cancer during pregnancy require further investigation.

Here, we present the first case report of a patient with metastatic non-small-cell lung cancer who experienced tumor progression as a result of an unplanned pregnancy during treatment with osimertinib. Following the patient's artificial induction of labor, her condition rapidly deteriorated with malignant pleural effusion and dyspnea. However, she was able to continue treatment with osimertinib and experienced a sustained tumor response.

Case presentation

A 29-year-old young woman who had never smoked presented with a history of chest pain and cough that lasted for 1 week. Physical examination revealed a body temperature of 36.9°C, a pulse rate of 105 beats/min, blood pressure of 103/69 mmHg, and respiratory rate of 22 breaths/min. Dual lung percussion was clear, and the breathing sound of both lungs was clear without any wetness. The serum tumor markers showed that the cancer antigen 15-3 (CA15-3) was 45.78 U/ml, and CA72-4 was 11.78 U/ml, while no abnormalities were observed in the remaining indicators. Chest computed tomography (CT) revealed a 2.5 × 2.2 cm solid nodule in the middle lobe of the right lung, along with multiple small nodules in both lungs, a small amount of pleural fluid on the right side, and several enlarged mediastinal lymph nodes (Figure 1A). The patient had menarche at the age of 14 with a menstrual cycle of 28 ± 3 days, lasting 3–5 days, normal menstrual volume and color, and no dysmenorrhea history. She was pregnant once, and a healthy male birth was born at the age of 27. The patient denied any history of previous tumor disease or family history of the same. Endoscopic ultrasound-guided fine-needle aspiration (FNA) pathology biopsy indicated scattered heterogeneous glandular epithelium. Immunohistochemistry (IHC) staining showed CK7 (+), CK20 (−), CDX2 (−), TTF-1 (8G7G3/1) (+), Napsin A (+), GATA3 (−), Ki67 (MIB-1) (+, 30%–40%), ALK-V (−), and ROS1 (−). These results supported the diagnosis of NSCLC of adenocarcinoma. Furthermore, second-generation genetic testing of the puncture specimen revealed a short deletion in exon 19 of the EGFR gene (del-19) and a mutation in L858R in exon 21. After a comprehensive evaluation, the oncologist assigned the staging as cT4N2M1a (IVa stage).

Following the diagnosis of adenocarcinoma due to the EGFR mutation, the patient was prescribed the EGFR-TKI gefitinib at a dosage of 250 mg p.o. q.d (Figure 2). Two months after treatment, a thoracic CT scan indicated a significant reduction in the nodule in the middle lobe of the right lung, which had decreased to 1.5 × 1.0 cm, without enlargement of the hilar and mediastinal lymph nodes (Figure 1B). The efficacy assessment showed a partial response (PR), and gefitinib was continued. However, 9 months later, the patient again experienced chest pain and coughing up blood with dyspnea, serum carcinoembryonic antigen (CEA) was 91.22 ng/ml, and neuron-specific enolase (NSE) was 16.77 ng/ml, and CT imaging indicated partial pulmonary atelectasis and solid changes in the middle and lower lobes of the right lung, moderate pleural effusion on the right side, and an increase in bilateral lung lesions and regional lymph nodes (Figure 1C). The response evaluation revealed progressive disease (PD). Additionally, the follow-up genetic sequencing revealed the addition of EGFR T790M mutation in exon 20, which indicated the resistance to gefitinib.

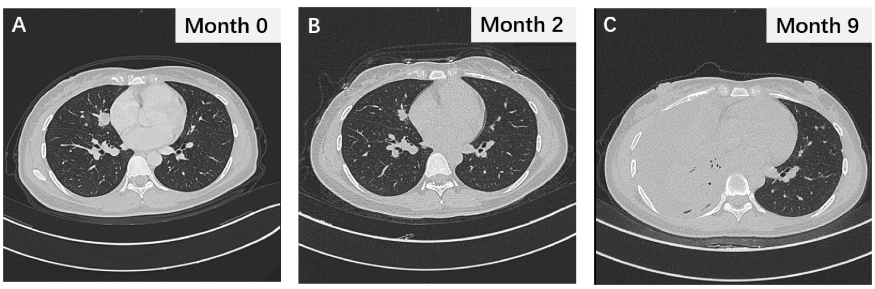

FIGURE 1
(A) The thoracic CT image displaying lung lesions during initial evaluation. **(B)** The thoracic CT scan showing the changes in lung lesions after 2 months of gefitinib treatment. **(C)** The chest CT image during gefitinib resistance.

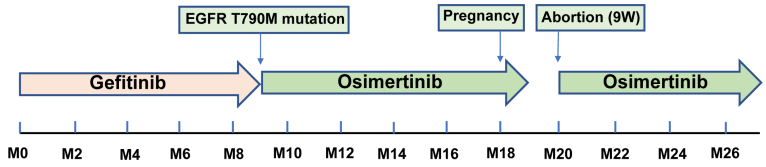

FIGURE 2
Flow-process diagram illustrating the patient's tumor management.

Following treatment with osimertinib, a third-generation EGFR-TKI, the patient's target lesions exhibited significant reduction after 2 months of dosing. The bilateral lung nodules were observed to have shrunk and decreased, the right pleural effusion disappeared, and the right hilar and mediastinal lymph nodes shrank, as confirmed by Figure 3A. The efficacy of the treatment was assessed as PR. Continuous administration of osimertinib for 8 months further reduced the tumor. However, the patient was unexpectedly found to be 4 weeks pregnant, and pregnancy termination was recommended due to the risks associated with treatment using osimertinib. Despite being fully informed of the potential risks of preterm delivery, fetal malformation, and late developmental complications associated with osimertinib treatment, the patient and her family decided to continue with the pregnancy. Targeted therapy was suspended in order to avoid potential risks of osimertinib to healthy fetal development. Unfortunately, the disease progressed upon assessment at 8 weeks of pregnancy.

We again informed the risks associated with continuing the pregnancy, and the patient ultimately decided to undergo an abortion at 9 weeks of gestation. However, an unforeseeable emergency arose after the procedure: the human chorionic gonadotrophin (HCG) levels rapidly dropped (Figure 4A). Shortly thereafter, the patient developed severe chest pain, respiratory distress, and moderate right pleural effusion. Red blood cell and lymphocyte counts decreased, and blood gas analysis revealed a pH of 7.452, oxygen level of 116.4 mmHg, potassium level of 3.37 mmol/L, glucose level of 6.60 mmol/L, oxygen saturation of 99.5%, and ion level of 1.02 mmol/L. Additionally, there was a significant increase in C-reactive protein (CRP), interleukin-6 (IL-6), and various tumor markers, indicating a rapidly deteriorating and urgent situation.

The patient was treated urgently with oxygen therapy and ultrasound-guided thoracentesis and drainage to relieve the pleural effusion. As gestation can lead to abnormal hormone secretion and immunosuppression, we believed that the rapid progression of the disease was not due to drug resistance to osimertinib. Therefore, 1 week after abortion, osimertinib targeted therapy was resumed, resulting in the disappearance of the pleural effusion and reduction in lung nodules and lymph nodes (Figure 3B). At the time of data collection, the patient had been on osimertinib treatment for over 16 months and was still benefiting from it (Figure 3C).

Throughout the course of treatment, we also monitored the patient's serum tumor marker levels, the NSCLC-specific marker cytokeratin fragment 19 (CYFRA21-1) (Figure 4B), and the broad-spectrum markers CEA, CA125, CA153, and CA724 (Figures 4C–F). These data were concordant with imaging findings and patient symptoms, to some extent, allowing to monitor the therapeutic effect, assess prognosis, and predict recurrence (9–11). Especially in the 20th month, after abortion at 9 weeks of pregnancy, serum levels of the above five tumor markers increased sharply, reflecting the critical situation caused by rapid tumor progression at that time; when continued treatment with osimertinib, the patient's serum tumor markers decreased rapidly, consistent with imaging findings (Figure 3C).

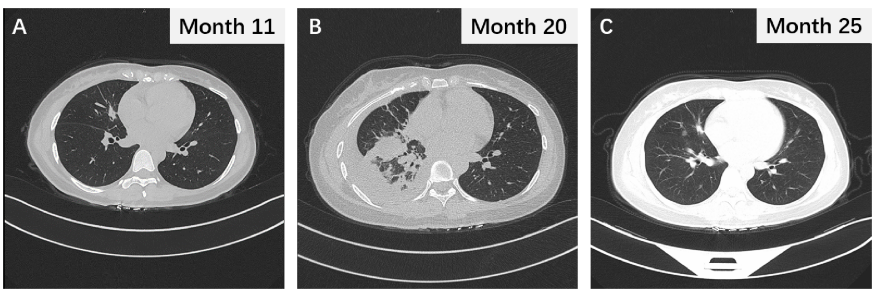

FIGURE 3
(A) The thoracic CT scan revealing the changes in lung nodules after 2 months of osimertinib treatment. **(B)** The chest CT image following termination of pregnancy. **(C)** Chest CT scan after 16 months of osimertinib treatment and demonstrating sustained partial response.

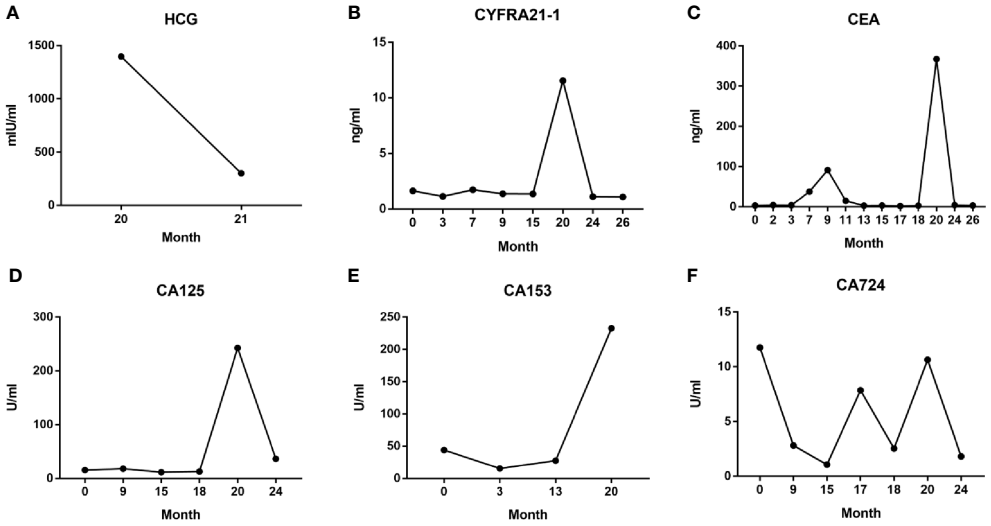

FIGURE 4
Serum HCG **(A)** and tumor markers CYFRA21-1 **(B)**, CEA **(C)**, CA125 **(D)**, CA153 **(E)**, and CA724 **(F)** levels during the entire diagnosis and treatment process.

Discussion

Lung cancer ranks third in prevalence among women and is the second most lethal tumor type worldwide (1). In recent years, lung cancer in pregnant women has been increasingly reported, and the majority of patients are diagnosed with progressive disease at stage III–IV (12). With advances in the study of lung cancer biology, molecular characteristics, and biomarkers, the treatment paradigm of lung cancer has undergone significant changes, leading to prolonged survival and improved the quality of life for patients (13). However, the management of pregnancy with lung cancer remains complicated. The challenge lies in balancing optimal treatment outcomes with fetal health, as treatment may potentially threaten the healthy development of the fetus, leading to serious ethical considerations (14).

We present a case report of a young non-smoking woman with NSCLC who had an unplanned pregnancy during osimertinib treatment, despite being advised to use strict contraception. After the diagnosis of tumor progression, the patient made the difficult decision to terminate the pregnancy. Unexpectedly, 2 weeks following the induced abortion, the patient developed severe chest pain and respiratory distress, and CT imaging revealed multiple patchy and solid shadows in the right lung, right pleural effusion, and enlarged mediastinal and bilateral axillary lymph nodes. Pulmonary vein embolism, pulmonary heart disease, and severe lung infection were all ruled out as potential causes, and the rapid progression of lung cancer was confirmed. However, with continued treatment of osimertinib, the patient achieved sustained remission.

In this case, three questions have arisen for our consideration. First is the efficacy and safety of drugs previously reported in patients with pregnancy-related driver gene-positive lung cancer, whether treated accordingly during pregnancy or after delivery, as compared to previous studies (15, 16). However, we noted that our report differed from previous cases, as most previous cases were diagnosed with lung cancer after pregnancy, whereas we reported an unplanned pregnancy during lung cancer treatment. After pregnancy, the body enters a state of immune escape from the fetus and placenta, which facilitates normal fetal growth and development. Unfortunately, tumor cells also simultaneously escape from immune cells with the help of the body's state of immune suppression and grow rapidly (17). Additionally, the increased estrogen and progesterone levels during pregnancy, in response to estrogen receptor-positive tumor cells, promote the proliferation of lung cancer cells, which may contribute to rapid tumor progression (18).

Second, what is the cause of rapid disease progression in patients after undergoing induced abortion? After termination of pregnancy, the immune-evasion mechanism of the fetus and malignant tumor ceases, and the organism restores normal immune function. This recognition of mutated tumor cells induces a strong anti-tumor immune response in a short period of time, and a large number of immune cells infiltrate, leading to acute tumor growth and pleural effusion. Moreover, abortion is an exogenous physical trauma that causes an inflammatory response in the body, attracting inflammatory cells and secretion of a large number of inflammatory factors. The healing process of the trauma further increases the expression of epidermal growth factor (19), thus accelerating tumor deterioration. Additionally, it has been demonstrated in NSCLC cell lines that estrogen can induce downregulation of EGFR expression in tumor cells (20), and this finding was also verified in mouse experiments that the administration of exogenous estrogen to male mice significantly inhibited the growth of lung cancer and attenuated NF-κB-driven immunosuppression (21). The rapid decrease in estrogen and progesterone levels *in vivo* after termination of pregnancy and the liberation of NF-κB immunosuppression, along with the upregulation of EGFR expression in response to estrogenic changes, may also be important for the disease progression.

Third, does pregnancy have different effects on lung cancer with different driver genetic alterations? Our report is similar to two other cases of lung cancer in pregnant patients delivered by cesarean

section, which exhibited rapid disease progression after delivery and followed a consistent clinical course (22, 23). One of the cases involved a 27-year-old woman who experienced fulminant respiratory failure on the third day after cesarean delivery. Despite the best supportive care, she succumbed to cardiopulmonary failure 4 days postoperatively (23). Notably, all three lung cancer cases, including our own, exhibited amplification or mutation of the EGFR driver gene. Another driver oncogenic molecule, the anaplastic lymphoma kinase (ALK) gene, is more commonly implicated in pregnancy-associated lung cancers (8). However, unlike EGFR mutations, pregnancy-associated lung cancers carrying ALK gene alterations did not show acute tumor progression after delivery; sustained disease remission was achieved through continued ALK-TKI therapy (24, 25). The observed differences in tumor behavior before and after delivery in pregnancy-associated lung cancers with different driver gene alterations may be related to dominant oncogenic pathways. Patients with EGFR mutations may be more sensitive to changes in hormonal and inflammatory responses *in vivo*, indicating the need for individualized formulation of management measures for lung cancer in pregnancy with specific driver mutations.

Therefore, termination of pregnancy in lung cancer patients requires heightened vigilance, especially in cases associated with EGFR mutations, as the disease may worsen dramatically following cesarean section or abortion. Adequate preparations should be made before termination of pregnancy to handle any unexpected emergencies, such as oxygenation, blocking driver gene signaling, suppressing immune response, and reducing the inflammatory response. Currently, there are no established guidelines for the clinical management of lung cancer during pregnancy, and treatment decisions are mostly based on case studies. Therefore, we strongly advocate the establishment of an international mutual support network platform dedicated to the study of pregnancy-related lung cancer, which can provide references for the standardized treatment of pregnancy-related lung cancer by sharing valuable experiences and insights.

Furthermore, strict contraception during treatment for female lung cancer patients of childbearing age is of utmost importance, as pregnancy can severely limit treatment options and delay the optimal tumor treatment. For lung cancer diagnosed during pregnancy, the main conflict between disease control of the mother and potential risks to the fetus should be carefully considered when choosing an optimal treatment. To provide an individualized treatment strategy for mothers with lung cancer during pregnancy, a multidisciplinary and integrated collaborative approach consisting of oncologists, obstetricians, and psychologists should be established, meanwhile respecting the patient's autonomous will.

Patient's perspective

Unexpectedly, I became pregnant while undergoing treatment for lung cancer. Despite being advised by my doctor about the possibility of treatment resistance, I chose to continue with the pregnancy. However, the disease progressed rapidly, and I made the decision to terminate the pregnancy. Following the procedure, I experienced a life-threatening complication that required prompt medical intervention. Thanks to the prompt and dedicated care provided by my medical team, the tumor was brought under control. I feel extremely fortunate to have received such excellent care.

Data availability statement

The original contributions presented in the study are included in the article/supplementary material. Further inquiries can be directed to the corresponding author.

Ethics statement

Written informed consent was obtained from the patient/guardian for all data and images in this study.

Author contributions

YW conceptualized the idea of this case. QM performed data and drafted the manuscript. PS and KZ revised and edited the manuscript. All authors read and approved the final manuscript.

Funding

This work was supported by National Natural Science Foundation of China (81872489).

Conflict of interest

The authors declare that the research was conducted in the absence of any commercial or financial relationships that could be construed as a potential conflict of interest.

The reviewer CW declared a shared affiliation with the authors to the handling editor at the time of review.

Publisher's note

References

1. Sung H, Ferlay J, Siegel RL. Global cancer statistics 2020: GLOBOCAN estimates of incidence and mortality worldwide for 36 cancers in 185 countries. *CA Cancer J Clin* (2021) 71(3):209–49. doi: 10.3322/caac.21660

2. Fidler-Benaoudia MM, Torre LA, Bray F, Ferlay J, Jemal A. Lung cancer incidence in young women vs. young men: A systematic analysis in 40 countries. *Int J Cancer* (2020) 147(3):811–9. doi: 10.1002/ijc.32809

3. Jemal A, Miller KD, Ma J, Siegel RL, Fedewa SA, Islami F. Higher lung cancer incidence in young women than young men in the United States. *N Engl J Med* (2018) 378(21):1999–2009. doi: 10.1056/NEJMoa1715907

4. Pentheroudakis G, Pavlidis N. Cancer and pregnancy: poena magna, not anymore. *Eur J Cancer* (2006) 42(2):126–40. doi: 10.1016/j.ejca.2005.10.014

5. Boussios S, Han SN, Fruscio R, Halaska MJ, Ottevanger PB, Peccatori FA, et al. Lung cancer in pregnancy: report of nine cases from an international collaborative study. *Lung Cancer* (2013) 82(3):499–505. doi: 10.1016/j.lungcan.2013.09.002

6. Rosell R, Moran T, Queralt C, Porta R, Cardenal F, Camps C, et al. Screening for epidermal growth factor receptor mutations in lung cancer. *N Engl J Med* (2009) 361 (10):958–67. doi: 10.1056/NEJMoa0904554

7. Cooper AJ, Sequist LV. Third-generation EGFR and ALK inhibitors: mechanisms of resistance and management. *Nat Rev Clin Oncol* (2022) 19(8):499–514. doi: 10.1038/s41571-022-00639-9

8. Mitrou S, Petrakis D, Fotopoulos G, Zarkavelis G, Pavlidis N. Lung cancer during pregnancy: A narrative review. *J Adv Res* (2016) 7(4):571–4. doi: 10.1016/j.jare.2015.12.004

9. Dal Bello MG, Filiberti RA, Alama A, Orengo AM, Mussap M, Coco S, et al. The role of CEA, CYFRA21-1 and NSE in monitoring tumor response to Nivolumab in advanced non-small cell lung cancer (NSCLC) patients. *J Transl Med* (2019) 17(1):74. doi: 10.1186/s12967-019-1828-0

10. Wang CF, Peng SJ, Liu RQ. The combination of CA125 and NSE is useful for predicting liver metastasis of lung cancer. *Dis Markers* (2020) 2020:8850873. doi: 10.1155/2020/8850873

11. Chen ZQ, Huang LS. Assessment of seven clinical tumor markers in diagnosis of non-small-cell lung cancer. *Dis Markers* (2018) 2018:9845123. doi: 10.1155/2018/9845123

12. Pavlidis NA. Coexistence of pregnancy and Malignancy. *Oncologist* (2002) 7 (4):279–87. doi: 10.1634/theoncologist.2002-0279

13. Thai AA, Solomon BJ, Sequist LV, Gainor JF, Heist RS. Lung cancer. *Lancet* (2021) 398(10299):535–54. doi: 10.1016/S0140-6736(21)00312-3

14. Weisz B, Schiff E, Lishner M. Cancer in pregnancy: maternal and fetal implications. *Hum Reprod Update* (2001) 7(4):384–93. doi: 10.1093/humupd/7.4.384

15. Yang L, He YT, Kang J, Zheng MY, Chen ZH, Yan HH, et al. Clinical features and intervention timing in patients with pregnancy-associated non-small-cell lung cancer. *J Thorac Dis* (2021) 13(7):4125–36. doi: 10.21037/jtd-21-234

16. Boudy AS, Grausz N, Selleret L, Gligorov J, Thomassin-Naggara I, Touboul C, et al. Use of tyrosine kinase inhibitors during pregnancy for oncogenic-driven advanced non-small cell lung carcinoma. *Lung Cancer* (2021) 161:68–75. doi: 10.1016/j.lungcan.2021.09.001

17. Hayakawa S. No cancer in cancers: evolutionary trade-off between successful viviparity and tumor escape from the adaptive immune system. *Med Hypotheses* (2006) 66(5):888–97. doi: 10.1016/j.mehy.2005.12.010

18. Nose N, Sugio K, Oyama T, Nozoe T, Uramoto H, Iwata T, et al. Association between estrogen receptor-beta expression and epidermal growth factor receptor mutation in the postoperative prognosis of adenocarcinoma of the lung. *J Clin Oncol* (2009) 27(3):411–7. doi: 10.1200/JCO.2008.18.3251

19. Zhang Y, Luo J, Zhang Q, Deng T. Growth factors, as biological macromolecules in bioactivity enhancing of electrospun wound dressings for diabetic wound healing: A review. *Int J Biol Macromol* (2021) 193:205–18. doi: 10.1016/j.ijbiomac.2021.09.210

20. Stabile LP, Lyker JS, Gubish CT, Zhang W, Grandis JR, Siegfried JM. Combined targeting of the estrogen receptor and the epidermal growth factor receptor in non-small cell lung cancer shows enhanced antiproliferative effects. *Cancer Res* (2005) 65 (4):1459–70. doi: 10.1158/0008-5472.CAN-04-1872

21. Deng S, Ramos-Castaneda M, Velasco WV, Clowers MJ, Gutierrez BA, Noble O, et al. Interplay between estrogen and Stat3/NF-κB-driven immunomodulation in lung cancer. *Carcinogenesis* (2020) 41(11):1529–42. doi: 10.1093/carcin/bgaa064

22. Watanabe T, Yamashita T, Sugawara H, Fukuchi T, Ishii A, Nagai Y, et al. Rapid progression of lung cancer following emergency caesarean section led to postpartum acute respiratory failure. *Intern Med* (2019) 58(7):991–7. doi: 10.2169/internalmedicine.1105-18

23. But Hadzic J, Secerov A, Zwitter M, Lamovec J, Kern I, Kavsek G, et al. Metastatic adenocarcinoma of the lung in a 27-year-old pregnant woman. *J Thorac Oncol* (2007) 2(5):450–2. doi: 10.1097/01.JTO.0000268680.33238.01

24. Carlier S, Carestia L, Marot JC, Wieërs G. Unplanned pregnancy in an HIV positive woman undergoing alectinib treatment for metastatic non-small-cell lung carcinoma. *BMJ Case Rep* (2022) 15(7):e247530. doi: 10.1136/bcr-2021-247530

25. Scarfone G, Fumagalli M, Imbimbo M, Ceruti T, Cribiù FM, Di Loreto E, et al. First case report of pregnancy on alectinib in a woman with metastatic ALK-rearranged lung cancer: A case report. *J Thorac Oncol* (2021) 16(5):873–7. doi: 10.1016/j.jtho.2021.02.005

Frontiers in Oncology

Advances knowledge of carcinogenesis and tumor progression for better treatment and management

The third most-cited oncology journal, which highlights research in carcinogenesis and tumor progression, bridging the gap between basic research and applications to imrpove diagnosis, therapeutics and management strategies.

Discover the latest Research Topics

See more →

Frontiers

Avenue du Tribunal-Fédéral 34
1005 Lausanne, Switzerland
frontiersin.org

Contact us

+41 (0)21 510 17 00
frontiersin.org/about/contact